Bronchoscopic assessment and management of children presenting with clinically significant airway obstruction due to tuberculosis

Dissertation presented by

Pierre Goussard

For a PhD degree in Paediatrics and Child Health

at

Stellenbosch University

Promoter: Prof RP Gie

March 2015

Declaration

I, the undersigned, hereby declare that the work contained in this dissertation is my own original work and that I have not previously in its entirety or in part submitted it at any other university for a degree.

Signature: Date

Summary

Tuberculosis (TB) in children is a common infectious disease in the world affecting approximately 550 000 children annually and contributing to approximately 10-15% of the TB caseload. The estimate is that 75% of the children who have TB live in the 22 countries that have the highest burden of TB disease. In these 22 countries, the technology required to make the diagnosis and manage complicated cases is limited. The epidemiological data required to estimate the proportion of children with severe disease requiring intervention at a global level are lacking.

Airway involvement is commonly seen in children with primary TB, but only in a small group of children the compression is severe, needing intervention. The incidence of children with airway obstruction requiring intervention due to primary TB in the chemotherapeutic era is not known. The incidence of complicated lymph node disease in two recent reports varied from 8-38% in children younger than 15 years of age.

Flexible bronchoscopy (FB) is an invasive procedure performed under general anesthetic is used to assess the airways of children. Few studies have been published on the use of FB in the diagnosis of paediatric TB and most have concentrated on the use of bronchoscopy as an intervention for obtaining samples to diagnose pulmonary TB (PTB). All previous studies only examined broncho-alveolar lavage (BAL) for Ziehl Neelsen (ZN) positive organisms and mycobacterial culture. All the published studies are from developed countries with a very low incidence of PTB in children. It has been postulated that HIV positive children with TB are more likely to have airway obstruction, but this hypothesis has not been studied. The same is true for children infected with drug-resistant strains of tuberculosis. Similarly, there have been few reports on the correlation between the findings at bronchoscopy and those found on chest computer tomography (CT).

The aim of this research project was to systematically determine airways involvement in childhood pulmonary TB and assess the role paediatric bronchoscopy plays in the diagnosis, sample collection and the management of severe airway obstruction.

The first part of the thesis describes the bronchoscopic assessment of airway obstruction due to pulmonary TB in children, specifically concentrating on the areas of the airway involved and the severity of the obstruction. We investigated which factors determine the severity of airway obstruction and this included age, sex, HIV status and drug sensitivities. We have shown that there was no difference in airway obstruction in HIV positive children

and in children with drug resistance TB. More severe airway obstruction was seen in the younger child.

The second question that was analysed is the value of flexible bronchoscopy in collecting samples for TB culture and drug sensitivity testing. It has previously been reported that BAL culture was inferior to gastric lavage in isolating the bacilli. We set out to evaluate which factors determine if a child will be culture-positive on BAL. Most childhood pulmonary TB is postulated to have a low yield of ZN positive cases. We found a higher yield from BAL as was previously reported, and the yield was increased if segmental or lobar pneumonia was present on the chest radiography. We developed novel interventions of finding the organism and increasing the yield from BAL. About 80% of children with PTB have enlarged subcarinal lymph nodes. We performed a trans-bronchial needle aspiration (TBNA) biopsy of these lymph nodes for culture. This technique enables us to differentiate the cause of enlarged mediastinal lymph nodes. This is especially important in children who are HIV positive, as they are prone to have other causes of enlarged lymph nodes. We successfully performed TBNA, even in very young infants, which resulted in a diagnostic yield of 55%. The use of Xpert has been described on other tissue, but not on BAL. We wanted to test if the use of Xpert on BAL is feasible in children, and determine if it will increase the diagnostic yield by using BAL samples.

The third aspect of this research was to compare flexible bronchoscopy findings with those of chest CT scan finding. Firstly, the aim was to describe the CT scan findings of mediastinal glands and lungs in children with significant airway obstruction due to PTB. The second aim was to investigate how these two investigations of airway obstruction compared, with particular emphasis on their advantages and disadvantages. The areas of airway obstruction as well as the severity of the obstruction as determined by CT scan were very similar to the findings with bronchoscopy. The final part under this aspect of the study was to analyze airway shape using a computer model to asses if this could predict TB. This was done by extracting components of the airway surface mesh and branch radius and orientation features. This method showed the potential of computer-assisted detection of TB and other airway pathology by using airway shape deformation analysis.

The fourth aspect investigated was to determine which children with severe airway obstruction would benefit from a surgical intervention. Surgical enucleation is done via a lateral thoracotomy in children with severe airway obstruction. We investigated which factors determine the need for surgical enucleation, the optimal timing of this intervention,

and – if surgical enucleation was done as an emergency intervention – which factors would predict for this. The combination of trachea, left main bronchus and bronchus intermedius involvement was the best predictor for children requiring surgical enucleation. Involvement of the smaller airway divisions did not play a significant role. Children needing enucleation were younger and had more severe airway obstruction.

The fifth aspect of this thesis was to measure the outcome following surgical enucleation. Measurements used included clinical measurements, radiological measurements and bronchoscopy. The response in children treated surgically were compared to those treated medically by estimating airway size with flexible bronchoscopy. Both groups showed significant improvement with the magnitude of improvement greater in those surgically treated.

We have demonstrated in this thesis that the site and severity of severe airway obstruction can be assessed by either bronchoscopy or chest CT scan. Approximately one third of children with severe airway compression due to TB lymph nodes can be successfully treated surgically with a low morbidity and mortality.

Opsomming

Tuberkulose (TB) by kinders is wêreldwyd ’n algemene siekte wat jaarliks ongeveer 550 000 kinders raak en sowat 10-15% van die algehele TB-siektelas uitmaak. Na raming kom 75% van alle kinders met TB van die 22 lande met die hoogste TB-siektelas. Hierdie 22 lande beskik oor beperkte tegnologie om die siekte te diagnoseer en ingewikkelde gevalle te bestuur. Die vereiste epidemiologiese data om te raam watter persentasie kinders wêreldwyd ernstig siek is en intervensie vereis, ontbreek ook.

Lugwegaantasting word algemeen by kinders met primêre TB aangetref. Tog is die kompressie by slegs ’n klein groepie kinders so erg dat dit intervensie vereis. Die voorkoms van kinders in die chemoterapeutiese era met primêre-TB-verwante obstruksie van die lugweë wat intervensie vereis, is onbekend. In twee onlangse verslae het die voorkoms van gekompliseerde limfkliersiekte by kinders jonger as 15 jaar van 8% tot 38% gewissel.

Buigbare brongoskopie is ’n indringende prosedure wat onder algemene verdowing uitgevoer word om kinders se lugweë te ondersoek. ’n Paar studies is reeds gepubliseer oor die gebruik van buigbare brongoskopie om pediatriese TB te diagnoseer. Die meeste daarvan het gekonsentreer op die gebruik van brongoskopie as intervensie vir die insameling van monsters om pulmonêre TB (PTB) te diagnoseer. Alle vorige studies het uitsluitlik ondersoek ingestel na brongo-alveolêre spoeling (BAS) vir die opsporing van Ziehl Neelsen- (ZN-)positiewe materiaal en vir kweking. Geen ander diagnostiese tegnieke is tot dusver ondersoek nie, wat die waarde daarvan vir populasies met ’n hoë siektelas beperk. Boonop is alle gepubliseerde studies in ontwikkelde lande met ’n baie lae voorkoms van PTB by kinders onderneem. Daar word aangevoer dat MIV-positiewe kinders met TB meer waarskynlik aan obstruksie van die lugweë sal ly, hoewel hierdie hipotese nog nie bestudeer is nie. Dieselfde geld vir kinders wat aan middelweerstandige vorme van TB ly. Daar is ook weinig verslae oor die verband tussen die bevindinge van brongoskopie en dié van rekenaartomografie (RT) van die borskas.

Die doel van hierdie navorsing was om stelselmatig vas te stel hoe pulmonêre TB by kinders die lugweë aantas, en watter rol pediatriese brongoskopie in diagnose, monsterinsameling en die hantering van ernstige obstruksie van die lugweë speel.

Die eerste deel van die tesis beskryf die brongoskopiese voorkoms van PTB-verwante obstruksie van die lugweë, met bepaalde klem op die aangetaste dele van die lugweg en

die erns van die obstruksie. Daar is ondersoek ingestel na watter faktore die erns van die obstruksie bepaal, onder meer ouderdom, geslag, MIV-status en middelsensitiwiteit. Die resultate toon geen verskil in obstruksie by MIV-positiewe kinders en kinders met middelweerstandige TB nie, hoewel ernstiger obstruksie van die lugweë by die jonger kind opgemerk is.

Die tweede kwessie wat ontleed is, is die waarde van buigbare brongoskopie in die verkryging van monsters vir TB-kweking en toetse vir middelsensitiwiteit. Daar is voorheen aangemeld dat BAS-kweking minder doeltreffend is as gastriese spoeling om die basille te isoleer. Hierdie studie was daarop toegespits om te beoordeel watter faktore bepaal of ’n kind kwekingspositief met BAS sal wees. Die meeste PTB by kinders toon na bewering ’n lae opbrengs van ZN-positiewe gevalle. Tog het BAS in hierdie studie ’n hoër opbrengs gehad as wat voorheen aangemeld is, welke opbrengs hoër was met die aanwesigheid van segmentale of lobêre pneumonie op die borskasradiogram. Innoverende intervensies is ontwikkel om die organisme op te spoor en die opbrengs met BAS te verhoog. Sowat 80% van kinders met PTB het vergrote subkarinale limfkliere. ’n Transbrongiale naaldaspirasie- (TBNA-)biopsie is gevolglik vir die doeleinde van kweking op hierdie kliere uitgevoer. Hierdie tegniek het die navorser in staat gestel om tussen die verskillende oorsake vir vergrote mediastinale limfkliere te onderskei. Dít is veral belangrik by MIV-positiewe kinders, wat geneig is om ander oorsake vir vergrote limfkliere te toon. Die TBNA-biopsies is selfs by baie jong babas suksesvol uitgevoer, wat tot ’n diagnostiese opbrengs van 55% gelei het. Die gebruik van Xpert op ander weefsel as BAS is al voorheen beskryf. Die navorser wou dus vasstel of die gebruik van Xpert by BAS haalbaar is by kinders, en of dit die diagnostiese opbrengs deur die gebruik van BAS-monsters sal verhoog.

Die derde aspek van hierdie navorsing was om die bevindinge van buigbare brongoskopie met dié van RT-skanderings van die borskas te vergelyk. Die doel was eerstens om die bevindinge van die RT-skanderings van mediastinale kliere en longe by kinders met beduidende PTB-verwante lugweg-obstruksie te beskryf. Tweedens wou die navorser vasstel wat die verskille tussen hierdie twee ondersoeke van lugweg-obstruksie is, met bepaalde klem op die voordele en nadele daarvan. Die RT-skandering en die bevindinge van brongoskopie lewer betreklik soortgelyke resultate op wat die aangetaste gedeeltes van die lugweg sowel as die erns van sodanige obstruksie betref. Die laaste doel onder hierdie studieaspek was om die vorm van die lugweg met behulp van ’n rekenaarmodel te ontleed om te bepaal of dit TB kan voorspel. Dít is gedoen deur komponente van die

lugwegoppervlaknetwerk en vertakkingsradius- en oriëntasiekenmerke te onttrek. Hierdie metode het daarop gedui dat rekenaargesteunde opsporing van TB en ander lugwegpatologie deur middel van ’n ontleding van lugwegvervorming wél potensiaal toon.

Die vierde aspek was om te bepaal watter kinders met ernstige obstruksie van die lugweë by intervensie sal baat vind. By sulke kinders word chirurgiese enukleëring deur ’n laterale torakotomie uitgevoer. Die studie het ondersoek ingestel na watter faktore die behoefte aan chirurgiese enukleëring bepaal, wat die optimale tyd vir sodanige intervensie sou wees, en – indien chirurgiese enukleëring as noodintervensie uitgevoer word – watter faktore so ’n noodintervensie sou vereis. Die kombinasie van aantasting van die tragea, linkerhoofbrongus en brongus intermedius was die beste voorspeller van kinders wat chirurgiese enukleëring benodig. Aantasting van die kleiner lugwegverdelings het nie ’n beduidende rol gespeel nie. Kinders wat enukleëring vereis, was jonger en het aan ernstiger obstruksie van die lugweë gely.

Die vyfde aspek van hierdie tesis was om die uitkoms na afloop van chirurgiese enukleëring te meet. Kliniese metings, radiologiese metings en brongoskopie is hiervoor gebruik. Die reaksie by kinders wat chirurgies behandel is, is vergelyk met diegene wat medies behandel is deur lugweggrootte met behulp van buigbare brongoskopie te raam. Albei groepe het beduidende verbetering getoon.

In die studie het ons getoon dat die ligging en die erns van ernstige lugwegobstruksie kan geassesseer word deur óf brongoskopie of rekenaartomografie van die borskas. Ongeveer een derde van kinders met 'n ernstige lugweg-obstruksie weens TB limfkliersiekte kan suksesvol chirurgies met 'n lae morbiditeit en mortaliteit behandel word.

Dedication

I dedicate this thesis to my family for their constant support and unconditional love. I thank the Lord for being present in good times and bad times.

Table of Contents

CHAPTER 1

Introduction

Introduction

During the last decade there has been a surge of interest in tuberculosis (TB) in children. In 2012 it was estimated that 82% of the approximately 8 million global cases of TB occur in 22 countries (high burden countries) and that 95% of the childhood TB cases live in these 22 countries. Furthermore, in 2012 the World Health Organization was able to calculate that 490000 children are annually treated for TB and that 64000 HIV uninfected children die from TB each year.[1] This data was obtained from national TB programs and is probably an underestimate as not only do the current diagnostic tests perform poorly in children but there is also limited resource capacity available for the diagnosis and management of complicated childhood TB in these high burden countries.

Pulmonary TB is the commonest clinical form of childhood TB and occurs in approximately 80% of cases. The clinical form of pulmonary TB in children differs from that seen in adults.[2] In children pulmonary TB is characterised by mediastinal lymph node enlargement and compression of the large airways by the enlarged mediastinal nodes.

The commonest form of pulmonary tuberculosis in children is uncomplicated lymph node enlargement.[3]The incidence of children with airway involvement due to primary TB in the chemotherapeutic era is not known. In two recent reports the airway compression varied from 8-38% in children under the age of 15 years.[3,4] Airway involvement, although relatively common in children, is seldom severe enough to warrant intervention for relief of airway obstruction.

An understanding of the pathogenesis of primary TB enables one to explain the clinical and radiological presentation of airway disease. When the primary infection is not contained the infected lymph nodes adjacent to the large airways, particularly the bronchi, increase in size, compressing the airway and infiltrating the airway wall. The clinical and radiological pictures that arise depend on the degree of airway narrowing and lymph node ulceration into the airway. If the lymph nodes ulcerate into the airway the caseating material can be inhaled into either the lobe or a lung segment. There is an initial hypersensitivity reaction to the inhaled tuberculous material. As the obstruction of the airway by the ulcerating lymph node increases and becomes complete, the reaction changes from a hypersensitivity reaction to caseation and liquefaction of the lung tissue.[4] The reaction in the lung is an expansile process, which is recognized radiologically as an expansile pneumonia.[4] These forms of TB are collectively called lymphobronchial

tuberculosis.

Flexible bronchoscopy (FB) is an invasive procedure performed under general anesthetic which is used to assess the airways of children. Only a few studies have been published on the use of FB in the diagnosis of pediatric TB [5,6] and most have concentrated on the use of bronchoscopy as a method for obtaining samples to diagnose pulmonary TB (PTB). All the published studies are from developed countries with a very low incidence of PTB in children. Bibi et al found that only 2 out of 80 children were culture positive on broncho-alveolar lavage (BAL) and that the opening of the right main bronchus was the most common area of obstruction.[7] De Blic et al evaluated 121 FB procedures in 54 children, aged between 3 months and14 years, who were suspected of having PTB.[6] They reported that FB was important in the management of children for the following reasons: (1) guided the use of adjuvant prednisone therapy, especially in the children with chest radiograph that were not suggestive of bronchial involvement; (2) indicated a need for the resection of granulation tissue by rigid bronchoscopy (three cases); and (3) guided the need for surgery (two children with persistent bronchial obstruction). Apart from these studies no other studies have systematically investigated the bronchoscopic findings of children with significant airway obstruction. There have also been no studies investigating TB airway involvement in children living with HIV or children with multidrug resistant TB. These studies reported on the yield from BAL but did not examine which factors determine whether or not a child will be culture positive on BAL.

Similarly there have been very few reports on the correlation of airway involvement in childhood TB between FB and chest computed tomography (CT). Arlaud et al in a study have reported a poor correlation between FB and chest CT. The limitation of their study was that at FB half of their study population had no airway involvement and only 10/53 had severe airway obstruction. In this study FB lead to change in therapy in 13 cases (steroids n=12, bronchoscopic extraction of a granuloma n=1) and permitted to isolate *Mycobacterium tuberculosis* in 3 patients (5.7%). Of interest was that there was no correlation between FB findings and clinical features or chest radiography. CT negative predictive value was 100% (95% confidence interval = 91- 100%). Based upon these CT results, FB could have been avoided in about 60% of patients.[7]

Study justification

Most of the research on the involvement of airways in childhood TB has been done in TB low prevalence countries where most of the children present early in the course of their disease. There is very little research on the clinical presentation, bronchoscopic appearance and the outcome of children with severe airway obstruction of the airways due to TB node involvement.

The aim of this dissertation is to evaluate the existing knowledge of TB node involvement of the airways, the bronchoscopic appearance and to describe the outcome of the children treated medically and surgically.

Research question

The clinical, radiological and bronchoscopic evaluation of children with severe airway obstruction of the airways due to TB nodes predicts which interventions are required to relieve the airway obstruction.

Research hypothesis

The outcome of children with TB node involvement of the airway resulting in severe airway obstruction is not influenced by the systematically applying interventions based on the degree of airway obstruction and can all be treated medically.

Primary outcome

The primary outcome is to determine which children require surgical intervention for severe airway obstruction

Research setting

A tertiary care children's hospital in a high TB prevalence country in Africa.

The research was carried out in a stepwise fashion with each step having specific aims:

1. To examine the published literature on the involvement of the airways in childhood tuberculosis and evaluate the possible interventions to relieve the airway obstruction.
   This aim is addressed in chapter two.

2. To describe the bronchoscopic appearance of TB node involvement of the airways in children with severe airway obstruction.
   This aim is addressed in chapter three.
3. Compare the accuracy of the radiological diagnosis of TB airway obstruction to those determined by flexible bronchoscopy in children.
   This aim is addressed in chapter four
4. Develop computer models to assist in the detection of obstructed airways in computer tomography scans of the chest in children with TB.
   This aim is addressed in chapter five.
5. Develop new diagnostic methods in children with severe TB lymph node obstruction of the airways.
   This aim is addressed in chapter six
6. Determine the optimal management of children with severe airway obstruction due to TB node involvement of the airways.
   The aim is addressed in chapter seven

References

1. Nelson LJ, Wells CD. Global epidemiology of childhood tuberculosis. Int J Tubercl Lung Dis 2004; 8: 363-647.
2. Marais BJ, Gie RP, Schaaf HS, Hesseling AC, Enarson DA, Beyers N. The spectrum of disease in children treated for tuberculosis in a highly endemic area. Int J Tubercle Lung Dis 2006 10: 1-7.
3. Theart A, Marais BM, Gie RP, Hesseling AC, Beyers N. Criteria used for the diagnosis of childhood tuberculosis at primary health care level in a high –burden, urban setting. Int J Tuberc Lung Dis 2005; 9: 1210-1214.
4. Goussard P, Gie RP, Kling S, Beyers N. Expansile Pneumonia in Children Caused by Mycobacterium tuberculosis: Clinical, Radiological, and Bronchoscopic appearances. Pediatr Pulmonol 2004; 38: 451-455.
5. Bibi H, Mosheyev A, Shoseyov D, Feigenbaum D, Kurzbart E, Weiller Z. Should bronchoscopy be performed in the evaluation of suspected pediatric pulmonary tuberculosis? Chest 2002; 122: 1604-1608.
6. De Blic J. The value of flexible bronchoscopy in childhood pulmonary tuberculosis. Pediatr Pulmonol 1995; S11: 24-25.

7. Arlaud K, Gorincour G, Bouvenot J, Dutau H, Dubus JC Could CT scan avoid unnecessary flexible bronchoscopy in children with active pulmonary tuberculosis? A retrospective study. Arch Dis Child 2010; 95: 125-129.

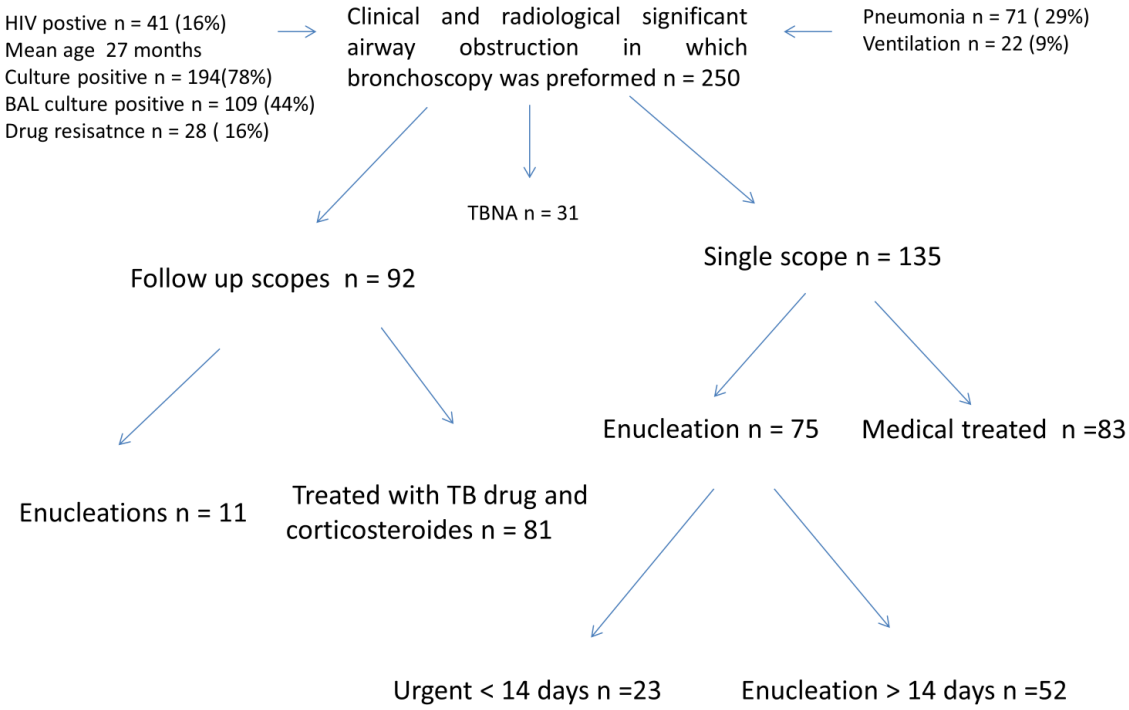

Surgical related complications n = 7 (8%)
Longterm outcome : Bronchiectasis n = 6 (4%)

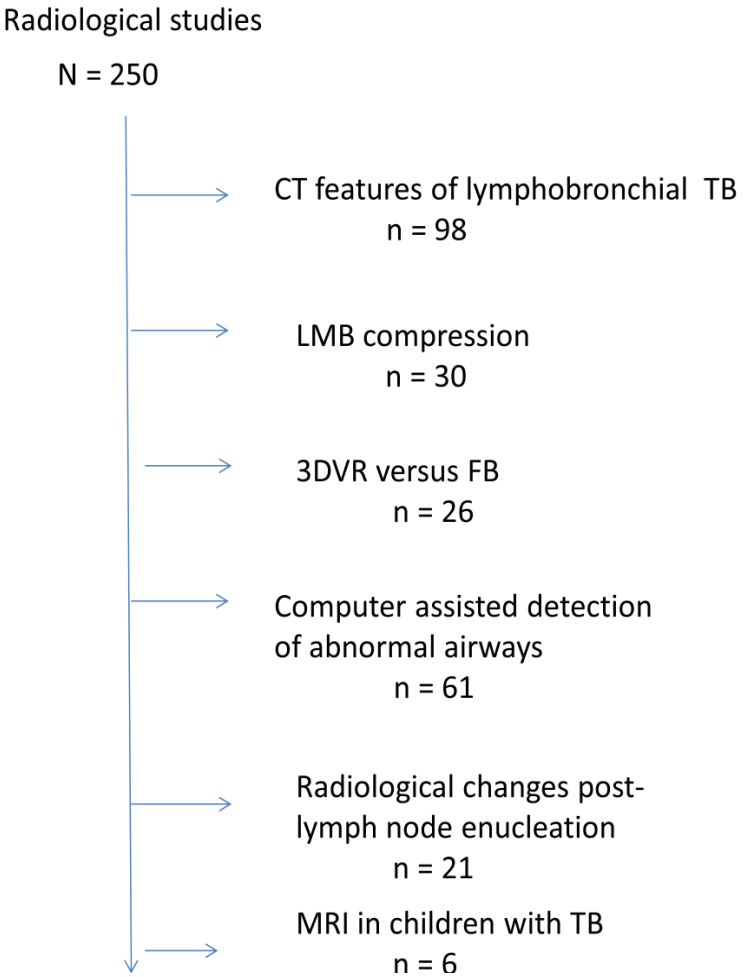

Declaration of work done:

I was responsible for the developing of the protocol for this thesis. I developed the concept of studying the bronchoscopic appearance of airway obstruction due to tuberculosis lymph node enlargement and by correlating the bronchoscopic findings to those imaged via chest computer tomography. I was actively involved in the management of all the cases and collected and analyzed the data. I did the bronchoscopy part of the study and I am the first author of the article reporting the bronchoscopy findings. The part on surgical intervention I developed the idea of investigation, the indications for enucleation and the systematic measurement of airway size prior and after the enucleation. I approached the department of cardiac thoracic surgery with this idea and was responsible for collecting, analyzing the data and writing the article. The diagnostic yield from Broncho-alveolar lavage has always been less than from gastric washings. I tried to develop methods to increase diagnostic power of bronchoscopy by sampling tissue that have not been previously studied. I developed the concept of using transbronchial needle aspiration (TBNA) for the diagnosis of tuberculosis in children. This idea was developed after discussions with Prof C Bollinger as TBNA have been routinely used in the evaluation of adults with lung cancer but has not been used in pediatric patients. I developed the question of what the value of Gene Xpert on BAL would be in childhood tuberculosis. This study was carried out with Dr E Waters and myself being co-principle investigators.

The radiological studies were evaluated by Prof Andronikou and Dr Lucas after we have managed these children and collected the data. The research question was to compare how this two investigations performed in childhood TB and if both investigations were needed in children with TB lymph node obstruction of the airways and if both were needed under which clinical conditions. The radiological articles were written in collaboration with these authors. I developed the idea of comparing MRI scan findings with CT scan findings; the reason for this is that due to the radiation CT scans cannot be used in the follow up management of airway complications. Previously very little data was available on the use of MRI in PTB.

The part of the thesis covering the development of computer models to assist the detection of airway abnormalities from chest CT images was done in collaboration with Dr B Irving. After identifying the pattern of airway obstruction on bronchoscopy, the research question was developed whether similar images could be generated using chest CT scan data as Chest CT scan are more freely available. The advantage is that if accurate this investigation could be used in regions where chest CT was freely available but childhood bronchoscopy and paediatric radiologist were not. This model would also serve as an independent measure to evaluate the accuracy of bronchoscopy. We have demonstrated that 3DVR has a good sensitivity and specificity when compared to bronchoscopy but this is a method that is time consuming and trained radiologist. I wanted to develop a model that can be used in any part of the world that after scanning generated computer images to aid in the management of childhood tuberculosis.

CHAPTER 2

Review of the Literature

EXPERT REVIEWS

The role of bronchoscopy in the diagnosis and management of pediatric pulmonary tuberculosis

Expert Rev. Respir. Med. Early online, 1–9 (2014)

Pierre Goussard* and Robert Gie

Department of Paediatrics and Child Health, Faculty of Medicine and Health Sciences, Stellenbosch University, Tygerberg Children's Hospital, PO Box 19063, Cape Town, South Africa
**Author for correspondence: pgouss@sun.ac.za*

Pulmonary tuberculosis (TB) is the commonest clinical form of childhood TB occurring in approximately 80% of cases. Traditionally, bronchoscopy in pediatric TB suspects was used to collect specimens for mycobacterial culture using especially bronchoalveolar lavage. New data have described the role of bronchoscopy as a more comprehensive instrument for the diagnosis and management of pulmonary TB in children. Flexible bronchoscopy is an important intervention to evaluated airways disease, collect samples for culture, relieve critical threatening airway obstruction and aid in the management of complicated pulmonary TB disease in children. Airway involvement in children suspected of pulmonary TB has been described in 41–63% of cases. The commonest airways involved are bronchus intermedius, left main bronchus and the trachea. Bronchoscopy is safe in children with severe airway obstruction. As bronchoscope images improve, the working channel size increases new applications for bronchoscopy will be developed making them more applicable in small children.

KEYWORDS: bronchoscopy • bronchoalveolar lavage • children • tuberculosis

During the last decade, there has been a surge of interest in tuberculosis (TB) in children. It was estimated in 2012 that 82% of the approximately 8 million global cases of TB occur in 22 countries (high-burden countries) and that 95% of the childhood TB cases live in these 22 high-burden countries. For the first time in 2012, the WHO, using data collected from national TB programs, calculated that 490,000 children are annually treated for TB and that 64,000 HIV-negative children annually die from TB [1]. This is probably an underestimate of children with TB as the present diagnostic tests perform poorly in children, and there is limited means to diagnose and manage complicated childhood TB in the 22 high-burden countries. Pulmonary TB (PTB) is the commonest clinical form of childhood TB occurring in approximately 80% of cases. The clinical form of pulmonary TB in children differs from that seen in adults [2]. In children, pulmonary TB is characterized by mediastinal lymph node enlargement and compression of the large airways by the enlarged mediastinal nodes.

The commonest form of pulmonary TB in children is uncomplicated lymph node enlargement [3]. The incidence of children with airway involvement due to primary TB in the chemotherapeutic era is not known. In two recent reports, the airway compression varied from 8 to 38% in children <15 years of age [3,4]. Airway involvement although relative common in children is seldom so severe that an intervention is required to relieve airway obstruction. The object of this review is to evaluate the role of bronchoscopy in the diagnosis and management of pulmonary TB in children.

Method of the review

A search of electronic databases was undertaken using PubMed and Google Advanced Scholar search engine limited to pediatrics, pulmonology, bronchoscopy and childhood TB for all articles in English on pediatric

 10.1586/17476348.2013.863712 ISSN 1747-6348

bronchoscopy published between 1990 and 2013 using the following key words: bronchoscopy, TB and fiber optic bronchoscopy. Hand searches were also carried out on the reference lists of retrieved articles.

Original articles on the use of both rigid and flexible bronchoscopy in the diagnosis and management of pulmonary TB in children <13 years were included. Articles comparing flexible bronchoscopy to chest CT scans in childhood TB were also examined. Between 1990 and 2013, 19 articles meeting these criteria were publish

Pathogenesis of pulmonary TB in children

To be able to understand the images as seen through the bronchoscope, the terminology used and the complications that develop it is useful to understand the pathogenesis of pulmonary TB in children.

On inhalation of the *Mycobacterium tuberculosis* bacilli, a localized pneumonia develops. Involved macrophages transport the bacilli to the regional and mediastinal lymph nodes. In the majority of cases, the primary infection is contained and the child does not develop disease. In young or immune suppressed children, the primary infection is not contained and the mediastinal lymph nodes especially those adjacent to the large airways, especially the main bronchi, increase in size. As the lymph nodes enlarge, they compress as well as infiltrate the airways and other surrounding mediastinal structures. The most common bronchoscopic images depend on the degree of airway compression and ulceration of the lymph glands into the airways. The ulcerating lymph nodes expel caseating material into the airway that in turn causes granulation tissue and polyps in the airway. Endobronchial involvement of the airway by the enlarge lymph nodes can result in the following bronchoscopic appearances: extrinsic bronchial compression, caesating lesions in the airway, intraluminal granulomas and polyps as well as mucosal erosion with ulceration. Although these images are highly suggestive of TB, they are suggestive but not diagnostic. Similarly, the enlarge inflamed lymph nodes can infiltrate any other mediastinal structure including the esophagus, superior vena cava, phrenic nerve, ductus thoracicus and even the chest wall. Involvement of these mediastinal structures distorts the bronchoscopic images and results in specific images.

Flexible bronchoscopy in the diagnosis & management of childhood TB

There are only a few studies published on the value of bronchoscopy in the diagnosis and management of pulmonary TB in children [5–14]. Most of the studies have concentrated on the use of bronchoscopy as a method for obtaining samples to diagnose pulmonary TB. These studies are limited by the fact that they have mostly been performed in developed countries with a low annual incidence of TB making the studies less applicable to the high-burden TB countries. Flexible bronchoscopy studies in children suspected of having TB have confirmed bronchial involvement in 41–63% [5–7]. The culture yield for *M. tuberculosis* from bronchoalveolar lavage (BAL) is always reported to be less than that obtained from gastric aspirates/lavages. Traditionally, bronchoscopy in pediatric TB suspects was used to collect specimens using especially BAL. Recently, new data have been published describing the role of bronchoscopy as a more comprehensive instrument to diagnose TB in children [8,13,14]. This enthusiasm for the bronchoscopic diagnosis of TB and other diseases have been made possible by the fact that newer bronchoscopes have improved imaging and larger working channels that add new diagnostic, interventional and therapeutic options to the pediatric bronchoscopy. With the worldwide increase incidence of multidrug-resistant TB and extremely resistant TB, it has become imperative to isolate *M. tuberculosis* to facilitate drug susceptibility testing to ensure children receive the appropriate TB antibiotics.

Indications for bronchoscopy in suspected & confirmed cases of TB in children

Bronchoscopy remains the gold standard for assessing the degree of airway compression and obstruction in pediatric pulmonary TB. Indications for bronchoscopy will vary according to the clinical presentation and the likelihood of TB occurring in a community. In the developed world, bronchoscopy is mostly used to collect diagnostic samples, whereas in the developing world, its value mainly lies in the management of complicated airway disease. The following are commonly used indications for bronchoscopy in children suspected of having pulmonary TB or requiring management of complicated pulmonary TB cases [15].

- Collect samples for *M. tuberculosis* culture from BAL, endobronchial tissue or transbronchial needle aspiration (TBNA) biopsy specimens.
- Assess the degree of airway obstruction in children with clinically and/or radiologically significant airway obstruction.
- Determine the cause and degree of life-threatening airway obstruction.
- Perform endoscopic enucleation as an emergency treatment for critical airway obstruction in children with TB lymph nodes ulcerating into the airways.
- etermine the cause of clinical and/or radiological failure in children being treated for TB.
- Perform transbronchial interventions to manage unusual complications of pulmonary TB. There are very few absolute contraindications for doing bronchoscopy. Absolute contraindications include a contraindication to have a general anesthetic, severe pulmonary hypertension and severe unresponsive hypoxia. Relative contraindications include a bleeding diathesis, significant hemodynamic cardiac lesions, significant upper airway pathology, superior cava syndrome, uncontrolled systemic hypertension and increased intracranial pressure [16].

The role of fiber optic & rigid bronchoscopy in children suspected of having pulmonary TB

In the majority of cases, bronchoscopy in children suspected of having TB with airway obstruction can be successfully carried

doi: 10.1586/17476348.2013.863712

out via a fiber optic bronchoscope. Rigid bronchoscopy is useful in removing endobronchial tissue caused by lymph nodes ulcerating into the airways, removing incidentally discovered foreign bodies and for controlling endobronchial bleeding. It is evident that these two methods of imaging and performing interventional procedures complement each other [17]. For this reason, it is advisable to perform childhood bronchoscopies in bronchoscopy suite where the facilities exist to perform both flexible as well as rigid bronchoscopy.

Method to perform fiber optic bronchoscopy

Shortly, the bronchoscopy techniques adjusted for children suspected or suffering from TB include the following. There is general agreement in the literature that both fiber optic and rigid bronchoscopy are best performed under general anesthesia. Children younger than 2 years of age are the most vulnerable group to develop TB (3). The accounts for the fact that 80% of bronchoscopies for TB are done in this young age group requiring the use of a 2.8 mm fiber optic or video scope. The working channel of a 2.8 mm bronchoscope is 1.2 mm limiting the procedures that can be performed. A fiber optic bronchoscope in a child suspected of having complicated pulmonary TB or TB not responding to treatment is not complete if samples are not collected for TB culture and drug susceptibility [6].

Fiber optic bronchoscopy can also be performed in the Intensive Care Unit on intubated and ventilated children. In these circumstances, bronchoscopy is done via an endotracheal tube or by extubating the child and performing the bronchoscopy through a laryngeal mask. The size of the endotracheal tube limits the size of the bronchoscope. During the bronchoscopy, the bronchoscope obstructs the lumen of the endotracheal tube increasing the risk of hypoxia and hypercapnia.

Diagnostic features of airway involvement in children with pulmonary TB

The commonest bronchoscopic image in children with culture-proven TB is lymph node compression of the airways. Most publish studies on airway involvement were done with a flexible bronchoscope with only one reported study on rigid bronchoscopy findings [10]. De Blic described that extrinsic compression of either the trachea or bronchus was the commonest visible abnormality [6]. In this study, the airway compression was either the only visible abnormality or coexisted with obstructive caseating material, granulation tissue and endobronchial mucosal inflammation of the airway [6]. Arlaud reported abnormalities in 49% of children with pulmonary TB [11]. The most frequent abnormality was extrinsic compression of <50% of the bronchus lumen in 24.5% of the cases and severe airway compression (>50%) in 18.9% [11]. Previously, Bibi *et al.* have reported that the right main bronchus was the most common area of compression [12]. Recently, the findings flexible bronchoscopy in a large series of infants and children (n = 250) with clinical and radiological signs of airway obstruction caused by TB was reported [13]. In this series of patients, compression of the right bronchial tree (85%) was more common than left-sided compression (66%) [13]. Compression of both the right and left bronchial trees was seen in 53% of the cases. The most common airways compressed were bronchus intermedius (72%) followed by left main bronchus (62%) and the trachea (57%) [13]. The right main bronchus was only compressed in 13%. In children with symptomatic airway obstruction, compression of the large airways (trachea, BI, LMB) was always present with the smaller airway compression playing a lesser role. In 95% of the cases with clinical airway obstruction, bronchus intermedius compression was visible. Cakir found TB airway involvement in 55% of children (n = 197) who had a flexible bronchoscope performed to determine the cause of treatment failure [14]. The common findings included an obstructive endoluminal polypoidal mass (42%), extrinsic compression (24%) and obstructive caseum (22%) with less common complications being intraluminal granulation tissue (9%) and mucosal erosion with ulceration (3%). Cakir reported that the risk factor for developing airway compression was resistance to treatment ($p = 0.002$). They also reported that airway involvement was more common in young children, primary TB and parenchymal involvement but this did not reach statistical significance [14].

These findings are in keeping with a previously published study by Lucas *et al.* on the chest CT scan findings of children with clinical significantly airway compression caused by pulmonary TB [18]. The lymph nodes had ulcerated into the airways in 49% of cases with the right side being involved in 64% and bronchus intermedius (31%), the most common airway where lymph nodes had ulcerated into the airway. There is a correlation between age and the severity of airway obstruction with children <24 months having statistically more severe airway obstruction. The correlation is the strongest when bronchus intermedius is >75% compressed [13]. Interestingly, there is no difference seen in the patterns or severity of airway obstruction in children who have drug-resistant TB and also TB in HIV-positive children. Previously, it was thought that children with drug resistance will have more severe disease than children with drug sensitive TB. The same assumption was suggested for HIV-positive children [13].

The cause of the airway obstruction is not always visible or appreciated on chest X-ray (CXR). The same is also true in children suspected of having pulmonary TB. De Blic has reported that bronchial involvement was found in 14 of 29 children in whom the enlarge lymph nodes was not seen on the CXR [6]. Chan reported on the bronchoscopic findings of 36 children with active pulmonary TB. Of the 36 children, 41.7% had endobronchial TB (ETB). The degree of airway involvement was underestimated on CXR as 28% of the children had no clinical or radiological signs of ETB but at bronchoscopy had endobronchial involvement [7]. Although there is a correlation between the degree of airway obstruction as seen on CXR and severity of disease, the degree of obstruction is underestimated on CXR [15]. Airway involvement of an individual lesion may not be diagnostic of pulmonary TB, but the

doi: 10.1586/17476348.2013.863712

pattern of airway obstruction makes the diagnosis of pulmonary TB very likely. This specificity of diagnosis is increased if lymph nodes have ulcerated into the airways. Bronchoscopy plays an important role in determining the severity of airway obstruction and in deciding which patients can be treated medically and which patients require surgery. Children with airway obstruction of <50% can be treated medically. In our opinion, the indications for surgery are:

- severe life-threatening airway obstruction on presentation requiring ventilation.
- critical airway obstruction as accessed at the initial bronchoscopy where the airway obstruction of both the main bronchi was >90%.
- severe airway obstruction treated with anti-TB drugs and oral prednisone for month where at bronchoscopic re-evaluation, the airway obstruction of one or both main bronchi remained >75%.
- The use of corticosteroids in ETB as an adjunct to anti-TB drugs have always been controversial as their effect remains uncertain. The balance of the studies indicated that adding corticosteroids to anti-TB drugs are beneficial in treating children with airway compression due to lymph node enlargement in pulmonary TB [19–21].

Repeated bronchoscopy may be needed in cases that do not respond to treatment or to re-evaluate cases with symptomatic airway obstruction. Some children may experience worsening airway obstruction after the initiation of anti-TB treatment due to a hypersensitivity reaction [22,23]. In our opinion, serial bronchoscopy may be necessary to evaluate if surgery is required to relieve the airway obstruction. ETB is treated with four first-line TB drugs to which methylprednisolone (2 mg/kg/day) is added for the first 30 days. The methylprednisolone is weaned over the next month. The child that responds to treatment and is asymptomatic does not require repeated bronchoscopy. The reported mean time before improvement on CXR is 5.3 ± 2.7 months, whereas bronchoscopic improvement closely follows (5.5 ± 2.7 months) [5]. De Blic on the other hand have reported that airway compression resolved in <100 days (range 14–98 days) in 11 of 20 children [6]. Of the remaining cases, in five children, the improvement took up to 120 days. Of the five children with delayed improvement, four developed bronchial stenosis. In the same report, endobronchial tissue, the result of lymph node ulceration into the airway, took between 3 and 10 weeks to resolve. Arlaud *et al.* have reported the results of a second bronchoscopy done after a mean time of 28.5 days after the initial bronchoscope in 12 children. In nine cases, the abnormalities had resolved, two had stable lesions and in one case the lesions had worsened. A third bronchoscope was done in the last three cases. One child had complete resolution, one had partial resolution and the remaining child had the persistent granuloma requiring removal via rigid bronchoscopy [11]. Early detection and treatment are thought to be important to prevent the long-term complications of bronchiectasis and bronchial stenosis. Bronchial stenosis, said to be complication of endobronchial TB in children, has been rarely reported. Choe has reported one case in a 5-year-old child [24]. De Blic described four cases that developed bronchial stenosis. These cases had both severe compression and marked inflammation of the airway visible at bronchoscopy [6].

Although TB is the most common cause of endobronchial obstruction in our setting, other causes must be considered [25]. In a series of 2555 flexible bronchoscopic procedures, Kut *et al.* reported the following intrinsic causes of endobronchial obstruction: foreign bodies (35.9%, n = 92), endobronchial TB (31.6%, n = 81), mucous plugs (16.7%, n = 43), granulation scars (6%, n = 16), hydatid cysts (n = 5), hemangiomas (n = 5), tumors (n = 5), submucosal nodules (n = 5) and polyps (n = 4). The most common areas of airway obstruction were the right bronchus 51% (n = 130), left bronchus 33% (n = 85) and trachea 8% (n = 20). Obstruction of both bronchi occurred in 8% (n = 21) [26].

Diagnostic procedures

Bronchoalveolar lavage

The commonest diagnostic procedure performed is BAL. Most studies have demonstrated that the culture yield from BAL is significantly less than that from GW [5,6,12,27–30]. Bibi *et al.* have reported a very low yield from BAL in children with suspected pulmonary TB [12]. The reported yield of culture varies with BAL specimens from 2.4 to 44% and gastric washings from 14 to 47% [5,6,12,27–30]. Cakir *et al.* have reported that the isolation rate from gastric washing was 10 and 12.8% from BAL, but cumulative yield is increased to 20% [5]. Somu *et al.* and Abadco *et al.* showed that the overall bacteriologic yield combining both procedures increased to 34 and 50%, respectively [27,29]. In Singh's study, overall mycobacterial isolation was possible in 20 patients (34.4%). The addition of BAL to the diagnostic workup increased the mycobacterial yield from 17.2% with GA alone to 34.4% when BAL was added [28]. Recently, Cakir *et al.* have published that the diagnostic yield increase to 41.9% if both BAL (32.6%) and GW (28.7%) are done [14].

It is also to be noted that in 47% of the culture-positive cases, they visualized ETB lesions [5]. Only one study has reported a higher yield from BAL compared with gastric washing. Menon *et al.* reported that a total of 52 children had both BAL and GA performed. Acid fast bacilli on smear was identified in 19 (36.5%), BAL was positive in 16 (30.8%) and GA positive in 11 (21.2%) [30]. Bronchoscopy is unlikely to be the investigation of choice in most patients and especially in the developing world as access to bronchoscopy services is limited. We recently demonstrated a higher culture yield than previously reported in children with complicated pulmonary TB [13]. Of the children investigated, 82% of these children were already on TB treatment, for a mean duration of 30 days, at the time of bronchoscopy. Even under these circumstances, bronchoscopy is a valuable tool for isolating the organism. In this sample, 44% of the children were culture positive for *M. tuberculosis* [13]. The diagnostic yield was higher in those

doi: 10.1586/17476348.2013.863712

children who had a pneumonic consolidation on CXR. For this reason, we recommended to lavage the most affected lobe. A surprising finding in this study was that the presence of lymph nodes ulcerating into the airway did not increase the BAL yield.

Endobronchial tissue biopsy

Few studies have looked at the value of endobronchial tissue as a source for culture. In children, lymph nodes ulcerate into the airway making it possible, in a percentage of these children, to biopsy the tissue. The size of the biopsy is limited by the size of the forceps able to pass through the working channel of the bronchoscope. We have not found the culture yield from endobronchial tissue biopsy to be higher than BAL [Goussard P, Unpublished Data]. The value of endobronchial tissue biopsy requires further investigation to determine its value in the diagnosis of pulmonary TB in children.

Transbronchial needle aspiration

TBNA biopsy has been used as a diagnostic technique in adult patients in whom it has been shown to be safe and effective in making the definitive diagnosis [31–36]. There is however a significant risk of causing a pneumothorax during the aspiration. The risk is reduced when central mediastinal lymph nodes are aspirated. In children, the use of TBNA has been limited due to the size of the working channel that did not allow the introduction of the aspiration needle. Recent pediatric bronchoscopes have larger working channels, making it possible to do TBNA in children via a laryngeal mask with 4.0 and 4.9 mm bronchoscopes. A laryngeal mask allows for ventilation during the procedure. In our opinion, to ensure that the procedure is performed safely, a proceeding chest CT scan is performed as only enlarged subcarinal lymph nodes can be aspirated in children as the safety of aspirating paratracheal and hilar lymph nodes in children has not been established. The technique used in adults described by Wang has been adapted for children [31,36]. Optimal results are achieved by having a cytologist in the theatre who immediately assesses the adequacy of the sample. Separate specimens are collected for cytology as well as fungal and *M. tuberculosis* (MTB) culture. The procedure is reported to be complication free with only small amount of self-limiting bleeding visible at the site of the TBNA. The advantage of TBNA is that it provides a rapid diagnosis based on the histology and culture without performing an open thoracotomy. It has been shown of value in HIV-positive children as well as those infected with drug-resistant TB. In a series of 30 children, a definitive diagnosis was made using TBNA in 54% of patients with a median age of 41 months (range 9–168 months); the diagnoses made were MTB lymph node enlargement (n = 13), metastatic nephroblastoma (n = 1) and fibrosing mediastinitis (n = 1). In 25% of the cases, the TBNA was the sole source of the specimens from which the diagnosis was made. No serious complications were encountered during or after the procedure [8]. Gilbert has reported the use of endobronchial ultrasound-guided TBNA (EBUS–TBNA) in patients with a mean age of 15.6 years. A definitive diagnosis was made in 66.7% of cases [37]. The use of EBUS–TBNA will be limited in small children due to the size of the EBUS bronchoscope and the cost of the apparatus.

Transbronchial biopsy

In children, TBBs are seldom performed as the risk of pneumothorax is approximately 10%. The use of TBB is further limited by the fact that pulmonary TB in children seldom involves alveoli adjacent to the large bronchi. TBB may be useful in diagnosing miliary TB or in HIV-positive children to distinguish miliary TB from lymphocytic interstitial pneumonia. This remains a theoretical possibility as there is no studies published on the use of TBB in the diagnosis of childhood TB.

The use of bronchoscopy in unusual forms of pulmonary TB

Expansile pneumonia

Expansile pneumonia is a radiological diagnosis that is characterized by increased volume of the affected lobe or segment resulting in bulging fissures. Expansile pneumonia caused by MTB has been described [22]. Severe airway compression (>75%) is seen in 83% of the cases where TB is the cause of the expansile pneumonia. In 13% of cases, endoscopic enucleation was required to re-establish the airway patency [22]. The value of bronchoscopy in the evaluation of expansile pneumonia in children is that the etiology can be rapidly established and if required the endoscopic enucleation can be performed.

Phrenic nerve palsy

Phrenic nerve palsy is a rare complication of complicated intrathoracic pulmonary TB [22,38–41]. All described cases involve the left phrenic nerve. The value of bronchoscopy is that lymph node compression of the left main bronchus is visible in 63% of cases and that appropriate samples can be collected.

Acquired broncho-esophageal fistula

In children, broncho-esophageal fistula (BOF) caused by *M. tuberculosis* is rare and in many cases fatal [42–48]. BOF is mostly only left sided and presents either as an acute perforation with respiratory failure or as a chronic problem with repeated aspiration. In patients with respiratory failure, bronchoscopy plays a role in making the diagnosis and determining the level of the perforation. In the acute situation, bronchoscopy also aids in the placement of an endotracheal tube in the right main bronchus as an emergency measure while the patient is prepared for an esophageal stent placement that successfully seals the leak. This is often the only available intervention as surgery in these acute circumstances is rarely successful. Post placement of the stent, the airways need to be evaluated to ensure that the stent does not cause airway compression. In the children with the chronic presentation, bronchoscopy is used to locate the fistula prior to surgery. Identification of the fistula can be problematic as there is significant infection in the left lower lobe and granulation tissue obscures the slit-like opening of the fistula.

doi: 10.1586/17476348.2013.863712

Tuberculosis of the upper airways

Laryngeal TB is rare in children but in TB, high prevalence areas should be included in the differential diagnosis of upper airway obstruction. Bronchoscopy is essential to confirm the diagnosis and determine the extent of the involvement. At bronchoscopy, extensive swelling of the epiglottis and larynx is seen [49].

Airway involvement in HIV-positive children

Endobronchial involvement due to *M. tuberculosis* is similar in HIV-positive children compared with HIV-negative children [13]. In HIV-positive children, there are other causes of airway involvement that need to be considered. These include Cryptococcus neoformans, Kaposi sarcoma, lymphoma, non*mycobacterium tuberculosis* disease and leiomyosarcomata. These children should be carefully evaluated including bronchoscopy and all the samples collected to establish the precise diagnosis. HIV-positive children receiving antiretroviral therapy may develop immune reconstitution inflammatory syndrome soon after the initiation of the antiretroviral therapy. The immune reconstitution inflammatory syndrome can lead to disease progression or reactivation of drug susceptible or resistant TB. Bronchoscopic assessment of the airways and extensive sample collection plays an essential part in the management of this problem.

Interventional bronchoscopy

Interventional bronchoscopy is very limited in young children due to the small working channel of the fiber optic bronchoscope. Interventional bronchoscopy is sometimes used in children with life-threatening airway obstruction where especially TB lymph nodes have herniated into the airway and causing critical airway obstruction. In these cases, it may be necessary to remove the caesating material obstructing the airway to re-establish airway patency. In most cases, this is a temporary measure until transthoracic surgical enucleation can be performed. Care must be taken not to injure the bronchial wall as this may create a bronchopleural fistula. Removal of the obstructing tissue from the airway can be done via a fiber optic or rigid bronchoscope. The reported number of children undergoing endoscopic enucleation is small. In a recently published report, only 9% of a cohort children with severe airway obstruction caused by TB lymph nodes in 250 children required this procedure [11]. Flexible bronchoscopy has been used to seal a persistent bronchopleural fistula following pneumonectomy in a patient with post-TB bronchiectasis. The fistula was localized, brushed and then human glue applied through a catheter that was inserted into the fistula via the working channel of the bronchoscope [50].

Complications of bronchoscopy in children with pulmonary TB

The reported complication rate of flexible bronchoscopy in children is very low but has the potential for significant morbidity and even mortality if not done correctly with the appropriate facilities and monitoring [51]. In our opinion, risk factors for complications is young age, significant airway disease especially with tracheal involvement and significant parenchymal disease. There is a small risk for bleeding during endobronchial biopsy or enucleation. The reported rate of complications during bronchoscopy for severe airway obstruction in children is 3.2% [13]. During TBNA, there is a small risk for pneumothorax and a chest X-ray must be done after the intervention to exclude the complication [32]. Complications in children with life-threatening airway obstruction can be minimized by performing the bronchoscopy in the thoracic surgery theatre so that transthoracic lymph node enucleation can immediately follow the bronchoscopy.

TB is a contagious disease and even if children have a paucity of bacilli, they are still infectious. During bronchoscopy, as there is direct access to the child's airway, this risk increases. The correct protective facemask (N95) must be used by all personnel during bronchoscopy [52].

Comparing chest CT scans to bronchoscopy in children with suspected airways disease

In middle-income countries, CT scan of the chest may be more freely available than pediatric bronchoscopy. CT scan of the chest should be carefully considered due to the radiation dose and the risk of developing cancer. Flexible bronchoscopy on the other hand is a safe procedure in skillful hands without major complications and has the additional advantage of enabling the collection of respiratory samples. Both require a general anesthetic to perform the investigation in young children. With the multidetector CT scanner, a multiplanar reconstruction of the chest is possible, allowing demonstration of airway pathology. In a large study of children with clinical symptoms of airway obstruction due to *M. tuberculosis*, Lucas *et al.* have shown that bronchus intermedius (75%) was the most common site of airway compression followed by left main bronchus (64%) and tracheal compression in 62% of cases [18]. They also demonstrated that obstruction occurs more commonly and is more severe in infants (0–12 months). Both Lucus *et al.* and Andronikou have confirmed that the subcarinal lymph node enlargement is the most common group of enlarged TB lymph nodes seen on CT scan [18,53]. Only two studies have compared flexible bronchoscopy to chest CT scan findings. Arlaud *et al.* have reported that bronchoscopy and chest CT scans have shown exactly the same localization of the abnormalities [11]. The CT scan had a sensitivity of 100% to predict severe bronchoscopic involvement (>50% extrinsic compression or obstructive endoluminal mass >25% of lumen), but the specificity was only 72%. The reason for this is on CT scan of the chest, clinically unimportant airway lesions were visible (<50% extrinsic compression or obstructive endoluminal mass <25% of lumen). The authors concluded that bronchoscopy could have been avoided in 57.7% of the cases if CT scans were done prior to bronchoscopy [11]. During this study, repeat CT scan was also done, which significantly increased the radiation risk. Du Plessis *et al.* compared three-dimensional volume-rendered CT

doi: 10.1586/17476348.2013.863712

scans (3D VR) with flexible bronchoscopy in 26 children with endobronchial TB (median age: 21 months) and demonstrated that 3D VR could determine airway narrowing in children caused by TB lymph nodes with a sensitivity of 92% and a specificity of 85% when using bronchoscopy as the gold standard [54]. The 3D VR was less accurate when the airway obstruction was <50%. The added advantage of the 3D VR was that in complete airway obstruction where access by bronchoscopy is limited beyond the point of obstruction, the 3D VR can measure the length of the obstruction. In the management of children with severe airway obstruction due to TB lymph node enlargement, chest CT scan and bronchoscopy should both be used to accurately determine the diagnosis and severity of disease. In the light of above data, we recommend that flexible bronchoscopy can be done first and if the airway obstruction is <50%, then chest CT scan is not indicated.

It is important that the chest CT scan must be done with contrast to demonstrate the diagnostic enhancement seen in lymph nodes in children with pulmonary TB. Andronikou described ghost-like and rim enhancement of TB lymph nodes [53].

Expert commentary

This article provides an extensive review of the role of pediatric bronchoscopy in the diagnosis and management of childhood TB. Fiber optic bronchoscopy allows for the visualization of airway compression and ulceration of lymph nodes into the airways in approximately 60% of children with pulmonary TB. Bronchoscopy in addition allows for the collection of respiratory samples for mycobacterial culture and sensitivity. The role of bronchoscope in sampling for TB culture is improving, resulting in a larger role for bronchoscopy in the diagnosis of childhood TB. As interventional bronchoscopy in children is evolving, its role in the diagnosis and management complicated pulmonary TB, and other lung diseases are becoming more important. Although pulmonary TB is common in low- and middle-income countries, facilities for the diagnosis and management of severe disease are sadly lacking. Facilities to perform pediatric bronchoscopy and training of bronchoscopists in these countries require urgent attention to ensure children are optimally managed.

Five-year view

New applications for flexible bronchoscopy are being developed and newer techniques are being developed to examine pulmonary disease in children. Many of these techniques are being carried over from adults to children such as endobronchial ultrasound and transbronchial needle biopsy aspiration of lymph nodes. Currently, many of these interventions are limited in children due to the size of the equipment but in future the bronchoscopes will be smaller making them more applicable in small children. Imaging and quality of imaging have significantly improved during the last number of years. This has made techniques such as virtual bronchoscopy and MRI of the chest more viable. These must be used in conjunction with bronchoscopy to improve the management of children with complicated intrathoracic TB. Pediatric bronchoscopy is still not freely available in the developing world and unfortunately this part of the globe has the highest burden of childhood TB. Equipment is expensive and infrastructure has to be developed to ensure that all children have the access to these essential services. As far as possible, bronchoscopy services should be centralized in low-income countries to limit the cost and buildup much needed pediatric bronchoscopic expertise.

Financial & competing interests disclosure

The authors have no relevant affiliations or financial involvement with any organization or entity with a financial interest in or financial conflict with the subject matter or materials discussed in the manuscript. This includes employment, consultancies, honoraria, stock ownership or options, expert testimony, grants or patents received or pending, or royalties.

No writing assistance was utilized in the production of this manuscript.

Key issues

- Flexible bronchoscopy is a useful instrument in the diagnosis and management of pulmonary tuberculosis (TB) in children.
- The commonest abnormality in children with pulmonary TB is lymph node compression of the airway and ulceration of the lymph node into the airway.
- The commonest airways involved are bronchus intermedius, left main bronchus and the trachea.
- TB airway involvement is more common in children <24 months of age.
- The bronchoscopic images of drug susceptible and drug-resistant TB are similar.
- The commonest diagnostic procedure performed is bronchoalveolar lavage with a diagnostic yield that is lower than that obtained from gastric aspirates. The diagnostics yield in childhood pulmonary TB is increased when both bronchoalveolar lavage and gastric aspirates are performed.
- Intervention bronchoscopy allows for endoscopic enucleation in critical airway obstruction and transbronchial needle aspiration of lymph nodes in pulmonary TB.
- The diagnostic yield of bronchoscopy and chest computer tomography is similar but bronchoscopy allows for respiratory sample collection and does not expose children to radiation. Bronchoscopy should be done before chest computer tomography.
- Bronchoscopy is safe in children with pulmonary TB.
- Bronchoscopy services need to be developed in low-income countries.

doi: 10.1586/17476348.2013.863712

References

1 WHO. *Global Tuberculosis Report 2012*. WHO Press, Geneva, Switzerland, 8–28 (2013).

2 Marais BJ, Gie RP, Schaaf HS *et al.* Appposed radiological classification of childhood intra-thoracic tuberculosis. *Pediatr. Radiol.* 34, 886–894 (2004).

3 Marais BJ, Gie RP Schaaf HS *et al.* The spectrum of disease in children treated for tuberculosis in a highly endemic area. *Int. J. Tuberc. Lung Dis.* 10, 1–7 (2006).

4 Theart A, Marais BM, Gie RP *et al.* Criteria used for the diagnosis of childhood tuberculosis at primary health care level in a high –burden, urban setting. *Int. J. Tuberc. Lung Dis.* 9, 1210–1214 (2005).

5 Cakir E, Uyan ZS, Oktem S *et al.* Flexible bronchoscopy for the diagnosis and follow – up of childhood endobronchial tuberculosis. *Pediatr. Infect. Dis. J.* 27(9), 783–787 (2008).

6 De Blic J, Azevedo I, Burren CP *et al.* The value of flexible bronchoscopy in childhood pulmonary tuberculosis. *Chest* 100, 688–692 (1991).

7 Chan S,Abadco DL, Steiner P. Role of childhood endobronchial tuberculosis. *Pediatr. Infect. Dis. J.* 13, 506–509 (1994).

8 Goussard P, Gie RP, Kling S *et al.* The diagnostic value and safety of transbronchial needle aspiration biopsy in children with mediastinal lymphadenopathy. *Pediatr. Pulmonol.* 45, 1173–1179 (2010).

9 de Blic J, Midulla F, Barbato A *et al.* Bronchoalveolar lavage in children. ERS Task Force on Bronchoalveolar Lavage in Children. *Eur. Respir. J.* 15, 217–231 (2000).

10 Gahouma D, Boguikouma JB, Mouba JF *et al.* [Rigid tube bronchoscopy in tuberculous children. Apropos of 24 cases]. *Ann. Pediatr. (Paris)* 37, 227–229 (1990).

11 Arlaud K, Gorincour G, Bouvenot J *et al.* Could CT scan avoid unnecessary flexible bronchoscopy in children with active pulmonary tuberculosis? A retrospective study. *Arch. Dis. Child.* 95, 125–129 (2010).

12 Bibi H, Mosheyev A, Shoseyov D *et al.* Should bronchoscopy be performed in the evaluation of suspected pediatric pulmonary tuberculosis? *Chest* 122, 1604–1608 (2002).

13 Goussard P, Gie RP, Kling S *et al.* Bronchoscopic assessment of airway involvement in children presenting with clinically significant airway obstruction due to tuberculosis. *Pediatr. Pulmonol.* 48, 1000–1007 (2013).

14 Cakir E, Kut A, Ozkaya E *et al.* Bronchoscopic evaluation in childhood pulmonary tuberculosis: risk factors of airway involvement and contribution to the bacteriologic diagnosis. *Pediatr. Infect. Dis. J.* 32, 921–923 (2013).

15 Dagli E, Gie RP, Uyan ZS *et al.* Endobronchial tuberculosis. In: *Paediatric Bronchoscopy (Progress in Respiratory Research)*. Priftis KN, Anthracopoulos MB, Eber E, Koumbourlis AC, Wood RE (Eds). Karger, Basel, Switzerland, 38, 173–181 (2010).

16 De Blic J, Telion C. Sedation and anaesthesia for bronchoscopy. In: *Paediatric Bronchoscopy (Progress in Respiratory Research)*. Priftis KN, Anthracopoulos MB, Eber E, Koumbourlis AC, Wood RE (Eds). Karger, Basel, Switzerland, 38, 22–29 (2010).

17 Hitter A, Karkas A, Schmerber S *et al.* Rigid bronchoscopy. In: *Paediatric Bronchoscopy. (Progress in Respiratory Research)*. Priftis KN, Anthracopoulos MB, Eber E, Koumbourlis AC, Wood RE (Eds). Karger, Basel, Switzerland, 38, 83–93 (2010).

18 Lucas S, Andronikou S, Goussard P *et al.* CT features of lymphobronchial tuberculosis in children, including complications and associated abnormalities. *Pediatr. Radiol.* 42, 923–931 (2012)

19 Nemir RL, Cordona J, Lacoius A *et al.* Prednisone as an adjunct in the chemotherapy of lymph node-bronchial tuberculosis in childhood: a double-blind study, *Am. Rev. Respir. Dis.* 88, 189–198 (1963).

20 Nemir RL, Cordona J, Vaziri F *et al.* Prednisone as an adjunct in the chemotherapy of lymph node-bronchial tuberculosis in childhood: a double-blind study. II. Further term observation. *Am. Rev. Respir. Dis.* 95, 402–410 (1967).

21 Toppet M, Malfroot A, Derde MP *et al.* Corticosteroids in primary tuberculosis with bronchial obstruction. *Arch. Dis. Child.* 65, 1222–1226 (1990).

22 Goussard P, Gie RP, Kling S *et al.* Expansile pneumonia in children caused by mycobacterium tuberculosis: clinical, radiological, and bronchoscopic appearances. *Pediatr. Pulmonol.* 38, 451–455 (2004).

23 Thampi N, Stephens D, Rea E *et al.* Unexplained deterioration during antituberculous therapy in children and adolescents: clinical presentation and risk factors. *Pediatr. Infect. Dis. J.* 31, 129–133 (2012).

24 Choe KO, Jeong HJ, Soh HY. Tuberculous bronchial stenosis : CT findings in 28 cases. *AJR* 155, 971–976 (1990).

25 Wood RE. The diagnostic effectiveness of the flexible bronchoscope in children. *Pediatr. Pulmonol.* 1, 188–192 (1985).

26 Kut A, Cakir E, Gokdemir Y *et al.* Intrinsic endobronchial obstruction in children from Turkey: Evaluation of 2555 flexible bronchoscopic procedures. *Respiration* 85, 43–48 (2013).

27 Abadco DL, Steiner P. Gastric lavage is better than bronchoalveolar lavage for the isolation of Mycobacterium tuberculosis in childhood tuberculosis. *Pediatr. Infect. Dis. J.* 11, 735–738 (1992).

28 Singh M, Moosa NV, Kumar L *et al.* Role of gastric lavage and broncho-alveolar lavage in the bacteriological diagnosis of childhood pulmonary tuberculosis. *Indian Pediatr.* 37, 947–951 (2000).

29 Somu N, Swaminathan S, Paramasivan CN *et al.* Value of bronchoalveolar lavage and gastric lavage in the diagnosis of pulmonary tuberculosis in children. *Tuber. Lung Dis.* 76, 295–299 (1995).

30 Menon PR, Lodha R, Singh U *et al.* A prospective assessment of the role of bronchoscopy and bronchoalveolar lavage in the evaluationof children with pulmonary tuberculosis. *J. Trop. Pediatr.* 57, 363–367 (2011).

31 Wang KP. Staging of bronchogenic carcinoma by bronchoscopy. Chest 1994; 106:588–593.

32 Holty JE, Kuschner WG, Gould MK. Accuracy of transbronchial needle aspiration for mediastinal staging of non-small cell lung cancer: a meta-analysis. *Thorax* 60, 949–955 (2005).

33 Hermens FH, Van Engelenburg TC, Visser FJ *et al.* Diagnostic yield of transbronchial histology needle aspiration in patients with mediastinal lymph node enlargement. *Respiration* 70, 631–635 (2003).

34 Ferna´ndez-Villar A, Leiro V, Blanco M *et al.* Efficacy and safety of the eXcelon transbronchial aspiration needle in mediastinal lymph node enlargement: a case-control study. *Respiration* 74, 208–213 (2007).

35 Diacon AH, Schuurmans MM, Theron J *et al.* Utility of rapid on-site evaluation of transbronchial needle aspirates. *Respiration* 72, 182–188 (2005).

doi: 10.1586/17476348.2013.863712

36 Wang KP, Terry PB. Transbronchial needle aspiration in the diagnosis and staging of bronchogenic carcinoma. *Am. Rev. Respir. Dis.* 127, 344–347 (1983).

37 Gilbert CR Feller-Kopman D, Akulian J *et al.* Interventional pulmonology prosedures in pediatric population. *Pediatr. Pulmonol.* doi:10.1002/ppul.22855 (2013) (Epub ahead of print).

38 Grenet P, Labram C. Phrenic paralysis caused by mediastinal adenopathy in primary tuberculous infection. *Med. Infant. (Paris)* 67, 53–55 (1960).

39 Mohan B, Jayaswal SN. Unilateral diaphragmatic paralysis due to tuberculous hilar adenitis. *Indian J. Pediatr.* 22, 468–470 (1985).

40 Dempers J, Bezuidenhout J, Schneider JW *et al.* Tuberculosis and phrenic nerve destruction. *S. Afr. Med. J.* 97, 572–573 (2007).

41 Goussard P, Gie RP, Kling S *et al.* Phrenic nerve palsy in children associated with confirmed intrathoracic tuberculosis: diagnosis and clinical course. *Pediatr. Pulmonol.* 44, 345–350 (2009).

42 Bhata R, Mitra DK, Mukkerjee S *et al.* Bronchoesophageal fistula of tuberculosis origin in a child. *Pediatr. Radiol.* 22, 154 (1992).

43 Coleman FP, Bunch GH. Acquired non-malignant esophagotracheo-bronchial fistula. *J. Thorac. Surg.* 19, 542–558 (1950).

44 Gie RP, Kling S, Schaaf HS *et al.* Tuberculous Broncho-esophageal fistula in children. *Pediatr. Pulmonol.* 25, 285–288 (1998).

45 Moersch HJ, Tinney WS. Fistula between the oesophagus and the tracheobronchial tree. *Med. Clin. North Am.*1001–1007 (1944).

46 Wychulis AR, Ellis FH, Andersen HA. Acquired non-malignant esophageo-tracheobronchial fistula. *JAMA* 196, 103–108 (1966).

47 Goussard P, Andronikou S. Tuberculous broncho-oesophageal fistula: images demonstrating the pathogenesis. *Pediatr. Radiol.* 40(Suppl. 1), S78 (2010).

48 Goussard P, Sidler D, Kling S *et al.* Esophageal stent improves ventilation in a child with a broncho-esophageal fistula caused by Mycobacterium tuberculosis. *Pediatr. Pulmonol.* 42, 93–97 (2007).

49 Gregg KK, Detjen AK, Goussard P *et al.* Gie R Laryngeal involvement in two severe cases of childhood tuberculosis. *Pediatr. Infect. Dis. J.* 28, 1136–1138 (2009).

50 Goussard P, Gie RP, Kling S *et al.* Fibrin glue closure of persistent bronchopleural fistula following pneumonectomy for post-tuberculosis bronchiectasis. *Pediatr. Pulmonol.* 43,721–725 (2008).

51 Wood RE. A Four – decade perspective on paediatric bronchoscopy-Where have we come from, and where are we going. In: *Paediatric Bronchoscopy (Progress in Respiratory Research).* Priftis KN, Anthracopoulos MB, Eber E, Koumbourlis AC, Wood RE (Eds). Karger, Basel, Switzerland, 38, 200–204 (2010).

52 Willeke K, Qian Y. Tuberculosis control through respirator wear: performance of National Institute for Occupational Safety and Health-regulated respirators. *Am. J. Infect. Control.* 26, 139–142 (1998).

53 Andronikou S, Joseph E, Lucas *et al.* CT scanning for the detection of tuberculous mediastinal and hilar lymphadenopathy in children. *Pediatr. Radiol.* 34, 232–236 (2004).

54 Du Plessis J, Goussard P, Andronikou S *et al.* Comparing three-dimensional volume-rendered CT images with fibreoptic tracheobronchoscopy in the evaluation of airway compression caused by tuberculouslymphadenopathy in children. *Pediatr. Radiol.* 39, 694–702 (2009).

doi: 10.1586/17476348.2013.863712

CHAPTER 3

Bronchoscopic assessment of airway involvement in children presenting with clinically significant airway obstruction due to tuberculosis

Introduction

Only a few studies have been published on the value of bronchoscopy in the diagnosis and management of pulmonary TB in children. Most of these studies have concentrated on the use of bronchoscopy as a method for obtaining samples to confirm the clinical diagnosis of pulmonary TB.[1-6] The studies are limited by the fact that they have mostly been performed in developed countries, with a low annual incidence of TB, making the studies less applicable to the high burden TB countries. The value of bronchoscopy in the diagnosis of pulmonary TB in HIV infected and children with drug resistant TB have not been studied. The culture yield for *Mycobacterium tuberculosis* from bronchoalveolar lavage (BAL) is reported to be less than that obtained from gastric aspirates/lavages.[1,5,7,8] Previously bronchoscopy in pediatric tuberculosis suspects was used to collect specimens using especially BAL but did not taken into consideration the site and severity of airway involvement which are highly suggestive of TB especially in high prevalence regions.

Goussard P, Gie RP, Kling S, Andronikou S, Lucas S, Janson JT, Roussouw GJ. Bronchoscopic assessment of airway involvement in children presenting with clinically significant airway obstruction due to tuberculosis. Pediatr Pulmonol 2013; 48: 1000-1007.

The aim of this study was to assess the site and severity TB lymph node involvement of airways in children with symptomatic airway obstruction by means of flexible bronchoscopy. A secondary outcome would be to compare airway obstruction in HIV-non-infected and HIV-infected children as well as comparing the bronchoscopic findings in children with drug sensitive to those with drug resistant TB. Age was an important variable with more severe airway compression occurring in children younger than 24 months of age. There was no difference in the site and degree of airway involvement in both HIV-infected and drug resistant cases.

We have identified that bronchus intermedius is the most common site of lymph node compression. The other important sites of airway compression were the trachea and left main bronchus. There was a correlation between age younger than 24 months and the degree of airway obstruction (>75%) of bronchus intermedius (P = 0.02). Obstruction of the right and left lower lobe bronchi was rare in this study.

The yield from BAL was higher (44%) than previously reported even though 82% of children were on antituberculosis treatment prior to the bronchoscopy. Children with radiological evidence of pneumonia had a statistically higher yield from BAL when compared to children with TB lymph node compression alone (P = 0.002). In 49% of cases the lymph nodes had ulcerated into the airway but this was not associated with an increase in yield from BAL.

Conclusion

Bronchoscopy is important in the evaluation of the degree and site of airway compression due to lymph node enlargement in children with pulmonary TB. This study describes the major sites of airway compression in childhood TB: bronchus intermedius, left main bronchus and the trachea. Airway compression was more severe in children younger than 24 months. Mycobacterium tuberculosis culture from BAL was higher than previously described and the yield higher when done from a region with pneumonia. Bronchoscopy does not only confirm the diagnosis but provides a functional and anatomical evaluation of the airway involvement in pulmonary TB which in addition to raising the suspicion of TB lymph node compression of the airway also guides treatment.

References

1. Bibi H, Mosheyev A, Shoseyov D, Feigenbaum D, Kurzbart E, Weiller Z. Should bronchoscopy be performed in the evaluation of suspected pediatric pulmonary tuberculosis? Chest 2002; 122: 1604-1608.
2. De Blic J. The value of flexible bronchoscopy in childhood pulmonary tuberculosis. Pediatr Pulmonol 1995; S11: 24-25.
3. Arlaud K, Gorincour G, Bouvenot J, Dutau H, Dubus JC Could CT scan avoid unnecessary flexible bronchoscopy in children with active pulmonary tuberculosis? A retrospective study. Arch Dis Child 2010; 95: 125-912.
4. Chan S, Abadco DL, Steiner P. Role of flexible fiberoptic bronchoscopy in the diagnosis of childhood endobronchial tuberculosis. Pediatr Infect Dis J 1994; 13: 506–509.
5. Somu N, Swaminathan S, Paramasivan CN, Vijayasekaran D, Chandrabhooshanam A, Vijayan VK, Prabhakar R. Value of bronchoalveolar lavage and gastric lavage in the diagnosis of pulmonary tuberculosis in children. Tuber Lung Dis 1995; 76: 295–299.

6. De Blic J, Azevedo I, Burren CP, Le Bourgeois M, Lallemand D, Scheinmann P. The value of flexible bronchoscopy in childhood pulmonary tuberculosis. Chest 1991; 100: 688–692.

7. Cakir E, Uyan ZS, Oktem S, Karakoc F; Ersu R, Karadag B, Dagli E. Flexible bronchoscopy for diagnosis and follow up of childhood endobronchial tuberculosis. Pediatr Infect Dis J 2008; 27: 783-787.

8. Cakir E, Kut A, Ozkaya E, Gedik AH, Midyat L; Nursoy M. Bronchoscopic evaluation in childhood pulmonary tuberculosis: risk factors of airway involvement and contribution to the bacteriologic diagnosis. Pediatr Infect Dis J. 2013; 32: 921-923.

Pediatric Pulmonology 48:1000–1007 (2013)

Bronchoscopic Assessment of Airway Involvement in Children Presenting With Clinically Significant Airway Obstruction Due to Tuberculosis

Pierre Goussard, MMed (Paed),[1]* Robert P. Gie, FC Paed,[1] Sharon Kling, FC Paed,[1] Savvas Andronikou, PhD,[2] Susan Lucas, MMed,[2] Jacques Janson, FC Cardio (SA),[3] and Gawie Roussouw, FC Cardio (SA)[3]

Summary. Introduction: The incidence of complicated lymph node disease in tuberculosis (TB) in children less than 15 years of age varies from 8% to 38%. There are few published studies on the bronchoscopic appearance and severity of airway obstruction caused by lymph node involvement of the airways resulting from *Mycobacterium tuberculosis* (*MTB*). The *primary aim* of the study was to describe the flexible bronchoscopic findings of lymph node involvement of the airways caused by *MTB* in children with severe airway obstruction. The *secondary aim* was to compare the degree of airway involvement in HIV negative to HIV positive children as well the airway involvement caused by drug susceptible and drug resistant *MTB*. Patients and Methods: All children between 1 month and 13 years of age presenting with clinical and radiological signs of significant airway obstruction suspected of being the result of *MTB* infection were studied. In addition to routine examination for *MTB* disease a flexible bronchoscope and bronchoalveolar lavage (BAL) for *MTB* culture were performed on all the children. Results: Two hundred fifty children (16% HIV positive) were studied. Median age was 14 months and the median weight 8.5 kg. *MTB* was cultured from 78% (n = 194) of children with the BAL positive in 44%. The BAL culture yield was significantly higher in children with radiological evidence of pneumonia when compared to children with airway involvement alone ($P = 0.004$). The bronchial tree was obstructed on the right in 85% (n = 212), the left in 66% (n = 164), and both sides in 53% (n = 132) of cases. The commonest sites of obstruction were bronchus intermedius (72%) and left main bronchus (62%). Drug resistance was present in 16% (n = 28). There was no difference in the site or severity of obstruction when comparing drug susceptible to drug resistant cases or HIV positive to HIV negative children. Conclusions: Bronchus intermedius and left main bronchus were the commonest sites of airway obstruction. The *MTB* culture yield from BAL was higher in children with pneumonia when compared to those with airway involvement alone. HIV positive or children with drug resistant TB did not have more severe airway obstruction. **Pediatr Pulmonol. 2013; 48:1000–1007.** © 2012 Wiley Periodicals, Inc.

Key words: tuberculosis; bronchoalveolar lavage; flexible bronchoscope; airway obstruction; lymph node disease.

Funding source: none reported.

INTRODUCTION

Tuberculosis (TB) in children is a common disease in the world affecting approximately 1 million children annually.[1] Airway involvement due to tuberculous lymph node compression is commonly seen in children with primary TB, but severe airway compression requiring intervention in only a small group of children. The

[1]Faculty of Health Sciences, Departments of Paediatrics and Child Health, Stellenbosch University, and Tygerberg Children's Hospital, Tygerberg, Cape Town, South Africa.

[2]Faculty of Health Sciences, Radiology Department, University of Witswatersrand, Johannesburg, South Africa.

[3]Faculty of Health Sciences, Cardio-Thoracic Surgery, Stellenbosch University and Tygerberg Children's Hospital, Tygerberg, Cape Town, South Africa.

Conflict of interest: None.

*Correspondence to: Pierre Goussard, MMed (Paed), Faculty of Health Sciences, Department of Paediatrics and Child Health, Stellenbosch University, PO Box 19063, Tygerberg 7505, South Africa.
E-mail: pgouss@sun.ac.za

Received 16 May 2012; Accepted 3 September 2012.

DOI 10.1002/ppul.22747
Published online 31 December 2012 in Wiley Online Library (wileyonlinelibrary.com).

incidence of complicated lymph node disease causing airway compression in two recent reports varied between 8% and 38% in children younger than 15 years of age.[2,3] The epidemiological data required to estimate the proportion of children with severe tuberculosis requiring invasive diagnostic procedures or surgery at a global level are lacking.

Flexible bronchoscopy (FB), an invasive procedure used to assess the airways of children, is mostly performed under general anesthesia. Few studies have been published on the use of FB in the diagnosis of pediatric TB[4–6] and most of these studies have concentrated on the use of bronchoscopy as a method for obtaining diagnostic samples. The majority of the published studies are from developed countries with a very low incidence of PTB in children, which complicates the applicability of the findings to high burden countries. Bibi et al.[5] found that only 2 out of 80 children were culture positive on broncho-alveolar lavage (BAL) and that the opening of the right main bronchus was the most common site of airway obstruction. De Blic et al.[6] evaluated 121 FB procedures in 54 children, aged 3 months to 14 years, suspected of having PTB. They found FB useful as a guide to direct the use of adjuvant steroids for airway compression, assessing the presence of granulation tissue in the airway requiring removal and the need for surgical intervention. Apart from these studies no other studies have systematically investigated the bronchoscopic findings of children with significant airway obstruction caused by *MTB*. There are also no published studies investigating TB airway involvement in children living with HIV or children with drug resistant TB. The correlation between FB findings and chest CT in children with airway compression caused by tuberculosis is poor suggesting that FB is essential investigation in assessing airway narrowing caused by *MTB*.[7]

The aim of this study was to assess TB lymph node involvement of airways in children with symptomatic airway obstruction by means of flexible bronchoscopy. A secondary outcome would be to compare airway obstruction in HIV-negative and HIV-positive children as well as in children with drug sensitive and drug resistant TB.

PATIENTS AND METHODS

This was a prospective, comparative study done from January 1, 2004 until December 31, 2011 at Tygerberg Children's Hospital, Western Cape, South Africa. The study population comprised all children between 1 month and 13 years of age presenting to the pediatric pulmonology service with clinical and radiological signs of significant airway obstruction suspected of being the result of TB lymph node involvement of the airways. The following definitions were used: Clinically significant airway obstruction was recognized by the presence of stridor or wheezing audible without the use of a stethoscope. The significant airway obstruction on a chest X-ray was defined as clearly visible narrowing of either the trachea or one of the main bronchi on a good quality chest X-ray. The following chest X-ray appearances also indicated significant airway obstruction: a ball valve effect with unilateral hyperinflation, expansile pneumonia, and atelectasis of a lobe or segment. The following children were excluded: Children with airway compression not due to TB, children who had lymph node enlargement and signs of airway obstruction on the chest X-ray but were not symptomatic, any child with a contraindication to FB or general anesthetic, and any child with hemodynamically significant cardiac disease and/or significant pulmonary hypertension.

The following routine tests were performed: full blood count with a differential cell count, Mantoux skin test (if the test had not been performed in the previous 3 weeks), two consecutive early morning gastric aspirates in infants and young children and sputum in older children for *Mycobacterium tuberculosis* (*MTB*) culture and sensitivity testing and an HIV test, with the appropriate test for the age of the child. Blood lymphocyte CD4 counts and plasma HIV viral loads were done in HIV positive children if the test had not been not performed in the previous 3 months. A chest X-ray, with a lateral view, was done in all children with the exception being those where a chest X-ray had been taken 7 days prior to the evaluation.

Flexible bronchoscopy was performed in the bronchoscopy theatre under general anesthesia using a combination of gas inhalation (halothane) and an intravenous agent (propofol), Children with life threatening airway obstruction who required intubation and ventilation for respiratory failure where done in the pediatric intensive care unit (PICU) under sedation. The consultant anesthetist evaluated all cases the day before FB and performed the anesthetic. Patients were routinely monitored during the procedure by pulse oximetry, continuous electrocardiography, capnography, and regular blood pressure monitoring. Staff in the bronchoscopy theatre was protected from the risk of infection by wearing a correctly fitted N95 mask. If following the bronchoscopy the degree of airway compression was assessed to be very severe or life threatening, the child was admitted to the PICU post-bronchoscopy.

The FB was systematically performed following the same protocol. During FB the areas of airway obstruction were recorded in a structured way. The degree of the airway obstruction was graded as either normal or obstructed with the following categories: (1) $\leq$30%, (2) 50–75%, (3) 75–90%, and (4) 100%. The anatomical areas that were assessed were the upper, middle, and

lower parts of the trachea, the left and right bronchial tree. On the left side the left main bronchus (LMB) left upper lobe, lingula and left lower lobe bronchi were examined while on the right the opening of the right main bronchus, bronchus intermedius (BI), and the right middle and the right lower lobe bronchi were similarly examined. Each site was checked for external compression and intraluminal involvement. All bronchoscopic images were digitally recorded for re-evaluation and comparison with the findings at follow-up bronchoscopy.

Following the evaluation of the airways a BAL was done in all the children for Ziehl–Neelsen staining and *MTB* culture. If lymph nodes had ulcerated into the airway the lavage was done from that specific airway. In cases where no ulceration had occurred the FB was wedged in the most involved lobe or segment as determined radiologically.[8] Visible intraluminal tissue was biopsied. If there was no positive *MTB* culture was available prior to bronchoscopy and the patient had large subcarinal lymph nodes visible on chest CT-scan a transbronchial needle aspiration (TBNA) was performed. Any complication of the FB or anesthetic adverse events were recorded.

Pulmonary TB was treated according to the recognized standard of care, consisting of four anti-tuberculous drugs (isoniazid, rifampicin, pyrazinamide, and ethambutol) during the 2-month intensive phase and two drugs (isoniazid, rifampicin) during the consolidation phase of 4 months. If multidrug TB (MDR TB) was suspected or confirmed the appropriate five to six-drug treatment was used for 18–24 months. In cases with significant airway obstruction (>50% obstruction) prednisone (2 mg/kg/day) was added to the initial treatment for 30 days and then weaned.

HIV infected children were referred to the Infectious Diseases department and had their antiretroviral treatment started 1–8 weeks after the initiation of the antituberculosis treatment.

In children with life threatening airway obstruction surgical relief via transthoracic glandular enucleation was performed by the Department of Cardiothoracic Surgery.

The Human Research Ethics Committee of the Faculty of Health Sciences, Stellenbosch University (N10/08/282), approved the study. The parents of the patients signed consent prior to enrolment in the study.

RESULTS

Two hundred fifty patients were enrolled into this study with 144 being male (58%). There was no relationship between gender and severity of airway obstruction. The median age was 14 months (range 2–156 months) and the median weight 8.5 kg (range 2.7–39 kg) with 50% of children below the 3rd percentile for age. Of the 41 patients (16%) that were HIV positive 65% had stage 3 disease according to the WHO classification. The median white cell count was 14×10^9/L with the median lymphocyte and neutrophil count 3.9×10^9 and 8×10^9/L, respectively. The median platelet count was 567×10^9/L, the median serum C-reactive protein 45 mg/L and the median serum globulin 35 g/L. The median CD4 lymphocyte count of the HIV positive patients was 1,116/μl. In addition to the large airway obstruction 37% (n = 92) additional clinical features included pneumonia 29% (n = 71), superior vena cava syndrome (n = 2), hemoptysis (n = 2), miliary TB (n = 4), TB meningitis (n = 2), TB of the vertebrae (n = 2), abdominal TB (n = 3), phrenic nerve palsy (n = 1), broncho-oesophageal fistula (n = 2), deep venous thrombosis (n = 1), lung abscess (n = 1), and chest wall TB (n = 1). Of the 71 children presenting with pneumonia 78% (n = 56) were classified as an expansile pneumonia. Of the children 9% (n = 22) had severe life threatening airway obstruction requiring intubation and ventilation.

There was a significant association between a platelet count $>450 \times 10^9$/L and >75% obstruction of the LMB ($P = 0.02$), but not for >75% obstruction of BI ($P = 0.15$).

TB Diagnosis

The culture results are summarized in Table 1. Of the whole cohort 78% (n = 194) were culture positive for *MTB* with 9 additional cases being ZN positive but culture negative. Nineteen percent (n = 48) of the culture positive cases were also ZN positive. Of the cases 82% had been on anti-tuberculous drugs prior to bronchoscopy. The mean duration of treatment prior to bronchoscopy was 31 days.

Of the 178 cases where drug susceptibility testing was performed 16% (n = 28) were drug resistant. The drug resistant patterns were as follows: isoniazid (H) mono resistant (n = 8), rifampicin (R) mono resistant (n = 5), H and R resistant (n = 12), H, R plus ethambutol resistant (n = 2), H, R, ethambutol, amikacin, and ofloxacin resistant (n = 1).

TABLE 1—The Source of the Specimens for Mycobacterium Tuberculosis Cultures and the Diagnostic Yield

Source of cultures	Positive, n (%)	Negative, n (%)
All cultures (n = 250)	194 (78%)	56 (22%)
BAL (n = 246)	109 (44%)	137 (56%)
Gastric aspirate (n = 210)	123 (59%)	87 (41%)
Tissue (n = 130)	72 (55%)	58 (45%)
Sputum (n = 37)	19 (51%)	18 (51%)
TBNA (n = 31)	14 (45%)	17 (55%)

BAL, bronchoalveolar lavage; TBNA, transbronchial needle aspiration.

Sixty-one percent (n = 153) of the cases were in contact with an adult infectious case, of which 11% (n = 17) were known to have drug resistant TB. Of the children in contact with an adult drug resistant index case 88% (n = 15) were culture positive with the following drug resistance patterns: drug susceptible (n = 4), mono drug resistance (n = 1), two drug resistance (n = 7), three drug resistance (n = 2), and four drug resistance (n = 1).

The Mantoux skin test was positive (>10 mm induration) in 62% (n = 139).

Bronchoscopy Findings

Airway involvement was divided into external compression of the airway 97% (n = 242) and those cases with glandular ulceration into the airway lumen without compression 3% (n = 8). External compression and intra luminal involvement were present in 50% of the cases. Compression of the right bronchial tree was seen in 85% (n = 212), left sided involvement in 66% (n = 164), and with both sides being compressed in 53% (n = 132). The anatomical sites and severity of airway compression are shown in Table 2. In 95% (n = 167) of cases with bronchus intermedius compression the airway was compressed from both the medial as well as the lateral side. The tracheal compression was seen in one of three anatomical sites: distal 64% (n = 91), mid tracheal 30% (n = 43), and whole length of the trachea 6% (n = 8). Isolated compression of the upper third of the trachea was not seen. Table 3 demonstrates the anatomical sites of airway compression, the degree of compression, and the combination of airways involved (Fig. 1).

In 49% (n = 171) of cases the lymph nodes had ulcerated into the airways of which 64% were into the right bronchial tree. Lymph nodes ulcerated into bronchus intermedius (31%), left main bronchus (25%), right upper lobe (21%), and right main bronchus (18%) of cases. Endoscopic enucleation was performed in 9% (n = 23).

Complications of bronchoscopy were recorded in eight cases and included: severe desaturation (n = 7) and severe airway obstruction requiring PICU admission (n = 1).

Age was correlated with: site of involvement, culture positivity, drug susceptibility, and HIV status (Table 4). There was an association between age and airway obstruction with young children having significantly more obstruction of the left main bronchus and bronchus intermedius. There was a correlation between age younger than 24 months and airway obstruction greater than 75% for bronchus intermedius only ($P = 0.02$). When more than one airway was significantly compressed, trachea and left main bronchus, trachea and bronchus

TABLE 2—The Site and the Degree of Obstruction of the Bronchial Tree Expressed as a Percentage

Site of obstruction	Obstruction present (n, %)	Obstruction absent (n, %)	Degree obstructed % (median)
Right bronchial tree	212 (85%)	38 (15%)	
Left bronchial tree	164 (66%)	86 (34%)	
Both left and right bronchial trees involved	132 (53%)	118 (47%)	
Trachea	142 (57%)	108 (43%)	50
Carina	192 (77%)	58 (23%)	
Bronchus intermedius	178 (72%)	68 (28%)	75
LMB	156 (62%)	94 (38%)	50
RMB	33 (13%)	217 (87%)	75
RULB	87 (35%)	159 (65%)	50
RMLB	44 (20%)	179 (80%)	75
RLLB	7 (3%)	221 (97%)	50
LULB	30 (12%)	214 (88%)	50
LINGULA	23 (9%)	220 (90%)	
LLLB	10 (4%)	232 (96%)	

LMB, left main bronchus; RMB, right main bronchus; RUL, right upper lobe bronchus; RMLB, right middle lobe bronchus; RLLB, right lower lobe bronchus; LULB, left upper lobe bronchus; LLLB, left lower lobe bronchus.

TABLE 3—Correlation Between the Site and Degree of Airway Compression and Age

	n	Age mean (months)	95% Confidence (months)	*P*-value
LMB				
No obstruction	94	37	28–45	<0.01
With obstruction	154	20.6	16–24	
Bronchus intermedius				
No obstruction	67	33	23–42	0.02
With obstruction	177	24	20–29	
LMB degree of obstruction				
<75%	94	22	17–28	0.11
>75%	60	18	12–24	
Bronchus intermedius degree of obstruction				
<75%	59	30	21–88	<0.01
>75%	118	22	17–28	
Tracheal and LMB compression				
No obstruction	160	30	24–36	0.33
With obstruction	88	21	17–26	
Tracheal and bronchus intermedius compression				
No obstruction	144	28	22–34	0.6
With obstruction	100	25	19–31	
Tracheal compression and LMB >75%				
Absent	119	27	16–26	0.63
Present	35	21	11–25	
Tracheal compression and Bronchus intermedius >75%				
Absent	77	24	17–31	0.39
Present	28	26	16–37	

LMB, left main bronchus.

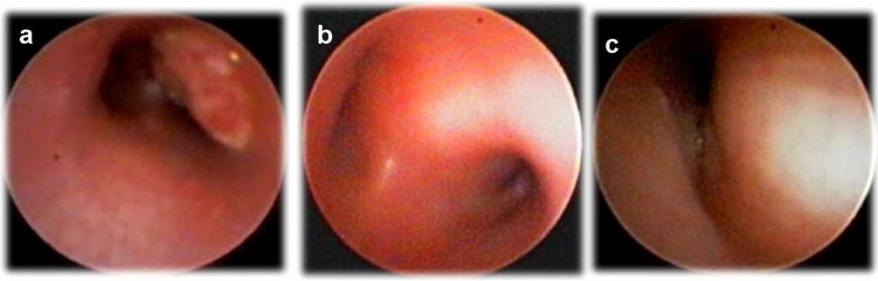

Fig. 1. Bronchoscopy images: (a) Gland ulcerating into airway, (b) Bronchus intermedius obstruction due to side to side compression, and (c) tracheal compression due to paratracheal glands.

intermedius, were compressed the correlation between age and airway compression was no longer present. Similarly there was no relationship between age and the degree of compression of the LMB or bronchus intermedius.

The severity of airway obstruction, lymph nodes ulcerating into the airway and the presence of pneumonia were studied as predictors of culture positivity (Table 5). Culture positivity did not correlate with severity of airway compression, site of obstruction or nodes ulcerating into the airways. The presence of pneumonic consolidation on chest radiology had significantly higher culture yield for all cultures ($P = 0.002$) as well as cultures from BAL (0.004) when compared to children were pneumonic consolidation was absent (Table 5).

There was no statistical difference between drug susceptible and drug resistant TB in regard to the bronchoscopic appearance and the degree or sites of airway compression. Similarly no difference could be demonstrated when the findings in HIV positive children were compared to HIV negative children with the exception that HIV positive children had more right sided involvement ($P = 0.03$).

DISCUSSION

The gold standard for the diagnosis of PTB is culture of *MTB* while the gold standard for the assessment of the degree of airway obstruction is flexible bronchoscopy. The patterns of airway obstruction caused by lymph node involvement of the airway caused by *MTB* have not previously been described in detail. Most previous articles have concentrated on evaluating bronchoscopy as a diagnostic tool for obtaining samples for *MTB* culture. This study carefully describes airway involvement resulting from PTB in children with symptomatic airway obstruction. The most common anatomical sites of TB lymph node obstruction are bronchus intermedius (72%) and the left main bronchus (62%) with children younger than 24 months having statistically more severe airway obstruction.

When the primary infection is not contained, the infected lymph nodes adjacent to the large airways, particularly the bronchi, increase in size, compressing the airway, and infiltrating the airway wall.[2] The clinical features, radiological pictures, and bronchoscopic appearances that arise depend on the degree of airway narrowing and lymph node ulceration into the airway. If the lymph nodes ulcerate into the airway, the caseous material can be inhaled into either the lobe or a segment. There is an initial hypersensitivity reaction to the inhaled tuberculous material. As the obstruction of the airway by the ulcerating lymph node increases and becomes complete, the reaction changes from a hypersensitivity reaction to an immune reaction that results in caseation and liquefaction of the lung tissue.[4]

Involvement of the right bronchial tree was more common (85%) than left sided involvement (66%) with both sides being compressed in 53%. Bronchus intermedius was the most common site of obstruction (72%), followed by LMB (62%), and tracheal compression (57%). The upper part of the trachea was seldom involved. Bibi et al.[5] have previously reported that the right main bronchus (RMB) was the most common area of obstruction. This is in contrast to the present study where RMB obstruction was only seen in 13% of cases. In cases where RMB obstruction was seen the degree of obstruction exceeded 75%. The reason for this difference is hard to explain. Obstruction of the right and left lower lobe bronchi was rare in this study. Bronchus intermedius obstruction was the most common site of airway compression. This is in keeping with recently published CT scan findings.[9,10] In a recent study Lucas et al.[9] reported BI compression in 75%, LMB in 64%, and tracheal compression in 62%. In the majority of cases bronchus intermedius was compressed both from medial and lateral sides by enlarged lymph nodes.

TABLE 4—The Stratification of Age Into Three Age Groups (<12 Months, 13–36 months, and >36 Months) and the Various Bronchoscopic Images, Drug Resistance, and HIV Status

	Present, n (%)	Absent, n (%)	*P*-value
Right involvement			
<12 Months	98 (90%)	11 (10%)	
13–36 Months	78 (86%)	13 (14%)	0.03
>36 Months	35 (73%)	13 (27%)	
Left involvement			
<12 Months	74 (68%)	35 (32%)	
13–36 Months	68 (75%)	23 (26%)	0.0005
>36 Months	20 (42%)	28 (58%)	
Both			
<12 Months	63 (58%)	46 (42%)	
13–36 Months	56 (62%)	35 (38%)	0.00006
>36 Months	12 (25%)	36 (75%)	
Trachea			
<12 Months	57 (52%)	52 (48%)	
13–36 Months	56 (62%)	35 (38%)	ns
>36 Months	28 (58%)	20 (42%)	
Bronchus intermedius			
<12 Months	86 (49%)	22 (33%)	
13–36 Months	61 (34%)	28 (42%)	ns
>36 Months	30 (17%)	17 (25%)	
LMB			
<12 Months	71 (40%)	38 (46%)	
13–36 Months	66 (43%)	25 (27%)	ns
>36 Months	17 (11%)	31 (33%)	
Culture positive			
<12 Months	86 (79%)	23 (21%)	
13–36 Months	68 (75%)	23 (25%)	ns
>36 Months	39 (81%)	9 (19%)	
Gland ulcerating into airway			
<12 Months	47 (43%)	62 (57%)	ns
13–36 Months	51 (56%)	40 (44%)	
>36 Months	25 (52%)	23 (48%)	
Resistant TB			
<12 Months	16 (20%)	65 (80%)	ns
13–36 Months	7 (12%)	53 (88%)	
>36 Months	5 (14%)	30 (86%)	
HIV status			
<12 Months	7 (6%)	102 (94%)	
13–36 Months	13 (14%)	78 (86%)	ns
>36 Months	21 (44%)	27 (56%)	

LMB, left main bronchus.

TABLE 5—Correlation Between the Bronchoscopic and Radiological Images and the Mycobacterium Tuberculosis Culture Yield

	Source of cultures	Culture positive (n)	Culture negative (n)	*P*-value
Obstruction of airway	All cultures			
>50% (n = 147)		112	35	NS
<50% (n = 27)		22	5	
Obstruction of airway	BAL			
>50% (n = 147)		62	83	NS
<50% (n = 27)		13	14	
Gland ulcerating into the airway	BAL			
Present (n = 123)		53	68	NS
Absent (n = 127)		56	69	
Pneumonia	All cultures			
Present (n = 71)		64	7	0.002
Absent (n = 176)		129	47	
Pneumonia	BAL			
Present (n = 71)		41	29	0.004
Absent (n = 176)		67	106	

BAL, bronchoalveolar lavage.

This finding was in keeping with CT scan studies that reported that bronchus intermedius is compressed medially by the enlarged subcarinal lymph nodes and laterally by the enlarged right-sided hilar lymph nodes. Both Andronikou et al.[10] and Lucas et al.[9] have also reported that subcarinal lymph nodes are the most commonly enlarged lymph nodes seen on CT scan in children with PTB, ranging from 92% to 100%. A possible explanation why bronchus intermedius obstruction is more common than LMB obstruction is the close relationship of the subcarinal lymph nodes and the hilar lymph nodes on the right side when compared to the left side. This may also be the reason why ulceration of lymph nodes into the right side was more common than on the left side. With right sided hilar lymph node enlargement (86%) being more common than left sided hilar lymph node enlargement (69%) it is not surprising the BI compression is more common than the left main bronchus compression. Lucas[9] also found the BI to be the airway most likely to show severe or complete compression. This is supported in the present study where the median degree of obstruction of BI was 75%.

There is a significant relationship between age and compression of both the LMB and bronchus intermedius with both the mean age below 24 months. The correlation between the degree of obstruction (>75%) and age only was significant for bronchus intermedius obstruction ($P < 0.01$). However if age were divided into less than 12 months, 13–36 months, and more than 36 months there were no statistical differences. In younger children the airways are more compliant and compressible which makes them more vulnerable to airway compression. This is compounded by the size of the airways in younger children. However not all children with PTB have airway compression, with the reported incidence between 28% and 38%.[3,11]

Du Plessis et al. have published that there is a good correlation when comparing three-dimensional volume-rendered CT images (3D VR) with flexible bronchoscopic findings. It was demonstrated that there was a 90% match with the sites identified with bronchoscope. The sensitivity and specificity of 3D VR was 92% and 85%, respectively. 3D VR can evaluated the airway past

the area of obstruction but does not add any value in determining the endobronchial lesions.[12] Similar correlations with chest X-ray images have not been published. This study was unable to examine this correlation as the entry criteria for this study included radiological evidence of airway compression. Objective evidence of the degree of airway obstruction on chest X-ray is also not available.

There is no clear reason why some children have airway obstruction during PTB and others do not. We postulate that in children with airway compression there is ongoing inflammation with the child unable to contain the infection. This might be an explanation why there is a correlation between the peripheral platelet count, serum globulin levels, and C-reactive protein and the degree of obstruction. These acute phase responses might indicate ongoing inflammation that could lead to enlarging lymph node and airway compression. This hypothesis needs to be further researched.

In this study 78% of children were culture positive for MTB. Previous reports in the literature have reported that the culture yield from BAL were low with specimens obtained from gastric aspirate having a higher yield.[5–7] In this study we report that MTB was cultured from 44% of BAL specimens which is higher than that previously reported. In spite of this high yield the culture yield from samples obtained from gastric aspirate were still higher than those obtained from BAL. It is surprising that the high culture positive yield was obtained as 82% of patients were already started on antituberculosis treatment prior to the bronchoscopy. The reasons for the high culture yield are uncertain but may include the following: high incidence of tuberculosis in this region where the study was conducted, late presentation resulting in severe disease and the high incidence of concurrent pneumonia. Another unexpected finding was that there were statistically more positive cultures obtained when pneumonia was present when compared to the culture yield for patients with lymph node involvement of the airway alone ($P = 0.004$). This was true for all forms of airway involvement that included compression and ulceration into the airway.

HIV positive children had a similar bronchoscopic appearance to HIV negative children with the exception that the right bronchial tree was slightly more involved in HIV positive children. This was surprising, as we had previously thought that due to the decreased ability of HIV positive children to contain the disease, compression of the airways would be more prominent in HIV positive children. This finding is similar to that previously reported in studies comparing the radiological picture of PTB in HIV positive when compared to HIV negative children. Similarly, due to a delay in the availability of drug susceptibility results the diagnosis of drug resistant tuberculosis is often delayed and for this reason one would postulate that there would be more airway involvement in this group of children. This study was not able to demonstrate a greater degree of airway involvement in patients with drug resistant TB as the bronchoscopic findings were similar to those found in children with drug susceptible TB.

Limitations: In this study we only investigated children with clinical or radiological signs of severe airway obstruction and not all children suspected of having TB. In our opinion it would have been unethical to subject all children to flexible bronchoscopy where there were no clear diagnostic and therapeutic advantages. We also interpret the findings in HIV positive patients and those with proven drug resistance with care, as the number investigated in both groups was limited. We were surprised by the high MTB culture yield for all samples including the BAL samples as we had included children who had been on antituberculosis treatment for up to 3 months prior to the bronchoscopy. The duration of antituberculosis treatment would certainly have influenced the percentage of children with culture proven TB and the yield from BAL might be greater. The mean duration of treatment prior to bronchoscopy of 31 days could certainly also have influenced the degree of lymph nodes obstruction of the airways. The degree of airway obstruction and culture yield from specimens in this study might therefore be an underestimate.

CONCLUSIONS

Bronchus intermedius is the most common site of lymph node obstruction caused by *MTB* as well as the site with the most significant degree of obstruction. Right-sided airway compression is more common than left sided compression. Children less than 24 months have more significant airway compression than older children. The yield from BAL was much higher than previously reported with the BAL statistically higher in children with TB pneumonia when compared to children with TB lymph node compression alone. HIV positive children and children suffering from TB caused by drug resistant strains have similar bronchoscopic appearances when compared to HIV negative children and those with drug susceptible TB. Further research is required to determine the pathogenesis of airway compression in children with lymph node enlargement due to *MTB*.

REFERENCES

1. Nelson LJ, Wells CD. Global epidemiology of childhood tuberculosis. Int J Tuberc Lung Dis 2004;8:363–647.
2. Marais BJ, Gie RP, Schaaf HS, Hesseling AC, Enarson DA, Beyers N. The spectrum of disease in children treated for tuberculosis in a highly endemic area. Int J Tuberc Lung Dis 2006;10:1–7.

3. Theart A, Marais BM, Gie RP, Hesseling AC, Beyers N. Criteria used for the diagnosis of childhood tuberculosis at primary health care level in a high-burden, urban setting. Int J Tuberc Lung Dis 2005;9:1210–1214.
4. Goussard P, Gie RP, Kling S, Beyers N. Expansile pneumonia in children caused by Mycobacterium tuberculosis: clinical, radiological, and bronchoscopic appearances. Pediatr Pulmonol 2004;38:451–455.
5. Bibi H, Mosheyev A, Shoseyov D, Feigenbaum D, Kurzbart E, Weiller Z. Should bronchoscopy be performed in the evaluation of suspected pediatric pulmonary tuberculosis? Chest 2002;122: 1604–1608.
6. De Blic J. The value of flexible bronchoscopy in childhood pulmonary tuberculosis. Pediatr Pulmonol 1995;S11:24–25.
7. Arlaud K, Gorincour G, Bouvenot J, Dutau H, Dubus JC. Could CT scan avoid unnecessary flexible bronchoscopy in children with active pulmonary tuberculosis? A retrospective study. Arch Dis Child 2010;95:125–129.
8. De Blic J, Midulla F, Barbato A, Clement A, Dab I, Eber E, Green C, Grigg J, Kotecha S, Kurland G, et al. Bronchoalveolar lavage in children. ERS task force on bronchoalveolar lavage in children. Eur Respir J 2000;15:217–231.
9. Lucas S, Andronikou S, Goussard P. Features of lymphobronchial tuberculosis in children, including complications and associated abnormalities Computed Tomography features of Lymphobronchial TB in children, including complications and associations. Pediatric Radiol 2012;42:923–931.
10. Andronikou S, Joseph E, Lucas S, Brachmeyer S, Du Toit G, Zar H, Swingler G. CT scanning for the detection of tuberculous mediastinal and hilar lymphadenopathy in children. Pediatr Radiol 2004;34:232–236.
11. Weber AL, Bird KT, Janower ML. Primary tuberculosis in childhood with particular emphasis on changes affecting the tracheobronchial tree. Am J Roentgenol Radium Ther Nucl Med 1968;103:123–132.
12. Du Plessis J, Goussard P, Andronikou S, Gie R, George R. Comparing three-dimensional volume-redered CT images with fibreoptic tracheobronchoscopy in the evaluation of airway compression caused by tuberculous lymphadenopathy in children. Pediatr Radiol 2009;39:694–702.

Bronchoscopic images of airway involvement due to Tuberculosis

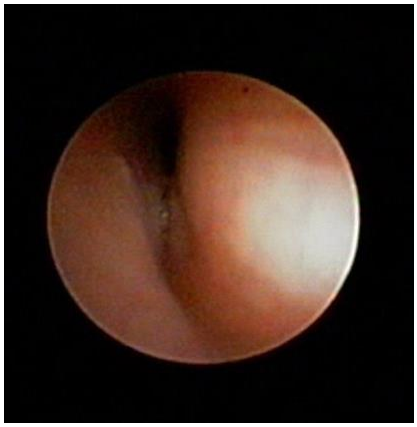

Figure 1: External compression of the trachea with more than 75% narrowing of the lumen

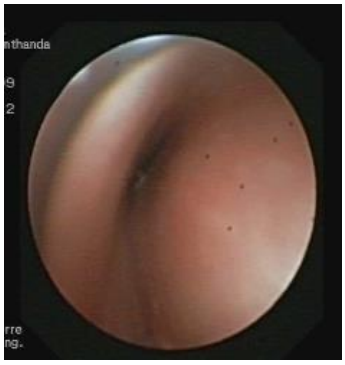

Figure 2: Compression of the opening of the left main bronchus with the medial compression due to enlarge subcarinal lymph nodes.

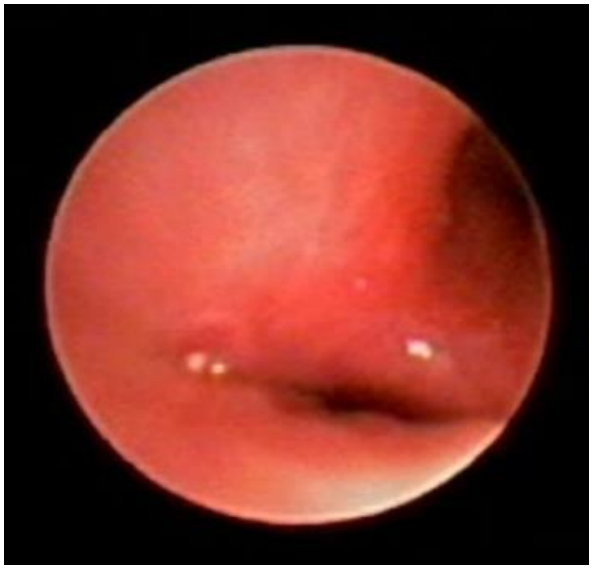

Figure 3 : Bronchus intermedius compression from both medial and lateral sides due to the subcarinal lymph nodes medial and the enlarge hiliar lymph nodes lateral.

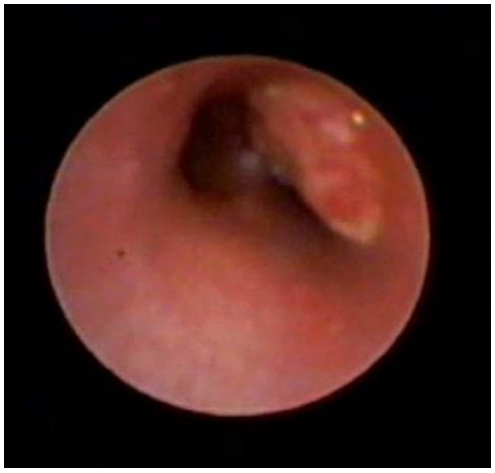

Figure 4 : Lymph nodes have herniated through the anterior wall of the trachea

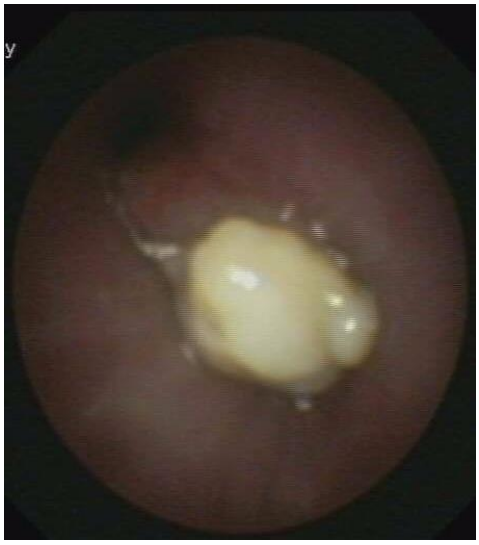

Figure 5 : Lymphnode have herniated into airway and caesating material is visible .

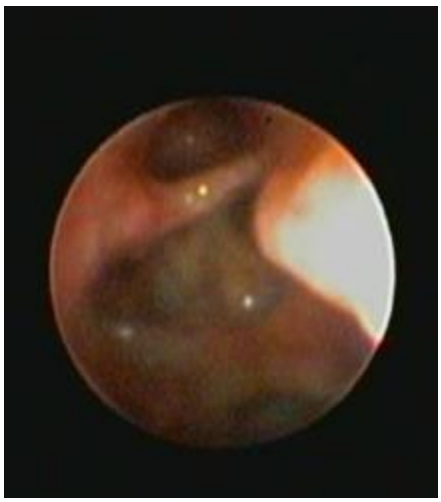

Figure 6: Bronchoscopic image taken from the left lower lobe bronchus demonstrating a very large cavity originating from a destroyed left lower lobe bronchus

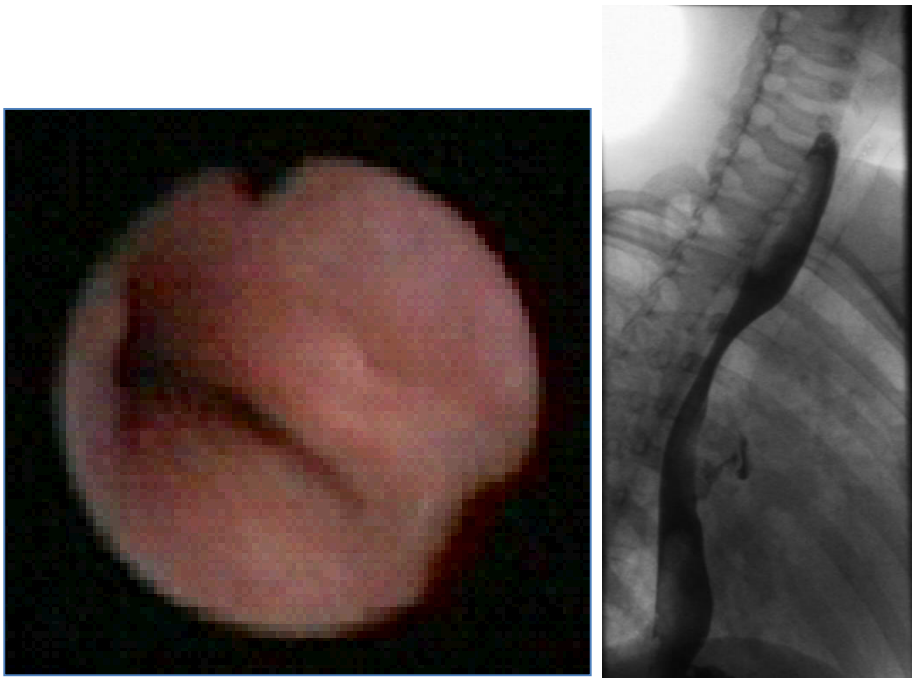

Figure 7: (a) Bronchoscopy demonstrates left sided fistula just below the carina. (b) Contrast study done with water-soluble contrast medium : demonstrating BOF to the left main bronchus

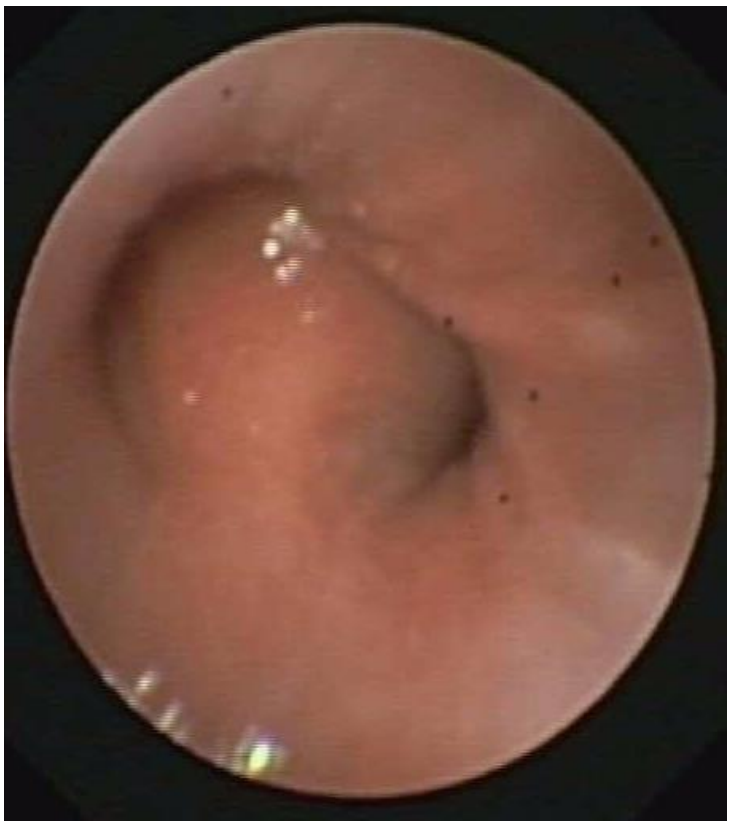

Figure 8: Bronchoscopic images of the right upper lobe bronchus of a child with right upper lobe expansile pneumonia. Tuberculosis granulomas is causing near complete obstruction of the bronchus.

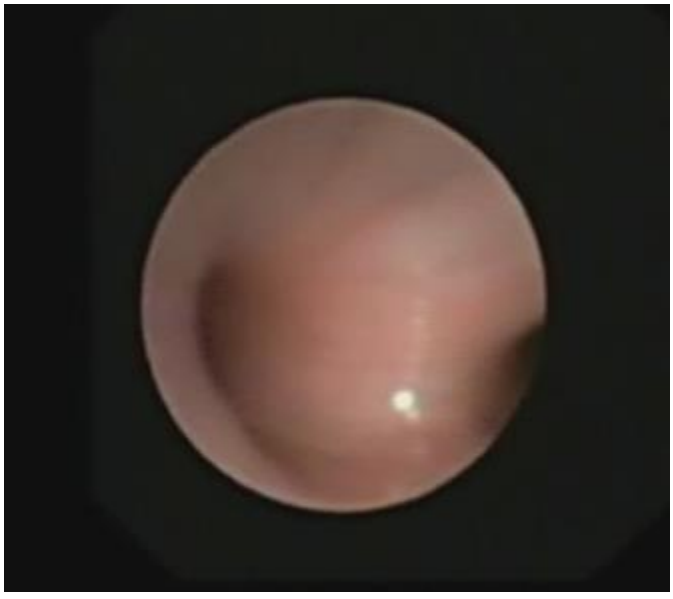

Figure 9: Bronchoscopy picture demonstrating a very swollen and enlarge carina due to enlargement of the subcarinal lymph nodes.

CHAPTER 4

Comparing the radiological diagnosis of airway obstruction to the finding at flexible bronchoscopy in childhood tuberculosis

Introduction

In middle-income countries computer tomography scan (CT-scan) of the chest may be more freely available than pediatric bronchoscopy. With the multi-detector CT scanner, it is possible to create a multiplanar reconstruction of the chest which, in turn is able to demonstrate of airway pathology due to TB mediastinal lymph node enlargement. Arlaud et al have reported that bronchoscopy and chest CT scan show the same localization of the abnormalities. The CT scan had a sensitivity of 100% to predict severe bronchoscopic involvement (> 50% extrinsic compression or obstructive endoluminal mass > 25% of lumen) with a specificity of 72%. The authors concluded that bronchoscopy could have been avoided in 57.7% of the cases if CT scans were done prior to bronchoscopy. These studies were performed on small numbers of children with minimal airway involvement. We performed a series of studies to examine the correlation between chest computer tomography scan and paediatric bronchoscopy in children with severe airway compression due to TB lymph node enlargement.

Lucas S, Andronikou S, Goussard P, Gie R. CT features of lymphobronchial tuberculosis in children, including complications and associated abnormalities. Pediatr Radiol 2012; 42: 923-931.

The aim of this study was to describe the features on CT scan of lymph node involvement of the airways in children with pulmonary tuberculosis, to document the parenchymal complications and to identify associated abnormalities. The study population was children younger than 13 years with known pulmonary tuberculosis and presenting with symptoms and signs of compression of large airways. All these cases had, in addition to the chest CT scan, a bronchoscopy performed. Bronchus intermedius (75%) was the commonest site of airway compression followed by left main bronchus (64%) and tracheal compression (62%). Bronchus intermedius was compressed by >75% in 47% of cases. The subcarinal lymph nodes were the commonest lymph node group involved (97%) Obstruction occurred more commonly and was more severe in infants (0-12 months). Parenchymal complications were present in 94% of patients.

Andronikou S, van Wyk MJ, Goussard P, Gie RP. Left main bronchus compression as a result of tuberculous lymphnode compression of the right-sided airways with right lung volume loss in children. Pediatr Pulmonol 2014; 49: 263-268.

The aim of this study was to report pediatric cases of right-sided airway involvement in childhood TB with volume loss, demonstrate the use of angle measurements to quantify mediastinal dynamics and support a pathogenetic theory for left main bronchus compression. Contrasted chest CT scans of children (<13 years of age) with culture confirmed pulmonary TB and symptoms of airway compression were studied. Patients with right-sided hilar, subcarinal lymph node enlargement and right lung volume loss were retrospectively identified and included in this study irrespective of the presence of left main bronchus compression. The ‘‘Pulmonary bifurcation angle’’ between the main pulmonary arteries reached statistical significance (P = 0.025). The ‘‘Pulmonary outflow tract rotation’’ angle (pulmonary trunk with the midsagittal plane) approached statistical significance (P = 0.078). In children with right lung volume loss from TB, the compression of the contralateral bronchus is due to narrowing of the pulmonary artery bifurcation angle as the main trunk rotates towards the midline.

Du Plessis J, Goussard P, Andronikou S, Gie R, George R. Comparing three-dimensional volume-rendered CT images with fibreoptic tracheobronchoscopy in the evaluation of airway compression caused by tuberculous lymphadenopathy in children. Pediatr Radiol 2009; 39: 694-702.

The aim of this study was to compare the site and degree of airway compression as determined by 3-dimensional volume-rendered CT scans (3-D VR) to those obtained by flexible bronchoscopy in children with airway compression due to TB lymph node enlargement. The study was performed in 26 children with endobronchial tuberculosis (median age: 21 months). The 3-D VR determined airway narrowing in children caused by TB lymph nodes with a sensitivity of 92% and a specificity of 85% when using bronchoscopy as the gold standard. The 3-D VR was less accurate when the airway obstruction was less than 50%. The added advantage of the 3-D VR was that in complete airway obstruction where access by bronchoscopy is limited 3-D VR can measure the length of the obstruction.

Conclusions

Chest CT scan findings in children with significant airway compression due to PTB correlate with bronchoscopy findings in children with airway narrowing due to TB lymph node involvement. Both demonstrate that bronchus intermedius is the most common and severely affected airway, especially in the young infant. The added advantage of CT scan is that additional information is gained concerning the characteristics of the enlarged lymph

nodes and the accompanying parenchymal complications. Both a chest CT scan and bronchoscopy require a general anesthetic. Although the chest CT scan findings correlated closely with findings at bronchoscopy we would recommend doing a bronchoscopy prior to the chest CT scan for the following reasons: there is no radiation risk, the specificity of bronchoscopy is higher and a bronchoalveolar lavage can be performed to confirm diagnosis in a percentage of cases. In regions where paediatric bronchoscopy does not exist, CT scan of the chest is a viable alternative.

Pediatr Radiol (2012) 42:923–931
DOI 10.1007/s00247-012-2399-x

ORIGINAL ARTICLE

CT features of lymphobronchial tuberculosis in children, including complications and associated abnormalities

Susan Lucas · Savvas Andronikou · Pierre Goussard · Robert Gie

Received: 20 July 2011 / Revised: 15 December 2011 / Accepted: 13 January 2012 / Published online: 30 May 2012

Abstract
Background Lymphobronchial tuberculosis (TB) is tuberculous lymphadenopathy involving the airways, which is particularly common in children.
Objective To describe CT findings of lymphobronchial TB in children, the parenchymal complications and associated abnormalities.
Materials and methods CT scans of children with lymphobronchial TB were reviewed retrospectively. Lymphadenopathy, bronchial narrowing, parenchymal complications and associations were documented.
Results Infants comprised 51% of patients. The commonest site of lymphadenopathy was the subcarinal mediastinum (97% of patients). Bronchial compression was seen in all children (259 bronchi, of these 28% the bronchus intermedius) with severe or complete stenosis in 23% of affected bronchi. Parenchymal complications were present in 94% of patients, including consolidation (88%), breakdown (42%), air trapping (38%), expansile pneumonia (28%), collapse (17%) and bronchiectasis (9%), all predominantly on the right side (63%). Associated abnormalities included ovoid lesions, miliary nodules, pleural disease and intracavitary bodies.
Conclusion Airway compression was more severe in infants and most commonly involved the bronchus intermedius. Numerous parenchymal complications were documented, all showing right-side predominance.

S. Lucas (✉) · S. Andronikou
Department of Radiology, Faculty of Health Sciences,
University of the Witwatersrand,
7 York Road, Parktown,
Johannesburg 2001, South Africa
e-mail: su.lucas@iburst.co.za

P. Goussard · R. Gie
Department Paediatrics, Stellenbosch University,
Stellenbosch, South Africa

Keywords Tuberculosis · Child · CT · Chest · Lymphadenopathy

Introduction

The incidence of tuberculosis (TB) is increasing globally. South Africa has the third highest incidence in the world with respect to both TB and multidrug-resistent (MDR) TB [1]. Lymphadenopathy is considered the hallmark of the radiological diagnosis of TB in children [2]. When primary tuberculous infection within the lymph nodes involves the airways, the result is lymphobronchial TB, historically known as epituberculosis [3, 4]. This term encompasses a spectrum of airways involvement and associated complications [5]. The lymph nodes enlarge, obstructing the airway by external compression, intraluminal occlusion by inflammatory change in the bronchial wall or herniation of caseating lymph nodes [4, 6, 7]. This usually affects the right main bronchus or bronchus intermedius [8]. The pathological process starts with partial occlusion of the lumen, with a ball-valve effect that leads to air trapping in the affected segment or lobe, which may in turn consolidate. In consolidated segments with completely occluded bronchi, the lung may fill with fluid, resulting in so-called "drowned lung" [9]. Other radiologically demonstrable parenchymal complications of obstruction include collapse, expansile pneumonia, necrotising pneumonia and liquefaction with or without cavitation [10]. Erosion of tuberculous lymph nodes into the airways can cause transbronchial spread, resulting in distant alveolar or bronchopneumonic consolidation [11]. Lymphobronchial TB is a complication of TB seen almost exclusively in children, who are at risk because of the small calibre and compressibility of their airways. Radiological demonstration of lymphobronchial TB and the initial or advanced parenchymal complications may prompt surgical

intervention to relieve the obstruction [12–14] and in some instances salvage of the lung.

Our purpose was to describe the features on CT of lymphobronchial TB in children, to document the parenchymal complications and to identify any associated abnormalities.

Materials and methods

A retrospective descriptive analysis of patient records, previously collated into an established database for use in a larger clinical project, was performed. The larger study group consisted of children who had had bronchoscopy, but not all these children had had CT. The number of children in the larger study was 212. The number of children with CT scans available for evaluation was 98. Ethics approval for this study was obtained from the Human Research Ethics Committee (Medical) of the University of the Witwatersrand, Johannesburg (clearance certificate M10441).

The database comprised children younger than 13 years with known TB, presenting to a paediatric pulmonologist with symptoms and signs of compression of large airways. These included persistent coughing and wheezing, unilateral hyperinflation, expansile pneumonia, pneumonia not responding to treatment, and lobar collapse. TB was confirmed either by culture or by demonstration of acid-fast bacilli in gastric or bronchial aspirates. The HIV status of all the patients was determined by PCR and was extracted from the available clinical data. The patients had been treated for 30 days with a quadruple anti-TB drug regimen, to which steroids were added. If, after 30 days of treatment, they had persistent clinical (e.g. coughing or wheezing) or radiologic (narrowed airway on radiographs, unilateral hyperinflation, persistent pneumonia, expansile pneumonia or lobar collapse) evidence of airways obstruction, fibreoptic tracheobronchoscopy and CT of the chest were performed to investigate the cause and level of obstruction. This was part of the routine clinical care.

CT was performed with a 4-slice multi-detector scanner (Aquilion, Toshiba, Nasu, Japan) using a routine chest CT protocol for children with 120-kVp tube voltage and 50-mA tube current. Intravenous iodinated contrast medium (low osmolar, non-ionic, 300 mg/ml iodine content) was used routinely at a dose of 2 ml/kg body weight, administered by hand injection. Standard image construction yielded soft-tissue images, standard lung images and high-resolution lung images. CTDI and DLP were not available.

All CT scans were reviewed by the same paediatric radiologist, who assessed:

- Airways stenosis: presence, distribution and diameter at the level of maximum stenosis
- Lymphadenopathy: presence and distribution of all lymphadenopathy. The size of the nodal group implicated in airway stenosis was measured
- Parenchymal complications: consolidation, breakdown, air trapping, expansile pneumonia, collapse and bronchiectasis
- Associated findings related to TB: ovoid focal bodies, miliary nodules, pleural disease and intracavitary bodies.

These radiologic findings were entered into the database as categorical and binary variables.

Our data collection regarding nodules included all varieties of nodules: larger nodules as well as ill-defined smaller nodules (tree-in-bud). We did not record tree-in-bud nodules as a separate entity. Nodules of any type at the periphery of a confluent area of consolidation were considered part of the airspace process and not as distinct nodules.

The measured value of the airway diameter at the level of maximum stenosis was compared to the normal value of the airway diameter for the child's age group [15, 16] and was expressed as a percentage of attenuation. This percentage was then stratified into a category of severity of compression as follows: mild (0–33%), moderate (34–66%), severe (67–99%) and complete (100%) for each airway in each age group.

Normal values for the diameter of the bronchial tree distal to the main bronchi, i.e. left upper lobe bronchus, bronchus intermedius (third order bronchi), and right lower lobe bronchus (fourth order bronchus), were not available and were therefore estimated by the formula [17, 18]:

$$d(z) = d_0.2^{\frac{-z}{3}}$$

where d = diameter of bronchus, z = generation of bronchus, and d_0 = diameter of trachea

The resulting estimated values for each age category were rounded off to the nearest millimetre to facilitate comparison with the calliper measurements on CT images. The data was analysed using STATISTICA 9.1; (a statistical software package by StatSoft, Inc.) with specific reference to the number of compressions by site, age and severity, as well as the number and type of parenchymal changes present including laterality. Results were expressed as frequencies and percentages for categorical variables.

Results

The study included 98 children with confirmed lymphobronchial TB. There were 55 males and 43 females, with ages ranging from 2 to 144 months (mean age, 26.6 months; median age, 12 months). The largest age category was that of infants, 50 patients (51%). The HIV status was positive for 17 children (17.3%), negative for 80 children (81.6%) and unknown for 1 (1%) child.

Table 1 Distribution of lymphadenopathy on CT in 98 children with lymphobronchial tuberculosis

Site of lymphadenopathy	Number of children with involvement (%)
Subcarinal	95 (96.9)
Right paratracheal	92 (93.9)
Right hilar	84 (85.7)
Right azygo-oesophageal	76 (77.6)
Left hilar	68 (69.4)
Right paracardiac	17 (17.3)
All sites	432[a]

[a] Representing 73.5% of all possible sites (6 sites in 98 children)

Lymphadenopathy was seen in all 98 children. Multiple sites were usually involved. Only one child had single-site involvement. The distribution of lymphadenopathy is summarised in Table 1. The most common site of lymphadenopathy was the subcarinal region, followed by the right paratracheal and right hilar regions. Of 588 possible lymph node sites (6 sites × 98 individuals), lymphadenopathy was documented at 432 sites (73.5%). The mean number of affected sites was 4.4 per child.

Tracheobronchial compression

CT revealed a total of 259 sites (37.8%) of large-airways compressions out of a possible 686 sites (7 sites × 98 individuals). The number and severity of airways compression is summarised by age group in Table 2.

In the infant age group, the largest age group, we found 140/259 of all compressions (54.1%). The number of compressions per child was similar across age groups ranging from 43/19 (2.3 compressions per patient) for the 2–6 year age group to 140/15 (2.8 compressions per patient) in the 0–1 year age group. Severe and complete stenoses formed 30/259 (11.6%) and 30/259 (11.6%), respectively, of all compressions. The infant group demonstrated the highest proportion of severe and complete compressions, 41/60 (68.3%). (Total of 41 severe and complete compressions in the infant age group; total of 60 severe and complete compressions in all patients.) 41/50 (82%) of the infants had severe or complete compression at some level. (Total of 41 severe and complete compressions in the infant age group; total of 50 infants with severe and complete compressions.) Only 4/60 (6.7%) of severe and complete compressions were in children older than 6 years. (Total of 4 severe and complete compressions in children older than 6 years; total of 60 severe and complete compressions in all patients.)

Levels of compression (by seven predetermined levels) were documented in the database and are summarised, by severity, in Table 3.

The most common site of compression was the bronchus intermedius comprising 73/259 sites (28.2%), followed by the left main bronchus (63/259; 24.3%) and trachea (62/259; 24%). Most (34/259; 13.1%) of the severe/complete compressions, and 56.7% of all severe and complete compressions (18+16/30+30) involved the bronchus intermedius. Severe and complete compressions made up 34/73 bronchus intermedius compressions (46.6%). Tracheal compression was most commonly mild or moderate (60/62; 96.8%).

Endoluminal lesions were seen in 14 children, ten on the right side and four on the left. It was not possible to differentiate granulomatous tissue from debris.

A total of 262 instances of parenchymal complication were identified in 92/98 children (93.9%). Table 4 shows the instances of specific parenchymal complications. The most common complication was consolidation (44.7%), followed by breakdown (16.4%) and air trapping (15.6%). Overall, parenchymal complications were more frequent in the right lung, (164/262; 62.6%) than in the left (98/262; 37.4%). All categories of complications were more frequent in the right lung. The mean number of complications per child was 2.8 (92/262).

The number of patients in the database with specific parenchymal complications that can be ascribed to lymphobronchial TB, together with laterality of the lesions, are summarised in Table 5. The most common complication was consolidation (87.7%), followed by breakdown (41.8%) and air trapping (37.8%). The majority of children

Table 2 Number of airway compressions by age and severity as detected by CT in 98 children with lymphobronchial tuberculosis

Age group	Number of children	Number of compressed segments					Compressed segments per child
		Mild	Moderate	Severe	Complete	Total	
0-12 months	50	58	41	22	19	140	2.8
13-24 months	19	26	15	4	8	53	2.8
25 months-6 years	19	20	20	2	1	43	2.3
>6<10 years	8	10	5	2	1	18	2.3
>10-13 years	2	3	1	0	1	5	2.5
All	98	117	82	30	30	259	2.6

Table 3 Number of airway compressions by site and severity as detected by CT in 98 children with lymphobronchial tuberculosis

Site	Severity of compression				Total compressions
	Mild	Moderate	Severe	Complete	
Trachea	44	16	2	0	62
Left main bronchus	22	25	7	9	63
Left upper lobe bronchus	3	0	1	1	5
Left lower lobe bronchus	7	2	0	1	10
Right main bronchus	10	9	1	0	20
Bronchus intermedius	15	24	18	16	73
Right lower lobe bronchus	16	6	1	3	26
All sites	117	82	30	30	259

(66/98) had multiple complications, either uni- or bilaterally. A total of 81 associated findings were documented in 56 children. These included ovoid focal lesions (Ghon focus, a classic radiological sign of primary TB), pleural disease, miliary nodules and intracavitary bodies. These findings are summarised in Table 6. The most common associated finding was ovoid focal lesions (33/81 = 40.1%), followed by pleural disease, 27.2% (16/81 = 19.8% on right + 6/81 = 7.4% on left) and miliary nodules, 24.7% (20/81).

Six children with lymphobronchial TB had no parenchymal complications. The mean age of these patients was 19 months (median 8 months) compared to the overall group who had an mean age of 26 months (median 12 months). None in the subgroup of six children without parenchymal complications had complete obstruction of any airway. There was a higher proportion of tracheal compression (83%) in comparison to the overall group (63%), with a higher proportion of severe obstruction of the trachea (20% of this subgroup vs 3% of the overall group). There was a lower proportion of bronchial involvement in the subgroup (BI 67% vs 75%; LMB 50% vs 64%; RMB 17% vs 20%) with no severe compressions of any of the bronchi in children without parenchymal complications. Ovoid focal bodies noted in three children of the subgroup (50% vs 34% in the overall group) were indistinguishable from the parenchymal complications of lymphobronchial TB.

Discussion

The incidence of TB is increasing worldwide, and children are at increasing risk of being exposed to the disease [19]. The subsequent increase in the number of children with TB has led to an increase in the number of children with complications such as lymphobronchial TB. Primary TB results from the inhalation of droplets containing the causative organism *Mycobacterium tuberculosis*. This initiates a localised pneumonic process called the Ghon focus. From here, the bacilli spread to regional lymph nodes via lymphatics. This local infective focus with associated lymphangitis and lymphadenopathy is known as the primary complex or Ghon complex [2, 20]. This regional lymphadenopathy is considered the hallmark of the radiologic diagnosis of primary TB in children [2, 21].

The radiologic findings of lymphobronchial TB on chest radiographs are well-established, but the findings on CT are not well-documented, nor is the prevalence of parenchymal complications. Similarly, CT findings in patients with TB are well-documented, but there is a paucity of published data regarding CT of lymphobronchial TB. Known findings include enlarged lymph nodes, hyperinflation, consolidation, wet lung, necrosis, bulging fissures and eventual cavitation [6, 8].

Contrast-enhanced chest CT may identify lymph nodes that are not visible on radiographs [4, 21–24]. All the

Table 4 Instances of specific parenchymal complications detected by CT in 98 children with lymphobronchial tuberculosis

Parenchymal complication	Number of instances (% of all parenchymal complications)	By laterality	
		Right	Left
Consolidation	117 (44.7)	71	46
Breakdown	43 (16.4)	28	15
Air trapping	41 (15.6)	28	13
Expansile pneumonia	29 (11.1)	19	10
Collapse	20 (7.6)	11	9
Bronchiectasis	12 (4.6)	7	5
Total	262	164	98

Table 5 Individuals with specific parenchymal complications as detected by CT in 98 children with lymphobronchial tuberculosis

Parenchymal complication	Number of children with complication (% of children)	By laterality		
		Unilateral right	Unilateral left	Bilateral
Consolidation	86 (87.8)	40	15	31
Breakdown	41 (41.8)	26	13	2
Air trapping	37 (37.8)	24	9	4
Expansile pneumonia	28 (28.6)	18	9	1
Collapse	17 (17.3)	8	6	3
Bronchiectasis	9 (9.2)	4	2	3

patients in our study had lymphadenopathy, and 99% had more than one site involved. The most common sites were the subcarinal, right hilar and paratracheal sites. This compares well with the known distribution of lymphadenopathy on radiographs [2, 20, 25].

The current study was compared to two previous studies that reported the prevalence and distribution of TB lymphadenopathy on CT. In the study by Andronikou et al. [21], the sample population included patients suspected but not proved to have TB, as was the case in the study by Mukund et al. [26] and our study. Both previous studies demonstrated airway disease in approximately one-third of patients whereas all patients in our study had airway involvement judged by our inclusion criteria. The median age of patients in the study by Mukund [26] was higher (11 years) than that found by Andronikou et al (21.5 months) [21] and the current study (12 months).

With regards to distribution of lymphadenopathy, our study demonstrates a higher prevalence overall and at specific sites when compared to both previous studies. In particular, we show a higher prevalence of hilar lymphadenopathy than the study by Mukund, and this can probably be explained by our preselection of childen with airway disease. This preselection in a predominantly infant population accounts for the higher prevalence of hilar lymphadenopathy, which is more likely to result in airway disease because bronchi in infants are more easily occluded due to their lack of cartilage and smaller diameter.

Table 6 Instances of findings associated with lymphobronchial tuberculosis as detected by CT in 98 children

Associated finding	Number of associated findings (% of all associated findings)
Ovoid focal bodies	33 (40.7)
Miliary nodules	20 (24.7)
Right pleural disease	16 (19.8)
Left pleural disease	6 (7.4)
Intracavitary body	6 (7.4)
Total	81

We show a higher prevalence of tracheal lymphadenopathy when compared to Andronikou et al. [21], who used a single-slice CT scanner. The use of MDCT in the our study presumably gave the reader (same reader as in the previous study) a higher confidence for distinguishing lymphadenopathy from the thymus and from poorly enhancing vasculature.

When tuberculous lymph nodes affect the airways, the resulting lesions define lymphobronchial TB. This may take the form of external airway compression, erosion, ulceration, infiltration, intraluminal caseating material or granulation tissue [6]. Not all children with TB develop lymphobronchial TB. The reported incidence of airway narrowing by tuberculous lymph nodes varies from 35% [21] to 40% [25]. The patient population in our study is a super-selected group of children presenting with symptoms of airway compression. It is not known what percentage they represent of all paediatric TB patients at our institution.

Younger children are more likely to develop TB, including lymphadenopathy, after infection with *M. tuberculosis* [2]. Younger children are also more likely to have tuberculous lymph nodes, probably because their immune systems are less mature [27], allowing organisms to proliferate within the reticulo-endothelial system. Younger children, by nature of their anatomical size, have narrower airways with less supportive cartilage, making them more compressible. This age-specific disease risk and the characteristic lymphadenopathy in primary TB offer plausible explanations why infants were more likely to develop lymphobronchial TB in our study. Although our patients ranged from 2 months to 12 years of age, the majority (51%) were younger than 1 year. This age group also demonstrated more severe compressions, with 82% of patients less than 1 year of age showing severe or complete compressions at least at one site.

The prevalence of HIV in our study population was 17%. This is in keeping with the prevalence of HIV co-infection with TB in children in other studies. Reported HIV prevalences in these studies vary from 11.2% in Ethiopia [28] and 18% in Zambia [29] in 2002, to 22.3% [30] and 21% [31] in more recent studies (2007, 2009) in South Africa. This similarity between the HIV prevalence of our study

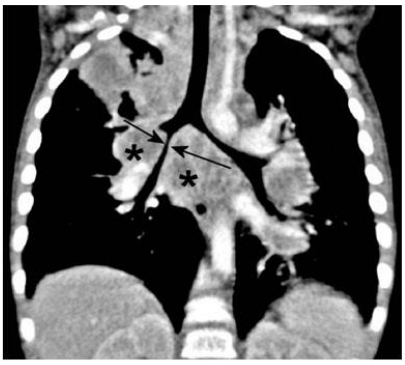

Fig. 1 11-month-old boy with lymphobronchial TB. Coronal minimum intensity projection from contrast-enhanced chest CT shows nutcracker-type compression of the bronchus intermedius (*arrows*) by tuberculous lymph nodes (*asterisks*)

population with lymphobronchial TB and other study populations with unspecified TB implies that HIV infection is not a specific predisposing factor for the development of lymphobronchial TB.

The children in our study showed a high percentage of lymphadenopathy at documented sites (73.5% of all possible sites showed nodal enlargement) but compression of the tracheobronchial tree was present at only 38% of sites. Although any of the airways may show compression by lymph nodes, our study showed that the bronchus intermedius is compressed most frequently (28% of all compressions). This is probably because it is a third-order bronchus and therefore narrower than the left and right main bronchi. It also is longer, more vertical and situated between two nodal groups that are often enlarged (subcarinal, 96.9% and right hilar, 85.7%). The predominant form of bronchus intermedius-compression was of a nutcracker-type, with combined medial and lateral

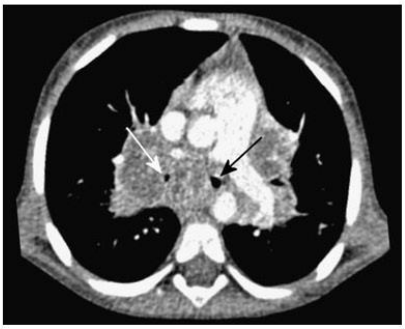

Fig. 2 Contrast-enhanced axial chest CT of an 11-month-old boy with lymphobronchial TB demonstrates right hilar and subcarinal lymphadenopathy resulting in severe circumferential compression of the bronchus intermedius (*white arrow*) and moderate compression of the left main bronchus (*black arrow*) against the left pulmonary artery

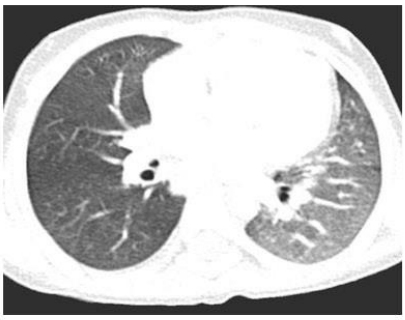

Fig. 3 Contrast-enhanced axial chest CT of 20-month-old male patient with lymphobronchial TB demonstrates relatively low density (air trapping) of the right middle and lower lobes secondary to mild to moderate compression of the bronchus intermedius

compression (Fig. 1). Less typical, larger, more extensive lymphadenopathy compressed it circumferentially (Fig. 2). The bronchus intermedius was also the most severely compressed airway segment (severe and complete in 47% of cases of involvement). Goussard and Gie [6] also found the bronchus intermedius a common site for complete obstruction.

The right and left main bronchi abut the pulmonary arteries, which may explain why they do not exhibit nutcracker-type compression by lymph nodes. When extensive lymphadenopathy encases the main bronchi, their larger calibre appears to initially protect them from significant compression. The longer and narrower left main bronchus accounted for 24% of total airway compressions, the right main bronchus for 8%.

The trachea accounted for 24% of nodal compressions; however, these were mostly (97%) mild or moderate, probably because the trachea is larger and more rigid than the

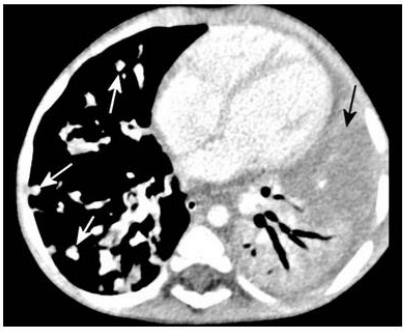

Fig. 4 19-month-old boy with lymphobronchial TB. Constrast-enhanced axial chest CT demonstrates parenchymal abnormalities in the left lung as a result of left main bronchus compression (not shown). There is consolidation posteriorly (enhancing viable consolidated lung with air-bronchograms) and lung necrosis (low-density non-enhancing lung without air-bronchograms, *black arrow*) anteriorly. Multifocal ovoid soft-tissue density interstitial lesions (*white arrows*) are seen in the right lung

bronchi and because it is not usually circumferentially involved and therefore responds by displacement rather than compression.

Nodal compression of airways leads to air trapping (Fig. 3), consolidation (Fig. 4), collapse, expansile pneumonia (Fig. 5), necrosis and breakdown (Fig. 6). The most common complication documented in our study was consolidation (88% of the children). Of note, however, is that it is not possible to differentiate consolidation secondary to lymphobronchial TB from that of primary TB, as the radiologic appearances are indistinguishable. Consequently, our results may overestimate the frequency of consolidation as a complication in lymphobronchial TB.

Evaluation of the subgroup of children that did not demonstrate any parenchymal complications of lymphobronchial TB (6% of all children) indicates that these children had a higher proportion of tracheal involvement rather than bronchial involvement and that there were no cases of severe or complete bronchial obstruction. We surmise that the lower proportion of severe and complete bronchial compression accounts for the absence of parenchymal complications of lymphobronchial TB. In addition we noted that there was a higher proportion of moderate and severe tracheal involvement in this subgroup without associated parenchymal complications.

The children in our study showed a predominance of right-side parenchymal complications, both overall and in each category of complication. This is to be expected, as lymphadenopathy was most commonly on the right and the most frequent and severe bronchial occlusions were also on the right. In addition, primary TB is reported to be more common on the right, which is thought to be related to the anatomy of the bronchial tree [32].

Other findings associated with TB, but not necessarily complications of lymphobronchial TB, were documented.

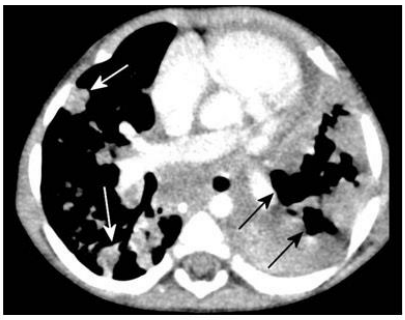

Fig. 6 10-month-old boy with lymphobronchial TB. Contrast-enhanced axial chest CT demonstrates multiple cavities (*black arrows*) within the consolidated left lung. This was secondary to compression of the left main bronchus (not shown). There are subcarinal lymphadenopathy and multifocal soft-tissue nodules in the right lung (*white arrows*)

These included pleural disease, ovoid focal bodies, miliary nodules and intracavitary bodies. All of these findings were also more common on the right.

TB is a progressively evolving, dynamic pathological process, and imaging findings depend on its stage. Our patients showed a variety of synchronous imaging abnormalities, e.g. features of primary TB (ovoid focal bodies) coexisting with abnormalities of advanced lymphobronchial TB (breakdown and cavitation; Fig. 6). Other children showed abnormalities of early lymphobronchial TB (air trapping) together with chronic lung disease in the form of bronchiectasis (Fig. 7). Interestingly, it has also been reported that treatment for TB can cause nodes to paradoxically enlarge [25], giving rise to more acute findings in patients with advanced (established) lymphobronchial TB.

Identifying the complications and associations of lymphobronchial TB has clinical relevance. These patients may need

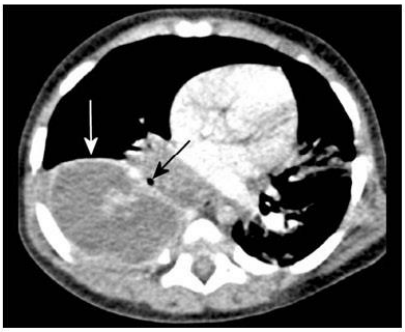

Fig. 5 Constrast-enhanced axial chest CT of a 7-month-old girl with lymphobronchial TB demonstrates right lower lobe necrotic expansile penumonia (*white arrow*) secondary to compression of the bronchus intermedius (*black arrow*) by subcarinal tuberculous lymph nodes. Less severe parenchymal abnormalities are seen in the left lung

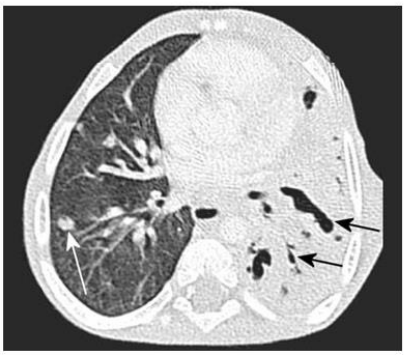

Fig. 7 Contrast-enhanced axial chest CT of a 10-month-old boy with lymphobronchial TB demonstrates bronchiectasis (*black arrows*) within the consolidated left lung distal to a focal compression of left main bronchus (not shown). An ovoid nodule is seen in the right lung (*white arrow*)

surgical intervention in the form of enucleation of an obstructing node to decompress a bronchus, or bronchoscopic removal of intraluminal obstructions [12–14]. Recovering patency of the airway and allowing resolution of the parenchymal disease associated with the obstruction to thus be achieved. In such cases, CT images serve as a road map for the surgical approach [33], and follow-up CT may confirm resolution [34]. Although CT may not replace bronchoscopy, it provides useful complementary information [35].

Our study was conducted purely from collected data without reviewing the CT scans. However, one author performed the original CT reporting from which the study data were compiled. The recorded data did not include sites of consolidation according to lobar distribution in detail, but recorded only the side of involvement. As a consequence, we could not draw direct conclusions from comparing of the site of the compression and the exact site of consolidation. CT is unable to differentiate consolidation of primary TB from consolidation as a complication of bronchial occlusion in lymphobronchial TB. The number of recorded instances of consolidation in our study may therefore include primary TB consolidations, falsely elevating the number of parenchymal complications of lymphobronchial TB in our study sample.

We identified a variety of future research questions including correlation of the degree of compression with nodal size. This study indicates that larger nodes are more likely to cause more severe airway compression. Determining whether there is a correlation between the consistency of lymph nodes identified at bronchoscopy, node density at CT and signal intensity at MRI may be interesting. So will further analysis to determine any relationship between lymph node consistency and likelihood of airway compression.

The hypothesis of pathogenesis developed from our study data may be confirmed by serial imaging of children with lymphobronchial TB, which may offer further insight into the disease process.

Conclusion

The most important CT finding in children with lymphobronchial TB is airway compression due to lymphadenopathy. Compression most frequently involves the right-side airways, most notably the bronchus intermedius. Compression is more frequent and more severe in infants. Parenchymal complications distal to an airway narrowing predominantly involve the right lung and include air trapping, consolidation/collapse, expansile pneumonia, breakdown and bronchiectasis. Associated findings in TB include miliary nodules, pleural disease, parenchymal ovoid focal bodies and intracavitary bodies, which are seen in a variety of combinations with the parenchymal complications.

CT of children with lymphobronchial TB is useful both for diagnosis and care planning. Recognition of lymphobronchial TB, identification of the location of airway compression, and identification of related parenchymal complications are relevant for paediatric radiologists, paediatric pulmonologists and thoracic surgeons and enable the planning of lung-sparing interventions. Development of protocols for scanning children with lymphobronchial TB, in collaboration with referring pulmonologists and thoracic surgeons, might be of multi-disciplinary benefit.

References

1. WHO (2010) Global tuberculosis control: a short update to the 2009 report. http://www.who.int/tb/publications/global_report/2009/update/en/index.html Accessed on 22/3/2010
2. Marais BJ, Gie RP, Schaaf HS et al (2004) The natural history of childhood intra-thoracic tuberculosis: a critical review of literature from the pre-chemotherapy era. Int J Tuberc Lung Dis 8:392–402
3. Beyers JA (1979) The radiological features of primary pulmonary tuberculosis. S Afr Med J 55:994–997
4. Daltro PA, Nunez-Santos E (2008) Pediatric tuberculosis. In: Lucaya J, Strife JL (eds) Pediatric chest imaging: chest imaging in infants and children. Springer, Berlin, pp 165–181
5. Marais BJ, Gie RP, Schaaf HS et al (2004) A proposed radiological classification of childhood intra-thoracic tuberculosis. Pediatr Radiol 34:886–894
6. Goussard P, Gie R (2007) Airway involvement in pulmonary tuberculosis. Paediatr Respir Rev 8:118–123
7. Gie RP, Goussard P, Kling S et al (2004) Unusual forms of intrathoracic tuberculosis in children and their management. Paediatr Respir Rev 5 Suppl A:S139–S141
8. Andronikou S, Vanhoenacker FM, De Backer AI (2009) Advances in imaging chest tuberculosis: blurring of differences between children and adults. Clin Chest Med 30:717–744
9. Venta LA, Shapir J (1985) Enhancement of pulmonary vasculature in pulmonary consolidation as seen by computed tomography. J Comput Tomogr 9:133–135
10. Andronikou S, Wieslthaler N (2009) Imaging for tuberculosis in children. In: Schaaf HS, Zumla A (eds) Tuberculosis: a comprehensive clinical reference. Saunders Elsevier, Philadelphia, pp 261–295
11. Griffith-Richards SB, Goussard P, Andronikou S et al (2007) Cavitating pulmonary tuberculosis in children: correlating radiology with pathogenesis. Pediatr Radiol 37:798–804
12. Papagiannopoulos KA, Linegar AG, Harris DG et al (1999) Surgical management of airway obstruction in primary tuberculosis in children. Ann Thorac Surg 68:1182–1186
13. Hewitson JP, Von Oppell UO (1997) Role of thoracic surgery for childhood tuberculosis. World J Surg 21:468–474
14. Freixinet J, Varela A, Lopez RL et al (1995) Surgical treatment of childhood mediastinal tuberculous lymphadenitis. Ann Thorac Surg 59:644–646
15. Hammer GB, Fitzmaurice BG, Brodsky JB (1999) Methods for single-lung ventilation in pediatric patients. Anesth Analg 89:1426–1429
16. Respiration and circulation (biological handbooks) (1971) Federation of American Societies for Experimental Biology. Bethesda, MD, pp 105–108
17. Weibel ER (1963) Morphometry of the human lung. Springer, Berlin
18. The lung: scientific foundations (1997) (2nd edn) Lippincott-Raven, Philadelphia, pp 1064–1066

19. Middelkoop K, Bekker LG, Morrow C et al (2009) Childhood tuberculosis infection and disease: a spatial and temporal transmission analysis in a South African township. S Afr Med J 99:738–743
20. Parisi MT, Jensen MC, Wood BP (1994) Pictorial review of the usual and unusual roentgen manifestations of childhood tuberculosis. Clin Imaging 18:149–154
21. Andronikou S, Joseph E, Lucas S et al (2004) CT scanning for the detection of tuberculous mediastinal and hilar lymphadenopathy in children. Pediatr Radiol 34:232–236
22. de Charnace G, Delacourt C (2001) Diagnostic techniques in paediatric tuberculosis. Paediatr Respir Rev 2:120–126
23. Delacourt C, Mani TM, Bonnerot V et al (1993) Computed tomography with normal chest radiograph in tuberculous infection. Arch Dis Child 69:430–432
24. Venkateswaran RV, Barron DJ, Brawn WJ et al (2005) A forgotten old disease: mediastinal tuberculous lymphadenitis in children. Eur J Cardiothorac Surg 27:401–404
25. Andreu J, Caceres J, Pallisa E et al (2004) Radiological manifestations of pulmonary tuberculosis. Eur J Radiol 51:139–149
26. Mukund A, Khurana R, Bhalla AS et al (2011) CT patterns of nodal disease in pediatric chest tuberculosis. World J Radiol 3:17–23
27. Newton SM, Brent AJ, Anderson S et al (2008) Paediatric tuberculosis. Lancet Infect Dis 8:498–510
28. Palme IB, Gudetta B, Bruchfeld J et al (2002) Impact of human immunodeficiency virus 1 infection on clinical presentation, treatment outcome and survival in a cohort of Ethiopian children with tuberculosis. Pediatr Infect Dis J 21:1053–1061
29. Chintu C, Mudenda V, Lucas S et al (2002) Lung diseases at necropsy in African children dying from respiratory illnesses: a descriptive necropsy study. Lancet 360:985–990
30. Schaaf HS, Marais BJ, Whitelaw A et al (2007) Culture-confirmed childhood tuberculosis in Cape Town, South Africa: a review of 596 cases. BMC Infect Dis 7:140
31. Hesseling AC, Cotton MF, Jennings T et al (2009) High incidence of tuberculosis among HIV-infected infants: evidence from a South African population-based study highlights the need for improved tuberculosis control strategies. Clin Infect Dis 48:108–114
32. Leung AN, Muller NL, Pineda PR et al (1992) Primary tuberculosis in childhood: radiographic manifestations. Radiology 182:87–91
33. Papaioannou G, Young C, Owens CM (2007) Multidetector row CT for imaging the paediatric tracheobronchial tree. Pediatr Radiol 37:515–529
34. Maydell A, Goussard P, Andronikou S et al (2010) Radiological changes post-lymph node enucleation for airway obstruction in children with pulmonary tuberculosis. Eur J Cardiothorac Surg 38:478–483
35. Lawler LP, Corl FM, Haponik EF et al (2002) Multidetector row computed tomography and 3-dimensional volume rendering for adult airway imaging. Curr Probl Diagn Radiol 31:115–133

Pediatric Pulmonology 49:263–268 (2014)

Left Main Bronchus Compression as a Result of Tuberculous Lymphnode Compression of the Right-Sided Airways With Right Lung Volume Loss in Children

S. Andronikou, PhD,[1]* M.J. van Wyk, FCRad (Diag),[1] P. Goussard, MMed,[2] and R.P. Gie, MMed[2]

Summary. Rationale: The superior mediastinal space is confined by the sterno-manubrium anteriorly and the vertebral column posterior. An abnormal relationship between the superior mediastinal structures may result in compression of the left main bronchus. In patients with right-sided pneumonectomy an exaggerated compensatory response may lead to stretching and compression of the remainder of the intra-thoracic airway. Lymphobronchial TB mimics pneumonectomy when it causes compression of the bronchus intermedius, between nodal lymphnode groups with resultant volume loss in the right lung and displacement of the mediastinum to the right. The left main bronchus may be at risk of compression due to rotation and displacement of the major vessels. Aim: To report pediatric cases of right-sided lymphobronchial TB with volume loss, demonstrate the use of angle measurements to quantify mediastinal dynamics and support a pathogenetic theory for left main bronchus compression. Materials and Methods: CT scans in children with TB and right lung volume loss, were compared retrospectively with controls using angle measurements based on descriptions of the aorta-carinal syndrome and the post-pneumonectomy syndrome. The Mann–Whitney *U*-test was used to compare groups. Results: The "Pulmonary bifurcation angle" between the main pulmonary arteries reached statistical significance ($P = 0.025$). The "Pulmonary outflow tract rotation" angle (pulmonary trunk with the mid sagittal plane) approached statistical significance ($P = 0.078$). The left main bronchus ranged from complete obliteration in two patients to 0.7 cm. In 16 of 30 patients the size was reduced to less than 75% of expected. Conclusion: In children with right lung volume loss from TB, the compression of the contralateral bronchus is due to narrowing of the pulmonary artery bifurcation angle as the main trunk rotates towards the midline. This is comparable to the post-pneumonectomy syndrome. **Pediatr Pulmonol. 2014; 49:263–268.** © 2012 Wiley Periodicals, Inc.

Key words: left main bronchus; lung volume; collapse; TB; post-pneumonectomy syndrome; aorta-carinal syndrome.

Funding source: none reported.

INTRODUCTION

The superior mediastinal space is confined by the sterno-manubrium anteriorly and the vertebral column posteriorly.[1] An abnormal relationship between the superior mediastinal structures may result in compression of the left main bronchus due to direct compression ("thoracic squeeze") or mediastinal stacking.[2,3] A descending aorta abnormally located in the midline, directly anterior to the vertebral body may cause compression of the carina and left main bronchus between the posterior midline aorta and the anterior right proximal pulmonary artery. This is referred to as aorta-carina compression syndrome.[3] In patients with right-sided pneumonectomy an exaggerated compensatory response may lead to stretching and compression of the remainder of the intra-thoracic airways against fixed structures.[4] This may be due to mediastinal stacking through

[1]Department of Diagnostic Imaging, Faculty of Health Sciences, University of the Witwatersrand, Johannesburg, South Africa.

[2]Department of Pediatrics and Child Health, University of Stellenbosch, Tygerberg Children's Hospital, Western Cape, South Africa.

Conflict of interest: None.

*Correspondence to: S. Andronikou, PhD, Department of Diagnostic Imaging, Faculty of Health Sciences, University of the Witwatersrand, York Road, Parktown, Johannesburg, South Africa.
E-mail: docsav@mweb.co.za

Received 9 July 2012; Accepted 29 October 2012.

DOI 10.1002/ppul.22728
Published online 28 November 2012 in Wiley Online Library (wileyonlinelibrary.com).

abnormal positioning of the aorta or due to stretching and compression of the left main bronchus.

Lymphobronchial TB (LBTB) occurs in children due to the presence of lymphadenopathy impressing on compressible airways.[5] This is found in over a third of children with suspected TB using CT[6] and is found in up to 100% of children with TB who present and airway symptoms, (almost a third of the latter affecting the bronchus intermedius).[5] This condition may mimic pneumonectomy when there is compression of the bronchus intermedius, between large matted lymphnode groups[7,8] causing volume loss in the right lung and displacement of the mediastinum to the right.

In both the aorta-carinal syndrome and the post-pneumonectomy syndrome, the left main bronchus compression contributes further to the airway embarrassment originating on the right. Defining this as an entity associated with tuberculosis in children with quantification of the degree and understanding the pathogenetic mechanism would contribute to radiological detection and strengthen the motivation for decompression of the bronchus intermedius through lymphnode enucleation in specific patients.[9] Right-sided nucleation would conceivably relieve both right and left airway after return of the mediastinum to the midline.

Aim

To report pediatric cases of right-sided lymphobronchial TB with volume loss, demonstrate the use of angle measurements to quantify mediastinal dynamics and support a pathogenetic theory for left main bronchus compression.

MATERIALS AND METHODS

Contrasted chest CT scans of children (<13 years of age) with culture confirmed pulmonary TB and airway symptoms referred to a pediatric pulmonologist form part of a larger retrospective study of lymphobronchial TB. CT was performed with a multi-detector scanner (Aquilion, Toshiba, Japan) using a routine chest CT protocol for children with 120 kVp tube voltage and 50 mA tube current. Intravenous iodinated contrast medium was used routinely. Studies were performed without sedation or anaesthesia during free breathing and there was no attempt to obtain an expiratory study. Only patients with reports of right-sided hilar and subcarinal lymphadenopathy and right lung volume loss were retrospectively identified and included in this paper, irrespective of the presence of left main bronchus compression. Nineteen children <13 years of age with normal CT reports, where CT was performed for other reasons were included as controls. For convenience and repeatability, the CT scans were evaluated in the axial plane at the level of the main pulmonary trunk (outflow tract) (Fig. 1a–c), by one radiologist. A "horizontal baseline" was created at this axial level on the computer monitor using OSIRIX DICOM reading software (freeware through Apple) by drawing a digital line between the transverse processes of the vertebra on each slice. A "sagital midline" was also created perpendicular to the "horizontal baseline" through the middle of the vertebral body. Measures were obtained using the digital cursor facility for measuring angles. Angle measures were created to represent aspects of aortic position, cardio-mediastinal rotation and distorted pulmonary artery bifurcation angle. The study is nested in a

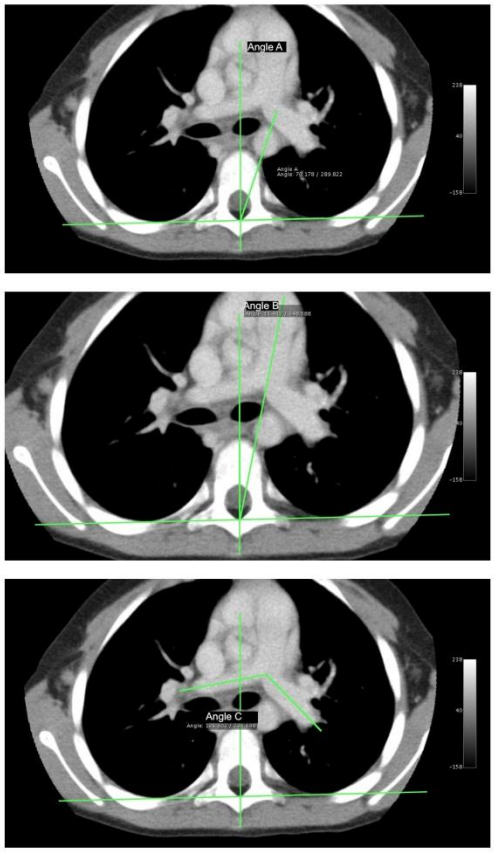

Fig. 1. a–c: CT scan measurements at the level of the main pulmonary trunk (outflow tract). The horizontal baseline represents a line between the transverse processes of the vertebra. a: "Anti-clockwise rotation of the aorta"—the angle between the midpoint of the aorta and the horizontal baseline (angle A). b: "Pulmonary outflow tract rotation"—the angle of the main axis of the pulmonary trunk with the mid sagittal plane (angle B). (c) "Pulmonary bifurcation angle"—the angle between the two main pulmonary arteries (angle C).

larger study of children with tuberculosis airway compression where CT scans were performed for clinical indications, with local ethical board clearance [clearance certificate M10441].

Angle measures included:

(a) "Anti-clockwise rotation of the aorta"—The angle between the midpoint of the aorta and the horizontal baseline at the sagital midpoint (angle A). (Fig. 1a).
(b) "Pulmonary outflow tract rotation"—The angle of the main axis of the pulmonary trunk with the mid sagital plane (angle B). (Fig. 1b).
(c) "Pulmonary bifurcation angle"—The angle between the two main pulmonary arteries (angle C) (Fig. 1c).

In addition, the left main bronchus was measured proximally (immediately distal to the carina and at its narrowest portion). A "percent of patency" was calculated by taking a proportion of the narrowest component to the proximal measurement.

Data was recorded in an Excel spreadsheet and statistical analysis was performed using Statistic 8.0 package. Data was summarized as mean (SD) or median (range) when distribution was normal or not normal respectively and variables were measured in a continuous scale. The Mann–Whitney *U*-test was used, as the data was not normally distributed along the mean to compare the two groups. Measurements were considered significant at a P-value < 0.05.

RESULTS

There were 30 patients (22 males and 8 females) and 19 controls (9 males and 10 females). Range, mean, median, and standard deviation values for the controls and the diseased patients as well as P-values of statistical significance are summarized in Table 1. Only one measure reached statistical significance. This was the "pulmonary bifurcation angle" (between the two main pulmonary arteries (angle C)) ($P = 0.025$). Angle B (the angle of the main axis of the pulmonary trunk with the mid sagital plane) approximated statistical significance ($P = 0.078$).

The left main bronchus measured from 0 to 0.7 (mean 0.4). The percentage patency ranged from 0% (in two patients) to 100% (in two patients). The mean patency was 70%. Six patients had <50% patency, 10 patients had patency ranging from 50% to 74% and 14 patients ranged from 75% to 100% [i.e. 16 patients (53%) had <75% patency].

Information on the timespan between the diagnosis and the CT scan was only available in 13 of the 30 patients and ranged from 1 day to 12 months from diagnosis. Surgery was undertaken in 13 of the 30 patients (43%).

DISCUSSION

Abnormal thoracic configuration or altered relationship of structures within thoracic space can lead to airway obstruction.[1] The trachea at the level of the thoracic inlet and the left main bronchus are the two most vulnerable sites of compression.[1]

Mechanisms of left main bronchus compression are varied. The mechanism of left main bronchus obstruction in thoracic distortion is either due to direct compression ("thoracic squeeze"), an abnormal relationship between the superior mediastinal structures (referred to as stacking), or both.[2,3] Vascular anomalies such as a double aortic arch, aberrant left or right subclavian artery, aberrant right innominate artery and pulmonary sling are causes of direct external compression. A descending aorta abnormally located in the midline, directly anterior to the vertebral body, is termed mediastinal stacking or aorta-carina compression syndrome[2,3] (the stimulus for measuring angle A). Abnormally stacked mediastinal structures are believed to cause compression of the carina and left main bronchus between the posterior midline aorta and the anterior right proximal pulmonary artery. This did not prove to be a statistically significant factor in our patients.

In patients with a right-sided pneumonectomy an exaggerated compensatory response may lead to stretching and compression of the remainder of the intra-thoracic airways against fixed structures.[4] Due to the fact that the right lung volume is larger than the left the effect is more pronounced after a right-sided pneumonectomy as

TABLE 1—Comparison of Angle and Distance Measures in Children With Right-Lung Volume Loss due to Tuberculosis Lymphadenopathy With Those of Normal Controls

	Control patients (N = 19)			Diseased patients (N = 30)				
	Mean	Median	SD	Mean	Median	SD	Z-value	*P*-value
Age	3.6	1.9	3.8	4.6	4.0	3.5	1.419	0.55
Angle A	66.8	69.3	8.1	66.2	71.3	23.1	1.405	0.159
Angle B	12.5	12.0	2.7	5.0	9.0	17.2	−1.760	0.078
Angle C	117.6	118.0	6.7	109.9	112.9	13.5	−2.226	0.025

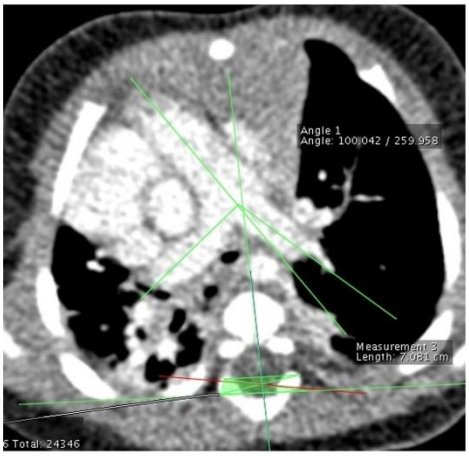

Fig. 2. A child with right lung volume loss demonstrates displacement of the mediastinal structures to the right with rotation of the pulmonary trunk to the right and narrowing of the bifurcation angle of the pulmonary arteries. The left main bronchus is compressed between the right pulmonary artery and the aorta, which in this patient lies anterior to the vertebral body.

there is greater mediastinal shift towards the right and the mediastinum is deviated posteriorly.[10] In addition there is counter-clockwise rotation of the heart along its main axis and herniation of the left lung towards the right[10,11] (the stimulus for measuring angle B). With this mechanism there is an increased chance of compression of the central airways between mediastial structures (Fig. 2). With right pneumonectomy and the ensuing mediastinal shift, the left main bronchus is stretched and pushed down by the left aortic arch and is then compressed inferiorly between the left pulmonary artery and the descending aorta[4] (the stimulus for measuring angle C).

Our results show that the rotation of the pulmonary trunk that occurs after right-sided bronchial compression with right lung volume loss in primary TB (much like the post-pneumonectomy syndrome) is less significant than the narrowing of the pulmonary artery bifurcation that results from this. The mechanism is more in keeping with the post-pneumonectomy syndrome rather then the aorto-carinal compression syndrome (malposition of the aorta and stacking of structures). Our measures show that the anatomical configuration in patients depends on the pulling of the main pulmonary trunk to the right with approximation of the main pulmonary arteries in what can be likened to a gymnast coming up from a "splits position"—where the gymnast's legs approximate each other. The left main pulmonary artery, which is then oriented less horizontally (and more vertically) and over to the right, would compress the left main bronchus against fixed structures including the vertebral body and aorta (not in itself significantly displaced in our patients). The left main bronchus is probably more prone to compression because it is also stretched during the right-sided midline shift[4] (Fig. 3a and b). The imaging in our patients demonstrates compression of the left main bronchus between the left pulmonary artery and the aorta (see Fig. 4a and b) with $<75\%$ patency in more than half of patients and $<50\%$ patency in a fifth of patients including two patients demonstrating complete obstruction.

TB infection in children leads to the development of a Ghon complex with involvement of regional lymph nodes and subsequent dissemination of bacilli throughout the body.[12] In general TB in children is pauci-bacillary which means that sputa are not available, requiring inducement or the use of gastric aspirates. Diagnosis therefore depends heavily on imaging.[12] Regional lymphadenopathy is considered the radiological hallmark of primary infection in childhood[12] but it is often difficult to detect confidently on radiographs. Right

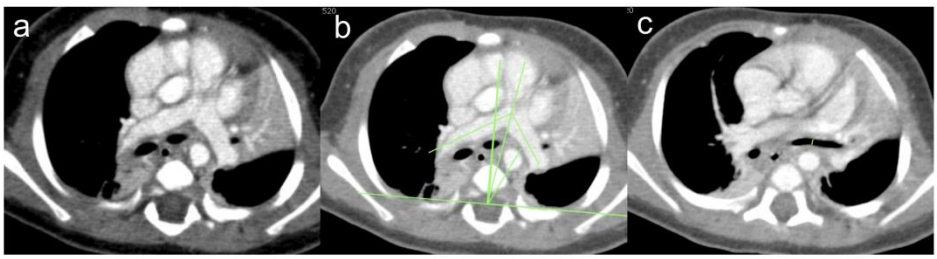

Fig. 3. a–c: Sequential CT slices of the chest at the level of the pulmonary outflow tract (a) without and (b) with lines and angles, and (c) at the pulmonary arteries. Right-sided displacement of the mediastinum due to right volume loss in this child with pulmonary TB, results in the left main pulmonary artery compressing the left main bronchus against the aorta. Note that the mediastinal displacement to the right also results in stretching of the left main bronchus making it vulnerable to compression.

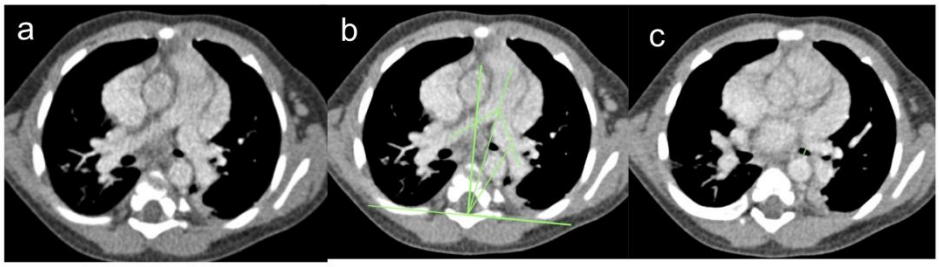

Fig. 4. a–c: Sequential CT slices of the chest at the level of the pulmonary outflow tract (a) without and (b) with lines and angles, and (c) at the pulmonary arteries. The narrow bifurcation angle resulting from mediastinal shift to the right in this child with pulmonary TB and right sided volume loss results in compression of the left main bronchus by the left main pulmonary artery against the aorta.

lung volume loss in primary TB may occur as a result of bronchial compression by lymphadenopathy in children and is termed "lymphobronchial TB".[7,8] This is found in about a third of patients suspected of having TB when imaged with CT[6] and almost all patients who have airway symptoms and TB.[5] Complications of lymph node compression include hyperinflation (partial obstruction), collapse (total obstruction), perforation into a bronchus with obstructive pneumonia/atelectasis (epituberculosis) and caseation with parenchymal destruction, cavitation and resultant fibrosis.[5,7,12] Lymphobronchial TB usually affects the right main bronchus or bronchus intermedius.[5,7]

Bronchoscopy demonstrates intraluminal narrowing or extrinsic compression of the airway, but cannot accurately determine the cause of the extrinsic compression, necessitating chest CT. du Plessis et al.[13] demonstrated the sensitivity and specificity of CT with volume rendered reconstructions against bronchoscopy and successfully measured stenotic airways even beyond sites where a bronchoscope could not be passed.[13] CT is the modality of choice, therefore, for demonstrating the cause of airway narrowing[13] and the parenchymal changes caused by it.[5] A progression from postobstructive air-space disease to bronchial filling by fluid (wet lung), progressive necrosis with loss of vascular markings, lack of lung parenchymal enhancement, bulging fissures, and eventual cavitation is visible with CT.[7] Removal of lymphadenopathy through enucleation has been shown to relieve the compression and allows salvageable lung to be recovered.[9]

As a result of right-sided bronchial compression and lung collapse, displacement of structures much like in the post-pneumonectomy syndrome occurs. The bronchus intermedius is the most common site of involvement in pediatric pulmonary TB, as it is compressed by the commonest and largest groups of lymphadenopathy.[5,6] This results in displacement of structures towards the right through rotation of the mediastinum in an anticlockwise direction, resultant narrowing of the bifurcation angle of the pulmonary artery which in turn leads to compression of the left main bronchus. This additional respiratory compromise is treatable by decompression of the right system, which will allow the mediastinum to centralize, the pulmonary angle to widen and the compression of the left main bronchus to be relieved also.

LIMITATIONS

Limitations of this study relate mainly to the retrospective nature of the work (which precluded universal availability of clinical information), and from the use of CT scans in controls as opposed to normal subjects (who were made up from children imaged for clinical indications thought to have normal CT scans). In addition the angles measured were generated based on a hypothesis that lymphadenopathy results in specific rotational displacement of structures. Furthermore we did not attempt to predict the degree of left main bronchus compression by comparing to the bronchial angle measurement. Instead the mechanical rotational changes on the mediastinal vessels with the potential for bronchial compression as a theory was being tested. This can later be translated into a clinical prediction tool prospectively testing degree of angle changes with degree of bronchial compression.

We did not have follow-up or post-operative imaging available to prove whether the left main bronchus narrowing could be relieved after decompression of the right airways. This must be the focus of future work.

CONCLUSION

Our measurements have demonstrated that children with right-sided compression of the airways due to tuberculosis lymphadenopathy and right lung volume loss put the contra-lateral left main bronchus at risk of

compression because there is narrowing of the pulmonary artery bifurcation angle. This happens as the main pulmonary trunk rotates towards the midline and beyond. This is comparable to the post-pneumonectomy syndrome. Knowledge of this phenomenon and an ability to identify and quantify this may serve to support a motivation for surgical enucleation either at first diagnosis or through follow-up measurements.

REFERENCES

1. Donnely LF, Frush DP. Abnormalities of the chest wall in pediatric patients. Am J Roentgenol 1999;173:1595–1601.
2. Donnelly LF, Bissett GS. Airway compression in children with abnormal thoracic configuration. Radiology 1998;206:323–326.
3. Donnely LF, Bissett GS, McDermott B. Anomalous midline location of the descending aorta: a cause of compression of the carina left mainstem bronchus in infants. Am J Roengenol 1995;164:705–707.
4. Kim EA, Lee KS, Shim YM, Kim K, Kim TS, Yang PS. Radiographic and CT findings in complications following pulmonary resection. Radiographics 2002;22:67–86.
5. Lucas S, Andronikou S, Goussard P, Gie R. CT features of lymphobronchial tuberculosis in children, including complications and associated abnormalities. Pediatr Radiol 2012;42:923–931.
6. Andronikou S, Joseph E, Lucas S, Brachmeyer S, du Toit G, Zar H, Swingler G. CT scanning for the detection of tuberculosis mediastinal and hilar lymphadenopathy in children. Pediatr Radiol 2004;34:232–236.
7. Andronikou S, Vanhoenacker FM, De Backer AI. Advances in imaging chest tuberculosis: blurring of differences between children and adults. Clin Chest Med 2009;30:717–744.
8. Goussard P, Gie R. Airway involvement in pulmonary tuberculosis. Paediatr Respir Rev 2007;8:118–123.
9. Maydell A, Goussard P, Andronikou S, Bezuidenhout F, Ackerman C, Gie R. Radiological changes post-lymph node enucleation for airway obstruction in children with pulmonary tuberculosis. Eur J Cardiothorac Surg 2010;38:478–483.
10. Shepard JO, Grillo HC, McLoud TC, Dedrick CG, Spizarny DL. Right-pneumonectomy syndrome: findings and CT correlation. Radiology 1986;161:661–664.
11. Chae EJ, Seo JB, Kim SY, Do KH, Heo JN, Lee JS, Song JW, Lim TH. Radiographic and CT findings of thoracic complications after pneumonectomy. Radiographics 2006;26:1449–1467.
12. Marais BJ, Gie RPH, Schaaf S, Starke JR, Hesseling AC, Donald PR, Beyers N. A proposed radiological classification of childhood intra-thoracic tuberculosis. Pediatr Radiol 2004;34:886–894.
13. du Plessis J, Goussard P, Andronikou S, Gie R, George R. Comparing three-dimensional volume-rendered CT images with fibreoptic tracheobronchoscopy in the evaluation of airway compression caused by tuberculosis lymphadenopathy in children. Pediatr Radiol 2009;39:694–702.

Pediatr Radiol (2009) 39:694–702
DOI 10.1007/s00247-009-1262-1

ORIGINAL ARTICLE

Comparing three-dimensional volume-rendered CT images with fibreoptic tracheobronchoscopy in the evaluation of airway compression caused by tuberculous lymphadenopathy in children

Jaco du Plessis · Pierre Goussard · Savvas Andronikou · Robert Gie · Reena George

Received: 4 October 2008 / Revised: 9 February 2009 / Accepted: 14 March 2009 / Published online: 28 April 2009

Abstract
Background Lymphobronchial tuberculosis (TB) causes airway compression in 38% of patients. The airway obstruction is conventionally assessed with fibreoptic tracheobronchoscopy (FTB). Multidetector-row spiral computed tomography (MDCT) with three-dimensional volume rendering (3-D VR) has significantly improved the imaging of the airways. No previous studies have assessed the accuracy of 3-D VR in determining the degree of airway compression in children due to TB lymphadenopathy.
Objective To compare 3-D VR CT to FTB for the assessment of airway compression due to TB lymphadenopathy in children.
Materials and methods Included in the study were 26 children presenting with symptoms of airway compression caused by pulmonary TB. MDCT of the chest and FTB were performed in all patients. Retrospective 3-D VR reconstruction of the major airways was performed from the original CT raw data and used to evaluate the tracheobronchial tree for site and degree of airway compression and then compared to the FTB findings. FTB was used as the reference standard
Results By FTB 87 sites of airway compression were identified. Using the 3-D VR technique, 138 sites of airway compression were identified, of which 78 (90%) matched with the sites identified by FTB. The sensitivity and specificity of 3-D VR when compared with that of FTB was 92% and 85%, respectively. In four patients (15%), severe narrowing of the bronchus intermedius made FTB evaluation of the right middle and right lower lobe bronchi impossible. VR demonstrated significant distal obstruction in three of these four patients
Conclusion 3-D VR demonstrates a very good correlation with FTB in determining airway compression caused by TB lymphadenopathy in children. In combination with FTB, 3-D VR adds confidence to the bronchoscopy findings and complements FTB by adding additional information on the status of the airway distal to severe obstructions unreachable by FTB.

Keywords Chest · Tuberculosis · CT · Children

J. du Plessis · R. George
Department of Radiology, University of Stellenbosch,
P.O. Box 19063, Tygerberg 7505, South Africa

J. du Plessis
e-mail: drjjdup@hotmail.com

P. Goussard · R. Gie
Department of Paediatrics, Tygerberg Children's Hospital,
Cape Town, South Africa

S. Andronikou (✉)
Department of Radiology, University of Cape Town,
Anzio Road, Observatory,
Cape Town, South Africa
e-mail: docsav@mweb.co.za

Introduction

In children, the diagnostic work-up for suspected airway obstruction traditionally includes chest radiography, CT and fibreoptic tracheobronchoscopy (FTB), with the latter considered the gold standard [1, 2]. FTB demonstrates intraluminal narrowing or extrinsic compression of the airway [2], but cannot accurately determine the cause of the

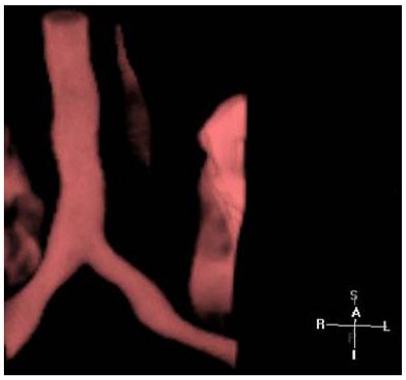

Fig. 1 Standard 3-D VR image of the distal trachea and proximal left and right main bronchi

extrinsic compression of the tracheobronchial tree, necessitating chest CT. Alternatively, CT of the chest is the modality of choice for demonstrating the cause of airway narrowing in children with pulmonary tuberculosis (TB) [3]. Three-dimensional volume-rendered (3-D VR) images depict airway compression more clearly than axial or multiplanar reconstructed (MPR) images [1]. Remy-Jardin et al. [4] found that the accuracy of demonstrating airway compression on 3-D VR images was 95.7%, compared to 91.5% with axial CT scans. 3-D VR allows better understanding of changes in airway calibre and complex tracheobronchial anomalies than axial CT scans [4]. This increases the diagnostic confidence and improves communication with referring physicians [1].

The aim of this study was to compare the site and degree of airway compression as determined by 3-D VR CT to those obtained by FTB in children with airway compression due to lymphadenopathy caused by *Mycobacterium tuberculosis* infection.

Materials and methods

The study was performed in Tygerberg Children's Hospital, a tertiary care hospital in the Western Cape, South Africa. The patients all presented with symptoms and signs of major airway compression, which included persistent coughing or wheezing, unilateral hyperinflation, or lobar collapse. The patients were all treated for TB with a quadruple anti-TB drug regimen to which steroids (prednisone 2 mg/kg per day for 30 days) was added. Children who failed to respond to treatment after 1 month and still had clinical symptoms and radiological evidence of significant airway obstruction were investigated by FTB and multidetector-row spiral CT (MDCT) scanning of the chest. The study cohort comprised 26 consecutive children with culture-confirmed pulmonary TB.

CT scanning of the chest was performed on a four-slice MDCT scanner at 120 kVp tube voltage and 50 mA tube current as part of a routine protocol in children. All patients received intravenous contrast medium by hand injection at a dose of 2 ml/kg. The delay before beginning the acquisition phase ranged from 30 to 35 s. All patients had only one CT scan of the chest performed.

FTB was performed under general anaesthesia by the same paediatric pulmonologist within 10 days of the chest MDCT scan. Flexible bronchoscopes of sizes 2.8 mm and 3.8 mm were used. In nine patients, the MDCT scan of the chest was performed prior to FTB with the results available to the bronchoscopist. The patients tolerated the procedure well and no complications related to the procedure or anaesthesia were recorded. The bronchoscopist commented on the site, degree and cause of the airway compression. The degree of airway compression was a visual impression of the calibre change of the narrowed airway segment. The degree of airway compression on FTB was recorded in categories of <50%, 50 75%, and 76 100%.

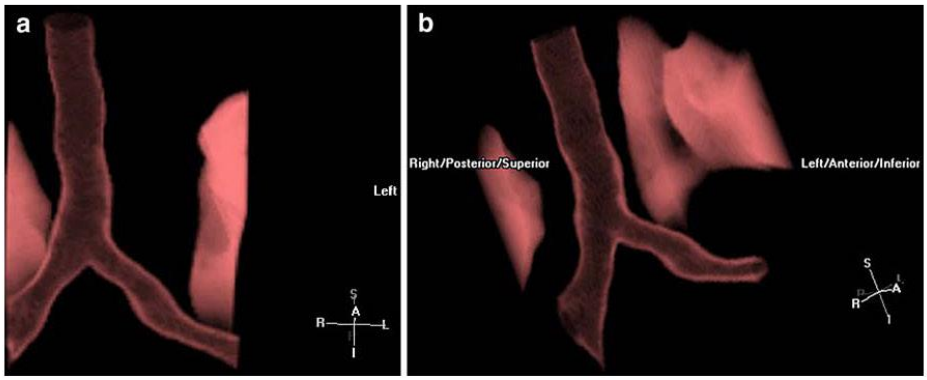

Fig. 2 Windowing of the airway is performed to obtain bronchographic images (**a**, **b**) with good transparency and wall homogeneity

The original MDCT dataset was used for reconstruction of the major airways using a 3-D VR technique. One patient was excluded as significant breathing artefact precluded accurate reconstruction of the airway. The same operator performed all the reconstructions and assessments of the airways. The software used was VOXAR 3-D version 4.1, service release 2 (Barco, Kortrijk, Belgium) (Fig. 1). The reconstructions were windowed to obtain an optimal 3-D bronchographic image and the reconstructions with the best (subjective) transparency, wall homogeneity and image sharpness were used in the evaluation (Fig. 2). The airway was segmented to remove irrelevant parts (Fig. 3).

The 3-D VR reconstructions were used to evaluate 11 sites, which included the trachea, main bronchi and lobar bronchi. The operator was blinded to the FTB findings. Each segment of the tracheobronchial tree was evaluated individually and sites of obstruction were recorded (Fig. 4). The length and degree of the obstruction were measured. The diameter of the compressed areas was measured from the outer aspect of the reconstructed airway. Measurements were taken at the most severe part of the compression and expressed as a ratio in relation to the diameter of the proximal 'normal' airway in the particular segment assessed. This matched the FTB technique for determining the proportion of compression, which was expressed as a percentage of airway compression. 3-D VR gives the exact percentage of compression. To enable comparison between 3-D VR and FTB the measurements and estimates from 3-D VR and FTB were grouped into three categories: mild (0 50%), moderate (51 75%) and severe (76 100%).

On identification of a compression using VR reconstructions, the axial images were used to document the cause of the obstruction at the particular site.

Ethical approval to perform this study was obtained from the Committee for Human Research, Stellenbosch Univer-

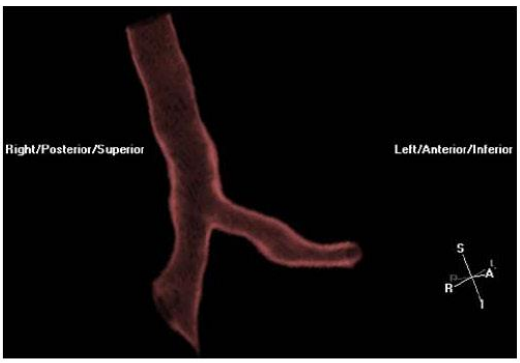

Fig. 3 Irrelevant parts of the reconstruction are removed by segmentation. Assessment of the segmented and windowed airway is performed in multiple planes (3-D)

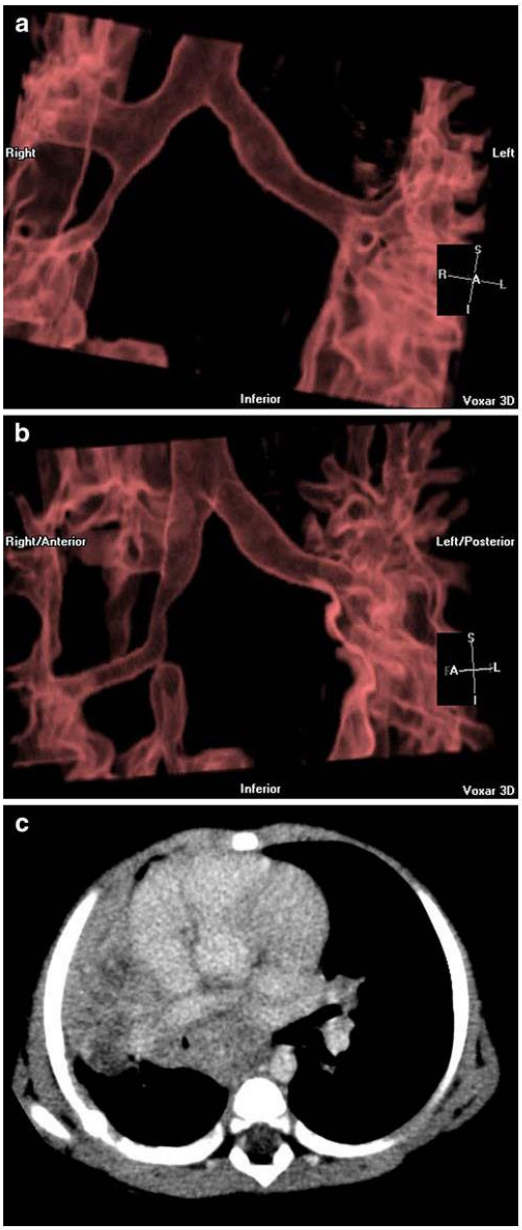

Fig. 4 Assessment of the bronchus intermedius. **a**, **b** Reconstructions demonstrate a significant (75%) stenosis with a length of 60% of the total length of the bronchus intermedius. **c** Axial image confirms lymphadenopathy as the cause of the airway compression

Table 1 Sites of compression identified by FTB and 3-D VR.

Site	FTB	3-D VR	Matching sites
Trachea	11	19	8
Carina	15	15	12
Right main bronchus	2	17	2
Right upper lobe	10	12	10
Bronchus intermedius	20	21	20
Right middle lobe	3	8	3
Right lower lobe	0	3	0
Left main bronchus	15	24	14
Left upper lobe	6	10	4
Lingula	4	7	4
Left lower lobe	1	2	1
Total	87	138	78

sity, and informed consent to perform the procedures from the parents or legal guardians of the patients was obtained.

Results

The study included a total of 26 patients with confirmed pulmonary TB (16 male; median age 21 months, range 3–84 months). All the patients had only one MDCT scan of the chest. A total of 45 FTB examinations were performed in this group (in 14 children more than one FTB examination was performed). FTB was repeated in 11 patients to assess response to treatment. Five patients underwent enucleation of lymph nodes to relieve the airway obstruction.

With 26 patients and 11 sites (the major airways), there were 286 possible sites evaluated. A total of 87 sites of bronchial compression were identified by FTB. FTB identified a single affected site in only three patients. 3-D VR identified 138 sites of bronchial compression of which 78 matched those identified by FTB (Table 1). FTB identified nine sites of airway compression, which were assessed as normal by 3-D VR (Table 2). At six of these nine sites, the compression was assessed by FTB as <50%. 3-D VR identified 60 sites of airway compression, which were assessed as normal by FTB. At four of these sites, the compression was assessed as 50–75% and at four sites as >76% (Table 3).

3-D VR demonstrated an overall sensitivity of 92% and specificity of 85% for the detection of airway narrowing when compared to the FTB findings. 3-D VR was able to assess the degree of airway compression at all 138 sites. FTB assessed the degree of compression in 67 of 87 compressed sites. In the remaining 20 sites the degree of compression was not recorded, with 15 of these located at the carina. In 85% of these 20 sites the airway compression measured by 3-D VR was <50%.

The study showed a further bias towards 3-D VR as in four patients compression of the bronchus intermedius was so severe that the distal airways could not be assessed by FTB. The compressed bronchi were clearly visible on the 3-D VR images (Fig. 5). Three of these four patients showed significant compression of the right middle lobe bronchus (100% occluded, two patients) and of the right lower lobe bronchus (80% and 100% occluded, two patients).

In addition, 3-D VR expressed the length of all compressions as a percentage of the full length of that segment of the airway. The agreement between the methods for the degree of overall narrowing was moderate (Cohen's kappa coefficient 0.39). The agreement for <50% compression was 92%, for 51–75% compression was 27%, and for 76–100% compression was 75% (Table 4). The 20 sites for which the degree of obstruction was not recorded on FTB were not used in the calculations.

Agreement between the two methods for the presence of compression was best for the bronchus intermedius (almost perfect agreement, kappa 0.88). Agreement for the degree of compression at the individual sites was best for the right upper lobe bronchus (substantial agreement, kappa 0.72).

The cause of compression was identified with the aid of the multiplanar reconstructions for all 138 sites demonstrated by 3-D VR. The left pulmonary artery, pulmonary veins and oesophagus were identified as the cause of compression in 20 of the 138 sites with the degree of airway compression estimated by FTB as >50% in 2 of the 20 sites. The cause of the obstruction in the two sites identified with compression by FTB was thought to be TB lymphadenopathy and other causes were not considered (one was due to the left pulmonary artery and the other due to the oesophagus).

Table 2 Sites assessed as normal by 3-D VR but compressed by FTB and the degree of compression.

Site	Number of sites missed by 3-D VR	Degree of compression by FTB (%)
Trachea	3	0–50
Carina	3	'Compressed'
Left main bronchus	1	0–50
Left upper lobe	2	0–50
Total	9	

Table 3 Sites assessed as normal by FTB but compressed by 3-D VR and the degree of compression.

Site	Number of sites missed by FTB	Degree of compression by 3-D VR		
		0–50%	51–75%	76–100%
Trachea	11	11		
Carina	3	2	1	
Right main bronchus	15	12	2	1
Right upper lobe	2	2		
Bronchus intermedius	1	1		
Right middle lobe	5	5		
Right lower lobe	3	3		
Left main bronchus	10	10		
Left upper lobe	6	5		1
Lingula	3		1	2
Left lower lobe	1	1		
Total	60	52	4	4

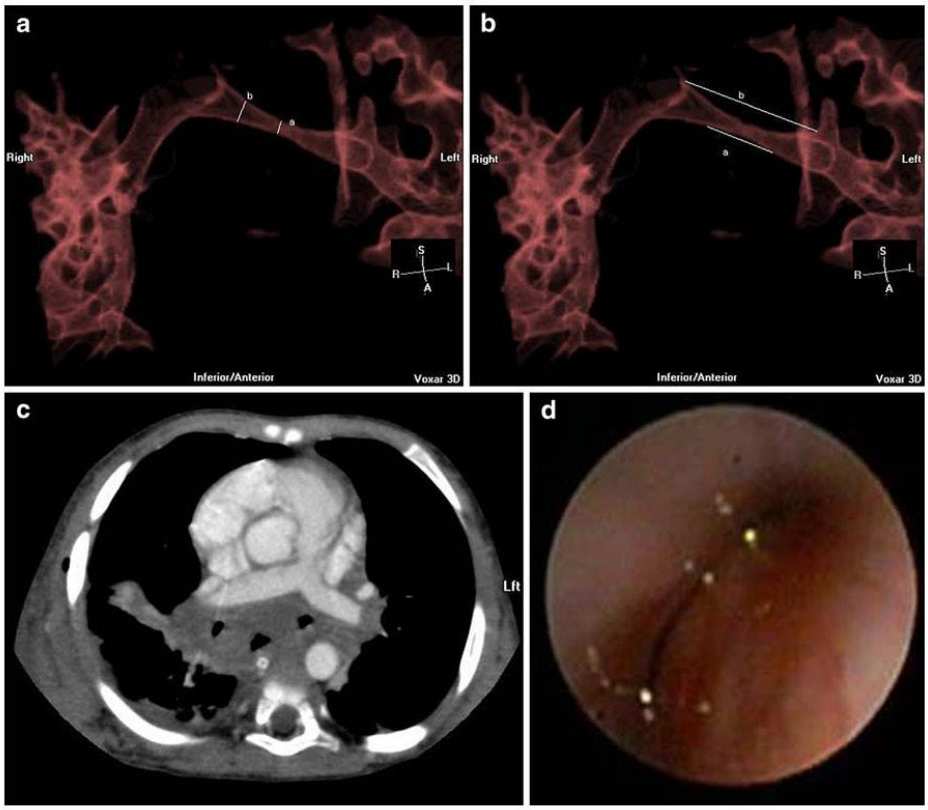

Fig. 5 Assessment of the left main bronchus. **a**, **b** 3-D VR reconstruction demonstrates 80% compression of the left main bronchus [1 $(a/b)\times100$] over 60% of the total length of the bronchus [$(a/b)\times100$]. The distal left upper lobe, lingula and left lower lobe bronchi can still be assessed despite the stenosis. **c** The axial image confirms the presence of lymphadenopathy. **d** Bronchoscopic view

Table 4 Agreement between the methods as to the degree of compression

Degree of compression: by FTB	Degree of compression: by 3-D VR				
	0–50%	51–75%	76–100%	'Compressed'	Total
0–50%	214 (92%)	8 (3%)	11 (5%)	0	233
51–75%	5 (45%)	3 (27%)	3 (27%)	0	11
76–100%	3 (15%)	2 (10%)	15 (75%)	0	20
'Compressed'	17 (85%)	1 (5%)	2 (10%)	0	20
Total	239	14	31	0	284

Discussion

In this study 3-D VR following MDCT had a sensitivity of 92% and a specificity of 85% for demonstrating airway compression due to lymphadenopathy caused by *M. tuberculosis* infection in children. This is probably an underestimation of the ability of 3-D VR as there were a number of sites in the distal airways with severe stenosis that could not be evaluated by FTB due to severe stenosis of the proximal airways.

In addition to the degree of stenosis, 3-D VR gave information concerning airway compression in these children. With 3-D VR the length of the compressed airway could be accurately measured, which was not possible with FTB. While the bronchoscopist assumed the cause of the airway compression in all the children was TB lymphadenopathy, in 14% the compression was due to other anatomical structures. Another advantage of MDCT is that the cause of the lymphadenopathy can be determined with greater certainty. Usually multiple sites are affected, but the subcarinal sites appear to be the most commonly affected [3]. This correlates well with our findings where the carina and bronchus intermedius were the most commonly compressed sites.

There is a global increase in the incidence of TB, with children being a high-risk group for acquiring the disease [3]. With 9 million new cases annually [5], TB is now considered to be the leading infectious cause of death in the world [6, 7]. Inhalation of an infectious droplet causes a localized pneumonic process (Ghon focus), from which the bacilli drain to regional lymph nodes. The Ghon focus, local lymphangitis and regional lymph node involvement are referred to as the Ghon complex. Lymph node involvement is the most common finding at presentation in children less than 5 years of age with pulmonary TB. Affected lymph nodes enlarge and can undergo central caseation [8]. These nodes can compress and infiltrate the airways causing intra- and extraluminal airway obstruction. Children then present with a persistent, unremitting cough and large-airway wheezing or stridor [9].

Chest radiographs are insensitive for lymph node detection. In up to 60% of patients with normal chest radiographs, CT scanning can demonstrate lymphadenopathy with a typical 'ghost-like' or low-density ring enhancement [10]. Tuberculous lymph nodes cause symptomatic airway obstruction in 38% of patients. If symptoms persist after 1 month of treatment (which includes anti-TB treatment and oral prednisone) reevaluation is recommended to determine the degree of airway compression. Evaluation is normally by FTB and MDCT of the chest. Where significant airway compression remains (obstruction >75%), enucleation of obstructing lymph nodes is considered [9]. Among our group of patients, airway compression was so severe in five (19%) that enucleation was performed.

FTB is a safe but invasive procedure, mostly performed under general anaesthesia [1, 2]. In the setting of lymphobronchial TB, the indications for FTB include confirmation of the diagnosis, evaluation of the degree of airway obstruction, aspiration of endobronchial contents, and evaluation of the response to anti-TB treatment. FTB is an excellent way to evaluate stridor and dynamic changes in airway calibre that cannot be done by MDCT. Complications of FTB occur in only a small percentage of patients and include hypoxaemia, hypercarbia, cardiac arrhythmias and subglottic oedema [11–13]. FTB has numerous limitations that include the inability to determine the cause of the stenosis or the relationship between the airway stenosis and the thoracic vessels [1, 2]. In addition, in patients with severe stenosis, FTB is unable to navigate the stenosis and determine the patency of the distal airways [2, 12]. The latter limitation was seen in four of the patients (Fig. 6). An area of concern raised by this study was the three patients in whom 3-D VR measured a significant stenosis (>76%) that was not identified by FTB. The reason for this discrepancy could be due to technical difficulties encountered during FTB, angular limitations of the bronchoscope or lack of recording of the stenosis in the light of accompanying severe stenosis in other parts of the airway. In these three patients the affected sites were the lingula and left upper lobe bronchus.

This study was performed retrospectively and, as such, had many limitations. It is possible that the bronchoscopist only recorded clinically relevant stenoses or that mild stenoses were less conspicuous on FTB. In our study, 3-D VR demonstrated 52 sites of mild (<50%) airway compression not seen on FTB. The presence and clinical signifi-

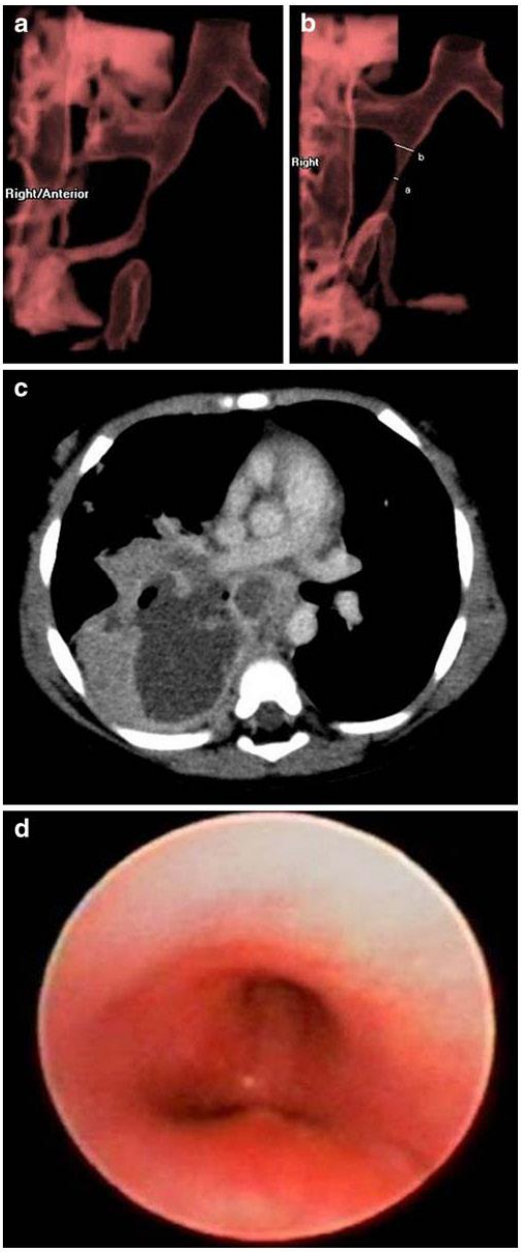

Fig. 6 Assessment of the bronchus intermedius and right lower lobe bronchus. **a**, **b** Severe stenosis of the proximal bronchus intermedius caused by TB lymphadenopathy, with complete compression of the right lower lobe bronchus at its origin. The right lower lobe bronchus is patent distally. The proximal stenosis of the bronchus intermedius could not be passed with the bronchoscope, making it impossible to assess the distal airway. **c** Axial image confirms lymphadenopathy as the cause of obstruction. **d** Bronchoscopic view demonstrates the narrowed bronchus intermedius at its origin below and the patent right upper lobe bronchus above

cance of these stenoses remains uncertain. It is also known that TB lymph nodes can enlarge during adequate antituberculous treatment, worsening airway obstruction [9]. In three of the four patients in whom severe obstruction of the airways was measured by 3-D VR but not recorded on FTB, the obstruction was in airways distal to the severe airway obstruction, making assessment by FTB impossible. All the measurements to determine the degree of stenosis were done by a single reader, which excluded interobserver error but not intraobserver bias.

The shortfalls of FTB necessitate MDCT of the chest, which also allows 3-D reconstructions of the airways and vasculature [1, 14]. MDCT with 3-D reconstructions is a safe, fast and noninvasive way of analysing the cause of airway compression in children [1, 2, 15]. The faster imaging capabilities of MDCT allow examinations to be performed without sedation, which improves the safety of the procedure [16]. The entire CT volume dataset of the tracheobronchial tree is converted into 3-D form, maintaining the original spatial relationships [12, 17, 18]. The reconstructions are based on differentiating between tissues on the basis of Hounsfield units [19]. By changing the window width and level the desired bronchographic image is obtained [20]. Due to its accuracy, VR has become the main technique for 3-D reformatting of the airways and mediastinal vascular structures that course into multiple planes [14, 16, 21]. Axial images remain necessary for extraluminal disease assessment, but 3-D VR can better demonstrate short focal areas of narrowing and the craniocaudal length of airway stenosis [15].

Abnormal airway calibre is more conspicuous, spatial relationships are better appreciated and measurements are more accurate with VR than with its two-dimensional reconstruction counterparts [17]. Three-dimensional VR reconstructions of the airways provide a more accurate assessment of the cause, degree and length of airway narrowing when compared to axial images, improving diagnostic confidence [1, 15, 22]. Over- or underestimation of the degree of airway stenosis is a known occurence [12, 21]. Possible causes for this would include windowing performed by the operator to obtain an ideal bronchographic image, the presence of mucus and airway secretions, and the dynamic changes of the airways during normal breathing. Some or a combination of these causes could have contributed to overestimation of the number of mild airway stenoses (<50%) not recorded by FTB (Tables 2 and 3). Axial images remain necessary to assess extraluminal disease and help identify artefacts [14]. Of VR images, 3% show disruptive stair-step artefacts, for which

vascular motion is considered to be the most likely explanation [4]. No stair-step artefacts were identified in our study.

The reported clinical applications for VR imaging of children's airways include congenital bronchial anomalies, tracheomalacia, tracheobronchial strictures, vascular airway compression, and bronchiectasis [1, 14, 22]. VR has been shown to produce high-quality diagnostic images in patients with congenital heart disease and obstruction of the major airways [2, 21]. In these studies, the airway compression affected single sites with no parenchymal lung disease. In our study, the airway disease was more complex, and in 23 patients multiple sites were affected. In adult patients, VR has been used to investigate lung metastases, bronchial carcinoma, laryngeal carcinoma and a variety of gastrointestinal tract pathologies [23–25].

A disadvantage of MDCT is the radiation dose to the patient. Lambert et al. [2] report that performing CT investigations in children at 80 kVp instead of 120 kVp decreases the radiation dose by 65% at a constant current tube setting. 3-D VR reconstruction of images is time consuming. Reconstructions took approximately 30 min per patient, but there was a definite learning curve seen in our study.

Conclusion

This study demonstrates that 3-D VR is valuable in investigating children suspected of having airway compression due to TB lymphadenopathy (sensitivity 92% and specificity 85%). MDCT has the additional advantages of allowing the length and the cause of the airway compression to be determined, and is also able to evaluate the airways distal to an area of severe stenosis. In children with airway compression due to TB lymphadenopathy the correlation between 3-D VR and FTB is moderate (kappa 0.51). In airways diagnosed with compression due to TB lymphadenopathy, a combination of MDCT with 3-D VR and FTB gives the most complete assessment. Future prospective studies are required to determine more accurately the degree of airway compression as determined by FTB and to correlate these findings with the degree of airway compression as determined by 3-D VR in children with compression of the airways due to TB lymphadenopathy.

References

1. Honnef D, Wildberger JE, Das M et al (2006) Value of virtual tracheobronchoscopy and bronchography from 16-slice multidetector-row spiral computed tomography for assessment of suspected tracheobronchial stenosis in children. Eur Radiol 16:1684–1691
2. Lambert V, Sigal-Cinqualbre A, Belli E et al (2005) Preoperative and postoperative evaluation of airways compression in paediatric patients with 3-dimensional multislice computed tomographic scanning: effect on surgical management. J Thorac Cardiovasc Surg 129:1111–1118
3. Andronikou S, Wieselthaler N (2004) Modern imaging of tuberculosis in children: thoracic, central nervous system and abdominal tuberculosis. Pediatr Radiol 34:861–875
4. Remy-Jardin M, Remy J, Artaud D et al (1998) Volume rendering of the tracheobronchial tree: clinical evaluation of bronchographic images. Radiology 208:761–770
5. McMaster P, Isaacs D (2000) Critical review of evidence for short course therapy for tuberculous adenitis in children. Pediatr Infect Dis J 19:401–404
6. Leung AN, Muller NL, Pineda PR et al (1992) Primary tuberculosis in childhood: radiographic manifestations. Radiology 182:87–91
7. Brown HM, Abbitt PL, Wilkinson EJ (2001) Diagnosis of clinically unsuspected extrapulmonary tuberculosis by fine needle aspiration: a case report. Acta Cytol 45:1032–1036
8. Marais BJ, Gie RP, Schaaf HS et al (2004) A proposed radiological classification of childhood intra-thoracic tuberculosis. Pediatr Radiol 34:886–894
9. Goussard P, Gie R (2007) Airway involvement in pulmonary tuberculosis. Paediatr Respir Rev 8:118–123
10. Bosch-Marcet J, Serres-Creixams X, Zuasnabar-Cotro A et al (2004) Comparison of ultrasound with plain radiography and CT for the detection of mediastinal lymphadenopathy in children with tuberculosis. Pediatr Radiol 34:895–900
11. Colin AA, Ali-Dinar T (2007) Endobronchial biopsy in childhood. Chest 131:1626–1627
12. Koletsis EN, Kalogeropoulou C, Prodromaki E et al (2007) Tumoral and non-tumoral trachea stenoses: evaluation with three-dimensional CT and virtual bronchoscopy. J Cardiothorac Surg 2:18
13. Labbé A, Meyer F, Albertini M (2004) Bronchoscopy in intensive care units. Paediatr Respir Rev 5 (Suppl A):S15–S19
14. Papaioannou G, Young C, Owens CM (2007) Multidetector row CT for imaging the paediatric tracheobronchial tree. Pediatr Radiol 37:515–529
15. Siegel MJ (2003) Multiplanar and three-dimensional multidetector row CT of thoracic vessels and airways in the paediatric population. Radiology 229:641–650
16. Lee EY, Siegel MJ, Hildebolt CF et al (2004) MDCT evaluation of thoracic aortic anomalies in paediatric patients and young adults: comparison of axial, multiplanar, and 3D Images. AJR 182:777–784
17. Lawler LP, Corl FM, Haponik EF et al (2002) Multidetector row computed tomography and 3-dimensional volume rendering for adult airway imaging. Curr Probl Diagn Radiol 31:115–133
18. Lawler LP, Fishman EK (2001) Multi-detector row CT of thoracic disease with emphasis on 3D volume rendering and CT angiography. Radiographics 21:1257–1273
19. Schertler T, Wildermuth S, Willmann JK et al (2004) Effects of ECG gating and post-processing techniques on 3D MDCT of the bronchial tree. AJR 183:83–89
20. Remy-Jardin M, Remy J, Artaud D et al (1998) Tracheobronchial tree: assessment with volume rendering – technical aspects. Radiology 208:393–398
21. Choo KS, Lee HD, Ban JE et al (2006) Evaluation of obstructive airway lesions in complex congenital heart disease using composite volume-rendered images from multislice CT. Pediatr Radiol 36:219–223

22. Salvolini L, Bichi Secchi E, Costarelli L, et al (2000) Clinical applications of 2D and 3D CT imaging of the airways – a review. Eur J Radiol 34:9–25
23. Peloschek P, Sailer J, Weber M et al (2007) Pulmonary nodules: sensitivity of maximum intensity projection versus that of volume rendering of 3D multidetector CT data. Radiology 243:561–569
24. Duan S, Zhang D, Lin Q, et al (2006) Clinical value of CT three-dimensional imaging in diagnosing gastrointestinal tract diseases. World J Gastroenterol 12:2945–2948
25. Wang S, Seo C, Chon K et al (2005) Clinical usefulness of 3-dimensional computed tomography laryngography in laryngeal and hypopharyngeal cancer. Am J Otolaryngol 26:314–323

CHAPTER 5

Developing computer models to assist in detection of abnormal airways in CT scan images related to paediatric tuberculosis

Introduction

Development of a computer based model to predict airway compression resulting from TB lymph nodes.

Airway deformation and stenosis can be important indicators of chest pathology such as lymph node enlargement. In paediatric pulmonary TB where a key sign is lymph node enlargement many cases show signs of airway compression or deformation due to the enlarged lymph nodes.

Bronchoscopy is currently seen as the gold standard for identifying signs of airway involvement with the limitation that the external cause of the airway compression cannot be determined by bronchoscopy. Studies have suggested that volume rendering of CT can be used as an alternative to bronchoscopy (du Plessis et al, 2009) solving a number of these issues.

We have proposed an automated framework that detects and delineates the airways from CT volumes, detects the airway branching structure and performs individual branch measurements. (Irving et al, 2014). Bronchi correspondence is found for a dataset of paediatric training cases containing tuberculosis and non-tuberculosis cases. These cases are used to train statistical classification algorithms to automatically detect airway deformation. We call this method the local airway point distribution model (LA-PDM) and is used to automatically assess normal and pathological variation in local regions of the airway. These point distribution models are effective for capturing variation that can be more complex than just airway narrowing. A classifier is trained using both the types of airway variation and the clinical diagnosis of each airway to detect pathology in unseen cases

This classifier is used to automatically distinguish between paediatric chest CT scans that are normal or have airway involvement related to tuberculosis. In addition, the type of abnormal changes to the airway is shown to the user.

This LA-PDM method was developed using 89 training cases and evaluated on a 90 CT test set from Tygerberg hospital, where each set includes paediatric tuberculosis (TB) cases (with airway involvement) and non-TB cases (without airway involvement). The LA-PDM was able to accurately distinguish cases with airway involvement with an AUC of the

ROC classification (and 95% confidence interval) of 0.87 (0.77–0.94) for the Trachea–LMB–RMB region and 0.81 (0.68–0.90) for the RMB–RUL–BI region.

Conclusions

By developing and training computer based models to determine the patterns of airway compression we were able to show that this model could accurately predict the airway compression resulting from enlarged TB lymph nodes. This model needs to be tested in children who have airway narrowing or compression from other causes of pathology. Extensions of this method have been also proposed for 2D X-ray analysis (Irving et al, 2013).

Related publications

1. Irving B, Goussard P, Gie R, Todd-Pokropek A, Taylor P. Identification of paediatric tuberculosis from airway shape features. Medical Image Computing and Computer-Assisted Intervention–MICCAI 2011. Springer Berlin Heidelberg, 2011. 133-140.

2. Irving B, Goussard P, Andronikou S, Gie R, Douglas TS, Todd-Pokropek A, Taylor P. Computer assisted detection of abnormal airway variation in CT scans related to paediatric tuberculosis. Medical Image Analysis 2014; 18: 963-976.

3. Andronikou S, Irving B, Tebogo Hlabangana L, Pillay T, Taylor P, Goussard P, Gie R. Technical developments in postprocessing of paediatric airway imaging. Pediatric Radiology 2013; 43: 269-284.

4. Irving B, Douglas T, Taylor P. 2D X-ray airway tree segmentation by 3D deformable model projection and registration. MICCAI - Workshop on abdominal imaging (2013)

Identification of Paediatric Tuberculosis from Airway Shape Features

Benjamin Irving[1], Pierre Goussard[2], Robert Gie[2], Andrew Todd-Pokropek[1], and Paul Taylor[1]

[1] University College London, London WC1E 6BT, UK
b.irving@ucl.ac.uk
[2] Tygerberg Hospital, Stellenbosch University, Western Cape 7530, South Africa

Abstract. Clinical signs of paediatric pulmonary tuberculosis (TB) include stenosis and deformation of the airways. This paper presents two methods to analyse airway shape and detect airway pathology from CT images. Features were extracted using (1) the principal components of the airway surface mesh and (2) branch radius and orientation features. These methods were applied to a dataset of 61 TB and non-TB paediatric patients. Nested cross-validation of the support vector classifier found the sensitivity of detecting TB to be 86% and a specificity of 91% for the first 10 PCA modes while radius based features had a sensitivity of 86% and a specificity of 94%. These methods show the potential of computer assisted detection of TB and other airway pathology from airway shape deformation.

1 Introduction

The prevalence of tuberculosis (TB) remains high in many developing countries while the accuracy of paediatric TB detection is low, and a combination of tests including imaging is used. Automated airway analysis has the potential to improve the detection of airway pathology such as TB. A common sign of primary TB in children is airway deformation caused by lymphadenopathy [1]. This can take the form of displacement and stenosis of airway branches, and widening of the carinal angle [1]. Hila, mediastinal, subcarinal and paratracheal lymph nodes are commonly affected and the most common sites for compression are: the trachea, left main bronchus (LMB), right main bronchus (RMB) and bronchus intermedius (BI) [1]. This sign is more sensitive in children because the airways are more malleable and primary TB tends to affect the lymph nodes. Lymphadenopathy can also indicate other pathology but is useful for detecting TB when used in conjunction with other tests and is likely to indicate TB in areas with a high TB prevalence.

Paediatric airways are considerably smaller than those of adult patients, which means a lower resolution using the same voxel size, and fewer branches can be identified. Movement artefacts are also more likely because it is not possible to perform a breath hold scan on infants [10].

G. Fichtinger, A. Martel, and T. Peters (Eds.): MICCAI 2011, Part III, LNCS 6893, pp. 133–140, 2011.

Point distribution models (PDM) are a common method of modelling shape variation. Anatomical landmarks or a mesh are used to represent a shape and the variation in position of corresponding points is calculated. Principal component analysis (PCA) can be applied to the PDM to reduce the dimensionality of the representation, identifying the principal modes of variation. These techniques have been applied successfully in a number of cases including facial morphology [5]. However, very little research has focussed on airway shape modelling. A previous study developing a shape model of the airways focussed on patient specific models and required manual interaction [4].

An alternative and more intuitive approach is to use features that correspond directly to clinical observations but this requires more background knowledge. In this paper we present a complete system for analysing pathological airway shape variation and compare two approaches for identifying TB cases: one using features generated using the principal modes of variation of a surface mesh, and another using features based on the branch radius and orientation. We test both on a dataset of TB and non-TB cases. Contributions of this work include a method to generate a shape model of normal and pathological airway variation (the authors are not aware of any previous method to model airway pathology and particularly to distinguish between TB and non-TB datasets) and methods focussed on paediatric datasets. Additional contributions include a novel method for automatically generating airway landmarks based on the airway topology and centreline, extension of mesh-warping to suit stenosed airway shape variation and the training of a classifier on airway shape data.

2 Method

An automated airway segmentation approach was used and the centreline and bifurcation points extracted. Corresponding landmark points were generated and a template mesh was warped to each airway. A shape model was then developed using the principal modes of the corresponding vertices. Cross-section diameter measurements were made for each branch and used to generate the second feature set.

2.1 Dataset and Airway Extraction

The dataset used in this study consists of TB and non-TB cases. 29 chest CT scans of paediatric patients diagnosed with definite or probable TB from a positive culture, or bronchoscopy and CT findings were acquired from Tygerberg Hospital in South Africa (mean age 22 ± 26 months) and 32 chest CT scans of paediatric patients with a non-TB diagnosis were acquired from Gt Ormond St Hospital, London (mean age 38 ± 22 months). Voxel size in the axial plane ranged from 0.3 - 0.5 mm and slice thickness 0.7 - 1 mm. 13 cases with completely obstructed branches were previously manually excluded from the dataset because these cases can be easily identified and are not of interest for building a shape model. The age difference between the groups is within one standard deviation and age does not influence airway proportions in children [8].

The airways were segmented using an existing method [6] . This method uses morphological closing and reconstruction to enhance possible airway locations in the axial, coronal and sagittal directions. A region growing method, seeded at the trachea, is then used to extract the airway region. The structure of the airways is found using centreline extraction, branch point detection and branch labelling. Palágyi et al. [9]'s skeletonisation method is used for the extraction of the centreline because of its previous application to the airways. This is an iterative thinning approach, where each surface voxel is analysed in terms of orientation and connectivity and simple points are iteratively removed.

False branching can occur because of surface deformation (particularly when pathology is present) and, therefore, branch pruning is required. We found that false branches connected to the trachea, LMB and RMB can be longer than true branches further down the tree, and false branches may bifurcate. Therefore, a multilevel pruning system was developed that removed branches less than a specified length (l) and removed larger false branches associated with the primary branches and smaller false branches associated with later generations. Three pruned trees ($T_{l_1}, T_{l_2}, T_{l_3}$) were created with pruning $l_1 > l_2 > l_3$. A final tree was constructed from T_{l_1} for the trachea, T_{l_2} for the LMB and RMB and from T_{l_3} for the remaining branches. A one voxel thick centre line was used to identify the branching structure, shown in Figure 1: a branch point was defined as a point with three neighbours in the 3x3x3 surrounding region.

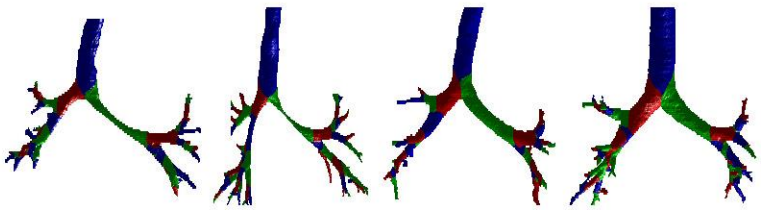

Fig. 1. Paediatric airway segmentation and branch-point identification. The two cases on the left show signs of TB while the others are non-TB cases.

2.2 Corresponding Surface Point Generation and Mesh Alignment

Surface point correspondence is required to derive features from a shape model while diameter based features require only regular sampling of the branch. Branch points are the only major anatomical landmarks and, therefore, corresponding points were generated by calculating the intersection between the surface and vectors orthogonal to the smoothed centreline at equidistant positions along each branch (Figure 2). The generated points take into account branch topology, medial line curvature and surface deformation. The analysis was performed on the trachea, RMB and LMB (commonly deformed by lymphadenopathy).

As discussed earlier, two sets of features are being considered, the principal modes of the surface deformation and branch radius/direction based features.

Fig. 2. Surface point placement using the centreline and bifurcation points

The surface points were used to calculate the two orthogonal diameters at each cross section along each branch. These points were generated from 60 equidistant points on the medial line of the trachea, 50 along the LMB and 30 along the RMB. A subset of the corresponding points (generated from 5 equidistant points on the Trachea and LMB, and 2 on the RMB) were used to warp a mesh onto each airway using Thin Plate Spline (TPS) warp. TPS warping is a common method of aligning objects using a set of landmark points [5]. TPS attempts to perform realistic deformation by minimising the bending energy [2]. The TPS function that minimises the energy is:

$$f_j(P_j) = \sum_{i=1}^{k} w_{ij} U(P_j - P_{ij}) + a_0 + a_x x + a_y y + a_z z \tag{1}$$

where f is the new position of the point and f_j is a component of f, $j \in (x, y, z)$, P are the landmark points on the shape and w_{ij} are the weighting factors. w_{ij} can be found from the corresponding landmark points.

Further matching is required so that the template mesh is aligned with each target mesh (as shown in Figure 3). The simplest method is to project the template mesh to the closest point on the target mesh [5] but this can lead to unrealistic deformation while not covering small deformations. Figure 4 shows this mesh misalignment because of narrow sections caused by stenosis and the proposed solution.

Kaus et al [7] optimise the fit based on the distance between the meshes while an additional force preserves the mesh structure. We add a third term based on surface orientation. For each vertex on the template mesh (t_i), a force ($F_{i,tot}$) is calculated to direct the warp. The closest point (r_i) on the object mesh component is included to align the meshes (Eqn 2) and an internal forcing component is included to preserve the size of the faces (change in the distance of each of the p neighbouring vertices to a vertex t_i from the initial distance v_{0j}) (Eqn 3). An expansion/contraction force is also added, based on the normal of each vertex $\hat{n}_i$ (calculated from the normal of the surrounding faces) controlled by the distance and direction of the target mesh to $F_{i,1}$ (Eqn 4). This improves performance for small surface indentations/protrusions associated with stenosis.

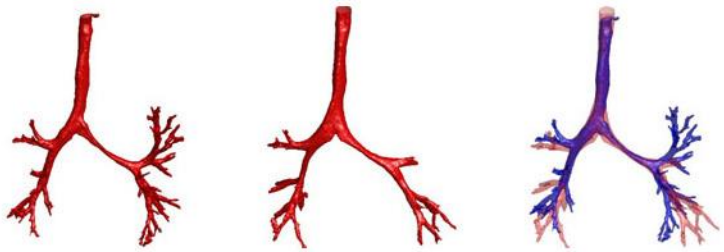

(a) Template image (b) Case to be matched (c) TPS warp

Fig. 3. TPS warp using landmarks on the trachea, LMB and RMB

(a) Matching to the closest point (b) Meshing procedure using F_1, F_2 and F_3

Fig. 4. Mesh matching

$$F_{i,1} = \boldsymbol{r}_i - \boldsymbol{t}_i \qquad \textit{nearest point ext. force} \quad (2)$$

$$F_{i,2} = \sum_j^p \hat{v_j}(||\boldsymbol{v}_j|| - ||\boldsymbol{v_0}_j||) \text{ where } \boldsymbol{v}_j = \boldsymbol{t}_j - \boldsymbol{t}_i \qquad \textit{internal force} \quad (3)$$

$$F_{i,3} = \hat{n}_i(\hat{n}_i \cdot F_{i,1}) \qquad \textit{normal ext. force} \quad (4)$$

$$F_{i,tot} = \alpha F_{i,1} + \beta F_{i,2} + \gamma F_{i,3} \quad (5)$$

In Equation 5, the forces are weighted with α, β and γ. This procedure is applied iteratively until stability is reached.

2.3 Feature Extraction and Classification

Each shape is represented as a $3n$ dimensional vector where n is the number of vertices in the mesh; $n \approx 1500$ was used in this study. Each shape was aligned using Generalised Procrustes analysis and PCA was applied to reduce the dimensionality and obtain a set of features for classification. PCA applies a linear transform that projects the PDM onto an uncorrelated space and can be used to extract relevant features [3]. PCA modes are ordered by the variance and, therefore, can be used to reduce the dimensionality of the feature vector. For PCA, it can be shown that the eigenvectors of the covariance matrix

$\sum = XX^T$ (where each column of X is a $3n$ vector for each airway) can be used to project the dataset into the uncorrelated space (b) represented by the eigenvectors $\boldsymbol{b} = \Phi^T(\boldsymbol{x} - \bar{\boldsymbol{x}})$ where the projection matrix (Φ^T) is the transpose of the eigenvector matrix (Φ). Therefore, a measurement vector $\boldsymbol{x} = \bar{\boldsymbol{x}} + \Phi\boldsymbol{b}$ can be represented in terms of the mean and displacement along each mode [3].

Three radius based features were calculated for each branch: the maximum ratio of the orthogonal diameters for each branch $\left(\max\left(\frac{d1}{d2}\right)\right)$, the ratio between the branch length and average branch diameter $\left(\frac{d_{ave}}{l}\right)$ and the maximum ratio of local minima and neighbouring local maxima of the diameter as a function of position on the branch $\left(\frac{lmax_1+lmax_2}{2lmin}\right)$. These features, based on advice from our clinical partners, were used as indicators of branch circularity, thickness and local stenosis, and were calculated for the trachea, RMB and LMB. The carinal angle was also calculated for each airway by fitting a line to the first third of the RMB and LMB and calculating the angle from bifurcation. All features were normalised.

Once a set of features was found to represent each airway in the dataset, a classifier was trained to distinguish between TB and non-TB cases. A Support Vector Machine (SVM) was chosen as the classifier because of its suitability for small datasets and the PRtools implementation of SVM was used. Leave-one-out cross validation (LOOCV) and nested CV were used to evaluate the classifier.

3 Results

Parameters for the mesh warp α, β and γ were determined by comparing the volume generated from both the template mesh and the original mesh ($V_{dif} = (V_{temp} \setminus V_{case}) \cup (V_{case} \setminus V_{temp})$. In order to focus on local errors instead of differences due to mesh face sizes, a morphological closing was applied ($V_{open} = V_{dif} \circ K$ where K is 6-connected kernel) in order to remove 1-voxel thick errors but retain larger local errors. Optimum parameters are around $\alpha = 0.2$ and $\gamma = 1$, where proportion of *general error* (without closing) is less than 0.022 and *local error* (with closing) is less than 0.002. Without the expansion force ($\gamma = 0$) then the minimum errors are 0.05 and 0.02 respectively. Fixed parameters were used for the whole dataset but could be chosen for each individual airway.

The SVM classifier was trained and tested on the two sets of features. Classification using PCA features were performed using the first 10 modes which represented 90% of the shape variation. Figure 5 shows the mean and variation from $-3\sqrt{\lambda_i}$ to $3\sqrt{\lambda_i}$ along the first 4 modes. Classification was also performed on the 10 radius and orientation based features. This classifier was optimised by adjusting the "trade-off parameter" C (between 5 and 500) and the degree of the polynomial kernel (between 1 and 13) while running LOOCV for each choice. These values were chosen to cover a reasonable range of parameters but further optimisation could be performed. LOOCV was used because the dataset was too small to divide into a testing and training set. However, adjusting the SVM parameters with LOOCV allows the best classifier to be selected but can lead to a biased measure of accuracy. Therefore, to determine an unbiased sensitivity

Table 1. Sensitivity and specificity using (1) the PCA and (2) the radius and orientation based feature set with LOOCV and Nested CV

	LOOCV		Nested CV	
	PCA	Rad	PCA	Rad
Sensitivity	93%	93%	86%	86%
Specificity	94%	94%	91%	94%

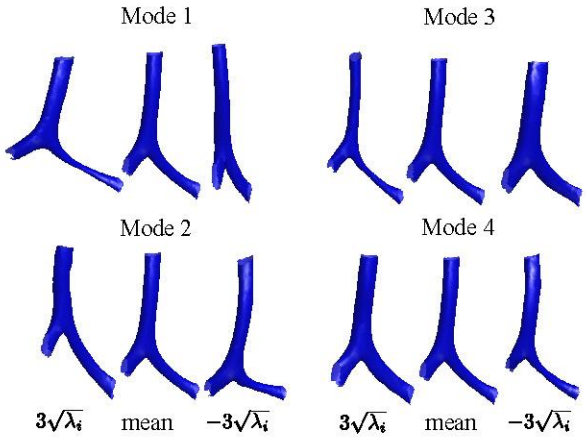

Fig. 5. Variation along the first four PCA modes

and specificity without an independent training set, nested CV was used [11]. Nested CV includes a second LOOCV loop with parameter optimisation inside the full LOOCV loop and results have been shown to be close to that of an independent testing set [11]. Using LOOCV, the classifiers performed the same and parameters of C=100 and 3 and polynomial degree of 3 and 1 were found for the PCA and radius based classifiers, respectively (Table 1). The radius based features performed slightly better when tested using nested CV (6 compared to 7 misclassified out of 61). The software was written in Matlab and C++ and tested on a 2.0 GHz quad-core processor. Generation of features from a segmented dataset and cross validation: ≈700s for the PCA based feature vector and ≈1200s for the radius based feature vector.

4 Discussion

In this paper we discuss two methods to quantify and detect airway shape deformation due to TB. Both these methods were able accurately to distinguish between paediatric cases with TB and without TB, and demonstrate the potential of these techniques to assist in the detection of airway pathology. PCA based features may be more generalizable and, more effective for differentiating other types of pathology without adjusting the feature choice.

The datasets were collected from two hospitals and it is possible that population differences also have an effect on the classification. However, the features extracted using PCA correspond to clinical signs of TB. Examining Figure 5, the modes correspond to stenosis and widening of the carinal angle, which is consistent with clinical signs of TB [1]. The other feature set was based on characteristics of airway pathology.

This paper shows the potential of automated airway analysis to assist in the identification of pathology with possible CAD applications. The model could be developed further by training on localised pathology, or applied to other areas such as airway deformation and narrowing caused by congenital cardiac disease.

References

1. Andronikou, S., Wieselthaler, N.: Modern imaging of tuberculosis in children: thoracic, central nervous system and abdominal tuberculosis. Pediatr. Radiol. 34, 861–875 (2004)
2. Bookstein, F.: Principal warps: Thin-plate splines and the decomposition of deformations. IEEE Trans. Pattern Anal. Mach. Intell. 11, 567–585 (1989)
3. Cootes, T., Taylor, C., Cooper, D., Graham, J., et al.: Active shape models-their training and application. Comput. Vis. Image. Und. 61, 38–59 (1995)
4. Deligianni, F., Chung, A., Yang, G.: Nonrigid 2-D/3-D registration for patient specific bronchoscopy simulation with statistical shape modeling: Phantom validation. IEEE Trans. Med. Imag. 25, 1462–1471 (2006)
5. Hutton, T., Buxton, B., Hammond, P., Potts, H.: Estimating average growth trajectories in shape-space using kernel smoothing. IEEE Trans. Med. Imag. 22, 747–753 (2003)
6. Irving, B., Taylor, P., Todd-Pokropek, A.: 3D segmentation of the airway tree using a morphology based method. In: Second International Workshop on Pulmonary Image Analysis, MICCAI (2009)
7. Kaus, M., Pekar, V., Lorenz, C., Truyen, R., Lobregt, S., Weese, J.: Automated 3-D PDM construction from segmented images using deformable models. IEEE Trans. Med. Imag. 22, 1005–1013 (2003)
8. Masters, I., Ware, R., Zimmerman, P., Lovell, B., Wootton, R., Francis, P., Chang, A.: Airway sizes and proportions in children quantified by a video-bronchoscopic technique. BMC Pulmonary Medicine 6, 5–13 (2006)
9. Palágyi, K., Tschirren, J., Hoffman, E., Sonka, M.: Quantitative analysis of pulmonary airway tree structures. Comput. Biol. Med. 36, 974–996 (2006)
10. du Plessis, J., Goussard, P., Andronikou, S., Gie, R., George, R.: Comparing three-dimensional volume-rendered CT images with fibreoptic tracheobronchoscopy in the evaluation of airway compression caused by tuberculous lymphadenopathy in children. Pediatr. Radiol. 39, 694–702 (2009)
11. Varma, S., Simon, R.: Bias in error estimation when using cross-validation for model selection. BMC Bioinformatics 7, 1–8 (2006)

Medical Image Analysis 18 (2014) 963–976

Contents lists available at ScienceDirect

Medical Image Analysis

journal homepage: www.elsevier.com/locate/media

Computer assisted detection of abnormal airway variation in CT scans related to paediatric tuberculosis

Benjamin J. Irving [a,*], Pierre Goussard [b], Savvas Andronikou [c], Robert Gie [b], Tania S. Douglas [d], Andrew Todd-Pokropek [e], Paul Taylor [a]

[a] Centre for Health Informatics and Multiprofessional Education, UCL, London, UK
[b] Desmond Tutu TB Center, Department of Paediatrics and Child Health, Stellenbosch University, Tygerberg, South Africa
[c] Department of Radiology, Faculty of Health Sciences, University of the Witwatersrand, South Africa
[d] MRC/UCT Medical Imaging Research Unit and the Biomedical Engineering Programme, University of Cape Town, South Africa
[e] Medical Physics, UCL, London, UK

ARTICLE INFO

Article history:
Received 28 October 2013
Received in revised form 13 April 2014
Accepted 23 May 2014
Available online 9 June 2014

Keywords:
Point distribution model
Airway
CT
Computer assisted detection
Classification

ABSTRACT

Airway deformation and stenosis can be key signs of pathology such as lymphadenopathy. This study presents a local airway point distribution model (LA-PDM) to automatically analyse regions of the airway tree in CT scans and identify abnormal airway deformation. In our method, the airway tree is segmented and the centreline identified from each chest CT scan. Thin-plate splines, along with a local mesh alignment method for tubular meshes, are used to register the airways and develop point distribution models (PDM). Each PDM is then used to analyse and classify local regions of the airway. This LA-PDM method was developed using 89 training cases and evaluated on a 90 CT test set, where each set includes paediatric tuberculosis (TB) cases (with airway involvement) and non-TB cases (without airway involvement). The LA-PDM was able to accurately distinguish cases with airway involvement with an AUC of the ROC classification (and 95% confidence interval) of 0.87 (0.77–0.94) for the Trachea–LMB–RMB region and 0.81 (0.68–0.90) for the RMB–RUL–BI region – outperforming a comparison method based on airway cross-sectional features. This has the potential to assist and improve airway analysis from CT scans by detecting involved airways and visualising affected airway regions.

1. Introduction

Tuberculosis is still prevalent – particularly in developing countries. The WHO estimates the annual number of new cases of TB to be 343/100,000 in Africa, higher than any other region (WHO, 2012). Childhood tuberculosis represents a large proportion of TB cases and is particularly difficult to diagnose; the disease is confirmed in less than 40% of cases (Schaaf et al., 1995). While most TB in adults is confirmed from sputum samples, childhood TB has a low sputum bacilli count, and, therefore, the diagnosis is based on a number of factors, with imaging playing a major role. Other indicators include: contact with an infected adult (often difficult to determine); symptoms and signs (vague and common); and tuberculin skin test (positive test only indicates exposure and false negatives can be attributed to HIV or other immune disorders). Each of these tests is imperfect but a combination is used to diagnose TB (Gie, 2003). Recent studies have highlighted increasing clinical interest and the need for further research into the diagnosis and treatment of paediatric TB (Sandgren et al., 2012).

Lymph node involvement is a key indicator of childhood TB, and as the lymph nodes enlarge the airways are compressed or deformed. This is because paediatric patients have smaller airways with less well developed cartilage – predisposing them to compression. This is known as lymphobronchial TB and is a current clinical focus in childhood TB research (Lucas et al., 2012; Goussard et al., 2013). Airway involvement due to lymphadenopathy is relatively common in children (between 29% (Andronikou et al., 2004) and 38% (Theart et al., 2005) of cases). This deformation can occur due to one enlarged lymph node, or compression can be due to an enlarged lymph node on both sides or a lymph node and a vessel, which can be used as an indicator of TB (Goussard and Gie, 2007; Andronikou et al., 2004). Fig. 1 shows a MinIP projection with airway stenosis caused by lymphadenopathy in a paediatric pulmonary TB patient. The most affected airways include the bronchus intermedius (BI), left main bronchus (LMB), trachea and right main bronchus (RUL) (Lucas et al., 2012; Goussard et al., 2013).

* Corresponding author. Tel.: +44 7723531777.
E-mail address: benjamin.irving@eng.ox.ac.uk (B.J. Irving).

http://dx.doi.org/10.1016/j.media.2014.05.007
1361-8415/

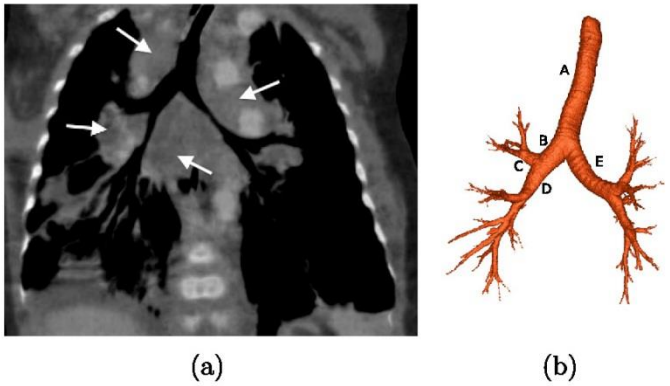

Fig. 1. (a) Coronal minimum intensity projection (MinIP) image with arrows indicating lymphadenopathy. Stenosis of the left main bronchus (LMB) and bronchus intermedius (BI) is visible. Arrows indicate locations of lymphadenopathy. (b) A diagram of the airway showing: (A) Trachea, (B) right main bronchus (RMB), (C) right upper lobe bronchus (RUL), (D) bronchus intermedius (BI) and (E) left main bronchus (LMB).

Determining airway involvement and cause is important for the treatment of paediatric TB and other diseases affecting the airways (Andronikou et al., 2013). Bronchoscopy is the "gold standard" for determining airway involvement but is invasive, general anaesthesia is often required and the external cause of the airway involvement cannot be seen. Recent studies suggest that CT with volume rendering can be used as an alternative to bronchoscopy (du Plessis et al., 2009) – offering the benefits of bronchoscopy while also allowing visualisation of the external cause of the airway involvement. This method allows manual measurements of airway cross-sections from the 3D rendering of the region, but requires considerable manual interaction in the form of setting thresholds, viewing parameters, and manual assessment of the airways, and a more automated approach to monitor airway involvement would be beneficial.

Thus, there is considerable value in automatically detecting airway involvement from lymphadenopathy to assist in the detection and assessment of paediatric patients with tuberculosis (and potentially other diseases). In this study we developed a method we call the local airway point distribution model (LA-PDM) to assess normal and pathological variation in local regions of the airway. Point distribution models are effective for capturing variation that is more complex than airway narrowing – where more complex variation is related to airway involvement from lymphadenopathy.

Section 2 discusses current methods used for airway analysis and Section 3 outlines our proposed LA-PDM method. This method performs a 3D airway segmentation using chest CT images, and then a branch labelling of the segmented airway (Section 3.1). Surface point correspondence is developed between the dataset of segmentations (Section 3.3 and 3.4) and used to create point distribution models for local regions of the airway (Section 3.6). The LA-PDM can then be used to distinguish normal and abnormal variation in local airway regions of a new CT image. Section 4 applies the LA-PDM to a 90 patient test dataset of paediatric chest CT scans. The results of the LA-PDM on the test set is shown in Section 5 and compared to simpler branch diameter based features, and show promising results for detection of airway pathology related to paediatric TB.

2. Airway shape analysis

A number of studies have developed methods that automate branch diameter measurements as well as the broncho-aterial ratio from segmented adult airways (Kiraly et al., 2008; Tschirren et al., 2005; Palágyi et al., 2006). Applications include detection of chronic obstructive pulmonary disease (COPD) and asthma identification (Petersen et al., 2010; Fetita et al., 2010; Wiemker et al., 2004). These methods are useful but rely on the identification of pathology from variation in local airway diameter.

External changes such as lymphadenopathy produce more global changes in airway shape that are difficult to identify from an analysis of local features. Point distribution models (PDM) allow more complex airway shape variation to be modelled. Deligianni et al., 2006 use a PDM of an airway phantom to model breathing but do not consider inter-patient variability or detection of pathology. Pinho et al., 2011 used a PDM to build individualised models of the healthy trachea for patients with stenosis. The difference between the models can be used to assist with stent implants. Given the global variability of the airway shape and the complexity of a branching airway tree, this method is not suitable for the analysis of airway bronchi (Pinho et al., 2011).

Initial steps in the development of our LA-PDM method were introduced in Irving et al. (2011) which provided a proof of concept by using the trachea and main bronchi to distinguish cases with TB (acquired from South Africa) from cases without TB (acquired from the UK). This paper presents a more detailed account of a refined method, extended to analyse multiple regions of the airway tree with improved region selection and correspondence detection. A full evaluation of the method is also presented, on a previously unseen dataset of cases with and without airway abnormalities that have been acquired from the same hospital. We analyse the shape model characteristics and compare the performance to features derived from airway cross sections. The authors are not aware of any previous methods that have detected abnormal airway variation from lymphadenopathy or paediatric TB.

3. Local airway point distribution models for abnormality detection

Fig. 2 shows our proposed method that uses a PDM of local regions of the airway to detect airway abnormalities. Airways are segmented and the branches are labelled. Surface mesh correspondence is developed using a reference airway, and PDMs with trained classifiers are used to detect airway abnormalities.

3.1. Segmentation and branch labelling

Initially the airway tree is segmented from each chest CT scan and each branch is labelled. There are a number of well established

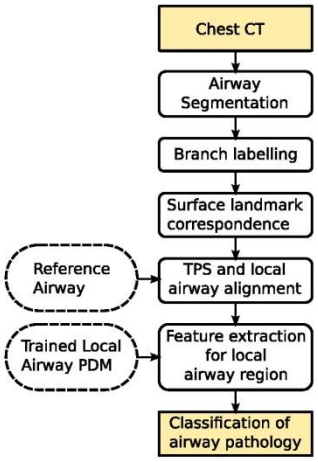

Fig. 2. The steps for airway shape analysis using local airway point distribution models. The airway is segmented from a chest CT and the airway structure is extracted. Surface landmarks are generated and a representative airway from the training set is warped onto the airway to create vertex–vertex correspondence. Features are generated using the airway PDM and are used to classify airway pathology.

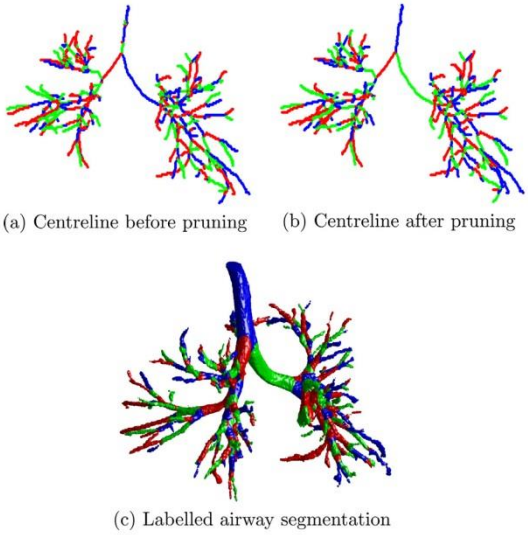

Fig. 3. Centreline identification of the a segmented airway tree using a chest CT of a 20 month patient. Red, green and blue are used to illustrate distinct airway branches. (For interpretation of the references to colour in this figure legend, the reader is referred to the web version of this article.)

methods for airway segmentation and labelling, and we implement existing algorithms (Lo et al., 2012; Palágyi et al., 2006). The first axial slice containing lung volume was used as a reference position from which the segmentation was initialised. The glottis could be a more reliable landmark on the trachea but was not present in the majority of chest CT volumes used in this study because of its position in the upper airway (Shi et al., 2006). In this study we use an existing morphology-based airway segmentation method (Irving et al., 2009; Lo et al., 2012). In this method, the trachea is detected in the initial slice using location, size and circularity. Morphological closing and reconstruction is used to enhance airway cross sections in 3 dimensions in the volume. A threshold is then applied to the filtered airways and a region growing method initialised from the trachea is used to segment the airway.

The Palágyi et al. (2006) iterative thinning approach is used to extract the centreline, identify branch points and label branches from the segmented airway. This method iteratively removes voxels from the segmentation that do not affect the topology to extract a 1-voxel thick branching centreline. A pruning method based on branch length and location is then used to remove false branches. Finally, starting from the trachea, voxel connectivity of the branching centreline is used to iteratively identify branch points and label each branch. Branch points are found when a voxel of the centreline has more than two 26-neighbours. The segmentation was then labelled using a distance transform from the labelled centreline. Original voxel size was used during skeletonisation, and voxel dimensions were taken into account when the skeleton was converted to smooth branch centrelines in the following steps.

Fig. 3 shows the labelled airway centreline before and after pruning of false branches and the labelled airway segmentation. Fig. 4 shows the segmentation and centreline in relation to the original CT volume. In some cases, due to the size of the airway and scan quality, the third generation of bronchi were not fully segmented. This does not affect our shape analysis method because the Trachea, LMB, RMB and BI are used for analysis in this study. These branches have been reported to contain 218 of all 259 compressions in a 98 patient study (Lucas et al., 2012). Improved image resolution and reduction in artefacts would allow further

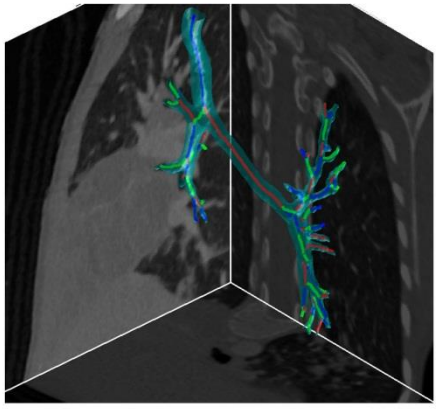

Fig. 4. Rendering of a paediatric airway segmentation and branch centrelines with intersecting slices of the original CT volume from the dataset. Red, green and blue are used to illustrate distinct airway branches. Each branch centreline is individually smoothed. (For interpretation of the references to colour in this figure legend, the reader is referred to the web version of this article.)

generations of bronchi to be accurately segmented. However, the segmentation does affect labelling and, therefore, 39 of the 179 cases required minimal user interaction (a single mouse click) to identify or remove a branch point from the centreline. The interaction is minimal, and fully automated branch labelling is not the focus for this study.

3.2. Surface point projection

A mesh of the airway surface was used to represent each airway and each face was labelled according to the branching structure of the airway. This triangular surface mesh was constructed from the

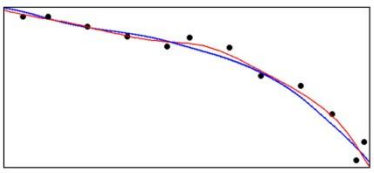

Fig. 5. A subsection of a smoothed centreline of a single branch with voxel coordinates (black) and two examples of smoothing: a 5 voxel moving average smoothed centreline (blue) and B-Spline interpolated centreline of degree 13 (red). (For interpretation of the references to colour in this figure legend, the reader is referred to the web version of this article.)

voxel segmentation, and then smoothed using an implicit fairing method (Desbrun et al., 1999). Implicit fairing uses curvature flow to remove noise and uneven edges while preserving the mesh geometry. The smoothing was used to remove noise due to the resolution of the CT scan. Voxel resolution has more of an impact in the segmentation of paediatric airways compared to those of adults because the smaller volume means that airways are represented by fewer voxels.

Corresponding landmarks are required to align the airways in the dataset in order to develop the PDM. However, the airways do not have clear landmarks between bifurcations, and instead pseudo-landmarks were projected onto the airway surface mesh using the topological structure of the airway and the tubular shape of the branches. This was performed using the following steps: the centreline was smoothed and resampled equidistantly and pseudo-landmark points were projected orthogonally to the centreline at these resampled centreline points.

The centreline of the airways is represented as a one-voxel thick branching medial line. Linear interpolation between each set of neighbouring voxels was used to achieve a more detailed representation of the centreline. A moving average smoothing filter was applied to the interpolated points to remove noise added to the centreline from the voxel resolution. B-Spline interpolation of the centreline voxels is an alternative but tends to show more sensitivity to voxel offset (as shown in Fig. 5). Nevertheless, either algorithm can be used for centreline smoothing. The branch is then resampled evenly m times to form landmark points (p_i) on the centreline.

At each resampled point (p_i), the tangent $T(p_i)$ to the centreline was estimated:

$$T(p_i) = \frac{p_i'(t)}{|p_i'(t)|} \tag{1}$$

$$p_i'(t) = \frac{p_i(t+h) - p_i(t-h)}{2h} \tag{2}$$

where each $p_i(t)$ can be represented as a function in the vicinity of the landmark and $p_i(t+h)$ is a small progression along the centreline. A set of orthogonal vectors $(\mathbf{r}_i)$ is then translated to each of the centreline points (p_i) and rotated to be orthogonal to the centreline (see Fig. 6). Euler angles (x-convention) were used to construct a rotation matrix that can be used to map each of these orthogonal vectors onto each branch centreline. The Euler angles are defined by three rotations (ϕ, θ, ψ). By setting $\phi = -\psi$ the orthogonal vectors are mapped to any orientation of the centreline while removing the ambiguity of rotation around the centreline.

The intersection of the vectors (r_{ij}) with the triangular surface mesh was found using Möller and Trumbore (2005) ray/triangle intersection method. This method determines if the vector falls inside each face when intersecting a plane (with the plane normal defined by the face). Each face must be checked individually. To improve the speed of the search, only faces that fall within a local sphere of intersection are analysed. The radius of the sphere is chosen to be larger than the branch radius, guaranteeing that the point of intersection falls in the sphere (see Fig. 8a). This representation allows a set of corresponding surface points to be mapped onto each branch of each segmented airway. Fig. 7 and 8 show the mapping of surface points onto the Trachea–LMB–RMB and RMB–RUL–BI regions, respectively, of example airway segmentations.

The benefit of this representation is that the surface landmarks are based on the most consistent features of the airway tree: the bifurcation points and centreline. Statistical analysis methods could be applied directly to these corresponding landmark points. This would simplify the method because registration of an airway surface mesh template is not required. However, by only representing an airway with landmark points projected from the centreline, concave regions will be represented by a larger number of landmarks and convex regions will be represented by fewer landmarks; this is not ideal. In addition, if a large number of landmarks are chosen there is also a risk that the orthogonal radii will overlap, due to the curvature of the centreline, causing folding in the surface representation. As an example, the first two projections of the Trachea in Fig. 7 show a region of larger curvature. Using a small number of landmarks to align a template mesh overcomes these challenges and a surface mesh provides a more detailed representation of the airway.

3.3. Mesh alignment step 1: thin-plate-spline warp

One airway from the control dataset was selected as a template and a thin-plate-spline (TPS) warp was applied to align the template with each airway in order to represent each airway in the dataset with a corresponding mesh. Fig. 9a shows a template warped by TPS to the RMB–RUL–BI region of the airway.

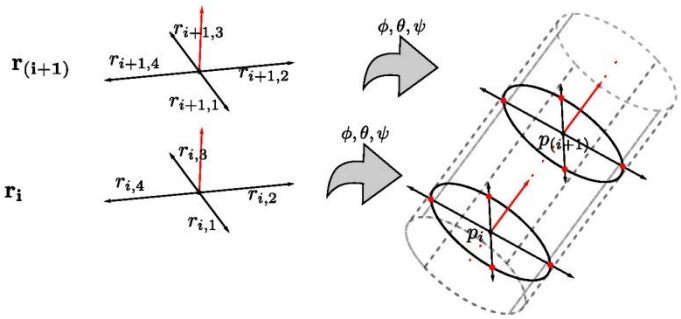

Fig. 6. Mapping landmark points to the airway surface. Each set of vectors is translated to p_i and Euler angles are used to align the central vector with the centreline tangent. The intersection between the vectors and the airway surface is then found by ray/triangle intersection.

TPS is a method of interpolation that minimises the bending energy of the surface (Bookstein, 1997; Bookstein, 1989). This method is also useful as a method of non-rigid registration; a surface with one set of landmarks is warped to a corresponding set of landmarks in a physically realistic way. The thin-plate spline function in 3D that transforms a point $\mathbf{p} = (x, y, z)$ is given by:

$$\mathbf{f}_j(\mathbf{p}) = \sum_{i=1}^{k} w_{ij} U(|\mathbf{p} - \mathbf{P}_i|) + a_0 + a_x x + a_y y + a_z z \quad (3)$$

where $\mathbf{f}(\mathbf{p}) = [f_x(\mathbf{p}), f_y(\mathbf{p}), f_z(\mathbf{p})]$ is the new position of the point $(\mathbf{p})$. $\mathbf{P}_i$ are the k landmark points on the shape, and w_{ij}, a_0, a_x, a_y and a_z are the weighting factors. $U(r) = |r|$ for the 3D case, where $r = \mathbf{p} - \mathbf{P}_i$. The weighting factors are found by writing Eq. (3) as a system of linear equations $H = LW$, where the landmark and transformed coordinates are input as p and $\mathbf{f}(\mathbf{p})$, respectively. The weights, $W = L^{-1}H$, can then be found (as explained in detail in Bookstein (1997)).

3.4. Mesh alignment step 2: local alignment

The TPS warp will only be exactly aligned at the landmarks and further matching is required to exactly align the template mesh with each target mesh (as shown in Fig. 9). The simplest method is to project the template mesh to the closest point on the target mesh (Paulsen et al., 2002; Hutton et al., 2003) but this can lead to unrealistic deformations and movement to the closest point while not representing small deformations.

Approaches such as Meller and Kalender (200) and Kaus et al. (2003) optimize the fit based on the distance between the meshes while an additional force preserves the mesh structure. Our method is based on these methods but is enhanced for deformed tubular objects by adding a third term based on the surface orientation. For each vertex (t_i) on the template mesh, a force $(F_{i,tot})$ is calculated to direct the warp. This consists of a component based on the closest point on the object mesh (r_i) (Eq. (4)) and an internal forcing component is included to preserve the size of the faces. The force is calculated by the change in the distance of each of the m neighbouring vertices to a vertex t_i from the initial distance v_{ij}^{init} (Eq. (5)). These two forces are not enough to match to small indentations or protrusions found in the airways. Therefore, a local *inflation/deflation* force is also applied based on the normal of each vertex $\hat{n}_i$ (calculated from the normal of the surrounding faces). The amount of inflation and deflation is controlled by the distance and direction of the target mesh to $F_{i,1}$ (Eq. (6)).

$$F_{i,1} = \overrightarrow{r_i} - \overrightarrow{t_i} \quad (4)$$

$$F_{i,2} = \sum_{j}^{m} \hat{v}_{ji} \left(||\vec{v}_{ji}|| - \left\| \vec{v}_{ji}^{init} \right\| \right) \quad (5)$$

where $\vec{v}_{ji} = \vec{t}_j - \vec{t}_i$

$$F_{i,3} = \hat{n}_i (\hat{n}_i \cdot F_{i,1}) \quad (6)$$

$$F_{i,tot} = \alpha F_{i,1} + \beta F_{i,2} + \gamma F_{i,3} \quad (7)$$

In Eq. (7), the forces are weighted with α, β and γ. This procedure is applied iteratively until stability is reached. An example mesh after this local alignment is also shown in Figs. 9b. This method enables any segmented airway to be registered to a template mesh, thus achieving vertex correspondence.

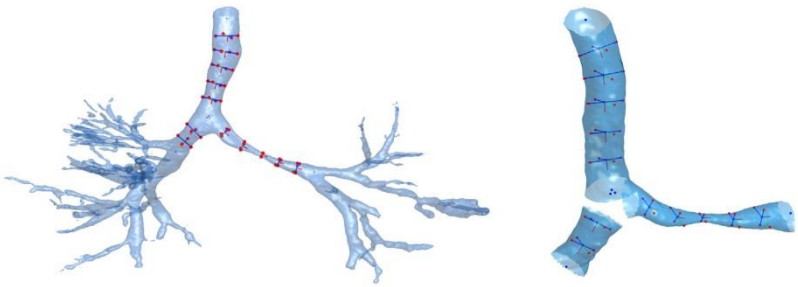

(a) Airway segmentation with landmark points for the Trachea-RUL-BI region

(b) Enlarged region showing the point mapping to individual branches

Fig. 7. Mapping corresponding points onto the surface mesh of an airway.

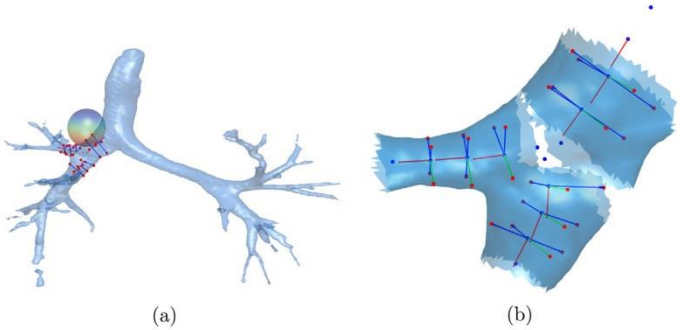

(a) (b)

Fig. 8. Mapping corresponding points onto the surface mesh of an airway. RMB–RUL–BI region (with a single sphere showing the area of search for an example vector).

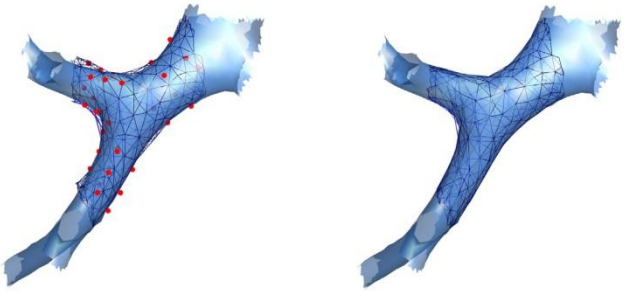

(a) Thin-plate spline warp by aligning landmark points (red) of a template mesh to the landmark points of a region of an airway

(b) Local alignment (performed after TPS warp) of each template vertex to the airway surface

Fig. 9. Registration of a template mesh to an airway mesh for the RMB–RUL–BI region.

3.5. Bifurcation region relabelling

The previous sections present a method to develop correspondence between the surface mesh of segmented airway trees. This method can be applied to the whole airway tree or to a region of the airway. Figs. 8 and 9 illustrate regional based airway analysis and this section discusses a method to refine the branch labelling at bifurcation.

Each face in the mesh was assigned a branch label by assigning the label of the closest voxel of the labelled skeleton. However, this labelling criterion leads to variation in label assignment in the branch bifurcation region. Mesh faces in a bifurcation region are assigned to the connected branches but this assignment is biased towards branches with a smaller diameter and is influenced by branch shape and orientation. This leads to irregular branch end points which adds additional complexity to the statistical shape representation. As an example, Fig. 3c shows how most of the bifurcation region is assigned to the trachea.

To produce consistent branch labels at bifurcation, adjustments are made to this label assignment. A face (m) is only labelled as belonging to a particular branch if:

(1) The centroid (c_m) of m falls between the two branch end points (creating a well defined branch end by cutting of the branch orthogonal to the centreline at the branch beginning and end bifurcation)

$$\hat{n}_{j1} \cdot \hat{n}_{m1} > \alpha \quad \text{and} \quad \hat{n}_{j2} \cdot \hat{n}_{m2} > \alpha \tag{8}$$

(2) It is near the branch centreline (ignore neighbouring branches)

$$|c_m - e_{j1}| + |c_m - e_{j2}| - |e_{j1} - e_{j2}| < \beta \tag{9}$$

where e_{j1} and e_{j2} are the start and end points of the branch, and therefore derived from the start and end positions of the extracted branch centrelines (shown in Fig. 3b). n_{m1}, n_{m2} are the directions from e_{j1} and e_{j2} to c_m (see Fig. 10). α and β are constants identified by qualitatively assessing the training set as 0.2 and 25 mm respectively. m that are not assigned to a branch are labelled as the bifurcation region. This method reduces variance due to region selection by creating consistent edges between branch labels as demonstrated in the branch endpoints of Fig. 11 and 12 introduced later.

3.6. Airway shape features

Feature vectors are derived from both LA-PDMs of airway regions and cross-sectional sampling of each branch in the airway tree.

3.6.1. LA-PDM features

Each airway is represented by a dense surface mesh. The corresponding vertices of each airway surface mesh can be used to build a PDM of the airway and extract a set of principal modes that represent the variation of each airway.

Some of the variation between airways in the dataset is due to size, position and rotation, which are related to patient age and scan position, and not of interest for the detection of airway pathology. Therefore, the airways are first aligned by generalised Procrustes analysis (GPA). GPA is used to iteratively align objects represented by a set of corresponding points using translation, scaling and rotation.

Principal component analysis (PCA) is an integral part of developing a point distribution model (PDM). PCA applies a linear transform that projects the vertices onto an uncorrelated space and can be used to extract relevant features (Cootes et al., 1995). PCA modes are ordered by the variance and, therefore, by selecting the subset of the modes with the most variance, each shape can be represented by a feature vector of lower dimensionality than the input feature vector.

As input into PCA, each object is represented as a $3n$ dimensional stacked vector of mesh vertices where n is the number of vertices in the mesh; for the Trachea-RMB-LMB regions $n \approx 1700$. Therefore, the GPA aligned 3D landmark points of the object $\mathbf{x} = [(x_1, y_1, z_1) \ldots (x_n, y_n, z_n)]$ are now represented as a single vector $\mathbf{x_i} = (x_1, y_1, z_1, \ldots, x_n, y_n, z_n)^T$ for object i.

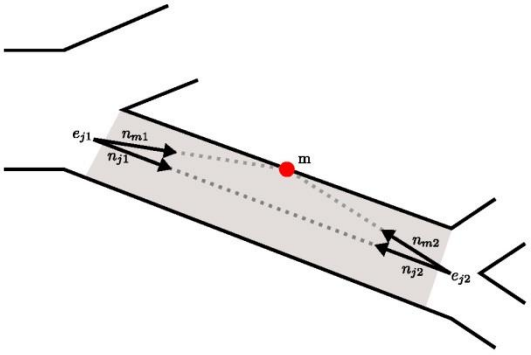

Fig. 10. Relabelling the surface mesh where m is the face to be relabelled. m is labelled according to the face's position in relation to the branch end points e_{j1} and e_{j2}.

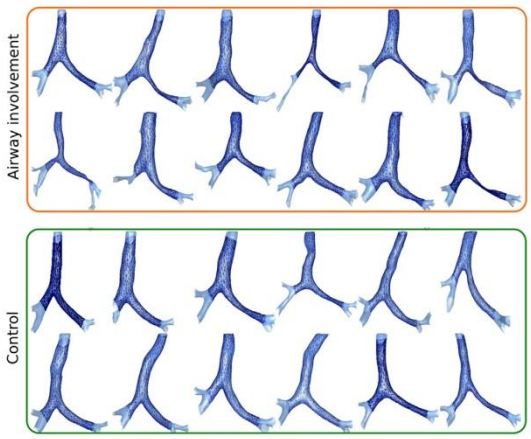

Fig. 11. Example cases of registration of the template mesh to the Trachea–RMB–LMB region. The first two rows are patients with airway involvement and the remainder are controls.

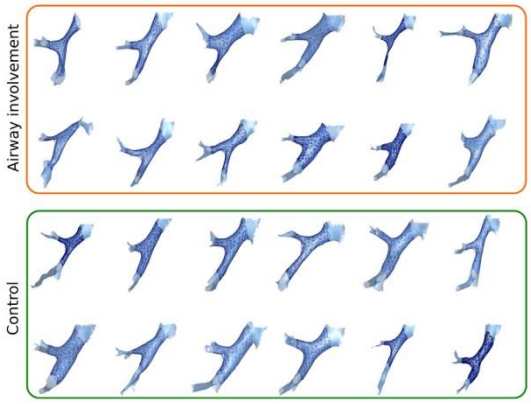

Fig. 12. Example cases of registration to the template mesh to the RMB–RUL–BI region. The first two rows are patients with airway involvement and the remainder are controls.

PCA is computed from the covariance matrix and it can be shown that the eigenvectors (Φ) of the covariance matrix can be used to project an airway ($\mathbf{x}$) into uncorrelated space, where the dimensions of the uncorrelated space are defined by the orthogonal eigenvectors. This projection is:

$$\mathbf{b} = \Phi^T(\mathbf{x} - \bar{\mathbf{x}}) \tag{10}$$

where $\mathbf{b}$ is the representation of the airway in the new space. Therefore, an airway can be represented in terms of the mean shape and a displacement along each principal component by $\mathbf{b}$:

$$\mathbf{x} \approx \bar{\mathbf{x}} + \Phi\mathbf{b} \tag{11}$$

Of particular interest is that PCA results in an ordered set of eigenvectors, where the contribution of the variance of each eigenvector (ϕ_i) is represented by the eigenvalues (λ_i). A shape can, therefore, be approximated by a set of m eigenvectors $\Phi = (\phi_1|\phi_2|\ldots|\phi_m)$ and $\mathbf{b} = (b_1, \ldots, b_m)$. This means that a dense surface mesh model of a shape is reduced to a much shorter feature vector represented in terms of the principal components of shape variation.

A common way of choosing the number of principal components (eigenvectors) that will represent the shapes is based on the amount of variance they represent. Typical choices range from 90% to 99.5% of the variance (van Ginneken et al., 2002). The variance represented by the first m eigenvectors can be calculated from the sum of the first m eigenvalues over the sum of all $3n$ eigenvalues:

$$f = \sum_{i=1}^{m}\lambda_i \Big/ \sum_{i=1}^{3n}\lambda_i \tag{12}$$

Each object is now represented by a vector $\mathbf{b}$ of length m. These vectors represent the object shape (with an accuracy of up to the chosen variance f) and can be used to distinguish and classify airway shapes.

3.6.2. Local region analysis

Variation in airway shape could potentially be modelled at a number of levels from the variation in a single cross-section of a branch to global variation of the entire airway. In this study, local regions of the airway are modelled individually, where each region consists of a parent branch, the bifurcation region and two child branches. Modelling each branch individually is not as effective because variation in the position of a branch relative to neighbouring branches is important; lymphadenopathy can lead to branch deformation as well as stenosis (an example of tracheal displacement by lymphadenopathy is presented in (Andronikou and Wieselthaler, 2004)).

Alternatively, shape models could be applied to the entire airway. However, PCA is a linear projection to a lower dimensional space and with each additional generation of a tree structure the variation of the airways becomes increasingly non-linear. While there are benefits to modelling the relationship between parent and child branches, there is limited value to modelling the relationship between the shape changes of second order connected branches. There are non-linear formulations of PCA (including Kernel PCA in (Schlkopf et al., 1997)), but modelling the airway as a set of 3-branch structures using PCA seems the most promising approach.

Therefore, this method creates a number PDMs of the airway for variation 3-branch regions. Each 3-branch region overlaps the previous region. For example, the RMB is represented in both the Trachea–RMB–LMB and RMB–RUL–BI regions. These regions are automatically identified, a point distribution model is built from the dataset and each 3-branch region is assigned a feature vector ($\mathbf{b}$) that can be used for classification.

In paediatric pulmonary TB, the most common locations of lymphadenopathy are subcarinal (90%), hila (85%), anterior mediastinum (79%) and paratracheal (63%) (Andronikou et al., 2004). Bronchial compression caused by lymphadenopathy is most apparent in the BI, LMB, RMB and trachea (Andronikou et al., 2004; Lucas et al., 2012). Therefore for identifying TB, two regions were modelled (Trachea–RMB–LMB and RMB–RUL–BI). This could be extended to the rest of the airway if useful for modelling additional airway pathology. The model is aligned using the branching structure and extracted mesh, and because three branches are modelled at any one time, no more complexity is added by analysing further generations.

3.6.3. Radius based features as an alternative to LA-PDM

LA-PDM provides a solution to a novel application and there are no comparison methods available. However, manual measurements of airway diameter are used clinically as an indicator of

airway involvement and are generally assessed in terms of proximal and distal involvement in each bronchi (du Plessis et al., 2009). The method that we have proposed in the previous sections can implicitly measure airway cross-sections as part of the landmark placement step (Section 3.2). Therefore, as a more conventional comparison to the LA-PDM, feature vectors based on cross-sectional measurements of the airway bronchi were also derived. As discussed in Section 3.2, vectors orthogonal to the branch centreline were projected to the surface and the intersection between the mesh and the vector was found. This provided radius measurements in four orthogonal directions for n equidistant samples along each branch. In this comparison we divide each bronchi into three regions: proximal, middle and distal and derive a single mean diameter ($\bar{d}$) for each region:

$$\bar{d} = \frac{1}{2(q-p+1)} \sum_{i=p}^{q} \sum_{j=1}^{4} ||\mathbf{r}_{ij}|| \tag{13}$$

where p and q are the scalars defining the start and end points of the region from the n centreline samples in the branch, and $\mathbf{r}_{ij}$ is the radius at position i and orientation j (as illustrated in Fig. 6). These features are normalised across airways by the branch length (l). As with the PDM derived features, the same 3-branch regions were used for this method, and therefore, 3 branches each with 3 mean region diameters, resulting in 9 features, were used for classification, and compared to classification using the LA-PDM derived features.

Linear discriminant analysis is used to classify these airway regions using these derived features with leave-one-out cross validation.

4. Application of the LA-PDM to clinical cases

This section describes the application of the LA-PDM method to the paediatric chest CT dataset.

4.1. Paediatric chest CT cases

A set of 89 paediatric non-TB and TB cases were acquired in 2010 from Tygerberg Hospital (South Africa) and Great Ormond Street Hospital (UK). These cases were used to develop the method and determine the parameters used in the algorithm. In 2012, a dataset of 90 patients with and without TB were all collected at Tygerberg Hospital. These were previously unseen and used only for evaluation in this study. Several cases with artefacts from tubes or severe movement were excluded from the study.

The test dataset included 42 non-TB patients with a mean age of 3.1 ± 3.8 years and 48 TB patients with a mean age of 2.4 ± 2.8 years. Patients under 5 years have more malleable airways and are, therefore, more predisposed to airway deformation. These images were acquired using the Siemens SOMATOM Sensation 40 and the Siemens SOMATOM Emotion 6. The pixel size in each slice varied from 0.21–0.54 mm and the slice thickness varied from 0.6 to 1.5 mm.

Patients with suspected TB only undergo a CT scan when there are signs or symptoms of airway involvement (du Plessis et al., 2009) and therefore, all TB cases in this dataset have suspected airway involvement. Suspected airway involvement is diagnosed from signs of obstruction of the large airways including stridor and wheezing or tracheal cough, or radiologically. Furthermore, all TB cases used in this study were classified as having probable or definite TB, where definite is culture confirmed and probable is not culture confirmed but combines clinical grounds, radiological assessment, Mantoux skin test and contact history.

In order for airway involvement to be compared to controls, a pulmonologist selected cases without airway involvement or tuberculosis. These cases include children with the following conditions: parenchymal lung disease such as interstitial lung disease, congenital lung malformations which affect the parenchymal tissue and not the airways; suspected lung metastases; and infective conditions other than TB. These will include cases of bronchiectasis, cystic fibrosis and pleural disease.

4.2. LA-PDM implementation

This section provides additional details on the experimental set-up and parameter settings.

For landmark generation, linear interpolation between the centreline voxel coordinates was performed and 100 points were sampled between each voxel. This was chosen to be suitably dense, from which, to derive resampled equally spaced landmark points. The centreline was then smoothed using a moving average. Five voxels were used to calculate the moving average at each point as this removed the appearance of individual voxel noise. Therefore, 500 points were used to calculate the smoothed centreline from the interpolated points.

A single case with no visible pathology (from the training set) was used as the template for registration. To improve computational efficiency, the airway mesh was reduced to 20% of the original number of vertices while maintaining vertex-to-vertex correspondence using a surface simplification method (Garland and Heckbert, 1997). Therefore, the Trachea–RMB–LMB region was represented by 3286 faces and 1733 vertices, and the RMB–RUL–BI regions were represented by 1093 faces and 618 vertices.

The number of resampled centreline points used to generate surface landmark points were: Trachea, 5; LMB, 5; RMB, 2; BI, 3 and RUL, 3. These were chosen to provide similar spacing for each branch. Each centreline point was used to generate four surface landmarks, resulting in 48 and 32 landmarks used to represent the Trachea–LMB–RMB and RMB–RUL–BI regions, respectively (as shown in Fig. 7 and 8), and were used to register the template mesh. These values were chosen so that the landmarks were suitably far apart that the orthogonal radii never intersected – which would cause folding in the surface representation. The number of resampled centreline points used, for radius based measurements, was [100 100 50] (number of points in each branch of a 3-branch section). At each of these equidistant points, 4 points were projected to the surface.

The accuracy of the mesh alignment was evaluated by comparing volumes generated from the template mesh and airway region of interest using the Jaccard distance (the complement of the Jaccard index). The proportion of error in the registration (V_{dif}) and an opening of the error using a 6-connected structuring element (V_{open}) as a function of α, γ and β (Eq. (7)) were used for evaluation using a grid search. The opening removes single voxel errors that may be introduced during re-voxelisation of the mesh for comparison, and, therefore, V_{open} represents larger local errors that have more impact on accuracy. For stability, only $\alpha < 1.0$ and $\gamma < 1.0$ were considered when choosing optimal values. A step size of 0.1 for α and γ, and $\beta = 0.5,\ 1.0,\ 1.5$ were used in the search. Optimal values were found to be $\alpha = 0.1$ and $\gamma = 0.8$ with a mean $V_{dif} = 0.021 \pm 0.009$ and $V_{open} = 0.0022 \pm 0.0049$. Just using closest point mapping (Eq. (4)), the errors were $V_{dif} = 0.029 \pm 0.019$ and $V_{open} = 0.009 \pm 0.015$. Using closest point mapping and the mesh structure term (Eqs. (4)), the errors were $V_{dif} = 0.027 \pm 0.018$ and $V_{open} = 0.006 \pm 0.011$. Therefore, including the *inflation/deflation* term improves the registration of the template and reduces the variance in the accuracy of the fit. This is particularly noticeable for V_{open} (larger local errors) and agrees with qualitative observations that adding the third term improves the registration for narrowed and stenosed branches. This optimisation could be performed on an individual basis to choose

parameters for each case. However, in this work the same fit parameters are used throughout the dataset.

Fig. 11 and 12 show alignment of a template mesh to the Trachea–RMB–LMB and RMB–RUL–BI regions of 24 example cases from the 90 patient test dataset. These cases are used to illustrate the typical variation found in the dataset and the template mesh alignment (the darker region is the aligned template mesh). As can be seen, differences between cases with airway involvement and controls are sometimes not clearly apparent.

4.3. Model variation and feature extraction

PCA modes of variation were extracted from the PDM model. The variation of the first 5 PCA modes for the Trachea–RMB–LMB and RMB–RUL–BI regions are shown in Figs. 13 and 14. The centre column shows the mean airway ($\bar{\mathbf{x}}$) with variation ($\mathbf{x} = \bar{\mathbf{x}} \pm \Phi_i b_i$). Using $b_i = \pm 3\sqrt{\lambda_i}$ shows the variation of one mode three standard deviations from the mean in the dataset (Cootes et al., 1995). These principal components exhibit a range of changes including branch narrowing, local stenosis, deformation, length and angular changes. These modes also include variation that is considered pathological such as deformation and stenosis of branches. For example, the fifth mode of Fig. 13 shows central narrowing of the LMB while the first and second modes of Fig. 14 show types of region based narrowing. Note that due to the perspective some of the 3D variation is not visible in the figures.

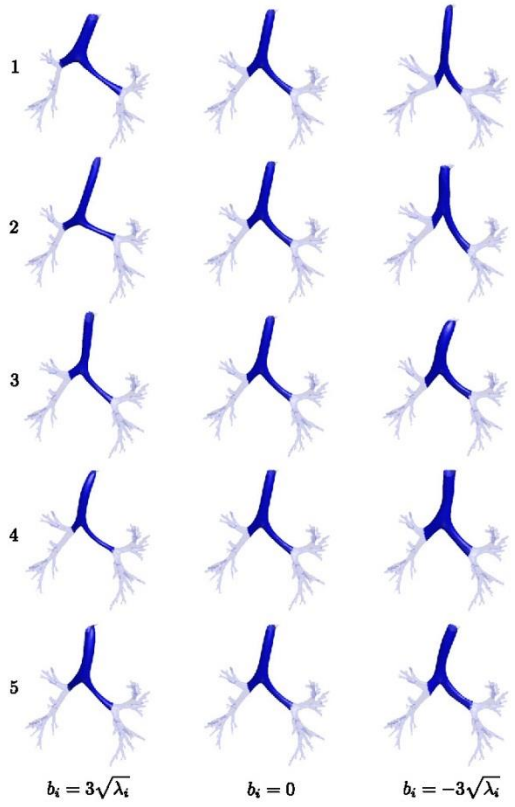

Fig. 13. Modes of variation 1–5 for the Trachea–LMB–RMB ($b_i = 0$ is the mean model and $b_i = \pm 3\sqrt{\lambda_i}$ represents the shape 3 standard deviations along each mode). Dark regions in the figures show the local PDM model and the light region is an example airway that is registered to the model to aid visualisation.

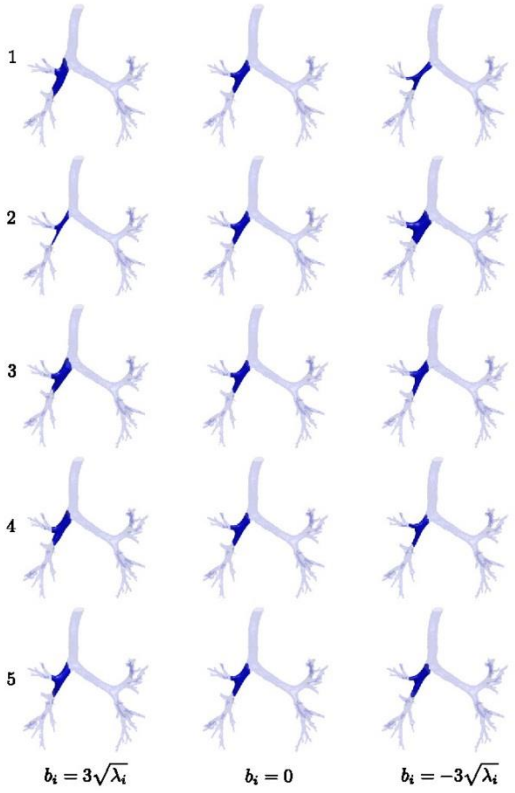

Fig. 14. Modes of variation 1–5 of the RMB-RUL-BI ($b_i = 0$ is the mean model and $b_i = \pm 3\sqrt{\lambda_i}$ represents the shape 3 standard deviations along each mode).

Fig. 15 shows two example airway segmentations from a TB patient and control. In this example there is narrowing of the LMB and BI for the TB case. The representation of the airway variation in this example by the LA-PDM is shown later in Fig. 21. Small differences are also visible between the 11 component representation of the Trachea–LMB–RMB region (dark blue) and the original airways (light blue). These differences are represented by the remainder of the principal components that are excluded from the model.

4.4. Model evaluation

Before analysis of the classification accuracy, the characteristics and performance of the point distribution model were analysed. Measures of compactness, generalisation and specificity, that are outlined by Styner et al. (2003), were used to evaluate the model.

A compact model can represent the variance within the dataset with only a few parameters. The variance can be calculated as a function of the number of shape parameters (modes of variation).

The model generalisation represents a model's ability to represent unseen cases (Styner et al., 2003). This was evaluated using leave-one-out reconstruction of the dataset. For each case in the dataset, the PDM was built without the case, and used to reconstruct the case using M modes of variation. The mean absolute

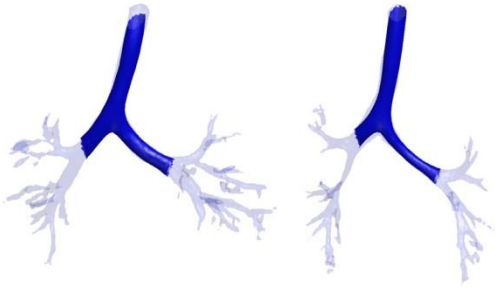

(a) non-TB case (b) TB case

Fig. 15. Example airways from the non-TB and TB datasets with overlaid 11 component representation of the first 3 branches.

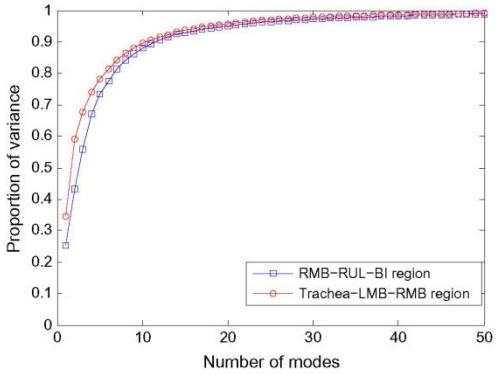

Fig. 16. The proportion of the total variance in the dataset that is represented by n principal modes for the Trachea–LMB–RMB and RMB–RUL–BI regions. Principal modes are ordered by variance and, therefore, higher modes will make smaller contributions. In this dataset, the first 11 modes represent $\approx 90\%$ of the variation.

distance (MAD)[1] was then used to approximate the error of the PDM representation of each case. The mean and standard deviation of the MAD values for the entire dataset was calculated. Confidence intervals were found by the Central Limit Theorem.

Model specificity evaluates the ability of the model to only generate shapes that are similar to those found in the dataset (Styner et al., 2003). A thousand new instances of the feature vector $\mathbf{b_i}$ were generated for each PDM. Monte Carlo simulations were used to randomly generate $\mathbf{b_i}$ from a multivariate normal distribution with standard deviation $\sigma_i = \sqrt{\lambda_i}$ and mean $\mu_i = 0$ (Hu et al., 2010). MAD from each instance to each case in the dataset was calculated, and the minimum distance was recorded, which represents to closeness of the instance to the nearest case in the dataset. The mean and standard deviation of the minimum MAD distances were calculated.

PCA produces modes of variation that are ordered by the contribution to the total variance within the dataset. Fig. 16 shows the contribution of each mode to the total variance. In both cases approximately 90% of the airway variation in the dataset is represented by the first 11 modes.

The model generalisation and model specificity for both PDMs are shown in Fig. 17 as a function of the number of modes of variation (M). As expected the model generalisation – the ability of the model to represent unseen cases – performs better (decreases) with increasing number of modes (using 11 modes $G(M) \approx 0.5$ mm). Also as expected, the specificity (the ability of the model to only represent similar cases) performs worse (increases) with increasing number of modes. The Trachea–LMB–RMB model outperforms the RMB–RUL–BI model both in terms of generalisation and specificity. This is probably because there is less variability in the latter region.

[1] The mean absolute distance is defined as the mean distance between the vertices of the model representation and the vertices of the corresponding case (Styner et al., 2003).

5. Detection of cases with airway abnormalities

The CAD pipeline that we have developed is able to detect airway deformation related to paediatric TB. The following steps are used for detection of an unseen case: a chest CT of a paediatric patient with suspected TB is acquired, the airway is automatically segmented, the airway centreline and branch points are identified, and landmarks are placed on the airway surface using the methods described in Section 3.1 and 3.2. The airway template mesh for each 3-branch region is then registered to the segmented airway surface to develop vertex to vertex correspondence with the training set (Sections 3.3 and 3.4). The point distribution model – created using the training set – is then used to project the mesh vertices of the test case, and the first 11 modes of variation are extracted as features. A classifier, trained on features from the training set, is then used to classify each 3-branch region of the airways. This allows automatic detection of airway abnormality in each 3-branch region based on variation of the shape of each bronchi as well as variation with respect to neighbouring bronchi.

Evaluation was performed using leave-one-out cross validation (LOOCV) on the test set where the classifier was tested on each case and trained on the remainder over the entire dataset. The receiver-operating-characteristic (ROC) was used to evaluate accuracy. Area-under-the-ROC curve (AUC) provided a single performance measure. Confidence intervals were used to assess the confidence in both the AUC and ROC curves, and were calculated using bootstrapping with 5000 replications. Bootstrapping was performed using the bias corrected and accelerated (BCa) method as this is the preferred approach (Altman et al., 2005).

Before classification, Fisher mapping was used as a useful visualisation of the linear separability between TB and non-TB cases for a set of features. Fig. 18 shows that separability of test cases with and without airway involvement can be achieved by 11 principal modes of variation (90% of the dataset variation) using Fisher mapping. Fisher mapping is an affine mapping that maximises the ratio of the inter/intra class variability (vanderHeijden et al., 2004).

The key outcome of this method is detection of airway abnormality in unseen cases. Fig. 19 shows ROC curves, for the two regions of interest, distinguishing cases with airway involvement from controls, using linear discriminant analysis (LDA) with leave-one-out cross validation on the test set. 95% confidence intervals for the sensitivity and AUC of the ROCs were estimated using bootstrap BCa with 1000 replications. The figure shows a comparison between classification using the LA-PDM derived features that we introduce and classification using features derived from mean airway cross-section. Using the LA-PDM achieved an AUC of $0.87(0.77-0.94)$ on the Trachea–RMB–LMB region (Fig. 19a). Fig. 19b shows that second order bronchi can also play a role in TB detection with an AUC of $0.81(0.68-0.90)$. Using the alternative set of features derived from mean airway cross-section an AUC of $0.72(0.59-0.83)$ was obtained for the first region but classification failed on the second region $0.59(0.46-0.73)$.

The significance of the AUC improvement was calculated using bootstrapping (BCa with 5000 replications) with a two-tailed Monte Carlo technique. Assuming a significance level of $\alpha = 5\%$,

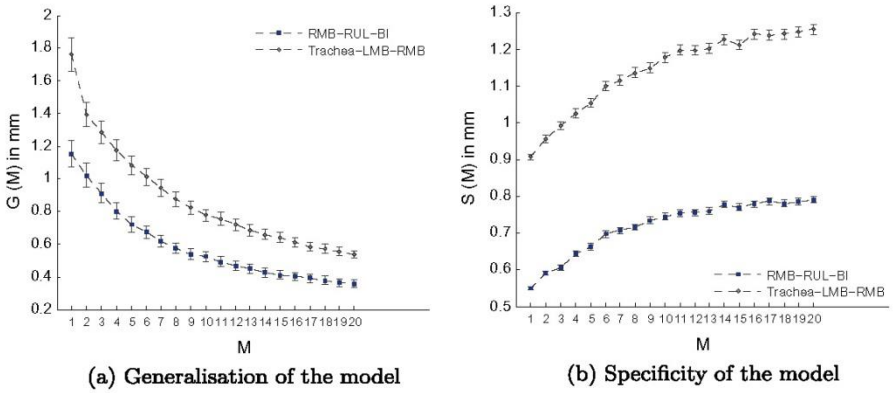

(a) Generalisation of the model (b) Specificity of the model

Fig. 17. Generalisation G(M) and specificity S(M) of the model with confidence intervals, as a function of the number of modes (M), for the Trachea–LMB–RMB and RMB–RUL–BI regions.

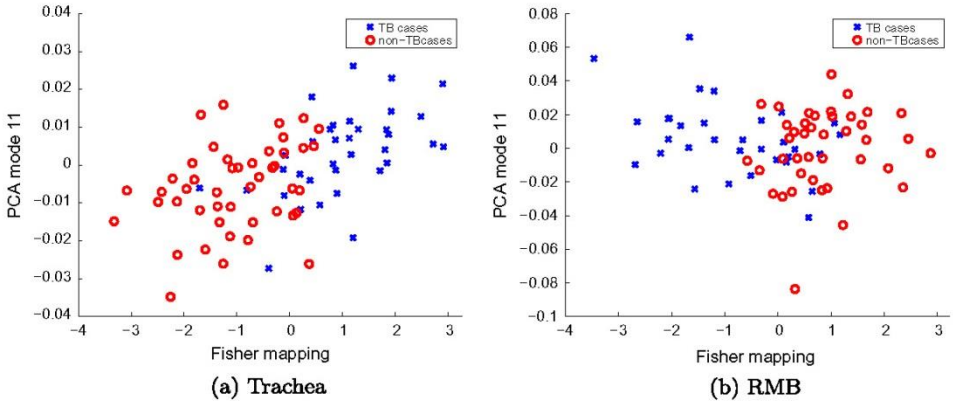

(a) Trachea (b) RMB

Fig. 18. Fisher mapping of first 10 modes of dataset versus the 11th mode on the test set.

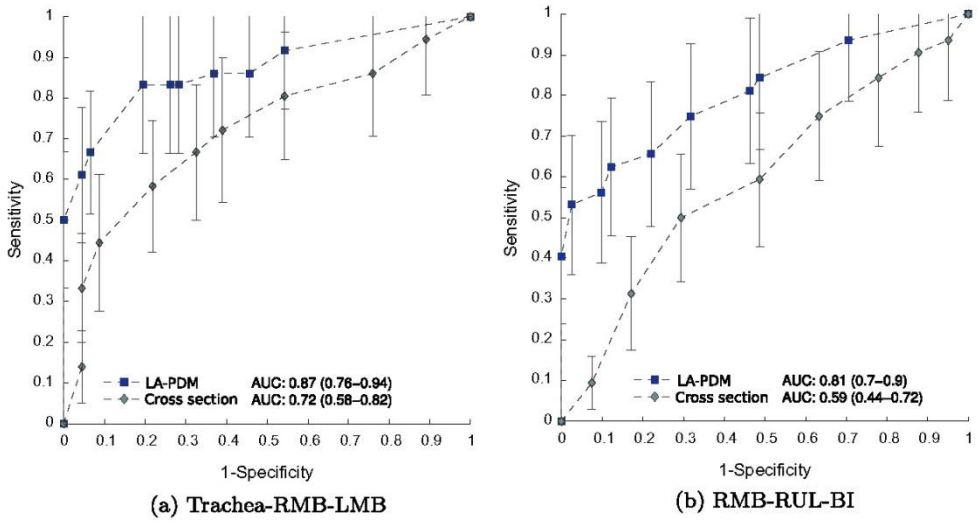

(a) Trachea-RMB-LMB (b) RMB-RUL-BI

Fig. 19. ROC curves for accuracy of detection of cases with airway involvement using LA-PDM and mean airway cross section features.

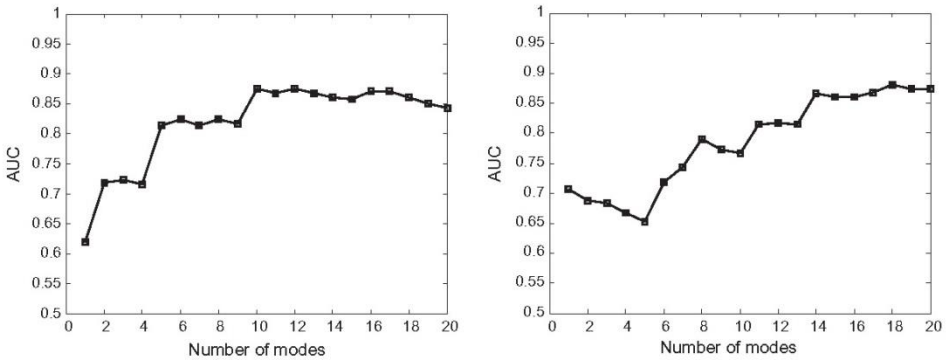

(a) Trachea-RMB-LMB region. Including modes 1, 2, 5 and 10 appears key to improving the accuracy of the classification.

(b) RMB-RUL-BI region. Including modes 1, 6, 7, 8, 11 and 14 appears key to improving the accuracy of the classification.

Fig. 20. AUC as a function of number of modes used in the classification.

the PDM derived features were significantly better than the average diameter derived features for both the Trachea–RMB–LMB ($p = 0.024$) and RMB–RUL–BI regions ($p = 0.013$).

This suggests that branch diameter is not enough for the detection of airway shape variation (due to paediatric TB), and that LA-PDM can considerably improve detection by accounting for variation in regions of the airway tree. The flexibility of the PDM to model variation automatically is also a considerable advantage.

So far we have shown the effectiveness of LA-PDM for the detection of airway involvement in unseen cases. However, analysis of more specific involvement could also be obtained from individual modes of variation and identifying the modes that have the most impact on classification. This method used 11 principal components, representing 90% of the variation for classification. Fig. 20 considers the impact of the number of components on the accuracy of detecting airway involvement and shows the key modes of variation that play a role in distinguishing airway involvement from normal variation. The AUC was calculated using LOOCV for each number of features on the validation set.

Interesting to note, is that large improvements in performance are seen when adding certain components while others offer no improvement. The modes that allow airway involvement to be identified include the modes 1, 2, 5 and 10 for the Trachea–RMB–LMB region and modes 1, 6, 7, 8, 11 and 14. Other modes may also contribute to the classification but only improve the classification when used in combination with one of the modes described above. Fig. 20b shows that the AUC could be improved further if more modes than those contributing to the 90% variance were included. The plots also show that adding certain modes can worsen the performance of the classifier; fitting a classifier to a feature that does not contribute to the distinguishing the datasets has the potential to be penalised by the cross validation.

This section shows that accurate classification of disease with airway involvement can be performed automatically. However, these modes could have more use beyond a automatic classification of the airway. By identifying the modes that are most important for detection of airway involvement, these modes could be used to illustrate the specific type of abnormal airway involvement to the viewer. Fig. 21 illustrates this point by including the key modes from the two regions along with the parameters of the example airway shown in Fig. 15b. The parameters of the example

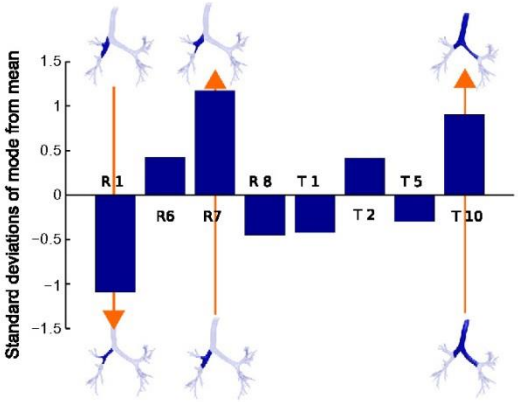

Fig. 21. The example airway (Fig. 15b) is shown in terms of the most important modes for classification (from Fig. 20) where R represents the modes from the RMB–RUL–BI and T is Trachea–RMB–LMB. R1, R7 and T10 show the largest deviation from the mean airway for this case and, therefore, the types of pathology found in this airway, including narrowing of the RMB and stenosis of the LMB.

airway are plotted in terms of the standard deviation of each mode. The figures show that the largest deviations (from the population mean) in the example have clinical importance because they illustrate the types of airway pathology, which, in this example, include narrowing of the bronchus-intermedius (R7) as well as local stenosis of the LMB (T10).

This software was written using a combination of Matlab R2011a and C++. C++ was incorporated to improve the speed at various bottlenecks. The software was evaluated on a system with a 2.80 GHz Intel quad-core processor and 6 GB of RAM. The mean time for segmentation of each airway was 168 ± 57 s. Extraction of the centreline, pruning and branch point detection for each airway took a mean time of 22 ± 18 s. Once each airway was segmented and the structure extracted, then mesh generation, registration, training and classification of the entire 179 patient dataset took 1162 s on a single run.

6. Discussion

The LA-PDM method introduced in this paper can accurately distinguish between airway involvement (from paediatric pulmonary TB) and normal airways by examining regions of the airway likely to be affected by lymphadenopathy (AUC of 0.87(0.77–0.94) and 0.81(0.68 – 0.90)). The LA-PDM derived features show more promise than features derived from the airway diameter, which is probably due to the ability to represent more complex variation in feature space. However, we are not aware of any previous studies that model the effect of lymphadenopathy on airway changes and are, therefore, not able to compare to previous methods. Instead we propose these results as a benchmark for future airway shape analysis.[2]

A training set of 89 patients was used during development of the method and determination of landmark point and registration methods. Because the training set was acquired from a number of hospitals, evaluation was performed on the previously unseen 90 patient test set (from a single hospital) using leave-one-out cross validation.

The classification based on shape aims to distinguish pathological shape variation from inter-patient variation, and variation due to age and breathing artefacts. The standard deviation of the patients' age is approximately 3 years. With a larger dataset, it would be possible to divide the dataset into age groups and possibly improve the performance by removing noise caused by age variation. However, studies have shown that the proportions of the airway do not change considerably with age in children (Masters et al., 2006). Breathing artefacts could also add noise to shape-based airway classification as it is not possible to perform a breath hold scan on young patients. The bronchi lengthen and dilate during inspiration but these changes are expected to be distinguishable from TB pathology. The accuracy of the classifier also indicates that breathing variation does not have a considerable effect. With newer 128 and even 256 slice CT, the whole chest volume could be imaged in less than a second, eliminating motion.

These results show that the LA-PDM has promise for detecting airway involvement in chest CT examinations and, thus, speeding up CT assessment. As demonstrated in the results section, the methods can also be used to provide key features of each airway being examined, providing information on the type of deformation from the modes of variation that each airway exhibits. If these key modes of variation were linked to the location or locations of lymphadenopathy then further information could be derived from shape changes.

This method could be used to provide additional automated analysis and visualisation for any patient undergoing a CT examination and might be applied to other diseases affecting the airway. Bronchoscopy is currently the "gold standard" for evaluating airway stenosis and deformation but is an invasive procedure. CT with techniques such as virtual bronchoscopy and virtual rendering, shows potential as an alternative to bronchoscopy. The method presented here has the potential to improve and automate analysis of airway shape deformation. Initial steps to extending the LA-PDM to X-ray examinations for routine X-ray screening are also being assessed (Irving et al., 2013).

Finally, CT scanners are increasingly being deployed, including in areas with a high TB prevalence such as South Africa. These are often not manned by radiologists or by junior trainees due to the shortage of radiologists in developing countries. Telereading is not always the solution because radiologists from low prevalence regions are not familiar with all the features of TB in children because of the limited number of cases in their countries. So there is a definite role for computer assisted detection in CT, and furthermore for screening in radiography.

[2] Supplementary data is available at: http://www.birving.com/supplementary/Irving_MEDIA_2014.html.

Acknowledgements

The authors would like to thank the Commonwealth Scholarship Commission (CSC) for funding this research.

References

Altman, D., Machin, D., Bryant, T., Gardner, M., 2005. Statistics with Confidence, second ed. BMJ Books, London.
Andronikou, S., Wieselthaler, N., 2004. Modern imaging of tuberculosis in children: thoracic, central nervous system and abdominal tuberculosis. Pediatr. Radiol. 34, 861–875.
Andronikou, S., Joseph, E., Lucas, S., Brachmeyer, S., Toit, G., Zar, H., Swingler, G., 2004. CT scanning for the detection of tuberculous mediastinal and hilar lymphadenopathy in children. Pediatr. Radiol. 34, 232–236.
Andronikou, S., Irving, B., Hlabangana, L.T., Pillay, T., Taylor, P., Goussard, P., Gie, R., 2013. Technical developments in postprocessing of paediatric airway imaging. Pediatr. Radiol. 43, 269–284.
Bookstein, F., 1989. Principal warps: thin-plate splines and the decomposition of deformations. IEEE Trans. Pattern Anal. Mach. Intell. 11, 567–585.
Bookstein, F., 1997. Shape and the information in medical images: a decade of the morphometric synthesis. Comput. Vis. Image Underst. 66, 97–118.
Cootes, T., Taylor, C., Cooper, D., Graham, J., et al., 1995. Active shape models-their training and application. Comput. Vis. Image Underst. 61, 38–59.
Deligianni, F., Chung, A., Yang, G., 2006. Nonrigid 2-D/3-D registration for patient specific bronchoscopy simulation with statistical shape modeling: phantom validation. IEEE Trans. Med. Imag. 25, 1462–1471.
Desbrun, M., Meyer, M., Schröder, P., Barr, A., 1999. Implicit fairing of irregular meshes using diffusion and curvature flow. Proc. SIGGRAPH, 317–324.
du Plessis, J., Goussard, P., Andronikou, S., Gie, R., George, R., 2009. Comparing three-dimensional volume-rendered CT images with fibreoptic tracheobronchoscopy in the evaluation of airway compression caused by tuberculous lymphadenopathy in children. Pediatr. Radiol. 39, 694–702.
Fetita, C., Ortner, M., Brillet, P., Hmeidi, Y., Prêteux, F., 2010. Airway shape assessment with visual feed-back in asthma and obstructive diseases. In: Proc. SPIE, pp. 76251E–76251E-12.
Garland, M., Heckbert, P.S., 1997. Surface simplification using quadric error metrics. In: Proceedings of the 24th Annual Conference on Computer Graphics and Interactive Techniques. ACM Press/Addison-Wesley Publishing Co., pp. 209–216.
Gie, R., 2003. Diagnostic Atlas of Intrathoracic Tuberculosis in Children: A Guide for Low Income Countries. International Union against Tuberculosis and Lung Disease, Paris.
Goussard, P., Gie, R., 2007. Airway involvement in pulmonary tuberculosis. South Afr. Med. J. 97, 986–988.
Goussard, P., Gie, R.P., Kling, S., Andronikou, S., Lucas, S., Janson, J., Roussouw, G., 2013. Bronchoscopic assessment of airway involvement in children presenting with clinically significant airway obstruction due to tuberculosis. Pediatr. Pulm..
Hu, Y., van den Boom, R., Carter, T., Taylor, Z., Hawkes, D., Ahmed, H.U., Emberton, M., Allen, C., Barratt, D., 2010. A comparison of the accuracy of statistical models of prostate motion trained using data from biomechanical simulations. Prog. Biophys. Mol. Biol. 103, 262–272.
Hutton, T., Buxton, B., Hammond, P., Potts, H., 2003. Estimating average growth trajectories in shape-space using kernel smoothing. IEEE Trans. Med. Imag. 22, 747–753.
Irving, B., Taylor, P., Todd-Pokropek, A., 2009. 3D segmentation of the airway tree using a morphology based method. In: Proc. of Second International Workshop on Pulmonary Image Analysis, pp. 297–307.
Irving, B., Goussard, P., Gie, R., Todd-Pokropek, A., Taylor, P., 2011. Identification of paediatric tuberculosis from airway shape features. In: Proc. Medical Image Computing and Computer Assisted Interventions, pp. 133–140.
Irving, B., Douglas, T., Taylor, P., 2013. 2D X-ray airway tree segmentation by 3D deformable model projection and registration. In: Proc. of Fifth International Workshop on Pulmonary Image Analysis, pp. 43–52.
Kaus, M., Pekar, V., Lorenz, C., Truyen, R., Lobregt, S., Weese, J., 2003. Automated 3-D PDM construction from segmented images using deformable models. IEEE Trans. Med. Imag. 22, 1005–1013.
Kiraly, A., Odry, B., Godoy, M., Geiger, B., Novak, C., Naidich, D., 2008. Computer-aided diagnosis of the airways: beyond nodule detection. J. Thorac. Imag. 23, 105–113.
Lo, P., van Ginneken, B., Reinhardt, J.M., Yavarna, T., de Jong, P.A., Irving, B., Fetita, C., Ortner, M., Pinho, R., Sijbers, J., Feuerstein, M., Fabijanska, A., Bauer, C., Beichel, R., Mendoza, C.S., Wiemker, R., Lee, J., Reeves, A.P., Born, S., Weinheimer, O., van Rikxoort, E.M., Tschirren, J., Mori, K., Odry, B., Naidich, D.P., Hartmann, I., Hoffman, E.A., Prokop, M., Pedersen, J.H., de Bruijne, M., 2012. Extraction of airways from CT (EXACT'09). IEEE Trans. Med. Imag. 31, 2093–2107.
Lucas, S., Andronikou, S., Goussard, P., Gie, R., 2012. Ct features of lymphobronchial tuberculosis in children, including complications and associated abnormalities. Pediatr. Radiol. 42, 923–931.

Masters, I., Ware, R., Zimmerman, P., Lovell, B., Wootton, R., Francis, P., Chang, A., 2006. Airway sizes and proportions in children quantified by a video-bronchoscopic technique. BMC Pulm. Med. 6, 5–13.

Meller, S., Kalender, W., 2004. Building a statistical shape model of the pelvis. In: Proc. Computer Assisted Radiology and Surgery, pp. 561–566.

Möller, T., Trumbore, B., 2005. Fast, minimum storage ray/triangle intersection. In: Proc. ACM SIGGRAPH.

Palágyi, K., Tschirren, J., Hoffman, E., Sonka, M., 2006. Quantitative analysis of pulmonary airway tree structures. Comput. Biol. Med. 36, 974–996.

Paulsen, R., Larsen, R., Nielsen, C., Laugesen, S., Ersboll, B., 2002. Building and testing a statistical shape model of the human ear canal. In: Proc. Medical Image Computing and Computer Assisted Intervention, pp. 373–380.

Petersen, J., Lo, P., Nielsen, M., Edula, G., Ashraf, H., Dirksen, A., De Bruijne, M., 2010. Quantitative analysis of airway abnormalities in CT. In: Proc. SPIE, p. 76241S.

Pinho, R., Tournoy, K., Sijbers, J., 2011. Assessment and stenting of tracheal stenosis using deformable shape models. Med. Image Anal. 15, 250–266.

Sandgren, A., Cuevas, L., Dara, M., Gie, R., Grzemska, M., Hawkridge, A., Hesseling, A., Kampmann, B., Lienhardt, C., Manissero, D., et al., 2012. Childhood tuberculosis: progress requires advocacy strategy now. Eur. Resp. J. 40, 294–297.

Schaaf, H., Beyers, N., Gie, R., Nel, E., Smuts, N., Scott, F., Donald, P., Fourie, P., et al., 1995. Respiratory tuberculosis in childhood: the diagnostic value of clinical features and special investigations. Pediatr. Infect. Dis. J. 14, 189–194.

Schlkopf, B., Smola, A., Mller, K., 1997. Kernel principal component analysis. In: Artificial Neural Networks – ICANN, vol. 1327, pp. 583–588.

Shi, H., Scarfe, W.C., Farman, A.G., 2006. Upper airway segmentation and dimensions estimation from cone-beam CT image datasets. Int. J. Comput. Assist. Radiol. Surg. 1, 177–186.

Styner, M., Rajamani, K., Nolte, L., Zsemlye, G., Szkely, G., Taylor, C., Davies, R., 2003. Evaluation of 3d correspondence methods for model building. In: Information Processing in Medical Imaging. In: Taylor, C., Noble, J. (Eds.), . Lecture Notes in Computer Science, vol. 2732. Springer, Berlin/Heidelberg, pp. 63–75.

Theart, A., Marais, B., Gie, R., Hesseling, A., Beyers, N., 2005. Criteria used for the diagnosis of childhood tuberculosis at primary health care level in a high-burden, urban setting. Int. J. Tuberc. Lung Dis. 9, 1210–1214.

Tschirren, J., Hoffman, E., McLennan, G., Sonka, M., 2005. Intrathoracic airway trees: segmentation and airway morphology analysis from low-dose CT scans. IEEE Trans. Med. Imag. 24, 1529–1539.

vanderHeijden, F., Duin, R., de Ridder, D., Tax, D., 2004. Classification, Parameter Estimation and State Estimation: An Engineering Approach Using MATLAB. Wiley, Chichester.

van Ginneken, B., Frangi, A., Staal, J., ter Haar Romeny, B., Viergever, M., 2002. Active shape model segmentation with optimal features. IEEE Trans. Med. Imag. 21, 924–933.

WHO, 2012. Summary for TB-HIV Estimates for 2005 by WHO Regions. <http://www.who.int/tb> (Accessed July 2012).

Wiemker, R., Blaffert, T., Blow, T., Renisch, S., Lorenz, C., 2004. Automated assessment of bronchial lumen, wall thickness and bronchoarterial diameter ratio of the tracheobronchial tree using high-resolution CT. In: Proc. Computer Assisted Radiology and Surgery, pp. 967 – 972.

Pediatr Radiol (2013) 43:269–284
DOI 10.1007/s00247-012-2468-1

MINISYMPOSIUM

Technical developments in postprocessing of paediatric airway imaging

Savvas Andronikou · Benjamin Irving · Linda Tebogo Hlabangana · Tanyia Pillay · Paul Taylor · Pierre Goussard · Robert Gie

Received: 15 May 2012 / Accepted: 9 July 2012

Abstract CT postprocessing allows more scan information to be viewed at one time allowing an accurate diagnosis to be made more efficiently, and is particularly important in paediatric practice where invasive clinical diagnostic tools can be replaced or at least assisted by modern postprocessing techniques. Four visualization techniques in clinical use are described in this paper including the advantages and disadvantages of each: multiplanar reformation, maximum and minimum intensity projections, shaded surface display and volume rendering. Volume-rendered internal visualization in the form of virtual endoscopy is also discussed. In addition, the clinical usefulness in paediatric practice of demonstrating airway compression and its causes are discussed. Advanced postprocessing techniques that must still find their way from the biomedical research environment into clinical use are introduced with specific reference to computer-aided diagnosis.

S. Andronikou · L. T. Hlabangana · T. Pillay
Radiology Department, Faculty of Health Sciences,
University of the Witwatersrand,
Johannesburg, South Africa

B. Irving · P. Taylor
CHIME, Division of Population Health,
University College London,
London, UK

P. Goussard · R. Gie
Department of Pediatrics and Child Health,
Faculty of Health Sciences, University of Stellenbosch,
Stellenbosch, South Africa

S. Andronikou (✉)
700 Harbouredge, 10 Hospital Str, Greenpoint,
Cape Town 8005, South Africa
e-mail: docsav@mweb.co.za

Keywords Minimum intensity projections · Multiplanar reconstruction · Volume rendering · Computer aided diagnosis · Paediatric

Introduction

Diagnostic methods for suspected airway obstruction in children include imaging in the form of chest radiographs and CT scanning as well as fibre-optic tracheobronchoscopy (FTB). FTB is an excellent way of evaluating stridor caused by airway compression and for visualizing the dynamic changes in airway calibre [1]. It is usually performed by a pulmonologist and represents the gold standard for airway investigation, but it has numerous limitations. Even though the procedure is considered a safe examination if performed by an experienced user, it is invasive and requires general anaesthesia, which carries further risks [1]. Complications such as hypoxaemia, hypercarbia, cardiac arrhythmia and subglottic oedema have resulted in the search for noninvasive diagnostic techniques [1]. Imaging is one of these solutions, but it must meet the aims of FTB. The main aims of FTB are to confirm airway narrowing, evaluate the degree of stenosis, aspirate endobronchial contents and perform transbronchial biopsy [1]. Imaging should also provide additional information acceptable as an alternative, particularly where FTB has limitations such as in demonstrating the cause of a stenosis, demonstrating relationships with surrounding structures and navigating airways that are difficult to access by FTB (such as the lingual and left lower lobe bronchi) and the airways beyond a tight stenosis [1].

CT has established its place in the evaluation of paediatric stridor as it is easy to perform and requires no sedation due to the speed of the procedure. It does, however, carry a radiation burden, which must be considered. Simple solutions such as reducing the kV and mAs can reduce the dose

by up to 65% [1]. CT volumes have traditionally been viewed as individual axial slices, but the availability of multidetector row CT (MDCT) has led to an increase in the clinical use of images in other planes. The advances in postprocessing have expanded the role of CT to a degree where it challenges other diagnostic techniques as the gold standard for diagnosis [2].

Postprocessing allows more scan information to be viewed at one time allowing an accurate diagnosis to be made more efficiently. The speed at which this can be done may be considered as a real-time interactive modification process. Therefore, understanding the need for routine thin-section axial MDCT to allow 3-D applications is critical for making clinical use of postprocessing [3]. Use of postprocessing including 3-D visualization has become a necessity [4] that is particularly important in paediatric practice where invasive clinical diagnostic tools can be replaced or at least assisted by modern postprocessing techniques.

This review describes the MDCT postprocessing tools in routine clinical use and identifies indications, advantages and disadvantages of each in relation to imaging the paediatric airways. It also explores more advanced postprocessing, more familiar to biomedical researchers, that will soon find their way into clinical practice, in particular in relation to computer-aided diagnostic tools.

Visualization techniques

Four visualization techniques are in clinical use on clinical workstations: multiplanar reformation (MPR) including curved plane reformation (CPR), maximum and minimum intensity projections (MIP/MinIP), shaded surface display (SSD) and volume rendering (VR). The first two techniques are limited to external visualization while SSD and VR can be used for both external and internal visualization [4].

Multiplanar reconstruction and curved plane reformation

MPR is the process of using the data from axial CT scans to create non-axial 2-D images. MPR images are coronal, sagittal, oblique or curved plane images generated from only one voxel thickness transecting a set or stack of axial images (Fig. 1). MPR images are in routine use, including for the evaluation of airways. Similar to MPR, CPR is a tomogram one voxel thick, but it is capable of demonstrating an uninterrupted longitudinal cross-section because the display plane curves along the structure of interest. A CPR can be created to include an entire structure on a single image [3]. CPRs are created along points that are manually positioned

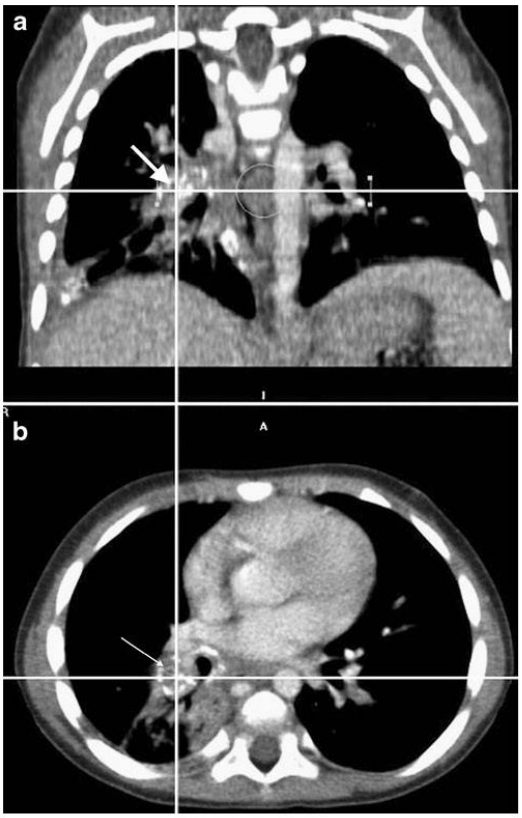

Fig. 1 Multiplanar reconstruction. Using a cross-hair on (**a**) the coronal image, it is possible to confirm the location and calcification of right hilar lymphadenopathy (*thick arrow*) on (**b**) the axial image (*thin arrow*)

over the structure of interest as viewed on transverse sections, MPRs, MIPs, SSDs or VRs. The points are connected to form a 3-D curve that is then extruded through the volume perpendicular to the desired view to create the CPR [4]. CPRs are very useful for displaying the interior of tubular structures such as blood vessels, airways and bowel. They are also useful for visualizing structures immediately adjacent to these lumina, such as mural thrombus [4]. Unlike SSDs or VRs, CPR images display the cross-sectional profile of a vessel along its length, facilitating characterization of stenosis or other intraluminal abnormalities [3].

Limitations

One major limitation of traditional MPR is that structures must lie in a plane, and almost all structures for which 3-D visualization is desired do not lie within a single plane.

MPR therefore cannot be used to demonstrate an entire structure at one time and pseudostenoses may appear on MPR images. One solution to this problem is to use CPR [4]. An important limitation of CPRs is that they are highly dependent on the accuracy of the curve. Inaccurately positioned or insufficient numbers of points can result in the curve slipping-off the structure of interest, again leading to pseudostenoses [3, 4]. A single curve also cannot accurately display eccentric lesions. Therefore, two orthogonal curves should always be created to provide a more complete depiction of eccentric lesions, particularly in stenosis [4]. Manual derivation of the curved plane is also time-consuming [3].

Maximum intensity projection

Multiplanar images can be thickened into slabs using projectional methods such as MIP, MinIP and average intensity projections/raysum (sum of all pixel values encountered by each ray to provide an image similar to a radiograph) [3, 4]. MIP is a widely used rendering tool particularly for evaluation and display in CT angiography, and has been shown to be more accurate than surface rendering for evaluating the vasculature. However, an understanding of how the MIP algorithm produces renderings and of the limitations of MIP is essential for the correct interpretation of MIP images [2].

MIPs are created when a specific projection is selected (e.g. anteroposterior) and rays are cast perpendicular to the view through the volume data MIP with only the brightest voxel being projected into the resultant image. The algorithm achieves this by selecting the voxels with the highest attenuation along lines projected through the volume dataset [4, 5]. The result is a 2-D image of 3-D information because the entire volume is collapsed with only the brightest structures being visible. Thick-slab MIPs can be applied to angiography data to include long segments of a vessel [3] (Fig. 2). There tends to be much less variability in MIP image reconstruction than in VR because fewer parameters are factored into the MIP algorithm [4] (Table 1). The application of MIP reconstructions for the lung has been shown to increase nodule detection and can help differentiate between small nodules and vessels [6]. This is not an ideal method for demonstrating the airway itself, but it is useful for evaluating the surrounding structures to determine a cause of airway compression.

Limitations

MIP images usually contain 10% or less of the original data [3]. The presence of high-attenuation voxels, other than those of interest, may obscure evaluation of the vasculature, but this is mainly a problem when evaluating atherosclerotic vessels in adults where there are large calcifications within the vascular lumen. The 2-D MIP display can also depict the 3-D relationships of structures inaccurately, causing misrepresentation, especially when there are overlapping structures, because there are no visual cues for depth perception [3]. This limitation can partially be overcome by thinner sliding slab MIP reconstructions [6, 7].

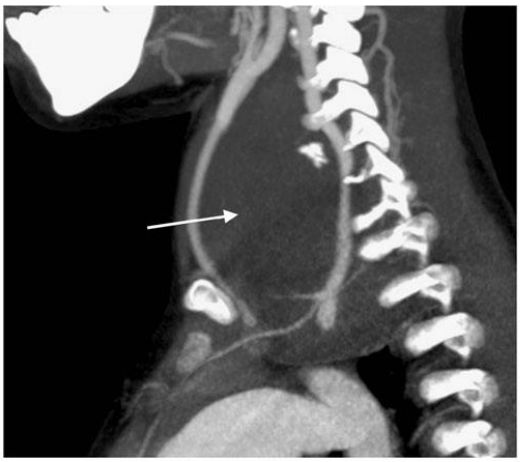

Fig. 2 Maximum intensity projection. When viewed parasagitally, the MIP image clearly demonstrates the contrast-enhanced blood vessels that are displaced and encased by a mass lesion (*arrow*) in the neck. Extension of the mass into the thorax is clearly demonstrated

Table 1 Comparison of advantages and disadvantages of VR and MinIP/MIP

Volume Rendering (VR)	MinIP/MIP
Accurate 3-D relationships demonstrated	Inaccurate 3-D relations
Shows additional structures (soft tissue, bone)	Only shows airways or vessels in detail
Colour display helps interpret complex relationships	Grey-scale windowing only
Calcified vessels not a major problem for depicting lumen size	Calcified vessels result in inaccurate representation of vessel size
Does not require editing	Requires editing
Does require adjustment of parameters, and interactive nature makes it subject to interobserver variability (speed depends on the user)	Simplicity makes it easy to master and does not require much interactivity
Advantages in ability to rotate a structure	Some advantages in demonstrating smaller vessels, especially collaterals

Minimum intensity projection

This is a particularly useful technique for imaging the major airways [4, 5]. MinIP images are a variation of the MIP approach where multiplanar slab images are produced by projecting only the lowest attenuation value when a ray is cast perpendicular to the view through the volume of data (Fig. 3) highlighting air-filled structures (as these have the lowest Hounsfield unit value). Most MinIP and MIP methods use only windowing parameters (window width and centre, specified in Hounsfield units) and not colour (Fig. 4). An advantage of MinIPs over MPRs is that structures that do not lie in a single plane, such as the bronchial tree, are visible in their entirety [5]. This allows determination of the length of airway strictures on one slice (Fig. 5). Thin-slab MinIP images (with section thickness less than 10 mm) viewed in sequence (much like scrolling through single-pixel MPR images), also known as a sliding slab, may provide more useful diagnostic information, as small structures are better detected [3] (Fig. 6).

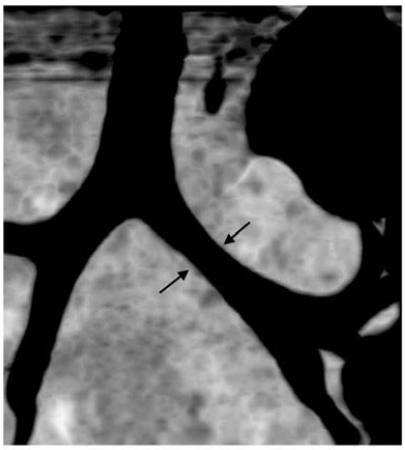

Fig. 4 Thick-slab coronal MinIP image using a soft tissue window demonstrates the full length of the major airways as well as lymphadenopathy, which is causing subtle compression of the left main bronchus (*arrows*)

Limitations

Limitations are the same as for MIP especially with regard to lack of appreciation of depth relationships [3].

Shaded surface display

SSD is termed a threshold-based classification technique. It provides 3-D views of the surface of an object by using grey-scale to demonstrate surface reflections from an imaginary source of light. SSD displays a single surface generated from thresholds selected by the user [4] (Fig. 7). The CT data are reduced to binary data to achieve this, defining each pixel as either in or out of the threshold range [3, 4]. Some versions allow several threshold ranges to be defined and displayed using different colours. In this setting, different tissue types or structures are coded as different colours to allow differentiation of adjacent structures, but for each classification, data segmentation is required, typically by using a threshold and editing, which dramatically increases postprocessing time. However, the main advantage of threshold-based rendering is its processing speed, since a comparatively small amount of computational power is needed [4].

Limitations

Much like MIP, SSD is flawed because it uses less than 10% of the acquired data [3]. The reduction to binary data limits

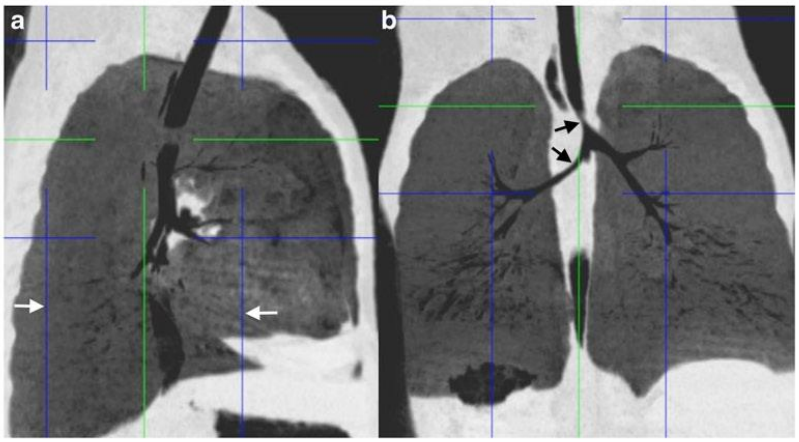

Fig. 3 Minimum Intensity projection. **a** The thickness of the coronal slab is decided on the sagittal image as a vertical thick slab selection (*white arrows*). **b** This yields a coronal MinIP image that includes the full thickness of all major branches of the tracheobronchial tree, thereby reliably demonstrating compression of the trachea and the right bronchus (*black arrows*) in this patient with situs inversus

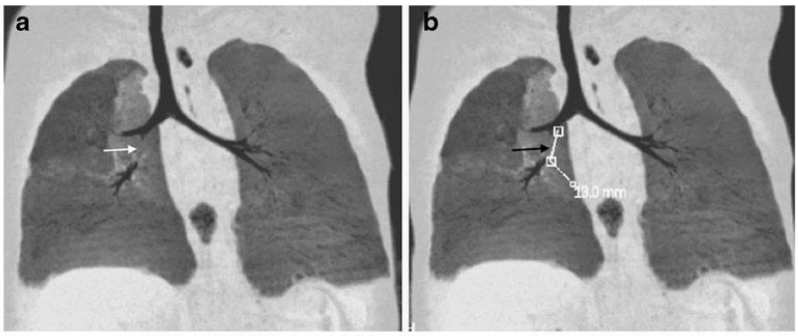

Fig. 5 Coronal MinIP images utilizing a lung window. The major airways are demonstrated on a single image, providing information on the degree of compression of the bronchus intermedius (**a** *white arrow*) as well as allowing measurement of the length of the compression (**b** *black arrow*), which has resulted from right hilar and subcarinal lymphadenopathy

flexibility and makes this postprocessing technique prone to artefacts. Regardless of the number of tissue groups or classes assigned, the selection of the threshold range that defines the groups is arbitrary and this limits accuracy [4]. Voxels that represent mixed tissue interfaces cannot be accurately classified. This makes the system incompatible with volume averaging and results in incorrect classification of voxels that contain volume averages [3]. The thresholding makes the technique susceptible to noise introduced during scanning. A small amount of noise can modify attenuation values and create the appearance of soft tissue in a voxel that actually represents mostly bone [2]. All of these disadvantages add up and many artefacts are described on the end image: "holes in structures, contours that represent voxel boundaries rather than true tissue interfaces, fragments of structures floating in space, and absence or exaggeration of details such as bone fractures" [2].

Volume rendering

VR is the most advanced of the rendering techniques and is the technique that allows the majority of clinically useful postprocessing. It refers to a 3-D volume reconstruction method that allows every voxel in the volume data to contribute to the reconstructed image [7]. The technique is termed a percentage classification (semitransparent volume-based/continuous technique). Simplistically, all voxel values are assigned an opacity level that varies from total transparency to total opacity. This can be applied to voxel values as a whole or to regions of the histogram that are classified as specific tissue types [4]. In percentage classification, it is assumed that a voxel may represent one or more tissue types and that the amount of each tissue as a percentage of the entire

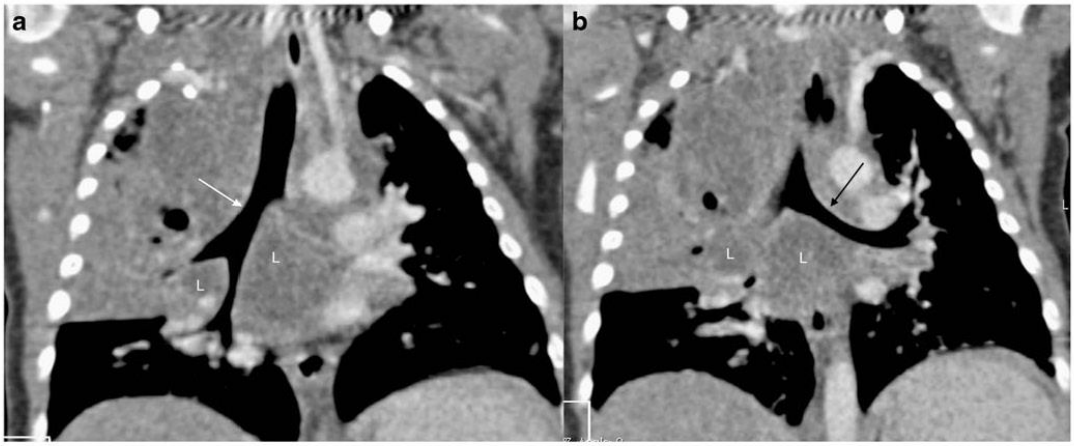

Fig. 6 Sequential coronal oblique thin-slice sliding slab MinIP images using soft-tissue window. Thin slab images do not demonstrate the airway on one single slab but rather demonstrate (**a**) the right major airways (*white arrow*) on an anterior slice and (**b**) the left airways (*black arrow*) on contiguous thin slabs. This is similar to scrolling through a coronal MPR but having a choice of slice thickness. In this patient, there is complete occlusion of the right upper lobe bronchus and moderate narrowing of the bronchus intermedius resulting from tuberculous lymphadenopathy (*L*). There is also extensive parenchymal disease distal to the right upper lobe obstruction with necrosis and breakdown

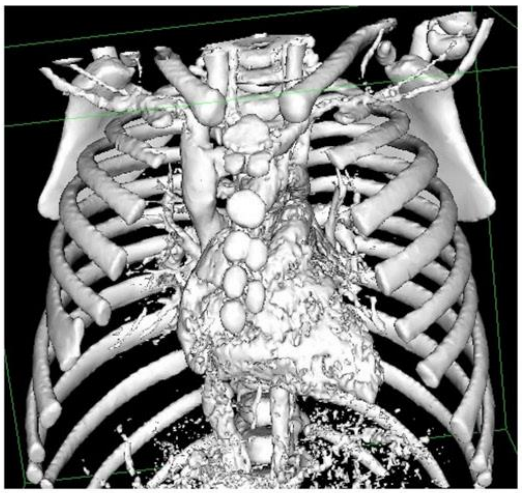

Fig. 7 Surface-shaded display image of the chest, anterior view. The image was generated using a threshold setting to preferentially demonstrate dense structures including bones, contrast-enhanced blood vessels and heart

voxel is between 0% and 100% [4, 7]. Once colour and transparency are assigned to each classified voxel, a 3-D image is produced by casting simulated rays of light through the volume. In addition, in VR there are adjustable parameters to change the way the image looks, including window setting, colour, degree of opacity and shading (Fig. 8). Angle and distance can also be determined. VR allows the operator to select a variety of viewing perspectives by rotating the 3-D reconstruction through a preset number of views or by manually customizing a desired view in real time (Fig. 9). VR images do not have many of the computer artefacts found with SSD. Most importantly, it has been shown that average reading time using VR images is significantly shorter than with MIP images [7].

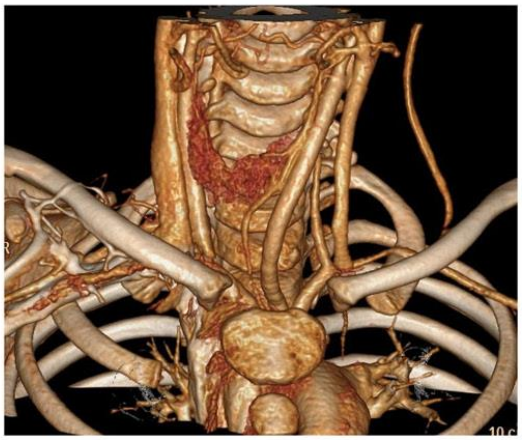

Fig. 8 3-D volume-rendered image generated using density, transparency and colour suited to demonstrating bone and blood vessels enhanced by contrast. As well as demonstrating these structures, the depth relationship of each can be appreciated as a possible cause of tracheal compression

Limitations

Inaccuracies in VR stem from mucus secretions, dynamic airway changes and artefacts such as the stair-step artefact encountered in up to 3% of images [1] (Fig. 10). VR also requires more computational power than SSD because each voxel must be projected into an image, while in SSD only the surface data need processing. On modern computers, even large datasets can be manipulated interactively, and the display can be instantaneously changed from VR to MIP as required. Interactive adjustment of VR parameters, rotation of the dataset and automated clip plane editing all can be performed in real time, but this places additional time constraints on the radiologist, who needs to be involved interactively.

Endoluminal visualization/virtual endoscopy

Both SSD and VR allow the production of images of the inner surface of tubular lumens, and the technique has been termed virtual endoscopy. This can be used to examine the bowel, airways, blood vessels and the urinary tract [4, 5]. The basic technique involves identification of threshold levels for SSD that exclude pixels of similar attenuation to the lumen (−900 to −1,000 HU for air-filled volume and 150 to 400 HU for contrast-enhanced volume) or an opacity curve for VR that results in complete transparency of the lumen. Rendering creates an image of the interface between luminal contrast and extraluminal attenuation and not the mucosa or intimal surface. The two methods widely in use are orthographic external rendering with cut planes and immersive perspective rendering [4].

Orthographic rendering

This is the most commonly used technique particularly for external visualization of a lumen from a viewpoint that is external to the data [3, 4]. It can, however, also be used for internal visualization when combined with cut planes positioned within the lumen of the structure of interest. This can be compared to cutting a "window into a piece of pipe to visualize its interior" [4].

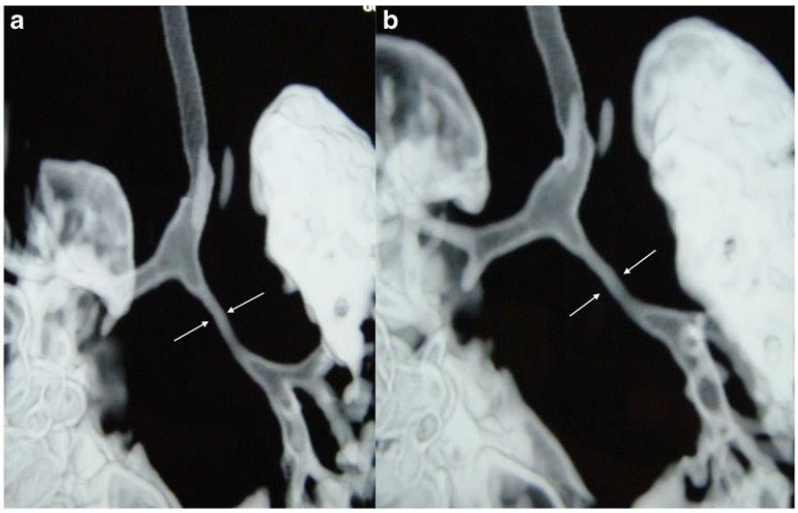

Fig. 9 3-D volume-rendered images generated using density and transparency settings suited to airway and lung visualization. Rotation of the dataset allows the degree and length of left main bronchus narrowing (*arrows*) to be visualized. In this patient, the left main bronchus compression was due to an anomalous artery

Limitations/disadvantages

This method only provides a regional snapshot; it cannot provide a continuous demonstration of all interior surfaces of a lumen [4].

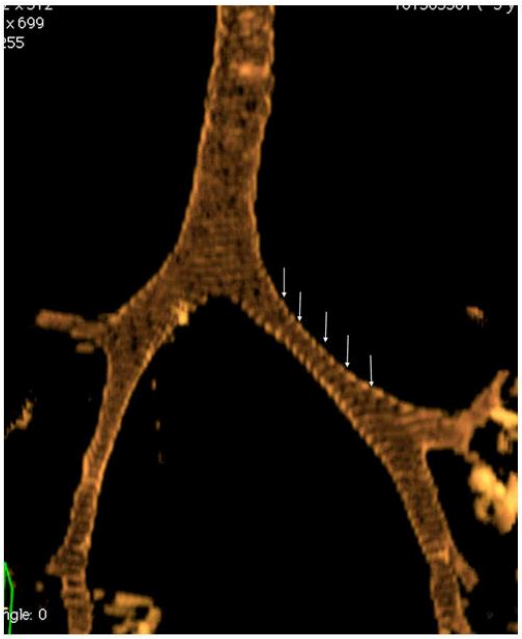

Fig. 10 3-D VR image showing the stair-step artefact (*arrows*) in a child with mild narrowing of the bronchus intermedius and left main bronchus

Immersive/perspective rendering

The viewpoint using this technique is from within the lumen (Fig. 11) mimicking fibre-optic endoscopy, and bypassing the limitations of the invasive technique that requires access to the lumen and has a restricted direction of viewing. For the viewer to have perspective on depth relationships at close range, a modelling technique is used that functions in a manner similar to the human visual system. In the same way that light rays are focused to converge on the retina, the viewer recognizes the distance of structures depending on their size. A structure close to the eye appears larger than a structure farther away. This effect is determined by the field of view of the virtual lens [4].

Limitations

Opacity and colour selection and the complexity of creating these visualizations can be daunting. The greatest problem with immersive visualization, however, is navigation. This is because there are three spatial degrees of possible position and three spatial degrees of possible view direction [4]. Without an external guide of the view position, it is easy to lose track of location within the lumen. Techniques that automatically create a flight path through the centre of a lumen are being developed to address this [4].

Advantages of CT postprocessing of the airway in children

Even though there is a shift away from the use of MDCT in children because of the radiation dose, it is important that,

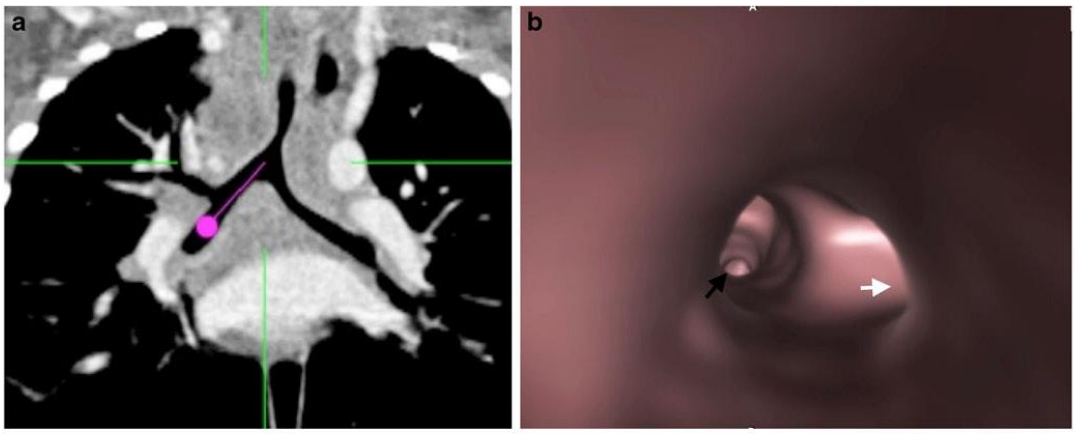

Fig. 11 The immersive (perspective) rendering technique results in images that mimic fibre-optic tracheobronchoscopy. Navigation tool image (**a**) and virtual endoscopy image (**b**) at the level of the right upper lobe bronchus (*white arrow*) and bronchus intermedius (*black arrow*)

having decided to use CT, a full volume of data is obtained after administration of intravenous contrast agent. This then represents a single and complete MDCT study that can be reconstructed as many times as necessary, in as many ways as desired and for as long as the raw data are stored.

To be useful, CT postprocessing must result in better anatomical detail and supply additional information relevant to diagnosis and management of the disease than the original axial images. A radiologist may, however, see the advantage of providing imaging information that is more easy to interpret and more easy to communicate to the referring clinician or parent even in situations where there is no further diagnostic value than the original axial views. For demonstrating airways, it is advantageous to depict the full tracheobronchial tree at once, the relationships of normal anatomical structures to the airway, any anomalies associated and any pathology that may be causing the airway compression in a way that clinicians and parents can understand. This can be achieved using postprocessing of images to mimic gross pathological specimens or endoscopic views. Thus, without additional imaging or radiation burden to a child, a clinician or a parent may be convinced of the benefits of further management or even of conservative management so that unnecessary interventions are avoided. Reconstructed CT views of the airway in children have been reported to have significantly reinforced the confidence in

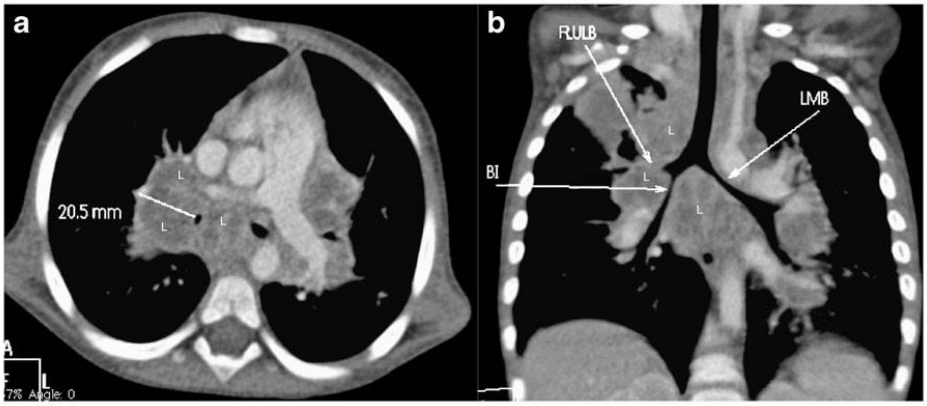

Fig. 12 Thick-slab MinIP in a child with primary lymphobronchial tuberculosis. Axial (**a**) and coronal (**b**) views demonstrate airway compression by lymphadenopathy (*L*) at multiple sites including the right upper lobe bronchus (*RULB*), the bronchus intermedius (*BI*) and the left main bronchus (*LMB*). This provides a practical means of demonstrating pathology to pulmonologists and thoracic surgeons who are contemplating lymph node enucleation for relieving the obstruction

diagnoses and improved communication with clinicians allowing more comprehensive surgical planning [8 11].

MPR is as accurate as axial CT, is easy to create and view, and improves perception as it displays information effectively [8, 9]. MinIP allows the detection of low-density structures and is therefore ideal for improving evaluation of paediatric airways [9, 10] (Fig. 12). MIP is ideally suited to demonstrating hyperdense pathologies such as vessel abnormalities, nodules, calcifications and foreign bodies that are associated with airway pathology [9]. VR techniques add value to imaging complex structures and interfaces that cross the traditional imaging planes [8, 9]. The 3-D images [9] simplify demonstration of pathology to the referring clinician and increase diagnostic confidence for all involved [8]. They are excellent for demonstrating a decrease in airway calibre, spatial relationships of structures, measuring stenoses to determine degree and length and identifying the cause of an airway stenosis [1]. The accuracy of detection of airway compression by 3-D VR has been reported to 95.7% compared to 91.5% for conventional CT [12].

Virtual bronchoscopy (VB) is a noninvasive endoluminal visualization technique that simulates bronchoscopy [9]. It provides a realistic endoscopic 3-D view of the tracheobronchial tree and is particularly useful in children. VB has additional advantages over true bronchoscopy in that it also allows simultaneous visualization of structures around the tracheobronchial tree, which helps in the identification of the cause of an obstruction [11]. VB is particularly attractive for imaging airway stenosis when traditional bronchoscopy presents a risk to a child, or when navigation of a bronchoscope is not possible due to a high-grade stricture [8], and VR is used to outline the bronchial lumen beyond this. The technique can

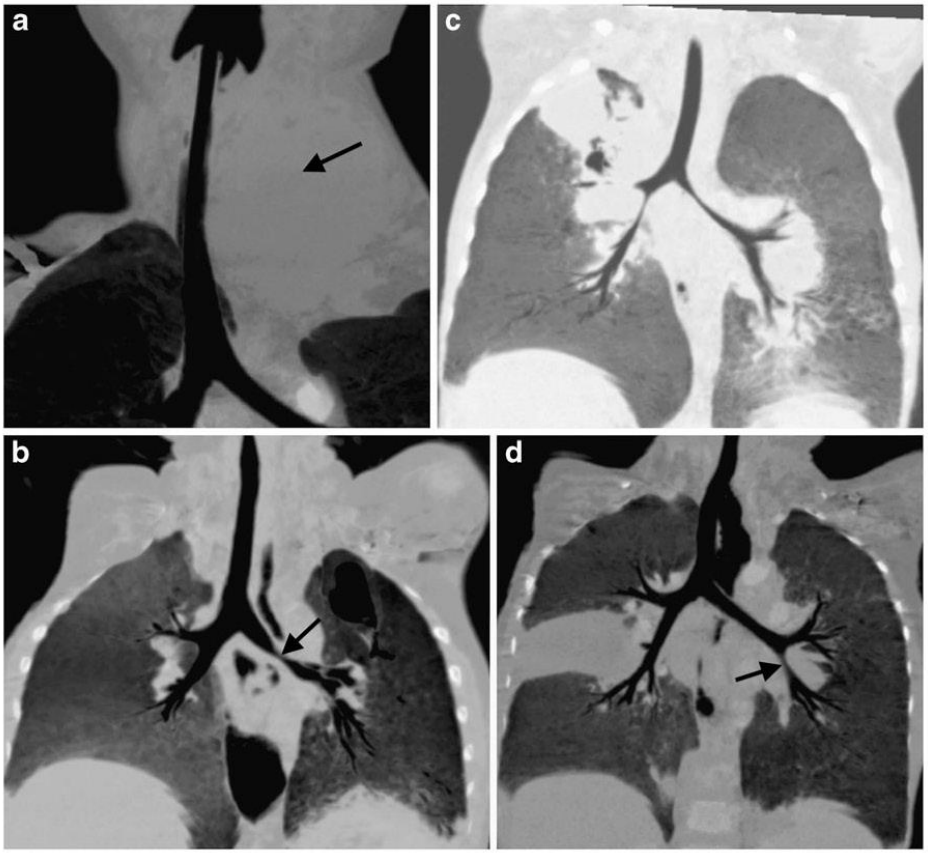

Fig. 13 MinIP images on lung window in children presenting with airway symptoms and signs. **a** Right tracheal displacement due to a left neck mass (*arrow*). **b** Focal left main bronchus compression by tuberculous lymphadenopathy. **c** Multifocal airway narrowing by tuberculous lymphadenopathy (right upper lobe, bronchus intermedius and left main bronchus). **d** Isolated narrowing of the left lower lobe bronchus (*arrow*) due to tuberculous lymphadenopathy

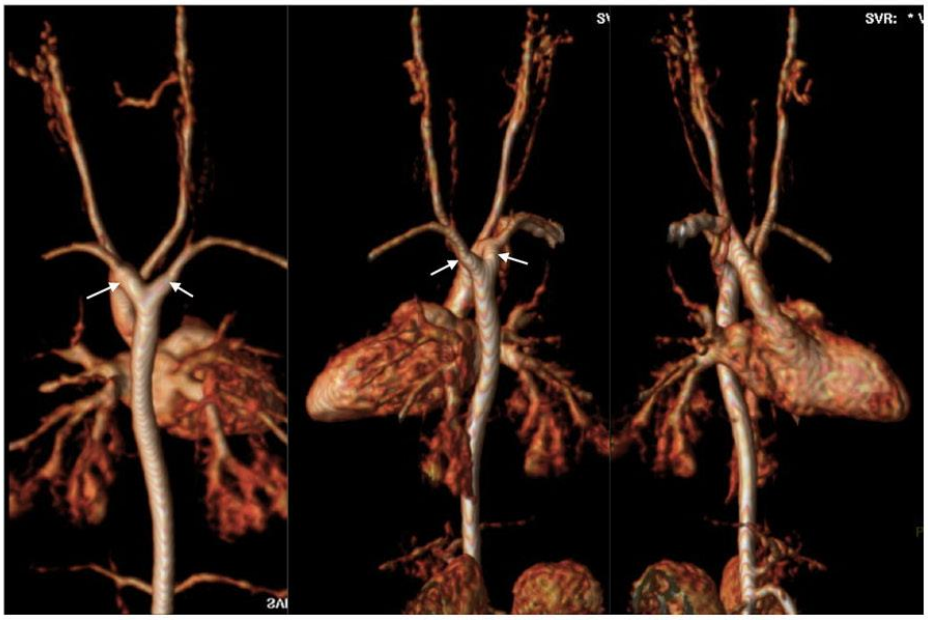

Fig. 14 3-D VR images. Multiple rotated views demonstrate the advantages of 3-D VR in the diagnosis and evaluation of this double aortic arch anomaly (*arrows*) as a cause for stridor and tracheal stenosis

also be used for planning transbronchial biopsy, endobronchial laser therapy and stenting [5].

Postprocessing for airway diseases in children

Identification and better characterization of tracheobronchial stenosis is the main indication for airway postprocessing techniques. Even though MPR and MinIP are extremely useful tools in evaluating tracheobronchial stenoses (Fig. 13), which are vertical or slightly oblique [8], it is 3-D VR that both allows 3-D reformatting of airways and demonstrates associated adjacent vascular structures [8]. It illustrates focal areas of narrowing, the craniocaudal length of tracheobronchial stenoses and even demonstrates the airway beyond the major stenosis. MinIP may demonstrate the airway equally as well, but VR is more useful when complex tracheobronchial congenital anomalies with vascular and other anatomical associations are being evaluated (Fig. 14) [8, 10].

Causes of tracheobronchial stenosis in children include tracheomalacia often associated with compressive vascular rings (Fig. 13), tracheooesophageal fistulas, hilar or mediastinal tumours, foreign bodies (Fig. 15) [8, 11] and mucoid impaction. In addition, reconstructions can be used for imaging the distal airways [8, 10], especially in suspected bronchiectasis (Fig. 16), for defining bronchoceles [8] and when planning a diagnostic lung biopsy [8].

For imaging lymphobronchial tuberculosis (i.e. the involvement of the airway by compressive lymphadenopathy of primary tuberculosis), the relationships between the bronchial walls and lymph nodes are extremely well demonstrated using reconstruction techniques [8]. The airway is most

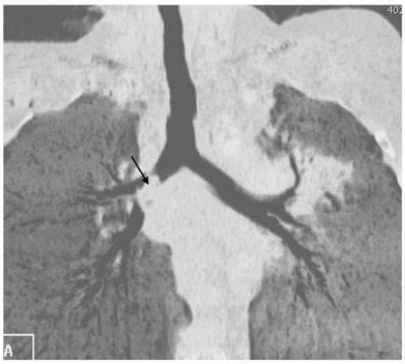

Fig. 15 Coronal MinIP image on lung window. MinIP adequately demonstrates endobronchial material (*arrow*) in the right main bronchus and bronchus intermedius (in this case granulation tissue from a tuberculous lymph node erosion into the airway). Fibre-optic tracheobronchoscopy was performed and the material was aspirated acting as both a therapeutic and a diagnostic procedure

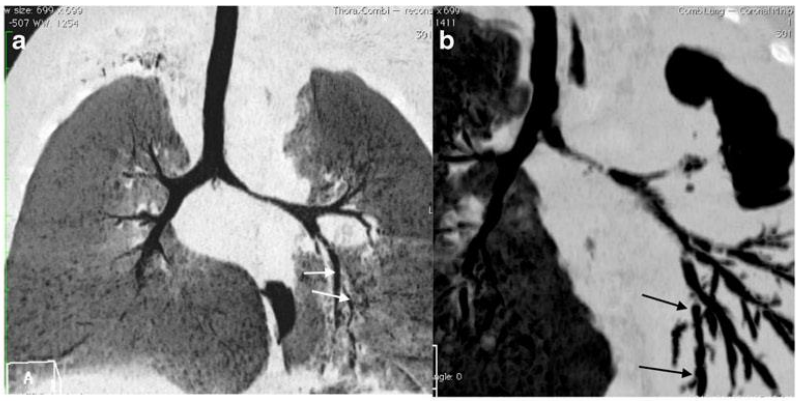

Fig. 16 Coronal MinIP images on lung window. MinIP demonstrates the distal airways and can distinguish air bronchograms related to an airspace process (*white arrows*) (**a**) from bronchiectasis (*black arrows*) (**b**)

easily compared to a chest radiograph using the MinIP technique, which is considered to be a useful training tool for tuberculosis workers restricted to the use of plain radiographs (Fig. 13). Du Plessis et al. [1] compared 3-D VR with FTB in 26 children with lymphobronchial tuberculosis (median age 21 months) and demonstrated a 92% sensitivity and 85% specificity for airway compression compared to traditional bronchoscopy. However, the VR technique was additionally successful in demonstrating a further 51 sites of stenosis, provided a description of the degree of stenosis in all patients, and in three of four patients even demonstrated stenotic airways beyond a proximal stenosis that the bronchoscope could not pass [1]. The readers also expressed the length of the stenosis and identified the cause of the stenosis in all children. FTB assumed the cause to be lymphadenopathy in all children, but

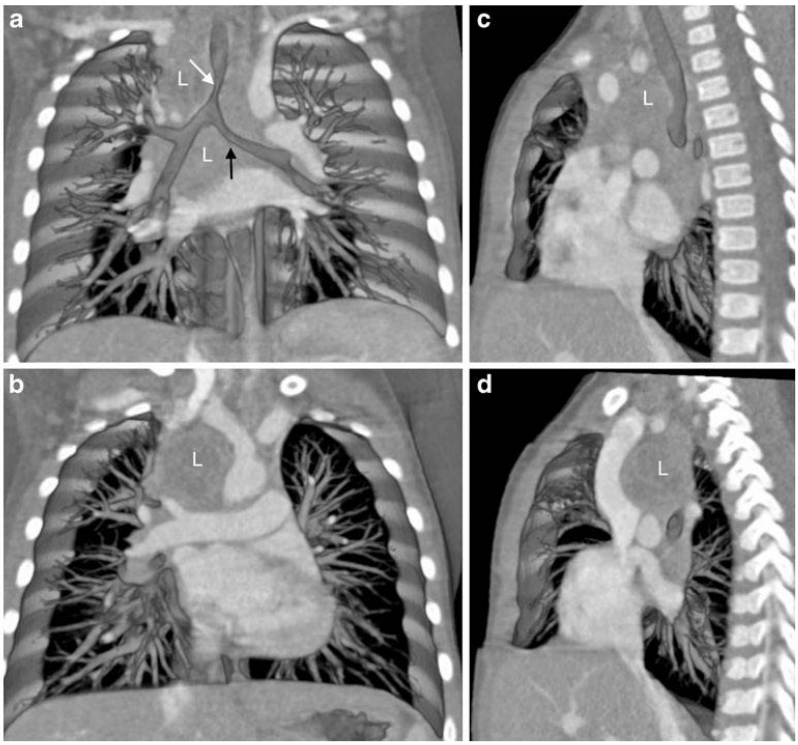

Fig. 17 3-D VR images. Multiple views demonstrate tracheal (**a** *white arrow*) and left main bronchus (**a** *black arrow*) narrowing caused by large mediastinal and subcarinal lymphadenopathy (**a**–**d** *L*) in a child with primary pulmonary tuberculosis

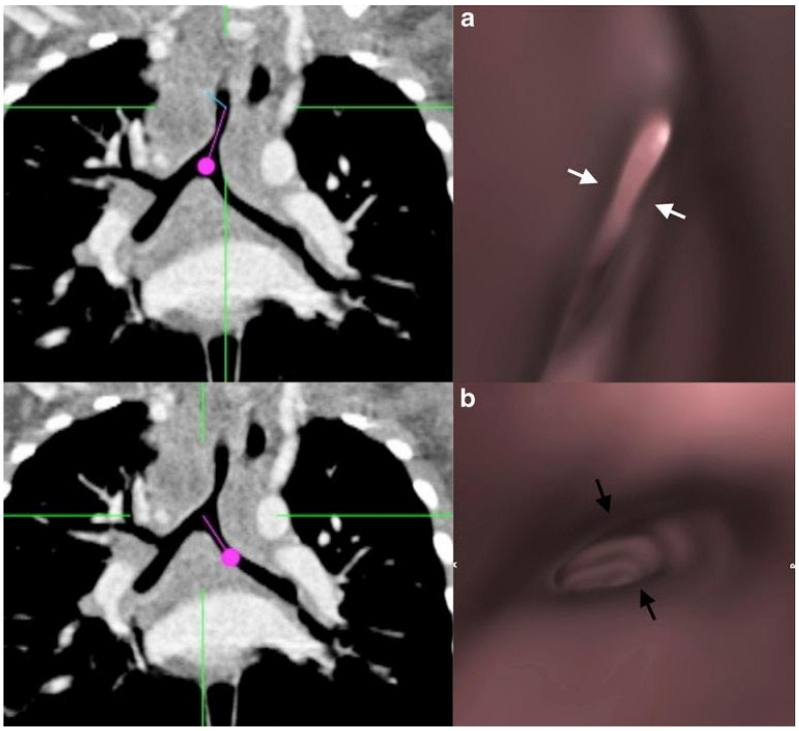

Fig. 18 Immersive virtual endoscopy in the same child as in Fig. 17 shows tracheal narrowing (**a** *white arrows*) and left main bronchus narrowing (**b** *black arrows*) adjacent to the respective navigation coronal images that help orientate the operator

VR demonstrated that 14% of the airway stenoses were from other causes [1].

Figure 17 demonstrates the usefulness of the 3-D VR technique in demonstrating tracheal and left main bronchus compression while also demonstrating the causative lymphadenopathy and relationships to blood vessels. Figure 18 demonstrates the navigation and endoscopic views in the same patient, which may assist in communicating the location and severity of stenosis to a bronchoscopist planning to perform a transbronchial biopsy.

Research tools: advanced postprocessing currently for research and CAD

Automatic segmentation of high-resolution CT images can extract and analyse the structure of the tracheobronchial tree and distinguish airway regions from surrounding tissue, including the lung. Improvements to these methods mean that smaller branches can be visualized. Postprocessing can be used to perform various measurements including identification of branching topology as well as branch dimensions and cross-section measurements. This technique can generate automated airway statistics at the click of a button. More sophisticated postprocessing can apply learning algorithms to develop models from entire datasets of CT scans. These models can then be used to automatically identify each anatomical airway branch and then detect normal and pathological variations related to a specific disease. Most postprocessing methods have been developed for and tested on adult airways, and limited work has focused on paediatric airways. Paediatric airway analysis

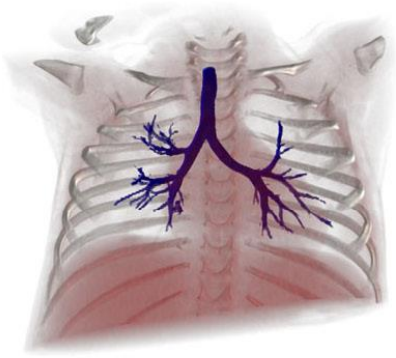

Fig. 19 Segmentation with bone rendering of the airway in a 20-month-old patient

introduces additional challenges to postprocessing. Smaller patient size and radiation dose considerations mean that the airways are extracted at a lower resolution and fewer branches are extracted [10]. In this section, we present general methods that can be applied to adults and children as well as specific methods and examples from our own work in paediatric airway analysis.

Segmentation

There are many airway segmentation algorithms that use a variety of mathematical techniques, but these methods usually comprise common steps. A typical airway segmentation algorithm would consist of the following steps: (1) identification of an initialization point within the airways, (2) application of filtering techniques to enhance the airways, (3) detection of connected airway regions from the initialization point, and (4) detection and removal of non-airway regions that have been mistakenly classified.

The main airways can be segmented more easily than smaller bronchi because they have a well-defined wall and therefore there is greater contrast between wall and lumen. Simple thresholding methods are often used to extract the larger airways while more sophisticated methods are used for the smaller bronchi. This saves processing time and allows the algorithm to be tailored more specifically to the smaller airways [13]. Airway segmentation methods include: adaptive thresholding [14], fuzzy connectivity [15], rule-based segmentation [13], morphology-based connection cost [16], and morphological filtering [17, 18]. The evaluation of these methods is a challenge because there is no common gold standard airway segmentation dataset. However, a number of state-of-the-art airway segmentation methods were evaluated as part of the EXACT'09 airway segmentation competition [19].

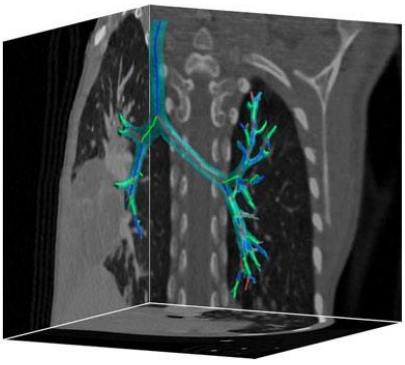

Fig. 20 Airway centre line and bifurcation point detection from a paediatric chest CT scan

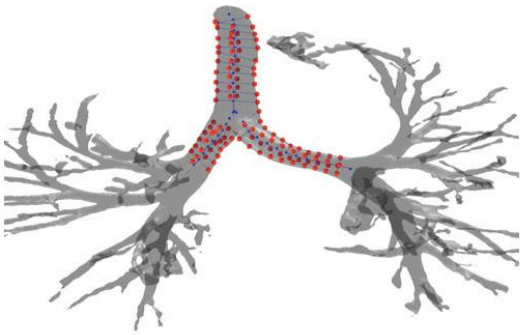

Fig. 21 Branch measurement by projection of points onto the airway surface from the medial line

Very few of the methods have been applied to paediatric CT volumes. Irving et al. [18, 20] developed a method targeted at paediatric airway volumes in which a threshold is applied to extract air-filled regions and therefore approximate the lung regions. The trachea is identified in the axial slices above the lung region and used to initialize the segmentation. The trachea is air-filled and therefore has a lower HU value than the surrounding tissue, and can be identified in cross-section. However, other objects within the same HU range may also be extracted so that a number of features, including the cross-sectional area, location and circularity, are used to identify the trachea [18]. A morphological filtering method is then applied to the CT volume in the axial, coronal and sagittal directions. This filter uses morphological closing and reconstruction to enhance regions with a circular appearance [21] and therefore enhances cross-sections of the airway in the three directions. Once a range of morphological filters have been applied to enhance airways of various sizes, a threshold value is applied to extract likely airway regions. Finally, a region-growing method is applied to extract just the connected airway. This region-growing method starts at the seed point located in the trachea and adds neighbouring voxels with 26-connectivity until no other voxels can be added [18].

Segmentation of the airway can be used to improve the rendering of the airway as well as to provide automated analysis of the airway that cannot be achieved with just rendering. An example of the resulting segmentation of the airways in a 20-month-old patient is shown in Fig. 19. Note also that some small regions have been misclassified as airway and there is a limit to the number of branches that are segmented. Each improvement in paediatric CT imaging and segmentation will lead to more accurate airway extraction.

The limitation of many segmentation algorithms is that in order to extract just the airways without additional regions being mistakenly included, the airway needs to be completely connected, i.e. branches are not obstructed. To include

obstructed branches, our algorithm performs a shape analysis of each section of the airway to identify obstructed branches and then searches for additional airway components beyond the obstruction [20].

Skeletonization

Once the airways have been segmented, centre-line extraction is an important intermediate step before more advanced airway processing can be performed.

Airway centre-line extraction algorithms produce a centre-line one voxel thick that bifurcates to form the centre line for each child branch (Fig. 20). The topological structure including branch start and end points and the relationships between parent and child branches can be extracted. The extracted medial line can also be used to direct VB and extract airway cross-sections. One method uses iterative "thinning" of the segmentation by removing voxels that do not affect the airway structure until only a one-voxel thick branching centre line remains [22]. The centre line extracted using this method in a child is shown in Fig. 20.

Branch measurements

Once the branching structure has been extracted, the start, endpoint and centre line of the branch are defined. This allows automatic measurement of the length, curvature and cross-section of the branch. The voxel size is used as a scaling factor for the volume. Branch length can be calculated from the skeleton length and branch volume is approximated as the number of voxels in the branch multiplied by the voxel dimensions [22]. From this, the approximate mean radius of the branch can be determined. Cross-sections can also be measured along each branch by projecting vectors orthogonal to the centre line to the branch surface [15]. This allows cross-sectional area and radius to be calculated, and can be extended to identify and measure branch local minima and maxima [23]. Figure 21 shows the projection of orthogonal vectors and calculation of the intersection of these vectors with the surface of the airways to measure a branch.

Branch labelling

The topological structure of the airway can be used to match each branch to its anatomical label. This can be used to provide annotated visualizations of the airway, present data about a branch of interest, and automatically compare branches in a dataset of airways. However, the labelling is made difficult by the variation in the shape and orientation of the branches, and the possibility of anomalous branches. Common methods use a template of the airway branching structure and match this to individual airway trees. Branch measurements such as branch length and orientation, angles between branches, and relationships between parent and child branches are used to match the template to the airways and a function is used to optimize these labels over the whole airway tree [24, 25].

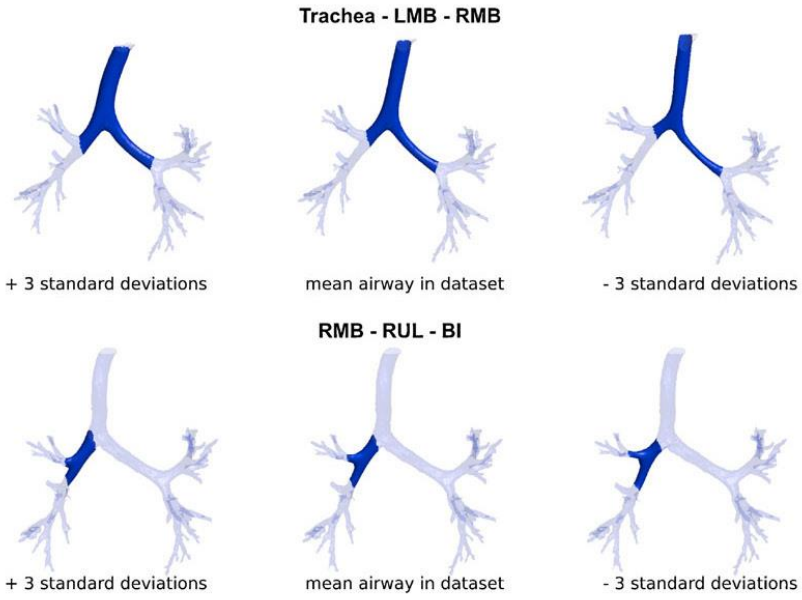

Fig. 22 Principal component analysis variation along one example mode of the trachea/right main bronchus/left main bronchus (*Trachea-LMB-RMB*) and one example mode of the right main bronchus/right upper lobe/bronchus intermedius (*RMB-RUL-BI*) regions

Computer-assisted detection of airway pathology

Automated segmentation and branch analysis can be used to evaluate and classify airways in a paediatric CT volume dataset. This procedure is used to differentiate airway deformation and stenosis from lymphadenopathy in children with tuberculosis. However, this can be extended to other airway pathologies and used in conjunction with other features of pathology.

Once a dataset of airways has been segmented and the structure analysed, the dataset can be used to train a classifier to distinguish between normal and abnormal airway variations. Irving et al. [23] created a point distribution model that represents the airways as a set of points each corresponding to a point on every other airway in the dataset. The point distribution model for each airway is automatically generated using a thin plate spline warp and localized matching to fit a template airway onto each airway segmentation. In the model of Irving et al. [23], three branch sections of the airway are represented by a set of about 1,500 (n) vertices. Each is a point in 3-D space and therefore each airway is represented by $(3\times n)$ features. Principal component analysis is a technique that can be used to reduce the dimensionality of this feature space and extract the main modes of variation from the covariance of the points within the airway dataset. This results in a more tractable number of features that can be used to classify normal and abnormal variations. Figure 22 shows one mode of variation from the trachea/right main bronchus/left main bronchus region and one from the right main bronchus/right upper lobe/bronchus intermedius region. Irving et al. [23] used ten modes of variation to represent each airway.

This method was evaluated using cross-validation on a dataset of 61 patients with and without tuberculosis. All the patients with tuberculosis showed symptoms and signs of major airway compression. The method was able to distinguish between patients with and those without tuberculosis with a sensitivity of 86% and a specificity of 91%.

Kiraly et al. [26] reviewed a number of other automated methods for airway assessment and visualization. Although these methods were evaluated on adult datasets, many methods could also be applied to paediatric airway analysis. These include methods to determine airway lumen size and wall thickness, identify mucus plugs and determine bronchus–artery ratios. These measurements can then be presented as colour-coded airway visualizations for assessment.

Conclusion

CT postprocessing techniques permit the demonstration of fine anatomical detail, provide additional information relevant to diagnosing and managing airway disease and supply images that are easily interpreted, specifically for improved communication with referring clinicians and parents. Postprocessing methods also have the potential to automate airway visualization, identify airway anatomy and detect regions of pathology. Improved airway segmentation will offer improved visualization of the smaller bronchi and allow automatic extraction of the airway structure. Branch measurements can then be automated and analysis of large datasets of images can be performed. These methods would allow clinicians to view the airways with overlays indicating airway properties or the likelihood of disease based on comparison to a dataset of airway images.

References

1. du Plessis J, Goussard P, Andronikou S et al (2009) Comparing three-dimensional volume-rendered CT images with fibreoptic tracheobronchoscopy in the evaluation of airway compression caused by tuberculous lymphadenopathy in children. Pediatr Radiol 39:694–702
2. Fishman EK, Ney DR, Heath DG et al (2006) Volume rendering versus maximum intensity projection in CT angiography: what works best, when, and why. Radiographics 26:905–922
3. Dalrymple NC, Prasad SR, Frecketon MW et al (2005) Informatics in radiology (infoRAD): introduction to the language of three-dimensional imaging with multidetector CT. Radiographics 25:1409–1428
4. Rubin GD (2003) 3-D imaging with MDCT. Eur J Radiol 45 (Suppl 1):S37–S41
5. Kirchgeorg MA, Prokop M (1998) Increasing spiral CT benefits with postprocessing applications. Eur J Radiol 28:39–54
6. Ueno J, Murase T, Yoneda K et al (2004) Three-dimensional imaging of thoracic diseases with multi-detector row CT. J Med Invest 51:163–170
7. Peloschek P, Sailer J, Weber M et al (2007) Pulmonary nodules: sensitivity of maximum intensity projection versus that of volume rendering of 3D multidetector CT data. Radiology 243:561–569
8. Papaioannou G, Young C, Owens CM (2007) Multidetector row CT for imaging the paediatric tracheobronchial tree. Paediatr Radiol 37:515–529
9. Perandini S, Feccioli N, Zaccarella A et al (2010) The diagnostic contribution of CT volumetric rendering techniques in routine practice. Indian J Radiol Imaging 20:92–97
10. Siegel M (2003) Multiplanar and three-dimensional multi-detector row CT of thoracic vessels and airways in the pediatric population. Radiology 229:641–650
11. Sodhi KS, Aiyappan SK, Saxena AK et al (2010) Utility of multidetector CT and virtual bronchoscopy in tracheobronchial obstruction in children. Acta Paediatr 99:1011–1015
12. Remy-Jardin M, Remy J, Artaud D et al (1998) Volume rendering of the tracheobronchial tree: clinical evaluation of bronchographic images. Radiology 208:761–770
13. Sonka M, Park W, Hoffman E (1996) Rule-based detection of intrathoracic airway trees. IEEE Trans Med Imaging 15:314–326
14. Mori K, Hasegawa J, Toriwaki J et al (1996) Recognition of bronchus in three-dimensional X-ray CT images with application to virtualized bronchoscopy system. In: Proceedings of the 13th International Conference on Pattern Recognition, vol 3. Vienna, Austria. IEEE Computer Society, Washington DC, pp 528–532

15. Tschirren J, Hoffman E, McLennan G et al (2005) Intrathoracic airway trees: segmentation and airway morphology analysis from low-dose CT scans. IEEE Trans Med Imaging 24:1529–1539
16. Fetita C, Preteux F, Beigelman-Aubry C et al (2004) Pulmonary airways: 3-D reconstruction from multislice CT and clinical investigation. IEEE Trans Med Imaging 23:1353–1364
17. Kiraly A, Higgins W, McLennan G et al (2002) Three-dimensional human airway segmentation methods for clinical virtual bronchoscopy. Acad Radiol 9:1153–1168
18. Irving B, Taylor P, Todd-Pokropek A (2009) 3D segmentation of the airway tree using a morphology based method. In: Brown M, de Bruijne M, van Ginneken B et al (eds) Proceedings of the second international workshop on pulmonary image analysis. London, pp 297–307
19. Lo P, van Ginneken B, Reinhardt J et al (2009) Extraction of airways from CT. In: Brown M, de Bruijne M, van Ginneken B et al (eds) Proceedings of the second international workshop on pulmonary image analysis. London, pp 175–189
20. Irving B, Goussard P, Gie R et al (2011) Segmentation of obstructed airway branches in CT using airway topology and statistical shape analysis. In: Proceedings of the eighth IEEE international symposium on biomedical imaging: from nano to macro. IEEE, Piscataway, NJ, pp 447–451
21. Vincent L (1993) Morphological grayscale reconstruction in image analysis: applications and efficient algorithms. IEEE Trans Image Process 2:176–201
22. Palágyi K, Tschirren J, Hoffman E et al (2006) Quantitative analysis of pulmonary airway tree structures. Comput Biol Med 36:974–996
23. Irving B, Goussard P, Gie R et al (2011) Identification of paediatric tuberculosis from airway shape features. Med Image Comput Comput Assist Interv 14:133–140
24. Tschirren J, McLennan G, Palágyi K et al (2005) Matching and anatomical labeling of human airway tree. IEEE Trans Med Imaging 24:1540–1547
25. Mori K, Hasegawa J, Suenaga Y et al (2000) Automated anatomical labeling of the bronchial branch and its application to the virtual bronchoscopy system. IEEE Trans Med Imaging 19:103–114
26. Kiraly A, Odry B, Godoy M et al (2008) Computer-aided diagnosis of the airways: beyond nodule detection. J Thorac Imaging 23:105

CHAPTER 6

New diagnostic methods in children with lymph node obstruction of the airway

Introduction

In this chapter three new techniques are described to enhance the diagnosis of pulmonary tuberculosis in children.

Transbronchial needle aspiration biopsy

Transbronchial needle aspiration (TBNA) has been used as a diagnostic technique in adult patients with enlarged mediastinal lymph nodes. The technique in adults has been shown to safe and effective in making a definitive diagnosis. There is however a significant risk of causing a pneumothorax during the procedure. The risk is reduced when central mediastinal lymph nodes are aspirated. In children the use of TBNA has been limited due to the size of the bronchoscope's working channel preventing the introduction of the aspiration needle. In this section of the chapter we describe performing TBNA in children with enlarged central lymph nodes.

Goussard P, Gie RP Louw M, Shubert P, Kling S, Nel ED, Rhode D,A Vanker A, Andronikou S. The diagnostic value and safety of transbronchial needle aspiration biopsy in children with mediastinal lymphadenopathy. Pediatr Pulmonol 2010; 45: 1173-1179.

The aim was to describe the diagnostic yield of TBNA in children with large subcarinal lymphadenopathy where the diagnosis of pulmonary TB could not be made by using conventional diagnostic tests and to determine the safety of TBNA in children. To limit the risk to children TBNA was only performed after chest CT-scan confirmed the presence of enlarged central mediastinal lymph nodes in children older than 6 months of age. Smaller children were excluded due to the limitations posed by airway size. A definitive diagnosis was made using TBNA in 54% of children with a median age of 41 months (range 9–168 months). In 25% of cases the TBNA was the sole source of the specimens from which the diagnosis was made. There was no difference in the diagnostic yield in HIV-uninfected children when compared to HIV-infected children (P=0.69). No serious complications were encountered during or after the procedure.

GeneXpert MTB/Rif assay

The Gene Xpert MTB/RIF assay (Xpert; Cepheid, CA, USA) has enabled rapid diagnosis and detection of drug resistance in children with pulmonary tuberculosis. Previously,

bronchoscopy in paediatric TB suspects was used to collect specimens for mycobacterial culture using especially bronchoalveolar lavage (BAL). The reported yield from BAL culture has always been inferior to those obtained by gastric lavage. Children with complicated intrathoracic tuberculosis require a rapid confirmation of the diagnosis of TB and of drug susceptibility to institute appropriate therapy.

Walters E, Goussard P, Bosch C, Hesseling AC, Gie RP. GeneXpert MTB/RIF on Bronchoalveolar Lavage Samples in Children With Suspected Complicated Intrathoracic Tuberculosis: A Pilot Study. Pediatr Pulmonol 2013; Dec 11. doi: 10.1002/ppul.22970.

The aim was to explore the value of GeneXpert as an add-on test to mycobacterial culture for the confirmation of TB in children suspected of having complicated intrathoracic TB. Children between 3 months and 13 years with complicated intrathoracic tuberculosis in which bronchoscopy were indicated, were investigated and a bronchoalveolar specimen collected during fibreoptic bronchoscopy. Fourteen children (2 HIV positive, median age 16 months) were investigated. TB was confirmed in 11 cases (78%), by either culture or GeneXpert . In 9/14 (64%) cases were confirmed by culture and BAL Xpert was positive in 7 cases (78% sensitivity). BAL GeneXpert confirmed 2 cases that had negative culture (14% additional diagnostic yield). BAL GeneXpert resulted in additional diagnostic yield in this study as well as the rapid detection of drug susceptibility in children with complicated intrathoracic tuberculosis

Magnetic resonance scanning

Children with complicated thoracic tuberculosis require advanced imaging to confirm the cause and extent of disease. Chest CT scan provides valuable information of not only the parenchymal tissue but also mediastinal lymph node involvement and their relationship to the large airways. High levels of radiation during chest CT scan remain a concern especially in young children. Magnetic Resonance Imaging (MRI) has been established as a radiation- free alternative to CT for several lung diseases. New MRI technologies now allow for fast scanning and better quality images to be collected and in addition complicated intrathoracic TB can be rescanned without increasing the radiation risk.

Peprah KO, Andronikou S, Goussard P. Characteristic Magnetic Resonance Imaging Low T2 Signal Intensity of Necrotic Lung Parenchyma in Children With Pulmonary Tuberculosis. J Thorac Imaging 2012; 27: 171-174.

The aim of this pilot study was to demonstrate that necrotic areas of the lung, as shown on CT scanning in children with primary pulmonary TB, might be of low signal intensity on T2 on MRI scanning. Chest CT scans of 6 children older than 6 years were compared to MRI Abnormalities included airspace consolidation in 6 children (100%); central necrosis in 6 children (100%); nodules in 2 children (33.3%); and lymphadenopathy in 6 children (100%). Low T2 signals in the areas of necrosis were demonstrated in all 6 children (100%). Airspace consolidation demonstrated T2 high signal in all the children (100%). Lung parenchymal necrosis in primary pulmonary TB in children may be of low signal intensity on T2 and STIR magnetic resonance imaging. These findings need to be confirmed in larger studies.

Conclusion

Performing other investigations, other than just collecting samples for TB culture, enhance the diagnostic value of bronchoscopy in children suspected of having pulmonary TB. Transbronchial needle aspiration can be safely performed in young children with enlarged subcarinal lymph nodes. It is possible to perform GeneXpert MTB/RIFon BAL samples in children suspected of having TB and this may increase the diagnostic yield of paediatric bronchoscopy. MRI scanning has the potential to replace CT scans in future but further research is necessary.

Further investigation is required to determine the value of GeneXpert MTB/Rif assay and MRI scanning in the diagnosis and management pulmonary tuberculosis in children.

Pediatric Pulmonology 45:1173–1179 (2010)

The Diagnostic Value and Safety of Transbronchial Needle Aspiration Biopsy in Children With Mediastinal Lymphadenopathy

P. Goussard, MMed (Paed),[1]* R.P. Gie, FCP (Paed),[1] S. Kling, FCP (Paed),[1] E.D. Nel, MMed (Paed),[1] M. Louw, MMed (Anat Path),[2] P.T. Schubert, FCPath (Anat),[2] D. Rhode, FCP (Paed),[1] A. Vanker, FCP (Paed),[1] and S. Andronikou, PhD[3]

Summary. Introduction: Anterior mediastinal masses in children can have different causes which includes, *Mycobacterium tuberculosis* (MTB) or malignant lymphadenopathy. Transbronchial needle aspiration (TBNA) has been described as a safe and effective diagnostic procedure in adult patients with lung cancer. Aim: To describe the use of TBNA as a diagnostic test in children with large subcarinal lymphadenopathy and to determine the safety of the procedure in children. Patients and Methods: Prospective descriptive study of children with subcarinal mediastinal lymph nodes who underwent TBNA. The majority of the children were referred due to treatment failure. Children were enrolled if the diagnosis remained unclear after computer tomography of the chest. Results: Thirty patients were enrolled in this study; TBNA was done in 28 patients. A definitive diagnosis was made by TBNA in 54% (n = 15) of patients; MTB lymphadenopathy (n = 13), metastatic nephroblastoma (n = 1), and fibrosing mediastinitis (n = 1). In seven (25%) cases the TBNA was the sole source of the specimens from which the definitive diagnosis was made. No serious complications were encountered during or after the procedure. Conclusion: TBNA is a safe procedure in children with mediastinal lymphadenopathy of unknown cause resulting in a definitive diagnosis in 57% of cases. TBNA adds additional value to flexible bronchoscopy in the diagnosis of mediastinal lymphadenopathy in children. **Pediatr Pulmonol. 2010; 45:1173–1179.** © 2010 Wiley-Liss, Inc.

Key words: transbronchial needle aspiration (TBNA); mediastinal lymphadenopathy; *Mycobacterium tuberculosis*; bronchoscopy.

Funding source: none reported.

INTRODUCTION

In children in a developing country, the most likely causes of mediastinal lymphadenopathy are chronic infections or malignancy. In most cases it is not possible to determine the cause of the mediastinal lymphadenopathy from the clinical and radiological findings. In adult patients, in whom lung malignancies are the most likely cause, this clinical problem is solved by performing a transbronchial needle aspiration (TBNA).[1] In these patients TBNA has been shown to be safe and effective in making the definitive diagnosis.[2–6] A further advantage is that the aspiration biopsy is taken from a centrally situated lesion, avoiding the risk of pneumothorax. In children TBNA has not been described and the diagnostic value is not determined largely due to the fact that the working channel of the flexible bronchoscopes are not large enough to allow for the introduction of an aspiration needle.

The aim of the study was to describe the diagnostic yield of TBNA in children with large subcarinal lymphadenopathy where the diagnosis could not be made by using conventional diagnostic tests and to determine if TBNA can safely be performed in children.

PATIENTS AND METHODS

This was a prospective descriptive study of cases of children with subcarinal mediastinal lymphadenopathy who underwent TBNA between January 2008 and August 2009. The study was carried out at, Tygerberg Children's

[1]Department of Pediatrics and Child Health, Stellenbosch University, Tygerberg Children's Hospital, Tygerberg, South Africa.

[2]Department of Anatomical Pathology, Stellenbosch University, Tygerberg Children's Hospital, Tygerberg, South Africa.

[3]Department of Radiology, University of Cape Town, Cape Town, South Africa.

*Correspondence to: P. Goussard, Faculty of Health Sciences, Department of Pediatrics and Child Health, Stellenbosch University, PO Box 19063, Tygerberg 7505, South Africa. E-mail: pgouss@sun.ac.za

Received 19 November 2009; Revised 4 March 2010; Accepted 29 April 2010.

DOI 10.1002/ppul.21303
Published online 17 August 2010 in Wiley Online Library (wileyonlinelibrary.com).

Hospital, a tertiary academic hospital, situated in the Western Cape, South Africa.

Study Population

All children, older than 6 months, with enlarged mediastinal lymph nodes diagnosed by computer tomography (CT scan) and where diagnostic uncertainty existed as to the cause of the lymphadenopathy, were included in the study. All chest CT-scans were done with contrast in order to clearly define the mediastinal structures and to exclude vascular structures in the subcarinal region. The children were only considered for TBNA if at coronal reconstruction of the CT scan of the chest, large lymph glands were visible in the subcarinal region immediately adjacent to the carina and abutting the airway and no vascular structures were visible in the target area (Fig. 1).

Exclusion Criteria

Children where fiberoptic bronchoscopy (FB) could not be safely performed and those with a coagulation abnormality were excluded. The TBNA was also not performed if an airway lesion suggestive of tuberculosis was visualized during flexible bronchoscopy and a biopsy of the lesion could be taken.

Study Methods

The majority of the children were referred to the hospital because of diagnostic uncertainty or the child failed to respond adequately to anti-tuberculous therapy when pulmonary tuberculosis (PTB) was suspected. Informed consent was obtained from the parents or legal guardian. Demographic data as well as data concerning previous treatment and the duration of treatment was collected. Prior to bronchoscopy a clotting profile, full blood, and platelet counts were performed and were required to be within normal limits for the procedure to proceed.

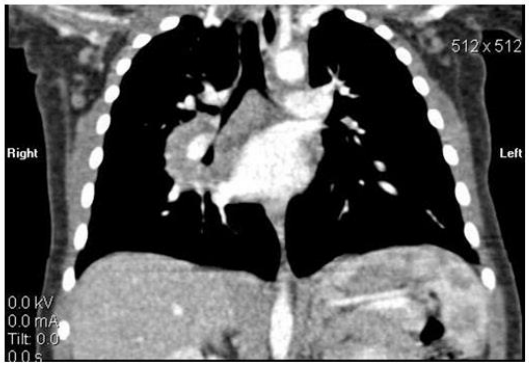

Fig. 1. Coronal reconstitution of a post-CT chest in a child demonstrating subcarinal, azygoesphageal, and right hilar lymphadenopathy causing severe glandular compression of bronchus intermedius.

Intervention

A 4.0 mm Olympus bronchoscope (BF-MP160F) with a 2 mm working channel was used to perform the bronchoscopy under general anesthesia. The bronchoscopies were done trough a laryngeal mask (LMA), which allowed the anesthetist to ventilate the patient during the intervention. The size of the LMA was determined by the weight of the patient. If during the procedure, especially in young children, there was airway obstruction caused by the bronchoscope, the bronchoscope was regularly removed to ensure adequate ventilation. At bronchoscopy glands compressing the large airways and broadening the carina confirmed the presence of mediastinal lymphadenopathy. The CT scan reconstruction and the visual appearance of the carina determined the site of the biopsy. If no enlarged subcarinal lymph nodes were visualized the TBNA was not performed. In this diagnostic study only the anterior subcarinal lymph glands were biopsied. No attempt was made to biopsy paratracheal or hilar lymphadenopathy. The technique used was that as described by Wang.[1,2] A Wang 21 gauge cytology needle was used. The needle and sheath were advanced through the working channel of the bronchoscope and the position visually confirmed. The needle was then ejected from the sheath. The length of the projected needle was 1.5 mm. A second operator then steadied the bronchoscope as close as possible to the carina to avoid movement of the bronchoscope when the needle was advanced into the gland (Fig. 2). The sample was generated by applying suction to the needle with a syringe. On site cytology was performed by a cytologist in the bronchoscopy suite. The aspirated material was immediately expressed on glass slides and processed as previously described (Figs. 3 and 4).[6] Three to five passes were made into the enlarged subcarinal glands. The number of passes was determined by a cytologist who evaluated the quality of the aspirated specimens. As soon as a suitable diagnostic specimen was obtained the procedure was stopped. A separate specimen was then collected for fungal and *Mycobacterium tuberculosis* (MTB) culture. The aspirated fluid was flushed from the needle with sterile saline into liquid culture medium. If the cytology confirmed ZN-positive material, the TBNA for MTB culture was done in the same position and if not MTB, cultures were done from the most prominent area of the carina. Following the aspirates the biopsy site was carefully observed to ensure that no bleeding was present. Routine samples taken at bronchoscopy included broncho-alveolar lavage (BAL), cultures for MTB, and viral and bacterial cultures. These

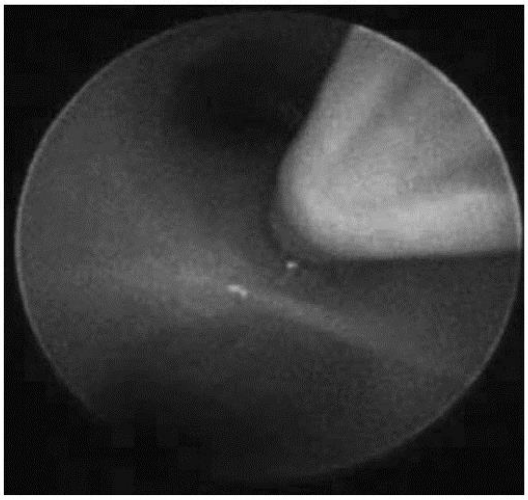

Fig. 2. Bronchoscopy picture of Wang needle puncturing the broadened carina.

procedures were done after the TBNA. The duration of bronchoscopy was recorded as from the time the bronchoscopy was introduced to the airway until the bronchoscope was finally removed.

The following diagnostic criteria were used. Tuberculosis was diagnosed if either MTB was cultured from the biopsy specimens or if at staining of the biopsy acid fast bacilli and granulomatous inflammation with necrosis were visualized.

Granulomas are diagnosed cytologically as loose aggregates of epithelioid histiocytes, which have classically elongated, slightly irregular, bent nuclei, and

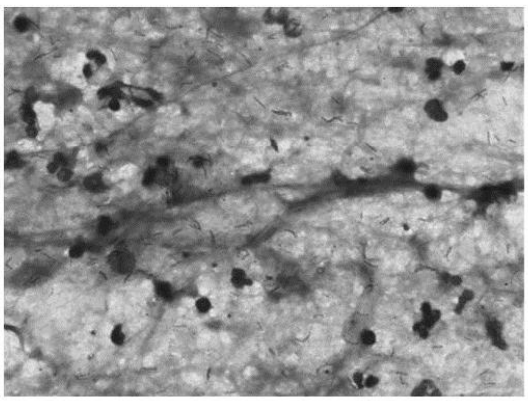

Fig. 3. Ziehl–Neelsen stain showing numerous acid fast bacilli. ZN 1,000×.

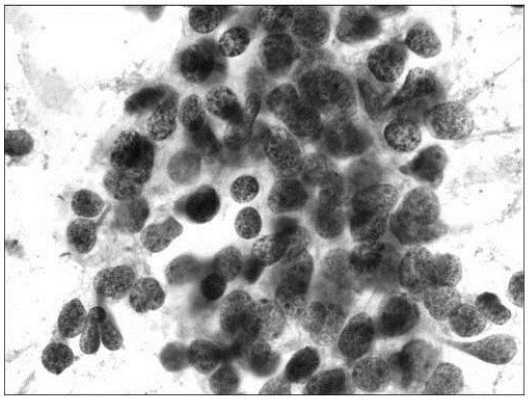

Fig. 4. Metastatic Wilm's tumor showing blastema with hyperchromatic nuclei, inconspicuous nucleoli, minimal cytoplasm, and focal nuclear molding. Papanicolaou stain 1,000×.

abundant cytoplasm. These may be seen on the background of necrosis, which, depending on the immune status of the patient may be amorphous, necrotizing, or suppurative.[7–9]

Malignancy was defined as the presence of cells diagnostic of malignancy in the TBNA sample by the cytologist.

Following the FB the children were observed for 24 hr postoperatively and a chest radiograph was taken 1 hr after the FB to exclude a pneumothorax and or pneumomediastinum. No child underwent a second TBNA.

Statistical Analysis

Data are expressed using standard descriptive statistics and the χ^2 test was used when comparing various groups with a $P < 0.05$ being considered significant.

Ethical Considerations

Ethics approval for the study was granted by the Human Research Ethics Committee of Stellenbosch University.

RESULTS

Thirty patients were enrolled into this study, but TBNA was only done in 28 patients (Fig. 5). The children's median age was 41 months (range 9–168 months) with 43% (n = 12) being female and 32% (n = 9) of the children were HIV PCR positive. Of the children 50% (n = 14) were younger than 3 years and 7% (n = 2) older than 12 years. The median weight was 11 kg (range 8.5–39 kg).

Diagnostic Outcome

A definite diagnosis was made by TBNA in 54% (n = 15) of patients. There were 13 cases of PTB and one

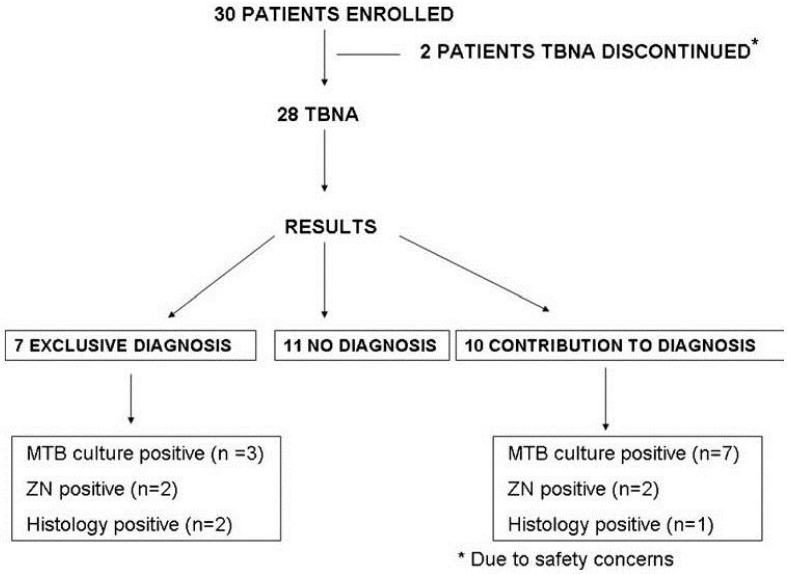

Fig. 5. Flow diagram: Patient selection and results.

each of metastatic nephroblastoma and fibrosing mediastinitis (FM). The definitive diagnosis was made by histology in 32% (n = 9) of cases. This included PTB (n = 7), and the cases of FM and nephroblastoma. Of the 15 patients with a definitive diagnosis 11 (73%) were HIV uninfected and 4 (27%) HIV infected. There was no difference in the diagnostic yield in HIV-uninfected children when compared to HIV-infected children ($P = 0.69$).

In seven (25%) cases the TBNA was the sole source of the specimens from which the definitive diagnosis was made. These included three culture positive specimens for MTB, two cases where the specimens were Ziehl–Neelsen positive with accompanying granulomas, and the cases of metastatic nephroblastoma and FM.

TBNA resulted in a definitive diagnosis by means of cytology performed in the bronchoscopy suite in 10 cases (36%).

Culture Results

Of the 26 children suspected of having PTB 14 (56%) were culture positive. MTB was cultured from the following specimens: Fine needle aspiration of a peripheral lymph node (n = 1), gastric washings (n = 3), sputum (n = 5), BAL (n = 9), and TBNA (n = 10). MTB was cultured from more than one site in seven patients but in three cases the TBNA was the sole source of the positive culture which included one of the two cases of multidrug-resistant TB. In five cases the TBNA specimens were ZN smear negative but culture positive. The mean duration of time from the TBNA to MTB culture positivity was 24 days (range 16–35 days), indicating a low bacillary load.

Of the 26 children suspected of having PTB prior to the biopsy 85% (n = 22) had been on anti-tuberculous treatment. In the culture positive group the mean duration of treatment prior to the TBNA was 15 days (0–60 days) while in the culture negative group the mean duration was 30 days (range 0–140 days). This was not statistically different. Similarly there was no statistical difference in the number of culture positive cases in the HIV-uninfected children when compared to the HIV-infected children. The duration of TB treatment was not an independent variable when comparing the number of TB cultures from HIV-infected to HIV-uninfected children ($P = 1$). When the number of culture positive specimens obtained by TBNA were compared to those obtained by BAL the kappa agreement was 0.42. If the TBNA specimens were taken as the sole source for the diagnosis of TB then three cases would have been missed. These three children had specimens taken from other sites that were culture positive for MTB. One of the three was HIV infected.

In all the HIV-infected children the histology was not suggestive of malignancy or fungal infections and the cultures for fungal infections were negative. The child with the metastatic nephroblastoma had an enlarged subcarinal mass, which on cytology was highly suggestive of a metastatic nephroblastoma. No further investigations were conducted.

In the remaining 11 cases the cause of the enlarged mediastinal glands could not be determined. The children remained on anti-tuberculous treatment to which they all responded well, suggesting MTB as the possible etiology.

Complications

No serious complications were encountered during or after the procedure. In all the cases a small amount of bleeding occurred at the site of the needle aspiration, which was self-limiting. The mean time duration of the bronchoscopy and TBNA was 40 min (range 15–65 min). Performing the TBNA increased the duration of the anesthetic but the exact increase in duration was not determined. There were no cases of pneumothorax or pneumomediastinum. No bronchoscope was damaged during the procedure.

In two cases TBNA was planned but not attempted due to safety considerations. The one case had significant tracheal compression, and the bronchoscope could only be advanced to the carina with difficulty, resulting in complete obstruction of the trachea. In the second case the descending aorta was demonstrated to be directly beneath the carina. Owing to the possibility of inadvertently puncturing the aorta, the TBNA was not done.

DISCUSSION

In this study we demonstrated that TBNA can be safely performed in a group of children with large mediastinal lymphadenopathy present in the anterior subcarinal region. A definitive diagnosis was made in 54% of the cases. No complications developed during or subsequent to the procedure. The youngest child in whom the procedure was performed was 9 months.

TBNA has been widely used in adult patients to confirm the diagnosis of bronchogenic carcinoma.[1] Subsequently TBNA has been used in the diagnosis of both malignant and benign mediastinal disease with success and a low complication rate.[2–6,10] The use of TBNA in the diagnosis of intrathoracic tuberculous lymphadenitis in adult patients has been published, but this technique has not been used in children.[11,12] Recently ultrasound-guided fine needle biopsy and endobronchial ultrasound have been used in the diagnosis of lung malignancy in adults.[13–15] Due to size constraints of the pediatric bronchoscopes this technique has not been widely used in children. There is one case report on its use in diagnosing sarcoidosis in a young child.[16] One of the major applications of TBNA in pediatric pulmonology would be in the diagnosis of tuberculosis, but the sophisticated equipment required is expensive and requires extensive training, making its use in resource-limited countries highly unlikely.[11]

The smallest working channel that will accept a transbronchial aspiration needle is 2 mm. Commonly used bronchoscopes in pediatric patients have a 1.2 mm working channel, which makes TBNA impossible. With the availability of a 4.0 mm scope with a 2 mm working channel, it is now possible to do TBNA in younger children. We preferred to do the bronchoscope via a LMA. The caliber of the LMA is large enough to allow the bronchoscope to pass through while simultaneously achieving adequate ventilation during the intervention. The size of the endotracheal tube which a child can safely be intubated with, limits the number of children in whom a 4.0 mm bronchoscope can be introduced. Due to the endotracheal tube lumen size, adequate ventilation cannot be sustained during the bronchoscopy, especially with a 4.0 mm bronchoscope in a small child.

The method we followed was described by Wang.[2] We only attempted to aspirate subcarinal lymphadenopathy in the anterior location due to the limitation of the apparatus we used. We do not consider this a limitation as the most common anatomical locations for TB lymphadenopathy in children is in the subcarinal (90%), right carinal (74%), and left carinal (72%) regions. It is therefore unlikely that we would have missed TB lymphadenopathy due to sampling limitations.[17,18] The anterior subcarinal lymph nodes could easily be aspirated through the carina. The other group of lymph nodes that would have been easy to aspirate are the posterior subcarinal lymph nodes, but due to safety concerns this was not attempted. Wang[2] has described TBNA of the other groups of lymph nodes that can be aspirated in adult patients.

The diagnosis of the etiology of mediastinal lymphadenopathy in children can be challenging. CT scan appearances are not diagnostic and the yield from sputum, gastric washings, and BAL are limited. In children where malignancy is considered as the cause of the lymphadenopathy this possibility can only be excluded if a tissue diagnosis is made. The problem is exacerbated in HIV-infected children where many chronic infections, as well as HIV-associated disease and malignancies have to be considered as possible causes of the mediastinal lymphadenopathy. Many of these children are extremely ill and the risk of performing an open thoracotomy needs to be taken into account. In these children TBNA is a viable option. Harkin et al.[19] agree that in HIV-positive adults TBNA is not only effective in the diagnosis of mediastinal lymph node disease but was the exclusive way of making the diagnosis in nearly a third of the patients.

In this cohort nine of the patients were HIV positive and in three of these patients the diagnosis of PTB was made by TBNA. In one case the diagnosis of TB in an HIV-infected child was not confirmed by TBNA. The true value of the TBNA cannot be determined from this study as the definitive diagnosis was not made in 11 cases, including 4 HIV-infected children.

It is argued that bronchoscopy is of limited value in the diagnosis of childhood tuberculosis due to the low

diagnostic yield for cultured MTB from BAL fluid. Numerous studies have demonstrated that the diagnostic yield of BAL is lower than that of gastric aspirate for the culture of MTB.[20–23] This approach does, however, not take into account the TB lymphobronchial airway involvement visualized during bronchoscopy. In a study where the culture yield for MTB by BAL was 20%, abnormalities of TB glandular disease were visible in 48% of the children.[23] To this we can now add the possibility of performing a TBNA in a subgroup of patients suspected of having TB and further improving the diagnostic yield. Additionally, endobronchial lesions can be biopsied to improve the diagnostic capabilities of flexible bronchoscopy in children, but there is very limited information about this diagnostic method.

There was a fair agreement in the culture yield for MTB in specimens collected by TBNA (38%) and BAL (35%). The diagnostic yield of positive cultures in this study is higher than reported in other studies even though most patients had been on anti-tuberculosis treatment prior to investigation. In this complicated group of patients with suspected TB the TBNA samples were the only source of a positive culture in 10% of the cases including one of the two cases of multi-drug-resistant TB.

No serious complications occurred during the study. A TBNA was safely performed in children as young as 9 months. The limitation to doing the procedure is the size of the working channel. A 2 mm working channel is needed to introduce the aspiration needle. TBNA cannot be performed in all children with subcarinal lymphadenopathy as was the case in two of our cases. The one case had severe tracheal lymph gland compression while the other had displacement of the aorta as demonstrated on CT scan of the chest.

Limitations

The study was designed to evaluate the usefulness and the practicality of TBNA in children with enlarged mediastinal lymph nodes. This was a diverse group of children with a varying spectrum of disease. There may be a number of reasons for the failure to make a diagnosis in 46% of patients and this includes possible sampling errors, failure to utilize the proper diagnostic test and the fact that a large number of children had been on anti-tuberculosis treatment prior to the TBNA. Owing to these factors it is not possible to accurately determine the value of this procedure. Only anterior subcarinal lymph nodes were attempted for TBNA which may also have limited the success rate.

We accept that the patients and settings may be unique to a developing world situation with a high burden of TB and HIV infection. In the developing world a large number of children are still diagnosed with advanced HIV disease which complicates the diagnosis as the large mediastinal lymph nodes may be related to their HIV disease and not TB. TBNA was also useful in children with malignancies and this is a universal problem.

Subcarinal lymph nodes are relative easy to biopsy and this may not only aid in the diagnosis of drug susceptible TB but is also an excellent sample area for culture material if drug-resistant TB is considered.

We conclude that TBNA is a safe procedure in children with mediastinal lymphadenopathy of unknown cause. It is clear that if the appropriate indications exist, this technology is applicable to children in whom a 4 mm or larger bronchoscope can be introduced to the airways. It adds additional value to flexible bronchoscopy in the search for the etiology of mediastinal lymphadenopathy. Not only does it provide a rapid diagnosis in some cases, but it may also prevent the necessity of an open thoracotomy. It is also useful in both HIV-infected and -uninfected children. More studies need to be performed to evaluate the value of the procedure in other causes of mediastinal lymphadenopathy, as the majority of the cases in this study had mediastinal lymphadenopathy caused by MTB.

REFERENCES

1. Wang KP, Terry PB. Transbronchial needle aspiration in the diagnosis and staging of bronchogenic carcinoma. Am Rev Respir Dis 1983;127:344–347.
2. Wang KP. Staging of bronchogenic carcinoma by bronchoscopy. Chest 1994;106:588–593.
3. Holty JE, Kuschner WG, Gould MK. Accuracy of transbronchial needle aspiration for mediastinal staging of non-small cell lung cancer: a meta-analysis. Thorax 2005;60:949–955.
4. Hermens FH, Van Engelenburg TC, Visser FJ, Thunnissen FB, Termeer R, Janssen JP. Diagnostic yield of transbronchial histology needle aspiration in patients with mediastinal lymph node enlargement. Respiration 2003;70:631–635.
5. Fernández-Villar A, Leiro V, Blanco M, Represas C, Botana M, González A, Piñeiro L. Efficacy and safety of the eXcelon transbronchial aspiration needle in mediastinal lymph node enlargement: a case-control study. Respiration 2007;74:208–213.
6. Diacon AH, Schuurmans MM, Theron J, Louw M, Wright CA, Brundyn K, Bolliger CT. Utility of rapid on-site evaluation of transbronchial needle aspirates. Respiration 2005;72:182–188.
7. Schubert PT, Cotton MF, Wright CA. Cytomorphological patterns of M. bovis BCG and M. tuberculosis on fine needle aspiration biopsies: does HIV make a difference. Diagn Cytopathol 2010; (in press).
8. Metre MS, Jayram G. Acid fast bacilli in aspiration smears from tuberculous lymphnodes. An analysis of 255 cases. Acta Cytol 1987;31:17–19.
9. Nayak S, Puranik SC, Deshmukh SD, Mani R, Bhore AV, Bolliger RC. Fine-needle aspiration cytology in tuberculous lymphadenitis of patients with and without HIV infection. Diagn Cytopathol 2004;31:204–206.
10. Trisolini R, Tinelli C, Cancellieri A, Paioli D, Alifano M, Boaron M, Patelli M. Transbronchial needle aspiration in sarcoidosis:

yield and predictors of a positive aspirate. J Thorac Cardiovasc Surg 2008;135:837–842.
11. Bilaçeroğlu S, Günel O, Eriş N, Cağirici U, Mehta AC. Transbronchial needle aspiration in diagnosing intrathoracic tuberculous lymphadenitis. Chest 2004;126:259–267.
12. Cetinkaya E, Yildiz P, Altin S, Yilmaz V. Diagnostic value of transbronchial needle aspiration by Wang 22-gauge cytology needle in intrathoracic lymphadenopathy. Chest 2004;125:527–531.
13. Herth FJ, Lunn W, Eberhardt R, Becker HD, Ernst A. Transbronchial versus transesophageal ultrasound-guided aspiration of enlarged mediastinal lymph nodes. Am J Respir Crit Care Med 2005;171:1164–1167.
14. Becker HD. EBUS: a new dimension in bronchoscopy. Of sounds and images—a paradigm of innovation. Respiration 2006;73:583–586.
15. Herth FJ, Eberhardt R, Vilmann P, Krasnik M, Ernst A. Real-time endobronchial ultrasound guided transbronchial needle aspiration for sampling mediastinal lymph nodes. Thorax 2006;61:795–798.
16. Wurzel DF, Steinfort DP, Massie J, Ryan MM, Irving LB, Ranganathan SC. Paralysis and a perihilar protuberance: an unusual presentation of sarcoidosis in a child. Pediatr Pulmonol 2009;44:410–414.
17. Hermens FH, Limonard GJ, Termeer R, van den Berg W, Visser FJ, Hol BE, Janssen JP. Learning curve of conventional transbronchial needle aspiration in pulmonologists experienced in bronchoscopy. Respiration 2008;75:189–192.
18. Andronikou S, Joseph E, Lucas S, Brachmeyer S, Du Toit G, Zar H, Swingler G. CT scanning for the detection of tuberculous mediastinal and hilar lymphadenopathy in children. Pediatr Radiol 2004;34:232–236.
19. Harkin TJ, Ciotoli C, Addrizzo-Harris DJ, Naidich DP, Jagirdar J, Rom WN. Transbronchial needle aspiration (TBNA) in patients infected with HIV. Am J Respir Crit Care Med 1998;157:1913–1918.
20. Abadco DL, Steiner P. Gastric lavage is better than bronchoalveolar lavage for isolation of *Mycobacterium tuberculosis* in childhood pulmonary tuberculosis. Pediatr Infect Dis J 1992;11:735–737.
21. Chan S, Abadco DL, Steiner P. Role of flexible fiberoptic bronchoscopy in the diagnosis of childhood endobronchial tuberculosis. Pediatr Infect Dis J 1994;13:506–509.
22. Somu N, Swaminathan S, Paramasivan CN, Vijayasekaran D, Chandrabhooshanam A, Vijayan VK, Prabhakar R. Value of bronchoalveolar lavage and gastric lavage in the diagnosis of pulmonary tuberculosis in children. Tuberc Lung Dis 1995;76:295–299.
23. Cakir E, Seda Uyan Z, Okten S, Karakoc F, Ersu R, Karadag B, Dagli El. Flexible bronchoscope for diagnosis and follow up of childhood endobronchial tuberculosis. Pediatr Inf Dis J 2008;27:783–787.

GeneXpert MTB/RIF on Bronchoalveolar Lavage Samples in Children With Suspected Complicated Intrathoracic Tuberculosis: A Pilot Study

Elisabetta Walters, MD,[1]* Pierre Goussard, MD,[2] Corne Bosch, BSc (Hon),[1] Anneke C. Hesseling, PhD,[1] and Robert P. Gie, MD[1,2]

Summary. Background: Children with complicated intrathoracic tuberculosis (TB) require rapid confirmation of TB diagnosis and of drug susceptibility to institute appropriate therapy. In a pilot study, we evaluated the feasibility and potential utility of GeneXpert (Xpert) on bronchoalveolar lavage (BAL) samples in children undergoing routine diagnostic bronchoscopy. Methods: We included children <13 years of age undergoing bronchoscopy for suspected complicated intrathoracic TB at Tygerberg Children's Hospital, October 1, 2012–May 15, 2013. A minimum of two respiratory specimens in addition to BAL were obtained from each child. In addition to fluorescent smear microscopy and automated liquid culture performed on all samples, BAL samples were analyzed by Xpert. Drug susceptibility was confirmed by GenoType® MTBDR*plus*. Results: Fourteen children (2 HIV positive, median age 16 months) were included. The Mantoux tuberculin skin test was positive in 11. On chest radiograph, six children had expansile pneumonia and nine had airway compression (one had both). The median duration of TB treatment before bronchoscopy was 8 days. TB was confirmed by either culture or Xpert from any sample in 11 (78%) children. Among 9/14 (64%) cases confirmed by culture, BAL Xpert was positive in 7 (78% sensitivity); in addition, Xpert confirmed 2 cases who had negative culture (14% additional diagnostic yield). Two drug resistant cases were identified: one by BAL Xpert and one from genotypic testing of a culture from gastric aspirate. All children were initiated on anti-TB treatment and responded well to therapy. Conclusion: BAL Xpert resulted in additional diagnostic yield and also in the rapid detection of drug resistance in children with complicated intrathoracic TB. The clinical impact of this modality should be further evaluated in children. **Pediatr Pulmonol.**

Key words: complicated tuberculosis; rapid diagnosis; bronchoscopy; children.

Funding source: none reported.

INTRODUCTION

Primary tuberculosis (TB) may become complicated when enlarged tuberculous lymph nodes result in large airway obstruction with or without herniation and bronchogenic spread of caseous material. Complicated intrathoracic TB has been reported in up to 38% of pediatric cohorts,[1] and is seen more frequently in young children because of smaller airway diameter. Children with complicated intrathoracic TB require rapid confirmation of a TB diagnosis to institute appropriate therapy, confirm drug susceptibility, and to guide management in the event of poor response to treatment. With intensive sampling, culture confirmation is possible in up to 78% of children with complicated intrathoracic disease, compared to <30% in children with uncomplicated pulmonary TB.[2] Bronchoscopy can be used both as a diagnostic and therapeutic procedure, with bronchoalveolar lavage (BAL) samples contributing up to 44% of total culture yield in severe cases.[3] However,

[1]Faculty of Medicine and Health Sciences, Department of Paediatrics and Child Health, Desmond Tutu TB Centre, Stellenbosch University, Cape Town, South Africa.

[2]Division of Paediatric Pulmonology, Faculty of Medicine and Health Sciences, Department of Paediatrics and Child Health, Tygerberg Academic Hospital, Stellenbosch University, Cape Town, South Africa.

E. Walters and P. Goussard contributed equally to this manuscript.

Conflict of interest: None.

*Correspondence to: E. Walters, MD, Faculty of Medicine and Health Sciences, Department of Paediatrics and Child Health, Desmond Tutu TB Centre, Stellenbosch University, Cape Town, South Africa.
E-mail: ewal@sun.ac.za

Received 13 July 2013; Accepted 3 November 2013.

DOI 10.1002/ppul.22970
Published online in Wiley Online Library (wileyonlinelibrary.com).

culture has long turnaround time, and empiric treatment is frequently necessary to prevent further progression of disease in children.

The GeneXpert MTB/RIF assay (Xpert; Cepheid Inc, Sunnyvale, CA), a rapid automated PCR-based test, detects *Mycobacterium tuberculosis* (MTB) complex, and simultaneously rifampicin resistance, within 2 hr. Sensitivity of Xpert on sputum in adults with smear positive pulmonary TB is >98%,[4] and 68% in smear negative TB, with a specificity of >97%. Published pediatric data suggest that, among children with varied spectrum of suspected pulmonary TB, Xpert analysis of two respiratory samples (induced sputum or nasopharyngeal aspirates) achieves sensitivity up to 70% compared to culture.[5–7] The proportion of total culture confirmed cases in these studies was 16–17% of children with suspected TB.

Children with severe forms of intrathoracic TB have higher culture yields, indicative of higher bacillary burden, typically coupled with more intense bacteriological sampling due to the clinical presentation.[2] Given the invasiveness of bronchoscopy, every effort should be made to optimize the diagnostic yield in children investigated with this modality for suspected TB. A recent retrospective study among smear negative adults with suspected pulmonary TB reported a sensitivity of 81% of Xpert on BAL compared to culture.[8] Xpert also confirmed 4 additional cases among 12 patients with a clinical diagnosis of TB (all culture negative), suggesting an additive potential of Xpert on total diagnostic yield.

There are currently no published data on the utility of Xpert on BAL samples from children.

We report a prospective pilot study to explore the value of Xpert as an add-on test to mycobacterial culture for the confirmation of TB in children presenting with suspected complicated intrathoracic TB.

METHODS

Children 3 months–13 years of age routinely admitted to Tygerberg Children's Hospital, Cape Town, South Africa, between October 1, 2012 and May 15, 2013 were included. Children were routinely investigated with bronchoscopy if TB was suspected based on chronic respiratory symptoms, contact with a known TB source case or a reactive Mantoux skin test and in combination with any of the following: (a) severe life-threatening intrathoracic large airway obstruction, (b) radiographic evidence of complicated intrathoracic disease, or (c) suspicion of drug-resistant TB based on the susceptibility pattern of an adult source case, and none of the bacteriological samples taken from the child to date had been positive. All children underwent HIV testing (HIV DNA PCR if <18 months, HIV antibody test if >18 months of age), and a minimum of two respiratory samples for smear microscopy and mycobacterial liquid culture (gastric aspiration in children <5 years, expectorated sputum in older children). Respiratory samples were analyzed by direct fluorescent microscopy (Auramine) and automated liquid culture (MGIT; Becton-Dickinson, Sparks, MD) at the hospital's National Health Laboratory Service according to standard protocols. Drug susceptibility was confirmed with the GenoType® MTBDR*plus* test (Hain Lifescience GmbH, Nehren, Germany).

Flexible bronchoscopy was performed in a dedicated bronchoscopy theatre under general anesthesia using gas inhalation (halothane) and an intravenous agent (propofol). Children were routinely monitored by the anesthetist during the procedure and for 30 min after bronchoscopy by pulse oximetry, continuous electrocardiography, capnography, and blood pressure monitoring. After the procedure, children were transferred back to the pulmonology ward for further observation. Bronchoscopy was systematically performed according to a standard protocol.[3] Observations made under direct bronchoscopic visualization were recorded in a standard data form. Any adverse events during and following bronchoscopy were systematically recorded. The degree of airway obstruction was recorded as either absent or graded according to the following categories: (1) 30%, (2) 50–75%, (3) 75–90%, and (4) 100% obstruction. The upper, middle, and lower parts of the trachea, the left and right bronchial tree were assessed. On the left, the left main bronchus, the left upper lobe, lingula and left lower lobe bronchi were examined; on the right, the right main bronchus, bronchus intermedius, and the right middle and the right lower lobe bronchi. Each site was assessed for external compression and intraluminal involvement. Following evaluation of the airways, a BAL was completed. If lymph nodes had ulcerated into the airway the lavage was done in that specific airway. In cases where no ulceration had occurred the bronchoscope was wedged in the most involved lobe or segment as determined radiologically, and the lavage was performed.[9] Visible intraluminal tissue was biopsied. Two BAL samples were obtained, one for mycobacterial smear microscopy and automated liquid culture, and one for Xpert. As lavage fluid was aspirated, it was collected into two separate sample containers: one for smear microscopy and culture, and one for Xpert. The order of the samples was not recorded (which of the first or second samples were analyzed by bacteriology vs. Xpert). Transbronchial biopsy was also completed on any subcarinal nodal tissue identified by computerized tomography of the chest.

For BAL Xpert, samples ≤1 ml were processed directly. Samples >1 ml were first concentrated by centrifugation at 2,163*g* for 20 min using a Multifuge 4 KR (Heraeus, Germany), then reconstituted to 1 ml by addition of phosphate buffer. Xpert buffer was added to raw and reconstituted samples at ratio 1:2 and transferred

into the Xpert cartridge for processing by the Xpert machine as recommended by the manufacturer.[10]

Lymph node tissue biopsy specimens were analyzed by histology, cytology, direct smear microscopy, and automated liquid culture.

Antituberculosis treatment for drug-susceptible TB included four drugs (isoniazid, rifampicin, pyrazinamide, and ethambutol) and in cases of suspected or confirmed multidrug resistant TB (MDR TB) an appropriate five to six drug treatment regimen. Oral prednisone at 2 mg/kg/day for 30 days was added for all cases with severe airway obstruction (>50% bronchial obstruction as visualized at bronchoscopy). Written informed consent was obtained for bronchoscopy from each child's parents or legal guardians and the study was approved by the Health Research Ethics Committee of the Faculty of Health Sciences, Stellenbosch University (N10/08/282 and N11/09/282).

RESULTS

During the study period, 46 children underwent bronchoscopy for suspected or confirmed complicated intrathoracic TB. Fourteen children (eight male, two HIV positive) did not have culture confirmed TB at the time of bronchoscopy and were included in this study (Table 1). The median age was 16 months (range: 5–132 months). Nine (64%) children had reported exposure to an adult culture positive source case (three with drug-resistant TB); one child had received prophylaxis for drug sensitive TB. The median duration of antituberculosis treatment before bronchoscopy was 8 days (range 0–85 days): for culture positive cases (n = 11), mean time on treatment before scope was 7 days versus 20.8 days for culture negative cases (n = 3). Only 3/14 (21%) children were not receiving antituberculosis treatment at the time of bronchoscopy. The Mantoux skin test was positive in 11 of 12 in whom it was performed. On chest radiograph, six children had expansile pneumonia and nine (64%) had airway compression (one had both).

At bronchoscopy, airway obstruction was demonstrated in 11 (79%) cases (bilateral in 3). Three children with severe and life-threatening airway obstruction underwent surgical enucleation of lymph nodes.

Ten children had gastric aspirates, and four had expectorated sputum obtained for direct smear and TB culture (2–4 samples per child), in addition to BAL. In total, 3/14 (21%) children had smear positive samples: on gastric aspirate in only one child (10%) and in two on BAL (14%); all sputum samples were smear negative. Nine of 14 (64%) children had positive TB cultures: 6 of 10 (60%) children on gastric aspirates, and 8 of 14 (57%) on BAL, while all the sputum samples were culture negative. One child had trans-bronchial fine needle aspiration of a mediastinal lymph node, and one had ulcerating caseating tissue sent for TB bacteriology: both were smear negative and culture positive.

Among the eight culture positive BAL samples, seven (88%) were also Xpert positive. In addition, Xpert was positive in two culture negative BAL samples; in these two cases BAL Xpert was the only confirmation of TB, as all other cultures were also negative. Compared to any positive culture (n = 9), BAL Xpert had a sensitivity of 7/9 (78%), while it had a sensitivity of 100% to detect children with any positive smear (3/3).

The mean time to positive culture for BAL samples was 20 days (range 10–42 days). Xpert results including DST were available within 48 hr of bronchoscopy.

Two drug resistant cases were identified: one by BAL Xpert (an adult contact had MDR TB) and one from culture of gastric aspirate (INH mono-resistant on GenoType® MTBDR*plus*), where Xpert was negative.

Xpert was not more frequently positive among children with uni- or multi-lobar pneumonia on chest radiograph. All of six children with lymph node ulceration into the airway were Xpert positive, while three of eight children without lymph node ulceration had positive Xpert results.

All 14 children received antituberculosis treatment and responded well within 1 month of therapy. Of the three children who did not have microbiological or Xpert confirmation of TB, one had surgical enucleation of intrathoracic lymph nodes with suggestive histology (caseating necrosis, Ziehl–Nielsen stain positive); one had a lung cavity with negative bacterial and TB cultures; the third had radiological and bronchoscopic evidence of large airway obstruction suggestive of pulmonary TB.

DISCUSSION

We report preliminary results of Xpert analysis of BAL in children with complicated intrathoracic TB, none of whom had culture confirmation before undergoing bronchoscopy. We show that Xpert may add to the clinical management of children with complicated intrathoracic TB by improving case ascertainment and rapid detection of rifampicin resistance.

The diagnostic value of mycobacterial culture from BAL is generally accepted to be limited in children with uncomplicated TB[11–13] with reported culture yields lower or equivalent to gastric aspirate. Higher BAL culture yield (44%) has recently been reported in children with significant airway obstruction,[3] reflecting the higher bacillary load typically associated with severe disease.[2]

Children with severe intrathoracic disease are frequently started on antituberculosis treatment before referral to a tertiary center, and the duration of treatment before bronchoscopy is variable. This could impact on culture results, thereby resulting in biased estimates of Xpert accuracy compared to culture. However, referring facilities frequently do not have the required resources for bacteriological investigation. We argue that Xpert may be

TABLE 1—Clinical, Imaging, and Bacteriological Characteristics of Included Children

						Chest radiography		Bronchoscopy	TB results					
	Age (months)	HIV	Adult index case	Time on anti-TB treatment before scope (days)	Mantoux	Pneumonia	Airway compression	Gland ulcerating into airways	Any TB culture	DST on culture	Source of positive culture	BAL culture	BAL Xpert	Rifampicin resistance on Xpert
1	17	Neg	Yes, MDR	0	Pos	Absent	Present	Absent	Neg			Neg	Pos	R
2	8	Pos	Yes, DS	6	Pos	Present	Present	Absent	Neg			Neg	Neg	
3	132	Neg	Yes, DS	1	Not done	Present	Absent	Present	Pos	DS	BAL/tissue	Pos	Pos	S
4	10	Neg	No	0	Pos	Present expansile	Present	Present	Pos	DS	BAL/GA	Pos	Pos	S
5	9	Pos	Yes, DS	12	Pos	Present expansile	Present	Absent	Pos	DS	BAL	Pos	Neg	
6	8	Neg	Yes, DS	8	Pos	Present	Absent	Present	Pos	DS	BAL/GA	Pos	Pos	S
7	14	Neg	Yes, MDR	5	Not done	Present expansile	Present	Absent	Neg			Neg	Neg	
8	5	Neg	Yes, DS	15	Pos	Present expansile	Present	Present	Pos	DS	BAL/GA	Pos	Pos	S
9	96	Neg	No	14	Pos	Present	Absent	Absent	Neg			Neg	Neg	
10	60	Neg	No	85	Pos	Present	Absent	Absent	Pos	INH mono	GA	Neg	Pos	S
11	84	Neg	No	15	Neg	Present expansile	Absent	Absent	Neg			Neg	Pos	S
12	26	Neg	Yes, DS	12	Pos	Present expansile	Present	Present	Pos	DS	BAL/GA/FNA	Pos	Pos	S
13	8	Neg	Yes, DS	8	Pos	Present	Present	Present	Pos	DS	BAL/GA	Pos	Pos	S
14	32	Neg	No	0	Pos	Absent	Present	Absent	Pos	DS	BAL/GA	Pos	Neg	

TB, tuberculosis; DST, drug-susceptibility testing; BAL, broncho-alveolar lavage; Neg, negative; MDR, multi-drug resistant TB; Pos, positive; R, Rifampicin resistant; DS, drug-susceptible; S, Rifampicin susceptible; GA, gastric aspirate; INH mono, isoniazid mono-resistant; FNA, Fine needle aspiration biopsy of mediastinal node.

particularly useful in this patient group, as culture of respiratory samples taken after treatment initiation is often negative. Since Xpert detects MTB DNA from both live and dead mycobacteria, it may therefore remain positive for longer than culture after initiation of treatment and may guide appropriate therapy.

In this study of children with complicated intrathoracic TB, Xpert was useful as an add-on test to routine culture on BAL samples, as it (a) enabled rapid diagnosis, including of drug-resistant TB in one case, and (b) added to the total diagnostic yield. Although a relatively large proportion of children in this study was confirmed by culture (9/14–64%), improving this to 79% through the addition of Xpert may have considerable clinical impact if confirmed by larger studies.

Xpert on one BAL sample had a high sensitivity (7/9, 78%) compared to BAL culture, particularly considering that most patients (11/14, 79%) were already on treatment at the time of bronchoscopy. Although numbers are small, this value compares favorably to the sensitivity reported for two induced sputum[5,7] and nasopharyngeal[6] samples, and may again reflect the high bacillary burden in children with complicated disease. In support of this argument, Xpert was also more frequently positive in cases where glands had ulcerated into the airway.

It is notable that gastric aspirate culture also contributed to the final diagnostic yield, supporting the evidence that obtaining different sample types, in addition to increasing the number of samples, is likely to improve case ascertainment in children with intrathoracic TB.

The study is limited by the small sample size. In addition, BAL sample volume was not consistent, and we therefore processed samples differently depending on the available volume, collected as part of routine care. Many samples were small volume, due to the relatively low volume of lavage fluid that can be used in children. We did not record the volume of individual BAL samples. Furthermore, only one sample was collected from each child. Current evidence supports the added benefit of multiple samples for improving diagnostic yield,[5,6] although there have been no studies evaluating the incremental yield of additional BAL samples in pediatric intrathoracic TB. In addition, the diagnostic utility of Xpert analysis of intrathoracic lymph node biopsy samples and caseating material should be investigated.

Another limitation is that in this study, being nested within a setting of routine clinical care, children were not all investigated in the same way. The number of routine respiratory samples was variable, precluding a fair comparison between sample types. However, this reflects how children with complicated intrathoracic TB are typically managed in the routine care setting. Future studies should evaluate the utility of BAL Xpert on a wider spectrum of complicated intrathoracic TB disease in children, specifically as an add-on test to other clinical specimens. Sample volume should be systematically recorded, as it is possible that larger volumes may result in improved sensitivity. Although useful, Xpert on BAL samples alone is unlikely to be sufficient for the evaluation of children with complicated intrathoracic TB, due to its imperfect sensitivity and the necessity for culture to confirm full drug susceptibility. The full clinical impact and cost-effectiveness of this diagnostic modality therefore also require further study.

REFERENCES

1. Theart AC, Marais BJ, Gie RP, Hesseling AC, Beyers N. Criteria used for the diagnosis of childhood tuberculosis at primary health care level in a high-burden, urban setting. Int J Tuberc Lung Dis 2005;9:1210–1214.
2. Marais BJ, Hesseling AC, Gie RP, Schaaf HS, Enarson DA, Beyers N. The bacteriologic yield in children with intrathoracic tuberculosis. Clin Infect Dis 2006;42:e69–e71.
3. Goussard P, Gie RP, Kling S, Andronikou S, Lucas S, Janson J, Roussouw G. Bronchoscopic assessment of airway involvement in children presenting with clinically significant airway obstruction due to tuberculosis. Pediatr Pulmonol 2013;48:1000–1007.
4. Steingart KR, Sohn H, Schiller I, Kloda LA, Boehme C, Pai M, Dendukuri N. Xpert® MTB/RIF assay for pulmonary tuberculosis and rifampicin resistance in adults (Review). Cochrane Database Syst Rev 2013; CD009593.
5. Nicol M, Workman L, Isaacs W, Munro J, Black F, Eley B, Boehme CC, Zemanay W, Zar HJ. Accuracy of the Xpert MTB/RIF test for the diagnosis of pulmonary tuberculosis in children admitted to hospital in Cape Town, South Africa: a descriptive study. Lancet Infect Dis [Online first] 2011;11:819–824.
6. Zar H, Workman L, Isaacs W, Munro J, Black F, Eley B, Allen V, Boehme C, Zemanay W, Nicol M. Rapid molecular diagnosis of pulmonary tuberculosis in children using nasopharyngeal specimens. Clin Infect Dis 2012;55:1088–1095.
7. Rachow A, Clowes P, Saathoff E, Mtafya B, Michael E, Ntinginya EN, Kowour D, Rojas-Ponce G, Kroidl A, Maboko L, et al. Increased and expedited case detection by Xpert MTB/RIF assay in childhood tuberculosis: A prospective cohort study. Clin Infect Dis 2012;54:1388–1396.
8. Lee HJ, Seong MW, Park SS, Hwang S-S, Lee J, Park YS, Lee CH, Lee S-M, Yoo C-G, Kim YW, et al. Diagnostic accuracy of Xpert® MTB/RIF on bronchoscopy specimens in patients with suspected pulmonary tuberculosis. Int J Tuberc Lung Dis 2013;17:917–921.
9. de Blic J, Midulla F, Barbato A, Clement A, Dab I, Eber E, Green C, Grigg J, Kotecha S, Kurland G, et al. Bronchoalveolar lavage in children. Eur Respir J 2000;15:217–231.
10. Helb D, Jones M, Story E, Boehme C, Wallace E, Ho K, Kop J, Owens MR, Rodgers R, Banada P, et al. Rapid detection of *Mycobacterium tuberculosis* and rifampin resistance by use of on-demand, near-patient technology. J Clin Microbiol 2010;48:229–237.
11. Abadco DL, Steiner P. Gastric lavage is better than bronchoalveolar lavage for isolation of *Mycobacterium tuberculosis* in childhood pulmonary tubersulosis. Pediatr Infect Dis J 11:735–738.
12. Somu N, Swaminathan S, Paramasivan CN, Vijayasekaran D, Chandrabhooshanam A, Vijayan VK, Prabhakar R. Value of bronchoalveolar lavage and gastric lavage in the diagnosis of pulmonary tuberculosis in children. Tuber Lung Dis 1995;76:295–299.
13. Singh M, Moosa NV, Kumar L, Sharma M. Role of gastric lavage and broncho-alveolar lavage in the bacteriological diagnosis of childhood pulmonary tuberculosis. Indian Pediatr [Comparative Study] 2000;37:947–951.

ORIGINAL ARTICLE

Characteristic Magnetic Resonance Imaging Low T2 Signal Intensity of Necrotic Lung Parenchyma in Children With Pulmonary Tuberculosis

Kwaku Oppong Peprah, MBChB, Savvas Andronikou, PhD,† and Pierre Goussard, MMed (Ped)‡*

Purpose: To show that necrotic areas of the lung demonstrated on computed tomographic scanning in children with primary pulmonary tuberculosis (TB) may be of low signal intensity on T2.

Materials and Methods: Review of magnetic resonance imaging scans (T1/T2/STIR/postgadolinium T1) in 6 children scanned because of low-density necrotic areas demonstrated on computed tomography scanning prior to bronchoscopic confirmation of pulmonary TB.

Results: Abnormalities included airspace consolidation in 6 children (100%); central necrosis in 6 children (100%); nodules in 2 children (33.3%); and lymphadenopathy in 6 children (100%). Low T2 signal in the areas of necrosis was demonstrated in all 6 children (100%) and in an area of at least 2 × 2 cm; 1 child also showed an area of high signal (16.67%). Airspace consolidation demonstrated T2 high signal in all the children (100%). Both children with nodules demonstrated at least 1 nodule with a low signal in addition to the majority of high-signal nodules. Post gadolinium, the consolidation and all high-signal nodules demonstrated enhancement, whereas the areas of lung necrosis and low signal nodules showed no enhancement.

Conclusion: Lung parenchymal necrosis in primary pulmonary TB in children may be of low signal intensity on T2 and STIR magnetic resonance imaging. This may be distal to lymphobronchial obstruction and is probably due to the caseating necrosis.

Key Words: tuberculosis, lung parenchyma, children, magnetic resonance imaging

(*J Thorac Imaging* 2012;27:171–174)

Primary pulmonary tuberculosis (TB) affects the lung parenchyma and regional lymph nodes.[1] Traditional imaging relies on chest radiographs (CXR) to demonstrate lymphadenopathy.[2] Primary TB typically manifests radiologically as parenchymal disease including airspace disease, focal granuloma, air trapping, collapse, expansile pneumonia, caseating consolidation, liquefaction necrosis (drowned lung), cavitation, and miliary interstitial nodules,[3,4] but none of these features are specific to TB.[1,5] The CXR may be normal, however.[4] Computed tomography (CT) is more sensitive than CXR for detecting lymphadenopathy.[6] On CT scanning, lung parenchymal involvement can typically present as airspace consolidation that is dense, homogeneous, and well defined,[4] or as ground-glass opacity, nodules or cavitation.[1,2]

Central airway involvement in TB can be the result of direct extension of tuberculous lymph nodes, endobronchial spread of infection, or lymphatic dissemination to the airway. This can manifest as persistent segmental or lobar collapse, lobar hyperinflation, obstructive pneumonia, or mucoid impaction.[4] Early reports of TB in children include the concept of "caseating consolidation" from compression and erosion of a bronchus by lymphadenopathy and secondary endobronchial spread of bacilli.[3] The airway compression and subsequent parenchymal disease is termed "lymphobronchial TB."[3] However, a CT scan cannot distinguish caseating necrosis relating to TB from other bacterial necrosis (Streptococcus, Staphylococcal pneumonias).

Magnetic resonance imaging (MRI) is especially attractive for pediatric radiology due to its lack of ionizing radiation.[7] Gd-DTPA-enhanced MRI in patients with tuberculoma has demonstrated enhancement of the peripheral portion of the tuberculoma, which was shown pathologically to consist mainly of a fibrous capsule and epithelioid granulomas, and a central zone, which showed no contrast enhancement, and which consisted of caseous necrotic material.[8] In brain lesions[9] and abdominal lymphadenopathy, the MRI signal of TB necrosis is hypointense on T2. Following the same principles, necrosis of the parenchyma in primary pulmonary TB may also have a low T2 signal helping to differentiate it from other causes of parenchymal necrosis.[1] MRI could therefore demonstrate "caseating necrosis" in vivo.

The aim of this study is to demonstrate that necrotic areas of the lung, as shown on CT scanning in children with primary pulmonary TB, may be of low signal intensity on T2.

MATERIALS AND METHODS

All children with symptoms of airway compression and a confirmed diagnosis of TB routinely undergo CT scanning prior to bronchoscopy in our institution. Included in this study are children who demonstrated lung necrosis on CT scanning (areas of low density > 2 × 2 cm demonstrating no enhancement, no vessels, and no bronchograms), and who were more than 6 years of age and could undergo MRI scan without sedation or anesthesia. Patients were excluded from the study when the CT scan demonstrated pockets of air indicating cavitation and/or areas of calcification, both of which can cause a low signal on

From the Departments of *Radiodiagnosis; ‡Paediatrics and Child Health, Faculty of Health Sciences, Stellenbosch University, Tygerberg, Cape Town; and †Department of Radiology, University of Witwatersrand, Johannesburg, South Africa.

The authors declare no conflicts of interest.

Reprints: Savvas Andronikou, PhD, Department of Radiology, University of Witwatersrand, York Rd, Parktown, Johannesburg, South Africa (e-mail: docsav@mweb.co.za).

T2-weighted MRI. MRI scans were performed on a 1.5-T MR scanner (Magnetom, Siemens, Erlangen, Germany). Sequences included T1, T2, STIR, and postgadolinium T1 in axial and coronal planes. One pediatric radiologist with more than 10 years of experience in TB and MRI evaluated the MRIs with regard to airspace consolidation (high T2 signal, enhancing lobar/segmental areas demonstrating air bronchograms); necrosis (areas central to an airspace process of T2 high or low signal corresponding to areas of CT necrosis—lacking air bronchograms and gadolinium enhancement); and nodules (discrete and oval parenchymal lesions). The reader recorded specifically whether the regions of necrosis determined on CT scanning demonstrated low or high signal on T2/STIR for the purposes of this study.

The results were analyzed and presented in a descriptive manner as frequencies and percentages.

RESULTS

The ages of the children ranged from 7 to 13 years. There were 3 boys and 3 girls. All patients had diagnostic confirmation of TB through bronchoscopic biopsy routinely performed through the transcarinal route into the subcarinal group of nodes.[10] Abnormalities included airspace consolidation in 6 children (100%) (Figs. 1, 2); central necrosis in 6 children (100%) (Figs. 1, 2); nodules in 2 children (33.3%); and lymphadenopathy in 6 children (100%). Low T2 signal in the areas of necrosis was demonstrated in all 6 children (100%) in an area of at least 2×2 cm (Figs. 1, 2); 1 child also showed an area of high signal (16.67%) (Fig. 1B). Airspace consolidation demonstrated T2 high signal in all children (100%). Both children with nodules demonstrated at least 1 nodule with a low signal in addition to the majority of high-signal nodules. Post gadolinium, the consolidation and high-signal nodules demonstrated enhancement, whereas the necrosis and low-signal nodules showed no enhancement (Figs. 1, 2).

DISCUSSION

This study demonstrates that areas of lung necrosis identified on CT scanning in children with primary TB may show a low signal on T2/STIR MRI. An inability to localize the primary TB infection results in a wide area of airspace consolidation.[2] If left untreated, the disease progresses to lobar or complete lung opacification and destruction.[4]

The enlarged regional lymph nodes draining the primary parenchymal focus may become hyperemic and edematous and may contain areas of caseation. These may impinge on the wall of a bronchus to occlude the lumen and cause atelectasis or air trapping of the lung distal to the obstruction,[11] termed lymphobronchial TB.[1,3,12] If the nodes rupture into a bronchus, this may lead to acute inhalation tuberculous bronchopneumonia.[11] Typically, parenchymal disease in primary TB manifests as dense, homogeneous parenchymal consolidation in any lobe.[1,13] In addition to airspace disease, oval focal granuloma, air trapping, collapse, expansile pneumonia, liquefaction necrosis ("drowned lung"), cavitation, and miliary interstitial nodules are also types of parenchymal involvement in children.[1,5,6,14] CXRs are effective in demonstrating airspace consolidation (one quarter of patients), the parenchymal nodule that represents the Ghon focus, diffuse

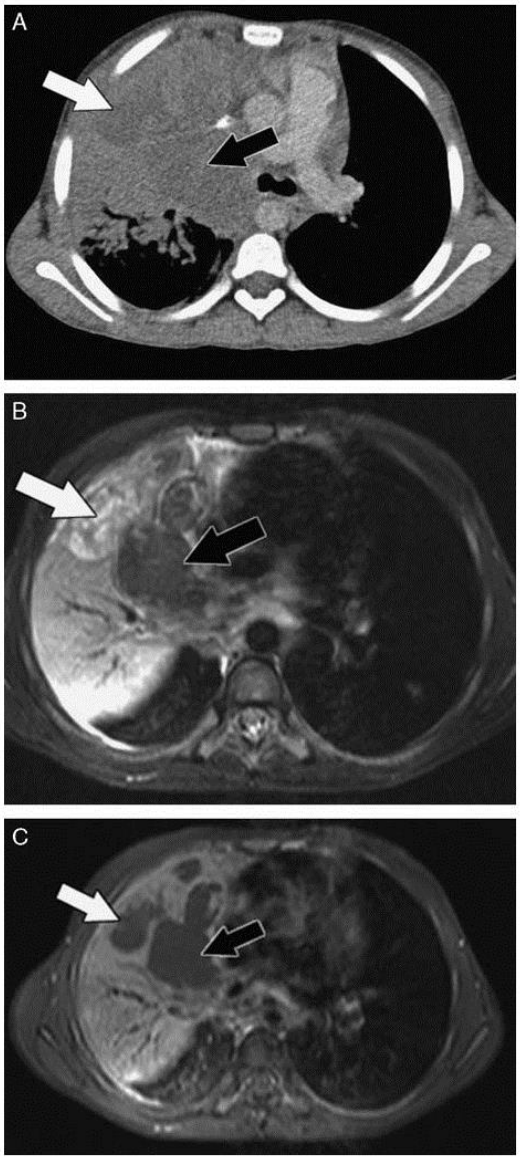

FIGURE 1. Axial images demonstrating lung necrosis on CT scanning and corresponding varying signal on MRI. A, Postcontrast CT scan of the lungs demonstrating central areas of low density (arrows) within an area of airspace consolidation. Note the lack of vessels, bronchograms, and enhancement in the areas of low density, representing lung necrosis. In contrast, the airspace consolidation demonstrates enhancement, vessels, and air bronchograms. B, STIR MRI demonstrates that one area of CT low density demonstrates high signal (white arrow) intensity, whereas the other demonstrates low signal intensity (black arrow) presumably due to different stages of necrosis. C, Postgadolinium T1-weighted MRI demonstrates that the areas of CT low density lack enhancement (arrows), whereas the airspace consolidation enhances.

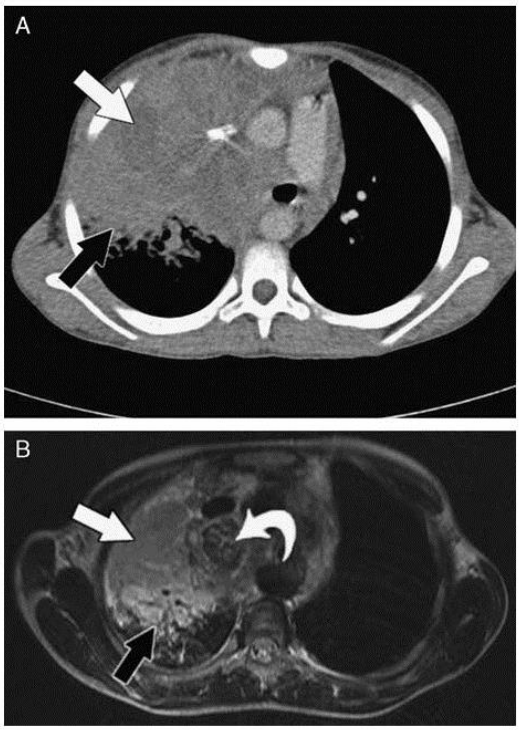

FIGURE 2. Axial images demonstrating airspace consolidation and lung necrosis on CT and STIR MRI. A, Postcontrast CT scan of the lung demonstrates a necrotic area of low density lacking enhancement and air bronchograms (white arrow), located centrally in an area of airspace consolidation (black arrow). B, STIR MRI demonstrates low signal intensity (white arrow) corresponding to the area of necrosis on CT. Also demonstrated are paratracheal lymphadenopathy (curved arrow) of even lower signal intensity and enhancing airspace disease with air bronchograms (black arrow), indicating consolidation without necrosis.

interstitial disease (one third of patients), and effusions.[15] CXRs, however, have been shown to be insensitive to the detection of lymphadenopathy, and there are significant interobserver and intraobserver differences in the detection of lymphadenopathy by film readers.[15] Advanced imaging is sometimes necessary as CXRs may remain normal (15%) in patients with proven primary TB, especially in patients with AIDS.[2]

MRI has successfully demonstrated chest wall, cardiac, mediastinal and vascular lung disease, as well as lung nodules and changes in cystic fibrosis.[7,16 19] MRI can demonstrate some of the features of pulmonary TB and can depict the mediastinal and hilar nodes equally as well as CT scanning.[11] Lymphadenopathy is well demonstrated on STIR imaging as high-signal masses in recognized regions.[15] The lack of ionizing radiation makes MRI a more attractive modality in children.[7]

Lung MRI has been neglected due to 3 technical difficulties: first, signal loss due to cardiac pulsation and respiration;[7] second, susceptibility artifacts caused by multiple air-tissue interfaces; and finally, low proton density of lung tissue.[17] MRI is not an adequate imaging methodology for the detection of small lung lesions, particularly in the vicinity of the diaphragm, because of its rather limited spatial resolution and due to respiratory or cardiac motion.[18] The usual appearance of the lung on conventional MR images is that of a black hole inside the thorax.[7] However, this may be favorable, as any pathology with higher proton density and therefore higher signal appears with a strong inherent contrast against the black surrounding lung tissue.[7] Subtle changes in lung signal due to small lesions or fine reticulations can be missed.[19] The use of MRI for demonstrating intrathoracic lymphadenopathy in children is limited because of the sedation/anesthesia and respiratory gating requirements, as well as the limited availability in countries where TB is endemic.[15]

A T2 low-intensity pulmonary lesion on MRI might contain calcification, air cysts, fibrous tissue, collagen tissue, and paramagnetic material, as these produce preferential T2 shortening or magnetic susceptibility effects on T2-weighted images.[7,18] In this study, all 6 patients had a low T2/STIR signal intensity on MRI in some parts of the involved parenchyma. The CT scans allowed preselection of patients for inclusion that did not demonstrate calcification or air pockets. A study by Chung et al[18] tested whether the hypointensity of lung lesions on T2-weighted imaging can serve as an indicator of tuberculoma in adults. In their study, tuberculomas of the lung ranged from hypointense to hyperintense on T2-weighted sequences according to their aging process.[18] The low T2 signal intensity in all of our patients correlates with these findings. The lung parenchyma surrounding the low T2 areas and other distant parenchymal airspace disease demonstrated a high T2 signal, consistent with airspace disease[7] without necrosis.

In solid, caseating granulomas found in the brain, the lesions are hypointense or isointense on T1-weighted images and isointense to hypointense on T2-weighted images. The reason for the shortening of the T2 signal is not clear, but may be the result of the presence of paramagnetic free radicals in the enclosed macrophages.[9] We speculate the same reason for the necrosis occurring in the parenchymal necrosis and nodular lesions of primary pulmonary TB in children. Limitations of this study include few patients, which make the results less robust; exclusion of patients less than 6 years of age because of the requirement of sedation/anesthesia in these patients; inclusion of only patients with airway symptoms, thereby preventing evaluation of a true prevalence of low T2 signal in children with primary TB; and finally, the lack of biopsy material of necrotic areas, as transbronchial lymph node biopsy (performed routinely) was sufficient for diagnosis.[10]

In conclusion, this study demonstrates that areas of lung necrosis identified on CT scanning in children with primary TB may show a low signal on T2/STIR MRI. Other than surgical pathologic specimens and postmortem studies, there has been no mechanism to demonstrate caseating consolidation described in classification systems of TB. To our knowledge, this is the first description of definitive MRI findings of the entity of caseating necrosis of the lung parenchyma in children with TB (correlated with CT imaging findings). This low signal on T2 is a known characteristic of tuberculous caseous necrosis at other sites. Further research comparing TB lung necrosis and other necrotizing pneumonias is needed to determine whether the low T2/STIR MRI signal can distinguish between the 2 conditions.

REFERENCES

1. Andronikou S, Vanhoenacker FM, De Backer AI. Advances in imaging chest tuberculosis: blurring of differences between children and adults. *Clin Chest Med*. 2009; 30:717–744.
2. Goo JM, Im JG. CT of tuberculosis and nontuberculous mycobacterial infections. *Radiolc Clin N Am*. 2002;40:73–87.
3. Marais BJ, Gie RP, Schaaf HS, et al. The natural history of childhood intra-thocacic tuberculosis: a critical review of the literature from the pre-chemotherapy era. *Int J Tuberc Lung Dis*. 2004;8:392–402.
4. Harisinghani MG, McLoud TC, Shepard JA, et al. Tuberculosis from head to toe. *Radiographics*. 2000;20: 449–470.
5. De Villiers RVP, Andronikou S, van de Westhuizen S. Specificity and sensitivity of chest radiographs in the diagnosis of paediatric pulmonary tuberculosis and the value of additional high-kilovolt radiographs. *Australas Radiol*. 2004;48: 148–153.
6. Andronikou S, Joseph E, Lucas S, et al. CT scanning for the detection of tuberculous mediastinal and hilar lymphadenopathy in children. *Pediatr Radiol*. 2004;34: 232–236.
7. Hirsch W, Sorge I, Krohmer S, et al. MRI of the lungs in children. *Eur J Radiol*. 2008;68:278–288.
8. Sakai F, Sone S, Maruyama A, et al. Thin-rim enhancement in Gd-DTPA-enhanced magnetic resonance images of tuberculoma: a new finding of potential differential diagnostic importance. *J Thorac Imaging*. 1992;7:64–69.
9. Bernaerts A, Vanhoenacker FM, Parizel PM, et al. Tuberculosis of the central nervous system: overview of neuroradiological findings. *Eur Radiol*. 2003;13:1876–1890.
10. Goussard P, Gie RP, Kling S, et al. The diagnostic value and safety of transbronchial needle aspiration biopsy in children with mediastinal lymphadenopathy. *Paediatric Pulmonology*. 2010;45:1173–1179.
11. Buxi TB, Sud S, Vohra R. CT and MRI in the diagnosis of tuberculosis. *Indian J Pediatr*. 2002;89:965–972.
12. Goussard P, Gie R. Airway involvement in pulmonary tuberculosis. *Paediatr Respir Rev*. 2007;8:118–123.
13. Burrill J, Williams CJ, Bain G, et al. Tuberculosis: a radiologic review. *Radiographics*. 2007;27:1255–1273.
14. Smuts NA, Beyers N, Gie RP, et al. Value of the lateral chest radiograph in tuberculosis in children. *Pediatr Radiol*. 1994;24: 478–480.
15. Andronikou S, Wieselthaler N. Modern imaging of tuberculosis in children: thoracic, central nervous system and abdominal tuberculosis. *Paediatr Radiol*. 2004;34:861–875.
16. Hatabu H, Gaa J, Tadamura E, et al. MR imaging of pulmonary parenchyma with a half-Fourier single-shot turbo spin-echo (HASTE) sequence. *Eur J Radiol*. 1999;29:152–159.
17. Kauczor HU, Kreitner KF. Contrast-enhanced MRI of the lung. *Eur J Radiol*. 2000;34:196–207.
18. Chung MH, Lee HG, Kwon SS, et al. MR Imaging of solitary pulmonary lesion: emphasis on tuberculomas and comparison with tumours. *J Magn Reson Imaging*. 2000;11:629–637.
19. Puderbach M, Hintze C, Ley S, et al. MR imaging of the chest: a practical approach at 1.5 T. *Eur J Radiol*. 2007;64: 345–355.

CHAPTER 7

Management of children with severe airway obstruction and the outcome

Introduction

Management and outcome of children with severe airway obstruction due to tuberculosis lymph node compression of the large airways.

Paediatric bronchoscopy plays an important role in determining the site and severity of airway obstruction in intrathoracic tuberculosis. The site and severity of the airway compression by enlarged TB lymph nodes determine which patients require medical or surgical treatment. The proportion of children with pulmonary tuberculosis requiring lymph node enucleation to relieve airway obstruction has been systematically investigated. A number of studies with small patient numbers have described the various procedures and complications that arise from the surgery to relieve TB lymph node compression of the airways. These studies did not evaluate the indications, the optimal timing for enucleation or determine which factors predicted for a surgical intervention.

Goussard, P, Gie RP, Janson JT, le Roux P, Kling S, Andronikou S, Roussouw GJ. Enucleation of enlarged mediastinal lymph nodes due to *Mycobacterium tuberculosis* causing severe airway obstruction in children. (Submitted to The Annals of Thoracic Surgery, September 2014)

The primary aim was to describe the indications and the effectiveness of lymph node enucleation in children presenting with clinical and radiological features of severe airway obstruction caused by TB lymph node enlargement. The secondary aims were to compare the indications for glandular enucleation in HIV-infected children and children infected with drug resistant *Mycobacterium* tuberculosis to those in HIV- uninfected children and those with TB caused by drug susceptible mycobacterium. An enucleation was done in 86 cases (34%). In 23 cases (27 %) the enucleation was done as an urgent procedure, within 14 days of presentation, to relieve acute life threatening airway obstruction. The patients requiring enucleation were significantly younger (18 months vs 32 months) ($p < 0,01$) and more likely to have a positive Mantoux skin test ($p = 0.004$). Culture positivity did not predict for enucleation ($p = 0.6$). The best predictors for lymph gland enucleation was airway compression (>75%) of either bronchus intermedius and/or the left main or significant airway narrowing of the combination of the trachea, bronchus intermedius and the left main bronchus. There was no significant difference in HIV status and drug susceptibility of the mycobacterial cultures when comparing patients. Lymph node enucleation resulted in a more rapid resolution of airway compression when compared to

medical treatment alone. Enucleation resulted in zero mortality and a low morbidity (8%). Most post-operative complications resolved spontaneously.

Maydell A, Goussard P, Andronikou S, Bezuidenhout F, Ackermann C, Gie R. Radiological changes post-lymph node enucleation for airway obstruction in children with pulmonary tuberculosis. Eur J Cardiothorac Surg 2010; 38: 478-483.

No study has investigated the change in the radiological picture post-enucleation. In this retrospective study of 21 paediatric cases that have undergone enucleation the chest radiological prior and subsequent to enucleation were compared. Resolution of bronchus intermedius stenosis and right lower lobe collapse/consolidation was the most consistent postoperative finding. In 43 % the mean time to resolution was 6.5 months postoperatively. The resolution of the complications of lymph node enlargement was more frequently seen than the resolution of the offending lymph node itself.

Conclusion

In children with severe airway obstruction due to TB lymph node enlargement approximately one third will need enucleation of lymph nodes. A significant number with life threatening airway obstruction require an urgent enucleation. Of the children with significant airway obstruction treated medical 27.7% have a poor response to treatment and require an enucleation. Severe obstruction (>75%) of the large airways (bronchus intermedius, left main bronchus and trachea) predict which children are at risk of requiring an enucleation. Enucleation results in significant relief of the airway obstruction and can be safely performed in children. Clinical, radiological and bronchoscopic outcome post enucleation is very good. The optimal duration of medical treatment prior to requiring an enucleation still needs to be determined.

Enucleation of enlarged mediastinal lymph nodes due to *Mycobacterium tuberculosis* causing severe airway obstruction in children

P. Goussard, MMed (Paed),[1] R.P. Gie, FC Paed,[1] J.T. Janson, FC Cardio (SA),[2] P. le Roux [3],
S. Kling, FC Paed,[1] S. Andronikou, PhD,[4] and G.J. Roussouw, FC Cardio (SA)[2]

[1]Departments of Paediatrics and Child Health and [2] Department of Cardio-Thoracic Surgery, [3]Department of Anesthesiology and Critical Care , Faculty of Medicine and Health Sciences, Stellenbosch University, and Tygerberg Children's Hospital, [4] Radiology Department, Faculty of Health Sciences, University of Witwatersrand, South Africa

Address for correspondence
Dr Pierre Goussard
Department of Paediatrics and Child Health
Faculty of Medicine and Health Sciences
Stellenbosch University
P O Box 19063
7505 Tygerberg
South Africa
e-mail: pgouss@sun.ac.za

Abstract

Background: Large airway compression by enlarged tuberculosis (TB) lymph nodes results in life threatening airway obstruction in a small proportion of childhood. The indications, safety and efficacy of lymph node decompression by enucleation are not adequately been described.

Aim: The aim of the study is to refined the indications and efficacy of TB lymph node enucleation in children with severe airway compression and determine the factors which influence the indications and outcome.

Patients and methods: In prospective cohort children (3 months-13 years) children with life threatening airway obstruction resulting from TB lymph node compression of the large airways attending a tertiary hospital were enrolled. The site and degree of airway obstruction were assessed by fibreoptic bronchoscopy and chest CT-scan.

Results: Of the 250 children enrolled 34% (n=86) required transthoracic lymph node enucleation, 29% as an urgent procedure and 71% (n=63) after failing one month's anti-tuberculosis treatment that included glucosteroids. Greater than 75% obstruction of bronchus intermedius (OR 2.28 95th CI 1.29- 4.02) and left main bronchus (OR 3.34 95th CI 1.73-6.83) where the best predictors for enucleation. HIV status, drug resistance, and malnutrition were not associated with enucleation. For enucleation there were few complications (self-limiting) (8%) or treatment failures (2%), and there were no fatalities.

Conclusion: In childhood TB severe airway obstruction caused by enlarged lymph nodes decompression via transthoracic enucleation is required in a third of cases. This procedure can be safely performed with low complication, failure and fatality rates.

Introduction

Surgery for acute pulmonary tuberculosis (TB) is rarely performed in children. There is however a small group of children who present with life threatening airway obstruction due to airway compression by enlarged lymph nodes caused by *Mycobacterium tuberculosis*. Transthoracic surgical decompression (enucleation) of the enlarged mediastinal lymph nodes is required to relieve the airway obstruction. The proportion of children with pulmonary tuberculosis requiring enucleation of the lymph nodes to relieve airway obstruction has not been reported. There have been a number of small studies describing the procedure and complications that arise from the surgery[1- 7]. These studies did not evaluate the indications for enucleation or the optimal timing for the intervention. A definite indication for enucleation is children requiring assisted ventilation due to critical airway obstruction. While relative indications include acute perforation of a lymph node into the airway with accompanying respiratory failure, obstruction of major airway resulting in lung or lobar collapse, a ball- valve effect with unilateral hyperinflation, permanent bronchial stenosis, superior vena cava obstruction and subcarinal oesophageal obstruction. These indications have not been tested in a prospective clinical trial and the degree of airway obstruction requiring surgery has not been determined. Surgical intervention to relieve airway obstruction is thought to prevent damage to the underlying lung parenchyma preventing bronchiectasis and recurrent lower respiratory tract infections [8- 10]

The primary aim of this study is to describe the indications and the effectiveness of lymph node enucleation in children presenting with clinical and radiological features of severe airway obstruction caused by TB lymph node enlargement. The secondary aim is to compare the indications for glandular enucleation in HIV-infected children and children infected with drug resistant *Mycobacterium* tuberculosis to those in HIV- uninfected children and those with TB caused by drug susceptible mycobacterium.

Patients and methods: This prospective, cohort study was done from January 2004 to December 2011 at Tygerberg Children's Hospital, Western Cape, South Africa. The study population and methods have been described in detail in a recently published paper.[11] Briefly, all children between the ages of 1 month and 13 years admitted to the hospital with clinical and radiological signs of severe airway obstruction were investigated and those with airway obstruction caused by TB lymph node compression of the airways enrolled in the study. Children were excluded if the lymph node compression of the airways was asymptomatic, not caused by *Mycobacterium tuberculosis*, or if there was a contraindication to fiber-optic bronchoscopy or general anesthetic. All participants

underwent HIV testing with appropriate pre- and post-test counseling. Other tests routinely performed were a Mantoux skin test, chest radiography and gastric aspirates for *Mycobacterium tuberculosis* culture and drug susceptibility testing. A fiber optic bronchoscopy under general anesthetic was performed in the bronchoscopy theatre to determine the site, degree and extent of the airway obstruction. During the fiber optic bronchoscopy the divisions of large airways were systematically examined and all sites of airway narrowing recorded. The degree of airway narrowing was estimated for each site. Bronchoalveolar lavage (BAL) samples were collected, from the site of greatest involvement, and transbronchial needle aspiration biopsies were collected for *Mycobacterium tuberculosis* culture and susceptibility testing as indicated.[12] Complications of the fiber optic bronchoscopy or anesthetic was recorded.

Children with life threatening airway obstruction requiring intubation and ventilator support prior to bronchoscopy were investigated in the paediatric intensive care unit using the same protocol.

The children diagnosed with TB were treated according to internationally recognised protocols and drug dosages. During the intensive phase of 2 months 4 anti-tuberculosis drugs (isoniazid 10mg/kg/day, rifampicin 10mg/kg/day, pyrazinamide 25mg/kg/day and ethambutol 20mg/kg/day) were given daily followed by the consolidation phase of 2 drugs (isoniazid and rifampicin) for 4 months. If multidrug resistant tuberculosis was either suspected or confirmed 5-6 drug treatment was prescribed for 18-24 months according to World Health Organization recommendations. All cases of significant airways obstruction (>50%), as estimated at bronchoscopy, were given prednisone (2mg/kg/day) for 30 days and then weaned.

The children were followed up after 1 month's treatment and re-evaluated. If the child had significantly improved as assessed clinically and radiologically medical treatment was continued. If however the child remained symptomatic and/or the chest radiological image showed no improvement the child was scheduled to have a second bronchoscopy. The second bronchoscopy was carried out in the same systematic way as the first bronchoscopy under general anesthetic.

Children with airway narrowing less than 75% of the airway caliber were continued on antituberculosis treatment while enucleation considered in those with a greater degree of airway obstruction.

The indications for enucleation used in this study were:

1. Children with severe life threatening airway obstruction requiring ventilation for respiratory failure due to TB lymph node obstruction of the airways.
2. Children with critical airway obstruction as accessed at the initial bronchoscopy where the airway obstruction of both the main bronchi or trachea was greater than 90%.
3. Children with severe airway obstruction who after one month's medical treatment who at bronchoscopic re-evaluation still had airway obstruction of one or both main bronchi of greater than 75%.

The children with significant parenchymal disease of the right upper lobe, especially those with expansile pneumonia, were not considered for transthoracic enucleation as the right upper lobe needed to be collapsed to perform the transthoracic enucleation. This posed an additional risk to the child during anaesthesia. These children were treated for an additional month and then re-evaluated. If the pneumonia had improved and significant airway compression (>75%) was still present enucleation was then performed.

All the children requiring surgery had a chest computer tomography performed under general anaesthetic prior to the enucleation to enable planning of the surgery.

Mediastinal node enucleation

Anesthetic technique

After a gas induction with sevoflorane endobronchial intubation of the non-operative side was attempted unless bronchoscopy revealed intraluminal node erosion. Complete lung separation was seldom achieved. Compression of the exposed lung during surgery resulted in profound desaturation, particularly where the dependent lung was significantly diseased. Increased F_iO_2 , PEEP (2-5 cmH_2O) and shortened surgical access time were used to manage the problem. When these failed frequent lung re-inflation was required to maintain oxygenation (arterial saturation > 85%). Intraluminal bleeding seldom occurred but airway plugging due to caseous necrotic material obstructing the airway was a frequent problem. The airway plugging was resolved by suction of the endotracheal tube.

Operative technique:

The pre-operative chest CT- scan was used to determine the site of the mediastinal lymph nodes required enucleation to relieve the airway obstruction.

A muscle sparing small right thoracotomy through the 4th or 5th intercostal space was the most common access used in children with airway compression of the distal trachea, right main bronchus, bronchus intermedius and proximal left main bronchus. The right upper lobe was gently compressed to expose the mediastinum. The capsule of the node was opened using a cautery with care taken not to injure the esophagus, vasculature or nerves. A sucker and/or forceps were used remove the nodal contents which varied from a cold abscess with pus to fleshy glandular tissue. Communication between the paratracheal nodes and subcarinal nodes was frequently observed. The subcarinal nodes were drained separately. The whole node was not removed since attempting this could injure the surrounding structures.

Where the mediastinal nodes had ulcerated into the airway an air leak sometimes resulted. This was dealt with by suturing the capsule of the lymph node. No additional measures were taken as air leaks usually sealed within 1 or 2 days. No sutures were placed in the eroded trachea or large airways as this could possibly lead to bronchial stenosis.

Isolated left main bronchus obstruction was uncommon and was dealt with via a left thoracotomy. The mediastinal pleura was opened over the aortopulmonary window and the aortopulmonary node and subcarinal nodes enucleated. If the bronchus was compressed between the left pulmonary artery and descending aorta, the ligamentum arteriosum was divided and a posterior aortapexy of the descending aorta performed.

The lung was expanded before closure and a single intercostal drain inserted.

Postoperatively early extubation and spontaneous ventilation was aimed for in all the patients. All children, even those extubated in theatre, were admitted to pediatric intensive care for respiratory support, monitoring and analgesia.

Pain management included: epidural analgesia and intravenous paracetamol or morphine. Chest radiographs were routinely performed after surgery to exclude surgery related complications. The intercostal drain was removed after 24 hours if there was no sign of a persistent air leak. Surgical complications together with the need for ventilation, the duration of ventilation as well as the duration of PICU and hospital stay were recorded.

Patients were continued on their antituberculosis regimen and followed up after 1 month. Any children with symptomatic airway obstruction or a worsening chest radiograph were re-admitted and clinically re-evaluated. If there were signs of significant airway obstruction the child underwent additional fibreoptic bronchoscopy.

Data analysis was performed using SAS (Statistical analysis system) version 9.1 (SAS Institute Inc., Cary, North Carolina, USA). Cross tabulations with the Chi-square test for comparing categorical variables, and one-way ANOVA for comparing means between groups was used.

Informed consent for the procedures were obtained from the parents or legal caregivers. The Human Research Ethics Committee of the Faculty of Health Sciences, Stellenbosch University (N10/08/282), approved the study.

Results:

Two hundred and fifty patients were enrolled (male: 58%) with a median age of 14 months (range: 2-156 months) and a median weight of 8.5kg (range 2.7-39 kg). Fifty percent were below the 3-percentile weight for age. Forty-one (16%) were HIV positive of whom 56% were stage 3 (WHO classification). In addition to the airway obstruction 92 (37%) had radiological features suggestive of pneumonia. Of those with pneumonia 56 (78%) had a radiological picture compatible with expansile pneumonia.

The Mantoux skin test was positive in 62% (>10mm induration) and *Mycobacterium tuberculosis* was cultured from 194 (77.6%) cases. In nineteen cases both the culture and Ziehl Neelsen stain were positive. Drug susceptibility testing was conducted on 178 (91%) cultures of which 28 (16%) were drug resistant. Of the drug resistant cases 13 were mono-resistant, 12 multi-drug resistant and 2 multiple drug resistant. Extensive drug resistance (XDR TB) was present in one case.

Bronchoscopic findings:

At bronchoscopy compression of the large airways by lymph nodes, exterior to the airway lumen, occurred in 242 (97%) of the cases. Glandular ulceration into the airway lumen without airway compression was present in 3% (n = 8). In 49% of cases the airway compression was complicated by glandular ulceration into the airways with the right side

involved in 64%. The main sites of airway compression were tracheal compression (56%), right bronchial tree (56%) and the left bronchial tree (66%). Both bronchi trees were narrowed in 53% of patients. Bronchus intermedius (78%) was the commonest site of airway narrowing on the right while on the left side it was the left main bronchus (64%). Bronchius intermedius was compressed from medial and lateral in 95% of cases implying compression between the enlarged hilar and subcarinal lymph nodes.
Only one adverse event, worsening airway obstruction, occurred during bronchoscopy requiring admission to the PICU.

Urgent lymph node enucleation:

Enucleation was done in 86 cases (34%). In 23 cases (27 %) the enucleation was done as an urgent procedure within 14 days of presentation to relieve acute life threatening airway obstruction. The mean duration of treatment prior to enucleation in the urgent group was 13 days (range: 1 – 157 days) which was significantly shorter than those requiring a planned enucleation 62 days (range 15 – 173 days) ($p< 0.01$). Comparing those requiring an urgent enucleation to those having a planned enucleation there was no significant difference in age, sex, weight, serum C-reactive protein, blood white cell count, HIV status and drug susceptibility of the mycobacterial cultures. Of interest was fact that there was no significant difference between the urgent compared to the planned enucleation groups regarding the sites and the degree of airway obstruction as determined at bronchoscopy or the presence of lymph nodes ulcerating into the airways. Multivariant analysis using a combination of the airways showed no difference in the site or degree of airway obstruction implying ill-defined lung pathology that contributed to the severity of airway obstruction.

Of the 22 children requiring ventilator support on admission 10 (45%) required an enucleation. This proportion was not different from the children not ventilated on admission that required enucleation.

Non-urgent lymph node enucleation:

Of the remaining 227 patients who were treated medically a single bronchoscope was performed in 135 cases and a second bronchoscope required in 92 (40%) cases following 1 month of medical treatment. Of the 227 patients treated medically 63 (27.7%) required transthoracic enucleation. Of the 63 patients requiring enucleation 52 showed no clinical or radiological improvement in spite of 1 month’s medical treatment and still had severe airway obstruction. A further 92 cases had shown clinical improvement but still had

symptomatic airway obstruction or had no radiological improvement and were subjected to a second bronchoscopy. Of the 92 cases that underwent a second bronchoscopy 11(12%) met the criteria for enucleation while in 81 the obstruction was less than 75% and they were continued on their medical treatment. In total 164 (66%) responded successfully to medical treatment. The mean duration of time between the initial scope and the second bronchoscope was 34 days (range 4 - 186 days). In those requiring a second bronchoscopy (n=92) a BAL sample for *Mycobacterium tuberculosis* culture was available in 83 (90%) cases. In spite of being adherent to treatment 14 (17%) were still culture positive although drug susceptible.

Factors predicting for lymph node enucleation:

The degree and sites of airway obstruction predicting enucleation is shown in Table 1 and 2

Left main bronchus (OR 2.28 (95th CI:1.29 – 4.02) and bronchus intermedius obstruction (OR 3.34 (95th CI:1.73 – 6.83) of greater than 75% were the best predictor for enucleation (Table 3). The combination of trachea, bronchus intermedius, left main bronchus obstruction also predicted for enucleation (Table 3) Lymph node ulcerating into the airway was not a predictor for enucleation.

The patients requiring enucleation were significantly younger (18 months vs 32 months ($p < 0,01$) and more likely to have a positive Mantoux skin test ($p = 0.004$). Malnutrition (weight below 3rd percentile for age) and contact with an adult infectious case, specimen smear positivity for ZN bacilli and culture positivity did not predict for enucleation ($p = 0.6$). Specimen culture results and the requirement for enucleation are shown in Table 3. The presence of an expansile pneumonia did not predict for enucleation (Table 4).

HIV infected and children with drug resistant tuberculosis:

There were 41 children that were HIV positive with a mean blood CD4 count of 1397/ul. The number of HIV positive children 13 (32%) requiring enucleation did was not significantly different from HIV negative children. Similarly in the 28 children with drug resistant TB 8 (29%) required an enucleation which was not significantly differently from children with drug susceptible TB.

Postoperative care:

Postoperative ventilation was required in 41 (47%) children. The median duration of ventilation was 0.5 hours (range 0 – 336 hours) and the median postoperative stay in the

pediatric ICU was 1 day (range 1 – 34 days). The median duration of stay in the PICU for those initially requiring an urgent enucleation was 3.4 days compared to the 1 day for children requiring a non-urgent enucleation. The median duration of hospital stay post surgery was 5 days (range3 – 58 days).

Treatment failures:

There were 2 treatment failures in this study. The one child had persistent severe airway obstruction and required a second enucleation 2 months after the initial enucleation. The second child had persistent severe tracheal compression following the enucleation requiring a tracheostomy for prolonged ventilation.

Postoperative complications:

Surgery related complications were seen in 7 cases (8%) that included: pneumothorax after removal of the intercostal drains (n = 3), chylothorax (n = 3) and broncho – oesophageal fistula (n=1). The three persistent air leaks resolved spontaneously after the insertion of an intercostal drain. The chylothoraces were self-limiting needing no further surgical intervention. The broncho-oesophageal fistula was probably related due to surgery and was surgically repaired without any long-term consequences. There were no bronchus or pulmonary vasculature tears, nerve injuries. No lobectomy or pneumonectomy were required.

Response to surgical treatment:

Children (n= 70) had a bronchoscopy following the enucleation. The results of this follow-up bronchoscopy are given in figure 1. This group (n=70) are compared to the children who were treated medically had a follow-up bronchoscopy (n=92) during the course of their treatment. The median duration of time between the initial bronchoscopy and the follow–up bronchoscopy was 33.5 days. When comparing the group requiring the enucleation to the group treated medically both groups showed a significant improvement when compared to the original bronchoscope. The degree of improvement was the largest in the group that had enucleation performed with both the enucleation and medical treated groups reaching similar endpoints regarding bronchial lumen diameter. (See Figure 1)

Long-term follow up and consequences:

During follow-up after 6 months on treatment (n = 165) 6 children developed bronchiectasis with 5 cases occurring in the medically treated group. (p = 0.3) Three of the

cases that developed bronchiectasis were HIV positive. Two children developed a broncho-oesophageal fistula between the left main bronchus and the oesophagus. The fistula was associated with lower lobe bronchiectasis in both cases. Of the 6 children with bronchiectasis two were severely symptomatic requiring a lobectomy. The one child had a right middle and right lower lobe lobectomy but remained symptomatic. The other child had left lower lobe bronchiectasis that was complicated by an acquired broncho-esophageal fistula. This child remained asymptomatic following a left lower lobe lobectomy.

Discussion

In this prospective cohort study of 250 infants and children who presented with severe airway obstruction due to lymph node compression of the large airways transthoracic enucleation of the lymph nodes were required in 34% of cases. Of the cases requiring enucleation 27% were required within the first 14 days of presentation to relieve life threatening airway obstruction. Of the patients treated medically 27.7% required enucleation one month after being enrolled as their severe airway obstruction had failed to respond to treatment. Short-term operative and postoperative complications occurred in 8% of cases. HIV infected children and children with MDR TB did not have an increased risk of requiring enucleation.

There is little written about the indications for transthoracic lymph node enucleation. Although there are a wide range of indications suggested in the literature in this cohort of 250 cases only 2 situations required enucleation: acute life threatening airway obstruction and chronic airway obstruction that failed to resolve after a month of medical treatment that included oral steroids. Other indications in the literature include superior cava syndrome, esophageal rupture and bronchial stenosis but these did not occur in this cohort.[5]

The best predictor for lymph node enucleation obstruction of both bronchus intermedius and the left main bronchus of greater than 75% or if there was significant airway narrowing of the trachea, bronchus intermedius and the left main bronchus. It was surprising that lymph node ulceration into the airways did not predict for enucleation in spite being present in 49% of the cases. One could postulate the as a result of the ulceration of the lymph node into the airway decompression occurred spontaneously. When comparing the degree and site of airway narrowing in children requiring an urgent enucleation to those who had a planned enucleation after failing medical treatment there was no difference. The most probable explanation is that those requiring an urgent enucleation had additional

pathology that precipitated the respiratory failure requiring admission. In previous studies up to 66% of those requiring enucleation were being ventilated [5]. This study of the 22 children being ventilated only 10 of these cases required urgent enucleation. The indications for enucleation remained the same for those being ventilated as for those not ventilated with greater the 90% obstruction of bronchus intermedius and left main bronchus being the commonest indication.

What predisposes some children to develop severe airway obstruction remains unclear. It is a well-known fact that young children develop more severe airway obstruction probably due to the size and compliance of the airways.[13] Children requiring enucleation were more likely to have positive Mantoux skin test suggesting an up regulated immune response but indicators of severe disease like culture or smear positivity were not statistically more common in the enucleated group. Similarly, malnutrition, HIV infected children and MDR TB known predictors of severe disease were however not predictors for severe airway compression requiring enucleation.

Previous studies have not systematically investigated the site and degree of airway obstruction. The sites and degree of airway involvement is in keeping with the findings of computer tomography studies on TB lymph node enlargement in children. In a recent study the commonest sites of airway compression where bronchus intermedius (75%), left main bronchus (64%) and trachea (62%).[14] Both Andronikou and Lucas et al have also reported that subcarinal nodes are the most commonly enlarged lymph nodes seen on CT scan in children with PTB, ranging from 92 – 100%. [14,15] Enlargement of the subcarinal lymph nodes contributes to compression of both bronchus intermedius and left main bronchus and is an important group of lymph nodes to decompress during surgery. This explains why most of the children had a right thoracotomy as this allows easier access to the subcarinal lymph nodes.

The outcome of children requiring enucleation was excellent with only 2% treatment failure and no deaths in this cohort. Short-term complications which included pneumothorax and chylothorax were all managed conservatively. Serious complications previously reported which included bronchial tear and pulmonary artery laceration were not experienced probably due to the surgical technique. Opening the capsule of the node and curettaging or sucking out the contents of the node decompressed the involved lymph nodes. No nodes were surgically removed. Long-term complications included bronchiectasis (3.5%) and broncho-esophageal fistula (1%). Both these complications have been previously described in studies with a limited number of patients. [6] Our study was also not powered to

determine if early enucleation prevented bronchiectasis. An interesting observation was that five of the six cases of bronchiectasis occurred in children who did not have an enucleation although the resulting lumen was similar in the enucleation and medically treated groups. This suggests that bronchial stenosis was not the cause of the bronchiectasis.

Although this is a large cohort there are a number of limitations to this study. Firstly children were not randomized to receive enucleation or be treated medically as this was thought to be unethical although there are no studies to support this contention. This study was carried out in a region with a high prevalence of HIV and MDR TB. In spite of this we were only able to include a limited number of children who were living with HIV or who had MDR-TB. Due to the limited numbers we could underestimate the effect of these 2 conditions. It could also be argued that if the medical treatment was continued for a longer period less children would have required surgical intervention. Finally, we were only able to follow up 66% of the enrolled patients due to logistical reasons, mainly transport. This could lead us to incorrectly underestimate estimate the long-term complications of this form of management.

In this large cohort of children with severe airway obstruction due to tuberculous lymph node obstruction of the airways 34% required enucleation to relieve the obstruction. Enucleation for life threatening airway obstruction was required in 27% and the remaining 73% after failing one month of medical treatment. Transthoracic enucleation was highly successful relieving the airway obstruction in 98% of cases with a low morbidity and no mortality. The investigation and management of severe airway obstruction requires sophisticated facilities that are not available to children in Africa and South East Asia where the majority of childhood TB occurs. Surrogate markers are required to simplify the management of this life threatening complication of childhood TB.

References

1. MacPherson AM, Lutwyche VU. Collapse of the lung associated with primary tuberculous lesion. Thorax 1950;5:1-4.
2. Freixinet J, Varela A, Lopez RL, Caminero JA, de Castro RF, Serrano A. Surgical treatment of childhood mediastinal tuberculous lymphadenitis. Ann Thorac Surg 1995;59:644-646.
3. Nakvi AJ, Nohl-Oser H.C. Surgical treatment of bronchial obstruction in primary tuberculosis in children: report of seven cases. Thorax 1979;34:464-469.
4. Huish DW. The surgical treatment of pulmonary tuberculosis in childhood and adolescence. Thorax 1956;11:186-200.
5. Papagiannopoulos KA, Linegar AG, Harris DG, Rossouw GJ. Surgical management of airway obstruction in primary tuberculosis in children. Ann Thorac Surg 1999;68:1182–1186.
6. Hewitson JP, von Oppell UO. Role of thoracic surgery for childhood tuberculosis. World J Surg 1997;21:468–474.
7. Worthington MG, Brink JG, Odell JA, Buckels J, de Groot MK, Klein M, Gunning AJ. Surgical relief of acute airway obstruction due to primary tuberculosis. Ann Thorac Surg 1993;56:1054-1062.
8. Cameron JK, Hay JD, Temple LJ. A critical examination of the role of surgery in the treatment of primary pulmonary tuberculosis in children. Thorax 1957;12:329-337.
9. Chesterman JT. The surgery of primary pulmonary tuberculosis in children. Thorax 1957;12:159-163.
10. Vosschulte K. Uber die Exstirpation tuberkulöser Mediastinoldeusen bei drohendem Bronchusdurchbruch. Chirurg 1951;22:310–316.
11. Goussard P, Gie RP, Kling S, Andronikou S, Lucas S, Janson J, Rossouw GJ. Bronchoscopic assessment of airway involvement in children presenting with clinically significant airway obstruction due to tuberculosis. Pediatr Pulmonol 2013;48:1000-1007.
12. Goussard P, Gie RP, Kling S, Nel ED, Louw M, Schubert PT, Rhode D, Vanker A, Andronikou S. The diagnostic value and safety of transbronchial needle aspiration biopsy in children with mediastinal lymphadenopathy. Pediatric Pulmonol 2010; 45:1173-1179.
13. Zucker EJ, Epelman M, Restrepo R, Lee EY. In Congenital and Acquired Large Airway Disorders in Pediatric Patients Garcia- Pena P, Guillerman PR. Pediatric Chest Imaging Heidelberg , Springer –Verlag Heidelberg , 2013; pp 219 – 240

14. Lucas S, Andronikou S, Goussard P, Gie RP. CT features of lymphobronchial tuberculosis in children, including complications and associated abnormalities. Pediatr Radiol 2012; 42:923-931.
15. Andronikou S, Joseph E, Lucas S, Brachmeyer S, Du Toit G, Zar H, Swingler G. CT scanning for the detection of tuberculous mediastinal and hilar lymphadenopathy in children. Pediatr Radiol 2004;34:232-236.

TABLE 1 - The site and degree of airway obstruction predicting enucleation

Site of the obstruction	Mean % of obstruction of airway	Enucleation no	Enucleation yes	p- value
Trachea	49%	(n = 84) 47%	(n = 58) 53%	ns
Left main bronchus	60%	(n = 92) 56%	(n = 64)65%	<0.01
Bronchus intermedius	73%	(n = 107) 65%	(n = 71) 84%	< 0.01
Right main bronchus	72%	(n = 18)70%	(n = 15) 74%	ns

TABLE 2 - The sites of airway involvement predicting enucleation

Airway involvement	Enucleation no	Enucleation yes	OR 95% CI	p - value
Right side involvement)				
Present (n= 212)	132	80	3.23 (1.34 –	0.005
Absent (n = 38)	32	6	7.77)	
Left side involvement				
Present (n= 164)	98	66	2.22 (1.24 –	0.004
Absent (n = 86)	66	20	3.95)	
Both right and left				
involvement	73	59	2.72 (1.58 –	0.0002
Present (n = 132)	91	27	4.68)	
Absent (n = 118)				
Trachea				
Present (n = 142)	84	58	1.97 (1.15 –	0.009
Absent	80	28	3.39)	
Bronchus intermedius				
Present (n = 178)	107	71	3.34 (1.73 –	0.0002
Absent (n = 68)	57	11	6.83)	
Left Main bronchus				
Present (n = 156)	92	64	2.28 (1.29 –	0.003
Absent (n = 94)	72	22	4.02)	
Right Main bronchus				
Present (n = 33)	18	15	1.71(0.82 –	ns
Absent (n = 217)	146	71	3.58)	
Right upper lobe				
bronchus	48	39	2.19 (1.27 –	0.003
Present (n = 87)	116	43	3.78)	
Absent (n = 159)				
Right middle lobe				
bronchus	29	15	1.26 (0.63 –	ns
Present (n = 44)	127	52	2.55)	
Absent (n = 179)				
Right lower lobe				
bronchus	5	2	1.11 (0.21 -	ns

Present (n = 7)	153	68	5.87)	
Absent (n = 221)				
Left upper lobe bronchus				
Present (n = 30)	21	9	1.18 (0.52- 2.71)	ns
Absent (n = 214)	142	72		
Lingula bronchus				
Present (n = 23)	19	4	2.51 (0.85 –	0.07
Absent (n = 220)	144	76	7.39)	
Left lower lobe bronchus				
Present	8	2	2.03 (0.43 –	ns
Absent	154	76	9.48)	

TABLE 3 - Specimen culture results and the requirement for enucleation

	Enucleation no	Enucleation yes	p-value
ZN positive all sources			
Yes (n = 48)	33	71	ns
No (n = 202)	131	15	
ZN positive on BAL			
Yes (n = 31)	20	11	ns
No (n = 209)	136	73	
Culture positive : all sources	123	71	ns
Yes (n = 194)	41	15	
No (n = 56)			
BAL culture positive			
Yes (n = 109)	77	32	0.08
No (n = 137)	84	52	
Gastric washing culture positive			
Yes (n = 123)	71	52	0.09
No (n = 87)	59	28	

TABLE 4 - Factors predicting for enucleation

	Enucleation no	Enucleation yes	p- value
Age (mean) 27 months	32 months	18 months	< 0.01
Sex			
Male (n 144)	97	47	ns
Female (n = 106)	67	39	
Weight(mean) 9.7 kg	10.6 kg	8 kg	< 0.01
Weight			
< 3p (n= 125)	76	49	0.06
>3p (n = 123)	87	36	
Mantoux			
Positive (n = 139)	101	38	0.004
Negative (n = 83)	45	38	
Contact			
Yes (n = 153)	99	54	ns
No (n = 97)	65	32	
HIV			
Positive (n = 41)	28	13	ns
Negative (n = 209)	136	73	
Resistant TB			
Yes (n = 28)	20	8	ns
No (n = 150)	97	53	
Ventilation			
Yes (n = 22)	12	10	ns
No (n = 228)	152	76	
Node open in airway			
Yes (n = 123)	80	43	ns
No (n = 127)	84	43	
Lmb			
<75%	81	50	ns
>75%	11	14	

Bronchus intermedius			
<75%	83	24	0.0001
>75%	24	47	
LMB < 75% and Bronchus intermeduis <	44	1	
75%	6	2	0.00001
LMB > 75% and bronchus intermedius <	8	24	
75%	1	10	
LMB < 75% and Bronchus intermeduis >	0	54	
75%			
LMB > 75% and Bronchus intermedius >			
75%			
Trachea and LMB and Bronchus			
intermedius involvement			

FIGURE 1 - Response to treatment as determine by follow – up bronchoscopy

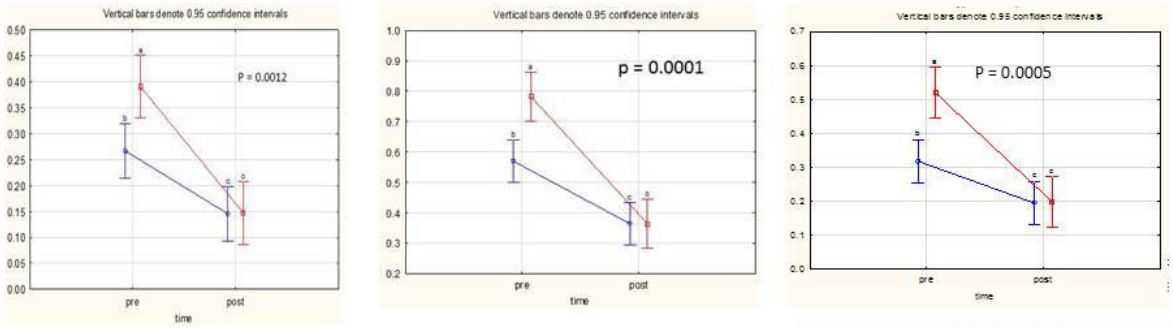

Trachea | Bronchus intermedius | Left main bronchus

Blue line : Medical treatment
Red line : Surgical treatment

ELSEVIER

European Journal of Cardio-thoracic Surgery 38 (2010) 478–483

EUROPEAN JOURNAL OF CARDIO-THORACIC SURGERY

www.elsevier.com/locate/ejcts

Radiological changes post-lymph node enucleation for airway obstruction in children with pulmonary tuberculosis☆

Arthur Maydell*, Pierre Goussard, Savvas Andronikou, Fourie Bezuidenhout, Christelle Ackermann, Robert Gie

Tygerberg Hospital, Cape Town, South Africa

Received 24 August 2009; received in revised form 31 January 2010; accepted 3 February 2010; Available online 25 March 2010

Abstract

Background: Tuberculous lymphadenopathy causing airway obstruction in children may be life threatening and may require surgical enucleation of the lymph glands. There are no studies investigating the radiological picture post-enucleation. We attempt to explore this area in our study. **Method:** A retrospective study of the imaging in 21 paediatric cases having undergone tuberculosis (TB) lymph node enucleation. **Results:** Bronchus intermedius (BI) stenosis was present in 95% of patients undergoing enucleation, followed by left main bronchus (LMB) (81%) and right main bronchus (RMB) (67%) stenosis. Right lung collapse/consolidation occurred more frequently (48–62%) than left-lung collapse/consolidation (10–14%). Resolution of BI stenosis and right lower lobe (RLL) collapse/consolidation is the most consistent postoperative finding. Nine children resolved at an average time of 6.5 months postoperatively, while 10 children were still resolving at an average time of 4.5 months. **Conclusion:** The resolution of the complications of lymph node enlargement (airway stenosis and lung collapse/consolidation) was seen more frequently than the resolution of the offending lymphadenopathy itself. Right-sided disease was necessary to produce complications severe enough to require enucleation. Subcarinal lymph node enucleation is sufficient for resolution of LMB stenosis and associated left-lung sequelae.

Keywords: Airway obstruction; Enucleation; Tuberculosis; Radiological changes

1. Introduction

Tuberculosis (TB) lymphadenopathy causing airway obstruction in children is a serious and sometimes life-threatening feature of the disease, with the prevalence of airway obstruction reported between 25% and 38.4% of children with pulmonary tuberculosis (PTB) [1,2]. Surgical management in the form of thoracotomy and enucleation of the offending groups of lymph glands is indicated in life-threatening airway stenosis.

Bronchoscopy is used mainly for the diagnosis of airway stenosis and the removal of herniating lymph glands and caseating material from the airways [3], but it is not able to relieve the pressure on the trachea and bronchi from the surrounding lymphadenopathy causing airway stenosis, which can only be achieved through enucleation. TB gland enucleation is an open-chest procedure, yet is minimal in terms of excision of tissue, serving mainly to incise and drain the enlarging masses of connecting caseating TB lymph nodes surrounding and compressing the major airways.

As yet there are no studies directly investigating the change in radiological picture post-enucleation of TB lymphadenopathy in the paediatric chest. Studies describing airway involvement and management in paediatric PTB [3,4], as well as surgical indications, options and outcomes [5–7], provide no detailed description outlining the expected appearances: whether there is a radiological improvement of airway compression and whether the sequelae (e.g., collapse and breakdown) resolve after enucleation.

Routine computed tomography (CT) of the chest is not performed for follow-up to minimise the exposure of these young paediatric patients to ionising radiation in keeping with modern paediatric radiology guidelines; hence, the chest X-ray (CXR) is the primary tool relied upon for monitoring disease improvement with the use of a repeat CT strictly reserved for cases requiring reassessment for surgical management for worsening clinical respiratory compromise and disease progression seen on bronchoscopy or the CXR.

The postoperative radiological changes in the CXR may reflect resolution of airway stenosis and a new imaging baseline must be set as follow-up X-rays need to be compared. No study has described temporary or permanent

☆ This article was presented on 3 June 2009 at the European Society of Paediatric Radiology Annual Congress in Istanbul, Turkey.

* Corresponding author. Address: Department of Radiology, University of Stellenbosch, Room 5019, Faculty of Health Sciences, Fransie van Zijl Drive, Cape Town 7505, South Africa. Tel.: +27 21 938 9320; fax: +27 21 931 5600.
E-mail address: atmaydell@hotmail.com (A. Maydell).

1010-7940/$ – see front matter
doi:10.1016/j.ejcts.2010.02.008

radiologic features found on CT and CXR post-enucleation in detail, which is the objective here.

2. Methods

A retrospective study was performed using the available imaging of a group of 21 paediatric TB cases having undergone enucleation at a tertiary referral centre between March 2004 and October 2007. Inclusion criteria were

(1) A frontal CXR taken within 5 days preoperatively (CXR 1).
(2) A standard contrasted CT scan of the chest taken preoperatively (CT).
(3) A frontal CXR taken at the last follow-up visit after discharge (CXR 2).

Cases that were missing imaging were excluded from the study. As outpatient clinic follow-up interval varied from case to case, it was not possible to systematically compare radiographs for the entire group at fixed points or periods in the follow-up timeline. As most patients showed a gradual clinical and radiological improvement over the course of their follow-up, it was decided to only consider the last CXR taken at the end of their follow-up period (i.e., the CXR most likely to show the greatest degree of improvement) before discharge from the outpatient clinic, regardless of the post-surgical duration. A lateral CXR was assessed, where available, together with the frontal CXR.

Preoperative bronchoscopy was performed in 19 of the 21 patients by a paediatric pulmonologist and findings relating to major airway stenosis and gland herniation were recorded. A postoperative CT scan of the chest performed in patients failing to improve after the enucleation was used to assess changes together with CXR 2 when available.

The imaging was evaluated by a dedicated paediatric radiologist with experience in TB imaging. Most imaging was available in film hard copy. CT scans were read in digital format from a picture archiving and communication system (PACS) workstation, where possible.

As lymphadenopathy on the right side is more frequently responsible for airway stenosis and lung sequelae, and access to the subcarinal glands is gained from this side, all the patients included in the study received a right posterolateral thoracotomy through the fifth intercostal space (muscle-sparing procedure as the serratus anterior muscle is not bisected) with the patient lying on the left side. A single lumen endotracheal (ET) tube was used. The capsule of the conglomerate of lymph glands was incised and the contents, usually soft caseous or partly fluid in the acute patient, and hard, sometimes calcified, fibrotic tissue in the chronic patient was evacuated or gently dissected out in a piecemeal fashion. The right hilar, subcarinal and right paratracheal groups of glands as well as those surrounding the right main bronchus (RMB) and bronchus intermedius (BI) were drained. No simultaneous pneumonectomy or other surgical procedure was performed in these patients.

Table 1
Criteria used for assessing imaging.

Presence of lymphadenopathy	Presence of airway stenosis	Presence of pulmonary collapse/consolidation
Right hilar	Right main bronchus	Right upper lobe
Subcarinal	Bronchus intermedius	Right middle lobe
Left hilar	Left main bronchus	Right lower lobe
		Left upper lobe (excl. lingula)
		Lingula
		Left lower lobe

Basic demographics as well as patient age at enucleation (years and months), combination and duration of anti-TB medical treatment prior to enucleation, number of enucleations and time span to last follow-up CXR (months) were recorded.

Each of the three studies was assessed according to the presence or absence of regional lymphadenopathy in the chest, main airway obstruction and collapse/consolidation of lung lobes as sequelae of the airway obstruction. Results were tabulated and compared using a spreadsheet structured similar to Table 1.

The prevalence of each finding in Table 1 was calculated for each of CXR 1, CXR 2 and CT, as well as the number of patients showing a change in positive findings between CXR 1 and CXR 2.

False-positive and false-negative findings on CXR 1 when compared with preoperative CTwere calculated to decide on reliability of CXR 1 (and hence CXR 2 findings compared with the more sensitive CT).

CXR 2 was also grouped into three outcome categories according to disease status (Table 2), with the patient mean age and the average time from enucleation for each group calculated in months.

Table 2
Outcome categories of disease status with description, number of patients, mean age and time after enucleation for each as seen on follow-up CXR (CXR 2). Standard deviation (SD) shown in brackets.

Category	Description	Number of patients	Mean age	Mean time after enucleation
Resolved	Marked improvement in radiological appearance, i.e., collapse consolidation completely resolved, stenosis resolved (mild residual airway narrowing and lymphadenopathy may still be present), no sign of active tuberculous disease	9	18 months (SD = 21 months)	6 months 2 weeks (SD = 3 months 2 weeks)
Resolving	Improvement from preoperative radiological picture but some degree of collapse/consolidation still remaining, no sign of active tuberculous disease	10	19 months (SD = 20 months 3 weeks)	4 months 2 weeks (SD = 4 months 3 weeks)
Unresolved or disease progression	No improvement in airway stenosis and sequelae thereof (collapse/consolidation), worsening in radiological picture, or active tuberculous disease present radiologically	2	Ages of 5 and a half years, and 5 months, respectively	2 weeks

Association between the occurrences of related changes was drawn out statistically in percentages.

3. Results

A total of 21 patients were investigated: 13 girls and eight boys, ages ranging from 2 months to 5 years and 9 months, and a mean age of 1 year and 8 months (standard deviation (SD) of 1 year and 10 months). Indications for enucleation were either acute presentation of life-threatening airway obstruction or worsening severe airway obstruction having failed to improve on TB and steroid therapy. Five cases from the same period were excluded due to incomplete imaging.

All patients undergoing enucleation were already receiving the standard oral first-line anti-TB treatment, a three-drug combination of isoniazid, rifampicin and pyrazinamide for the first 2 months, and then isoniazid and rifampicin for a further 4 months thereafter (dosages of medication according to patient weight). Ethambutol was added to the combination when lung cavitation was present. Oral steroids were added when airway obstruction was present. Enucleation did not influence the treatment drug combination or duration unless it was performed late in the medical treatment period, in which case treatment duration was extended by 3 months for a total of 9 months of pharmacological therapy. Mycobacterial drug sensitivity was determined via culture and the drug treatment combination adjusted in cases where drug resistance was present.

Seven children presented with acute severe airway obstruction and were diagnosed with TB on a combination of radiological findings and positive purified protein derivative (PPD), and all had either positive smears for acid-fast bacilli or positive cultures from tracheal or gastric aspirates. One child had congenital TB. The duration of oral anti-TB treatment before enucleation in this acute group ranged from 1 week to 1 month.

Eleven children presented with previously diagnosed PTB and worsening severe airway obstruction and lung complications; all were on TB treatment and five were already receiving additional oral steroid therapy for airway obstruction. One child was later found to have multidrug-resistant TB (MDR-TB) on culture. One patient in this group was human immunodeficiency virus (HIV) positive and was receiving antiretroviral therapy. The duration of oral anti-TB treatment in this chronic group ranged from 1 month to 4 months.

Fifty-seven percent of patients were under the age of 1 year at the time of enucleation. Nine children (mean age of 18 months) resolved at an average time of 6.5 months after surgery, while 10 children (mean age of 19 months) were resolving at an average time of 4.5 months, and two children (aged 5.5 years and 5 months, respectively) were both unresolved or progressing 2 weeks after surgery (Table 2). An example of a patient's preoperative imaging of CXR 1 and CT included in the study is shown in Figs. 1 and 2.

Table 3 describes the preoperative findings of bronchoscopy, CXR 1 and CT for the entire group. All three main airways (RMB, BI and left main bronchus (LMB)) were stenosed in 48% of patients, while a bilateral stenosis (LMB plus either RMB or BI) was present in 33%, and combined

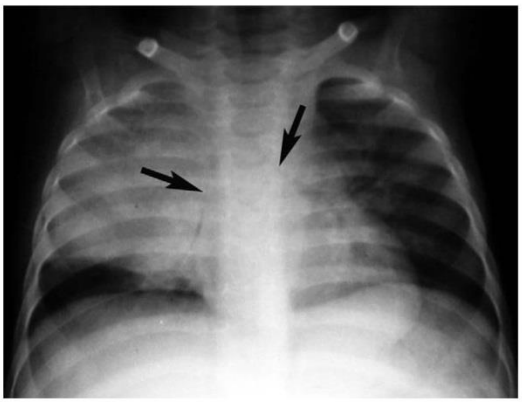

Fig. 1. Eleven-month-old male infant – CXR 1 shows severe LMB and BI stenosis (black arrows) with RUL consolidation.

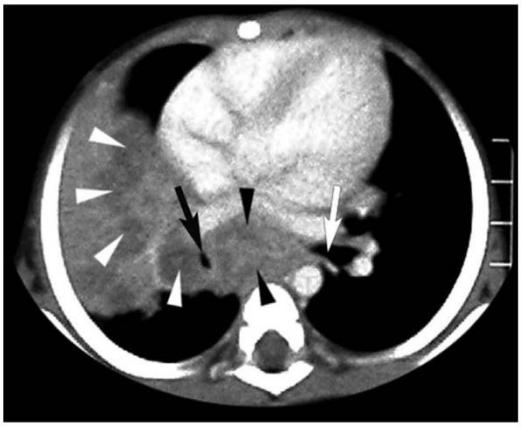

Fig. 2. Same patient as in Fig. 1 – CT shows BI (black arrow) and LMB (white arrow) stenosis with extensive 'ghost-like' enhancing subcarinal, precarinal (black arrowheads) and R hilar (white arrowheads) lymphadenopathy, with RUL consolidation.

right-sided only (RMB and BI) airway stenosis was present in 14%. One patient had a single major airway stenosis (RMB). There were no patients with exclusive left-sided involvement (LMB stenosis with or without left-lung collapse/consolidation).

Subcarinal lymphadenopathy was present in all BI stenoses, 90% of RMB stenoses and in 86% of LMB stenoses. Right hilar lymphadenopathy was present in 90% of BI and 78% of RMB stenoses. Left hilar lymphadenopathy was present in only 35% of LMB stenosis. In the presence of precarinal lymphadenopathy, 90% of patients had associated RMB and BI stenoses, respectively, and 86% had LMB stenosis. Precarinal lymphadenopathy was the responsible factor in the patient with single airway (RMB) stenosis.

Preoperative bronchoscopy performed in 19 of the 21 patients reported BI stenosis in 90%, LMB stenosis in 53%, RMB

Table 3
Prevalence of pathology seen on each set of imaging reported as percentages with the last column showing improvement in radiological findings on CXR 2 (postoperative) when compared to CXR 1 (preoperative) reported as a percentage, values for the McNemar Chi-square test and p included. Numbers in brackets relay number of patients, $n = 21$ for imaging and $n = 19$ for bronchoscopy.

	Bronchoscopy preoperative	CXR 1 preoperative	CT preoperative	CXR 2 postoperative	Improvement in CXR 2 (CXR 1 – CXR 2)/CXR 1
Airway stenosis					
Right main bronchus	21% (4)	57% (12)	67% (14)	24% (5)	67% Chi-square = 4; $p = 0.0455$
Bronchus intermedius	90% (17)	90% (19)	95% (20)	24% (5)	74% Chi-square = 12.07; $p = 0.00051$
Left main bronchus	53% (10)	90% (19)	81% (17)	38% (8)	58% Chi-square = 9.091; $p = 0.00257$
Collapse/consolidation					
Right upper lobe		86% (18)	62% (13)	29% (6)	67% Chi-square = 10.0833; $p = 0.0015$
Right middle lobe		43% (9)	48% (10)	19% (4)	67% Chi-square = 2.286; $p = 0.1306$
Right lower lobe		62% (13)	62% (13)	10% (2)	85% Chi-square = 9.091; $p = 0.00257$
Left upper lobe		24% (5)	10% (2)	5% (1)	80% Chi-square = 2.25; $p = 0.13362$
Lingula		10% (2)	14% (3)	0% (0)	100% Chi-square = 0; $p = 1.000$
Left lower lobe		24% (5)	14% (3)	10% (2)	60% Chi-square = 0.800; $p = 0.3711$
Lymphadenopathy					
Right hilar		95% (20)	86% (18)	52% (11)	45% Chi-square = 7.111; $p = 0.00766$
Subcarinal		95% (20)	95% (20)	65% (11)	37% Chi-square = 5.143; $p = 0.02334$
Left hilar		76% (16)	33% (7)	52% (11)	44% Chi-square = 1.7778; $p = 0.18243$

stenosis in 21% and distal tracheal stenosis in 63% (Table 3), with various combinations and degrees of lobar and segmental bronchial stenosis. Enlarged lymph glands herniating into the airway lumen (not distinguished from simple airway stenosis on CT or CXR) was observed in 53% of patients and predominated in the LMB as seen in 37% of patients undergoing preoperative bronchoscopy. The results of the positive findings from the postoperative CXR 2 are shown in the last column of Table 3 with imaging from the same patient shown in Fig. 3. Relative improvement in the studied aspects compared with CXR 1 is reported in the last column of Table 3 as percentages.

The patient age at enucleation was plotted against the time to CXR 2 in months as shown in Fig. 4, to determine whether patient age had an influence on duration of

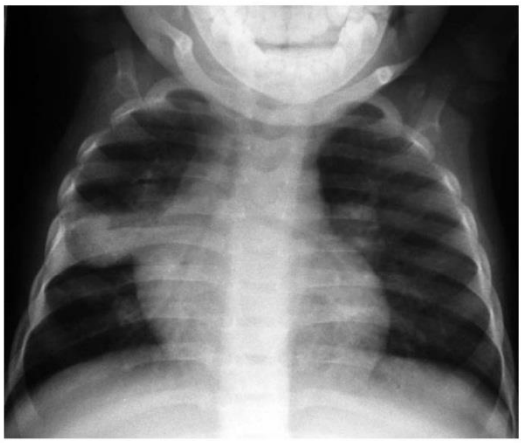

Fig. 3. Same patient as in Figs. 1 and 2 – CXR 2 at 8 months after two enucleations shows complete resolution of airway stenosis with some residual RUL opacification.

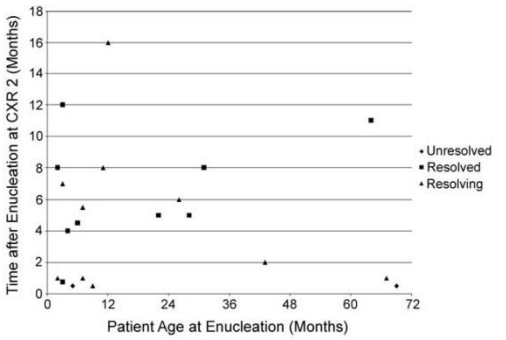

Fig. 4. A graph demonstrating time of CXR 2 (in months) related to age of patient at time of the enucleation surgery (in months).

Table 4
False-positive and false-negative findings on CXR 1 when compared to CT done during the same time period, reported as number of findings (percentage in brackets).

	False-positive findings	False-negative findings
Airway stenosis		
Right main bronchus	2 (10%)	4 (20%)
Bronchus intermedius	0	1 (5%)
Left main bronchus	2 (10%)	0
Collapse/consolidation		
Right upper lobe	5 (24%)	0
Right middle lobe	2 (10%)	3 (14%)
Right lower lobe	3 (14%)	2 (10%)
Left upper lobe	3 (14%)	0
Lingula	0	1 (5%)
Left lower lobe	4 (19%)	1 (5%)
Lymphadenopathy		
Right hilar	3 (14%)	1 (5%)
Subcarinal	0	0
Left hilar	9 (43%)	0

recovery, but no age-related association in recovery time could be established.

One patient, who showed poor clinical response after the first enucleation, received a second CT performed a few days before a second enucleation 2 months after the first surgery; there was no change in the radiological findings when compared with the first preoperative CT. Two children had complications due to surgery: one patient developed a bronchopleural and broncho-oesophageal fistula, and the second a chylothorax.

False-positive and false-negative rates were relatively low on CXR 1 compared with CT as shown in Table 4.

There were no anatomical changes (such as pneumonectomy and rib excision) and no surgical clips or remaining surgical implements present on the postoperative X-rays.

4. Discussion

The World Health Organization (WHO) reports the incidence and prevalence of TB in South Africa for the year 2007 as 948 and 692 per 100 000, respectively, with a TB mortality rate of 230 per 100 000 [8].

A 2002–2003 clinic-based study of 256 children under 15 years of age in the local area documenting the criteria used at primary health-care level to diagnose childhood TB, reported a 38.4% prevalence of lymph node disease complicated by visible alveolar consolidation, airway compression and/or segmental/lobar collapse [2]. A second similar 2003–2004 community-based study, also in the local area, describing the spectrum of TB disease in 439 children under 13 years, reported airway obstruction in 25% of patients [1].

In a study of 100 children admitted to hospital with suspected PTB, the most common locations for TB lymph gland enlargement on CT were subcarinal (90%), right hilar (74%), left hilar (72%) and bilateral hilar (61%). The largest group of nodes was located in the subcarinal area. The most common sites of airway compression were described as the LMB (21%), RMB (14%) and BI (8%) [9].

The only clear indications for urgent surgical enucleation include children requiring assisted ventilation for airway obstruction and children with life-threatening airway obstruction. Children with airway obstruction at bronchoscopy estimated to be greater than 75% should also be considered for enucleation.

Other indications for surgical enucleation include

- acute perforation of a lymph gland into a major airway causing respiratory failure;
- occlusion of a major airway with pulmonary collapse or hyperinflation;
- permanent bronchial stenosis due to fibrosis;
- rarely, superior vena cava obstruction; and
- subcarinal oesophageal obstruction [10].

In a study at Red Cross Children's Hospital (Cape Town, South Africa) of 168 children under 13 years receiving therapeutic surgical interventions for proved intrathoracic TB and its related complications, obstruction of the major airways was the indication for 38% of all procedures, with surgical intervention resulting in radiologic and symptomatic improvement in 73% of patients. Airway stenosis due to TB lymphadenopathy was described as acute or chronic, with the majority (69%) of patients requiring surgical intervention presenting with acute major airway obstruction [11].

The reported complication rate resulting from enucleation is low and includes bronchial tear, pulmonary artery laceration, bronchopleural and broncho-oesophageal fistula [11,12]. Caution is taken not to probe or dissect too aggressively during the procedure. Airway wall breach causing a tracheo- or bronchopleural fistula may occur as the pathological lymph nodes and surrounding inflammatory tissue weaken and sometimes directly erode the walls of the airways. Lymph nodes or their caseous contents may herniate through the wall of the airway directly into the lumen, causing further obstruction.

Preoperative radiographs and CTs of the chest compared favourably in our patients and showed that airway stenosis with associated collapse/consolidation was seen most commonly involving the right side. The absence of exclusive left-sided involvement suggests that it is either not prevalent or that lymphadenopathy affects the airways less severely, and that right-sided disease was necessary to produce severe enough clinical respiratory compromise to require surgical management.

BI stenosis was present in 90% or more of cases as reported on bronchoscopy, CXR 1 and CT indicating excellent correlation between these different investigations. LMB and RMB stenoses were reported more frequently on imaging than bronchoscopy, likely due to differences in the definitions of terms such as 'stenosis' and 'obstruction', as well as inter-observer variability. When LMB stenosis was present, it was associated with a much lower rate of left-lung collapse/consolidation, and a better response to surgery relative to that of the right side. This supports the routine use of a right-sided surgical approach.

Resolution of BI stenosis with associated resolution in collapse/consolidation of the right lower lobe (RLL) is the most consistent finding postoperatively, followed closely by RMB stenosis and associated right middle lobe/right upper lobe (RML/RUL) collapse/consolidation improvement. Resolution of the stenosed LMB is seen in just over 50% of affected patients, with most of left-lung collapse/consolidation present in the entire group resolving, suggesting that subcarinal lymph node clearance is sufficient for left-sided resolution (as the left hilar and left paratracheal groups are not drained during the right-sided thoracotomy approach).

The improvement in lung collapse/consolidation related closely to resolution of related airway stenosis, and less so to the poorer degree of resolution of related lymphadenopathy on the postoperative CXR. This is thought to be due to the conglomerate of lymph glands not being excised during surgery but merely having their contents evacuated, leaving behind the surrounding fibrous capsule, which would be unlikely to resolve completely. The resolution of the complications of lymph node enlargement (airway stenosis and lung collapse/consolidation) is thus seen more frequently than the resolution of the offending lymphadenopathy itself.

5. Limitations

Due to the small group of patients, it is not possible to study the population in age-specific groups, where it is possible that different trends exist relating to airway maturity and size of lymphadenopathy. As only one patient was HIV positive in this group, the presentation and response to enucleation of TB lymphadenopathy in the HIV-positive population cannot be reported on. HIV-positive patients may well have a different outcome than seen in this group as lymphadenopathy consistency may differ owing to the altered immunological response. The ideal scenario for evaluation would involve the availability of CT postoperatively for true comparisons.

6. Conclusion

Postoperative radiographs commonly correspond with the surgical enucleation procedure in children with airway stenosis due to TB lymphadenopathy. CXR is a useful technique for pre- and postoperative evaluation of the cause and resolution of airway stenosis in children with PTB. Resolution of BI stenosis with associated improvement in collapse/consolidation of the RLL is the most consistent finding, followed closely by RMB stenosis resolution with associated RML/RUL collapse/consolidation improvement. Exclusive left-sided disease was not present, and thus was either not prevalent or severe enough to require enucleation. Resolution of the stenosed LMB is seen in just over 50% of affected patients with most of left-lung sequelae in the entire group resolving, suggesting that subcarinal lymph node enucleation is sufficient for left-sided resolution of LMB stenosis and associated lung sequelae. The improvement in lung collapse/consolidation related closely to the resolution of related airway stenosis, and less so to the poorer resolution of related lymphadenopathy. The resolution of the complications of lymph node enlargement (airway stenosis and lung collapse/consolidation) is thus seen more frequently than the resolution of the offending lymphadenopathy itself.

References

[1] Marais BJ, Gie RP, Schaaf HS, Hesseling AC, Enarson DA, Beyers N. The spectrum of disease in children treated for tuberculosis in a highly endemic area. Int J Tuberc Lung Dis 2006;10:732–8.
[2] Theart A, Marais BM, Gie RP, Hesseling AC, Beyers N. Criteria used for the diagnosis of childhood tuberculosis at primary health care level in a high-burden, urban setting. Int J Tuberc Lung Dis 2005;9:1210–4.
[3] Goussard P, Gie R. Airway involvement in pulmonary tuberculosis. Paediatr Respir Rev 2007;8:118–23.
[4] Awad WI, Graves TD, White VC, Wong K. Airway obstruction complicating mediastinal tuberculosis: a life-threatening presentation. Ann Thorac Surg 2002;74:261–3.
[5] Papagiannopoulos KA, Linegar AG, Harris DG, Rossouw GJ. Surgical management of airway obstruction in primary tuberculosis in children. Ann Thorac Surg 1999;68:1182–6.
[6] Nakvi AJ, Nohl-Oser HC. Surgical treatment of bronchial obstruction in primary tuberculosis in children: report of seven cases. Thorax 1979;34(4):464–9.
[7] Iwamoto Y, Miyazawa T, Kurimoto N, Miyazu Y, Ishida A, Matsuo K, Watanabe Y. Interventional bronchoscopy in the management of airway stenosis due to tracheobronchial tuberculosis. Chest 2004;126(4):1344–52.
[8] World Health Organization Global Tuberculosis Control: WHO Report. Country Profile for South Africa; 2009.
[9] Andronikou S, Joseph E, Lucas S, Brachmeyer S, Du Toit G, Zar H, Swingler G. CT scanning for the detection of tuberculous mediastinal and hilar lymphadenopathy in children. Pediatr Radiol 2004;34:232–6.
[10] Konstantinos A, Papagiannopoulos KA, Linegar AG, Harris DG, Rossouw GJ. Surgical management of airway obstruction in primary tuberculosis in children. Ann Thorac Surg 1999;68:1182–6.
[11] Hewitson JP, van Oppel UO. Role of thoracic surgery for childhood tuberculosis. World J Surg 1997;21:468–74.
[12] Worthington MG, Brink JG, Odell JA, Buckels J, de Groot MK, Klein M, Gunning AJ. Surgical relief of acute airway obstruction due to primary tuberculosis. Ann Thorac Surg 1993;56:1054–62.

CHAPTER 8

Conclusion

The aim of this dissertation was to study airway involvement in children with pulmonary tuberculosis presenting with severe airway obstruction, determine the factors which influence the degree of airway obstruction and to determine what the indications are for surgical relief of the airway obstruction.

We describe the airway involvement in children with severe clinical and radiological airway obstruction due to TB lymph node enlargement as assessed by bronchoscopically evaluating of the airways. The commonest large airways compressed were bronchus intermedius and the left main bronchus. At these sites the airways are compressed between the hilar and subcarinal lymph nodes. This is the first time that this has been reported which is different from airway involvement previously reported. With previously reported that the opening of the right main bronchus was the most common area of obstruction.[1]

It is fortunate that the main sites of severe airway obstruction is bronchus intermedius and left main bronchus and that the lymph nodes involves are the right hilar and subcarinal lymph nodes as these lymph nodes are accessible via a right thoracotomy enabling surgical relief. This justifies the surgical approach to the relief of children with severe airway obstruction that is life threatening or not responding to medical treatment to which steroids have been added.

As a secondary outcome we attempted to determine which children had a higher risk of developing severe airway obstruction. Severe airway obstruction was more common in young children. This is ascribed to the smaller and more compliant airways. What however was surprising was that there was no correlation between degree and site of airway obstruction and HIV status. HIV infected children were not more likely to have severe airway obstruction. Similarly we hypothesized that the diagnosis that drug resistant TB would be delayed resulting in severe airway obstruction. We could however not show that children suffering from drug resistant children had more severe airway obstruction. What was however unexpected was that the a positive Mantoux skin test predicted for severe airway obstruction while acute phase inflammatory markers failed to do so. This leads to the hypothesis that the upgrading of the immune response as indicated by a positive Mantoux skin test results in severe airway obstruction. This hypothesis we did not test but would be an interesting area of research.

Previously culture yield from BAL has always been reported to be low (10 - 28.7%); in this study we found a significant higher yield (44%) even with a large percentage of children

already on TB treatment.[2–4] The yield from broncho-alveolar lavage (BAL) was significantly higher if the lavage was done from a lobe with pneumonic consolidation on the chest x-ray. The finding that *Mycobacterium tuberculosis* could be isolated from BAL weeks to months after starting anti-tuberculosis treatment is interesting, as this has not been reported. This finding has a practical application, as children often with uncertain tuberculosis not responding to treatment require investigation including bronchoscopy. In these children based on this finding BAL remains an important investigation. We have demonstrated in this study that the value of bronchoscopy is more than just a way of finding the collecting specimens for culture but it also allows one to evaluate the airways, determine if the pattern of airway compression which is highly suggestive of TB especially if the lymph nodes have ulcerated through the airway wall into the airways. Bronchoscopy has an additional role in that it allows one to determine the degree and site of airway obstruction that determines the medical and/or surgical treatment. It is these uses of paediatric bronchoscopy in the investigation of children suspected of having pulmonary TB.

The accuracy of chest computer tomography (CT scan) in the diagnosis of severe airway obstruction due to tuberculosis is poorly described. In a series of articles we compared the chest CT scan findings to the findings visualized during paediatric fiber-optic bronchoscopy. All children with severe airway obstruction had a fiber-optic bronchoscopy and contrast enhanced chest CT scan. We describe a very good correlation between the findings of the two diagnostic techniques. CT scan data confirmed that the most common and severely affected airways was bronchus intermedius and the left main bronchus and that young children had the most severe involvement. Subcarinal lymph nodes were enlarged in 97% of pulmonary TB cases. This helps explains why both the left and right main bronchus is compressed in children with severe obstruction. In addition, chest CT scan demonstrated that the right hilar lymph node enlargement was common. This explains why bronchus intermedius compression with the bronchus compressed between the enlarged right hilar and subcarinal lymph nodes. This explanation has not previously been raised in the literature. We used 3-dimensional volume-rendered chest CT scans (3-D VR) and found that when compared to bronchoscopy3-D VR had a good sensitivity (92%) and specificity (85%). This is an important observation as bronchoscopy is not freely available, especially in the developing world, and in its absence CT scan is an important modality in assessing the site and degree of airway obstruction provide important information in children with airway compression. Form these studies we were able to

calculate that very little additional information is obtained from an additional chest CT scan if the airway obstruction is less than 50%. For this reason I would advocate that bronchoscopy be done prior to chest CT scan and if there is no significant airway obstruction chest CT scan is not needed.

The diagnostic yield of specimens to confirm tuberculosis is low. We have explored additional diagnostic tests to improve the diagnostic yield. We have described the use of transbronchial needle aspiration (TBNA) in children, a test not previously described in children, to confirm the diagnosis, especially that of tuberculosis. We were able to demonstrate that TBNA was safe and effective even in very young infants. A definitive diagnosis was made using TBNA in 54% of patients; the diagnoses made were MTB lymph node enlargement (n = 13), metastatic nephroblastoma (n = 1) and fibrosing mediastinitis (n = 1). In 25% of the cases TBNA was the sole source of the specimens from which the diagnosis was made.

The second strategy we have studied is the use of GeneXpert as an additional test to confirm tuberculosis in children. Initial studies have been done on mostly sputum, nasopharyngeal aspirates and gastric aspirates. In a pilot study we demonstrate that GeneXpert can be successfully be performed on BAL specimens. Using this approach an increase in the number of cases with pulmonary TB can be increased. This adds further value to bronchoscopy, as GeneXpert is a rapid way of confirming the diagnosis and identifying RIF resistance.

This dissertation was design to determine the optimal management of children with severe airway obstruction due to TB lymph node enlargement. This was the first study determining the incidence of children with severe airway obstruction due to tuberculous lymph node compression of the airways requiring transthoracic enucleation to relieve severe airway obstruction. We identified 3 important groups of children needing enucleation (1) children with severe life threatening airway obstruction, (2) children with critical airway obstruction as accessed at the initial bronchoscopy, (3) children with severe airway obstruction not responding to TB treatment and corticosteroids. In a cohort of 250 children, 34% needed enucleation with 27% of then needing urgent enucleation, within 14 days of presentation with the remaining 73% indicated after failing one month of medical treatment. We a showed a 98% success rate with transthoracic enucleation and a low morbidity and no mortality. The children in which enucleation were done were significantly younger (18 months vs. 32 months ($p < 0, 01$) and more likely to have a positive Mantoux

skin test (p =0.004). Severe airway obstruction (>75%) of bronchus intermedius (OR 2.28 95th CI 1.29- 4.02) and left main bronchus (OR 3.34 95th CI 1.73-6.83) where the best predictors for enucleation. There was no increased risk of requiring an enucleation in children with drug resistant TB when compared to children with and drug susceptible TB. Similarly HIV –infected children were at no greater risk of requiring an enucleation than children that were HIV non-infected.

Bronchoscopy was done after enucleation to determine the improvement in airway caliber enucleation had. There was a significant improvement in airway caliber of the large airways that followed enucleation. We were able to demonstrate that enucleation resulted in a more rapid improvement in airway size compared to medical treatment. The low postoperative complication rate was most probably related to the surgical approach used to enucleate the enlarged lymph nodes. In contrast to other surgical reports the approach we use was to decompress the lymph node by opening the capsule and removing the content by suction or curettage. No lymph nodes were removed. None of the patients we subjected to enucleation required a lobectomy or pneumonectomy and there was no major bleeding episodes from torn pulmonary vessels. Treatment failure seldom occurred in children that required enucleation with only 2% requiring re-evaluation for unresolved severe airway obstruction. An interesting observation was that bronchiectasis following the treatment of the pulmonary TB occurred in 6 patients, 5 in the medically treated group and 1 in the group requiring enucleation. This observation did not achieve statistical significance possible due to the sample size. This requires further investigation. I would advocate that children with enlarge lymph nodes and airway obstruction which is still symptomatic after one month's treatment of TB treatment and corticosteroids needs to be referred for further investigation and advance imaging as these children may have significant airway obstruction and will benefit from possible surgical intervention. The important areas to inspect on the chest x ray is the subcarinal area and any deviation of the trachea to the left. In the absence of advanced imaging these areas may yield important information about the presence and the significance of airway compression. This may be even more important in children younger than 24 months as they seen to be more often and more severely affected. These children have smaller airways, and they may become more symptomatic during intercurrent viral infection bringing them to medical attention. During the study period bronchoscopy was done after enucleation but this proved not to be necessary if the child was asymptomatic. This has led to a change in management and bronchoscopy is only done in child still symptomatic after enucleation.

Irving et al used a database of 61 chest CT scans of children with airway obstruction due to tuberculosis. This is the first computer-assisted detection model developed to detect tuberculosis in children by using airway obstruction patterns. He used automated segmentation and branch analysis to evaluate and classify airways in this database. This procedure is used to differentiate airway deformation and stenosis from lymphadenopathy in children with tuberculosis and can be used as a computer-assisted detection of airway pathology. Once a dataset of airways has been segmented and the structure analysed, the dataset can be used to train a classifier to distinguish between normal and abnormal airway variations. This method was tested using cross-validation on a dataset of 61 patents with and without tuberculosis. The method was able to distinguish between patients with and those without tuberculosis with a sensitivity of 86% and a specificity of 91%. This method may be of significant advantage in areas where bronchoscopy is not available or patients too sick to be investigated by bronchoscopy. In future it may be possible to apply these methods to chest x rays in helping with the diagnosis of tuberculosis

Conclusion

In this thesis I was able to demonstrate that paediatric bronchoscopy has an important role to play in accurately assessing the site and degree of airway narrowing due to TB lymph node compression. The correct assessment is essential in determining whether the affected child requires surgical or medical treatment. There was a statistically significant correlation between bronchoscopic and Chest CT scan findings with both of these investigations identifying bronchus intermedius and the left main bronchus as the most common sites as well as the most severely compressed regions of the airways. One third of children with clinical and radiologically significant airway narrowing will need surgical intervention. The outcome of surgery was excellent resulting in significant improvement in airway size with low morbidity and no mortality. The diagnostic yield during bronchoscopy was been improved by the application of TBNA and GenXpert, although there is still significant room for improvement. Computer-assisted modeling of airway narrowing may in future a useful addition to the diagnosis of pulmonary TB in children as well as determining the site and degree of airway narrowing. Developing computer-assisted diagnostic models could potentially be of tremendous benefit to children residing in regions where paediatric bronchoscopy is not available. New diagnostic tests are urgently needed and especially non-invasive tests. The new tests will have to be evaluated against a gold standard and this where the increased diagnostic yield of paediatric bronchoscopy will, amongst other

diagnostic tests, continue to play an important role. New diagnostic and the studies to determine their accuracy are urgently required

Future/on-going research

Future studies will evaluated the role of GeneXpert on BAL to determine what it role is in the diagnosis of PTB, especially in children that is already on TB treatment. Since Xpert detects MTB DNA from both live and dead mycobacteria, it may therefore remain positive for longer than culture after initiation of treatment and may guide appropriate therapy. We will also look at other factors that determine a positive GeneXpert. As BAL is unlikely to be repeated as with other samples used for GeneXpert it is important to determine what the correct volume of samples is for the best possible results and also where this samples was taken from.

Chest CT scans is associated with significant risk of radiation and because of this reason Chest CT-scans cannot be repeated in the management of patients. MR scan is not associated with risk of radiation and in future studies we want to evaluate the information gained from MR scanning in children with significant airway obstruction and if this scans can in future replace the use of CT scans.

Positron emission tomography (PET) with 2-[fluorine-18]fluoro-2- deoxy-d-glucose (FDG) is use in adult and pediatric oncology patients and its use is well documented 18F FDG is a glucose analog labeled with a positron- emitting isotope, F (fluorine)–18, this is transported into cells by glucose transporters and trapped within the cell. This happens in malignant tissue but also in nonmalignant inflammation and infection. The role of FDG scan in children with tuberculosis need to be studied. These scans may be used to localize lesions for biopsy, may determine if PTB is present or active and may exclude PTB. These scans may be expensive and may expose the patient to radiation but may be of important value if drug resistance is expected.

Endobronchial ultrasound guided transbronchial needle aspiration (EBUS-TBNA has been preformed in older children as an alternative to invasive surgical biopsy in children with mediastinal pathology.[5] The EBUS scope has an outer diameter of 6.9 mm which limits its use to adults and adolescents. Although there is no EBUS bronchoscope currently available for children, it is possible to use ultrasound probes are passed via the working channel. This needs to be studied in comparison to blind TBNA if this increases the yield of TBNA. Secondly we sampled only the subcarinal area and not the other lymph node

groups. With the use of ultrasound probes it may be possible to sample these groups of lymph nodes and increase the yield from this intervention. Repeating the GeneXpert after TBNA may be theoretically of value as more bacilli may be released in the airway lumen after TBNA but this need to be tested.

References

1. Bibi H, Mosheyev A, Shoseyov D, Feigenbaum D, Kurzbart E, Weiller Z. Should bronchoscopy be performed in the evaluation of suspected pediatric pulmonary tuberculosis? Chest 2002; 122: 1604-1608.

2. Cakir E, Uyan ZS, Oktem S, Karakoc F; Ersu R, Karadag B, Dagli E. Flexible bronchoscopy for diagnosis and follow up of childhood endobronchial tuberculosis. Pediatr Infect Dis J 2008; 27: 783-787.

3. Somu N, Swaminathan S, Paramasivan CN, Vijayasekaran D, Chandrabhooshanam A, Vijayan VK, Prabhakar R. Value of bronchoalveolar lavage and gastric lavage in the diagnosis of pulmonary tuberculosis in children. Tuber Lung Dis 1995; 76: 295–299

4. Cakir E, Kut A, Ozkaya E, Gedik AH, Midyat L; Nursoy M. Bronchoscopic evaluation in childhood pulmonary tuberculosis: risk factors of airway involvement and contribution to the bacteriologic diagnosis. Pediatr Infect Dis J. 2013; 32: 921-923.

5. Gilbert CR, Feller-Kopman D, Akulian J, Hayes M, Yarmus L. Interventional pulmonology procedures in the pediatric population. Pediatr Pulmonol 2014; 49: 597-604.

OTHER TUBERCULOSIS-RELATED MANUSCRIPTS

Pediatric Pulmonology 38:451–455 (2004)

Expansile Pneumonia in Children Caused by *Mycobacterium tuberculosis*: Clinical, Radiological, and Bronchoscopic Appearances

P. Goussard, MMed (Ped),* R.P. Gie, FCP (Paed), S. Kling, FCP(Paed), and N. Beyers, PhD

Summary. A cohort of 24 children with expansile pneumonia caused by *Mycobacterium tuberculosis* is described in mostly HIV-noninfected children (n = 22). The children presented with nonresolving pneumonia and a swinging fever (83%). On chest radiography, they had dense opacification with bulging fissures mainly in the upper lobes (75%). On computed tomography, the lobes are consolidated, with areas of liquefacation. Other features visible are enlarged mediastinal lymph adenopathy with ring enhancement (100%), cavities (63%), and tracheal compression (71%). On bronchoscopy, bronchi were obstructed by more than 75% in 20 (83%) of cases. Lymph gland enucleation was required in 42% of cases. Phrenic nerve palsy was present in 3 children, of whom 2 underwent diaphragmatic plication. The children received standard antituberculous therapy, to which prednisone (2 mg/kg/day) was added for 1 month. The mortality was 4% after 6 months of therapy. **Pediatr Pulmonol. 2004; 38:451–455.** © 2004 Wiley-Liss, Inc.

Key words: tuberculosis; expansile pneumonia; childhood tuberculosis; tuberculous pneumonia.

INTRODUCTION

Expansile pneumonia is characterized by increased volume of the involved lobe or segment during a bout of pneumonia, resulting in the radiological appearance of a densely consolidated lobe or segment with bulging fissures. It rarely presents in childhood. The most common bacterial causes of expansile pneumonia are *Klebsiella pneumoniae* and *Staphylococcus aureus*. Expansile pneumonia caused by *Klebsiella pneumoniae* usually involves the upper lobes.[1,2] Fungal pneumonia in immunocompromised and neutropenic children presents as expansile pneumonia that has a characteristic computed tomography (CT) appearance of a halo sign and is caused by *Aspergillus fumigatus*.[3,4] The aim of this paper is to describe the clinical, radiological, and bronchoscopic characteristics of expansile pneumonia in children caused by *Mycobacterium tuberculosis* (MTB), and the clinical course of the disease on therapy.

PATIENTS AND METHODS

This is a descriptive study of cases of expansile pneumonia collected prospectively from September 2000–June 2002 in a tertiary care hospital, situated in a province of South Africa with an extremely high incidence of tuberculosis (TB) (840 new cases/100,000 population per annum). The tertiary hospital serves as a referral hospital for a population of approximately 2 million persons. The study patients were referred from surrounding regional and district hospitals. All children with expansile pneumonia were included in the study. Twenty-six patients with expansile pneumonia were treated during the study period; in 24, the cause was MTB. These 24 patients constituted the cohort that was investigated. All children were examined clinically and had the following investigations: chest radiograph (CXR), HIV test, Mantoux skin test, gastric washings for MTB culture, chest CT with contrast, and a rigid bronchoscopy with bronchoalveolar lavage (BAL). If on bronchoscopy the TB glands were herniating into the airway, specimens of the caseating material were sent for culture. On bronchoscopy, the degree of obstruction of the involved airways was estimated. In all cases, the bronchoscopist was not always blinded to the CT findings, which could have influenced the estimated degree of obstruction.

Pulmonary tuberculosis was diagnosed using modified WHO criteria.[5] The children were treated with isoniazid (INH) (10 mg/kg/day), rifampicin (10 mg/kg/day), pyrazinamide (25 mg/kg/day), and ethambutol (15 mg/kg/day) for 2 months, and with INH and rifampicin for a further

Department of Paediatrics and Child Health, Stellenbosch University, Tygerberg, South Africa.

*Correspondence to: Dr. P. Goussard, Department of Paediatrics and Child Health, Stellenbosch University, PO Box 19063, Tygerberg 7505, South Africa. E-mail: pgouss@sun.ac.za

Received 19 March 2004; Revised 7 May 2004; Accepted 8 May 2004.

DOI 10.1002/ppul.20119
Published online 16 September 2004 in Wiley InterScience (www.interscience.wiley.com).

4 months during the continuation phase. Prednisone (2 mg/kg) was added for the first 30 days. The prednisone was weaned over the next month.

The children were clinically followed up after 1, 3, and 6 months, and chest radiographs were performed after 1 and 6 months.

If there was no improvement in the clinical and/or radiological condition of the child after 1 month, an additional rigid bronchoscopy was performed and an attempt was made to enucleate the obstructing lymph glands. If the enucleation was unsuccessful, the child was referred for thoracotomy and glandular enucleation.

A review of the modern English-language literature for similar cases was done using PubMed. Ethical approval for the study was granted by the Stellenbosch University Ethics Committee.

RESULTS

The median age of the children was 19 months (range, 4 96 months), with 63% younger than age 24 months. Fifteen were male. Two were HIV-seropositive: one child was older than 18 months, and in the younger child the diagnosis was confirmed by PCR.

Clinical Presentation

The children were referred with four distinct presentations: nonresolving pneumonia (n — 20); large airway obstruction with unremitting monotonic wheezing (n — 1); tuberculous meningitis (TBM) with convulsions (n — 1); and persistent lobar collapse (n — 2).

Diagnosis of TB

Forty-two percent of the children had been in contact with a known adult index case. The Mantoux skin test was positive (>15 mm induration) in 63% of patients. The greatest majority (88%) were culture-positive for MTB. Early morning gastric lavage (79%) and bronchoalveolar lavage (46%) were the most common specimens to yield a positive culture. In 39% of the children, one of the specimens yielded visible acid-fast organisms. BAL yielded only one additional positive culture that was not cultured from a gastric washing. One child died, and MTB was cultured from lung tissue obtained at postmortem. All MTB cultures tested (n — 8) were drug-sensitive strains. In three children, probable TB was diagnosed on the basis of a positive Mantoux skin test (n — 2), glandular airway compression on bronchoscopy (n — 3), herniation of the TB gland into the airway (n — 1), and the characteristic chest radiograph (n — 3). All 3 cases of probable TB responded to therapy.

Chest Radiographic Features

Homogeneous opacification with displacement of the fissures of the affected lobe or lobes was visible in all cases. Air bronchograms in the consolidated lobe were visible in only 4 cases. Hilar lymphadenopathy was not visible in any of the cases, as the hilar regions were obscured by the consolidated lobe or lobes. Indirect evidence of mediastinal lymphadenopathy resulting in compression of the large airways was visible in 22 cases (92%). In 8 (33%), cavities were visible on the chest radiograph. The upper lobes were involved in 75% of cases, with 42% and 33% affecting the left and right upper lobes, respectively (Fig. 1), with the middle lobe (21%) and lower lobes (17%) involved less often. Left-sided phrenic nerve palsy with an elevated left diaphragm was seen in 3 (13%) patients and confirmed by fluoroscopy. Pleural effusion was not visible in any of the cases.

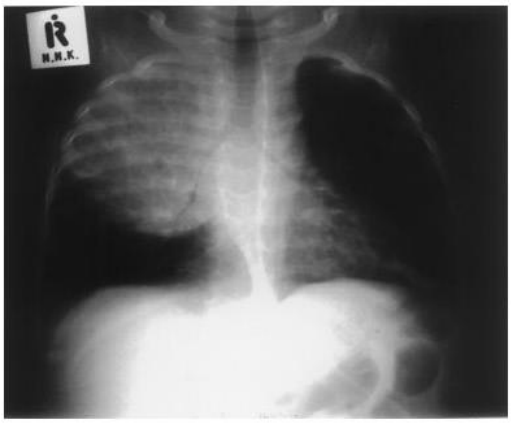

Fig. 1. Chest radiograph showing typical radiological appearance of expansile tuberculous pneumonia. Densely opacified right upper lobe with bulging upper lobe fissure and compression of both right and left main bronchi are visible.

Computed Tomography Appearance

Three patterns of CT images were seen. The first was that of a dense homogeneous opacification with no evidence of liquefaction of the affected lobe and patent airways and air bronchograms visible (17%). The second, the most common picture, consisted of homogeneous opacification with areas of necrotic liquefaction in the opacified lobe, together with glandular obstruction of the airways and absence of air bronchograms (67%) (Fig. 2). The third picture consists of a combination of the foregoing, with a homogeneously opacified lobe and areas of necrotic liquefaction and lobes with homogeneous opacification, with patent airways and visible air bronchograms (17%). In all cases, the CT scan provided additional information that was not apparent on routine chest radiograph. Hilar lymphadenopathy with ring enhancement was also visible in all cases. Other additional information obtained

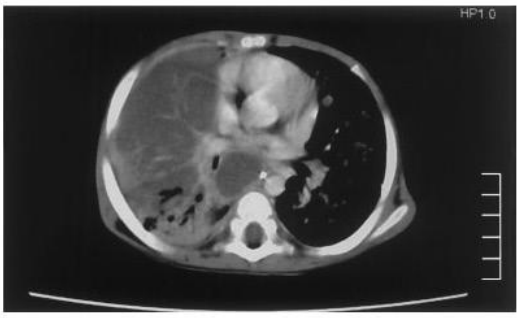

Fig. 2. Computed tomography showing massive enlarged subcarinal lymphadenopathy and densely opacified right upper lobe, with liquefaction in both glands and lung tissue. Compression of airways is also visible.

included tracheal compression (71%), subcarinal lymphadenopathy (96%), and cavitation (63%).

Bronchoscopy Findings

Airway compression was bronchoscopically confirmed in 96% of the patients. In all cases, the bronchus to the affected lobe was narrowed. In 20 cases, the narrowing was estimated to be greater than 75% of the original lumen. Severe compression of the airways in the contralateral lung was visible in 33% of cases. In addition, tracheal compression (63%) and glands herniating into the airway (29%) were observed. There was a correlation between the CT scan findings and bronchoscopic findings. All patients with necrotic liquefaction of the lobe had greater than 75% obstruction of the bronchus supplying the involved lobe. In 21%, the obstruction was complete. In contrast, those with homogeneous opacification without evidence of liquefaction and patent airways on CT scan had less than 75% obstruction of the lobar bronchus.

Surgical Enucleation of Glands

Ten children (42%) required glandular enucleation. In half, the glandular enucleation was done on admission for severe life-threatening large airway obstruction. Bronchoscopic enucleation of glands was successful in 3 cases (13%); 7 children (29%) needed transthoracic glandular enucleation. Neither bronchoscopic nor transthoracic enucleation of glands was associated with any complications.

Phrenic Nerve Palsy

Three of the 9 left upper lobe pneumonias had associated phrenic nerve palsy. Two children were severely symptomatic with respiratory failure at presentation, while the other was asymptomatic, presenting with tuberculous meningitis. None of these phrenic nerve palsies resolved on antituberculous therapy. One child died, and one patient who required ventilation did not respond to conventional ventilation and was changed to high-frequency oscillatory ventilation. She was only successfully extubated after transthoracic glandular enucleation. All 3 patients had the same CT scan appearance, with homogeneous opacification with areas of liquefaction of the left upper lobe and glandular obstruction of the airways. Massive subcarinal and left-sided paratracheal lymph glands were present, resulting in a mediastinal shift to the right.

Outcome

Only one patient in this study died, and 2 required ventilation. Both ventilated children survived. Two patients were lost to follow-up. Chest radiographs were done in 92% of the cases after completion of 6 months' therapy. In 2 (10%), the chest radiographs were normal, while in all the other cases there had been considerable improvement (Fig. 3). Cystic changes compatible with parenchymal damage were seen in 4 (18%), and volume

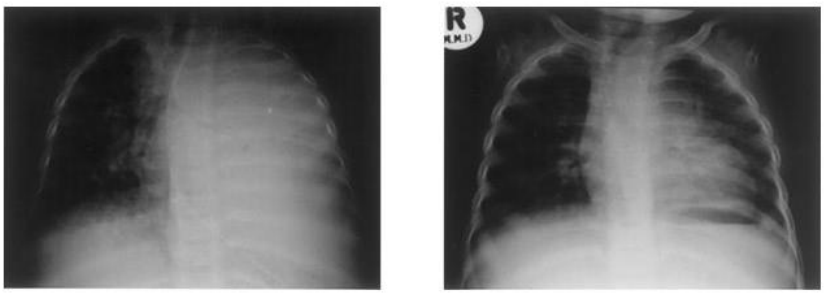

Fig. 3. Chest radiographs showing dense opacification of left lung prior to treatment (left), and follow-up chest radiograph after 6 months of treatment (right).

loss of the affected lobe in 68%. One patient had a massive calcified Ghon focus visible. Two children had recurrent episodes of pneumonia ascribed to underlying lung damage.

DISCUSSION

In this study, we describe the clinical and radiological picture of expansile pneumonia caused by *Mycobacterium tuberculosis*, as well as the response to therapy. We found that most children were referred to the tertiary care hospital with pneumonia not responding to treatment. The radiological picture was one of dense opacification of mostly the upper lobes with bulging fissures. *Mycobacterium tuberculosis* was cultured in most cases. The CT scan pictures were mostly of homogeneous opacification with areas of necrotic liquefaction, with enlarged mediastinal glands. Approximately 40% of the children required enucleation of the intrathoracic lymphadenopathy. In all cases, the lung lesions improved on standard antituberculosis therapy. This picture of expansile pneumonia caused by *Mycobacterium tuberculosis* and its response to modern antibiotics was not previously described.

There is confusion in the literature as to what the correct terminology is for describing the combination of airway and parenchymal disease in children with TB. Initially the clinical term "epituberculosis" was used to describe a chronic illness in children with indefinite clinical signs but a homogeneous opacity extending from the hilar region into part of the whole lobe on chest radiograph. These children were not very ill, and in most cases the lesion resolved without therapy.[6] It was also termed "endobronchial tuberculosis" when the lymph node involvement of the bronchus led to obstruction of the bronchus. Seal and Thomas described tuberculous pneumonia as aspiration due to perforation of caseous lymph nodes distal to lobar or segmental bronchial obstruction.[7] It was thought that the lobe became congested and edematous, and these enlarged lobes on chest radiography were termed a "wet" or "drowned lung."[8]

Others used the term "lymphobronchial tuberculosis" to describe the lesions that result from lymph gland involvement with the airways in children.[9] Expansile pneumonia is one of the radiological pictures of lymphobronchial tuberculosis.[9] The term "lymphobronchial tuberculosis" is useful, as it partially explains the pathogenesis of the disease. Other radiological pictures of lymphobronchial tuberculosis are bronchial compression, unilateral hyperinflation, and lobar or segmental collapse.

The most common cause of expansile pneumonia in children was stated to be caused by *Klebsiella pneumoniae* and to affect mostly the upper lobes.[1,2] Rarely, expansile pneumonia is caused by *Staphylococcus aureus* and even less commonly by *Aspergillus fumigatus* in neutropenic immunocompromised patients.[3,4] Expansile pneumonia caused by MTB was not well-described, even in the literature prior to the availability of modern chemotherapy.

The clinical picture is characteristic, with most (83%) of the children presenting as nonresolving pneumonia. One child presented with wheezing as a result of severe obstruction of the major airways. As in other studies published from the same high prevalence area, the history of contact was present in only 42%, and the Mantoux tuberculin skin test was positive in 63%.[10] In contrast with other studies, MTB was cultured from 88% of cases. Normally studies report that *M. tuberculosis* is cultured in only 30–40% of cases.[10] As previously reported, early morning gastric aspirates had the highest yield, while BAL contributed very little to the yield.[2,11]

On chest radiograph, the upper lobes were most frequently involved. The lobes were densely involved without air bronchograms, and with cavities visible in 33%. Hilar lymph glands were not visible, as the hilar region was obscured by the enlarged lobe, but indirect evidence of lymph gland enlargement was airway compression, seen in 92% of cases. Computed tomography was shown to be superior in the identification of enlarged lymph glands.[12] This was also the case in this study, where mediastinal lymph gland enlargement was observed in all cases.

It is speculated that the pathogenesis of these lesions follows narrowing of the airways by mediastinal glands. The enlarged glands infiltrate the bronchial wall, eventually rupturing into the bronchus. The caseating material containing both viable organisms and tuberculous material (tuberculoprotein) is aspirated into the affected lobe. In the lobe, an allergic response develops, causing the expansile pneumonia. This hypothesis is supported by the observation that lesions similar to those seen in these children develop after the injection of tuberculoprotein into the lobes of rabbits.[13]

An interesting exercise was the correlation of the degree of airway obstruction and the computed tomography picture. All patients with obstruction greater than 75% had liquefaction on CT scan, while in those with less than 75% obstruction, no liquefaction was observed. Utilizing the CT scan appearance and bronchoscopic findings, we propose the following pathogenesis. The tuberculous infection causes glandular involvement of the bronchus wall, with the gland rupturing into the airway. This leads to the inhalation of tuberculoprotein, and a hypersensitivity response develops and leads to expansile pneumonia. This is the hypersensitivity phase which correlates with the CT scan appearance of opacification with air bronchograms with patent airways. As progression of the disease occurs, severe to complete obstruction of the airways develops, with caseating necrosis of the lung parenchyma; this leads to tissue breakdown of the lung parenchyma with liquefaction. This correlates with the CT scan appearance of airway obstruction and homogeneous opacification with

areas of liquefaction and glandular obstruction. The proposed pathogenesis is very similar to that proposed by Seal and Thomas, who described three categories of lung involvement: noncaseating pneumonia, caseating pneumonia, and a combination of the two forms.[7] These authors also pointed out that these lesions are not paucibacillary, but have a high bacillary load and are usually culture-positive. This is similar to our finding that MTB was cultured in the majority of cases (88%).

The treatment of expansile pneumonia caused by MTB is unclear and controversial. We treated the children with a standard four-drug TB regimen, to which we added prednisone for a month. In approximately 60% of cases, this was successful in relieving airway obstruction, allowing the pneumonia to resolve. The value of adding steroids remains uncertain, and indications for the use of steroids in pulmonary disease remain controversial.[14,15]

Three children had bronchoscopic enucleation, and after the airway obstruction was improved, chest X-rays showed dramatic improvement, with the affected lobe losing its expansile appearance and numerous cavities becoming visible. This suggests that if it is possible to open the airway, the lobe will drain. Transthoracic enucleation was shown to be safe and effective in relieving airway obstruction, provided that only incision, evacuation, and curettage of lymph nodes was done, and not aggressive dissection and removal of the glands.[16] The indications for enucleation are uncertain. Life-threatening airway obstruction is a clear indication. Other indications are less clear. We treated children for 1 month and evaluated the improvement clinically and radiologically. If there was no improvement, we repeated the bronchoscopy, and if the gland could not be enucleated transbronchoscopically, transthoracic enucleation was performed. The timing of 1 month was based on personal experience that if the enucleation is postponed, the enlarged glands will start to organize, and relief of airway obstruction is seldom obtained. The position of steroids and the role of transbronchoscopic or transthoracic enucleation are unlikely to be resolved, as a large randomized trial would be required.

Three children had associated phrenic nerve palsy, with none of them recovering phrenic nerve function. Diaphragmatic plication was required in the two surviving children.

The long-term outcome of expansile pneumonia in the studied children was surprisingly good. Only two children had repeated respiratory infections ascribed to underlying bronchiectasis. No children were treated for longer than 6 months, although only 10% had a normal chest radiograph at this time.

Here we have described expansile pneumonia caused by *M. tuberculosis*, which can be recognized from clinical and radiological appearances and which can be successfully treated medically in the majority of cases. We have too few patients with dual infection with *M. tuberculosis* and HIV to speculate how dual infection and immunosuppression will influence the outcome of expansile pneumonia in HIV-infected children.

ACKNOWLEDGMENTS

We thank our colleagues in the Departments of Radiology and Cardiothoracic Surgery for their assistance in the management of these children.

REFERENCES

1. Feldson B, Rosenberg L, Hamburger M. Roentgen findings in acute Friedlander's pneumonia. Radiology 1949;46:559–565.
2. Korvick JA, Hackett AK, Yu VL, Mulder RR. *Klebsiella pneumonia* in the modern era: clinicoradiographic correlations. South Med J 1991;84:200–204.
3. Winer-Muram HT, Arheart KL, Jennings SG, Rubin SA, et al. Pulmonary complications in children with hematological malignancies: accuracy of diagnosis with chest radiography and CT. Radiology 1997;204:643–649.
4. Caillot D, Couaillier JF, Bernard A, Casasnovas O, et al. Increasing volume and changing characteristics of invasive pulmonary aspergillosis on sequential thoracic computed tomography scans in patients with neutropenia. J Clin Oncol 2001;19:253–259.
5. World Health Organisation. Provisional guidelines for primary health care, surveillance and special studies. EPI/GEN/83/4. Geneva: World Health Organisation; 1983.
6. Eliasberg H, Neuland W. Zur Klinik der Epituberkulosen und gelatinosen Infiltration der kindlichen Lunge. Jahrb Kinderheilkd 1920;93:88.
7. Seal RME, Thomas DME. Endobronchial tuberculosis in children. Lancet 1956;271:995–996.
8. Jones EM, Rafferty TN, Willis HS. Primary tuberculosis complicated by bronchial tuberculosis with atelectasis (epituberculosis). Am Rev Tuberc 1942;46:392.
9. Beyers JA. Radiographic manifestations. In: Coovadia HM, Benatar SR, editors. A century of tuberculosis. Cape Town: Oxford Press; 1991. p 203–233.
10. Schaaf HS, Beyers N, Gie RP, Nel ED, et al. Respiratory tuberculosis in childhood: the diagnostic value of clinical features and special investigations. Pediatr Infect Dis J 1995;14:189–194.
11. Abadco DL, Steiner P. Gastric lavage is better than bronchoalveolar lavage for the isolation of *Mycobacterium tuberculosis* in childhood tuberculosis. Pediatr Infect Dis 1992;11:735–738.
12. Kim WS, Moon WK, Kim IO, Lee HJ, et al. Pulmonary tuberculosis in children: evaluation with CT. AJR 1997;168:1005–1009.
13. Oppenheimer EH. Experimental studies on the pathogenesis of epituberculosis. Bull Johns Hopkins Hosp 1935;57:247.
14. Nemir RL, Cardona J, Vazairi F, Teledo R. Prednisone as an adjunct in the chemotherapy of lymph node-bronchial tuberculosis in childhood: a double blind study II. Further term observation. Am Rev Respir Dis 1967;95:402–410.
15. Toppet M, Malfoot A, Dedre MP, et al. Corticosteroids in primary tuberculosis with bronchial obstruction. Arch Dis Child 1990;65:1222–1226.
16. Papagiannopoulos KA, Linegar AG, Harris DG, et al. Surgical management of airway obstruction in primary tuberculosis in children. Ann Thorac Surg 1999;68:1182–1186.

PAEDIATRIC RESPIRATORY REVIEWS (2004) **5(Suppl A)**, S139–S141
Available online at www.sciencedirect.com
SCIENCE DIRECT®
Paediatric Respiratory Reviews

Unusual forms of intrathoracic tuberculosis in children and their management

R.P. Gie*, P. Goussard, S. Kling, H.S. Schaaf and N. Beyers

Department of Paediatrics and Child Health, Faculty of Health Sciences, Stellenbosch University, Tygerberg, Cape Town, South Africa

Intrathoracic tuberculosis (TB) usually develops after a child has been in contact with an adult index case with newly diagnosed pulmonary TB. The child may present with chronic non-specific or respiratory symptoms, and have a positive tuberculin skin test, while on a chest radiograph mediastinal lymphadenopathy is normally seen with or without complications of the lymphadenopathy.

The most common radiological features are mediastinal lymphadenopathy (49–70%), lobar opacification (56%), lobar or segmental collapse (17%), pleural effusion (12%), miliary opacification (6%) and lung cavities (6%).[1,2,3] There are a number of unusual presentations, the incidence of which is difficult to estimate. The cases presented in this paper have occurred in a region where the incidence of TB is extremely high (>700 new cases/100000 annum) but the prevalence of HIV is relatively low. None of the cases described were HIV seropositive.

BRONCHO-OESOPHAGEAL FISTULA ($n = 5$)

Broncho-oesophageal fistulae have two main clinical pictures in children. It may firstly present as a patient with known intrathoracic TB who then develops symptoms of aspiration during feeding ($n = 3$). The second clinical picture ($n = 2$) is of a child with severe hypoxic respiratory failure. During assisted ventilation the presence of an air leak through the oesophagus becomes evident. At bronchoscopy the fistula was seen in the left main bronchus ($n = 4$) with the other site in bronchus intermedius. Although the literature suggests that these fistulae heal on antituberculous therapy[4,5] this has not occurred in the children we have managed. All the children required surgical closure after 6 months of antituberculosis therapy. In one ventilated case a Sengstaken–Blakemore tube was used to seal the fistula so that surgery could be performed.[6] Both children with respiratory failure died.

PHRENIC NERVE PALSY ($n = 6$)

This is an extremely rare complication with a single case in a child described in the literature. In all the cases that we have seen phrenic nerve palsy, the involvement occurred on the left side. Phrenic nerve palsy presents either co-incidentally in asymptomatic children previously treated for TB or as part of extensive intrathoracic TB. In the asymptomatic group ($n = 2$) diaphragmatic plication was required to stabilise lung function. In the group with extensive intrathoracic TB ($n = 4$) diaphragmatic function was absent on initial evaluation. In no case did phrenic nerve function return on anti-tuberculous treatment to which steroids had been added. In one case surgical decompression of the glandular mass was performed but phrenic nerve function failed to return. A complicating factor in the group with extensive intrathoracic TB was that the left main bronchus had glandular obstruction of varying degree in all the cases. One child died and at autopsy the phrenic nerve was infiltrated by the tuberculous process.

CHYLOTHORAX ($n = 1$)

Chylothorax is a rare complication of TB described in adult patients. A single child with chylothorax has been seen. The 2 year old boy presented with bilateral pleural effusions. The aspirated pleural fluid had the characteristics of a true chylothorax. *M. tuberculosis* was cultured from the gastric aspirate. The chest radiograph showed bilateral pleural effusions with a broad mediastinum due to

*Correspondence to: R.P. Gie. Tel.: +27-(21)-938-9444; Fax: +27-(21)-938-9138; E-mail: rpg1@sun.ac.za

1526-0542/$ – see front matter

lymphadenopathy and the computerised tomography confirmed these findings. The boy was treated with a 3 drug antituberculous regimen, steroids (prednisone 2 mg/kg/day) and a diet of medium chain triglycerides. During the first month the effusions repeatedly recurred causing great discomfort to the patient. Percutaneous needle drainage was performed on numerous occasions to relieve shortness of breath. After a month the effusions stabilised. The patient required 6 months of therapy before the effusions disappeared. There was no residual pleural pathology.

INTRATHORACIC COLD ABSCESS FORMATION ($n = 2$)

Two children, one 5 months of age (boy) and the other 3 years of age (girl) were evaluated for pulmonary TB that was not responding to therapy. After 6 and 3 months, respectively, of therapy the patients still had a high swinging fever and were not gaining weight. Both children were severely malnourished. The boy had features of widely disseminated TB with generalised lymphadenopathy and hepatosplenomegaly. The girl had an upper motor neuron lesion of her legs and was unable to walk. On computerised tomography of the brain she had a TB granuloma in the temporal region. The boy had a miliary picture on chest radiography while the girl had widespread bronchopneumonic involvement as well as large thin walled cysts in both lungs. In the boy tuberculosis was proven by histology of the lung and liver while in the girl *M. tuberculosis* was cultured from gastric aspirate. Computerised tomography of the chest in both cases confirmed the widespread alveolar involvement and mediastinal lymphadenopathy but in addition both patients had large liquified glands present in the anterior and posterior mediastinum. These children required surgery to drain the liquified glands. The pus in the glands was still Ziehl–Neelsen positive on microscopy but *M. tuberculosis* was not cultured. After drainage of the abscesses, both patients' fever resolved and they gained weight.

EXPANSILE PNEUMONIA

It is extremely common for glands to involve the airways either by compression of the airway, infiltration of the airway or erosion of the gland into the lumen of the airway. These lesions have been referred to as endobronchial TB, epituberculosis or lymphobronchial TB. The term lymphobronchial TB as propagated by Beyers[7] seems to be the preferred term as it focuses on the lymph gland and its effect on the airways. The term also differentiates this form of TB in children from endobronchial TB in adult patients which has a different clinical picture, pathogenesis, bronchoscopic findings and outcome. TB glandular obstruction of the airways can cause a check valve effect causing a large hyperinflated lung or lobe. If the airway is completely obstructed the lobe or segment may collapse. Another presentation that is not well recognised is the clinical and radiological picture of an expansile pneumonia caused by *M. tuberculosis*. TB expansile pneumonia mostly occurs in children younger than 2 years of age. Almost all children are referred for evaluation as they have a lobar pneumonia that is not responding to antibiotic therapy. Almost all cases occur in the upper lobes with middle lobe or lingula involvement also frequently being present. These children do not appear toxically ill, although some have fever spikes, are often not tachypnoeic, are dull to percussion and have decreased air entry over the affected lobe. They rarely require supplementary oxygen. On chest radiograph the affected lobe is homogeneously opacified with no air bronchograms visible. The lobe is enlarged causing downward displacement of the fissures. In some of the cases breakdown with cavities can be seen in the area of opacification. At bronchoscopy the airway is completely occluded from either external compression or by erosion of the gland through the wall of the bronchus. These children are treated with the standard three drug TB regimen to which steroids (prednisone 2 mg/kg) are added for one month and then weaned. After 6 months of treatment lobar or segmental opacification is still present in 24% but improvement continues after stopping therapy with bronchiectasis developing in 7%.[8]

OTHER UNUSUAL FORMS

Other unusual forms have also been seen and include pleural effusion with a chest wall mass and TB of the thoracic vertebrae causing an unusual mediastinal mass and compression of the left main bronchus.

REFERENCES

1. Smuts NA, Beyers N, Gie RP, Schaaf HS, et al. Value of the lateral chest radiograph in tuberculosis in children. *Pediatr Radiol* 1994; **24**: 478–480.
2. Donald PR, Ball J, Beyers JA. Bacteriologically confirmed pulmonary tuberculosis in children. *S Afr Med J* 1985; **65**: 588.
3. Schaaf HS, Beyers N, Gie RP, Nel ED, et al. Respiratory tuberculosis in childhood: the diagnostic value of clinical features and special investigations. *Pediatr Inf Dis J* 1995; **14**: 189–194.

4. Wychulis AR, Bunch GH. Acquired non-malignant esophago-tracheo-bronchial fistula. *JAMA* 1996; **196**: 103–108.
5. Danino EA, Evans CJ, Thomos JH. Tuberculous broncho-esophageal fistula in a child. *Thorax* 1955; **10**: 351–353.
6. Gie RP, Kling S, Schaaf HS, Beyers N, et al. Tuberculous broncho-esophageal fistula in children. *Pediatr Pulmonol* 1998; **25**: 285–288.
7. Beyers JA. Radiographic manifestations. In: Coovadia HM, Benatar SR, eds., *A Century of Tuberculosis*. Cape Town: Oxford Press, 1991: pp. 203–233.
8. Gie RP, Beyers N, Schaaf HS, Donald PR, et al. The outcome of children with endobronchial tuberculosis. *Tubercle Lung Dis* 1995; **76**: s53.

PAEDIATRIC RESPIRATORY REVIEWS (2004) **5(Suppl A)**, S147–S149
Available online at www.sciencedirect.com
SCIENCE DIRECT®
Paediatric Respiratory Reviews

The challenge of diagnosing tuberculosis in children: a perspective from a high incidence area

R.P. Gie*, N. Beyers, H.S. Schaaf and P. Goussard

Department of Paediatrics and Child Health, Faculty of Health Sciences, Stellenbosch University, Tygerberg, Cape Town, South Africa

Tuberculosis (TB) is a common disease in children living in the developing world. It is estimated that 95% of the 1.4 million childhood TB cases and 450.000 deaths occur in the developing world. It is in these resource-poor countries that the diagnosis is extremely challenging. This article will review some of the difficulties in diagnosing intrathoracic TB in children living in these parts of the world.

Children live in communities where the reported annual incidence of TB can be as high as 1297 cases/100.000 population/annum with certain areas in such a community having a reported incidence of greater than 3000 cases/100.000 population/annum.[1] It is not surprising that children living in these communities have an annual risk of TB infection of 3.5%.[2] In low incidence areas children make up a small portion (2 to 5%) of the caseload. In high incidence areas children can contribute up to 39% of the annual caseload[3] and have a notification rate of 3.5-fold greater than that of adults.[3] In these communities it is mostly young children who are infected and develop disease with 79% of the children in this community that develop disease being younger than 5 years.[3]

It is generally accepted that most transmission takes place within a household. When a child is infected the index case is usually a household member or close family friend. In communities with a low incidence of TB the presence of a newly diagnosed adult case of TB is an important clue to the diagnosis of TB in a child. In a community with a high TB incidence this seems to be more complex. In a provisional report evaluating the transmission of TB to children using restricted fragment length polymorphism (RFLP) to characterise *M. tuberculosis* isolated from adults and children with TB it was shown that 56% of transmission occurred outside the household but within the community.[4] This increases the difficulty of diagnosis in children living in high incidence areas, as the children do not necessarily have a known adult index case.

In normal circumstances 5–10% of adults infected with TB will develop disease. In children living in resource-poor countries with a high incidence of TB this transition has been reported to be as high as 34%.[5] The reasons for this high disease rate are unknown but in this study did not relate to HIV infection. The most likely explanation is that all the children studied were under 5 years of age where the risk of disease after infection is estimated to be 24%.[6] While it was originally assumed that children in contact with multidrug resistant (MDR) TB would be less likely to be infected and develop disease. It has recently been shown that in communities with a high incidence of MDR TB the rate of infection is as high as children exposed to drug-susceptible strains although less developed disease.[7]

The symptoms of TB disease are chronic in nature and are non-specific. When comparing the symptoms of children with culture proven TB to those who were initially suspected of having TB but shown to have other lung diseases it was shown that weight loss, chronic cough, duration of symptoms or weight less than the third percentile did not differ between the two groups.[8] The only clinical factors which differentiated between the groups were contact with an adult index case and a positive tuberculin skin test. Children infected with HIV often have similar symptoms related to their HIV infection without being

*Correspondence to: R.P. Gie. Tel.: +27-(21)-938-9444. Fax: +27-(21)-938-9138; E-mail: rpg1@sun.ac.za

1526-0542/$ – see front matter

infected with TB. The overlapping nature of the symptoms and the higher prevalence of non-reactive tuberculin skin tests makes the diagnosis of TB in a HIV-infected child very complex. Furthermore, TB in HIV-infected children can present as an acute respiratory disease, more often associated with fever than in HIV-uninfected children.

Tuberculin skin testing is particularly useful in identifying children infected with TB. The interpretation of the test is very complex as only 70% of children with culture-proven TB had a positive tuberculin skin test.[8] It is further complicated in regions with a high incidence of HIV infection and malnutrition as these children are less likely to have a positive test. On the other hand it has been reported that up to 28% of healthy children (5–9 years) living in a high incidence area have a Mantoux skin test of greater than 15 mm induration.[4]

The chest radiographic findings diagnostic of intrathoracic TB are enlarged mediastinal glands and complications resulting from the glands compressing airways or other structures. Many radiologists would be reluctant to diagnose TB in the absence of adenopathy. In studies of culture-proven TB adenopathy is visible in 49 to 60% of cases.[8,9] Lateral chest radiographs improve the diagnostic yield by 11%.[9] TB may present only with alveolar opacification making it difficult to distinguish from other causes of pneumonia. In children with a positive tuberculin skin test and a normal chest radiograph glands were seen in 60% when a computerised tomography of the chest was performed.[10] In an area with a high HIV incidence it can be very difficult to distinguish lymphocytic interstitial pneumonia (LIP) from TB as both cause significant mediatinal lymphadenopathy and a fine interstitial nodular pattern (miliary) on chest raadiography.

Culture of the *M. tuberculosis* is the gold standard for the diagnosis of TB. Early morning gastric aspirates are the commonest method of obtaining samples for cultures. The reported number of children likely to have TB and positive culture is approximately 28–40%.[11,12] More intensive methods of obtaining samples such as bronchioalveolar lavage and hypertonic induced sputum with nasopharyngeal aspiration have been used to increase the yield. While induced sputum increases the yield by 4.3% it has yet to be shown that this technique is widely applicable in resource-poor countries.[13]

Serological testing and polymerase chain reaction (PCR) of specimens have failed to live up to their initial promise, are expensive and require sophisticated laboratory services which are not available in resource-poor countries.

As diagnosing TB in children is relatively expensive, scoring systems have been developed to aid in the screening and diagnosis of TB. Of the 17 published scoring systems very few are based on prospective studies, have quantifiable sensitivities, specificities and positive predictive values.[14] Yet, it is these scoring systems than are used in the diagnosis of childhood TB in resource poor countries. Most of the scoring systems were developed before HIV became common and only 2 of the scoring systems have been adapted for children living in areas where the incidence of both TB and HIV are high.[14]

In resource-poor countries active contact tracing is seldom practised. Children often present late with severe and disseminated disease requiring hospitalisation and even admission to an ICU. In a high incidence area TB was responsible for 3% of annual admissions to the PICU with 70% requiring assisted ventilation for respiratory failure.[15] The mortality in the group as a whole was 23%.

The diagnosis TB is extremely complex and difficult especially in resource-poor countries with limited access to even the most basic investigations. When the incidence of TB is high and HIV infection increases, the diagnosis is even more challenging. Research into childhood TB is urgently required to improve diagnostic accuracy and to develop tools, which are applicable to children living in resource-poor countries. The need for this is especially urgent as the incidence of TB is rising as a result of the HIV epidemic in resource-poor countries.

REFERENCES

1. Beyers N, Gie RP, Zietsman HL, Kunneke M, et al. The use of a geographical information system to evaluate the distribution of tuberculosis in a high incidence community. *S Afr Med J* 1996; **86**: 40–44.
2. Ussery XT, Valway SE, Mckenna M, Cauthen GM, et al. Epidemiology of tuberculosis in the United States. *Pediatr Inf Dis J* 1996; **15**: 697–704.
3. Van Rie A, Beyers N, Gie RP, Kunnecke M, et al. Childhood tuberculosis in an urban population in South Africa: burden and risk factor. *Arch Dis Child* 1999; **80**: 433–437.
4. Schaaf HS, Michaelis IA, Richardson M, Booysen CN, et al. Adult to child transmission of tuberculosis: household or community contact? *Int J Tubercl Lung Dis* 2003; **7**: 426–431.
5. Beyers N, Gie RP, Schaaf HS, Van Zyl S. A prospective evaluation of children under 5 years living in the same household as adults with recently diagnosed pulmonary tuberculosis. *Int J Tuberc Lung Dis* 1997; **1**: 38–43.
6. Miller FJW, Seal RME, Taylor MD. Tuberculosis in Childhood. Boston: Little, Brown and Co., 1963.
7. Schaaf HS, Vermeulen HAS, Gie RP, Beyers N, Donald PR. Evaluation of young childen in household contact with adult multidrug-resistant pulmonary tuberculosis cases. *Pediatr Inf Dis J* 1999; **18**: 494–500.
8. Schaaf HS, Beyers N, Gie RP, Nel ED, et al. Respiratory tuberculosis in childhood: the diagnostic value of clinical features and special investigations. *Pediatr Inf Dis J* 1995; **14**: 189–194.

9. Smuts NA, Beyers N, Gie RP, Schaaf HS, et al. Value of the lateral chest radiograph in tuberculosis in children. *Pediatr Radiol* 1994; **24**: 478–480.
10. Delacourt C, Mani TM, Bonnerot V, de Blic J, et al. Computed tomography with normal chest radiograph in tuberculous infection. *Arch Dis Child* 1993; **69**: 430–432.
11. Lloyd AVC. Bacteriological diagnosis of tuberculosis in children. A comparative study of gastric lavage and laryngeal swab methods. *East Afr Med J* 1968; **2**: 140–143.
12. Starke JR, Yaylor-Watts KT. Tuberculosis in the pediatric population of Houston Texas. *Pediatrics* 1989; **84**: 28–35.
13. Zar HJ, Tannenbaum E, Apolles P, Roux P, et al. Sputum induction for the diagnosis of pulmonary tuberculosis in infants and young children in an urban setting in South Africa. *Arch Dis Child* 2000; **82**: 305–308.
14. Hesseling AC, Schaaf HS, Gie RP, Starke JR, et al. A critical review of diagnostic approaches used in the diagnosis of childhood tuberculosis. *Int J Tubercl Lung Dis* 2002; **6**: 1038–1045.
15. Heyns L, Gie RP, Kling S, Samaai P, et al. Management of children with tuberculosis admitted to a pediatric intensive care unit. *Pediatr Inf Dis* 1998; **17**: 403–407.

Acta Pædiatrica, 2006; 95: 535–539

Taylor & Francis
Taylor & Francis Group

Nosocomial transmission of *Mycobacterium tuberculosis* in kangaroo mother care units: A risk in tuberculosis-endemic areas

LOUIS HEYNS[1], ROBERT P. GIE[1], PIERRE GOUSSARD[1], NULDA BEYERS[1], ROB M. WARREN[2] & BEN J. MARAIS[1]

[1]*Desmond Tutu TB Centre and the Department of Paediatrics and Child Health, Tygerberg Children's Hospital and the Faculty of Health Sciences, Stellenbosch University, Tygerberg, South Africa, and* [2]*Medical Research Council (MRC) Centre for Molecular and Cellular Biology, Department of Medical Biochemistry, Stellenbosch University, Tygerberg, South Africa*

Abstract

Background and aim: Kangaroo mother care (KMC) has become the standard of care for low-risk preterm babies born in developing countries. However, the potential risk of nosocomial transmission of *Mycobacterium tuberculosis* within KMC units, particularly in tuberculosis-endemic areas, has not been explored. We report an infant (sentinel case) who was admitted to our paediatric intensive care unit (PICU) with extensive pulmonary tuberculosis. *Methods and results:* When interviewed, the mother reported no household contact with a tuberculosis source case, but mentioned that she shared a KMC room with someone who had symptoms suspicious of tuberculosis. We found molecular evidence that nosocomial transmission of *M. tuberculosis* occurred within the KMC unit and conducted a contact investigation of all infants exposed to this infectious source case during her stay in the KMC unit.

Conclusion: We present the findings of the contact investigation and discuss the implications of these findings for KMC units, particularly in tuberculosis-endemic areas.

Key Words: *Kangaroo mother care, nosocomial transmission, tuberculosis*

Introduction

Kangaroo mother care (KMC) has become the standard of care for low-risk preterm babies born in developing countries [1]. Strong evidence supports its benefits and safety in these settings [2], and it has been suggested as the optimal neonatal care model even in developed countries [3]. In South Africa, KMC units have become an integral part of routine neonatal care, and experience with these units has been very positive, being associated with improved neonatal outcomes and a drastic reduction in the cost of neonatal care.

It has been documented that KMC reduces the risk of nosocomial transmission of common bacterial pathogens [4]. However, the potential risk of nosocomial transmission of *Mycobacterium tuberculosis* within KMC units, particularly in tuberculosis-endemic areas, has not been explored. In tuberculosis-endemic areas it is not uncommon for pregnant mothers to develop active tuberculosis and, if untreated, these mothers pose an obvious transmission risk within the healthcare setting. The transmission risk within KMC units is of particular concern, as mothers and babies spend prolonged periods of time in small, often poorly ventilated rooms. In South Africa, it is standard practice for groups of 4–8 mothers and their preterm infants to share a single room for extended periods. In addition to the high transmission risk posed by the confines of KMC units, infants represent an exceptionally vulnerable group, who frequently develop severe forms of tuberculosis following exposure and infection with *M. tuberculosis*. The vulnerability of infants was clearly documented by studies that described the natural history of tuberculosis in children.[5] The combination of both these factors, the high transmission risk posed by KMC units and the exceptional vulnerability of those exposed, indicate the potential gravity of the situation.

We present a case report of an infant (sentinel case) who was admitted to our paediatric intensive care unit (PICU) with extensive pulmonary tuberculosis. When interviewed, the mother reported no household contact with a tuberculosis source case, but mentioned

Correspondence: B. J. Marais, Department of Paediatrics and Child Health, Faculty of Health Sciences, Stellenbosch University, PO Box 19063, Tygerberg, 7505, South Africa. Tel: +27 21 938 9155. Fax: +27 21 838 9138. E-mail: bjmarais@sun.ac.za

(Received 23 December 2005; accepted 15 February 2006)
ISSN 0803-5253 print/ISSN 1651-2227 online
DOI: 10.1080/08035250600636560

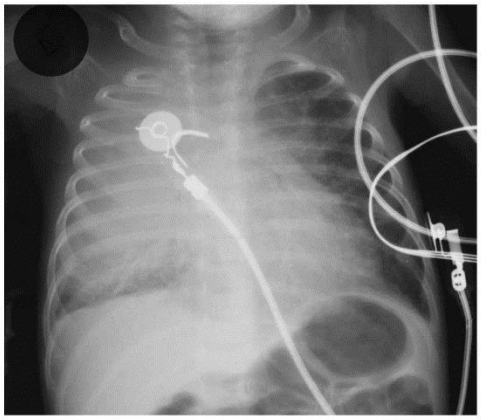

Figure 1. Chest radiograph of the sentinel case on admission to the intensive care unit (ICU), showing widespread alveolar opacification of the right lung, extensive hilar adenopathy and airway compression

that she shared a KMC room with someone who coughed continuously. This initiated an investigation into the possibility of nosocomial transmission within the KMC unit. We present the findings of this investigation and discuss the general implications for KMC units, particularly in tuberculosis-endemic areas.

Sentinel case

A 3-mo-old baby was admitted to the PICU of Tygerberg Children's Hospital with respiratory failure,

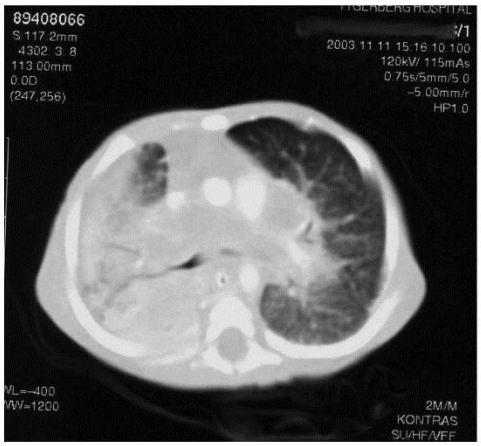

Figure 2. Chest computed tomograph (CT) scan of the sentinel case on admission to the intensive care unit (ICU), confirming extensive hilar adenopathy with central low attenuation, indicative of tuberculous caseation, and near-total obstruction of the right main bronchus.

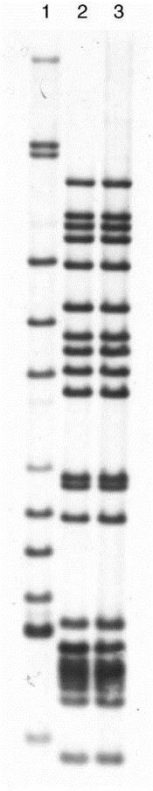

Figure 3. Comparative restriction fragment length (RFLP) fingerprints of the sentinel case and the source case, providing evidence of nosocomial transmission. Lane 1: reference strain; lane 2: source case; lane 3: sentinel case.

which required assisted ventilation. The chest radiograph showed extensive alveolar consolidation of the right lung with hilar adenopathy and compression of the airways (Figure 1). A computed tomography (CT) scan of the lung confirmed the presence of multiple hilar lymph nodes and near-total obstruction of the right main bronchus (Figure 2). The severe degree of airway obstruction necessitated surgical intervention. At surgery, the largest glands were enucleated to remove the caseated contents and to reduce the degree of airway obstruction; *M. tuberculosis* was subsequently cultured from the enucleated material. Following surgery, the baby was weaned off the ventilator within 1 d, and made a remarkable recovery on standard anti-tuberculosis chemotherapy.

On interview, no household member, or other family/friends that had close contact with the baby, reported suggestive symptoms or a recent diagnosis of tuberculosis. The baby was born prematurely (29 wk gestation, birthweight 1.4 kg), and the mother spent a

considerable time (23 d in total) in two local kangaroo units. The only possible source case that could be identified was another mother with whom she and her baby shared a KMC room at one of these units. The mother reported that the potential source case coughed continuously and looked ill.

Source case

We traced the potential source case and discovered that she was diagnosed with sputum smear-positive tuberculosis shortly after discharge from the KMC unit. We were able to collect a viable *M. tuberculosis* culture to establish if she was the source case by comparing the restriction fragment length polymorphism (RFLP) patterns (fingerprint) found, to that of the sentinel case. RFLP fingerprinting was done using previously reported methodology [6]. The fact that the fingerprints were identical provided molecular evidence that she was indeed the source case (Figure 3). Circumstantial evidence indicated that transmission could only have occurred in the KMC unit as the two families reside in different communities and have not been in contact outside the hospital. Comparison of the RFLP fingerprint to a reference database showed that the *M. tuberculosis* organism belonged to the Beijing strain family.

The source case reported classic symptoms of active tuberculosis coughing, weight loss, night sweats and lethargy but she attributed these to her pregnancy. These symptoms persisted for more than 3 mo before she gave birth prematurely (32 wk gestation, birthweight 1.4 kg). After delivery, she spent 15 d in a local KMC unit without ever being screened or tested for tuberculosis, despite reporting a persistent cough with severe lethargy and weight loss during this time. After discharge from the KMC unit, she presented to the local primary healthcare clinic due to progressive symptoms and a single episode of haemoptysis. A sputum sample was collected for smear microscopy, and she was diagnosed with sputum smear-positive tuberculosis. By this time, she was already very ill and she made a slow, but complete, recovery on standard anti-tuberculosis chemotherapy.

Contact investigation

It was established that 11 infants shared a room with the source case during her stay in the KMC unit. Of these 11 children, eight were traced and it was discovered that four of them received anti-tuberculosis treatment in the first 6 mo following discharge from the KMC unit. The exposure duration, age at tuberculosis diagnosis and disease outcome are reflected in Table I. We were unable to trace three of the exposed neonates, as the phone numbers provided were non-functional and they were not known at the addresses provided. Two of them had very limited exposure (<1 d) to the source case, and to our knowledge none of them received anti-tuberculosis treatment within the first year of life.

Discussion

This study demonstrates that the potential risk of nosocomial *M. tuberculosis* transmission within KMC units may be very high. A previous report documented transmission from an infectious source case within a maternity unit in Modena, Italy [7]. Infection (as measured by a positive ELISPOT result) was well correlated with the amount of time that room air was shared with the source case [6]. As mothers in KMC units share room air for extensive periods of time, it is important to take cognizance of the transmission risk that this poses.

The risk of nosocomial transmission of tuberculosis is well documented [8], although we tried to emphasize the particularly favourable environment that KMC units provide to facilitate transmission. In our study, 4/6 (66.7%) of the neonates who shared a room with the source case for 10 d or more developed disease within 6 mo. However, it is not only the high transmission risk that is a concern, but the fact that infants are extremely vulnerable to develop severe forms of disease following infection with *M. tuberculosis*. This is supported by our findings that three of the four diseased infants developed extensive pulmonary tuberculosis, although none of them developed miliary tuberculosis or tuberculous meningitis.

We do not believe that this episode represents an isolated incident. Since admission of the sentinel case to our ICU, two other infants have been admitted to the ICU with extensive pulmonary tuberculosis. Both of these infants spent time in KMC units and reported no known contact with a tuberculosis source case outside the hospital. It remains difficult to prove the link between their disease and exposure within the KMC unit, as it is known that a lot of transmission in this highly endemic community occurs outside the household [9]. However, infants are usually protected against community exposure due to their limited social contact and, in our experience, known household or family/friend contact is reported in nearly every instance where an infant develops tuberculosis. In our study, we have convincing molecular evidence that the sentinel case developed disease following infection within the KMC unit. Of the other three infants that developed tuberculosis, none reported known exposure to a tuberculosis source case outside the hospital, and in every instance the disease manifested within 6 mo after the exposure they had in the KMC unit. According to the natural history of tuberculosis in children, this

Table I. Duration of exposure, tuberculosis (TB) diagnosis and outcome in all infants exposed to an infectious tuberculosis source case in a kangaroo mother care (KMC) unit.

Patient number	Exposure duration	TB diagnosis	Time since KMC exposure	TB disease manifestation[a]	Outcome
1	>15 d	TB (baby of source case)	2 mo	Complicated lymph node disease with expansile TB pneumonia	Good
2	15 d	TB	5 mo	Uncomplicated lymph node disease	Good
3	12 d	No TB			
4	10 d	TB (sentinel case)	3 mo	Complicated lymph node disease with airway compression	Good
5	10 d (twin no. 1)	TB	4 mo	Complicated lymph node disease with airway compression	Good
6	10 d (twin no. 2)	No TB			
7	5 d	Not found			
8	4 d	no TB	Mother diagnosed with TB <1 y		
9	2 d	no TB			
10	<1 d	Not found			
11	<1 d	Not found			

[a] TB disease manifestation according to a recently proposed radiological classification of intrathoracic tuberculosis in children [12].

establishes the KMC exposure as the most likely time of infection [5,10].

Mother and infant demonstraing Kangaroo mother care. The infant was born at 30 weeks gestation, weighing 1.21 kg; spent the first 3 days in an incubator and was then nursed by his mother; the baby is currently 25 days old, weighs 1.53 kg and is fully breast fed.

An interesting observation was that one of the mothers also developed tuberculosis within 1 y of sharing a KMC room with the source case, although her baby did not develop disease. In highly endemic areas, the tuberculosis epidemic is primarily driven by transmission [11], and adult tuberculosis frequently follows after fairly recent exposure; unlike the classic scenario in non-endemic areas where adult disease is usually ascribed to re-activation of a distant primary infection. Therefore, the tuberculosis that this mother developed may have resulted from exposure to the source case, but as no culture specimen was collected we were unable to confirm this by molecular means.

The value of KMC units is not disputed, and this report does not question their important contribution to improve neonatal care in resource-limited settings. However, the potential risk for nosocomial *M. tuberculosis* transmission in endemic areas is high, and we believe that this requires more emphasis. The institution of simple measures, such as symptom-based screening, may be sufficient to identify mothers who require further testing to exclude tuberculosis. To prevent nosocomial transmission of *M. tuberculosis*, healthcare workers should remain vigilant to identify and treat suspected tuberculosis cases promptly [12].

In KMC units, it is particularly important to identify and isolate suspect cases, but, in addition, preventive chemotherapy should be provided to all neonates that were exposed to a source case with confirmed tuberculosis.

Acknowledgements

We want to thank the mother of the sentinel case for her kind assistance and understanding; the doctors and nursing staff in the Tygerberg Children's Hospital PICU for their dedication and for the care they provided to the sentinel case; and the TB in the 21st Century Consortium, an international network supported by the Norwegian Research Council and the Centre for Prevention of Global Infections, University of Oslo, for scientific input.

References

[1] Kirsten GF, Bergman NJ, Hann FM. Kangaroo mother care in the nursery. Pediatr Clin North Am 2001;48:443–52.

[2] Charpak N, Ruiz-Pelaez JG, Figuera de CZ, Charpak Y. Kangaroo mother versus traditional care for the newborn infant ≤2000 grams: a randomised, controlled trial. Pediatrics 1997;100:682–8.

[3] Ruiz-Pelaez JG, Charpak N, Cuervo LG. Kangaroo mother care, an example to follow from developing countries. Br Med J 2004;329:1179–81.

[4] Conde-Agudelo A, Diaz-Rosello JL, Belizan JM. Kangaroo mother care to reduce morbidity and mortality in low birthweight infants. Cochrane Database Syst Rev 2003;2: CD002771.

[5] Marais BJ, Gie RP, Schaaf HS, Hesseling AC, Obihara CC, Starke JJ, et al. The natural history of disease of childhood intra-thoracic tuberculosis – a critical review of the pre-chemotherapy literature. Int J Tuberc Lung Dis 2004;8: 392–402.

[6] Van Rie A, Warren RM, Richardson M, Victor TC, Gie RP, Enarson DA, et al. Exogenous reinfection as a cause of recurrent tuberculosis after curative treatment. N Engl J Med 1999;341:1174–9.

[7] Richeldi L, Ewer K, Losi M, Bergamini BM, Roversi P, Deeks J, et al. T cell-based tracking of multidrug resistant tuberculosis infection after brief exposure. Am J Resp Crit Care Med 2004;170:288–95.

[8] Schaaf HS, Michaelis IA, Richardson M, Booysen CN, Cie RP, Warren RM, et al. Adult-to-child transmission of tuberculosis: household or community contact? Int J Tuberc Lung Dis 2003;7:426–31.

[9] Marais BJ, Donald PR, Gie RP, Schaaf HS, Beyers N. Diversity of disease manifestations in childhood pulmonary tuberculosis. Ann Trop Paed 2005;25:79–86.

[10] Kellerman SE, Simonds D, Banerjee S, Towsley J, Stover BH, Jarvis W, et al. APIC and CDC survey of Mycobacterium tuberculosis isolation and control practices in hospitals caring for children. Part 1: Patient and family isolation policies and procedures. Am J Infect Control 1998;26:478–82.

[11] vd Spuy GD, Warren RM, Richardson M, Beyers N, Behr MA, van Helden PD, et al. Use of genetic distance as a measure of ongoing transmission of Mycobacterium tuberculosis. J Clin Microbiol 2003;41:5640–4.

[12] Centers for Disease Control and Prevention (CDC). Tuberculosis outbreak in a community-hospital: District of Columbia, 2002. MMWR 2004;53:214–6.

[13] Marais BJ, Gie RP, Schaaf HS, Starke JR, Hesseling AC, Donald PR, et al. A proposed radiologic classification of childhood intra-thoracic tuberculosis. Pediatr Rad 2004;33: 886–94.

Pediatric Pulmonology 42:93–97 (2007)

Esophageal Stent Improves Ventilation in a Child With a Broncho-Esophageal Fistula Caused by *Mycobacterium tuberculosis*

P. Goussard, M Med,[1]* D. Sidler, FCP,[2] S. Kling, FCP,[1] S. Andronikou, FCP,[3] G. F. Rossouw, M Med,[4] and R. P. Gie, FCP[1]

Summary. The deployment of an esophageal stent to aid in the ventilation of a child who had developed an acquired broncho-esophageal fistula caused by *Mycobacterium tuberculosis* (MTB) is described. The 12-month-old boy presented with respiratory failure requiring ventilation. The air leak via the fistula led to inadequate mechanical ventilation. The deployment of the stent resulted in successful ventilation, closure of the fistula, and eventual successful treatment. **Pediatr Pulmonol. 2007; 42:93–97.** © 2006 Wiley-Liss, Inc.

Key words: ***Mycobacterium tuberculosis*; broncho-esophageal fistulae; esophageal stent; ventilation.**

INTRODUCTION

Fifty percent of acquired esophagorespiratory fistulae in adult patients are due to benign causes.[1] The most common causes are prolonged mechanical ventilation, iatrogenic injuries, trauma, foreign body ingestion, prior tracheal or esophageal surgery, indwelling stents, granulomatous mediastinal infections, and AIDS.[1,2] In adults, 10–19% of acquired non-malignant broncho-esophageal fistulae (BEF) are caused by *Mycobacterium tuberculosis* (MTB). In children, BEF caused by MTB are rare and mostly fatal. This complication has been described in seven children in the English language literature.[3–7] BEF caused by MTB present as one of three clinical pictures: acutely with severe respiratory distress requiring ventilation, a chronic picture with repeated aspiration, and following surgery for tuberculous gland enucleation. The previous six children presenting to us with acute respiratory failure requiring ventilation did not survive because of ineffective ventilation caused by the air leak through the BEF.

In this article, we describe the successful management with the aid of an esophageal stent of a child with BEF requiring ventilation.

CASE REPORT

A 12-month-old boy presented with acute onset respiratory failure requiring ventilation. He was referred from a rural hospital where he presented with a 1-week-history of a lower respiratory tract infection with accompanying weight loss. He had been in contact with a recently diagnosed adult case of pulmonary tuberculosis and had not received chemoprophylaxis. He had a normal neonatal history, a previously uneventful medical history, and had received BCG vaccination at birth.

On physical examination, he was acutely ill, with tachypnea and intercostal retraction. His weight was 5.2 kg, which is less than 60% of expected weight for age. He appeared anemic, but was not clubbed and did not have signs of chronic lung disease. He had a tracheal cough and monophonic bilateral wheezing, indicating large airway obstruction. Hepatomegaly of 5 cm was present; there was no splenomegaly.

[1]Department of Pediatrics and Child Health, University of Stellenbosch and Tygerberg Children's Hospital, Cape Town, South Africa.

[2]Department of Pediatric Surgery, University of Stellenbosch and Tygerberg Children's Hospital, Cape Town, South Africa.

[3]Department of Radiology, University of Stellenbosch and Tygerberg Children's Hospital, Cape Town, South Africa.

[4]Department of Cardiothoracic Surgery, University of Stellenbosch and Tygerberg Children's Hospital, Cape Town, South Africa.

*Correspondence to: Dr. P. Goussard, Department of Paediatrics and Child Health, Faculty of Health Sciences, Stellenbosch University, PO Box 19063, Tygerberg 7505, South Africa. E-mail: pgouss@sun.ac.za

Received 17 March 2006; Accepted 28 July 2006.

DOI 10.1002/ppul.20532
Published online in Wiley InterScience (www.interscience.wiley.com).

The complete blood count showed a hemoglobin of 6.8 g/dl, MCV 95 fl, a white cell count of 19.4×10^9 L ^{1} and platelet count of 253×10^9 L ^{1}. The C-reactive protein was 214 µg/ml. The child was HIV antibody negative and no other causes of immune deficiency could be demonstrated.

The boy's respiratory status deteriorated rapidly and he required urgent intubation. The initiation of ventilation resulted in severe abdominal distension, which further compromised ventilation. An audible air leak, which disappeared once the endotracheal tube was advanced into the right main bronchus, could be heard over the abdomen. A plain chest radiograph revealed extensive bilateral parenchymal disease and gastric distension. The BEF originating in the left main bronchus was demonstrated by a bronchogram using water-soluble contrast medium (Fig. 1). The size of the BEF was so large that a 2.8 mm flexible bronchoscope could pass from the left main bronchus through the fistula into the esophagus. Other bronchoscopic findings were tracheal compression and a broadened carina with tuberculous gland herniation into the left main bronchus.

Ventilation was inadequate due to the air leak caused by the fistula. A Sengstaken-Blakemore tube was inserted into the esophagus and the esophageal bulb inflated to reduce the air leak for adequate ventilation. The pressure required to reduce the air leak was greater than the recommended maximum of 25 cm water. Above this pressure, ischemic necrosis of the esophagus becomes an increasing risk. For this reason, we decided to remove the Sengstaken-Blakemore tube and place a stent in the esophagus. A self-expanding, nitinol-alloy-covered esophageal stent (18 mm by 6 cm) (Taewoong Medical, Korea) was deployed in the esophagus via a rigid scope in an attempt to decrease the air leak (Fig. 2). Although the air leak decreased the airway obstruction worsened. Under direct observation, the endotracheal tube was positioned via a flexible bronchoscope just above the carina. The endotracheal tube served as a stent for the airway, which was compressed by the esophageal stent and tuberculous lymph glands. If the endotracheal tube dislodged from this optimal position, ventilation became difficult with the arterial pC02 episodically rising to above 180 mmHg.

Initially, the child's tuberculosis was treated by intravenous rifampicin, amikacin, and ciprofloxacin. After placing the esophageal stent, it was possible to pass a duodenal tube and feed the child via this route. The tuberculosis treatment was then changed to the more conventional therapy of rifampicin (20 mg/kg/day), isoniazid (20 mg/kg/day), pyrazinamide (25 mg/kg/day), and ethionamide (20 mg/kg/day). Prednisone (2 mg/kg/day) was added to this therapy.

A chest computerized tomography scan (CT) confirmed large right-sided paratracheal glands causing tracheal compression (Figs. 3 5). As extubation was not possible, a right thoractomy was performed under general anesthesia to enucleate the paratracheal glands, which contained large amounts of caseating material. After enucleation, the child was rapidly weaned but extubation was still not possible. At further flexible bronchoscopy, compression

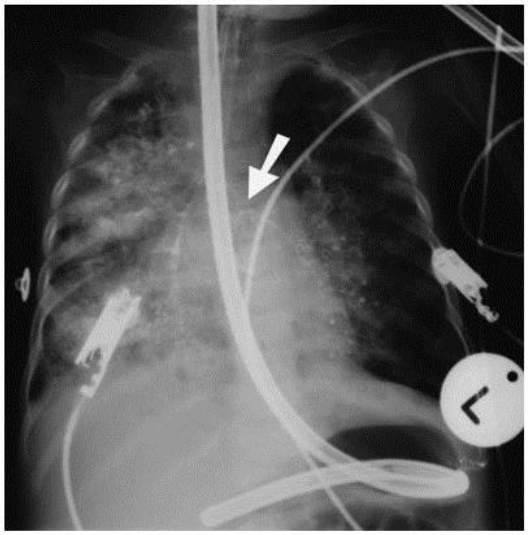

Fig. 1. Water-soluble bronchography performed via the endotracheal tube demonstrates the contrast leaking from the left main bronchus and entering the esophagus (arrow). A Sengstaken-Blakemore tube is in situ in an attempt to limit leakage from the esophagus. Advanced air-space disease is present on the right.

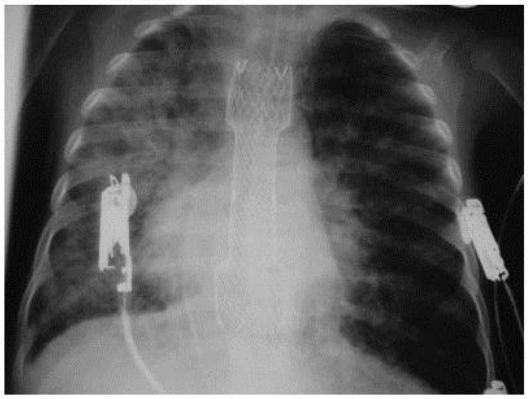

Fig. 2. Post-esophageal stent insertion. The radiograph demonstrates the stent, an endotracheal tube, a naso-gastric tube, and a central venous line inferiorly. There is persistent extensive air-space disease in the right lung and less marked lingular and left lower lobe disease.

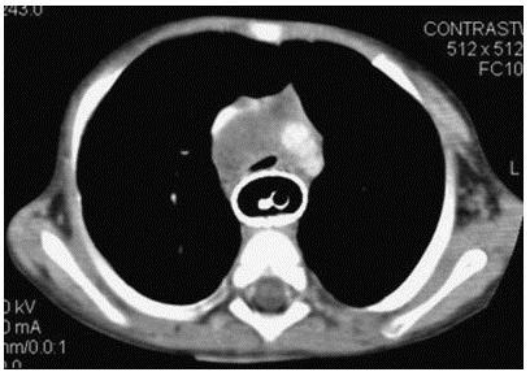

Fig. 3. Axial post-contrast CT at the level of the superior mediastinum demonstrates the radio-dense esophageal stent which is impressing on the dorsal aspect of the trachea. There is a large pre- and para-tracheal lymph node group impressing on the trachea from the right anteriorly. A nasogastric tube and a Replogle tube are seen adjacent to each other within the stent lumen.

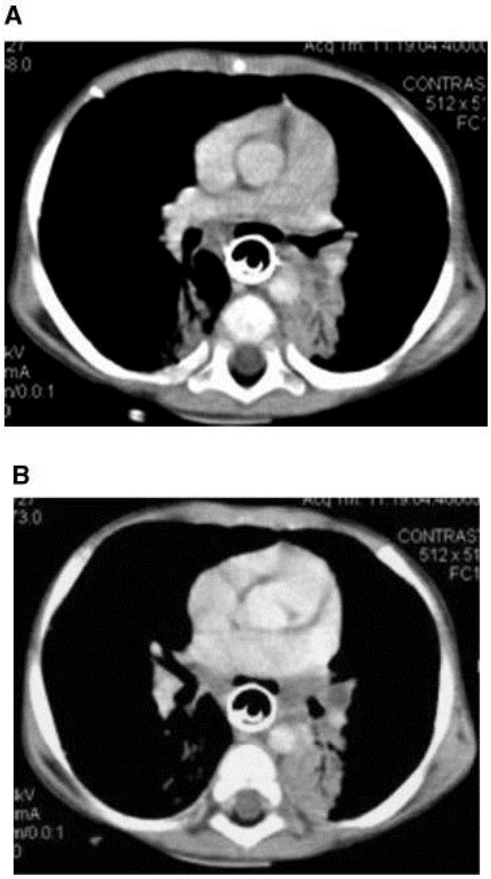

Fig. 4. A, B: Axial, consecutive CT scans below the level of the carina demonstrate air anterior to the esophageal stent inferring a fistulous communication between the esophagus and left main bronchus. Left hilar and subcarinal lymphadenopathy is present as well as posterior segment air-space disease bilaterally.

of the trachea by the esophageal stent was visible. For this reason, it was decided to remove the stent via a flexible gastroscope 3 weeks after it had been inserted. Following uncomplicated removal of the stent, extubation was possible. The boy required ventilation for 24 days and was discharged from the PICU after 6 weeks.

Drug susceptible MTB was cultured from both the bronchial washings and the material enucleated from the mediastinal glands.

The boy was fed via the duodenal tube until a barium swallow done after 6 weeks confirmed that the fistula was closed. Flexible bronchoscopy confirmed that the fistula was no longer patent although the site of the fistula was still visible and the bronchoscope could enter the tract. The left main bronchus was narrowed by 50% and there was tracheomalacia of the anterior part of the trachea where the trachea had been compressed by the glands.

The child spent 4 months in the hospital before discharge. After 2 months, his TB treatment was adjusted so that he received only rifampicin and isoniazid. After 6 months of TB treatment, the child was doing very well; he had no swallowing difficulties, and had doubled his weight. A follow-up chest radiograph confirmed fibrotic changes in the right upper lobe, but no volume loss or bronchiectatic changes were visible. The child completed 9 months of antituberculous therapy and is presently asymptomatic and developing normally.

DISCUSSION

Broncho-esophageal fistulae (BEF) caused by MTB are mostly left-sided, although one case of right-sided BEF has been reported.[5] Tuberculous BEF result from the erosion of tuberculous peribronchial lymph nodes into both the esophagus and bronchus. They may also result from direct extension of tuberculous ulceration or perforation of a tuberculous abscess. Less frequently, a fistula may follow direct spread from thoracic vertebral TB[6] or be a complication of endotracheobronchial TB. Esophageal TB is rare and is almost always secondary to pulmonary tuberculosis.

This patient with an acquired BEF caused by MTB, requiring ventilation for respiratory failure is probably the first survivor documented in the literature. The previous patients died because adequate ventilation could not be achieved by either conventional mechanical ventilation (CMV) or high frequency oscillatory ventilation (HFOV). The reasons for the difficult ventilation possibly include

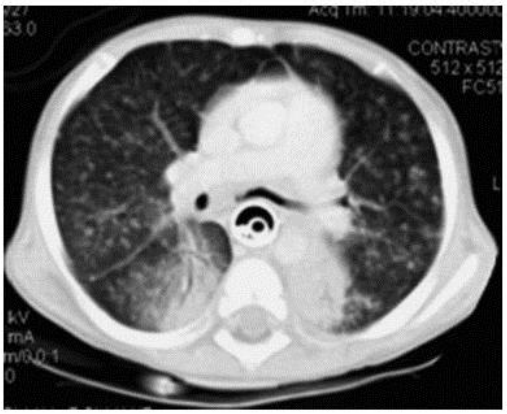

Fig. 5. Axial CT ("lung window" view) at the level of the carina confirms the bilateral, dependent air-space disease, and also demonstrates bilateral scattered interstitial nodules consistent with miliary TB.

the fact that not only is there a large air leak between the airway and the esophagus, but these children also have glandular compression of the large airways in addition to their significant parenchymal disease. This results in very ineffective ventilation with hypercarbia and severe hypoxia. Previous interventions included attempts to ligate these fistulae surgically during the acute phase but the patients succumbed during surgery. Other attempts included passing a Sengstaken-Blakemore tube which provided short-term improvement, but the tube could not be left in position because of the risk of necrosis of the esophagus.[5] Selective intubation into the right main bronchus was also not successful and these children became severely hypoxic because of the degree of parenchymal lung disease. In this case, the stent provided time for the parenchymal lung disease to improve and made successful extubation possible. The covered stent was able to seal the airleak by compressing the fistula between the endotracheal tube and the stent. This made it possible to isolate the esophageal content from the fistula as it is postulated that this promotes healing.[10] Extracorporeal membrane oxygenation (ECMO) is not available in South Africa, but this might be an alternative form of treatment. Ideally, the stent in the esophagus should be left in situ, but in this case a large stent was used, as it was the only one available. This resulted in posterior compression of the trachea, making extubation difficult. This complication was previously reported in an adult patient where the tracheal compression resolved after removal of the stent.[11]

Because Berger and Donato[12] in 1972 described the successful use of a Celestin tube to manage leaks in the esophagus, the use of self-expanding plastic esophageal stents for various causes of fistulae and leakages have been well established in adults. Radecke et al.[13] have shown that in 73.3 % of patients the leak in the esophagus could be successfully sealed by stent placement. They have also shown that this is a safe, technically feasible, effective, and relatively inexpensive option to treat esophageal fistulae, perforations, and anastomotic leaks. In their study, the fistulae closed between 1 and 3 months after stent placement. Esophageal stents were successful in closing fistulae or perforations ranging in size from a few millimeters to a couple of centimeters. Even anatomic dehiscence of more than 50% of the anatomic circumference healed successfully.[14]

It was recently suggested that esophageal stenting is the treatment of choice for children with esophageal strictures following the ingestion of corrosive agents.[15] There is, however, no guidance for the use of stents in children with esophageal perforations in children. Although there is a considerable body of evidence that esophageal stents are successful in the treatment of esophageal perforations and anastomotic leaks in adults, this evidence is not available for children.[16] Although we used a metal, partially covered stent, it seems that a Polyflex (woven plastic stent made of polyester mesh and embedded in silicone) might have been a more appropriate choice. The Polyflex stents are fully covered, have a decrease likelihood of migration, and result in less proliferation of inflammatory issue.[16]

In contrast to the adult literature, our previous cases of BEF did not close on TB treatment alone and needed surgical intervention after 6 months of TB treatment.

In this reported case, the BEF closed on TB treatment alone. Previously, the children who survived presented with symptoms that indicated that the fistula had been patent for a prolonged period of time. It could be that the described case had an acute presentation and thus was able to close on therapy.

This patient has helped us to formulate a treatment plan for children with an acquired broncho-esophageal fistula needing ventilation. In children with BEF not requiring ventilation, the role of esophageal stenting is unclear, but it is possible that self-expanding stents might have a role to play in the treatment of these patients.

CONCLUSION

The previous patients with BEF who required ventilation died because adequate ventilation could not be achieved. In such cases, stenting the esophagus is a treatment option during the acute phase where ECMO is not available. The use of stents to close the fistula in the long-term management of BEF has yet to be determined.

REFERENCES

1. Chauhan SS, Long JD. Management of tracheoesophageal fistulas in adults. Curr Treat Options Gastroenterol 2004;7:31–40.

2. Reed MF, Mathisen DJ. Tracheoesophageal fistula. Chest Surg Clin N Am 2003;13:271–289.
3. Bhata R, Mitra DK, Mukkerjee S, Berry M. Bronchoesophageal fistula of tuberculosis origin in a child. Pediatr Radiol 1992;22:154.
4. Coleman FP, Bunch GH. Acquired non- malignant esophago-tracheo-bronchial fistula. J Thorac Surg 1950;19:542–558.
5. Gie RP, Kling S, Schaaf HS, Beyers N, Moore S, Schneider J. Tuberculous Broncho-esophageal fistula in children. Pediatr Pulmonol 1998;25:285–288.
6. Moersch HJ, Tinney WS. Fistula between the oesophagus and the tracheobronchial tree. Med Clin North Am 1944;July:1001–1007.
7. Wychulis AR, Ellis FH, Andersen HA. Acquired non-malignant esophageo-tracheobronchial fistula. JAMA 1966;196: 103–108.
8. Danino EA, Evans CJ, Thomas JH. Tuberculous bronchoesophageal fistula in a child. Thorax 1955;10:351–353.
9. Lucaya J, Sole S, Badora J, Manjanares R. Bronchial perforation and broncho-esophageal fistulas: tuberculous origin in children. AJR 1980;135:525–528.
10. Adler DG, Pleskow DK. Closure of benign tracheoesophageal fistula by using a coated self-expanding plastic stent in a patient with a history of oesophageal atresia. Gastroint Endosc 2005;61: 765–768.
11. Evrard S, Le Moine O, Lazaraki G, Dormann A, Nakadi IE, Deviere J. Self-expanding plastic stents for benign esophageal lesions. Gastrointest Endosc 2004;60:894–900.
12. Berger RL, Donato AT. Treatment of esophageal disruption by intubation. A new method of management. Ann Thorac Surg 1972;13:27–35.
13. Radecke K, Gerken G, Treichel U. Impact of a self-expanding, plastic esophageal stent on various esophageal stenoses, fistulas and leakages: a single-center experience in 39 patients. Gastrointest Endosc 2005: 61; 812–818.
14. Gelbmann CM, Ratiu NL, Rath HC, Rogler G, Lock G, Scholmerich J, Kullman F. Use of self-expandable plastic stents for the treatment of esophageal perforations and symptomatic anastomotic leaks. Endoscopy 2004;36:695–699.
15. Zhang C, Yu J-M, Fan G-P, Shi C-R, Yu S-Y, Wang HP, Zhang W-X. The use of retrievable self-expanding stent in treating childhood benign esophageal strictures. J Pediatr Surg 2005;40: 501–504.
16. Siersema PD. Treatment of esophageal perforations and anastomotic leaks: the endoscopist is stepping into the arena. Gastroint Endosc 2005;61:897–900.

Pediatr Radiol (2007) 37:636–639
DOI 10.1007/s00247-007-0482-5

ORIGINAL ARTICLE

Oesophageal perforation as a complication of primary pulmonary tuberculous lymphadenopathy in children

Anita Erlank · Pierre Goussard · Savvas Andronikou · Robert Gie · Daniel Sidler · Christelle Ackermann · Jaco Parsons · Jaco Greyling

Received: 6 October 2006 / Revised: 11 March 2007 / Accepted: 25 March 2007 / Published online: 25 May 2007

Abstract
Background Involvement of the oesophagus by tuberculosis is rare, and erosion and perforation of the oesophagus by tuberculous lymphadenopathy is an unusual complication of primary pulmonary tuberculosis. There are very few reports describing both CT and contrast swallow appearances of these lesions.
Objective To describe the CT and contrast swallow appearances of oesophageal erosion and perforation by lymphadenopathy as a complication of primary pulmonary tuberculosis in children.
Materials and methods Imaging of three children with confirmed pulmonary tuberculosis and oesophageal perforation was retrospectively reviewed.
Results Tuberculosis was confirmed by culture in all three patients. Contrast swallow demonstrated a contained leak in two patients and a tracheo-oesophageal fistula in one. Two patients had mediastinal air and one patient had a mediastinal collection on CT. All patients had features diagnostic of pulmonary tuberculosis on CT.
Conclusion The imaging features comprise leakage of contrast medium with or without fistula formation on contrast swallow, large low-density lymph nodes on CT, and mediastinal air. The use of retrievable stents is a promising idea in this condition.

Keywords Oesophagus · Perforation · Tuberculosis · Stent · Children

A. Erlank · S. Andronikou (✉) · C. Ackermann · J. Parsons · J. Greyling
Department of Radiology, Stellenbosch University Medical School, P.O. Box 19063, Tygerberg 7505, South Africa
e-mail: docsav@mweb.co.za

P. Goussard · R. Gie
Department of Paediatrics, Tygerberg Hospital, University of Stellenbosch, Cape Town, South Africa

D. Sidler
Department of Paediatric Surgery, Tygerberg Hospital, University of Stellenbosch, Cape Town, South Africa

Introduction

Involvement of the oesophagus by tuberculosis (TB) is rare (0.15%) and erosion and perforation of the oesophagus by lymphadenopathy is an unusual complication of primary pulmonary TB (PTB) [1]. Characteristic contrast swallow and CT features of three children with oesophageal erosion due to tuberculous lymphadenopathy are described.

Materials and methods

The medical records and imaging of three known patients with oesophageal perforation as a result of tuberculous lymphadenopathy were reviewed, with particular reference to the contrast swallow and CT images. All contrast swallows were performed using water-soluble contrast medium and with the patients supine and oblique. TB was confirmed in all three children by positive cultures from lymph-node biopsies obtained by bronchoscopy or oesophagoscopy.

Results

Case 1

A 10-year-old girl who had been treated for PTB 2 years previously re-presented with a 3-month history of cough productive of yellow sputum, night sweats and loss of

weight. Her HIV status was negative. A chest radiograph was in keeping with primary PTB and bronchiectasis. Chest CT demonstrated mediastinal air and significant lymphadenopathy (right paratracheal, subcarinal, bilateral hilar; Fig. 1). Some of these nodes were calcified. There was significant compression of the right main bronchus and 90% compression of the bronchus intermedius, as well as consolidated right middle and lower lobes. Bronchiectasis was confirmed. Calcified granulomas in the liver compatible with abdominal TB were also noted. A contrast swallow was performed to determine whether the cause of the mediastinal air was oesophageal perforation and this showed a tracheo-oesophageal fistula at the level of the tracheal bifurcation (Fig. 1).

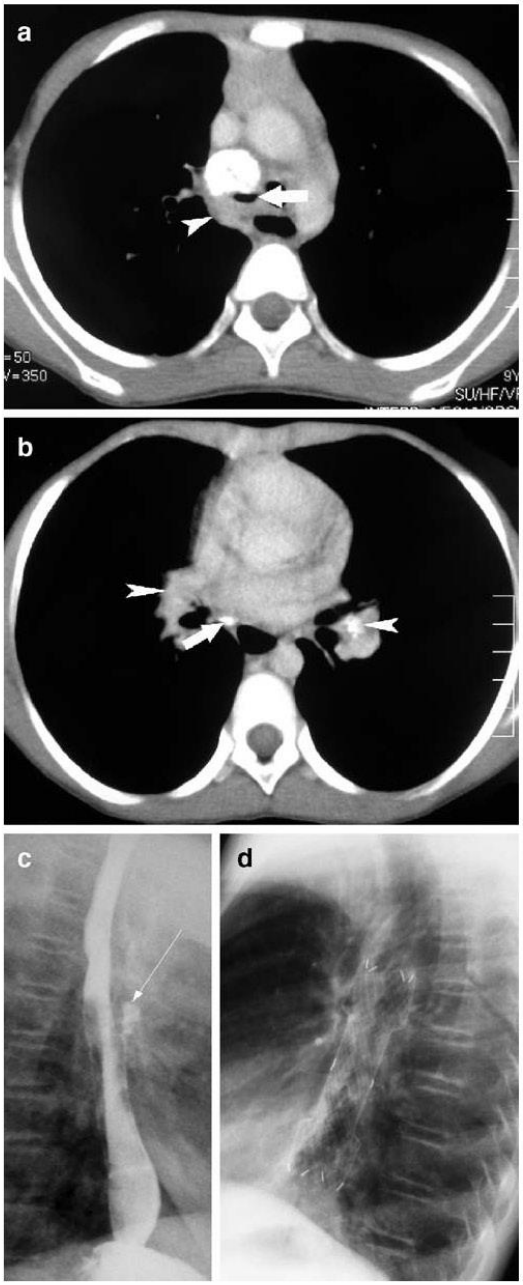

Fig. 1 Patient 1. **a** Axial contrast-enhanced chest CT image shows mediastinal air (*arrow*) and right paratracheal lymphadenopathy (*arrowhead*). **b** Axial contrast-enhanced chest CT image shows calcified subcarinal (*arrow*) and bilateral hilar (*arrowheads*) lymphadenopathy. **c** Contrast swallow shows a tracheo-oesophageal fistula at the level of the tracheal bifurcation with contrast medium entering the trachea (*arrow*). **d** Lateral chest radiograph demonstrates the oesophageal stent

Bronchoscopy identified lymph nodes herniating into the right main bronchus with complete obstruction of the bronchus intermedius. Endoscopic curettage was performed and biopsies of the lymph nodes were taken. A retrievable oesophageal stent was inserted a few days later as treatment for the tracheo-oesophageal fistula (Fig. 1). TB culture of the lymph-node biopsy was positive. At the time of this report, the patient was still receiving anti-TB treatment, the stent had been removed with successful closure of the fistula, and she was doing well.

Case 2

A 10-month-old HIV-positive baby presented with failure to thrive. Chest radiography demonstrated bronchopneumonia. Clinically the patient also had oral candidiasis and hepatosplenomegaly. A contrast swallow was performed to investigate for possible aspiration and demonstrated oesophageal perforation with contrast medium tracking between the oesophagus and the trachea (Fig. 2). Chest CT demonstrated low-density mediastinal lymphadenopathy consistent with TB (Fig. 2). The patient underwent oesophageal stenting because of mediastinal tissue friability and the risk for mediastinal abscess formation, but unfortunately died soon after the procedure due to HIV-related illness. TB culture of gastric washings was positive.

Case 3

An 11-year-old girl presented with a few months' history of loss of weight, cough and symptoms suggesting tracheo-oesophageal fistula. Chest radiography demonstrated primary PTB. A contrast swallow was performed to investigate for a tracheo-oesophageal fistula and demonstrated a contained

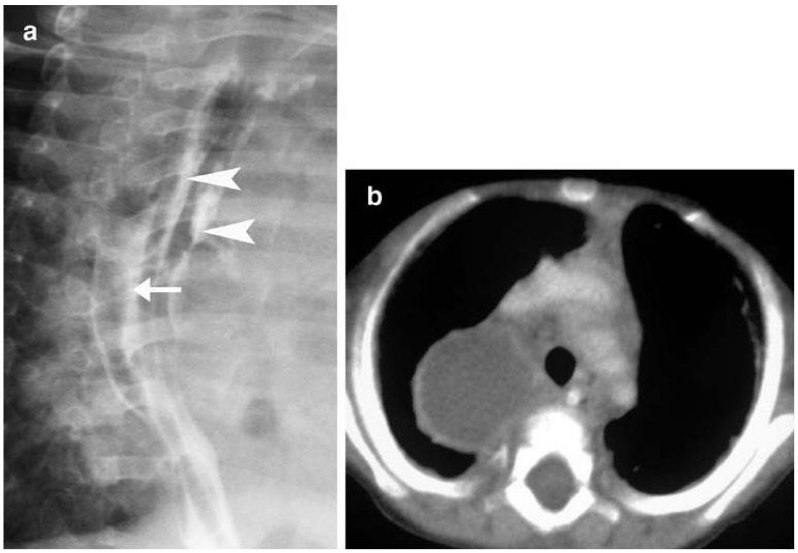

Fig. 2 Patient 2. **a** Contrast swallow shows oesophageal perforation with contrast medium tracking between the oesophagus and trachea (*arrow* oesophageal contrast medium, *arrowheads* contrast medium around the trachea). **b** Axial contrast-enhanced chest CT demonstrates low-density mediastinal lymphadenopathy consistent with TB. This is difficult to differentiate from a ring-enhancing collection

leak posteriorly, just above the carina, tracking superiorly, consistent with oesophageal perforation related to TB lymphadenopathy (Fig. 3). Chest CT demonstrated features in keeping with TB, namely mediastinal lymphadenopathy, and features suggesting erosion of the oesophagus (Fig. 3). Mediastinoscopy was performed and two large nodes in the right mediastinum were biopsied. Oesophagoscopy showed erosion of the oesophagus by large lymph nodes. An oesophageal stent was inserted due to the friability of the mediastinal tissue. Biopsies of the mediastinal lymph nodes

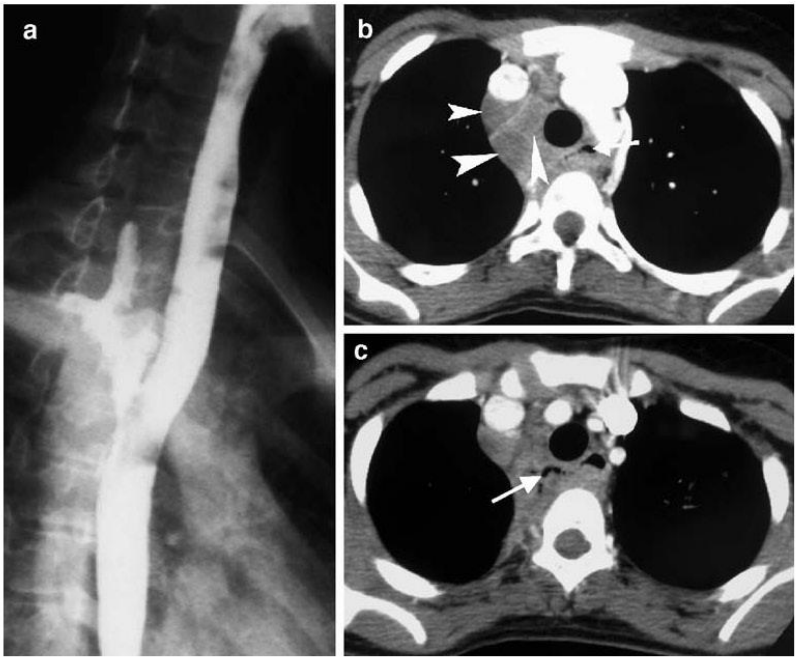

Fig. 3 Patient 3. **a** Contrast swallow demonstrates a contained leak posteriorly just above the carina, with contrast medium tracking superiorly in the mediastinum, consistent with oesophageal perforation. **b**, **c** Axial contrast-enhanced chest CT shows low-density mediastinal lymphadenopathy (**b**, *arrowheads*) consistent with TB and mediastinal air (**c**, *arrow*) secondary to mediastinal nodes eroding the oesophagus

confirmed TB by positive cultures. At the time of this report the patient was still receiving anti-TB treatment and her clinical status had improved; the stent was successfully removed a few months after insertion.

Discussion

Oesophageal perforation due to TB is a rare clinical entity, being described in only 0.15% of cases [1]. In the literature, isolated or primary TB of the oesophagus in adults is restricted to a few case reports. An English language literature search on oesophageal involvement in children with PTB revealed only seven previously reported cases of oesophageal erosion by lymphadenopathy with tracheo-oesophageal fistula formation [2–5]. Our report is unique in that two of our three patients demonstrated oesophageal perforation without fistula formation and imaging (contrast swallow and CT) was available.

Oesophageal perforation in TB may be due to rupture of a mediastinal abscess into the oesophagus [6], the formation of a traction diverticulum secondary to tuberculous mediastinitis [7]. Tuberculous lymph nodes lead to erosion and eventual perforation by pressure necrosis in combination with an inflammatory reaction [8]. This condition rarely causes symptoms as the perforation is often walled off by the mediastinal lymph nodes and the delay in diagnosis significantly increases mortality [9]. In contrast, involvement of the oesophagus in adult TB has a different pathogenesis. Primary TB in children is characterized by lymphadenopathy that is necrotic (low density on CT) whereas lymphadenopathy is not a feature of adult post-primary TB or reactivated TB.

The imaging features in the three reported cases comprised the following:

- Leakage of contrast medium with or without fistula formation on contrast swallow
- Large low-density lymph nodes on CT
- Mediastinal air on CT

Correlation with bronchoscopy in two of our patients confirmed erosion of the oesophagus by lymph nodes.

Conclusion

Oesophageal erosion and perforation by lymphadenopathy in paediatric primary PTB is described using diagnostic contrast swallows and CT in three patients. Endoscopy confirmed the cause to be erosion by lymph nodes in primary PTB. The use of retrievable stents is a promising idea in this condition.

References

1. Kotanidou A, Andrianakis I, Mavrommatis A et al (2003) Mediastinal mass with dysphagia in an elderly patient. Infection 31:178–180
2. Gie RP, Kling S, Schaaf HS et al (1998) Tuberculous bronchoesophageal fistula in children: a description of two cases. Pediatr Pulmonol 25:285–288
3. Bhata R, Mitra DK, Mukkerjee S et al (1992) Bronchoesophageal fistula of tuberculosis origin in a child. Pediatr Radiol 22:154
4. Danino EA, Evans CJ, Thomas JH (1955) Tuberculous bronchoesophageal fistula in a child. Thorax 10:351–353
5. Lucaya J, Sole S, Badora J et al (1980) Bronchial perforation and bronchoesophageal fistulas: tuberculous in origin. AJR 135:525–528
6. Ghandour Z, al Karami MA, Mohamed AE (1997) Spontaneous oesophageal perforation: unusual presentation of tuberculosis. Endoscopy 29:143–144
7. Tucker LE, Aquino T, Sasser W (1994) Mid-esophageal traction diverticulum: rare cause of massive upper gastrointestinal bleeding. Mo Med 91:140–142
8. Adkins MS, Raccuia JS, Acinapura AJ (1990) Esophageal perforation in a patient with acquired immunodeficiency syndrome. Ann Thorac Surg 50:299–300
9. Gupta NM, Goenka MK, Vaiphei K (1995) Isolated esophageal tuberculosis. Indian J Gastroenterol 14:25–26

Pediatr Radiol (2007) 37:798–804
DOI 10.1007/s00247-007-0496-z

ORIGINAL ARTICLE

Cavitating pulmonary tuberculosis in children: correlating radiology with pathogenesis

Stephanie Barbara Griffith-Richards · Pierre Goussard · Savvas Andronikou · Robert P. Gie · Stefan J. Przybojewski · Melanie Strachan · Yousuf Vadachia · David L. Kathan

Received: 28 November 2006 / Revised: 20 March 2007 / Accepted: 9 April 2007 / Published online: 26 May 2007

Abstract
Background Cavitating pulmonary tuberculosis (PTB) is generally known as a disease of adults, with children typically having features of primary PTB.
Objective To group children with PTB and cavities according to possible pathogenesis by evaluating the clinical and radiological findings.
Materials and methods The clinical and radiological findings in ten randomly selected children with PTB and cavitations on chest radiographs were retrospectively reviewed and evaluated.
Results Three groups emerged: group 1 (four children) had cavities, usually single and unilateral in the classic upper lobe distribution of postprimary PTB; group 2 (three children) developed progressive primary spread of disease with extensive and bilateral pulmonary cavities; and group 3 (three children) developed cavities secondary to airway obstruction by mediastinal lymph nodes with consequent distal collapse and consolidation. Children in group1 responded well to treatment and had unremarkable recoveries. Children in group 2 were all below 2 years of age with complicated recoveries. Children in group 3 had frequent complications resulting in one fatality.
Conclusion Cavities in PTB in children may arise by one of three possible mechanisms with a relatively equal incidence. A study is underway to determine the incidence of cavity formation associated with mediastinal lymphadenopathy and airway obstruction.

Keywords Lung · Tuberculosis · Cavitation · Children

S. B. Griffith-Richards (✉) · S. Andronikou · S. J. Przybojewski · M. Strachan · Y. Vadachia · D. L. Kathan
Department of Radiology,
Tygerberg Hospital and University of Stellenbosch,
P.O. Box 19063, Tygerberg 7505, South Africa
e-mail: drsteph21@hotmail.com

P. Goussard · R. P. Gie
Department of Paediatrics,
Tygerberg Children's Hospital and University of Stellenbosch,
Tygerberg, South Africa

Introduction

While intrathoracic lymphadenopathy is the commonest radiographic feature of primary pulmonary tuberculosis (PTB) in children, parenchymal abnormalities do occur, the commonest findings being alveolar consolidation and linear interstitial opacification [1]. Primary PTB, the most common form in childhood, is radiologically distinct from postprimary TB, the most common form occurring in adults [2]. In primary pulmonary infection, a Ghon complex is formed with a primary parenchymal focus (Ghon focus) and lymphadenopathy occurs in the draining regional lymph nodes [3].

The reported incidence of lymphadenopathy seen on chest radiographs is very variable, ranging from 63% to 95% in different studies [4]. Lymphadenopathy occurs most frequently in the right hilar and right paratracheal positions, which represent the draining nodes of the lower and upper lobes of the right lung [4]. In 5–10% of children with primary PTB, the primary focus can enlarge and undergo caseous necrosis; this is called progressive primary PTB [5]. This can lead to endobronchial spread and miliary dissemination. The lymph nodes themselves may undergo disease progression, enlarging due to central caseation, and the result is lymphobronchial TB [3]. The airways may become obstructed with distal collapse/consolidation [3] and subsequent breakdown. They may also erode into the

airways and cause intrabronchial spread with distal alveolar or bronchopneumonic consolidation [3].

In adults, cavitation results from reactivation of a dormant focus, the degree of tissue destruction being proportional to the severity of the hypersensitivity response [6].

Children have also been shown to develop adult-type postprimary PTB, with the characteristic distribution of cavities in the upper lobes and apices of the lower lobes of the lung [5]. This is rarely seen in prepubescent children [4]. The incidence of cavitation on chest radiography is between 5% and 16%; however it is frequently missed on plain radiographs alone, with CT demonstrating areas of cavitation or breakdown not seen on radiographs [4].

Understanding the pathological progression of the disease is essential in understanding the pathogenesis of the cavities, which may occur in a variety of clinical settings. We evaluated the clinical and radiological findings on plain chest radiographs of ten children found to have parenchymal cavitations as a result of PTB. In describing the patterns of cavitating lesions and associated chest radiograph findings and correlating with the clinical findings, we sought to group the lesions according to possible pathogenesis.

Materials and methods

Ten children with cavitating PTB were randomly chosen from children encountered in the radiology department of a tertiary hospital in a region where the incidence of TB is high. The children were all under the age of 16 years. The clinical picture and chest radiographic findings were documented and tabulated. This included initial and follow-up plain chest radiographs, if available, as well as contrast-enhanced CT chest scan if performed. Each image was evaluated for multiplicity, mural thickness and distribution of cavities, and the presence of associated findings, such as associated airspace disease, lymphadenopathy, with or without airway obstruction, and the presence of complications.

Results

The ten children included six girls and four boys; their ages ranged from 3 months to 15 years. Of the ten children, seven were culture-positive for *Mycobacterium tuberculosis* on gastric washings, sputum culture or lymph node aspiration; two were found to have multidrug-resistant PTB. In the other three children the diagnosis was based on a combination of the presence of constitutional symptoms, a positive tuberculin skin test (Mantoux or Tine

Table 1 Demographic data

	Group 1				Group 2			Group 3		
	FM	JP	NX	VH	DG	CP	LM	FS	LM2	TL
TB diagnosis[a]	NTP	Bacteriology	Bacteriology	NTP	Bacteriology	NTP	Bacteriology	Bacteriology	Bacteriology	Bacteriology
Multidrug-resistant TB	No	No	Yes	No	No	No	No	Yes	Yes	No
HIV status	Negative	Not tested	Negative	Negative	Not tested	Negative	Not tested	Negative	Positive	Positive
Age	6 years	10 years	14 years	4 years	3 months	2 years	4 months	15 years	5 months	5 years
Gender	Female	Female	Male	Male	Female	Female	Female	Female	Male	Male
ICU admission	No	No	No	No	Yes	No	Yes	No	Yes	No
Deceased	No	No	No	No	No	No	Yes	No	Yes	No

[a] *NTP* diagnosis as per National Tuberculosis Program guidelines [7]; *bacteriology* diagnosis made on bacteriological grounds, sputum/gastric washings/lymph node aspiration either positive for acid-fast bacilli or culture-positive for *Mycobacterium tuberculosis*

Table 2 Imaging findings

	Group 1						Group 2						Group 3					
	FM		JP		NX		VH		DG		CP		LM		FS		LM2		TL	
	Radiography	CT	Radiography	CT	Radiography	CT	Radiography	CT	Radiography	CT	Radiography	CT	Radiography	CT	Radiography	CT	Radiography	CT	Radiography	CT
Single	+	+	+		−		−		−	−	−		−	−	−		−	−	+	−
Multiple	−	−	−		+		+		+	+	+		+	+	+		+	+	−	+
Unilateral	+	+	+		+		+		−	−	−		−	−	−		+	+	+	+
Bilateral	−	−	−		−		−		+	+	+		+	+	+		−	−	−	−
Thick-walled	+	+	+		+		+		+	+	+		−	−	+		+	+	+	+
Thin-walled	−	−	−		−		−		−	−	−		+	+	−		−	−	−	−
Associated airspace disease	−	+	+		+		+		+	+	+		−	−	+		+	+	+	+
Associated disease elsewhere	−	+	−		+		+		+	+	+		−	−	+		+	+	−	−
Lymphadenopathy	−	+	−		n/a		n/a		n/a	+	n/a		n/a		n/a		+	+	+	+
Associated obstruction	−	−	−		−		−		n/a	−	n/a		n/a		+		+	+	+	+
Air/fluid level	−	−	−		−		−		−	+	−		−		−		−	+	+	+
Complications	−	Pe	−		−		−		−	Pe	−		−		Pt		Op/Bpf	Op/Bpf	−	−

Bpf bronchopleural fistula, *n/a* not applicable, *Pe* pleural effusion, *Pt* pneumothorax, *Op* oesophageal perforation

test) and a positive TB contact according to National Tuberculosis Programme (NTP) guidelines [7]. Seven children had an HIV test, two of which were positive and five negative. The remaining three were not tested for HIV.

The children were divided into three groups on the basis of chest radiographic and CT findings. Their demographic data are summarized in Table 1, and their imaging findings are presented in Table 2.

Three children required ICU admission for respiratory complications and two subsequently died.

Only five of the ten children had CT scans performed; these were those whose clinical course was complicated and for whom surgical intervention might be required. The rest had an unremarkable recovery or were too unwell to undergo scanning.

Group 1

These four children were initially symptomatic, but responded rapidly to treatment. CT was performed in one child only. The cavities, visible on plain chest radiographs in all children, were thin-walled, mostly single and unilateral with half having associated airspace disease and half not. Their course was unremarkable and most were managed on an outpatient basis. There were no visible lymph nodes on plain radiographs (Fig. 1); however, on CT scans one child did have lymphadenopathy not visible on plain radiographs.

Group 2

These three children were below 2 years of age and were unwell. They presented with multiple, bilateral thin- or thick-walled cavities. Two of these children had CT scans; the third child died from respiratory failure before a scan could be performed (Fig. 2). On CT scans, lymph nodes were present in both children, but there was no associated obstruction. In two of the children there was also associated airspace disease (Fig. 3); in the third the lung destruction was so extensive that there was little remaining parenchyma.

Group 3

These three children were also unwell, and one child in this group died after a long and complicated course on a ventilator in intensive care. They developed cavitations as a consequence of lymphadenopathy causing airway obstruction with caseous liquefaction of the lung distal to the obstruction. Two of the three children had CT scans in view of the complications or for surgical planning (Fig. 4). In both these children, the adenopathy was visible on plain chest radiographs. One of the children was less symptomatic and while she had multiple bilateral cysts, no CT was

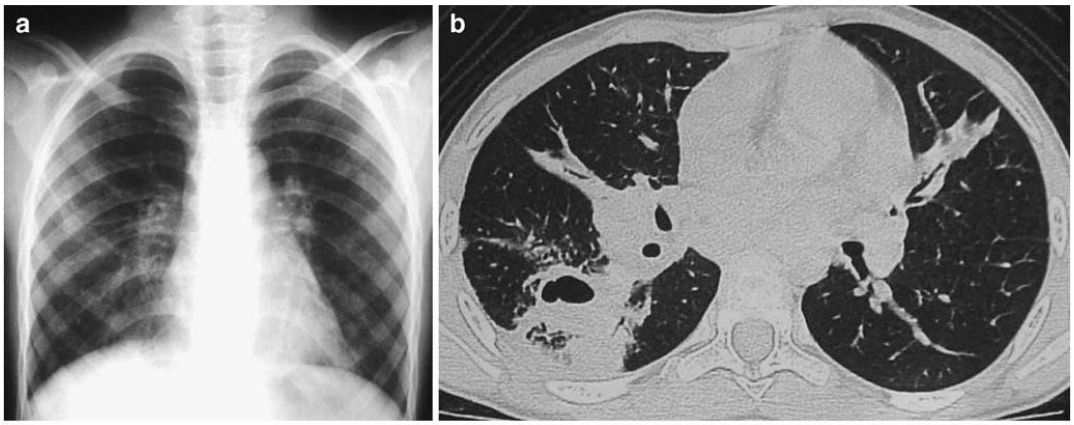

Fig. 1 A 6-year-old girl (CP) with constitutional symptoms and a positive tuberculin skin test. **a** Chest radiograph shows a thin-walled cavity in the right mid-zone. **b** CT (lung windows) demonstrates cavitation of the lung parenchyma posteriorly at the level of the right hilum. Note also the bulky right pulmonary hilum in keeping with hilar lymphadenopathy

done and lymph nodes were inferred from the presence of obvious bronchial obstruction on plain radiographs. She may well represent a child who lies somewhere between the first and the third group.

Discussion

In Cape Town, Western Cape, South Africa, a high TB burden area, children under 13 years of age contribute 13.7% to the total TB burden with the incidence of TB in children at 441/100,000/year [8]. The children in this study were all treated at the tertiary level after being referred from smaller clinics in this catchment area.

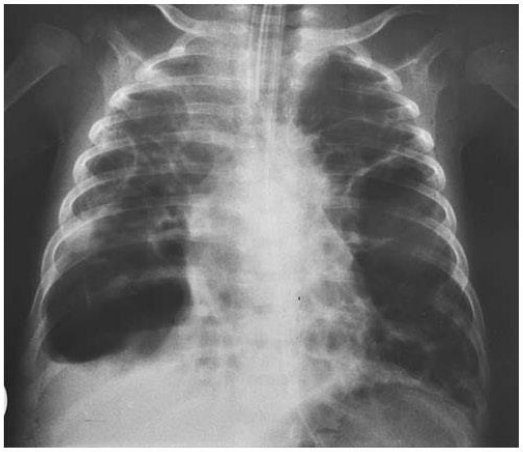

Fig. 2 A 4-month-old girl (LM) with worsening cough, dyspnoea and fever for 3 weeks was intubated and on intermittent positive pressure ventilation. The chest radiograph demonstrates bilateral, diffuse, air-filled cystic spaces of various sizes and large lung volumes. The child subsequently died and a post-mortem examination confirmed the diagnosis of PTB

In children the chest radiograph is of major importance in early diagnosis as bacteriology is hampered by the difficulty in obtaining suitable sputum specimens [1]. Diagnosis is usually made and treatment instigated on the basis of high clinical suspicion especially in children who have been exposed to an adult with PTB. A tuberculin skin test and chest radiograph are routinely done and treatment started as per NTP guidelines [7]. Seven of the ten children in our series had the diagnosis of tuberculosis confirmed, with sputum or gastric washings either positive for acid-fast bacilli (AFB) or culture-positive for *Mycobacterium tuberculosis*.

HIV-positive patients appear to have an eight-times higher risk of infection by *Mycobacterium tuberculosis*. Such children acquire primary TB and then go on to develop a rapid and fulminating form of the disease [4]. They are also prone to develop other mimickers of PTB, namely lymphoid interstitial pneumonia and opportunistic infections such as *Pneumocystis jiroveci* pneumonia (PCP), viral and atypical *Mycobacterium* pneumonias. This has led to the over-diagnosis of PTB in HIV-positive children with 40% of HIV-positive children treated for the disease being incorrectly diagnosed [8].

Lymphadenopathy is the commonest single manifestation of PTB in children [1] and, with or without concomitant parenchymal abnormality, is the radiological hallmark of primary TB in children [2]. Cavitations are reported in children; however, the aetiology and pathogenesis is somewhat more complex than in adults. In a study done of 80 children with PTB, cavitation was found in 7 (9%) on initial chest radiographs [9]. CT is more sensitive in demonstrating any cavitation that may occur [10]; our

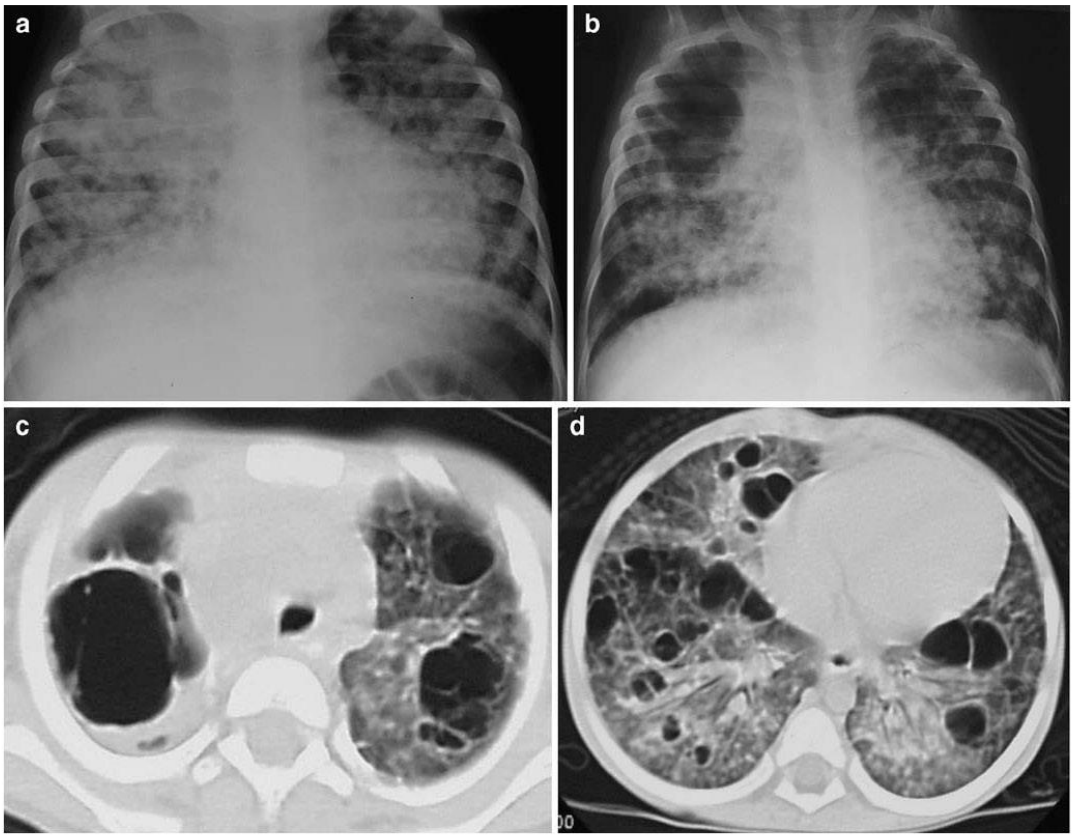

Fig. 3 A 2-year-old HIV-negative girl (CP) with severe adenopathy, clubbing and malnutrition and a positive TB contact. **a** The initial chest radiograph demonstrates bilateral airspace disease with areas of confluence and some early breakdown. **b** A follow-up chest radiograph shows progression of disease with bilateral cyst development; a large thin-walled cavity is identified in the right upper zone. **c**, **d** CT scans show multiple, bilateral thin-walled cavities of various sizes, some unicameral and others multicameral

children were recruited on the basis of cavitation on plain radiographs.

There are three groups into which children with cavitation due to PTB can be placed. These relate to the clinical presentation, radiological characteristics and distribution of the cavities, and associated findings, for example mediastinal lymph nodes.

Group 1

The adult form of PTB does occur in children, but prior to 14 years of age, primary PTB is more likely to be seen, and thereafter cavitation becomes progressively more common [11]. In our study, three children in this group were older than 10 years of age. Cavitations were single or multiple, almost always unilateral and often associated with airspace disease (three out of four).

Postprimary PTB results from reactivation of a dormant focus with cavitation being the radiographic hallmark [5]. Evidence of previous primary PTB is frequently seen on chest radiographs in children [5]. The cavities usually already exist on presentation, surrounded by alveolar consolidation and fibrosis [3]. The common sites are apical and posterior segments of the upper lobe and apical segments of the lower lobe [3].

Group 2

Why some children go on to develop progressive primary PTB may be related to the number and virulence of the organisms in the setting of a child with poor resistance to infection [12]. Poor containment of the primary infection is more common in children under the age of 2 years who are immunocompromised [3]. These children are usually very

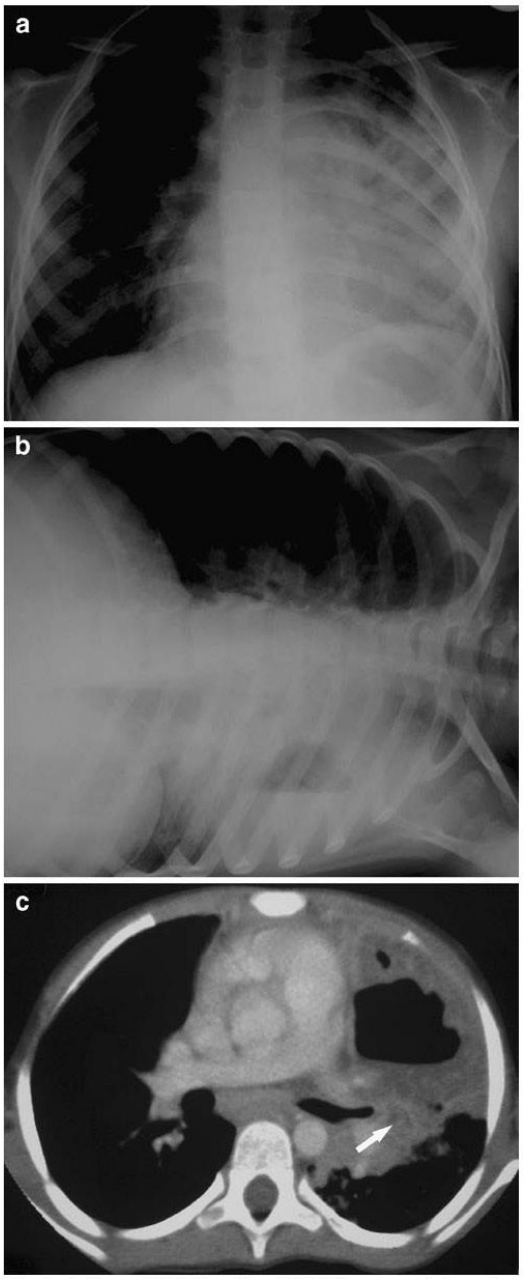

Fig. 4 A 5-year-old HIV-positive child (TL) not receiving antiretroviral therapy. **a** The chest radiograph demonstrates dense airspace consolidation with breakdown in the left lower zone. **b** A decubitus view confirms an air-fluid level within a large thick-walled cavity. **c** CT demonstrates breakdown in an area of dense consolidation in the lingular region secondary to airway obstruction. Low-density rim-enhancing nodes (*arrow*) are seen at the left hilum

ill. The cavities develop as a result of enlargement of the Ghon focus with eventual caseous liquefaction at the centre of the focus. When this focus ruptures into an airway, cavitation occurs and endobronchial spread of disease results. Distal bronchopneumonic consolidation occurs.

Group 3

Newborn children up to 3 years of age have a higher prevalence of adenopathy and a lower prevalence of parenchymal abnormalities [2]. This, along with a small airway size makes young children most vulnerable to develop lymphobronchial TB [3]. Airway compromise due to extraluminal compression of an airway is a recognized complication of adenopathy in primary PTB. If the airway is only partially obstructed, a ball-valve effect may occur giving distal hyperinflation. However, should the airway be completely obstructed, distal air becomes resorbed and collapse occurs [3]. Destructive caseating pneumonia may result with bulging fissures and cavitation.

Lymph nodes are a frequent cause of complications as they erode into adjacent structures, for example, causing oesophageal perforation or bronchopleural fistula [4]. The cavities are thick-walled and often difficult to separate from surrounding consolidated lung on plain radiographs. CT confirmed the airway compromise and the associated thick-walled cavities were seen to enhance and contain air-fluid levels.

It is often technically difficult to see lymphadenopathy on plain radiographs and especially AP chest radiographs [3]. Lateral chest radiographs were not always available in our patients making the detection of nodes more difficult. The use of high-kVp radiography to demonstrate airway compression, or better still contrast-enhanced CT, is of great benefit in confirming the presence of adenopathy. CT scanning was only performed in two of the three children in the obstruction group. In both these children, however, the nodes were visible on plain radiographs.

Among children who present with expansile pneumonias caused by *Mycobacterium tuberculosis*, 83% have significant airway obstruction (more than 75% occlusion) on bronchoscopy and all have enhancing mediastinal lymph nodes on CT. Cavities are present in 63% of children with expansile pneumonia [13].

Conclusion

Cavitation is a frequent finding on initial chest radiographs in children with PTB. There are three possible mechanisms involved in the formation of cavities: 'adult-type' post-primary PTB, progressive primary spread of disease, or cavities arising as a consequence of bronchial obstruction by lymph nodes. In our small sample there were equal

numbers of children in all three groups. Some children do not quite fit the described groups and these children are probably those who present in the first group, i.e. well children who developed cavities as result of nodal obstruction or progressive primary disease and who subsequently recovered. Many variables, including the dose and the virulence of the organism, the age of the patient and, therefore, the predilection for certain sites of progression, and lastly the immune competence of the host all determine the presentation on chest radiographs. It was not possible to determine the role of immune status in cavity formation in this study as not all children were tested and the resistance of the organisms, whether they were multidrug-resistant (MDR) tuberculous bacilli, was not explored.

A larger study involving all children with PTB who have undergone CT scanning is underway and will better determine the true incidence of parenchymal cavitation and the association with the presence of mediastinal lymphadenopathy and airway obstruction.

References

1. Lamont AC, Cremin BJ, Pelteret RM (1986) Radiological patterns of pulmonary tuberculosis in the paediatric age group. Pediatr Radiol 16:2–7
2. Leung AN, Muller NL, Pineda PR et al (1992) Primary tuberculosis in childhood: radiographic manifestations. Radiology 182:87–91
3. Marais BJ, Gie RP, Schaaf HS et al (2004) A proposed radiological classification of childhood intra-thoracic tuberculosis. Pediatr Radiol 34:886–894
4. Cremin BJ, Jamieson DH (1995) Childhood tuberculosis: modern imaging and clinical concepts. Springer, Berlin, pp 11, 20, 26, 33, 37, 46, 109
5. Shewchuk JR, Reed MH (2002) Paediatric postprimary pulmonary tuberculosis. Pediatr Radiol 32:648–665
6. McAdams HP, Erasmus J, Winter JA (1995) Radiological manifestations of pulmonary tuberculosis. Radiol Clin North Am 33:655–678
7. South African Department of Health (2000) The S.A. tuberculosis control programme-practical guidelines. Pretoria, South Africa, pp 32–37 http://www.capegateway.gov.za/text/2003/tb_guidelines2000.pdf Cited 16/01/2007
8. Marais BJ, Hesseling AC, Gie RP et al (2006) The burden of childhood tuberculosis and the accuracy of community-based surveillance data. Int J Tuberc Lung Dis 10:259–263
9. Kisembo HN, Kawooya MG, Zirembu G et al (2001) Serial chest radiographs in the management of children with a clinical suspicion of pulmonary tuberculosis. J Trop Paediatr 47:276–283
10. Koh DM, Bell JR, Burkill GJ et al (2001) Mycobacterial infections: still a millennium bug – the imaging features of mycobacterial infections. Clin Radiol 56:535–544
11. Weber HC, Beyers N, Gie RP et al (2000) The clinical and radiological features of tuberculosis in adolescents. Ann Trop Paediatr 20:5–10
12. Agrons GA, Markowitz RI, Kramer SS (1993) Pulmonary tuberculosis in children. Semin Roentgenol 28:158–172
13. Goussard P, Gie RP, Kling S et al (2004) Expansile pneumonia in children caused by Mycobacterium tuberculosis: clinical, radiological and bronchoscopic appearances. Pediatr Pulmonol 38:451–455

PAEDIATRIC RESPIRATORY REVIEWS (2007) **8**, 118–123

ELSEVIER

Paediatric Respiratory Reviews

MINI-SYMPOSIUM: CHILDHOOD TUBERCULOSIS

Airway involvement in pulmonary tuberculosis

Pierre Goussard* **and Robert Gie**

Department of Paediatrics and Child Health, Faculty of Health Sciences, Stellenbosch University, Tygerberg, South Africa

KEYWORDS
tuberculosis;
expansile pneumonia;
childhood tuberculosis;
airway obstruction;
bronchoscopy

Summary Lymph gland involvement of the airways is common in young children with pulmonary tuberculosis. This lymph gland involvement leads to lymphobronchial tuberculosis, which presents with varying degrees of airway obstruction. These children are best assessed by fibreoptic bronchoscopy and are treated with the normal anti-tuberculosis regimens to which corticosteroids are added for a month and then weaned off over the next month. If, after a month, the children remain symptomatic, they must be re-evaluated by bronchoscopy and chest computed tomography. Surgery must be considered in children with severe airway obstruction still present at the time of the second evaluation. Surgical intervention consists of endoscopic or transthoracic enucleation of the lymph nodes. Only a small percentage of those with lymphobronchial tuberculosis will require surgery to relieve their airway obstruction.

Lymph gland disease involving the airways is common following primary tuberculosis infection in children younger than 5 years of age, whose small airway size causes them to be vulnerable to airway obstruction.[1–3] In the pre-chemotherapeutic era, compression syndromes (68%) and bronchial perforation (28%) were common in children.[4] Risk factors for this form of tuberculosis are a young age[5] and severe malnutrition.[6]

The exact incidence of children with airway obstruction caused by primary tuberculosis in the chemotherapeutic era is not known. The incidence of complicated lymph node disease in two recent reports varied from 8% to 38% in children less than 15 years of age.[7,8] The study reporting the 8% incidence was a community-based study that included all children diagnosed with tuberculosis, whereas the higher percentage was recorded in a hospital-based study.[7,8] Both the upper and lower airways can be compromised by tuberculosis, but involvement of the upper airways is rare and is seldom seen in isolation from tuberculous parenchymal disease. Severe airway involvement occurs in both HIV-infected and uninfected children.

* Corresponding author. Department of Paediatrics and Child Health, Faculty of Health Sciences, Stellenbosch University, PO Box 19063, Tygerberg. 7505, South Africa. Fax: +27 21 9389138.
E-mail address: pgouss@sun.ac.za (P. Goussard).

1526-0542/$ – see front matter © 2007 Elsevier Ltd. All rights reserved.
doi:10.1016/j.prrv.2007.04.007

PATHOGENESIS

The pathogenesis of airway involvement in primary intrathoracic tuberculosis is explained when the primary infection is not contained in the infected lymph nodes. The lymph nodes adjacent to the large airways enlarge, compress and infiltrate the airway wall. Airway obstruction can either be extraluminal or intraluminal. Extraluminal obstruction is due to compression by the enlarged lymph nodes with associated inflammatory oedema. Intraluminal obstruction results from polyps or granulomatous tissue, which follows inflammatory changes in the bronchial wall or when a caseating lymph node herniates into the airway.[4] In children with clinical symptoms, the trachea and the two main bronchi are the most frequently involved airways.

The clinical picture caused by airway involvement depends on the degree of airway narrowing and on whether

KEY POINTS

- Younger children (<5 years of age) with a smaller airway are more inclined to have symptoms and signs of airway obstruction.
- Complicated disease follows involvement of the infected lymph nodes and the adjacent large airways.
- In young infants, the only sign of enlarged lymph nodes is the visualisation of airway compression on the chest radiograph.
- The yield for positive culture via bronchoscopy is less than that of gastric aspirate culture.
- During adequate anti-tuberculosis treatment. the size of the lymph nodes may increase and airway obstruction worsen.
- Surgical intervention will be necessary only in a small group of children with complicated airway obstruction.
- The only clear indication for surgery is a child requiring assisted ventilation for airway obstruction.

the infected gland has infiltrated the airway wall, herniated into the lumen and discharged caseous material into the lumen of the airway. Children with airway narrowing present with signs of airway obstruction. As the obstruction increases, a point is reached at which the incomplete obstruction causes a 'ball-valve effect', which leads to unilateral hyperinflation of the lobe or lung. If the obstruction is complete, collapse of a lobe or segment of a lobe occurs.

Ulceration of the lymph gland into the airway can lead to the inhalation of tuberculous material. An initial hypersensitivity response to the inhaled tuberculoprotein occurs, which presents as a lobar pneumonia not responding to conventional antibiotics. As the lymph gland obstruction of the airway increases and becomes complete, the reaction in the lobe or segment changes from a hypersensitive reaction to one which leads to caseation and liquefaction. This leads to an expansile process that is recognised radiologically as an expansile pneumonia.[9] These forms of tuberculosis are collectively called lymphobronchial tuberculosis.

CLINICAL PRESENTATION

The clinical picture depends on a number of factors. First, younger children with smaller airways are more inclined to have the symptoms and signs of airway obstruction. Second, the anatomical part of the airway that is involved is important. The airway involvement can be supraglottic, extrathoracic, intrathoracic or combinations of these. Third, the clinical signs and symptoms depend on the degree of external compression and internal obstruction. Finally, the clinical picture differs when there is bilateral involvement.[10–12]

Children frequently present with a persistent unremitting cough. As the disease progresses, the cough will become more prominent and can become brassy or biphonal, often with associated large airway wheezing or stridor.[1] Classically, large intrathoracic airway obstruction presents with monophonic wheezing; the wheeze is harsh, low-pitched and audible without a stethoscope. Hyperinflation and subcostal retraction are not as prominent as in small airway obstruction.[13] The wheeze of large airway obstruction may be audible on one side of the chest or on both sides, depending on the area and the degree of obstruction. This clinical presentation is often confused with asthma, but these children do not respond to inhaled steroids, and the airway obstruction might be worsened by the use of β_2 agonists. When the presentation is that of a 'ball-valve' obstruction, children have unilateral hyperinflation, hyperresonance and decreased breath sounds on the affected side of the chest. In some cases, monophonic wheeze with prolonged expiration is heard. When the obstruction is complete, lung or lobar collapse will develop with accompanying reduced or lack of ventilation to the affected part of the lung. Expansile pneumonia presents as a lobar pneumonia that has not responded to a course of antibiotics. The children may have a high swinging fever but are not toxically ill. Extrathoracic airway obstruction presents with stridor that may be either inspiratory or present during both inspiration and expiration.

Children with airway obstruction can be relatively asymptomatic, but they become very symptomatic during intercurrent viral infections, especially young infants. During adequate anti-tuberculosis treatment, the size of the lymph nodes may increase in size and airway obstruction worsen. This has also been seen in children concurrently receiving anti-tuberculosis and antiretroviral drugs.[14,15]

Luminal involvement of the airway is very rare in children. In these cases, the lumen of the airway is involved and airway disease is not caused by external compression or herniation of glands into the airways.

CHEST RADIOGRAPHIC APPEARANCES

Airway compression

The most important groups of glands that lead to large airway obstruction are those located in the paratracheal and subcarinal regions (Fig. 1). In young infants, the only sign of enlarged lymph nodes is the visualisation of airway compression on the chest radiograph.[6] Deviation of the trachea to the left may possibly indicate lymph node enlargement. Subcarinal glands can be detected directly or indirectly. Direct signs on the chest radiograph include a double shadow below the carina and a shift to the right of the para-oesophageal adhesion line. Compression of both main bronchi is an indirect sign of subcarinal lymph node enlargement.

The frontal high-kilovolt radiograph has been used to assess the effect of tuberculous lymph glands on the

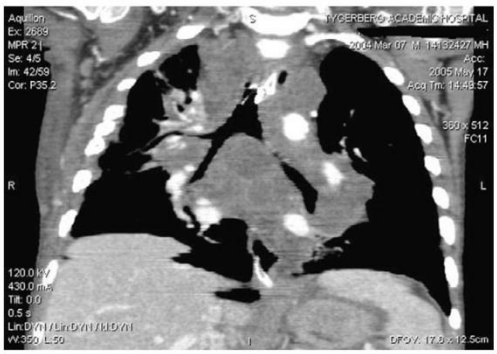

Figure 1 A coronal reconstruction of a chest computed tomography scan of a child with lymphobronchial tuberculosis. The major lymph gland groups are clearly visible in the subcarinal and paratracheal regions, with compression of the left main bronchus.

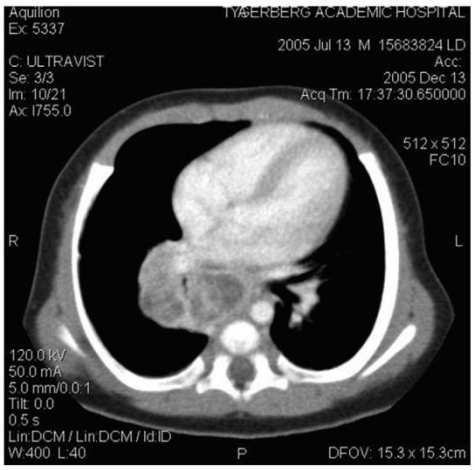

Figure 2 A contrasted chest computed tomography scan demonstrating the subcarinal lymph glands with ghost-like ring enhancement of the lymph glands and entrapment of the bronchus intermedius by the lymph glands.

tracheobronchial tree. By using high-kilovolt radiology, the specificity for detecting mediastinal lymph glands increased from 74% to 87%.[16] The authors thought that, although there was this increase, it did not warrant the routine use of high high-kilovolt radiographs.[16]

Collapse will be visible on the chest radiograph if external compression of the lumen is complete or if glands have herniated into the airway. The bronchus intermedius is a common region for complete airway obstruction, resulting in collapse of the right middle and right lower lobes.

Unilateral hyperinflation

This is not a common radiological picture seen in childhood tuberculosis. The chest radiographic presentation is unilateral hyperinflation with a flattened hemi-diaphragm and reduced vascularity (Fig. 2). In severe air-trapping, the ipsilateral lung herniates across the midline. The compressed main bronchus and mediastinal lymph glands causing the compression are normally visible.

Expansile pneumonia

The radiological picture is that of dense opacification of left (42%) and right (33%) upper lobes of the lung, with downward displacement of the fissures.[9] Air bronchograms are visible in only a few cases (16%). The lymph glands responsible for compressing the airway are seldom directly visible owing to the expanded lobe overlying the hilar regions, but airway compression is a common finding. Associated findings are cavities (33%) and left-sided phrenic nerve palsy (13%).[9]

BRONCHOGRAPHY

Bronchography is seldom used but can be performed with non-ionic water-soluble contrast medium in intubated patients. Transient desaturation is sometimes experienced, but it is a safe and reliable investigation if bronchoscopy is not available or indicated.[17]

COMPUTED TOMOGRAPHY SCAN APPEARANCES

Chest computed tomography (CT) scanning should be carried out in children with clinically and radiologically significant airway compression to determine the location of the glandular involvement and the relationship of these glands to the airways. CT scanning is useful to establish the nature of the mediastinal glands and to demonstrate the typical ghost-like enhancement of the rims of the lymph glands after contrast administration (Fig. 3). The most common locations for tuberculous lymph gland enlargement in children are the subcarinal (90%), right hilar (74%), left hilar (72%), bilateral hilar (61%), anterior mediastinal (79%), precarinal (64%) and right paratracheal positions (63%).[18] The largest group of nodes is located in the subcarinal area (87%). The most common sites of airway compression are described as the left main bronchus (21%), right main bronchus (14%) and bronchus intermedius (8%).[18]

In children with expansile pneumonia, three radiological pictures are seen.[9] The first (17%) is dense opacification of the lobe with no obstruction of the airways and visible air bronchograms. In these cases, no liquefaction of the lung parenchymal tissue is seen on CT scan. The second picture (67%) is dense opacification of the lobe with areas of liquefaction of the lung parenchymal tissue and complete

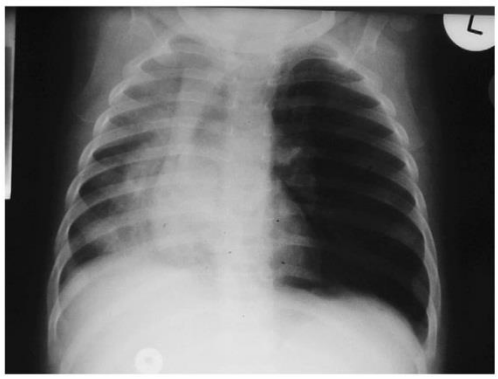

Figure 3 A chest radiograph demonstrating unilateral hyperinflation of the left lung, flattening of the diaphragm and herniation of the left lung across the midline. Tuberculous lymph gland obstruction of the left main bronchus was the cause of the 'ball-valve' effect.

obstruction of the airways. No air bronchograms were present in these cases described in a study from our centre. The last group has a combination of the described pictures.

CT scan in conjunction with flexible bronchoscopy is used to determine the severity of airway obstruction and extent of parenchymal involvement. This information is used to determine whether a child will benefit from further intervention.

BRONCHOSCOPY

In children with airway obstruction, flexible bronchoscopy is mainly used for diagnostic purposes. The advantage is that the smaller divisions of the airways can be reached and airway obstruction bypassed, enabling an evaluation of the distal airway. Rigid bronchoscopes are better suited to transbronchial lymph gland enucleation as the patient can be ventilated during the procedure and the instruments used are larger. Bronchoscopy is not indicated for routine specimen collection as the yield from bronchoscopically performed bronchoalveolar lavage for tuberculosis cultures is less than the culture from gastric lavage.[19–21]

Indications for bronchoscopy are as follows:

- To confirm the diagnosis of pulmonary tuberculosis. Bronchial obstruction may be present in the absence of visibly enlarged hilar and mediastinal lymph nodes on a chest radiograph.
- To determine the degree of airway obstruction in complicated disease.
- For the endoscopic enucleation of glands that have ulcerated into the airway, and for the removal of granulation tissue and caseous material causing airway obstruction.
- To evaluate the response to treatment in children with complicated airway disease.[22]

The most common bronchoscopic finding is extrinsic compression (37%) of the bronchi or trachea.[23] Bronchial involvement, granulation tissue, obstructing caseous material and mucosal inflammation have been found in 48% of children with no detectable lymph gland enlargement on the chest radiograph.[23]

MANAGEMENT OF AIRWAY COMPRESSION

All children with airway obstruction are treated with a standard three-drug anti-tuberculosis regimen. If, however, cavities are present on the chest radiograph, a fourth drug, ethambutol, is added because of the higher bacillary load in the cavities.

Corticosteroids are recommended in children with airway compression caused by mediastinal lymph node enlargement, although there is very little scientific information supporting this practice. Most data originates from adult studies. Childhood studies are lacking. Reports from the 1960s suggested that corticosteroids were effective in decreasing airway obstruction if given early in the course of the disease.[24–26] These claims were not supported by an initial double-blind randomised study looking at the effect of prednisone on lymph node disease.[27] In a subsequent follow-up study, 36% of those who had received corticosteroids had an improved outcome compared with the placebo group ($P < 0.05$).[28] It was suggested that those receiving corticosteroids had more rapid improvement and less glandular ulceration into the airways than those receiving conventional treatment, but the eventual outcome was similar.[29]

Corticosteroids have a significant side effect profile requiring careful monitoring of the children. The effective dose of corticosteroids is also unknown. We currently prescribe corticosteroids (prednisone 2 mg/kg per day) in children who are symptomatic due to airway obstruction. Higher doses could be used because rifampicin influences corticosteroid metabolism. The prednisone is given for a month and then weaned over the next month. During this time, children are closely monitored by routine clinical examination and chest radiography.

Symptomatic children or those with a worsening chest radiograph after 1 month of treatment require further evaluation. These children are investigated by bronchoscopy and chest CT scanning to see whether surgical intervention is indicated. Surgical intervention – lymph gland enucleation – will be necessary in only a small group of children with complicated airway obstruction. Lymph gland enucleation can be done either endoscopically or by thoracotomy.

Endoscopic enucleation is indicated in children when the glands have herniated or ulcerated into the airways, result-

ing in granulomas and caseous material obstructing the airways. The caseous material and some of the granulomas can be endoscopically removed. This intervention often has to be repeated as the lymph gland situated adjacent to the airway continues to deposit fresh caseous material into the airway. For this reason endoscopic enucleation is best suited to children with single lesions causing lobar collapse. Only a small group of children will benefit from endoscopic enucleation.

Acute perforation of a lymph node into a major airway presenting with severe respiratory failure is rare. In these cases, bronchoscopic removal of the caseating material from the airways can be life-saving.[30] Endoscopic enucleation of the glands is safe, but care must be taken not to remove too much tissue. Complications include bleeding, perforation of the bronchus wall with a resulting pneumothorax, or the creation of a broncho-oesophageal fistula.

Endoscopic enucleation is usually carried out through a rigid bronchoscope. No studies have been published looking at the long-term outcome of endoscopic enucleation or comparing transthoracic with endoscopic enucleation. Four studies on transthoracic enucleation in children have been published. Comparing the studies is difficult as there were no clearly defined indications for enucleation. The presence of mediastinal lymph nodes alone is not an indication for surgery.

Indications for surgical enucleation include:[30]

- acute perforation of a lymph gland into a major airway, causing respiratory failure;
- occlusion of a major airway with pulmonary collapse or hyperinflation;
- permanent bronchial stenosis due to fibrosis;
- rarely, superior vena caval obstruction;
- subcarinal oesophageal obstruction.

A number of factors have to be taken into account when considering surgery. These include the age of the child, the degree of airway involvement, the position and character of the lymph nodes causing the obstruction, and the clinical response to anti-tuberculosis therapy together with corticosteroids. The only clear indications for surgical enucleation include children requiring assisted ventilation for airway obstruction and children with life-threatening airway obstruction. In these circumstances, urgent enucleation is required to relieve the airway obstruction. Children in whom the airway obstruction at bronchoscopy is estimated to be greater than 75% should be considered for enucleation.

Prior to surgery, a chest CT scan should be performed to determine the size, site and character of the lymph glands. Calcified lymph glands will not be successfully enucleated. The location of the lymph glands will determine from which side the thoracotomy will be done. The most common groups of lymph glands obstructing the main bronchi are the subcarinal and paratracheal groups, compressing the proximal main bronchi or the distal trachea between them.[31] Decompression of the subcarinal lymph glands is important if both the left and right main bronchus are compressed.

The lymph glands are easier to enucleate early in the disease process because they are still soft, but once the glands become organised, enucleation becomes technically more difficult. The procedure entails partial resection of the lymph nodes and careful curettage of caseous material out of the gland. During enucleation, overzealous dissection must be avoided to prevent complications. Lung resection during enucleation should be avoided at all cost as nearly all children improve with time.[30] The reported complication rate resulting from enucleation is low and includes bronchial tear, pulmonary artery laceration, bronchopleural fistula and broncho-oesophageal fistula.[31,32] Bronchopleural fistulas resolve with intercostal drainage.

The role of surgery in airway compression is not only to relieve the airway compression, but also to preventing ongoing damage to the lung parenchyma. Relieving the airway obstruction prevents complete obstruction, which leads to lung collapse and eventual bronchiectasis.

Indications for surgery for the long-term complications of airway involvement include symptomatic bronchiectasis not controlled by conservative measures, destroyed lung parenchyma that is the site for recurrent or chronic infection and infected pulmonary cavities with or without fungal infection.[31] Pulmonary surgery other than enucleation of glands is best done well after the completion of anti-tuberculosis treatment. Bronchiectasis of the lower lobes is the most common indication for lung resection. Chronic bronchus intermedius obstruction can lead to right middle and lower lobe destruction requiring resection. Bronchial stenosis is a rare complication of glandular airway obstruction and is mostly seen in adults.

CONCLUSION

Lymph node involvement of the airways is a relatively common complication of primary tuberculosis, especially in children younger than 5 years of age. In the majority of cases, the obstruction of the airways clears on conventional anti-tuberculosis regimens. The optimal therapy for lymphobronchial tuberculosis has still to be determined. The role of corticosteroids and surgery in the treatment of lymphobronchial tuberculosis remains uncertain and controversial. These, together with the role of bronchoscopy and chest CT scanning in the management of lymphobronchial tuberculosis, need to be further researched.

REFERENCES

1. Lincoln EM, Sewell EM. *Tuberculosis in children*. New York: McGraw-Hill, 1963.

2. Wallgren A. Primary pulmonary tuberculosis in childhood. *Am J Dis Child* 1935; **49**: 1105–1363.
3. Miller FJ, Seal RM, Taylor MD. *Tuberculosis in children*. London: Churchill, 1963.
4. Marais BJ, Gie RP, Schaaf HS *et al.* The natural history of childhood intra-thoracic tuberculosis – a critical review of the literature from the prechemotherapy era. *Int J Tuberc Lung Dis* 2004; **8**: 392–402.
5. Forstad S. Segmental atelectasis in children with primary tuberculosis. *Am Rev Tuberc* 1959; **79**: 597–605.
6. Schaaf HS, Gie RP, Beyers N, Smuts N, Donald PR. Tuberculosis in infants less than 3 months of age. *Arch Dis Child* 1993; **69**: 371–374.
7. Marais BJ, Gie RP, Schaaf HS *et al.* The spectrum of disease in children treated for tuberculosis in a highly endemic area. *Int J Tuberde Lung Dis* 2006; **10**: 1–7.
8. Theart A, Marais BM, Gie RP, Hesseling AC, Beyers N. Criteria used for the diagnosis of childhood tuberculosis at primary health care level in a high-burden, urban setting. *Int J Tuberc Lung Dis* 2005; **9**: 1210–1214.
9. Goussard P, Gie RP, Kling S, Beyers N. Expansile pneumonia in children caused by *Mycobacterium tuberculosis*: clinical, radiological, and bronchoscopic appearances. *Pediatr Pulmonol* 2004; **38**: 451–455.
10. Rich A. *The pathogenesis of tuberculosis*. 2nd edn.. Springfield, IL: Charles C Thomas, 1951.
11. High RH, Nelson WE. Experiences with intra- and extraluminal bronchial tuberculous lesions. *Am Rev Tuberc* 1955; **74**: 256–266.
12. Freiman I, Geefhuysen J, Solomon A. The radiological presentation of pulmonary tuberculosis in children. *S Afr Med J* 1975; **49**: 1703–1706.
13. Finder JD. Primary bronchomalacia in infants and children. *J Pediatr* 1997; **130**: 59–66.
14. Amodio J, Abramson S, Berdon W. Primary pulmonary tuberculosis in infants. A resurgent disease in Urban United States. *Paediatr Radiol* 1986; **16**: 185–189.
15. Fishman JE, Saraf-Lavi E, Narita M *et al.* Pulmonary tuberculosis in AIDS patients; transient chest radiographic worsening after initiation of antiretroviral therapy. *AJR* 2000; **174**: 43–49.
16. De Villiers RVP, Andronikou S, Van de Westhuizen S. Specificity and sensitivity of chest radiographs in the diagnosis of paediatric pulmonary tuberculosis and the value of additional high-volt radiographs. *Australas Radiol* 2004; **48**: 148–153.
17. Cheun YF, Lee SL, Leung MP, Yung TC, Chau AKT, Hu HKY. Tracheobronchography and angiocardiography of paediatric cardiac patients with airway disorders. *J Paediatr Child Health* 2002; **38**: 258–264.
18. Andronikou S, Joseph E, Lucas S *et al.* CT scanning for the detection of tuberculous mediastinal and hilar lymphadenopathy in children. *Pediatr Radiol* 2004; **34**: 232–236.
19. Chan S, Abadco DL, Steiner P. Role of flexible fiberoptic bronchoscopy in the diagnosis of childhood endobronchial tuberculosis. *Pediatr Infect Dis J* 1994; **13**: 506–509.
20. Somu N, Swaminathan S, Paramasivan CN *et al.* Value of bronchoalveolar lavage and gastric lavage in the diagnosis of pulmonary tuberculosis in children. *Tuber Lung Dis* 1995; **76**: 295–299.
21. Abadco DL, Steiner P. Gastric lavage is better than bronchoalveolar lavage for isolation of *Mycobacterium tuberculosis* in childhood pulmonary tuberculosis. *Pediatr Infect Dis J* 1992; **11**: 735–737.
22. De Blic J. The value of flexible bronchoscopy in childhood pulmonary tuberculosis. *Ped Pulmonol* 1999; (Suppl 11): pp. 24–25.
23. de Blic J, Azevedo I, Burren CP, Le Bourgeois M, Lallemand D, Scheinmann P. The value of flexible bronchoscopy in childhood pulmonary tuberculosis. *Chest* 1991; **100**: 688–692.
24. Gerbeaux J. *Tuberculose primaire de infant*. Paris: Edition Medicale Flammarion, 1967.
25. Gerbeaux J, Baculard A, Couvreur J. Primary tuberculosis in childhood. *Am J Dis Child* 1965; **110**: 507–518.
26. Rosenzweig DY, Stead WW. The role of tuberculosis and other forms of bronchopulmonary necrosis in the pathogenesis of bronchiectasis. *Am Rev Respir Dis* 1965; **92**: 769–785.
27. Nemir RL, Cordona J, Lacoius A, David M. Prednisone as an adjunct in the chemotherapy of lymph node-bronchial tuberculosis in childhood: a double-blind study. *Am Rev Respir Dis* 1963; **88**: 189–198.
28. Nemir RL, Cordona J, Vaziri F, Toledo F. Prednisone as an adjunct in the chemotherapy of lymph node-bronchial tuberculosis in childhood: a double-blind study. II. Further term observation. *Am Rev Respir Dis* 1967; **95**: 402–410.
29. Toppet M, Malfroot A, Derde MP, Toppet V, Spehl M, Dab I. Corticosteroids in primary tuberculosis with bronchial obstruction. *Arch Dis Child* 1990; **65**: 1222–1226.
30. Konstantinos A, Papagiannopoulos KA, Linegar AG, Harris DG, Rossouw GJ. Surgical management of airway obstruction in primary tuberculosis in children. *Ann Thorac Surg* 1999; **68**: 1182–1186.
31. Hewitson JP, van Oppel UO. Role of thoracic surgery for childhood tuberculosis. *World J Surg* 1997; **21**: 468–474.
32. Worthington MG, Brink JG, Odell JA *et al.* Surgical relief of acute airway obstruction due to primary tuberculosis. *Ann Thorac Surg* 1993; **56**: 1054–1062.

Pediatr Radiol (2008) 38:224–226
DOI 10.1007/s00247-007-0634-7

CASE REPORT

Chylothorax as a complication of pulmonary tuberculosis in children

Marie Grobbelaar · Savvas Andronikou · Pierre Goussard · Salomine Theron · Ayanda Mapukata · Reena George

Received: 9 May 2007 / Revised: 29 July 2007 / Accepted: 23 August 2007 / Published online: 11 October 2007

Abstract Chylothorax is a rare clinical entity characterized by a milky white aspirate with increased triglyceride levels. The commonest aetiology is malignancy and trauma. Pulmonary tuberculosis is an extremely rare cause of chylothorax. Two children with chylothorax and pulmonary tuberculosis are described. One child had bilateral and the other unilateral chylous effusions. Extensive mediastinal and hilar lymphadenopathy was demonstrated. Diseased lymph nodes may infiltrate other intrathoracic structures such as the thoracic duct, and they can also obstruct the cisterna chyli and thoracic duct. A possible explanation for the development of a chylothorax in our patients is obstruction of the thoracic duct by tuberculous lymphadenopathy with subsequent increase in pressure in the surrounding lymphatic system and leaking of chyle into the pleural space.

Keywords Chest · Tuberculosis · Chylothorax · Children

M. Grobbelaar · S. Andronikou (✉) · S. Theron · A. Mapukata · R. George
Department of Radiology,
University of Stellenbosch and Tygerberg Hospital,
Francie van Zijl Drive,
Tygerberg 7505, South Africa
e-mail: docsav@mweb.co.za

P. Goussard
Department of Child Health,
University of Stellenbosch and Tygerberg Hospital,
203 Mullerhof, 15 Belle Ombre Road,
Cape Town Tamboerskloof 8001, South Africa

Introduction

Chylothorax is a rare clinical entity characterized by a milky white aspirate with an increased triglyceride level in the fluid [1]. Diagnosis can be made when triglyceride levels in the pleural fluid are >1.2 mmol/l (110 mg/dl) [2]. The commonest aetiology is malignancy (commonly lymphoma) and trauma (due to cardiothoracic surgery) [1, 3]. Other causes include thrombosis of the superior vena cava or subclavian veins, constrictive pericarditis, pulmonary lymphangiomyomatosis, filariasis, Kaposi sarcoma in AIDS, heart failure, amyloidosis, tuberculosis (TB) and sarcoidosis [1–3]. Chylothorax has been described in a patient infected with the human immunodeficiency virus and pulmonary TB [2]. Chylothorax is a rare complication of TB in both adults and children [4–7].

Case reports

Case 1

A 35-month-old boy presented with a cough. His mother was receiving treatment for pulmonary TB. The chest radiograph showed a large right-sided pleural effusion and multilobar pneumonia. Gastric aspirate was positive for acid-fast bacilli and *Mycobacterium tuberculosis* was cultured from it. The pleural effusion on the left was tapped and found to be chylous with a triglyceride level of 16.2 mmol/l. CT scan of the chest was performed due to symptoms and signs of airway compression and confirmed a large right-sided pleural effusion (mean attenuation 10.2 HU) as well as a smaller left-sided pleural effusion (Fig. 1). Tuberculous lymphadenopathy was demonstrated

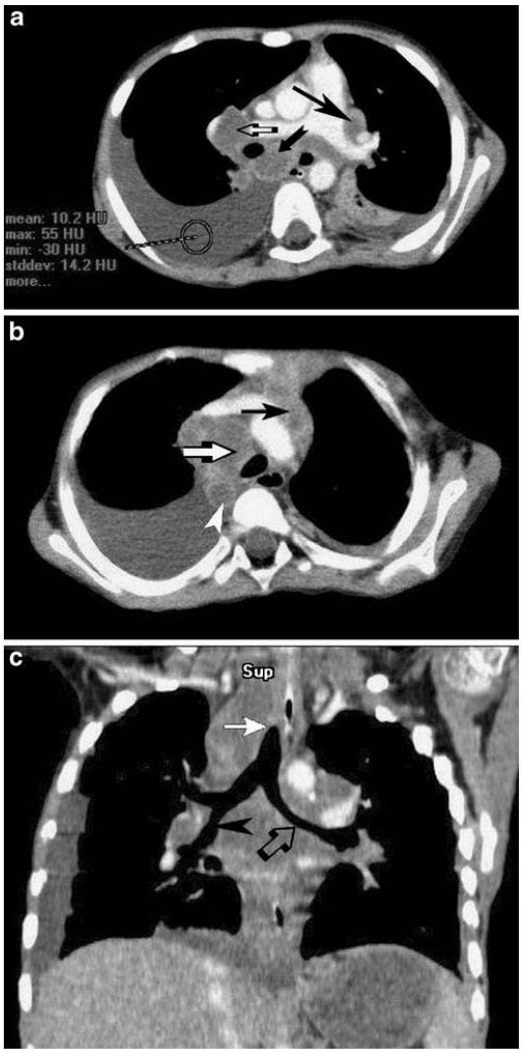

Fig. 1 Case 1: CT of the thorax in a 35-month-old boy. **a** A large right-sided pleural effusion (10.2 HU) and a small left-sided effusion are demonstrated. The patient has extensive mediastinal lymphadenopathy: subcarinal (*short black arrow*), right hilar (*open arrow*) and aortopulmonary window (*long black arrow*) nodes are visible. The nodes demonstrate central necrosis with rim enhancement, typically found in tuberculous lymphadenopathy. Thoracic duct compression is likely. **b** There is extensive right paratracheal lymphadenopathy (*white arrow*) with compression on the trachea. Nodes are also present in the aortopulmonary window (*black arrow*). The nodes demonstrate ghost-like (*white arrow*) and ring (*white arrowhead*) enhancement. Large right-sided and smaller left-sided effusions are visible. **c** Coronal reconstruction demonstrates the large right-sided and smaller left-sided pleural effusions. Extensive mediastinal and bilateral hilar lymphadenopathy demonstrating ghost-like and ring enhancement patterns is visible. There is compression of the distal trachea (*white arrow*), left main bronchus (*open arrow*) and bronchus intermedius (*arrowhead*)

in the right paratracheal, pretracheal, subcarinal, aortopulmonary window and both hilar regions. The patient was negative for retroviral disease.

Case 2

A 14-month-old boy was diagnosed with pulmonary TB (gastric aspirate positive for acid-fast bacilli and *Mycobacterium tuberculosis* cultured). The child also had tuberculous meningitis and was malnourished. He had been exposed to retroviral disease, but his ELISA test was negative at that stage. A left-sided pleural effusion was visible on the chest radiograph and tapped. It was found to be chylous with a

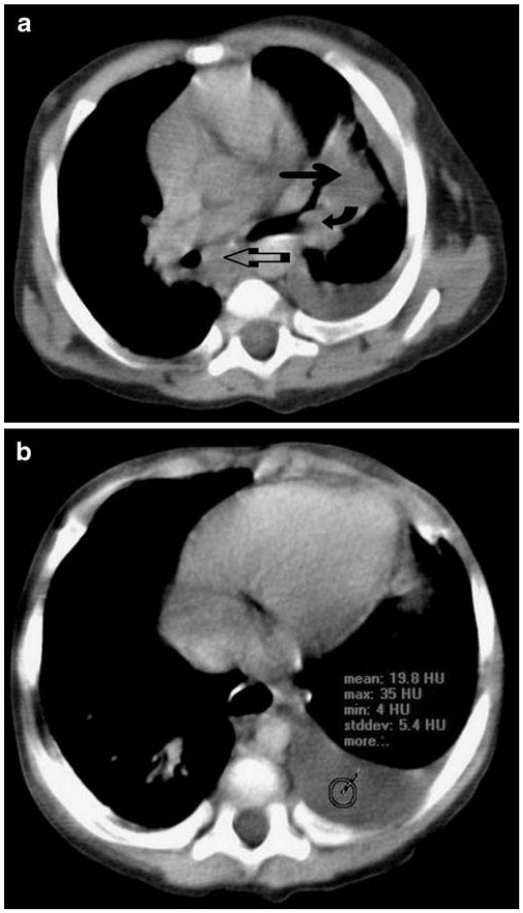

Fig. 2 Case 2: CT of the thorax in a 14-month-old boy. **a** Large subcarinal (*open arrow*) and left hilar (*curved arrow*) tuberculous lymphadenopathy with consequent bronchial narrowing are demonstrated. The patient has a left-sided pleural effusion and air-space opacification involving the lingula (*solid arrow*). **b** Large left-sided chylothorax with a mean attenuation of 19.8 HU

triglyceride level of 17 mmol/l. CT scan of the chest was performed due to symptoms and signs of airway compression and confirmed the pleural effusion (mean attenuation 19.8 HU) as well as tuberculous lymphadenopathy in the right paratracheal, subcarinal and both hilar regions (Fig. 2).

Discussion

Pulmonary TB is an extremely rare cause of chylothorax, with only a few cases reported in the literature [2]. Enlarged lymph nodes are a primary feature in childhood tuberculous disease [4, 8]. The most common location reported for tuberculous lymphadenopathy in the chest is subcarinal, followed by the hila, the anterior mediastinum, the precarinal nodes and the right paratracheal nodes. The subcarinal position harbours the largest nodes, followed by the anterior mediastinum and the right paratracheal position [8]. Tuberculous lymphadenopathy is most common following primary infection in children younger than 3–5 years of age [6, 8]. Diseased lymph nodes may infiltrate other intrathoracic structures such as the oesophagus, phrenic nerve and thoracic duct [6]. Enlarged lymph nodes can also obstruct the cisterna chyli and thoracic duct [2]. A possible explanation for the development of chylothorax in our two patients is obstruction of the thoracic duct by tuberculous lymphadenopathy in the right paratracheal region with subsequent increase in pressure in the surrounding lymphatic system and leaking of chyle into the pleural space [2, 5].

References

1. Singh P, Shah KV, Shah NT et al (2005) Chylothorax: a rare presentation of constrictive pericarditis. Indian J Tuberc 52:207–210
2. Singh S, Girod JP, Ghobrial MW et al (2001) Chylothorax as a complication of tuberculosis in the setting of the human immunodeficiency virus infection. Arch Intern Med 161:2621
3. Doerr CH, Allen MS, Nichols FC et al (2005) Etiology of chylothorax in 203 patients. Mayo Clin Proc 80:867–870
4. Gie RP, Goussard P, Kling S et al (2004) Unusual forms of intrathoracic tuberculosis in children and their management. Paediatr Respir Rev 5(Suppl A):S139–S141
5. Vennera MC, Moreno R, Cot J et al (1983) Chylothorax and tuberculosis. Thorax 38:694–695
6. Marais BJ, Gie RP, Schaaf HS et al (2004) A proposed radiological classification of childhood intrathoracic tuberculosis. Pediatr Radiol 34:886–894
7. Anton PA, Rubio J, Casán P et al (1995) Chylothorax due to Mycobacterium tuberculosis. Thorax 50:1019
8. Andronikou S, Joseph E, Lucas S et al (2004) CT scanning for the detection of tuberculous mediastinal and hilar lymphadenopathy in children. Pediatr Radiol 34:232–236

Airway involvement in pulmonary tuberculosis

Pierre Goussard, Robert Gie

Airway involvement is relatively commonly seen in children with primary tuberculosis (TB), but in only a small group of children is the compression severe, needing intervention. The incidence of children with airway obstruction due to primary TB in the chemotherapeutic era is not known. In two recent reports the incidence of complicated lymph node disease varied from 8% to 38% in children less than 15 years of age.[1,2]

The trachea and the two main bronchi are the airways most often affected by the enlarged glands. Upper-airway involvement is rare in children; most reports of upper-airway TB have been in adults. However, two forms of upper-airway TB have been described in children: laryngeal TB and retropharyngeal TB abscess.

In children other conditions also cause airway compression and it is important to include these in the differential diagnosis. External airway compression can be caused by congenital malformations, vascular compression and enlarged mediastinal lymph nodes. Airway compression can also be confused with airway obstruction, with foreign-body inhalation a common cause of intraluminal obstruction.

Clinical presentation

Children with airway compression present with a wide variation of symptoms and signs. The clinical presentation depends on a number of factors:

1. **Age of the child**. Younger children with relatively smaller airways have the largest risk of being symptomatic. Their airway obstruction, which can be quite severe, is often precipitated by an acute viral infection with the viral-induced inflammation causing additional obstruction.

2. **Anatomical site of the involved airway.** The involvement can be supraglottic, extrathoracic, intrathoracic, or combinations of these. The most severe forms of obstruction are seen when both the trachea and one or both of the main bronchi are involved. Extrathoracic airway obstruction presents with stridor, which may be present during inspiration or both inspiration and expiration. Intrathoracic obstruction presents with monophonic wheezing.

3. **The degree of luminal obstruction**. TB lymph gland enlargement involves the airways in various pathological ways. The enlarged glands may only cause external compression of the airways. Further involvement leads to herniation of the glands into the airways causing worsening obstruction but rarely complete obstruction of the airway. The degree of obstruction leads to different clinical presentations. Airway compression causes wheezing audible on one or both sides of the chest depending on the degree of obstruction. These children are misdiagnosed as asthmatics but respond poorly to asthma treatment. Children with partial obstruction of the airway may develop a ball-valve effect, where air can enter the lung but is trapped on expiration. There is hyperinflation and hyper-resonance of the affected side of the chest, the breath sounds over the involved lung are decreased, and prolonged expiration is audible. When the obstruction is complete, lung or lobar collapse can develop with reduced or no ventilation to the affected part of the lung. Bronchus intermedius is the most vulnerable part of the airway, and collapse of the right middle and lower lobes may occur. Airway compression is common in children with expansile pneumonia caused by *Mycobacterium tuberculosis* (MTB).[3]

4. **Other factors.** Airway obstruction occurs in both HIV-infected and HIV-uninfected children. The size of the lymph nodes may increase during anti-TB treatment and airway obstruction may worsen. This also occurs in children receiving both TB and antiretroviral drugs.[4] Luminal TB is rare in children and is mostly seen in adults with TB. In these cases there is no compression of the airway but involvement of the luminal wall.

Diagnosis of airway compression

Most severe forms of airway compression can be diagnosed from plain chest X-rays (CXRs) and further investigation is only necessary in complicated cases.

Four patterns of airway obstruction can be recognised on CXR: (*i*) airway narrowing; (*ii*) ball-valve effect; (*iii*) expansile pneumonia; and (*iv*) lobar collapse.

Airway narrowing

The most important groups of lymph nodes causing airway compression are the paratracheal, hilar and subcarinal lymph nodes. Lymph gland obstruction of the airways is commonly clearly visible on a CXR. Paratracheal lymph glands can cause tracheal compression. Any deviation of the trachea to the left is abnormal, except when a right-sided aortic arch is present, and can indicate paratracheal lymph gland compression of the trachea. Subcarinal glands may also be difficult to detect, but if both main bronchi are narrowed, enlarged subcarinal lymph nodes may be present. Shifting of the para-oesophageal

Department of Paediatrics and Child Health, Desmond Tutu Tuberculosis Centre, Stellenbosch University, Tygerberg, W Cape
Pierre Goussard, MMed (Paed)
Robert Gie, FCP (Paed)

Corresponding author: *P Goussard (pgouss@sun.ac.za)*

adhesion line may also indicate enlarged subcarinal lymph nodes.

The frontal high kilovolt (kV) radiograph may be useful to assess the effect of enlarged TB lymph glands on the tracheobronchial tree. It has been demonstrated that the specificity for the detection of TB lymph nodes increases from 74.4% to 86.6% with the addition of high-kV radiographs.[5]

Ball-valve effect

This is seen on a CXR as unilateral hyperinflation because of the fact that air is trapped by the 'check valve' effect of an incompletely obstructed airway. The involved lung or lobe is enlarged, has reduced vascularity and can herniate across the midline if severe air trapping is present.

Expansile pneumonia

Expansile pneumonia caused by MTB affects mostly the upper lobes. Expansile pneumonia is characterised by the dense opacification of the enlarged lobe with displacement of the fissures. Air bronchograms are usually not visible. Airway compression is seen in 92% of cases on plain CXR.

Lobar collapse

Lobar collapse is uncommon with the right middle and lower lobes being most commonly involved.

Management of airway obstruction

Children with airway obstruction caused by MTB are treated with the standard 3-drug regimen to which corticosteroids (prednisone 2 mg/kg/d) are added for the first month of treatment. If there is clinical and radiological improvement, the treatment is continued and the corticosteroids are weaned over the next month. There is very little information on the use of corticosteroids in the treatment of TB glandular obstruction of the airways. Early reports from the 1960s were that corticosteroids were effective in decreasing airway obstruction if given early in the course of the disease. These claims were not supported in a double-blind study looking at the effect of prednisone on lymph node disease.[6] In a follow-up study the group receiving prednisone had an improved outcome when compared with the placebo group (in 36% of cases, $p < 0.05$).[7] It seems that corticosteroids give a more rapid improvement and less glandular ulceration into the airways than conventional treatment, but the eventual outcome is similar.

If there is no improvement after 1 month of treatment with TB drugs and corticosteroids, these patients are subjected to bronchoscopy. Bronchoscopy is used to determine the degree of airway obstruction and indicate whether further intervention is required. During bronchoscopy endoscopic enucleation of glands that have ulcerated into the airway and the resulting granulation tissue and caseating material can be removed. If at bronchoscopy severe airway compression is diagnosed, computed tomography (CT) of the chest is indicated.

CT scan is also useful to determine the anatomical location and nature of mediastinal glands (Fig. 1). Typical ghost-like enhancement of the rims of the lymph glands is visualised after contrast administration. The largest group of lymph nodes as identified by CT scan is located in the subcarinal area (87%), and the most common sites of airway compression are the left main bronchus (21%), right main bronchus (14%) and bronchus intermedius (8%).[8]

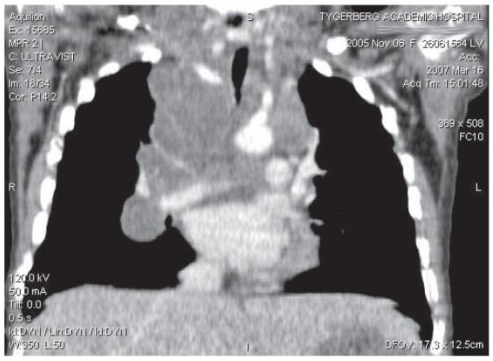

Fig. 1. A coronal reconstruction of a chest computed tomography scan demonstrating the large hilar, subcarinal and mediastinal tuberculosis lymph glands with compression of the trachea.

Surgical intervention in the management of complicated airway obstruction is only required for a small group of children. Clear indications for surgical enucleation are children requiring assisted ventilation for airway obstruction and children with life-threatening airway obstruction. Children with airway compression greater than 75% of the airway lumen, after 1 month of treatment to which corticosteroids have been added, should be considered for enucleation. Children with calcified lymph glands on CT scan are not good candidates as surgical enucleation will not be successful. The presence of lymph nodes alone is not an indication for surgery. Suggested indications include acute perforation of a major airway with severe respiratory embarrassment, pressure and occlusion of a major airway with lung collapse or hyperinflation, bronchial stenosis due to fibrosis and, rarely, superior vena cava obstruction or subcarinal oesophageal obstruction.[9]

The reported complication rate resulting from enucleation is low. Reported complications include bronchial tear, pulmonary artery laceration and bronchopleural fistula.

Conclusion

Most children with airway compression caused by TB lymph gland enlargement will respond favourably to medical treatment. A small percentage will need further investigation which includes bronchoscopy and chest CT scan. An even smaller percentage will benefit from surgical intervention.

References

1. Marais BJ, Gie RP, Schaaf HS, *et al*. The spectrum of disease in children treated for tuberculosis in a highly endemic area. *Int J Tuberc Lung Dis* 2006; 10: 1-7.
2. Theart A, Marais BJ, Gie RP, Hesseling AC, Beyers N. Criteria used for the diagnosis of childhood tuberculosis at primary health care level in a high-burden, urban setting. *Int J Tuberc Lung Dis* 2005; 9: 1210-1214.
3. Goussard P, Gie RP, Kling S, Beyers N. Expansile pneumonia in children caused by mycobacterium tuberculosis: clinical, radiological, and bronchoscopic appearances. *Pediatr Pulmonol* 2004; 38: 451-455.
4. Fishman JE, Saraf-Lavi E, Narita M, *et al*. Pulmonary tuberculosis in AIDS patients; transient chest radiographic worsening after initiation of antiretroviral therapy. *AJR* 2000; 174: 43-49.
5. De Villiers RVP, Andronikou S, van der Westhuizen S. Specificity and sensitivity of chest radiographs in the diagnosis of paediatric pulmonary tuberculosis and the value of additional high-volt radiographs. *Australas Radiol* 2004; 48: 148-153.
6. Nemir RL, Cordona J, Lacoius A, David M. Prednisone as an adjunct in the chemotherapy of lymph node-bronchial tuberculosis in childhood: a double-blind study. *Am Rev Respir Dis* 1963; 88: 189-198.
7. Nemir RL, Cordona J, Vaziri F, Toledo F. Prednisone as an adjunct in the chemotherapy of lymph node-bronchial tuberculosis in childhood: a double-blind study. II. Further term observation. *Am Rev Respir Dis* 1967; 95: 402-410.
8. Andronikou S, Joseph E, Lucas S, *et al*. CT scanning for the detection of tuberculous mediastinal and hilar lymphadenopathy in children. *Pediatr Radiol* 2004; 34: 232-236.
9. Konstantinos A, Papagiannopoulos KA, Linegar AG, Harris DG, Rossouw GJ. Surgical management of airway obstruction in primary tuberculosis in children. *Ann Thorac Surg* 1999; 68: 1182-1186.

Pediatric Pulmonology 43:505–510 (2008)

The Outcome of Infants Younger Than 6 Months Requiring Ventilation for Pneumonia Caused by *Mycobacterium tuberculosis*

P. Goussard, MMed (Paed), MD,[1]* R.P. Gie, FCPaed,[1] S. Kling, FCPaed,[1] H.S. Schaaf, PhD,[1] F. Kritzinger, FCPaed,[1] S. Andronikou, PhD,[2] N. Beyers, PhD,[1] and G.J. Rossouw, MMed[3]

Summary. Introduction: The outcome of young infants (<6 months) being ventilated for respiratory failure caused by *Mycobacterium tuberculosis* (MTB) has not been recorded. Patients and Methods: A descriptive study of children <6 months admitted to the PICU from 1 February 1999 to 31 December 2005 with MTB causing respiratory failure. Results: Seventeen infants were ventilated for respiratory failure caused by MTB: ten had ventilatory respiratory failure and seven had hypoxic failure. An index case was found in 47%. All chest radiographs (CXRs) were highly suggestive of tuberculosis. MTB was cultured in 15 cases. In the other two cases MTB was confirmed by histopathology. The median duration of ventilation was 6 days (range: 1–35 days) with a median PaO2/FiO2 of 85 and ventilatory index of 58. Transthoracic glandular enucleation was required to facilitate extubation in six babies. All the infants survived. At 6-month follow-up 35% had a normal CXR and all were asymptomatic. One child had CXR changes suggestive of bronchiectasis but was asymptomatic. Conclusion: The outcome of infants <6 months ventilated for respiratory failure caused by MTB is very good if TB is recognized timeously and appropriate management started. The diagnosis of TB in these infants can be made with a high index of suspicion and careful evaluation of the CXR. **Pediatr Pulmonol. 2008; 43:505–510.** © 2008 Wiley-Liss, Inc.

Key words: tuberculosis; infant tuberculosis; tuberculous pneumonia; ventilation.

INTRODUCTION

Although the consequences of the ongoing tuberculosis (TB) epidemic are well known, there is very little data on the outcome of young infants with tuberculosis. Prior to the advent of modern antibiotics, the case fatality from TB in infants <6 months of age varied between 30% and 55%.[1,2] As the prevalence of HIV infection increases in the developing world the attributable fraction of TB related to HIV in pregnancy rises by 71.7%.[3] Despite the increase in TB prevalence the outcome of infants infected shortly after birth has been poorly documented. In infants less than 3 months of age with TB, which included cases of congenital TB, the case fatality was 13%.[4] The mortality for infants with congenital tuberculosis varies between 22% and 46%.[5] The aim of this case series is to report on the clinical and radiological presentation, management and outcome of infants younger than 6 months of age requiring ventilation for respiratory failure caused by *Mycobacterium tuberculosis* (MTB).

PATIENTS AND METHODS

Setting

This is a descriptive study of pulmonary tuberculosis in infants younger than 6 months of age requiring assisted ventilation in a tertiary care hospital from 1 February 1999 to 31 December 2005. The hospital is situated in the Western Cape Province of South Africa, a province with an extremely high incidence of TB (917 new cases/100,000 population per annum in 2003). The tertiary

[1]Department of Paediatrics and Child Health, Faculty of Health Sciences, Stellenbosch University, Tygerberg Children's Hospital, Tygerberg, South Africa.

[2]Department of Radiology, Faculty of Health Sciences, Stellenbosch University, Tygerberg Children's Hospital, Tygerberg, South Africa.

[3]Department of Cardiothoracic Surgery, Faculty of Health Sciences, Stellenbosch University, Tygerberg Children's Hospital, Tygerberg, South Africa.

*Correspondence to: P. Goussard, M.Med. (Paed), M.D., Department of Paediatrics and Child Health, Faculty of Health Sciences, Stellenbosch University, P.O. Box 19063, Tygerberg 7505, South Africa.
E-mail: pgouss@sun.ac.za

Received 9 July 2007; Revised 28 December 2007; Accepted 28 December 2007.

DOI 10.1002/ppul.20812
Published online in Wiley InterScience (www.interscience.wiley.com).

hospital serves as a referral hospital for a population of approximately 2 million people.

Study Population

All infants under 6 months of age admitted to the pediatric intensive care unit (PICU) with respiratory failure due to underlying pneumonia and who required ventilation were included in the study (n = 387). The 17 (4.4%) infants who had respiratory failure caused by *M. tuberculosis* constitute the case series. All 17 infants were referred for ventilation from surrounding district and regional hospitals.

Indications for Ventilation

The infants were intubated if warranted by their clinical picture, if they remained hypoxic ($paO_2 < 5.5$ kPa) on supplemental oxygen or if they were hypercapneic ($paCO_2 > 6.5$ kPa) with uncompensated respiratory acidosis.

Clinical Examination and Investigations

All the children were clinically examined and had the following investigations performed: full blood count, liver enzymes, chest radiograph (CXR), HIV test (ELISA) after informed consent, Mantoux tuberculin skin test (5 units S-PPD intradermally), gastric washings for MTB culture, and non-directed tracheal aspirate for viral, bacterial, and MTB culture. A chest computed tomogram (CT) with contrast and a rigid or flexible bronchoscopy were performed in those infants who could not be weaned from the ventilator within a few days or who had life threatening airway obstruction.

Blood cultures and viral studies from nasopharyngeal aspirates were done to diagnose co-infections.

All patients were ventilated with conventional pressure cycled ventilation according to standard protocols. Ventilation data on admission, duration of ventilation and duration of PICU stay were recorded. The children were classified as survivors if they were discharged from hospital.

Pulmonary tuberculosis was diagnosed using modified WHO criteria.[6] The children were treated with isoniazid (INH; 10 mg/kg/day), rifampicin (10 mg/kg/day) and pyrazinamide (25 mg/kg/day) during the initial intensive phase of 2 months. In infants who had specimens that were smear-positive for acid-fast bacilli or had disseminated TB either ethambutol (15 mg/kg/day) or ethionamide (20 mg/kg/day) was added for the duration of the intensive phase. Ethionamide was preferred if there was widespread dissemination due to its superior penetration into the central nervous system compared to ethambutol. INH and rifampicin were continued for a further 4 months. All infants were treated under direct observation and no infant received intermittent treatment. Patients with severe airway compression received prednisone (2 mg/kg) for 30 days. The prednisone was weaned over the next month. All children were treated for bacterial co-infections with appropriate antibiotics for community acquired or nosocomial pneumonia.

The children were clinically followed up after 1, 3, and 6 months and chest radiographs were performed after 6 months.

A prospective register is maintained at the hospital of all culture-confirmed childhood TB cases. This database was accessed to identify all infants less than 6 months of age, not admitted to the PICU with culture-confirmed TB during the study period.

Ethical approval for the study was granted by the Stellenbosch University Ethics Committee.

RESULTS

The 17 infants, 11 boys and 6 girls, with respiratory failure as a result of MTB, had a median age of 4 months (range: 2–5 months). TB was not suspected by the referring hospitals in any of the cases, but the possibility of TB was considered in seven cases on admission.

None of the infants had a history of being ill at birth. The most prominent presenting symptoms on admission were a cough (n = 11), grunting and tachypnoea (n = 2), wheezing (n = 3) and apnoea (n = 1). Weight loss was an additional complaint in only one case.

All children had evidence that they had received BCG during the neonatal period although a BCG scar was visible in only two cases.

On clinical examination 88% of the infants were below the 3rd percentile weight for age (National Center for Health Statistics percentile chart). On examination hepatomegaly (n = 15), splenomegaly (n = 11), and generalized lymphadenopathy (n = 2) were the most common extrapulmonary findings. None of the children had signs of TB meningitis.

There were two distinct clinical presentations. In 10 (59%) cases the infants had large airway obstruction causing ventilatory failure while in 7 (41%) cases there was extensive alveolar disease causing hypoxic failure (Table 1).

All the patients were HIV seronegative. The one child born to an HIV infected mother was HIV uninfected as confirmed by polymerase chain reaction (PCR). Mild liver dysfunction was present in seven children. The only significant other findings were lymphopenia ($<2 \times 10^9$/L; n = 7) and thrombocytopenia (n = 4).

Two of the 16 blood cultures performed on admission were positive and cultured *Shingomonas paucimobilis* and *Streptococcus pneumoniae*. All rapid tests for respiratory syncytial virus were negative and of the 15 viral cultures requested only parainfluenza type 3 (n = 2) was cultured.

TABLE 1— Comparing the 2 Presentations of Infants With PTB Needing Ventilation

	Airway obstruction, n 10	Pneumonia, n 7
Age (months) median (range)	3 (2–5)	4 (3–4.5)
Sex (male)	7	4
Contact	6	2
ZN positive	6	3
Culture positive	9	6
Duration of ventilation (days) median (range)	8.5 (1–17)	4 (1–35)
ICU stay (days) median (range)	11.5 (2–18)	7 (2–37)
PaO_2/FiO_2 median (range)	84.5 (54–375)	85 (65–322)
V I median (range)	59 (23–94)	46 (32–73)

ZN, Ziehl Neelsen; VI, ventilatory index.

Diagnosis of TB

Eight of the children had contact with a known adult TB index case. Not-one infant had received chemoprophylaxis as recommended by the National TB Programme. Mantoux tuberculin skin test was positive (>15 mm induration) in one infant with no induration recorded in the other infants.

Tuberculosis was proven in all 17 cases. *M. tuberculosis* was cultured in 15 cases with the source being tracheal aspirate (n — 9), gastric lavage (n — 4) or both (n — 2). The remaining two cases were confirmed by histopathology from a lung biopsy and tissue obtained at enucleation of tuberculous glands. In seven cases either the tracheal aspirate or gastric lavage was smear-positive for acid-fast bacilli. The 17 ventilated children made up 15% of the 113 culture-confirmed cases in infants younger than 6 months of age during the study period. Cultures were not routinely tested for drug susceptibility due to financial constraints. The drug susceptibility tests of the source cases were not available. In the six cases tested the bacilli were susceptible to INH and rifampicin.

Chest Radiographic Findings

The major abnormalities were mediastinal lymphadenopathy (n — 15), miliary tuberculosis (n — 2) and TB bronchopneumonia (n — 7; Fig. 1). In 9 of the 14 cases with airway obstruction significant narrowing of both main bronchi was visible (Fig. 2). Paratracheal lymph node enlargement was visible in four cases. One case had a combination of an expansible TB pneumonia and complicating miliary picture. In all cases the chest radiograph was highly suggestive of TB.

Before a neonatal bronchoscope became available to us for use in ventilated patients, tracheobronchograms were done using water soluble contrast medium. In two patients in this study severe airways obstruction was clearly demonstrated using this method (Fig. 3).

At the end of 6 months' treatment the chest radiographic findings were normal in six children. Nine children had fibrotic changes and two had cavities. Additional findings included calcification (n — 2) and signs of early bronchiectasis (n — 1).

Computed Tomography Findings

Chest computed tomography (CT) scans (n — 12) were performed to define the extent of the nodal compression of the airways. Tuberculous liquefaction of the lymph nodes with ring enhancement was present in 11 cases and severe large airways compression in 12 cases (Figs. 3 and 4). Massive subcarinal glands were present in all the cases of airway obstruction. Unsuspected tracheal compression was observed in seven patients. Although the CT scans confirmed the diagnosis of pulmonary TB and the severity of disease, very little new information that changed the management of the patients was gained.

Bronchoscopic Findings

Bronchoscopy was done in nine patients with suspected airway obstruction. Two further bronchoscopies were

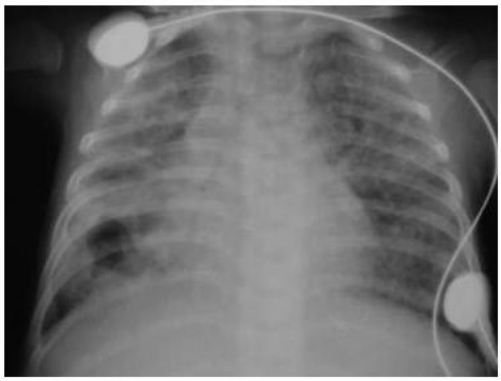

Fig. 1. Chest radiograph. Extensive confluent air-space disease is present involving most of the right lung with some lower zone breakdown. The left lung also demonstrates extensive, but patchy air-space disease. The bronchus intermedius is narrowed and the left main bronchus is not well demonstrated.

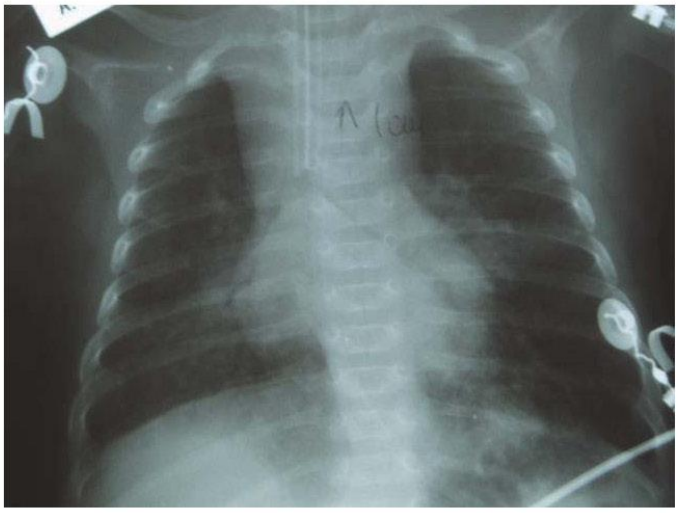

Fig. 2. Chest radiograph. There is an endotracheal tube in situ. Both bronchus intermedius and left main bronchus are markedly narrowed. The parenchyma is difficult to evaluate but even so, the left cardiac margin is obscured by lingular air-space disease.

indicated but not performed as a neonatal bronchoscope was not available. Severe large airways obstruction was confirmed in seven cases, while in two cases bronchoscopic examination was normal. The bronchus intermedius was severely obstructed in six cases. Three cases had severe obstruction of both main bronchi. In one of these cases the airways were obstructed by caseous material from lymph nodes that had perforated into the airways. Suctioning out the caseous material from the airways relieved a large degree of obstruction, but the patient still subsequently required transthoracic lymph nodal enucleation. Bronchoscopic findings were valuable in determining the extent of the airway obstruction which was not always clear on CT scan of the chest.

Ventilation Data

The median duration of ventilation was 6 days (range: 1–35 days). Nine children with ventilatory respiratory failure were ventilated for a median duration of 8.5 days

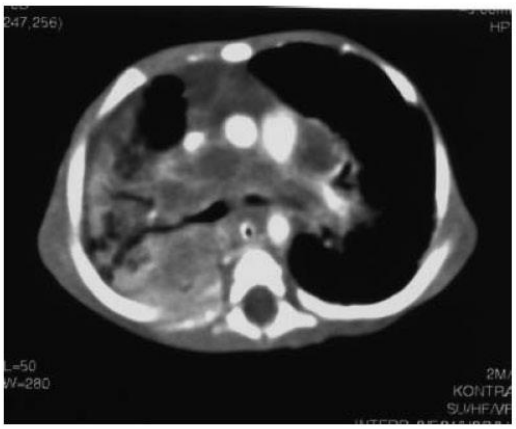

Fig. 3. Axial contrasted CT of chest. There is extensive low density (necrotic) lymphadenopathy with "ghost-like" and ring enhancement, causing compression and displacement of the right middle lobe and left main bronchi. The right lung shows air-space disease with lung parenchymal liquefaction and cavity formation.

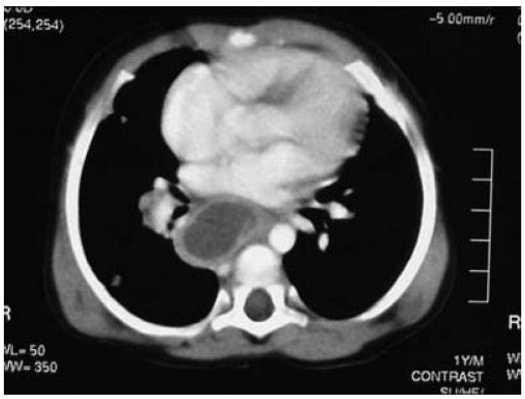

Fig. 4. Axial contrasted CT can of the chest. A characteristic large low density ring-enhancing azygoesophageal TB lymph node is present.

compared to the eight children with hypoxic failure who were ventilated for a median duration of 4 days. The median PaO_2/FiO_2 ratio for all infants was 85 (range: 57–346) and the median ventilatory index (VI) was 58 (range: 27–94) on admission to the PICU.

Surgical Procedures

In one infant a lung biopsy was done to confirm the diagnosis of tuberculosis, as all the other tests were not diagnostic of TB. Six infants required transthoracic enucleation of the mediastinal lymph nodes under general anesthesia, because large airways obstruction prevented them from being weaned from ventilation. Those requiring enucleation had large subcarinal nodes visible on both chest radiograph and CT-scan. The transthoracic enucleation of the obstructing glands was performed after a median of 4 days (range: 1–8 days). One case was complicated by a post-operative bronchopleural fistula, which resolved spontaneously. These six patients required ventilation for a median duration of 2 days (range: 0.5–5) post-surgery.

TB Treatment

All the infants received INH, rifampicin and pyrazinamide during the intensive phase of treatment. Ethambutol (n = 4) or ethionamide (n = 8) was added to the treatment. Not one of the children developed side effects related to their antituberculosis treatment.

Outcome

Children stayed in the PICU for a median duration of 7 days (range: 2–37 days). One child required readmission to the PICU for 37 days. All the children survived the PICU and were discharged from hospital. No child required readmission to hospital following discharge. All the patients were asymptomatic after 6 months of therapy.

DISCUSSION

The diagnosis of TB in young infants is particularly challenging as demonstrated by this study. The diagnosis was not made by the referring physician in a single case of the 17 children referred for ventilation. The infants presented with non-specific symptoms and only 47% had a known contact with an infectious case of TB. Although most infants with TB are symptomatic,[7] the non-specific nature of the symptoms and signs has been widely noted, and especially so in congenital TB.[8] According to the current series the presence of hepatosplenomegaly with or without the presence of generalized lymphadenopathy should raise the suspicion of a chronic infection. The diagnosis was further complicated in these very sick infants by the non-reactive Mantoux tuberculin skin tests in all but one infant, but this poor response in young infants has previously been documented by others.[4,9]

The diagnosis was aided by the fact that seven infants had tracheal or gastric aspirates smear-positive for acid-fast bacilli and the high culture yield of *M. tuberculosis* (n = 15). Because the infants were all intubated, tracheal aspirates were easy to obtain and were more often done than gastric aspirates. Despite this the proportion of cases cultured from tracheal aspirates or gastric aspirates were similar. The high proportion of smear-positive aspirates indicates that these infants had severe disease with a high bacillary load. Young infants are seldom considered to be smear positive, but in this study 41% of them were. Consideration must be given to the fact that these children are a risk not only to the other children in the PICU, but also to medical personnel. For this reason most infants were treated with four drugs during the intensive phase. This is in accordance with recommendations that when a high bacillary population is present in children, four drugs are indicated during the intensive phase.[10] Visual acuity could not be tested in these infants, but ethambutol in a dose of 15 mg/kg/day is regarded as safe even in very young children.[11,12] Ethionamide is a relatively safe drug, with gastrointestinal symptoms the most common side-effects. The use of ethionamide is more controversial, but it was used when disseminated TB was present, as the cerebrospinal fluid (CSF) penetration is superior to that of ethambutol.[13]

All children with large airway obstruction received steroids as part of their therapy although the value of adding steroids remains uncertain and indications for the use of steroids in pulmonary disease remain controversial.[14,15]

Transthoracic enucleation of obstructing mediastinal lymph nodes was required in six children to aid their weaning from assisted ventilation. No controlled trials have been undertaken to establish the indications for this invasive procedure. In children with life threatening airway obstruction this procedure yielded encouraging results in this limited study. All six patients were weaned from ventilation within 5 days of the operation and only one developed a complication, a bronchopleural fistula, which sealed off spontaneously. Of interest was that all infants that were ventilated for airway obstruction had enlarged subcarinal nodes, similar to the observation made by others that subcarinal lymph nodes play an important part in large airway obstruction.[16]

In this study there are three unusual observations. Although all the infants had received BCG only two had BCG scars, not one of the infants was HIV infected and no infant had extrapulmonary TB. We have no logical explanations for the above observations but they might indicate a certain immune response leading to the clinical pictures we encountered. None of the children had proven immune deficiency and all were thriving following therapy. The absence of HIV infected infants might be a reflection of admission policies but there was no

systematic exclusion of HIV infected children with respiratory failure with many infants during the period of the study being ventilated for *Pneumocystis jiroveci* and cytomegalovirus pneumonia.

We report the favorable outcome of children younger than 6 months ventilated for respiratory failure caused by MTB pneumonia. Only a few reports are available on tuberculosis in infants[4,7,8] and although some reports refer to assisted ventilation and surgery in infants with intrathoracic TB,[8,17] no report specifically addresses the management and outcome of young infants requiring assisted ventilation for intrathoracic TB-associated respiratory failure.

The mortality reported from TB in infants at different ages varies widely. Before the availability of antituberculosis treatment it varied from 55% in infants less than 6 months of age to 30% in those from 1 to 2 years of age.[2] Even after the introduction of antituberculosis drugs, the mortality due to congenital TB remained high, while deaths in infants less than 3 months of age (including some congenital TB cases) was 13%.[4] However, in a developed setting, the death rate in infants under 1 year of age was reported as only 2%. We have previously reported that children admitted to a PICU with TB have a case fatality of 23% with the most common cause of death being TB meningitis.[18] Compared to all of these outcomes, the young infants in this study had a good short and long-term outcome. Possible reasons for the improved outcome in these infants are that not one of the infants had TB meningitis, none had congenital TB and all were HIV-seronegative. Further this study illustrates that children requiring assisted ventilation for respiratory failure because of TB do not necessarily have a poor outcome. A limitation of this study is that we cannot be sure that all infants with pneumonia or glandular obstruction of the airway caused by TB were recognized and referred for ventilation. We could therefore be overestimating the favorable outcome of infants with extensive pulmonary TB.

The outcome of infants less than 6 months of age requiring assisted ventilation for respiratory failure caused by TB need not be as guarded as previously reported if TB is timeously recognized and appropriate management started. With a high index of suspicion and careful evaluation of the chest radiograph TB can be suspected in most infants. Further studies are required to confirm these findings and examine if these outcomes can be achieved in infants dually infected with TB and HIV.

ACKNOWLEDGMENTS

We would like to thank our colleagues in the Departments of Radiology and Cardiothoracic Surgery for their assistance in the management of these children.

REFERENCES

1. Marais BJ, Gie RP, Schaaf HS, Hesseling AC, Obihara CC, Nelson LJ, Enarson DH, Donald PR, Beyers N. The clinical epidemiology of childhood pulmonary tuberculosis: a critical review of the literature from the pre-chemotherapy era. Int J Tuberc Lung Dis 2004;8:278–285.
2. Lincoln EM. Course and prognosis of tuberculosis in children. Am J Med 1950;9:623–632.
3. Pillay T, Khan M, Moodley J, et al. The increasing burden of tuberculosis in pregnant women, newborns and infants under 6 months in Durban, Kwazulu-Natal. S Afr Med J 2001;91:983–987.
4. Schaaf HS, Gie RP, Beyers N, Smuts N, Donald PR. Tuberculosis in infants less than 3 months of age. Arch Dis Child 1993;69:371–374.
5. Weisoly DL, Khan A, Elidemir O, Connelly Smith K. Congenital tuberculosis requiring extracorporeal membrane oxygenation. Pediatr Pulmonol 2004;37:470–473.
6. World Health Organization. Treatment of tuberculosis: guidelines for national programmes, 3rd edition. Geneva: World Health Organization; 2003. (WHO/CDS/TB/2003.313).
7. Vallejo JG, Ong LT, Starke JR. Clinical features, diagnosis, and treatment of tuberculosis in infants. Pediatrics 1994;94:1–7.
8. Kim K, Lee JW, Park JH, Kim SY, Choi PJ, Lee KN, Kim HJ, Lee SH. Pulmonary tuberculosis in five young infants with nursery exposure: clinical, radiographic and CT findings. Pediatr Radiol 1998;28:836–840.
9. Hageman J, Schulman S, Shreiber M, et al. Congenital tuberculosis: critical reappraisal of clinical findings and diagnostic procedures. Pediatrics 1980;66:980–984.
10. American Thoracic Society, Centers for Disease Control and Prevention, Infectious Disease Society of America. Treatment of tuberculosis. Am J Respir Crit Care Med 2003;167:603–662.
11. Trebucq A. Should ethambutol be recommended for the routine treatment of tuberculosis in children? Review of the literature. Int J Tuberc Lung Dis 1997;1:12–15.
12. Graham SM, Daley HM, Banerjee A, Salaniponi FM, Harries AD. Ethambutol in children: time to reconsider. Arch Dis Child 1998;79:274–278.
13. Donald PR, Seifart HI. Cerebrospinal fluid concentrations of ethionamide in children with tuberculous meningitis. J Pediatrics 1989;115:483–486.
14. Toppet M, Malfroot A, Derde MP, Toppet V, Spehl M, Dad I. Corticosteroids in primary tuberculosis with bronchial obstruction. Arch Dis Child 1990;65:1222–1226.
15. Nemir RL, Cardona J, Vazairi F, Teledo R. Prednisone as an adjunct in the chemotherapy of lymph node-bronchial tuberculosis in childhood: a double blind study II. Further term observation. Am Rev Respir Dis 1967;95:402–410.
16. Andronikou S, Joseph E, Lucas S, Brachmeyer S, Du Toit G, Zar H, Swingler G. CT scanning for the detection of tuberculous mediastinal and hilar lymphadenopathy in children. Pediatr Radiol 2004;34:232–236.
17. Kim K, Lee JW, Park JH, Kim SY, Choi PJ, Lee KN, Kim HJ, Lee SH. Pulmonary tuberculosis in five young infants with nursery exposure: clinical, radiographic and CT findings. Pediatr Radiol 1998;28:836–840.
18. Heyns L, Gie RP, Kling S, et al. Management of children with tuberculosis admitted to a pediatric intensive care unit. Pediatr Infect Dis J 1998;17:403–407.

routinely used in adult radiology practices. The primary advantage is the increased signal-to-noise ratio.
Objective To review the utility of 3-T MRI in improving the diagnostic quality of paediatric studies. In particular, to overcome certain challenges unique to imaging children—from smaller structures, faster heart rates, movement and difficulties with breathhold.
Materials and methods A retrospective review of 121 MRI studies performed on the 3T scanner of a tertiary paediatric hospital, from 2005–2007. The studies were assessed for advantages of the higher resolution imaging for specific indications, including cortical dysplasia, metabolic white matter diseases, and obstetric brachial palsy. Also, diagnostic issues arising from the altered T1 and T2 relaxation times, increased chemical shift and susceptibility effects were considered.
Results The increased SNR translates to superior spatial resolution, providing high quality images of small structures e.g., inner ear, peripheral nerves, articular cartilage and biliary system. In addition, the increased temporal resolution is useful to reduce scan times, increasing patient co-operation. Whole body MRI for total tumour burden; sickle cell disease etc. can be performed. The improved separation of metabolite peaks provides a distinct advantage for MR Spectroscopy. Also the susceptibility effect can be exploited to increase sensitivity for haemorrhage in diffuse axonal injury and the BOLD effect of de-oxyhaemoglobin.
Conclusion A 3-T MRI has definite advantages in paediatric imaging for specific indications, including specialised applications such as arterial spin labelling and fMRI.

O47

Genomic changes after routine magnetic resonance imaging in children. A pilot study

Alvhild Bjorkum[1], Beate Kluge[2], Sigrun Kjaerstad[3], Cecilie Myhre[4], *Karen Rosendahl*[5]
1. Faculty of Engineering, Biomedical Laboratory Science Program, Bergen University College, Bergen, Norway
2. Medical Research Centre, University of Bergen, Bergen, Norway
3. Laboratory Unit, Children's Clinic, Haukeland University Hospital, Bergen, Norway
4. Laboratory Unit, Children's Clinic, Haukeland University Hospital, Bergen, Norway
5. Great Ormond Street Hospital, London, UK

Objective To identify genomic changes in white blood cells from girls after routine 3T MR examination.
Material and methods After Regional Ethical Committee approval six healthy females aged 6–10 years subjected to a routine MR-scan were sampled for 2.5 ml blood immediately before and after an unenhanced 3-T MR examination. RNA was extracted and the microarray experiments were performed using the Applied Biosystems 1700 Expression Array system. The AB human microarray contains 31,700 probes against 27,868 genes, and around 1,000 control probes. The chemiluminescent signal detection, image acquisition and image analysis of the microarrays were performed using the Applied Biosystems 1700 Chemiluminescent Microarray Analyzer.
Results Changes were seen in 205 of approximately 14,000 genes in all six girls. The five most commonly involved functional biological processes were: (1) cell cycle (G1-S Growth factor regulation and mitosis), (2) immune (antigen presentation and TCR signalling), (3) inflammation (IgE signalling and NK cell cytotoxicity), (4) development (skeletal muscle) and (5) cell adhesion (leukocyte chemotaxis and cell junctions). Further the microarray screening showed distinct changes in gene groups defined as members of specific gene functional pathways (canonical pathways), amongst them the G-Protein mediated regulation p38 and JNK signalling pathways. The changes were consistent using two different software packages for analysis and visualization of microarray data (J-express Pro and GeneGo).
Conclusion Our pilot suggests changes involving canonical pathways for cell cycle and immune response, amongst others. The clinical implication of these findings remains unclear.

O48

MRI for characterization of tuberculous lymphadenopathy in children

Reena George[1], *Savvas Andronikou*[1], Pierre Goussard[2], Salomine Theron[1], Ayanda Mapukata[1], Jaco Du Plessis[1], Murray Hayes[1], Robert Gie[2], Marie Grobbelaar[1]
1. Department of Radiology, University of Stellenbosch, Stellenbosch, South Africa
2. Department of Child Health, University of Stellenbosch, Stellenbosch, South Africa

Background CT scanning is currently the gold standard for demonstration of mediastinal lymphadenopathy, in the diagnosis of Primary Pulmonary Tuberculosis in children. Apart from the characteristic ring enhancement and suggestive calcification, there are no defined diagnostic criteria that differentiate tuberculous nodes from other causes of lymphadenopathy. MRI may have advantages in demonstrating specific signal in TB nodes. To the best of our knowledge MRI characteristics of tuberculous lymph nodes have not been published in the literature.
Objective To determine the MRI signal characteristics and enhancement pattern in tuberculous lymphadenitis and to correlate MRI appearance with the CT appearance.
Materials and methods Four children with culture proven Pulmonary TB were examined with MRI. Two observers blinded to CT and Chest X-ray reported the MRI. These findings were then correlated with the CT appearance and histological pattern of the nodes.
Results The patients in the study group had ring enhancing nodes typical of tuberculosis as well as nonspecific solid uniformly enhancing nodes on contrasted CT. However both these lymph node groups had a strikingly low signal on T2 and STIR sequences.
Conclusion MRI signal characteristics of TB lymph nodes are defined. We speculate that the low signal noted in T2/STIR characteristic of TB lymphadenitis is due to gummatous necrosis. MRI can be used instead of CT in evaluating these children and has the significant advantage of no exposure to ionizing radiation. This is a pilot study and we intend to carry out this study in a larger population to confirm our findings.

Conclusion The diagnostic performance characteristics of the D-dimer assay are not high enough to exclude or confirm venous thromboembolism detectable by imaging in the pediatric population. Use of the D-dimer assay for stratifying children according to adult protocols for imaging of venous thromboembolism is not advocated.

O103

Radiation exposure of obese children from body CT: are they appropriately treated as adults?

Sjirk Westra, Mannudeep Kalra, Bob Liu
Massachusetts General Hospital, Boston, MA, USA

Background Longitudinal automatic exposure control (AEC) modulates the CT radiation dose according to attenuation factors calculated from the scanogram. Because of the increased radiosensitivity of children, risk estimates in obese children for future cancer induction are increased compared to lean children and adults.
Objective To assess dose and image quality of scans performed with AEC on obese children and compare them to fixed mA techniques.
Materials and methods In a sample of 150 pediatric body CT scans, nine were identified as dose outliers (>2 SD above group mean). We recorded kV, mA range and $CTDI_{vol}$. In scans obtained with AEC, we compared $CTDI_{vol}$ with that from a corresponding age-adjusted fixed mA acquisition at 120 kV. We measured image noise as standard deviation of attenuation values within a homogeneous region of interest placed in the subcutaneous fat. We compared dose and noise of scans performed with AEC with historic scans performed with fixed mA, when available.
Results All dose outliers occurred in obese children. Five of six abdominal CT and 1/3 chest CT dose outliers were scanned at 140 kV. Dose in these outliers was between 1.6 and 3.6 times dose calculated for scans performed at 120 kV and with fixed mA. Noise varied between 7–24, and did not interfere with diagnostic image quality.
Conclusion Obese children are getting substantially higher doses when using 140 kV and/or AEC without specified maximum mA, than when using age-based fixed mA settings, but these higher doses may be required in order to limit noise.

O104

64-Slice multidetector spiral computed tomography: radiation dose and image quality depending on the tube current in an anthropomorphic paediatric phantom

Dagmar Honnef[1], Andreas Mahnken[1], Christoph Suess[2], Rosemarie Banckwitz[2], Marco Das[1], Rolf Günther[1], Christian Hohl[1]
1. University Hospital RWTH, Aachen, Germany
2. Siemens Medical Solutions, CT, Forchheim, Germany

Purpose To evaluate the influence of tube-voltage-reduction on effective dose (ED) and image noise compared to a standard pediatric 120 kVp-protocol in thoracic and abdominal 64-slice MDCT.
Materials and methods A tissue-equivalent anthropomorphic phantom representing a 5-year-old child was used. The scans were performed on a 64-slice-MDCT scanner (SOMATOM Sensation 64, Siemens, Germany) with a 64×0.6 mm collimation and 500 ms tube-rotation time. Reconstructed slice thickness was 5 mm. Based on 120 kVp-protocols the mAs of the 100-kVp and 80-kVp scans were selected keeping the $CTDI_{vol}$ displayed at the scanner console constant. For chest CT, 120 kVp and 20 mAs (1.52 mGy $CTDI_{vol}$) and for abdomen CT 120 kVp and 50 mAs were used (3.82 mGy $CTDI_{vol}$). A total of 141 thermoluminescent dosimeters at 47 measuring points were placed in the phantom. Calculation of ED was according to ICRP60 for boys (m) and girls (f). Objective image quality was determined by ROI-measurements.
Results Keeping the $CTDI_{vol}$ constant, a decrease of tube voltage causes an increase of ED compared to 120 kVp protocol: chest-CT 8.05% (m)/8.95% (f) (100 kVp); 14.64% (m)/15.06% (f) (80 kVp); abdomen CT 4.23% (m)/5.71% (f) (100 kVp); 9.55% (m)/9.20% (f) (80 kVp). Noise measurements were as followed: thoracic 12.7 HU (120 kVp), 13.0 HU (100 kVp), 13.7 HU (80 kVp); abdominal 12.7 HU (120 kVp), 12.9 HU (100 kVp), 14.5 HU (80 kVp).
Conclusion A reduction of tube voltage while keeping $CTDI_{vol}$ constant results in an increase in ED and in a slight increase of image noise. Therefore a decrease of tube voltage cannot be recommended in children in general for reasons of radiation protection and image quality as long as the desired low dose levels can be reached at 120 kVp.

O105

Does the routine availability of a high-resolution CT (multidetector CT) of the chest in children add significant information? An African setting

Anita Erlank, *Savvas Andronikou*, Christelle Ackermann, Stephanie Griffith-Richards, Pierre Goussard
Stellenbosch University, Stellenbosch, South Africa

Background HRCT in children has traditionally been performed as an individual procedure (specific indication) or as an addition to routine post contrast contiguous slice CT for imaging airways and interstitium. It involves production of fine slices (1 mm) with large gaps between and reconstruction using a bone algorithm. The value of routine HRCT availability (produced as a Combi-scan on MDCT by reconstruction of contiguous fine slices) for all chest imaging has not been evaluated in children, particularly in developing nations where replacement of existing single slice spiral CT scanners with more expensive MDCTs must be motivated for strongly. However, the prevalence of HIV and TB in our population and their effects on the interstitium and airway warrants investigation of routine HRCT availability yield in addition to contiguous post contrast CT. This would either create a strong motivation for replacing existing equipment or result in performance of additional HRCT on every child referred for chest CT.
Objective To determine sensitivity and specificity of routine use of contiguous slice CT for detecting interstitial and small airways disease versus HRCT available routinely (considered the Gold Standard) in developing countries.
Materials and methods One hundred Combi-scans retrospectively reviewed (contiguous slice evaluated independently from HRCT component) for presence of nodules, septal lines, bronchiectasis, air trapping and ground glass.

Results One hundred patients (age range 1 month to 14 years). Fifty-two female, 48 male. Nodules: sensitivity 83%, specificity 100%; septal lines: sensitivity 75%, specificity 100%; ground glass: sensitivity 71%, specificity 93%; bronchiectasis: sensitivity 68%, specificity 100%; air trapping: sensitivity 34%, specificity 98%.
Conclusion Moderate/low sensitivity of contiguous slice CT for interstitial disease. HRCT should be routinely used in the African setting in the context of TB and HIV. Conventional CT is cost effective but investment in MDCT scanners would offer a clinical advantage with regard to time saving and radiation exposure.

RESERVE

O106

Implementation of paediatric automatic exposure control CT protocols which are based on weight, clinical indication and number of prior CTs

Sjirk Westra, Mannudeep Kalra, Sarabjeet Singh, Ellen Grant
Massachusetts General Hospital, Boston, MA, USA

Background Weight based colour-coded protocols for CT dose reduction have been reported, using fixed mA settings. With automatic exposure control (AEC), noise index (NI) has to be specified for every scan.
Objective To introduce colour-coded paediatric CT protocols with AEC, based on patient weight, clinical indication and number of prior CTs, and evaluate technologist compliance, reduction in dose and effect on image quality.
Materials and methods Pediatric chest and abdomen CT protocols were divided into six colour zones: pink (routine or rule out situation), green (low-dose or follow-up CT), red (second follow-up CT or ultra-low-dose indications), yellow (bone protocol), blue (high-dose indications for subtle lesions), and grey (CT angiography). NI, milliampere range, and peak kilovoltage were adapted differently for each zone based on weight, babies (<20 lbs), cuties (21–60 lbs), kiddies (61–100 lbs) and teenagers (>101 lbs, <18 years). Radiation doses were compared with non-compliant and historical scans.
Results Compliance with recommended zones was 53% for chest and 75% for abdomen scans. Non-compliance occurred mainly in obese adolescents, who were dosed as adults. Compliant scans reduced dose by 56% in the chest, and 24% in the abdomen. Green zone protocols were most frequently used (57%), followed by pink (31%) and yellow (8%). Image quality remained diagnostic for the purpose of the scan, regardless of the zone used.
Conclusion CT protocols with NI, mA range and kVp tailored to weight, clinical indication and number of prior CTs are easy to implement and can help in reducing radiation dose to children.

Pediatric Pulmonology 43:721–725 (2008)

Case Report

Fibrin Glue Closure of Persistent Bronchopleural Fistula Following Pneumonectomy for Post-Tuberculosis Bronchiectasis

P. Goussard, MMed (Paed),[1]* R.P. Gie, FCPaed,[1] S. Kling, FCPaed,[1] F.E. Kritzinger, FCPaed,[1] J. van Wyk, FC Cardio(SA),[2] J. Janson, FC Cardio(SA),[2] and S. Andronikou, PhD[3]

Summary. We report a case of a persistent bronchopleural fistula following a pneumonectomy for post-tuberculosis bronchiectasis. The patient had two unsuccessful surgical attempts at closing of the fistula. Further surgical attempts were technically were not possible. Bronchoscopic closure was achieved by injecting human fibrin glue into the fistula via a catheter. Closure of the bronchopleural fistula was confirmed by repeated ventilation scan over a period of 2 months. Endoscopic closure of small bronchopleural fistulae is an attractive option in children with significant underlying lung disease. **Pediatr Pulmonol. 2008; 43:721–725.** © 2008 Wiley-Liss, Inc.

Key words: bronchopleural fistula; fibrin glue; tuberculosis; pneumonectomy; bronchoscopy.

INTRODUCTION

The reported incidence of bronchopleural fistula (BPF) following pneumonectomy varies between 1.5% and 28%[1–5] with a resulting mortality rate of 16.4–71.2%.[6–8] Surgical closure of BPF includes the following methods: thoracotomy with debridement of the pleural cavity and manual closure of the bronchial stump, sternotomy with transpericardial closure of the bronchial stump, thoracotomy with transposition of a pedicle of skeletal muscle or omental flap, video-assisted closure through short cervicotomy, and open thoracotomy.[9–12] Unsuccessful closure of a BPF poses a dilemma as repeated thoracotomy is not always possible.

The successful closure of a BPF in adults using fibrin sealant administered through a bronchoscope has been described.[13,14] Similarly, endoscopic closure of BPF in a small number of older children has been reported.[15]

We describe the use of fibrin glue to close a persistent BPF in a child following pneumonectomy for post tuberculosis bronchiectasis.

CASE

A 16-year-old girl with previously diagnosed agammaglobulinaemia had been previously diagnosed with bronchiectasis complicating culture proven tuberculosis, and a right sided pneumonectomy was performed in 2001. In August 2005 she presented with empyaema and a chronic stump leak was diagnosed. She underwent right thoracotomy and debridement of the pleural space and the BPF was closed by direct repair. The BPF recurred and a second repair was performed in November 2005. On this occasion a right sided thoracoplasty was done through a posterior thoracotomy and a serratus anterior muscle flap was transposed into the chest cavity. Shortly after

[1]Department of Paediatrics and Child Health, Faculty of Health Sciences, Stellenbosch University, Tygerberg Children's Hospital, Tygerberg, South Africa.

[2]Department of Cardio-Thoracic Surgery, Faculty of Health Sciences, Stellenbosch University, Tygerberg Children's Hospital, Tygerberg, South Africa.

[3]Department of Radiology, Faculty of Health Sciences, Stellenbosch University, and Tygerberg Children's Hospital, Tygerberg, South Africa.

*Correspondence to: P. Goussard, Department of Paediatrics and Child Health, Faculty of Health Sciences, Stellenbosch University, P.O. Box 19063, Tygerberg 7505, South Africa. E-mail: pgouss@sun.ac.za

Received 7 December 2007; Revised 7 March 2008; Accepted 30 March 2008.

DOI 10.1002/ppul.20843
Published online in Wiley InterScience (www.interscience.wiley.com).

the operation she had a recurrence of culture proven pulmonary tuberculosis. She received 6 months' anti-tuberculosis treatment and was regarded as cured as the sputum cultures for *Mycobacterium tuberculosis* were negative.

On this occasion the patient presented with a 3-week history of lethargy, weight loss, fever, and rigors. On examination she was tachypnoeic and pale with normal oxygen saturation in room air. Her weight for age was 57% of expected, her height for age 85% of expected, and her weight for height 87% of expected. She did not have digital clubbing. On examination of the chest the scars of the previous thoracotomies were visible. She had mild scoliosis to the right with decreased chest wall expansion on the right side. The trachea deviated to the right and the right hemithorax was dull to percussion. The breath sounds were normal over the left hemithorax but absent on the right side. Signs consistent with cor pulmonale were present. She had a port system venous catheter in situ and *Serratia marcescens* was cultured on two separate occasions from the line before it was removed. Chest radiograph demonstrated a thoracic rib deformity with a small right hemithorax and displacement of the mediastinal structures to the right. An unexpected tubular shaped, vertically oriented air collection was present within the right hemithorax in keeping with an air leak (Fig. 1). A CT scan demonstrated a connection between the right main bronchus stump site and the air collection which also contained a fluid level (Fig. 2), leading to the diagnosis of stump breakdown and leakage. The leak was confirmed with 81m Kr ventilation scintigraphy (Fig. 3A D). During normal tidal breathing the leak was not visualized (Fig. 3A,B), but when the patient was asked to cough the leak was clearly visible on the posterior view (Fig. 3D).

The BPF on the left side of the carina with air bubbles at its origin was visualized by means of a flexible bronchoscope. Surgical closure of the BPF was thought not to be feasible following the previous 3 thoractomies. There was also concern that the patient's pulmonary hypertension posed an anaesthetic risk. For these reasons an alternative method to close the BPF was attempted using fibrin glue (Tisseel®) via the working channel of a flexible bronchoscope. Tisseel® is a two-component liquid sealant. It contains freeze-dried human sealer protein in Aprotinin solution (protein, fibrinogen, plasmafibronectin, factor XIII, plasminogen) and 500 U of thrombin in a calcium chloride solution.

Under general anaesthesia a 4.9 mm flexible videobronchoscope with a 2 mm working channel was advanced to the level of the BPF. A brush was pushed through the working channel into the fistula to roughen up the epithelial lining to enhance adhesion of the fibrin glue. The brush was removed and a catheter was advanced into the fistula. A duploject plunger was used to inject the two compounds through the catheter simultaneously, while the patient was not being ventilated for 60 sec. The fistula visibly sealed during the 60 sec. There were no short or long term complications. The patient improved clinically and the closure was confirmed by ventilation scintigraphy on three subsequent occasions in the 6 months following

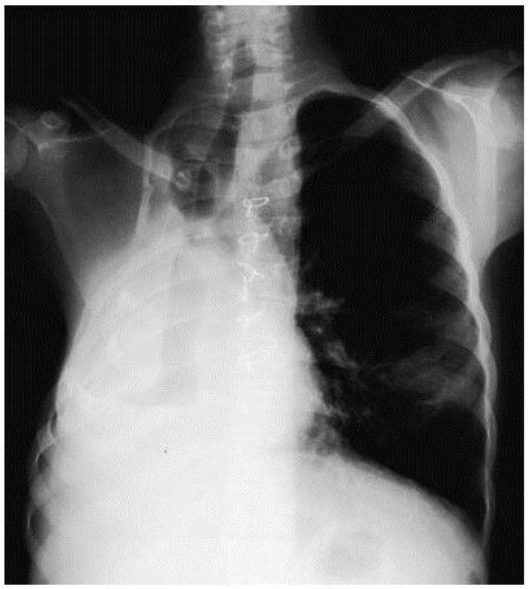

Fig. 1. Chest radiograph demonstrates the sternotomy wire sutures, thoracic deformity and volume loss due to the previous surgery. The mediastinum is deviated to the right and there is air within the right hemithorax, indicating an air leak.

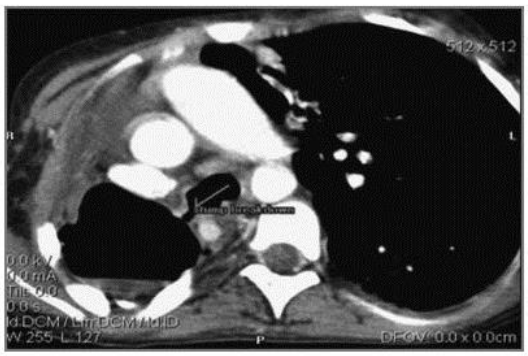

Fig. 2. Post contrast CT scan demonstrates the area of stump breakdown, just distal to the carina, which communicates with an air-containing right hemithorax. Note also the presence of an air-fluid level. The mediastinum is displaced towards the side of the pneumonectomy.

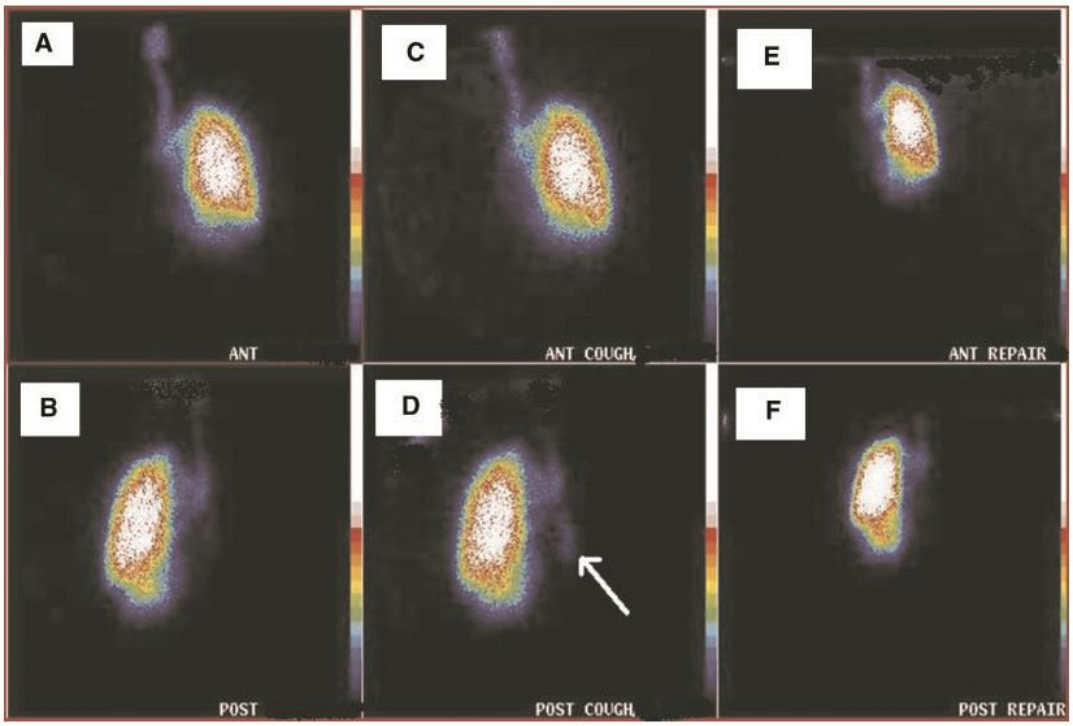

Fig. 3. Krypton 81-M ventilation scintigraphy series (A–F) demonstrating bronchopleural fistula (D) before surgery and demonstrating the absence of the bronchopleural fistula 3 months after the procedure (Fig. 2E,F). [Color figure can be viewed in the online issue, which is available at www.interscience.wiley.com.]

the procedure (Fig. 3E,F). She remained well with no subsequent lower respiratory tract infections.

DISCUSSION

In this article we report the successful closure of a BPF with fibrin glue following a pneumonectomy for post tuberculosis bronchiectasis. The closure of the fistula was complicated as two previous surgical attempts to close the BPF failed. Bronchopleural fistula following pneumonectomy for inflammatory diseases is associated with a high morbidity, which includes complications such as post-pneumonectomy space empyaema. Although there are only a few published studies on the outcome of pneumonectomy in children a complication rate of as high as 20% has been reported.[16,17,18] Factors that increase the risk of developing BPF include tuberculosis, preoperative empyaema, complete pneumonectomy and right sided pneumonectomy.[19–21] In the early chemotherapy era, pneumonectomy for tuberculosis carried a 28% risk for a BPF.[22] The risk with the use of modern antituberculosis drugs has not been reported.

The aetiology of the BPF in this case was initially thought to be secondary to the surgery but the possibility of it occurring as a complication of reactivated tuberculosis merits consideration. Factors favoring it being a complication of the second episode of tuberculosis include the position of the BPF and that culture proven tuberculosis was diagnosed following the second surgical closure of the BPF. The incidence of BPF in children after pneumonectomy for post-TB bronchiectasis is unknown. It is interesting to speculate if chemoprophylaxis following the surgical closure of the initial BPF would have prevented the reactivation of tuberculosis and so the development of a BPF as a complication.

The best treatment for BPF following surgery is always to prevent the complication in the first instance. It has been shown that pre-operative fever, steroids, peripheral leucocytosis, tracheostomy, long residual stump and excessive dissection increase the risk of developing a postoperative BPF.[23] All these factors increase the postoperative risk of ischaemic necrosis of the residual stump. Increased pooling of secretions in the stump results in colonisation and bacterial overgrowth. The risk is also increased when a right sided pneumonectomy is preformed.[19–21]

BPF most commonly occurs 8 12 days after the pneumonectomy but can occur at any time following

surgery.[9] In the early period following surgery the most likely causes of BPF are mechanical failure, following a suppurative pneumonia or secondary to an infarction.[9] The sudden reappearance of air in the obliterated space on the side of the pneumonectomy suggests either a BPF or gas forming infection. Flexible bronchoscopy is valuable in determining the site of the leak and assessing if bacterial infection or tuberculosis is present. Radioisotope ventilation scintigraphy is a valuable non-invasive diagnostic tool which can be repeated without exposing the patient to a high dose of radiation. The reported sensitivity and specificity of this test using ^{133}Xe gas are 83% and 100%, respectively.[24,25] Various other radioactive aerosols have been used to demonstrate BPF.[26–29] In this case the BPF was not visible on spontaneous breathing (Fig. 3A,B) but was easily visualized on the posterior view when the patient was asked to cough (Fig. 3D). Other diagnostic techniques used to demonstrate BPF include bronchography and the instillation of methylene blue into the chest cavity.[30,31] Methylene blue is no longer available for medical use in many parts of the world including the USA.

The successful treatment of chronic BPF depends on the aggressive control of infection, adequate drainage of the chest cavity, closure of the fistula with vascularized tissue and obliteration of the chest cavity.[9] The reported success rate of surgical closure of a BPF is 80–95% in adults.[10–12]

In adult patients flexible bronchoscopy has been used to apply sealants directly into the fistula. The first successful cases of endoscopic closure of a BPF with tissue glue were reported by Hartmann and Rausch[13] and Ratliff et al.[14] Multiple sealing compounds have been used which include polyethylene glycol, cyanoacrylate glue, fibrin glue, coils, and even stents.[9] Most leaks are in the peripheral part of the lung and not in the large airways which explains why this method is successful. Other factors which determine success are infection and fistula size. BPF larger than 8 mm are not suitable for endoscopic closure, while fistulas of 1 mm and less have the best closure rate.[9]

In two paediatric patients (18 and 20 years of age) endoscopic closure of their BPF was achieved.[15] Both of these patients had a large fistula between the pleural cavity and a segmental bronchus of the right upper lobe. Both were sealed with a methacrylate adhesive.[15] In recent publication a bronchoplearal fistula following lobectomy in an 8-year-old patient was successfully closed using porcine small intestinal mucosa and fibrin glue.[32] The technique used was similar to the one described in this article.

CONCLUSION

BPF is a rare complication in children following pneumonectomy, but it has a high mortality and morbidity. To our knowledge this is the youngest patient reported to have undergone successful endoscopic closure of a BPF. Endoscopic closure of bronchopleural fistulae is an attractive option in children with significant underlying lung disease, but is limited by the size of the working channel of paediatric flexible bronchoscopes.

REFERENCES

1. McManigle JE, Fletcher GL, Tenholder MF. Bronchoscopy in the management of bronchopleural fistula. Chest 1990;97:1235–1238.
2. Cerfolio RJ. The incidence, etiology and prevention of postresectional bronchopleural fistula. Semin Thorac Cardiovasc Surg 2001;13:3–7.
3. Sirbu H, Busch T, Aleksic I, Schreiner W, Oster O, Daliciau H. Bronchopleural fistula in the surgery of non-small cell lung cancer: incidence, risk factors and management. Ann Thorac Cardiovasc Surg 2001;7:330–336.
4. Turk AE, Karanas YL, Cannon W, et al. Staged closure of complicated bronchopleural fistulas. Ann Plastic Surg 2000;45:560–564.
5. Puskas JD, Mathisen DJ, Grillo HC, Wain JC, Wright CD, Moncure AC. Treatment strategies for bronchopleural fistula. J Cardiovasc Surg 1995;109:989–996.
6. Malave G, Foster E, Wilson J, Munro D. Bronchopleural fistula—Present-day study of an old problem: a review of 52 cases. Ann Thorac Surg 1971;11:1–10.
7. Asamura H, Naruke T, Tsuchiya R, Goya T, Kondo H, Suemasu K. Bronchopleural fistulas associated with lung cancer operations: univariate and multivariate analysis of risk factors, management, and outcome. J Thorac Cardiovasc Surg 1992;104:1456–1464.
8. Williams N, Lewis C. Bronchopleural fistula: a review of 86 cases. Br J Surg 1976;63:520–522.
9. Lois M, Noppen M. Bronchopleural fistula. An overview of the problem with special focus on endoscopic management. Chest 2005;128:3955–3965.
10. Stamatis G, Freitag L, Wencker M, et al. Omentopexy and muscle transposition: two alternative methods in the treatment of pleural empyema and mediastinitis. Thorac Cardiovasc Surg 1994;42:225–232.
11. Hollaus PH, Huber M, Lax F, et al. Closure of bronchopleural fistula after pneumonectomy with a pedicled intercostal muscle flap. Eur J Cardiothorac Surg 1999;16:181–186.
12. Sabanathan S, Richardson J. Management of postpneumonectomy bronchopleural fistula. J Cardiovasc Surg 1994;35:449–457.
13. Hartmann W, Rausch V. A new therapeutic application of the fiberoptic scope [letter]. Chest 1977:237.
14. Ratliff JL, Hill J, Tucker H, et al. Endobronchial control of bronchopleural fistula. Chest 1977;71:98–99.
15. Wood RE, Lacey S, Azizkan RG. Endoscopic management of large, postresection bronchopleural fistulae with methacrylate adhesive (super glue). J Pediatr Surg 1992;27:201–202.
16. Eren S. Pneumonectomy in children for destroyed lung and the long-term consequences. J Thorac Cardiovasc Surg 2003;126:574–581.
17. Campbell DN, Lilly JR. The changing spectrum of pulmonary operations in infants and children. J Thorac Cardiovasc Surg 1982;83:680–685.
18. Tsukada G, Stark P. Postpneumonectomy complications. Am J Roentgenol 1997;169:1363–1370.
19. Conlan AA, Scott EK. Pneumonectomy for benign disease. In: Deslauries J, Faber LP, editors. Chest surgery clinics of North America. Philadelphia: Saunders; 1999. pp. 311–325.

20. Halezeroglu S, Keles M, Uysal A, et al. Factors affecting postoperative morbidity and mortality in destroyed lung. Ann Thorac Surg 1997;64:1635–1638.
21. Blyth DF. Pneumonectomy for inflammatory lung disease. Eur J Cardiothorac Surg 2000;18:429–434.
22. Floyd R, Hollister W, Sealy W. Complications in 430 consecutive pulmonary resections for tuberculosis. Surg Gynecol Obstet 1959;109:467–472.
23. Sato M, Saito Y, Fujimura S, et al. Study of postoperative bronchopleural fistulas: analysis of factors related to bronchopleural fistulas. Nippon Kyobu Geka Gekkai Zasshi 1989;37:498–503.
24. Raja S, Rice TW, Neumann DR, et al. Scintigraphic detection of post-pneumonectomy bronchopleural fistulae. Eur J Nucl Med 1999;26:215–219.
25. Greyson ND, Rosenthal L. Detection of postoperative bronchopleural fistulas by radionuclide fog inhalation. Can Med Assoc J 1970;103:1366–1368.
26. Hollett P, Wright E, Wesolowski C, Harris R. Aerosol ventilation scintigraphy in the evaluation of bronchopleural fistula: a case report and literature review. Can J Surg 1991;34:465–467.
27. James R, Ahmad M, William P. Demonstration of a bronchopleural fistula by ventilation lung scanning. Cleve Clin Q 1979;46:67–70.
28. Vincken W, Schandeyl W, Sonstabo R, et al. Demonstration of a bronchopleural communication by inhalation of Kr-81m gas. Clin Nucl Med 1981;8:117–119.
29. Glen AL, Robert PS, Gerald LD. Bronchoscopic location of bronchopleural fistula with xenon-133. J Nucl Med 1982;23:322–323.
30. Nielsen KR, Blake LM, Mark JB. Localization of bronchopleural fistula using ventilation scintigraphy. J Nucl Med 1994;35:867–869.
31. York EL, Lewall DB, Hirji M, et al. Endoscopic diagnosis and treatment of postoperative bronchopleural fistula. Chest 1990;97:1390–1392.
32. Keckler SJ, Spilde TL, St Peter SD, Tsoa K et al. Tretment of bronchopleural fistula with small intestinal mucosa and fibrin glue sealant. Ann Thorac Surg 2007;84:1383–1386.

Pediatric Pulmonology 44:345–350 (2009)

Phrenic Nerve Palsy in Children Associated With Confirmed Intrathoracic Tuberculosis: Diagnosis and Clinical Course

P. Goussard, MMed (Paed),[1]* R.P. Gie, FC Paed,[1] S. Kling, FC Paed,[1] S. Andronikou, PhD,[2] J.T. Janson, FC Cardio (SA),[3] and G.J. Roussouw, FC Cardio (SA)[3]

Summary. In this descriptive retrospective cases series of eight cases phrenic nerve palsy in children caused by tuberculosis lymph gland infiltration of the phrenic nerve. The lymph gland enlargement was in all cases caused by culture confirmed Mycobacterium tuberculosis. The phrenic nerve palsy was on the left side in all eight cases with the presenting feature a raised diaphragm on chest radiography that was accompanied by consolidation of the left upper lobe (88%) The diagnosis of phrenic nerve palsy was confirmed by fluoroscopy of the chest. On computer tomography the outstanding features were left sided hilar and paratracheal lymph gland enlargement with displacement of the mediastinum to the right. Mediastinal displacement lead to anterior displacement of the descending aorta, which further compressed the left main bronchus. Two children had accompanying respiratory failure requiring assisted ventilation and in two additional cases the airway compression was so severe that glandular enucleation of the enlarged glands was indicated. Of the eight children five remained symptomatic after completion of TB treatment to which steroids were added for the initial month. Diaphragmatic plication was indicated in all five cases. On clinical follow-up two children had repeated respiratory tract infections secondary to underlying lung damage while the other six remained asymptomatic. **Pediatr Pulmonol. 2009; 44:345–350.** © 2009 Wiley-Liss, Inc.

Key words: phrenic nerve palsy; *Mycobacterium tuberculosis*; expansile pneumonia; diaphragm; plication.

INTRODUCTION

Phrenic nerve palsy, characterized by elevation of the hemi-diaphragm, rarely occurs in children. Phrenic nerve palsy following cardiac surgery is a recognized complication with increasing frequency the more complex the surgery. The incidence of unilateral phrenic nerve paralysis following pediatric cardiac surgery have been reported to vary between 0.46% and 4.6% with the highest risk occurring after Blalock–Taussig shunt surgery.[1,2] Other rare causes include chest-tube trauma to the phrenic nerve and as a complication of indwelling subclavian vein catheters.[3,4] Pulmonary tuberculosis is not considered as a common cause of phrenic nerve palsy in children with three reports of phrenic nerve paralysis caused by tuberculosis mediastinal adenopathy found in the English literature.[5–7] We have previously described phrenic nerve palsy in association with left upper lobe expansile pneumonia caused by *Mycobacterium tuberculosis* (MTB).[8]

The aim of this article is to describe the clinical, radiological, and pathological characteristics of phrenic nerve palsy associated with confirmed intrathoracic tuberculosis as well as the clinical course and response to therapy. We describe the short- and long-term outcome as well as the role of diaphragm plication in the management of this condition.

PATIENTS AND METHODS

This is a descriptive study of all cases of phrenic nerve palsy associated with MTB was retrospectively collected from October 1999 to June 2008 in a tertiary care hospital, situated in the Western Cape, South Africa. This region has

[1]Faculty of Health Sciences, Departments of Paediatrics and Child Health, Stellenbosch University, and Tygerberg Childrens' Hospital, Tygerberg, South Africa.

[2]Faculty of Health Sciences, Department of Radiology, Stellenbosch University, and Tygerberg Childrens' Hospital, Tygerberg, South Africa.

[3]Faculty of Health Sciences, Department of Cardio-Thoracic Surgery, Stellenbosch University, and Tygerberg Childrens' Hospital, Tygerberg, South Africa.

*Correspondence to: Dr. P. Goussard, Department of Paediatrics and Child Health, Stellenbosch University, PO Box 19063, Tygerberg 7505, South Africa. E-mail: pgouss@sun.ac.za

Received 22 September 2008; Revised 25 November 2008; Accepted 27 November 2008.

DOI 10.1002/ppul.21007
Published online 12 March 2009 in Wiley InterScience (www.interscience.wiley.com).

an extremely high incidence of tuberculosis with 840 new cases/100,000 population per annum. The tertiary hospital serves as a referral hospital for a population of ~2 million persons. All children with phrenic nerve palsy associated with culture proven MTB were included in the study. During the study period eight cases were collected. All the children were examined clinically and had a chest radiograph taken. The following investigations: HIV test, Tuberculin skin test, and gastric washings for the culture of MTB were performed in all the cases. When indicated chest computer tomography (CT-scan) with contrast and a rigid or flexible bronchoscopy under general anesthetic were performed. If at bronchoscopy the TB lymph glands had eroded into the airway then biopsy specimens of the caesating material were sent for culture.

Pulmonary tuberculosis was diagnosed using modified WHO criteria.[9] The children were treated with an isoniazid (INH) (10 mg/kg/day), rifampicin (10 mg/kg/day) and pyrazinamide (25 mg/kg/day) during the initial 2 months (intensive phase). Ethambutol (15 mg/kg/day) was added during the intensive phase if cavities were visible of the chest X-ray or CT-scan. During the 4 months of the continuation phase patients received INH and rifampicin. Prednisone (2 mg/kg) was added for the first 30 days if there was glandular compression of the airways. The prednisone was weaned over the next month. One child, in contact with an adult index case with proven multidrug resistant tuberculosis, was treated according to the adult index cases' drug susceptibilities.

Ethical approval for publication of this study was granted in retrospect by the Institutional Review Board of the Health Science Faculty of Stellenbosch University.

RESULTS

All children with phrenic nerve palsy associated with culture proven MTB were included in the study. During the study period eight cases were collected. The clinical picture of the eight cases are summarized in Table 1. Four of the cases were female and 755 were younger than 2 years.

Clinical Presentation

Six (75%) children were malnourished. On examination the mediastinum was deviated to the right in all eight children. The clinical sign of phrenic nerve palsy, winging, as well as reduced breath sounds over the left chest was present in all the children. Bronchial breathing (n = 4) was heard over the left hemithorax. The two children who presented with vomiting had severe gastro-oesophageal reflux as demonstrated on barium swallow.

The Diagnosis of TB

In 50% there was a known adult index case with one case known to have multidrug resistant tuberculosis.

TABLE 1—Clinical Details and Management

n	Agemonths	HIV	Symptoms	Ventilation	TB culture	CXR	CT-scan	Enucleation	Plication	Outcome
1	22	Negative	Expansile pneumonia	No	Positive on lung tissue	Elevated left diaphragm plus LUL disease	Airway compression mediastinal shift, displaced aorta	No	No	Died
2	17	Negative	TB meningitis	No	Positive on BAL	Elevated left diaphragm plus LUL disease	Airway compression mediastinal shift, displaced aorta	No	No	Alive
3	24	Negative	TB meningitis	No	Positive on gastric washings	Elevated left diaphragm, bilateral bronchopneumonia	Airway compression mediastinal shift, displaced aorta	Yes	Yes	Alive
4	33	Negative	Expansile pneumonia	No	Positive on gastric washings	Elevated left diaphragm plus LUL disease	Airway compression mediastinal shift, displaced aorta	No	No	Alive
5	16	Negative	Respiratory symptoms and vomiting	Yes	Positive on gastric washings	Elevated left diaphragm plus LUL disease	Airway compression mediastinal shift, displaced aorta	No	Yes	Alive
6	10	Negative	Failure to thrive	No	Positive on gastric washings	Elevated left diaphragm plus LUL disease	Not done	No	Yes	Alive
7	14	Negative	Respiratory symptoms and vomiting	Yes	Positive on gastric washings	Elevated left diaphragm plus LUL disease	Airway compression mediastinal shift, displaced aorta	Yes	Yes	Alive
8	20	Negative	Expansile pneumonia	No	Positive on gastric washings	Elevated left diaphragm plus LUL disease	Airway compression mediastinal shift, displaced aorta	No	Yes	Alive

Tuberculin skin test (Mantoux) was positive (>15 mm induration) in 63% of patients. In only one specimen examined by microscopy were acid-fast bacilli seen (Ziehl Nielsen positive). All of the children were culture positive for MTB. All the cultures were from gastric lavage specimens except for one child, who unfortunately died, was the organism was cultured from post-mortem lung tissue. Drug susceptibility testing was done on three of the cultures with one being resistant to both INH and Rifampicin.

Chest Radiographic Features

In all the cases the left diaphragm was markedly raised. The left upper lobe was consolidated 7 (88%) in cases with half the cases involving all the lobes on the left lung (Fig. 1). Although all the children had left sided disease, airspace disease consistent with bronchopneumonia was visible on the right side in 5 (63%) cases. Left sided hilar lymphadenopathy was only visible in one case as the hilar regions were opacified by the consolidated lobe or lobes. Subcarinal glands were clearly visible in one case. Large airway compression by the enlarged mediastinal lymph nodes was evident in five cases (63%) while cavities on the left side were present in four cases. The trachea deviated to the right in 6 (75%) cases but no children had evidence of tracheal compression. There was no pleural disease.

Fluoroscopy

Fluoroscopy confirmed phrenic nerve palsy in all of the cases with paradoxical movement of the hemidiaphragm on inspiration clearly visible.

Computer Tomography Features

Chest CT-scan was done in seven children. Tracheal and left main bronchus compression was seen in all of the cases as was mediastinal deviation to the right. The descending aorta was displaced to a position anterior to the vertebral column in the seven cases (Fig. 2). The displaced aorta was responsible for partial compression of the left main bronchus, which was the most severe in the children requiring ventilation and in the child that died. Lymph gland enlargement with features typical of TB were seen in the hilar (n – 7), paratracheal (n – 6), and subcarinal (n – 7) areas of the mediastinum. In five cases there was homogenous opacification of the left upper lobe with areas of necrotic liquefaction visible in the opacified lobe (Fig. 3). In all the cases there was accompanying glandular obstruction of the airways (Fig. 4).

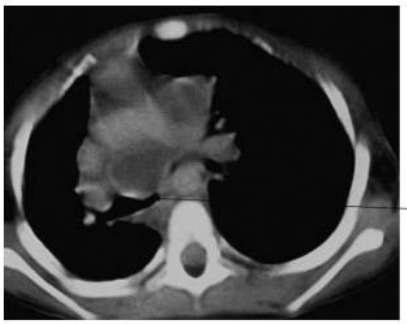

Fig. 2. Computer tomography of the chest demonstrating the mediastinal shift to the right and anterior displacement of the descending aorta to a position anterior to the vertebral body. Compression of the left main bronchus between the enlarged lymph gland with shadow enhancement and the anterior displaced descending aorta is clearly visualized.

Bronchoscopy Findings

Bronchoscopy was performed in five children where airway compression was suspected. The left main bronchus was narrowed in all five cases with the narrowing

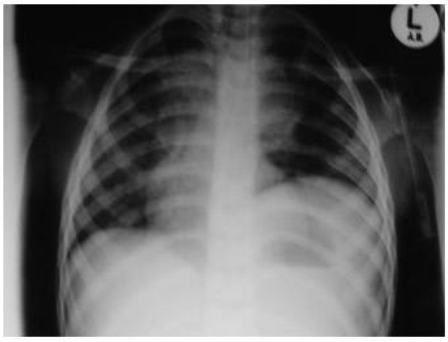

Fig. 1. Chest-radiography demonstrating the evaluated left diaphragm with accompanying mediastinal shift to the right and prominent mediastinal glands on the left.

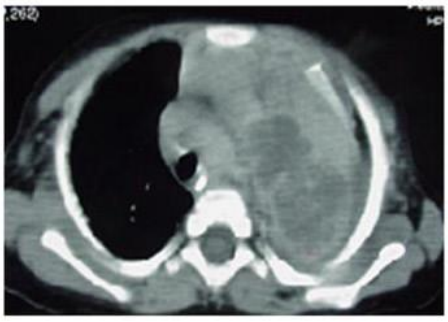

Fig. 3. Computer tomography of the chest with opacification of the left upper lobe with areas of tissue breakdown and liquefaction.

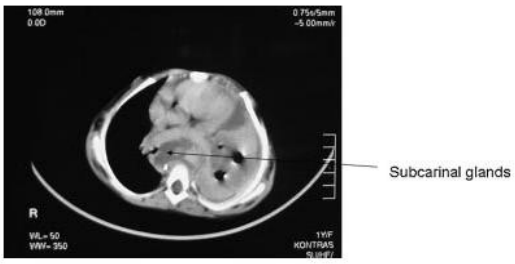

Fig. 4. Computer tomography of the chest with opacification of the left upper lobe and lingula with areas of tissue breakdown and liquefaction. Large subcarinal glands causing compression of both main bronchi.

estimated to be between 30% and more than 90% of the original lumen. Severe compression of the right main bronchus was visible in one case. In one case lymph glands had eroded into the airway (Fig. 5).

Outcome

Two children develop respiratory failure, which required assisted ventilation. Both the ventilated children survived. Two children had severe airway obstruction, which failed to respond to the anti-tuberculosis treatment and steroids. After 1 month of treatment the children required transthoracic enucleation of the glands to relieve the airway obstruction. Both responded well to the enucleation and did not develop any further complications.

Five children (63%) remained symptomatic after completion of TB treatment. They remained tachypneic and developed repeated respiratory tract infections. These children were referred for plication of the diaphragm. Diaphragm plication was performed using a purse-string stitch to reduce the dome of the diaphragm followed by mattress sutures placed in radial orientation on the paralyzed hemidiaphragm. Following placation no complications were noted.

One patient died during hospitalization. The child's post-mortem findings have previously been published.[7] At post-mortem, this child had extensive TB involvement of left lung but also extra pulmonary involvement. The phrenic nerve was clearly infiltrated by the subcarinal lymphnodes. Histology confirmed that the phrenic nerve had been infiltrated and destroyed by the MTB mediated inflammatory process (Fig. 6).

Follow-up chest radiographs were done on all the survivors after completion of therapy. In 4 (57%) the chest radiographs were normal while in all the other cases there had been considerable improvement compared to the initial lesions. In the three cases changes compatible with parenchymal damage and volume loss of the affected lobe was seen. One patient had a massive calcified Ghon focus visible. Two children had recurrent episodes of pneumonia ascribed to underlying lung damage.

DISCUSSION

In this study we describe the clinical, radiological, and clinical outcome of children with phrenic nerve palsy associated with infiltration of the phrenic nerve by MTB infected lymph glands. All cases involved the left phrenic nerve. The phrenic nerve function did not in a single case improve after a full course of TB treatment to which corticosteroids were initially added for a month.

This is a rare clinical condition in children with only three case reports on phrenic nerve palsy caused by MTB in the English literature found.[5–7]

Mohan et al.[6] postulated that phrenic nerve palsy was caused by pressure from the enlarged hilar lymph glands

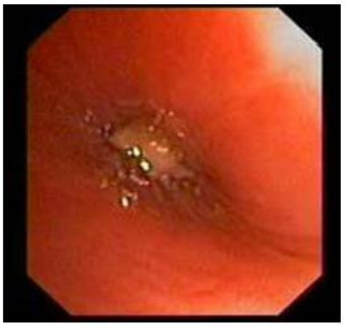

Fig. 5. Bronchoscopy image of the left main bronchus demonstrating narrowing of the bronchus and also a gland that is eroding into the airway. [Color figure can be viewed in the online issue, which is available at www.interscience.wiley.com.]

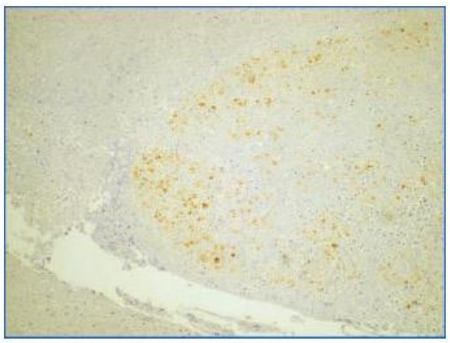

Fig. 6. Histology of the phrenic nerve showing positive neurofilament immunohistochemical staining of the destroyed phrenic nerve in the granulomatous tissue in the left hilar area. [Color figure can be viewed in the online issue, which is available at www.interscience.wiley.com.]

on the phrenic nerve. This implied that the phrenic nerve function would return after treatment. In our experience this is unlikely as this did not occur in any of our cases following treatment. Secondly, the post-mortem finding in the one case demonstrated that the phrenic nerve was infiltrated and destroyed by infiltration from the TB lymph gland.[7]

We previous have published our experience with expansile pneumonia cause by MTB. We reported nine cases with left upper lobe expansile pneumonia where 3 (30%) of the cases were associated with phrenic nerve palsy.[8] The left phrenic nerve is particularly vulnerable as it descends between the left common carotid and subclavian artery, crossing in front of the left vagal nerve from where it passes lateral to the aortic arch and continuing down along the pericardium to just above the diaphragm.[10] The left phrenic nerve is more commonly infiltrated by the TB glands due to the closer relationship to the mediastinal glands to the phrenic nerve when compared to the right side. All the cases we describe were associated with extensive mediastinal gland involvement.

The CT-scan demonstrated the mediastinum displacement to the right with severe compression of the left main bronchus. The descending aorta was displaced to a position anterior to the vertebral column adding to the compression of the left main bronchus. This was especially evident in the two children requiring ventilation and the case that died. These three children had in addition extensive alveolar disease.

Phrenic nerve palsy associated with MTB had a mortality of 13% while and additional two children (25%) required ventilation and two children (25%) required surgery for glandular enucleation to relieve airway obstruction. In children with phrenic nerve palsy respiratory function is more compromised when compared to adults with the same condition. Reasons for this greater compromise include weaker intercostals muscles, horizontal orientated ribs, a very mobile mediastinum and greater compliance of the chest wall.[11,12]

Fluoroscopy have been used to demonstrated paradoxical diaphragm movement during inspiration but Miller et al.[13] have shown that echocardiography is an appropriate and accurate method for assessing diaphragm function in pediatric cardiac patients. Both these diagnostic methods are limited as they are unable to differentiate between phrenic nerve paralysis and paradoxical motion of the diaphragm.[13]

In 63% of the cases there were persistent symptoms or a severe elevation of the diaphragm. These cases were referred for diaphragm plication. Diaphragm plication was performed using a purse-string stitch to reduce the dome followed by mattress sutures placed in radial orientation on the paralyzed hemidiaphragm. Diaphragm plication is done to decrease lung compression, stabilize the thoracic cage and mediastinum and to strengthen the respiratory action of the intercostals and abdominal muscles.[14] Diaphragm plication have been used since 1954 for the treatment of hemidiaphragm paresis.[15,16]

Baker et al.[17] published data suggesting that diaphragm function improves over time after plicaction, but this may be to the nonpermanent nature of the thermal or stretch injury to the phrenic nerve in post-cardiac surgery patients. In not one of the patients that had plication of the diaphragm performed, was there any evidence of improved diaphragm of function. Although 75% of children had persistent volume loss of the left lung after treatment only children had persistent had persistent symptoms and suffered from recurrent infections.

One of the limitations of the study is that we cannot prove that these children had normal phrenic nerve function prior to developing TB. None of these children had thoracic surgery or the placement of intercostals tubes, which could have injured the phrenic nerve. Taking the severity of the initial involvement into account it is unlikely that the children had another cause of phrenic nerve palsy. This is supported by the case describing infiltration and destruction of the phrenic nerve. Another limitation is that we were due to technical limitations not able to do phrenic nerve conduction studies to proven the phrenic nerve dysfunction.

We describe a case series of children with phrenic nerve palsy associated with MTB. Children with this complication are at risk of developing life-threatening disease requiring either early surgical intervention and or ventilatory support. In phrenic nerve palsy associated with TB glandular enlargement did spontaneous recovery after successful anti-tuberculosis treatment occur resulting in a large proportion of the children requiring diaphragm plication.

REFERENCES

1. Simansky DA, Paley M, Refaely Y, Yellin A. Diaphragm plication following phrenic nerve injury: a comparison of paediatric and adult patients. Thorax 2002;7:613–616.
2. Kunovsky P, Gibson GA, Pollock JC, Stejskal L, Houston A, Jamieson MP. Management of postoperative paralysis of diaphragm in infants and children. Eur J Cardiothorac Surg 1993;17:342–346.
3. Nahum E, Ben-Ari J, Schonfeld T, Horev G. Acute diaphragmatic paralysis caused by chest-tube trauma to the phrenic nerve. Pediatr Radiol 2001;6:444–446.
4. Aggarwal S, Hari P, Bagga A, Mehta SN. Phrenic nerve palsy: a rare complication of indwelling subclavian vein catheter. Pediatr Nephrol 2000;3:203–204.
5. Grenet P, Labram C. Phrenic paralysis caused by mediastinal adenopathy in primary tuberculous infection. Med Infant (Paris) 1960;67:53–55.
6. Mohan B, Jayaswal SN. Unilateral diaphragmatic paralysis due to tuberculous hilar adenitis. Indian J Pediatr 1985;22:468–470.
7. Dempers J, Bezuidenhout J, Schneider JW, van Rensburg MJ. Tuberculosis and phrenic nerve destruction. S Afr Med J 2007;97:572–573.

8. Goussard P, Gie RP, Kling S, Beyers N. Expansile pneumonia in children caused by Mycobacterium tuberculosis: clinical, radiological, and bronchoscopic appearances. Pediatr Pulmonol 2004; 38:451–455.
9. Stop TB Patnership Childhood Subgroup, World Health Organization. Guidance for national tuberculosis programmes on the management of tuberculosis in children. Chapter 2: anti-tuberculosis treatment in children. Int J Tuberc Lung Dis 2006;10: 1205–1211.
10. Fell S. Surgical anatomy of the diaphragm and the phrenic nerve. Chest Surg Clin N Am 1998;8:281–294.
11. Commare MC, Kurstjens SP, Barois A. Diaphragmatic paralysis in children. Pediatr Pulmonol 1994;18:187–193.
12. Muller NL, Bryan AC. Chest wall mechanics and respiratory muscles in infants. Pediatr Clin North Am 1979;26:503–516.
13. Miller SG, Brook MM, Tacy TA. Reliability of two-dimensional echocardiography in the assessment of clinically significant abnormal hemidiaphragm motion in pediatric cardiothoracic patients: comparison with fluoroscopy. Pediatr Crit Care Med 2006;5:441–444.
14. Affatato M, Villagra F, de Leon JP, Vellibre D, Sanchez P, Diez Balda JI, Brito JM. Phrenic nerve paralysis following pediatric cardiac surgery. Role of a diaphragmatic plication. J Cardiovasc Surg 1988;29:606–609.
15. de Leeuw M, Williams JM, Freedom RM, Williams WG, Shemie SD, McCrindle BW. Impact of diaphragmatic paralysis after cardiothoracic surgeryin children. J Thorac Cardiovasc Surg 1999;118:510–517.
16. Langer JC, Filler RM, Coles J, Edmonds JF. Plication of the diaphragm for infants and young children with phrenic nerve palsy. J Pediatr Surg 1988;23:749–751.
17. Baker CJ, Boulom V, Reemtsen BL, Rollins RC, Starnes VA, Wells WJ. Hemidiaphragm plication after repair of congenital heart defects in children: quantitative return of diaphragm function over time. J Thorac Cardiovas Surg 2008;135:56–61.

CHAPTER
33

Management of complicated intrathoracic and upper airway tuberculosis in children

Pierre Goussard, Sharon Kling, and Robert P Gie

AIRWAY DISEASE

An understanding of the pathogenesis of primary TB enables one to explain the clinical and radiological presentation of airway disease. When the primary infection is not contained, the infected lymph nodes adjacent to the large airways, particularly the bronchi, increase in size, compressing the airway and infiltrating the airway wall. The clinical and radiological pictures that arise depend on the degree of airway narrowing and nodal ulceration into the airway. If the nodes ulcerate into the airway the caseous material can be inhaled into either the lobe or a segment. There is an initial hypersensitivity reaction to the inhaled tuberculous material. As the obstruction of the airway by the ulcerating node increases and then becomes complete, the reaction changes from a hypersensitivity reaction to caseation and liquefaction of the lung tissue. The reaction in the lung is an expansile process, which is recognized radiologically as an expansile pneumonia.[1] These forms of TB are collectively called *lymphobronchial tuberculosis*. Lymphobronchial TB was more common in the prechemotherapeutic era with compression syndromes detected in up to 67.8% and bronchial perforation in 27.8% of the patients studied.[2] Other risk factors for this type of TB are a young age and severe malnutrition.[3,4]

CLINICAL PRESENTATION

The clinical presentation depends on which anatomical part of the airway is involved. The involvement can be supraglottic, extrathoracic, intrathoracic or a combination of these. The clinical signs and symptoms will also depend on the degree of external compression and whether the nodes have ulcerated through the airway wall. Bilateral airway involvement especially of the large bronchi will present differently from unilateral involvement. Airway obstruction can be either complete or incomplete.

Extrathoracic airway obstruction presents with stridor, which may be either inspiratory or present during both inspiration and expiration. Intrathoracic obstruction presents with monophonic wheezing. The wheeze may be audible on one or both sides of the chest, depending on the degree of obstruction. Occasionally the involved nodes obstruct the bronchi, causing a clinical picture that may be confused with asthma, but responds poorly to bronchodilators. Children with partial obstruction of the airway may develop a ball-valve effect, where air can enter the lung but is trapped on expiration. These children have hyperinflation and hyperresonance of the affected side of the chest. Air entry over the involved lung is decreased on auscultation and wheezing with prolonged expiration is heard. When the obstruction is complete, lung or lobar collapse can develop, with reduced or no ventilation to the affected part of the lung.

CHEST RADIOGRAPHIC APPEARANCES

Airway compression

Lymphadenopathy may be clearly visible on a chest radiograph (CXR), or there may be indirect evidence of its presence indicated by airway narrowing or deviation. Mediastinal lymph nodes are usually visible in cases of bronchial obstruction. In younger patients often the only sign of lymph node airway compression is narrowing of the major airways.[3] Tracheal deviation to the right is normal and a shift to the left is abnormal except when a right-sided aortic arch is present. Tracheal deviation to the left might be the only sign of paratracheal lymph node enlargement. Subcarinal nodes may also be difficult to detect. In a patient without cardiac disease a double shadow below the carina is often a sign of subcarinal lymph node enlargement especially if there is also a shift in the para-oesophageal adhesion line. Further evidence of subcarinal lymph node enlargement is compression of both main bronchi.

The frontal high-kilovolt (kV) radiograph has been used to assess the effect of TB lymph nodes on the tracheobronchial tree. It has been demonstrated that the specificity for the detection of TB lymph nodes increased from 74.4% to 86.6% with the addition of the high-kV radiographs (Fig. 33.1).[5] However, the authors felt the data did not support the routine use of high-kV radiographs in the diagnosis of childhood pulmonary TB.

If the airway obstruction is complete, lung collapse with volume loss will be seen on the CXR. Bronchus intermedius is a common region for complete airway obstruction, resulting in collapse of the right middle and lower lobes. In most cases the obstruction clears on treatment.

Unilateral hyperinflation (Fig. 33.2)

This is not a common radiological picture. As the airways start to narrow, a point is reached where the narrowing acts as a 'check valve' allowing air to be trapped in the affected lobe or lung. On the CXR unilateral hyperinflation with a flattened hemidiaphragm is seen. The involved lung has reduced vascularity and herniates across the midline if severe air trapping is present. The bronchus of the involved lung is narrowed and enlarged lymph nodes may be visible. On the lateral chest radiograph air is visible in the anterior mediastinum. The diagnosis is best made by combining the clinical examination with the radiological picture.

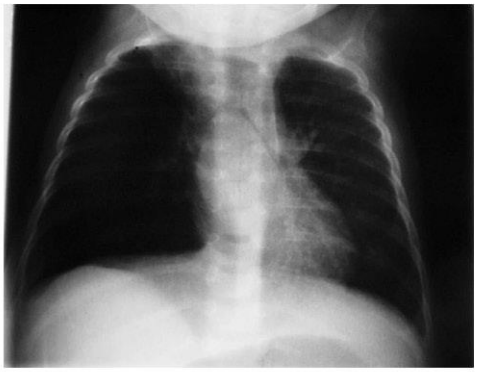

Fig. 33.1 High-kilovolt chest radiograph demonstrating TB lymph node compression of both main bronchi.

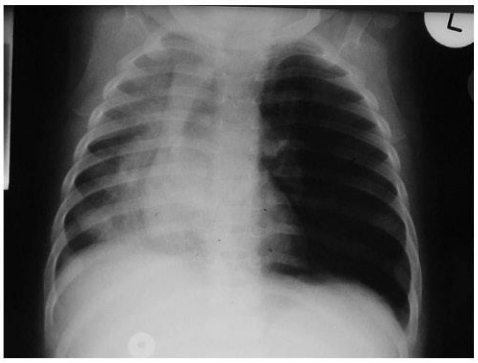

Fig. 33.2 Chest radiograph of a child with a ball-valve effect (left-sided hyperinflation) caused by lymph node compression of the left main bronchus.

A bronchogram (Fig. 33.3) can be performed with non-ionic, water-soluble contrast medium in intubated patients and is useful when bronchoscopy is not available. The procedure is safe, but can cause transient desaturation.[6]

COMPUTED TOMOGRAPHY (CT) SCAN APPEARANCE

A chest CT scan should be done in children with clinically and radiologically significant airway compression. The CT scan shows the location of nodal involvement and the relationship of these nodes to the airways, and will assist in assessing whether a patient will benefit from lymph node enucleation. Patients with small lymph nodes or lymph nodes that have already calcified will not benefit from enucleation. The CT scan also guides the surgeon in deciding from which side the thoracotomy must be done. Andronikou et al.[7] have shown that the most common locations for tuberculous lymph node enlargement are the subcarinal area (90%), right hilum (74%), left hilum (72%), both hila (61%), anterior mediastinum (79%), precarinal (64%) and right paratracheal

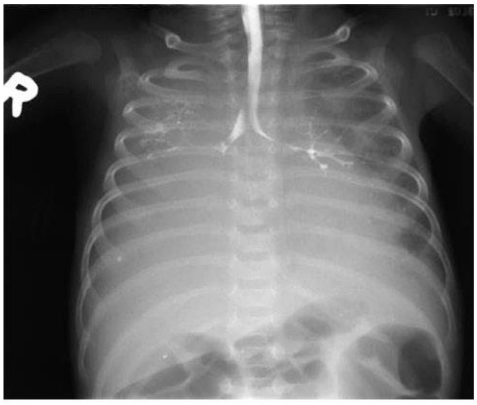

Fig. 33.3 Tracheobronchogram performed with non-ionic, water-soluble contrast medium in an intubated patient suspected of having TB nodal obstruction, showing obstruction of bronchus intermedius, splaying of the carina and narrowing of the left main bronchus.

(63%). The largest group of nodes was located in the subcarinal area in 87% of cases. The most common site of airway compression was the left main bronchus (21%), followed by the right main bronchus (14%) and bronchus intermedius (8%).

BRONCHOSCOPIC FINDINGS

Both flexible and rigid bronchoscopy play a role in the management of children with airway obstruction. The advantage of the flexible bronchoscope is that the smaller airways can be reached and the airway obstruction bypassed to evaluate the airway distal to the area of obstruction. Rigid bronchoscopes are best used for transbronchial lymph node enucleation, as the patient can be ventilated during the procedure and larger instruments can be used (Fig. 33.4). It is possible to remove tissue via a flexible bronchoscope, but this is limited by the size of the forceps that can be passed through the working channel (Fig. 33.5).

Indications for bronchoscopy

Bronchoscopy is not indicated for routine specimen collection in TB. The yield for positive culture via bronchoscopy is less than that of gastric aspirate culture.[8–10]

Bronchoscopy can be used to confirm the diagnosis of TB, as well as the site and extent of airway obstruction. Chest radiographs underestimate the presence and the degree of airway obstruction, which may be present without visibly enlarged hilar and mediastinal lymph nodes. Tuberculous lymph nodes may cause obstruction by compression of or ulceration into the airways, with granulation tissue and caseating material obstructing the airway. The granulation tissue and caseating material can be removed via a rigid bronchoscope. Repeated bronchoscopies may be required to remove the material if the patient's clinical condition or radiological picture fails to improve.[11]

Bronchoscopy findings

The most common bronchoscopic findings are extrinsic compression of the bronchi or the trachea (37%) (Fig. 33.6).[12] Bronchial involvement, with granulation tissue and caseous material causing obstruction

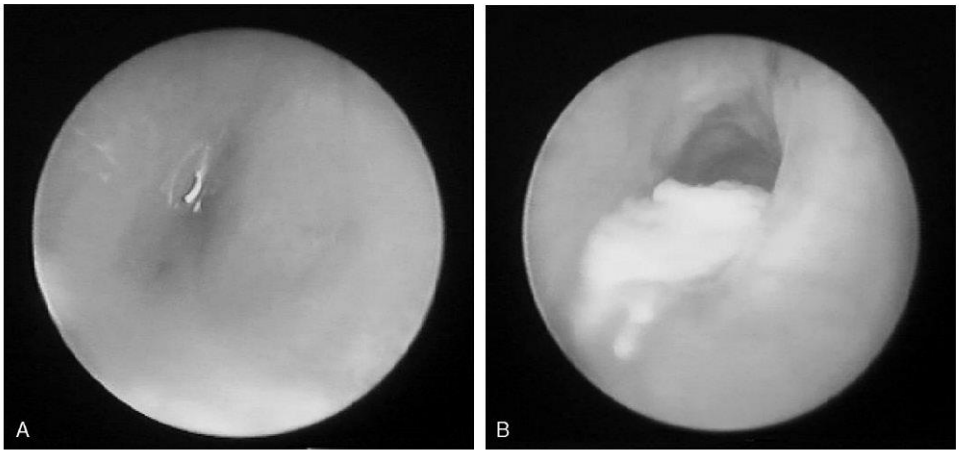

Fig. 33.4 Nodal compression of the left main bronchus (A) before and (B) during bronchoscopic enucleation, demonstrating drainage of caseating material from the left upper lobe.

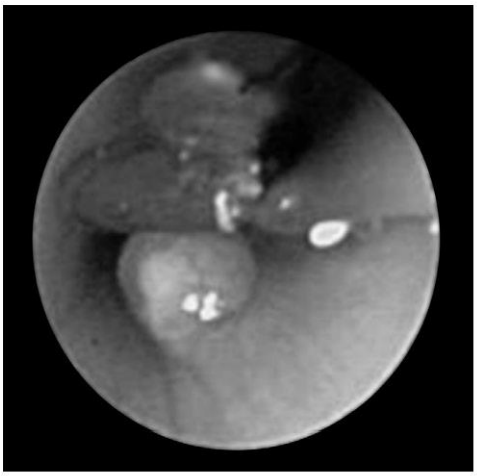

Fig. 33.5 Lymph node herniating into the left main bronchus, being removed with flexible bronchoscope.

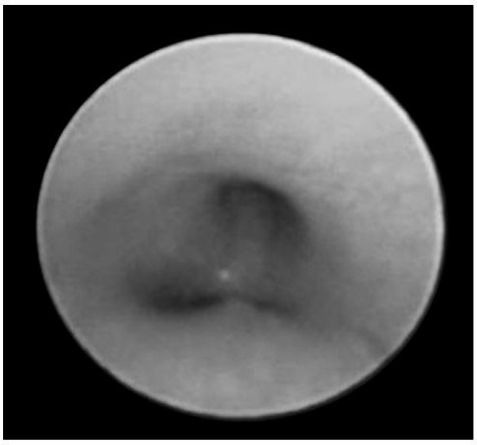

Fig. 33.6 Bronchoscopic picture of near complete obstruction of bronchus intermedius.

and mucosal inflammation, was found in 48% of children without detectable lymphadenopathy on the chest radiographs.[12]

MEDICAL MANAGEMENT

Standard three-drug anti-TB treatment (isoniazid, rifampicin, pyrazinamide) is used in children with airway obstruction. A fourth drug is added when cavities are present on chest radiograph.

There is very little information about the use of corticosteroids in the treatment of lymph node obstruction of the airways. There are conflicting data in the literature. Early reports from the 1960s were that corticosteroids were effective in decreasing airway obstruction if given early in the course of the disease.[13–15] These claims were not supported in a double-blind study looking at the effect of prednisone on lymph node disease.[16] In a follow-up study the 36% of the group receiving prednisone had an improved outcome when compared with the placebo group.[17] It seems that corticosteroids give a more rapid improvement and less nodal ulceration into the airways than conventional treatment, but the eventual outcome is similar.[18] In view of the potential side-effects of corticosteroids, care should be taken with their use in childhood TB. We prescribe prednisone (2 mg/kg/day) in children who are symptomatic due to airway obstruction. The prednisone is given for 1 month and then weaned over the next month. The children are followed up every 2 months. If the child is still symptomatic after 1 month's therapy, bronchoscopy is indicated. Children with unilateral hyperinflation due to a ball-valve effect do respond to

medical treatment, but they may become very symptomatic with severe airway obstruction if superimposed infection develops. This is usually seen in infants less than 6 months of age.

SURGICAL MANAGEMENT

Surgical intervention can be used as adjuvant treatment for tracheobronchial complications stemming from mediastinal tuberculous lymphadenitis. The surgical intervention can be either endoscopic or via thoracotomy.

Endoscopic enucleation is indicated in children where the lymph nodes have herniated through and ulcerated into the airways (Figs 33.7 and 33.8). The advantage of endoscopic enucleation is that tissue can be sent for culture. Only a small group of children benefit from endoscopic enucleation. The reason for this is that the enucleated lymph nodes, which are situated outside the airway, continue to leak caseous material into the airways and granulation material continues to form. Endoscopic enucleation is best suited for children with single lesions causing lobar collapse. Acute perforation of a major airway is rare but can present with severe respiratory embarrassment. Bronchoscopy for removal of the caseous material and relief of the obstruction is indicated.[19] Endoscopic enucleation of nodes is safe, but care must be taken that too much tissue is not removed. Complications include bleeding, perforation of the bronchus wall with a pneumothorax and creation of a broncho-oesophageal fistula. Endoscopic enucleation is mostly done through a rigid bronchoscope, but can also be done via a flexible bronchoscope. No studies looking at the outcome of endoscopic enucleation have been published.

Four studies on surgical transthoracic enucleation have been published. There are no clear indications when to perform enucleation. The presence of lymph nodes alone is not an indication for surgery unless they cause complications, such as acute perforation of a major airway with severe respiratory embarrassment, pressure and occlusion of a major airway with lung collapse or hyperinflation, bronchial stenosis due to fibrosis and, rarely, superior vena cava obstruction or subcarinal oesophageal obstruction.[19]

A number of factors must be taken into account when considering surgery. These include the age of the child, the degree of airway involvement as assessed by bronchoscopy, the position and character of the lymph nodes causing the obstruction and the clinical response to antituberculous therapy together with corticosteroids. Clear indications for surgery include assisted ventilation for airway obstruction and life-threatening airway obstruction. A symptomatic child who has received 1 month's therapy should have a repeat bronchoscopy performed. If at bronchoscopy the airway narrowing is judged to be more than 75%, enucleation should be considered. Prior to bronchoscopy a CT scan of the chest should be done to determine the size, site and character of the lymph nodes. Lymph nodes that are calcified will not be successfully enucleated. The situation of the lymph nodes will determine the side from which the thoracotomy will be done (Fig. 33.9). The most common lymph nodes obstructing the main bronchi are the subcarinal and paratracheal groups, compressing the proximal main bronchi or the distal trachea between them.[20] Decompression of the subcarinal lymph nodes is important if both the left and right main bronchus are compressed (Fig. 33.10). The lymph nodes are easier to enucleate earlier in the disease process. During enucleation overzealous dissection must be avoided. The procedure entails partial resection of the lymph nodes and evacuation of mucopus within the gland by careful curettage. Lung resection

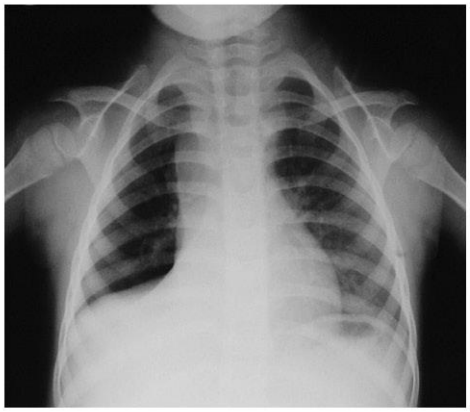

Fig. 33.7 Chest radiograph showing collapse of the right middle and lower lobe. The right hilar nodes are enlarged.

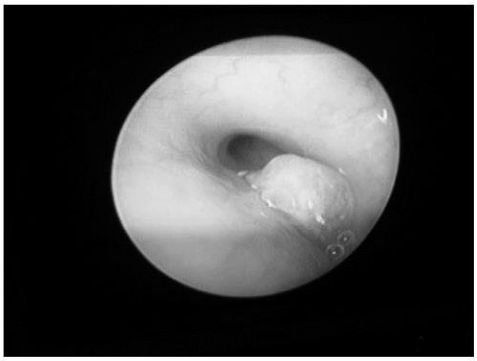

Fig. 33.8 Bronchoscopy showing lymph nodes, which have herniated into bronchus intermedius.

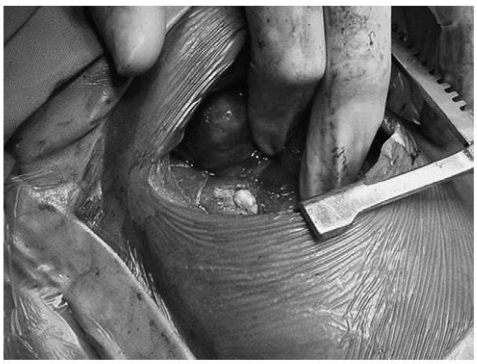

Fig. 33.9 Transthoracic surgical enucleation of TB nodes, caseating material visible.

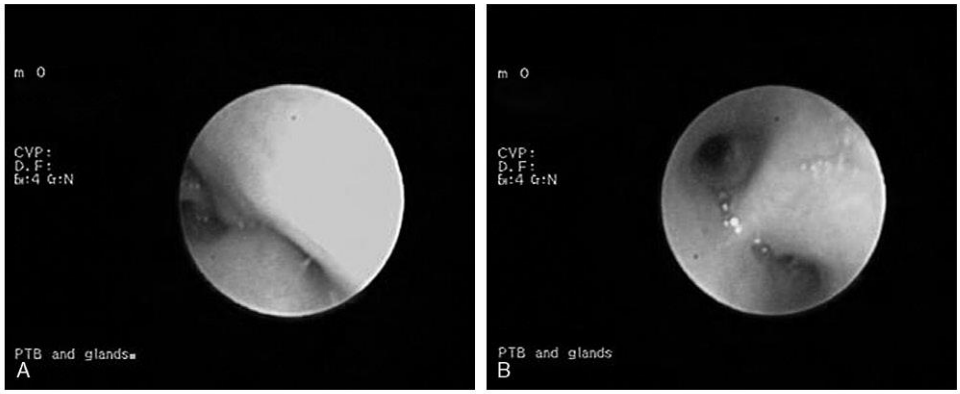

Fig. 33.10 Bronchoscopic pictures (A) before and (B) after surgical transthoracic enucleation of nodes.

should be avoided at all cost as nearly all children improve with time.[19] The reported complication rate resulting from enucleation is low and includes bronchial tear, pulmonary artery laceration and bronchopleural fistula.[20,21] Bronchopleural fistulae mostly resolve with intercostal drainage; if unsuccessful, surgery may be necessary.

COMPLICATIONS

The role of surgery in airway compression caused by TB is not only to relieve airway compression but also to prevent future damage to the lung parenchyma. Untreated airway compression can lead to lung collapse and bronchiectasis. Hewitson and van Oppel[20] reported that the indications for pulmonary resection are symptomatic bronchiectasis not controlled with conservative measures, destroyed lung parenchyma that is the site for recurrent or chronic infection and infected pulmonary cavitation with or without fungal infection. Pulmonary resection is best avoided during the acute phase, as the surgery is difficult and resulting bronchiectasis rare. The lung heals by fibrosis with a small risk of infection. Bronchiectasis of the lower lobes is the most common indication for resection. Chronic bronchus intermedius obstruction can lead to right middle and lower lobe destruction requiring resection. Gross parenchymal destruction may be the source of secondary bacterial or fungal suppurative infections, which result in bronchiectasis.

PLEURAL DISEASE

CLINICAL PRESENTATION

Pleural effusion due to *Mycobacterium tuberculosis* is categorized as extrapulmonary TB.[22,23] It develops as a complication of primary TB in 2–38% of children with pulmonary TB. Effusion is not a common feature of primary TB in young children. As adolescence approaches the number of children presenting with large pleural effusions becomes more common. An effusion occurs when the primary focus ruptures into the pleural cavity, releasing the tuberculoprotein and a small number of bacilli. The pleural effusion results from a hypersensitivity immune response to the tuberculoprotein in the pleural cavity. It is usually unilateral.

Children with pleural effusions usually present with fever and an insidious onset of shortness of breath. Clinically the TB effusion can be differentiated from other causes of empyema in that the children are not toxically ill, although they can have a high fever. These large pleural effusions are difficult to differentiate radiologically from other causes of pleural effusion, as hilar adenopathy is seldom visible. The effusion can vary in size from complete opacification of the hemithorax to obliteration of the costophrenic angle. After draining the effusion the enlarged glands or primary focus may become visible. Parenchymal consolidation (59%) is the most common associated radiographic finding.[24] In younger children the effusion is mostly part of complicated lung disease. The pleural effusion is normally an inconsequential part of miliary TB, or lobar or bronchopneumonic TB.

The diagnosis of TB pleural effusion is made from the clinical and radiological pictures. The diagnosis can be further substantiated by doing a diagnostic tap, with TB characterized by the predominance of lymphocytes in the fluid.

In nearly all cases the TB effusion clears up rapidly on treatment. After 3–4 weeks of treatment the pleural effusion will have cleared with only slight pleural thickening still being present.

Complicated pleural TB is rare in children. Chest CT scan features of complicated pleural effusions include pleural thickening and enhancement, and fluid collections with associated parenchymal lesions and lymphadenopathy (Fig. 33.11).

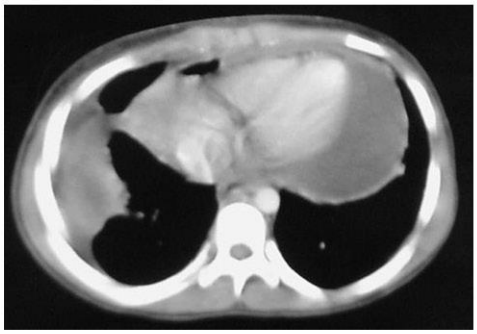

Fig. 33.11 Chest CT scan demonstrating complicated pleural disease caused by TB. A pericardial effusion is also visible.

Chronic tuberculous empyema is characterized by persistent and grossly purulent pleural fluid. This fluid contains numerous tubercle bacilli. Chest CT scan is used to differentiate between pleural thickening and a chronic loculated effusion or empyema, as they have the same appearance on chest radiograph.[25]

MANAGEMENT

The approach to children presenting with an effusion suggestive of TB is as follows. If the effusion is small, only a diagnostic tap may be necessary. If the effusion is large and the child is symptomatic, the fluid can be aspirated, with either a needle or a pigtail catheter. Very large effusions must be drained slowly because of the risk of re-expansion pulmonary oedema. If it is not possible to drain the fluid, it is either loculated or an organized pleural effusion. If the fluid is loculated, an ultrasound-guided aspiration can be attempted.

Tuberculosis effusions are exudative with protein > 30 g/L or lactate dehydrogenase (LDH) > 200 U/L, with a lymphocytic predominance. The fluid must be sent for Ziehl–Neelsen (ZN) stain and TB culture. The ZN recovery rate from pleural fluid is very low (5.5%).[24]

Several biochemical markers have been used for the diagnosis of tuberculous pleural effusions including adenosine deaminase (ADA), lysozyme, interferon-γ and *M. tuberculosis* DNA detected with polymerase chain reaction (PCR). The most extensively studied have been ADA.[26] Ena et al.[27] have confirmed in a meta-analysis that ADA has a high sensitivity and a high negative predictive value in the diagnosis of TB pleural effusion.

A pleural exudate with high ADA levels (40 U/L) is usually due to TB or rheumatoid arthritis; other possibilities are haematological malignancies and empyema. If the pleural fluid is rich in lymphocytes and has a high ADA, the most likely diagnosis is TB. If the ADA is low, haematological malignancies are the most likely cause. A high ADA in a neutrophil-predominant pleural effusion suggests parapneumonic effusion, particularly empyema.[26]

The combination of culture and histological examination has been described as the most sensitive diagnostic test for pleural TB. The histological changes seen on pleural biopsy are granulomatous inflammation.

Several adult studies on tuberculous pleurisy have suggested that corticosteroid therapy may reduce morbidity, decrease pleural thickening and cause more rapid absorption of the pleural fluid.[8,29–32] Randomized controlled trials of corticosteroid therapy failed to show clinically relevant earlier symptom relief or a beneficial effect on residual pleural thickening after early complete drainage of the effusion.[33,34] No childhood studies on the use of corticosteroids are available.

Chronic tuberculous empyema must be drained surgically, and decortication may be necessary to expand the lung. Biopsies should be taken for culture and histology. Radiographic clearing of chronic TB empyema may take up to 1 year.

EXPANSILE PNEUMONIA

Expansile pneumonia is a radiological diagnosis. It is characterized by increased volume of the affected lobe or segment due to pneumonia. It has the appearance of a densely consolidated lobe or segment with bulging fissures and is rare in childhood. The most common bacterial causes of expansile pneumonia are *Klebsiella pneumoniae* and *Staphylococcus aureus*. Expansile pneumonia caused by *K. pneumoniae* usually involves the upper lobes.[35,36]

Fungal pneumonia in immunocompromised and neutropenic children caused by *Aspergillus fumigatus* presents as expansile pneumonia with the characteristic halo sign appearance on CT scan.[37,38] Tuberculosis is seldom considered as a cause of expansile pneumonia in countries with a low incidence of TB, but in areas with a high incidence this clinical presentation is relatively common. In the literature there is confusion as to what the correct terminology is for describing the combination of airway and parenchymal disease in children with TB. Initially the clinical term 'epituberculosis' was used to describe a chronic illness in children with indefinite clinical signs but with a homogeneous opacity extending from the hilar region into part of the lobe on the chest radiograph. These children were not very ill, and in most cases the lesion resolved without therapy.[39] The term 'endobronchial TB' was used when lymph node involvement of the airway led to obstruction of the bronchus. Seal and Thomas[40] described tuberculous pneumonia as aspiration of caseous material due to perforation of the airway by lymph nodes distal to lobar or segmental bronchial obstruction. It was thought that the lobe became congested and oedematous, and these enlarged lobes on chest radiography were termed a 'wet' or 'drowned' lung.[41] Others used the term 'lymphobronchial TB' to describe the lesions that result from lymph node involvement of the airways in children. Expansile pneumonia is one of the radiological pictures of lymphobronchial TB.[42]

PATHOLOGY

The term lymphobronchial TB is useful, as it partially explains the pathogenesis of the disease. Other radiological pictures of lymphobronchial TB are bronchial compression, unilateral hyperinflation and lobar or segmental collapse. It is speculated that the pathogenesis of these lesions follows narrowing of the airways by mediastinal lymph nodes. The enlarged nodes infiltrate the bronchial wall, eventually rupturing into the bronchus. The caseating material, containing both viable organisms and tuberculous material (tuberculoprotein), is aspirated into the affected lobe. In the lobe, an allergic response develops, causing the expansile pneumonia. This hypothesis is supported by the observation that lesions similar to those seen in these children develop after the injection of tuberculoprotein into the lobes of rabbits.[43]

CLINICAL PRESENTATION

Children with expansile pneumonia caused by *M. tuberculosis* are mostly younger than 24 months but this presentation can also be seen in older children. The children present with three distinct clinical pictures: non-resolving pneumonia, large airway obstruction with unremitting monotonic wheezing and persistent lobar collapse. Most patients will be referred with pneumonia that has not responded to antibiotics. The great majority of these children will be culture positive for *M. tuberculosis*.[1]

CHEST RADIOGRAPHIC FEATURES

Homogeneous opacification with displacement of the fissures of the affected lobe or lobes is seen in all cases (Fig. 33.12). The involvement is usually lobar, but segmental involvement has also been seen. Air bronchograms are seldom visualized in the consolidated lobe. Hilar lymphadenopathy is difficult to see because the hilar regions are obscured by the consolidated lobe or lobes. Indirect evidence of mediastinal lymphadenopathy resulting in compression of the large airways can be seen in most cases. The upper lobes are most frequently involved, with the left upper lobe more commonly

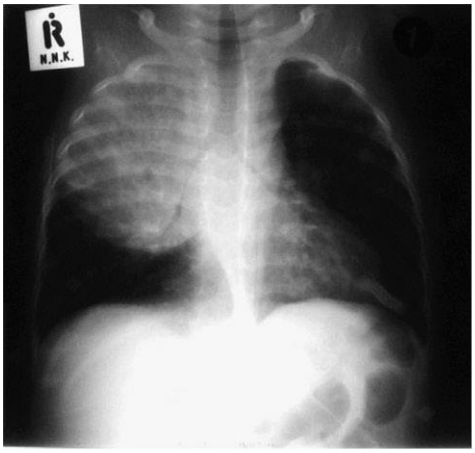

Fig. 33.12 Expansile pneumonia of the right upper lobe with bilateral bronchial compression.

involved than the right upper lobe. The middle lobe, lingula and lower lobes are less frequently involved. Pleural effusions in combination with expansile pneumonia are rare.[1]

COMPUTED TOMOGRAPHY APPEARANCE

Three patterns of CT appearance have been identified. The first is that of a dense homogeneous opacification with no evidence of liquefaction of the affected lobe and patent airways, so that air bronchograms are visible. The second, the most common picture, consists of homogeneous opacification with areas of necrotic liquefaction in the opacified lobe, together with nodal obstruction of the airways and absence of air bronchograms (Fig. 33.13). The third picture consists of a combination of the foregoing, with a homogeneously opacified lobe and areas of necrotic liquefaction as well as lobes with homogeneous opacification, patent airways and visible air bronchograms. Chest CT scan provides additional information regarding subcarinal lymphadenopathy and tracheal compression not seen on routine chest radiographs (Fig. 33.14). Hilar lymphadenopathy with ring enhancement is also visible in all cases.[1]

BRONCHOSCOPY FINDINGS

Severe airway compression is seen in a large number of children with expansile pneumonia caused by *M. tuberculosis*. These infants are also at risk of these nodes herniating into the airways. There is a correlation between the chest CT scan findings and the bronchoscopic findings. In one study, patients with necrotic liquefaction of the lobe had a degree of airway obstruction greater than 75%, compared with those with homogeneous opacification without evidence of liquefaction and patent airways on CT scan who had less than 75% obstruction of the lobar bronchus.[1]

MANAGEMENT

Bronchoscopy must be done in children with signs and symptoms of severe large airway obstruction. Children with expansile pneumonia on chest radiograph but without signs and/or symptoms of airway obstructions do not warrant bronchoscopy. Chest CT scan can be done to confirm the diagnosis and to determine the cause and degree of airway obstruction.

These children are treated with isoniazid (INH) (5–10 mg/kg/day), rifampicin (10 mg/kg/day), pyrazinamide (25 mg/kg/day) and ethambutol (20 mg/kg/day) for 2 months (intensive phase) and with INH and rifampicin for a further 4 months during the continuation phase. Prednisone (2 mg/kg/day) is added for the first 30 days and then weaned over the next month.[18] During the first month of treatment children must be closely monitored. If there is no or very little improvement in the clinical and/or

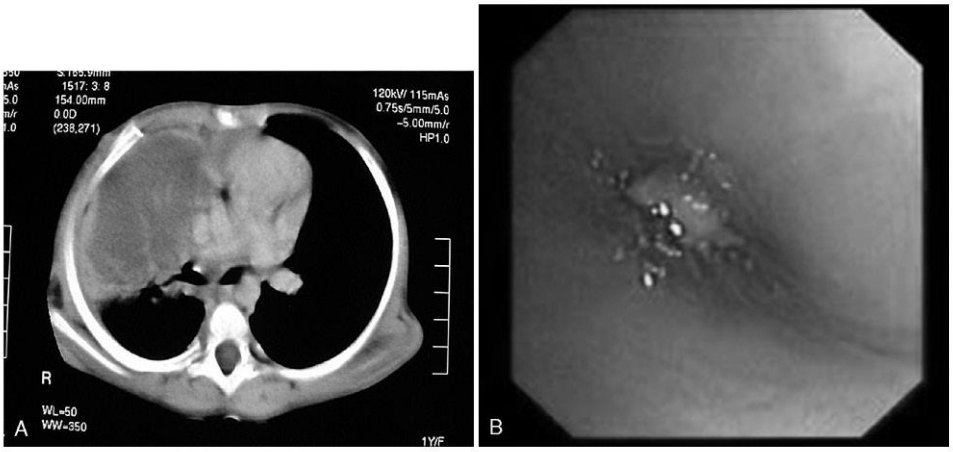

Fig. 33.13 (A) Chest CT scan demonstrating homogeneous opacification of right upper lobe. In the opacified lobe, extensive areas of liquefaction are visible. (B) The right upper lobe bronchus is also obstructed.

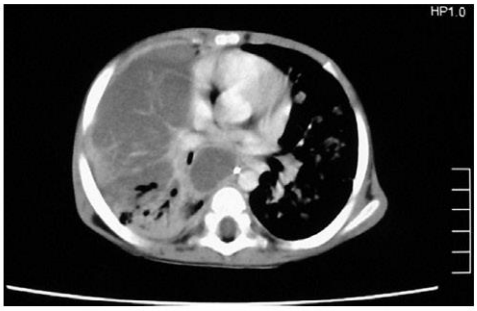

Fig. 33.14 Chest CT scan demonstrating homogeneous opacification with areas of liquefaction of the right upper lobe. Large subcarinal lymph nodes causing airway compression are also present.

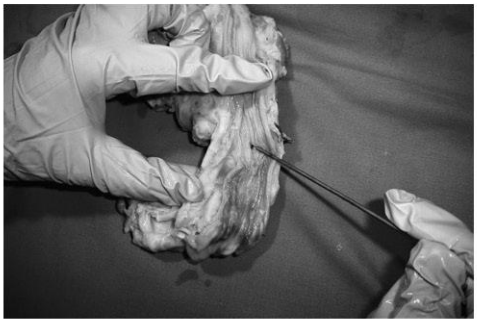

Fig. 33.15 Postmortem specimen showing a broncho-oesophageal fistula opening in the oesophagus.

radiological condition of the child after 1 month, bronchoscopy is indicated. The airways must be evaluated for obstruction by lymph nodes and where possible an attempt made to enucleate the obstructing lymph nodes. If bronchoscopic enucleation is not possible or unsuccessful, and the child's clinical condition warrants it, surgical nodal enucleation via thoracotomy is indicated. Expansile pneumonia caused by *M. tuberculosis* has a good short- and long-term prognosis, if treated correctly. Most children will have considerable improvement in their chest radiographic appearance after 6 months of TB treatment. Although volume loss has subsequently been seen in the affected lobe in 68% of cases, recurrent infection and bronchiectasis are rare.

BRONCHO-OESOPHAGEAL FISTULA

CLINICAL PRESENTATION

The sudden onset of coughing following ingestion of fluids, in particular if combined with symptoms and signs of acute pneumonia or a history of repeated respiratory tract infections, should alert the physician to the possibility of a tracheo- or broncho-oesophageal fistula. Congenital tracheo-oesophageal fistulas are often considered in the differential diagnosis, while acquired fistulas are seldom thought of, as they are rare. Fifty per cent of acquired oesophago-respiratory fistulae in adult patients are due to benign causes.[44] In adults, 10–19% of acquired non-malignant broncho-oesophageal fistulae (BOF) are caused by *M. tuberculosis*. In children, acquired broncho-oesophageal fistula is an uncommon complication of trauma, foreign body ingestion and pulmonary TB.[45,46] In children, BOF caused by *M. tuberculosis* are rare and mostly fatal. This complication has been described in seven children in the English language literature.[45–51] BOF caused by *M. tuberculosis* present as one of three clinical pictures: acutely with severe respiratory distress requiring ventilation, a chronic picture with repeated aspiration and following surgery for tuberculous node enucleation. BOF caused by *M. tuberculosis* are mostly left-sided, although one case of right-sided BOF has been reported.[47] Tuberculous BOF results from the erosion of tuberculous peribronchial lymph nodes into both the oesophagus and bronchus (Fig. 33.15). They may also result from direct extension of tuberculous ulceration or perforation of a tuberculous abscess. Less frequently, a fistula may follow direct spread from thoracic vertebral TB or be a complication of endotracheobronchial TB.[46] Oesophageal TB is rare and is almost always secondary to pulmonary TB.

DIAGNOSIS

In many cases in which a tracheobroncho-oesophageal fistula is clinically suspected, the diagnosis can be confirmed by barium swallow (Fig. 33.16). Water-soluble contrast medium must be used to reduce the complication of aspiration. These fistulas are mostly left-sided and are seen on contrast studies, just distal to the origin of the left main bronchus. Bronchoscopy is a useful additional investigation for a suspected fistula. When *M. tuberculosis* is the cause of the fistula the origin is mostly in the bronchus, and not in the trachea as with congenital tracheo-oesophageal fistulas. The origin of the fistula is close to the carina. Visualization of the

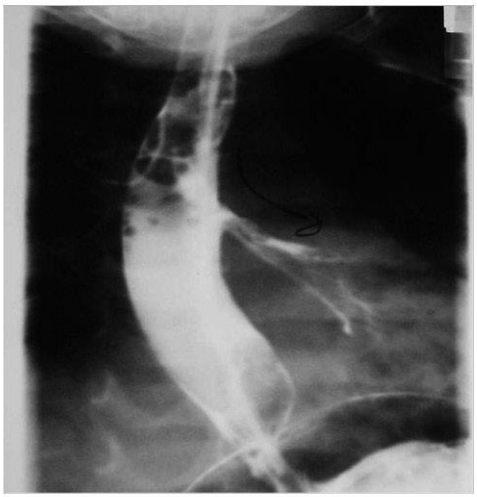

Fig. 33.16 Barium study demonstrating a broncho-oesophageal fistula between the left main bronchus and the oesophagus.

origin might be difficult as it is hidden in a granuloma caused by caseating lymph nodes that have herniated into the airway. Communication between the tracheobronchial tree and the oesophagus can be demonstrated by instilling methylene blue into the oesophagus and visualizing the dye in the tracheobronchial tree. In ventilated children a tracheobronchogram can be used to demonstrate the fistula by means of radiocontrast medium being instilled via the endotracheal tube.[47]

MANAGEMENT

The management depends on the clinical presentation. The child presenting with a chronic picture with repeated episodes of aspiration is managed conservatively. These children must be treated with INH, rifampicin and pyrazinamide for 2 months and with INH and rifampicin for a further 4 months during the continuation phase. Although there is no evidence to support it, it is thought advisable to treat these patients for a longer period of time. To prevent repeated episodes of aspiration the child must be fed via a nasogastric tube. In contrast to the adult literature, the cases of broncho-oesophageal fistula in children failed to close on anti-TB treatment alone. Surgical intervention after 6 months of TB treatment was required.[47] Ligation of the fistula can be difficult because of all the adhesions that have formed.

Treating children with a broncho-oesophageal fistula who present with respiratory failure needing ventilation can be a major challenge. The survival rate of children with BOF requiring ventilation is very poor, with only one survivor reported.[52] The patients died because adequate ventilation could not be achieved by either conventional mechanical ventilation or high-frequency oscillatory ventilation (HFOV). The reasons for not achieving adequate ventilation include the fact that not only is there a large air leak between the airway and the oesophagus, but these children also have nodal compression of the large airways in addition to their significant parenchymal disease. This results in very ineffective ventilation with hypercarbia and severe hypoxia. Previous interventions included attempts to ligate these fistulae surgically, passing a Sengstaken–Blakemore tube and selective intubation into the right main bronchus during the acute phase. These efforts were all unsuccessful as the patients succumbed during surgery. Extracorporeal membrane oxygenation (ECMO) might be an alternative form of treatment if it is available. Recently the use of an oesophageal stent to aid in the ventilation of a child with an acquired broncho-oesophageal fistula caused by *M. tuberculosis* was described (Fig. 33.17).[52] The covered stent was able to seal the air leak by compressing the fistula between the endotracheal tube and the stent. In this case the stent provided time for the parenchymal lung disease to improve, and made successful extubation possible. Radecke et al.[53] have shown that in 73.3% of adult patients the leak in the oesophagus could be successfully sealed by stent placement. They have also shown that this is a safe, technically feasible, effective and relatively inexpensive option to treat oesophageal fistulae, perforations and anastomotic leaks. Studies on the use of these stents in children with TB are lacking.

The management of a child with a broncho-oesophageal fistula requiring ventilation includes the following:

1. Intubate with a cuffed endotracheal tube.
2. Pass a nasogastric tube to decompress the stomach. Place the nasogastric tube on suctioning.
3. Confirm BOF with flexible bronchoscopy.

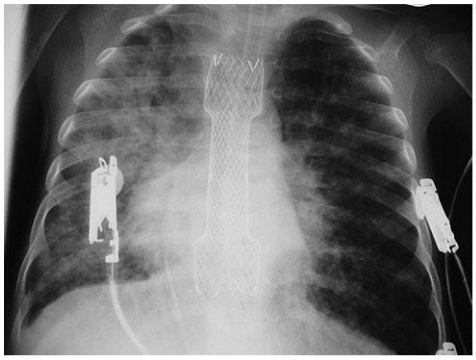

Fig. 33.17 Chest radiograph demonstrating the placement of a stent in the oesophagus of a child with a broncho-oesophageal fistula.

4. Place a Sengstaken–Blakemore tube for short-term relief.
5. Place a covered stent in the oesophagus.
6. Oral feeding is not possible in the first couple of days. This complicates the use of standard TB treatment. Alternative intravenous therapy, which could include rifampicin, ofloxacin (ciprofloxacin) and amikacin, should be prescribed.
7. Add prednisone 2 mg/kg/day to the treatment.

The optimal duration of stenting is unknown. In the cases of BOF that present with respiratory failure requiring ventilation the stent mst be removed before the child can be extubated. The use of stents to close the fistula in the long-term management of BOF has yet to be determined, but they might have a role to play in the treatment of these patients.

OESOPHAGEAL PERFORATION

CLINICAL PRESENTATION

Tuberculous involvement of the oesophagus is rare in both adults and children.[54] Oesophageal TB is the least common of all tuberculous lesions of the gastrointestinal tract.[55] Erosion and perforation of the oesophagus is an unusual complication. Oesophageal TB can be either primary or secondary. Secondary oesophageal TB results from the swallowing of infected sputum, direct involvement from the lungs, mediastinal lymph nodes or thoracic spine, retrograde lymphatic spread or haematogenous spread.[56] The commonest causes of oesophageal perforation in tuberculous disease is thought to be from a mediastinal abscess bursting into the oesophagus[47] or the formation of a traction diverticulum secondary to adjacent inflammation in the mediastinum.[57] Tuberculous lymph nodes may lead to erosion and eventual perforation by pressure necrosis in combination with an inflammatory reaction.[58] This condition rarely causes symptoms because the perforation is often walled off by the mediastinal lymph nodes.[59]

Symptoms and signs include dysphagia, cough, chest pain, fever and weight loss.[60]

The imaging features that have been described include the leaking of contrast with or without fistula formation on contrast swallow, and large low-density lymph nodes and mediastinal air visible on chest CT scan.

MANAGEMENT

These children are managed conservatively with anti-TB drugs and prednisone. If there is perforation into the airway, they are managed in the same way as a broncho-oesophageal fistula. In children with mediastinal abscesses surgical drainage can be considered if the perforation of the oesophagus does not respond to medical treatment alone and for persistent fever. The use of an oesophageal stent can be considered if there is a significant leak into the mediastinum.

CHYLOTHORAX

Chylothorax is a rare complication of TB described in adult patients.[61,62] A small number of cases have been seen in both human immunodeficiency virus (HIV)-uninfected and -infected children. They present with a combination of mediastinal lymph node enlargement and pleural effusions (Fig. 33.18). Left- and right-sided as well as bilateral chylothoraces have been seen. The aetiology is not known but it is postulated that it is secondary to infiltration of the main lymphatic vessels by TB lymph nodes. The aspirated pleural fluid has the characteristics of a true chylothorax. The pleural fluid appears milky with very high lymphocyte counts and triglyceride levels.

Chest CT scan is indicated to exclude other causes of chylothorax. On CT scan large mediastinal nodes typical of those seen in TB are visualized. The treatment consists of the standard three-drug anti-TB regimen to which prednisone (2 mg/kg/day) is added. The child's diet must be adjusted to include mostly medium chain fatty acids and the pleural fluid must be tapped if the child is symptomatic. Children treated with this regimen showed complete resolution of the chylothorax with no residual pleural disease.[63]

PHRENIC NERVE INVOLVEMENT

This is an extremely rare complication of TB with only a single case previously described in a child.[64] We have described seven cases in children (Goussard P, personal communication). In all our cases of phrenic nerve palsy the involvement occurred on the left side. Phrenic nerve palsy presents either coincidentally in asymptomatic children previously treated for TB or as part of extensive intrathoracic TB. A third of left upper lobe expansile pneumonia cases in one study were associated with phrenic nerve palsy.[1] Phrenic nerve palsy should be suspected if the diaphragm on the left side is elevated on the chest radiograph (Fig. 33.19). Phrenic nerve palsy must be confirmed with fluoroscopy, which will show paradoxical movement of the diaphragm. In our patients with extensive intrathoracic TB diaphragmatic function was absent on initial evaluation. Phrenic nerve function did not recover on anti-tuberculous treatment and steroids. In one case surgical decompression of the glandular mass was performed but this also failed to improve phrenic nerve function. A complicating factor in the group with extensive intrathoracic TB was that the left main bronchus had nodal obstruction of varying degrees in all the cases. At autopsy in the one child who died, infiltration of the phrenic nerve by the tuberculous process could be demonstrated. These children are at high risk of developing respiratory failure, especially if they also have severe parenchymal disease.

Spontaneous recovery of phrenic nerve function does not occur after infiltration by tuberculous nodes.

Plication of the diaphragm might be necessary to stabilize lung function in symptomatic children;[65] this is best delayed until after completion of anti-TB treatment.

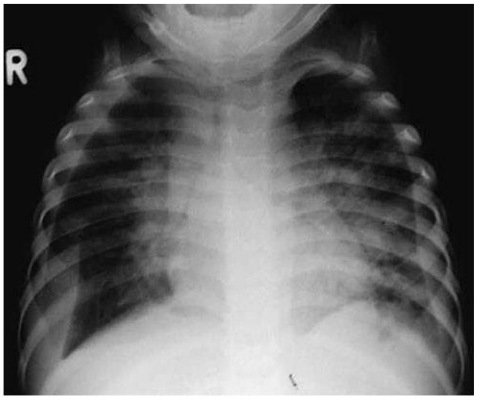

Fig. 33.18 Bilateral pleural effusions visible on chest radiograph. Aspirated fluid was milky and fulfilled the criteria for a chylothorax. Nodal compression of both main bronchi is present.

TUBERCULOSIS OF THE UPPER AIRWAYS

Tuberculous involvement of the upper airways in children is rare and most of the reports of upper airway TB have been in adults.[66] Two forms of upper airway TB have been described: laryngeal TB and retropharyngeal abscess.

LARYNGEAL TUBERCULOSIS

Laryngeal TB is well recognized in the adult population, but is rare in children. Children present with stridor, dysphagia and hoarseness. The pathogenesis of laryngeal TB in children is postulated to be different from that in adults. In adults it is secondary to cavitating pulmonary disease, while in children it is postulated to be primary infection of the larynx. The modes of infection in laryngeal TB are through bronchogenic spread by direct infection via highly infectious sputum from active pulmonary TB, or by haematogenous or lymphatic spread.[67] Many children with laryngeal TB do not have pulmonary disease.[68] Laryngoscopy and bronchoscopy with biopsy are necessary to confirm the diagnosis. Tuberculosis tends to be localized to the vocal cords and posterior larynx.[69] The most frequently encountered types of laryngeal lesions are infiltrative mucosal hypertrophy, a gross tumour-like surface appearance and ulcerative mucosal lesions. These lesions can mimic laryngeal cancer, and the laryngoscopic appearances often simulate malignancy. CT scan findings of laryngeal TB include bilateral involvement, thickening of the free margin of the epiglottis and good preservation of the pre-epiglottic and para-laryngeal fat spaces.[70]

Management depends on the severity of the upper airway obstruction. In severe cases tracheostomy may be lifesaving, but most children respond to anti-TB treatment and oral corticosteroids. Standard three-drug therapy is used. Biopsy may be necessary to confirm the diagnosis. Tissue must be sent for culture and histology.

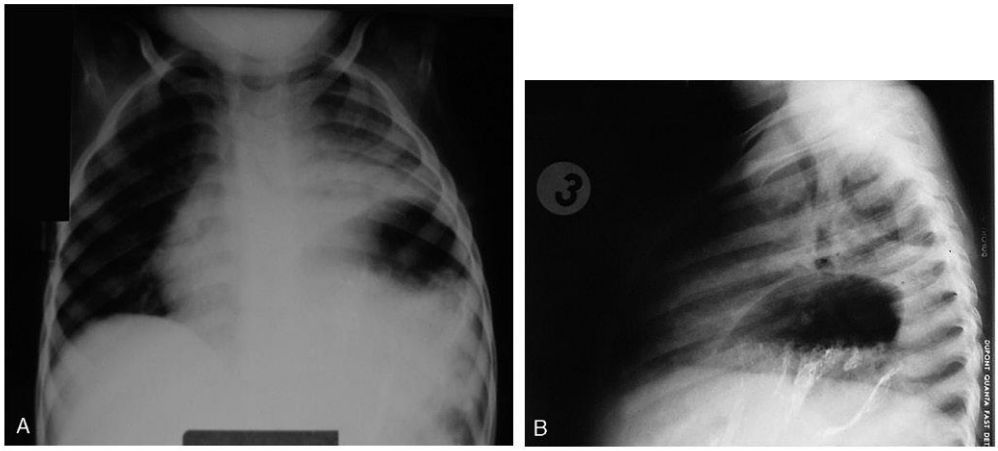

Fig. 33.19 Left phrenic nerve palsy with elevated left hemidiaphragm on (A) anteroposterior and (B) lateral chest radiographs.

TUBERCULOUS RETROPHARYNGEAL ABSCESS

This is a very rare presentation in children. A cold abscess develops in the retropharyngeal space and causes severe airway obstruction with stridor. These children are not toxically ill when compared with those with other bacterial causes of retropharyngeal abscess. The enhancing abscess can be seen on CT scan of the neck.

Management includes surgical decompression if the airway is compromised. Standard three-drug anti-TB treatment is used.

OTHER UNCOMMON CHILDHOOD PRESENTATIONS OF TUBERCULOSIS

HAEMOPTYSIS

Haemoptysis is an uncommon problem in childhood pulmonary TB, but can be a potentially serious problem. It may be the presenting sign of pulmonary TB in adults and older children, but seldom in infants. Most patients presenting with haemoptysis will have cavities on their chest radiographs. Salazar et al.[71] found that 12% of definite paediatric TB cases presented with haemoptysis. Children presenting with severe haemoptysis are treated with cough suppressants, antibiotics to cover infection and four-drug anti-TB treatment. In severe cases bronchoscopy may be indicated to determine the location of the bleeding. Transcatheter embolization of bronchial vessels and lobectomy may be necessary if conservative measures have failed to control the bleeding. Before surgery is done it is important to have localized the zone of bleeding by means of bronchoscopy.[72]

INTRATHORACIC COLD ABSCESS FORMATION

A small number of children not responding to antituberculous therapy were found to have intrathoracic cold abscess formation on CT scan, and they improved only after drainage of the pus. These children had been on treatment for 3–6 months, were severely malnourished and not gaining weight and had a persistent high swinging fever. Chest CT scan confirmed widespread alveolar involvement and mediastinal lymphadenopathy, but the patients also had large liquefied nodes in the anterior and posterior mediastinum (Fig. 33.20).[63] The children required surgery to drain the liquefied nodes. The pus from the nodes was Ziehl–Neelsen positive on microscopy but *M. tuberculosis* was not cultured. After drainage of the abscesses the patients' symptoms resolved. This condition has been seen in both HIV-uninfected and -infected children.

Management

In children with persistent swinging fever not responding to anti-TB treatment, intrathoracic cold abscess must be considered. The diagnosis is confirmed by chest CT scan. In addition to anti-TB treatment surgical drainage of the abscesses is required.

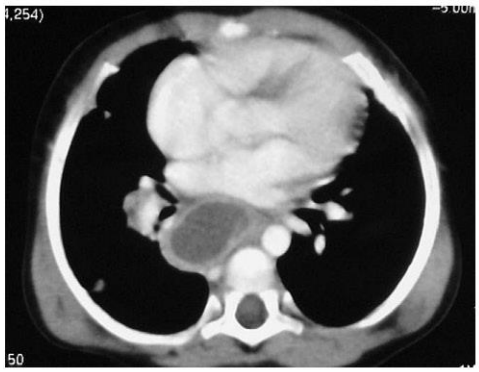

Fig. 33.20 Large subcarinal lymph nodes with ring enhancement. At surgery pus was drained from these nodes. This picture represents a large intrathoracic cold abscess.

CHEST WALL TUBERCULOSIS

The chest wall is an uncommon site for osteoarticular TB.[73] It is usually secondary to haematogenous spread and less commonly due to direct spread from the underlying pleural or parenchymal disease.[74] Radiographic changes include bone erosion, periosteal reaction, bone sequestrum and soft-tissue masses.[74] The affected areas are the rib shaft, the costovertebral joint and the posterior arch.[73,74] Sternal involvement is very rare.[75] CT scan findings of the chest wall are similar to those seen on chest radiography.[3]

The diagnosis can be made by fine needle aspiration or with CT scan-guided biopsy, which are sent for histology and culture. Children with a chest wall mass need biopsy or fine needle aspiration to exclude unusual causes of chest wall masses such as actinomycosis.

Treatment is medical but sometimes it is necessary to drain the soft-tissue abscess.

OTHER UNUSUAL CLINICAL PICTURES

Other unusual forms of TB have also been seen and include pleural effusion with a chest wall mass and TB of the thoracic vertebrae causing an unusual mediastinal mass and compression of the left main bronchus.

Airway compression associated with spinal TB is rare in children. Rarely airway obstruction can be caused by extensive paravertebral mediastinal abscess in children with TB of the spine.[76]

REFERENCES

1. Goussard P, Gie RP, Kling S, Beyers N. Expansile pneumonia in children caused by *Mycobacterium tuberculosis*: clinical, radiological and bronchoscopic appearances. *Pediatr Pulmonol* 2004;38:451–455.
2. Forstad S. Segmental atelectasis in children with primary tuberculosis. *Am Rev Tuberc* 1959; 79:597–605.
3. Schaaf HS, Gie RP, Beyers N, et al. Tuberculosis in infants less than 3 months of age. *Arch Dis Child* 1993;69:371–374.
4. Marais BJ, Gie RP, Schaaf HS, et al. The natural history of childhood intra-thoracic tuberculosis: a critical review of literature from the pre-chemotherapy era. *Int J Tuberc Lung Dis* 2004;8:392–402.
5. De Vilhers RVP, Andronikou S, Van der Westhuizen S. Specificity and sensitivity of chest radiographs in the diagnosis of paediatric pulmonary tuberculosis and the value of additional high-kilovolt radiographs. *Australas Radiol* 2004;48:148–153.
6. Cheung YF, Lee SL, Leung MP, et al. Tracheobronchography and angiocardiography of paediatric cardiac patients with airway disorders. *J Paediatr Child Health* 2002;38:258–264.
7. Andronikou S, Joseph E, Lucas S, et al. CT scanning for the detection of tuberculous mediastinal and hilar lymphadenopathy in children. *Pediatr Radiol* 2004;34:232–236.
8. Chan S, Abadco DL, Steiner P. Role of flexible fiberoptic bronchoscopy in the diagnosis of childhood endobronchial tuberculosis. *Pediatr Infect Dis J* 1994;13:506–509.
9. Somu N, Swaminathan S, Paramasivan CN, et al. Value of bronchoalveolar lavage and gastric lavage in the diagnosis of pulmonary tuberculosis in children. *Tuber Lung Dis* 1995;76:295–299.
10. Abadco DL, Steiner P. Gastric lavage is better than bronchoalveolar lavage for isolation of *Mycobacterium tuberculosis* in childhood pulmonary tuberculosis. *Pediatr Infect Dis J* 1992;11:735–737.
11. De Blic J. The value of flexible bronchoscopy in childhood pulmonary tuberculosis. *Pediatr Pulmonol* 1995;11(Suppl):24–25.
12. De Blic J, Azevedo I, Burren CP, et al. The value of flexible bronchoscopy in childhood pulmonary tuberculosis. *Chest* 1991;100:688–692.
13. Gerbeaux J. *Tuberculose Primaire de Infant*. Paris: Edition Medicale Flammarion, 1967.
14. Gerbeaux J, Baculard A, Couvreur J. Primary tuberculosis in childhood. *Am J Dis Child* 1965;110:507–518.
15. Rosenzweig DY, Stead WW. The role of tuberculosis and other forms of bronchopulmonary necrosis in the pathogenesis of bronchiectasis. *Am Rev Respir Dis* 1966; 93:769–785.
16. Nemir RL, Cordona J, Lacoius A, David M. Prednisone as an adjunct in the chemotherapy of lymph node-bronchial tuberculosis in childhood: a double-blind study. *Am Rev Respir Dis* 1963; 88:189–198.
17. Nemir RL, Cardona J, Vaziri F, et al. Prednisone as an adjunct in the chemotherapy of lymph node-bronchial tuberculosis in childhood: a double-blind study. II. Further term observation. *Am Rev Respir Dis* 1967;95:402–410.
18. Toppet M, Malfroot A, Derde MP, et al. Corticosteroids in primary tuberculosis with bronchial obstruction. *Arch Dis Child* 1990;65:1222–1226.
19. Papagiannopoulos KA, Linegar AG, Harris DG, et al. Surgical management of airway obstruction in primary tuberculosis in children. *Ann Thorac Surg* 1999;68:1182–1186.
20. Hewitson JP, van Oppel UO. Role of thoracic surgery for childhood tuberculosis. *World J Surg* 1997;21:468–474.
21. Worthington MG, Brink JG, Odell JA, et al. Surgical relief of acute airway obstruction due to primary tuberculosis. *Ann Thorac Surg* 1993;56:1054–1062.
22. Seibert AF, Haynes J Jr, Middleton R, et al. Tuberculous pleural effusion. Twenty-year experience. *Chest* 1991;99:883–886.
23. Waagner DC. The clinical presentation of tuberculous disease in children. *Pediatr Ann* 1993; 22:622–628.
24. Merino JM, Carpintero I, Alvarez T, et al. Tuberculous pleural effusion in children. *Chest* 1999;115:26–30.
25. Moon WK, Kim WS, Kim IO, et al. Complicated pleural tuberculosis in children: CT evaluation. *Pediatr Radiol* 1999;29:153–157.
26. Segura RM. Useful clinical biological markers in the diagnosis of pleural effusions in children. *Paediatr Respir Rev* 2004;5(suppl A):S205–S212.
27. Ena J, Valls V, Perez de Oteyza C, et al. Utilidad y limitaciones de la adenosina desaminasa en el diagn' ostico de la pleures'ia tuberculosa. Estudio metaanal'itico. *Med Clin (Barc)* 1990;95:333–335.
28. Aspin J, O'Hara H. Steroid-treated tuberculous pleural effusions. *Br J Tuberc* 1958;52:81–83.
29. Grewal KS, Dixit RP, Sil DR. A comparative study of therapeutic regimens with and without corticosteroids in the treatment of tuberculous pleural effusion. *J Indian Med Assoc* 1969;52:514–516.
30. Damany SJ, Shah KT. Treatment of pleural effusion with and without triamcinolone in addition to usual antituberculosis chemotherapy. *J Indian Med Assoc* 1968;51:391–393.
31. Mathur KS, Prasad R, Mathur JS. Intrapleural hydrocortisone in tuberculous pleural effusion. *Tubercle* 1960;41:358–362.
32. Lee CH, Wang WJ, Lan RS, et al. Corticosteroids in the treatment of tuberculous pleurisy. A double blind, placebo-controlled randomized study. *Chest* 1988;94:1256–1259.
33. Wyser C, Walzl G, Smedema JP, et al. Corticosteroids in the treatment of tuberculous pleurisy. A double-blind, placebo-controlled, randomized study. *Chest* 1996;110:333–338.
34. Galarza I, Canete C, Granados A, et al. Randomised trial of corticosteroids in the treatment of tuberculous pleurisy. *Thorax* 1995;50:1305–1307.
35. Feldson B, Rosenberg L, Hamburger M. Roentgen findings in acute Friedlander's pneumonia. *Radiology* 1949;46:559–565.
36. Korvick JA, Hackett AK, Yu VL, et al. Klebsiella pneumonia in the modern era: clinicoradiographic correlations. *South Med J* 1991;84:200–204.
37. Winer-Muram HT, Arheart KL, Jennings SG, et al. Pulmonary complications in children with hematological malignancies: accuracy of diagnosis with chest radiography and CT. *Radiology* 1997; 204:643–649.
38. Caillot D, Couaillier JF, Bernard A, et al. Increasing volume and changing characteristics of invasive pulmonary aspergillosis on sequential thoracic computed tomography scans in patients with neutropenia. *J Clin Oncol* 2001; 19:253–259.
39. Eliasberg H, Neuland W. Zur Klinik der Epituberkulosen und gelatinosen Infiltration der kindlichen Lunge. *Jahrb Kinderheilkd* 1920;93:88.
40. Seal RME, Thomas DME. Endobronchial tuberculosis in children. *Lancet* 1956;271:995–996.
41. Jones EM, Rafferty TN, Willis HS. Primary tuberculosis complicated by bronchial tuberculosis with atelectasis (epituberculosis). *Am Rev Tuberc* 1942;46:392.
42. Beyers JA. Radiographic manifestations. In: Coovadia HM, Benatar SR (eds). *A Century of Tuberculosis*. Cape Town, South Africa: Oxford University Press, 1991:203–233.
43. Oppenheimer EH. Experimental studies on the pathogenesis of epituberculosis. *Bull Johns Hopkins Hosp* 1935;57:247.
44. Chauhan SS, Long JD. Management of tracheoesophageal fistulas in adults. *Curr Treat Options Gastroenterol* 2004;7:31–40.
45. Bhatia R, Mitra DK, Mukherjee S, et al. Bronchoesophageal fistula of tuberculosis origin in a child. *Pediatr Radiol* 1992;22:154.
46. Coleman FP, Bunch GH. Acquired non-malignant esophagotracheo-bronchial fistula. *J Thorac Surg* 1950;19:542–558.
47. Gie RP, Kling S, Schaaf HS, et al. Tuberculous broncho-esophageal fistula in children. *Pediatr Pulmonol* 1998;25:285–288.
48. Moersch HJ, Tinney WS. Fistula between the oesophagus and the tracheobronchial tree. *Med Clin North Am* 1944; July:1001–1007.
49. Wychulis AR, Ellis FH, Andersen HA. Acquired non-malignant esophageo-tracheobronchial fistula. *JAMA* 1966;196:103–108.
50. Damino EA, Evans CJ, Thomas JH. Tuberculous bronchoesophageal fistula in a child. *Thorax* 1955;10:351–353.
51. Lucaya J, Sole S, Badora J, et al. Bronchial perforation and broncho-esophageal fistulas: tuberculous origin in children. *Am J Radiol* 1980;135:525–528.
52. Goussard P, Sidler D, Kling S, et al. Esophageal stent improves ventilation in a child with a broncho-esophageal fistula caused by *Mycobacterium tuberculosis*. *Pediatr Pulmonol* 2007;42:93–97.
53. Radecke K, Gerken G, Treichel U. Impact of a self-expanding, plastic esophageal stent on various esophageal stenoses, fistulas and leakages: a single-center experience in 39 patients. *Gastrointest Endosc* 2005;61:812–818.

54. Kotanidou A, Andrianakis I, Mavrommatis A, et al. Mediastinal mass with dysphagia in an elderly patient. *Infection* 2003;31:178–180.
55. Sood A, Sood N, Kumar R, et al. Primary tuberculosis of esophagus. *Indian J Gastroenterol* 1996;15:75.
56. Gordon AH, Marshall JB. Esophageal tuberculosis: definitive diagnosis by endoscopy. *Am J Gastroenterol* 1990;85:174–177.
57. Ghandour Z, al Karawi MA, Mohamed AE. Spontaneous oesophageal perforation: unusual presentation of tuberculosis. *Endoscopy* 1997; 29:143–144.
58. Tucker LE, Aquino T, Sasser W. Mid-esophageal traction diverticulum: rare cause of massive upper gastrointestinal bleeding. *Mo Med* 1994; 91:140–142.
59. Adkins MS, Raccuia JS, Acinapura AJ. Esophageal perforation in a patient with acquired immunodeficiency syndrome. *Ann Thorac Surg* 1990;50:299–300.
60. Sathiyasekaran M, Shivbalan S. Esophageal tuberculosis. *Indian J Pediatr* 2004;71:457–458.
61. Vennera M, Moreno R, Cot J, et al. Chylothorax and tuberculosis. *Thorax* 1983;38:694–695.
62. Anton PA, Rubio J, Casan P, et al. Chylothorax due to *Mycobacterium tuberculosis*. *Thorax* 1995;50:1019.
63. Gie RP, Goussard P, Kling S, et al. Unusual forms of intrathoracic tuberculosis in children and their management. *Paediatr Respir Rev* 2004;5(Suppl A): S139–S141.
66. Nishiike S, Irifune M, Doi K, et al. Laryngeal tuberculosis: a report of 15 cases. *Ann Otol Rhinol Laryngol* 2002;111:916–918.
67. Travis LW, Hybels RL, Newman MH, et al. Tuberculosis of the larynx. *Laryngoscope* 1976; 86:549–558.
68. Ramadan HH, Wax MK. Laryngeal tuberculosis. *Arch Otolaryngol Head Neck Surg* 1995;121:109–112.
69. Soda A, Rubio H, Salazar M, et al. Tuberculosis of the larynx: clinical aspects in 19 patients. *Laryngoscope* 1989;99:1147–1150.
70. Kim MD, Kim DI, Yune HY, et al. CT findings of laryngeal tuberculosis: comparison to laryngeal carcinoma. *J Comput Assist Tomogr* 1997;21:29–34.
71. Salazar GE, Schmitz TL, Cama R, et al. Pulmonary tuberculosis in children in a developing country. *Pediatrics* 2001;108:448–453.
72. Shields TW. Pulmonary tuberculosis and other mycobacterial infections of the lung. In: Shields TW (ed.). *General Thoracic Surgery*, 4th edn. Baltimore: Williams & Wilkins, 1994: 968–985.
73. Tatelman M, Drouillard EJP. Tuberculosis of the rib. *Am J Roentgenol Radium Ther Nucl Med* 1953;70:923–935.
74. Khalil A, Le Breton C, Tassart M, et al. Utility of CT scan for the diagnosis of chest wall tuberculosis. *Eur Radiol* 1999;9:1638–1642.
75. Mulloy EMT. Tuberculosis of the sternum presenting as metastatic disease. *Thorax* 1995;50:1223–1224.
76. Ochoa TJ, Rojas R, Gutierrez M, et al. Severe airway obstruction in a child with Pott's disease. *Pediatr Infect Dis J* 2006;25:649–651.

eighth, and 12th rib. A magnetic resonance imaging of the spine also revealed signal abnormalities in the T6, T7, T12, and L4 vertebrae bodies without bony destruction.

Culture from the lesions over her left forearm grew fully drug susceptible *M. tuberculosis*. An immunologic work-up including HIV serology and IL-12 and gamma interferon gene analysis revealed no abnormalities. She received treatment with standard antituberculous therapy for 1 year with resolution of the cutaneous masses. Her mother was investigated and found to have pulmonary tuberculosis and treated.

DISCUSSION

Cutaneous lesions from *M. tuberculosis* occurs from several possible routes (Table 1). The clinical features of cutaneous tuberculosis are diverse and result from exogenous and endogenous spread of *Mycobacterium tuberculosis* and from immune-mediated mechanisms.[2] Direct inoculation of *Mycobacterium tuberculosis* usually produces nodules or plaques which can ulcerate. These lesions typically heal with scar formation. Endogenous infections can spread to the skin producing several different lesions. For example, scrofuloderma is the extension to skin of *Mycobacterium tuberculosis*, usually from an underlying infected lymph node or bone. Often the deeper infected structure forms a sinus and drains to the skin. Plaque-like or nodular forms also exist from endogenous spread. In the miliary variant, multiple tiny papules develop from bacteremia, usually secondary to lung involvement. Finally, tuberculids are immune reaction in the skin secondary to a *M. tuberculosis* infection. This group includes a papule-pustular variant with central necrosis, a perifollicular variant (lichen scrofulosorum) and a with panniculitis and vasculitis.[3]

Sporotrichoid-like cutaneous tuberculosis is a rare form of cutaneous tuberculosis.[4] As the name suggests, it mimics the chronic granulomatous mycotic infection of the skin and subcutaneous tissue by the dimorphic fungi *Sporothrix schenckii*.[5] The lesions often have a linear arrangement as a result of retrograde lymphatic spread of an exogenous infection from a primary cutaneous entry point. There are also reports that endogenous spread of tuberculosis can produce similar cutaneous lesions, as was seen in our second case.[6]

The infection is often misdiagnosed initially due to the striking similarities to pyogenic infection caused by *Streptococcus pyogenes* or *Staphylococcus aureus* as well as other chronic granulomatous lesions such as cutaneous leishmaniasis, nocardiosis, tularemia, atypical mycobacterial infection, deep fungal infections, and sarcoidosis.[7,8] Definitive diagnosis of the lesion is usually delayed for weeks to months until a skin biopsy is taken. The lesions are usually paucibacillary: the discharge may be culture negative and smear negative.[9] The diagnosis cannot always be made from histopathology alone and culture of the biopsied section of skin is recommended.

The 2 different presentations and disease patterns of sporotrichoid-like tuberculosis illustrated by our patients emphasize the importance of history taking and high index of suspicion of tuberculosis. This is especially important when encountering a skin lesion in a child who comes from, or has visited a tuberculosis-endemic region. A prompt biopsy of the lesion for histopathology and tuberculosis culture is necessary to allow early diagnosis and treatment and to prevent any further complications. Once the diagnosis of sporotrichoid-like tuberculosis is made, investigations are required to rule out pulmonary or disseminated disease.

TABLE 1. Pathogenesis and Forms of Cutaneous Tuberculosis

Direct inoculation
Tuberculous chancre
Tuberculosis verrucosa cutis
Spread from endogenous *Mycobacterium tuberculosis*
Scrofuloderma
Acute miliary TB
Tuberculous gumma
Lupus vulgaris
Oroficial tuberculosis
Tuberculids (Cutaneous immune reactions from internal *Mycobacterium tuberculosis*)
Papulonecrotic tuberculid
Lichen scrofulosorum
Nodular vasculitis

REFERENCES

1. Pandhi D, Reddy BS, Chowdhary S, et al. Cutaneous tuberculosis in Indian children: the importance of screening for involvement of internal organs. *J Eur Acad Dermatol Venereol*. 2004;18:546–551.
2. Tappeiner G. Tuberculosis and infections with atypical mycobacteria. In: Fitzpatrick TB, Eisen AZ, Wolff K, et al, eds. *Dermatology in General Medicine*. 7th ed. New York, NY: McGraw-Hill, 2008.
3. Ramos-e-Silva M, Ribeiro de Castro MC. Mycobacterial infections. In: Bolognia JL, Jorizzo JL, Rapini RP, eds. *Dermatology*. 2nd ed. Vol 74. New York, NY: Mosby, 2008:1114–1118.
4. Ramesh V. Sporotrichoid cutaneous tuberculosis. *Clin Exp Dermatol*. 2007; 32:680–682.
5. Hay RJ, Robert SO, MacKenzie DW. Mycology. In: Champiann RH, Barton JL, Ebling FJ, eds. *Rook's Textbook of Dermatology*. 5th ed. Oxford, MA: Blackwell Scientific Publication, 1992:1127–1216.
6. Lai-Cheong JE, Perez A, Tang V, et al. Cutaneous manifestations of tuberculosis. *Clin Exp Dermatol*. 2007;32:461–466.
7. Tobin EH, Jin WW. Sporotrichoid lymphocutaneous infections: etiology, diagnosis and therapy. *Am Fam Physician*. 2001;63:326–332.
8. Kampur S, Nanda S, Reddy BS. An unusual episode of lupus vulgaris masquerading as sporothrichosis. *Int J Dermatol*. 2001;40:336–339.
9. Sharma S, Choudhary R, Juneja M, et al. Cutaneous tuberculosis mimicking sporotrichosis. *Indian J Pediatr*. 2005;72:86–88.

LARYNGEAL INVOLVEMENT IN TWO SEVERE CASES OF CHILDHOOD TUBERCULOSIS

Katharine K. Gregg, MD, Anne K. Detjen, MD,† Pierre Goussard, MD,† and Robert Gie, MD†*

Abstract: Laryngeal tuberculosis in children is seldom reported in the literature. We present 2 children from Cape Town, South Africa who had disseminated tuberculosis involving the cervical lymph nodes and the larynx. The cases emphasize the pathophysiology, the clinical picture, the bronchoscopic appearance, and the response to therapy in laryngeal tuberculosis.

Key Words: pediatric, larynx, tuberculosis, miliary, lymph node

Accepted for publication April 30, 2009.

From the *Department of Pediatrics, University of California San Francisco, San Francisco, CA; and †Desmond Tutu TB Centre, Department of Paediatrics and Child Health, Faculty of Health Sciences, Stellenbosch University, Cape Town, South Africa.

Supported by UCSF Dean's Office Medical Student Research Program (to K.K.G.) and by Alexander von Humboldt Foundation (to A.D.D.).

Address for correspondence: Robert Gie, Desmond Tutu TB Centre, Department of Paediatrics and Child Health, Faculty of Health Sciences, Stellenbosch University, P.O. Box 19063, Tygerberg 7505, South Africa. E-mail: rpg1@sun.ac.za.

DOI: 10.1097/INF.0b013e3181ac7b26

Tuberculosis (TB) affects approximately 1 million children worldwide, with children from developing countries carrying the largest burden of disease.[1] It is estimated that 21% to 44% of

pediatric TB cases are extrapulmonary, involving the cervical lymph nodes in the majority of cases.[1] In the era before anti-TB chemotherapy, laryngeal TB in adults was usually associated with severe pulmonary disease. The pathogenesis of laryngeal disease is thought to include direct inoculation of expectorated sputum onto the larynx, and lymphogenic or hematogenous spread.[2] The latter could be especially applicable to the pediatric population given the paucibacillary nature of sputum and the higher incidence of TB lymphadenitis and disseminated disease.[3] We present 2 cases of laryngeal TB associated with disseminated disease and cervical lymph node involvement.

CASE REPORTS

Case 1. A 4-year-old girl presented with a 5-month history of progressive neck swelling. Her parents reported occasional dysphagia, snoring at night, intermittent fevers, and short episodes of apnea while asleep. She had lost 4 kg in the past 2 months. She had been exposed to a neighbor with newly diagnosed TB. The patient was previously treated twice for drug susceptible TB, though adherence to these regimens was uncertain.

Physical examination revealed an afebrile, chronically ill-appearing child with a "bull neck," and distended anterior chest wall vasculature, suggesting superior vena cava syndrome. The patient had severely enlarged, matted cervical lymph nodes, as well as generalized lymphadenopathy. Bacillus Calmette-Guérin scar was not present. She was breathing comfortably with intermittent stridor and wheezes audible on auscultation. The induration following a Mantoux tuberculin skin test (TST) was 20mm. Fine needle aspiration of the left cervical node revealed acid-fast bacilli. HIV serology was negative.

Chest radiograph showed enlarged lymph nodes and a miliary infiltrate. Computer tomography of the chest demonstrated deep cervical and superficial neck lymph nodes and extensive hilar and mediastinal lymphadenopathy. The trachea was narrowed above the thoracic inlet, and the lung fields were consistent with miliary TB. While awaiting culture results, the patient was treated with a 4-drug anti-TB regimen consisting of rifampin, isoniazid, pyrazinamide, and ethionamide. Prednisone was started to decrease inflammation and airway obstruction. Bronchoscopy revealed severe glottic and supraglottic swelling with nodules on the supraglottic tissue. There was 30% stenosis of the proximal trachea. *M. tuberculosis* was cultured from a gastric washing specimen, which was susceptible to rifampin and isoniazid. The patient's acute signs and symptoms resolved within 2 months of treatment, and she completed a 6-month regimen at a TB hospital.

Case 2. A 6-year-old boy presented with a 1-month history of hoarse voice, difficulty breathing, dysphagia, vomiting, and increased neck swelling. His mother noted loud snoring while sleeping. No specific TB source case could be identified.

On physical examination, the patient was afebrile, thin, pale, with audible breathing. Bacillus Calmette-Guérin scar was not present. He had massive matted, nontender, bilateral cervical node enlargement. Swollen axillary and inguinal lymph nodes were also present. He had subcostal retractions and stridor. Bilateral monophonic wheezes were heard on auscultation. The TST had an induration of 20 mm and chest radiograph revealed a miliary picture. Fine needle aspiration of the cervical nodes showed granulomatous inflammation with positive staining for acid-fast bacilli. HIV serology was negative.

CT of the chest showed features consistent with miliary TB with extensive cervical, hilar, and mediastinal lymph node enlargement. There was narrowing of the upper airways with edema of the laryngopharynx and proximal trachea. Bronchoscopy showed a severely swollen epiglottis and lymphoid hyperplasia of the supraglottic tissue. The proximal trachea was stenosed >30%. Gastric washing culture was positive for *M. tuberculosis* susceptible to rifampin and isoniazid. He was initially treated with a 4-drug anti-TB regimen of rifampin, isoniazid, pyrazinamide, and ethionamide. Prednisone was given to decrease airway inflammation. The patient remained in the hospital for 4 weeks to ensure resolution of his compromised airway. He was then transferred to a community hospital and completed 6 months of treatment as an outpatient with complete clinical recovery.

DISCUSSION

Laryngeal involvement in TB is rarely described, even in high burden populations as in Cape Town, South Africa. Early in the 20th century, the larynx was involved in 25% of all cases of TB but decreased to 1% following the introduction of anti-TB medication.[4] The current incidence is rising with increases in overall TB disease.[5] Laryngeal TB should be among the differential diagnoses for children with upper airway obstruction, especially in areas with high prevalence of TB.

There are several possibilities for the pathophysiology of laryngeal disease. Prior to the advent of anti-TB chemotherapy, most patients with TB laryngitis had severe cavitary lung disease with smear positive sputa that would collect in the posterior larynx and directly inoculate the laryngeal mucosa. Recently however, there appears to be an increase in the number of anterior laryngeal lesions.[2,6] The lesions are usually associated with pulmonary TB, but isolated cases without pulmonary pathology are described.[6,7] These findings point towards a lymphogenic or hematogenous spread of disease to the larynx. Such explanations especially apply to children, who often have negative sputum for acid-fast organisms.

The clinical signs and symptoms of laryngeal TB are varied. In adults, common presentations include hoarse voice, dysphagia, and cough.[7] Airway compression is usually not associated with disease in adults, but there have been several reports of stridor in children with laryngeal TB.[8,9] Both children discussed above showed signs of significant airway compression, particularly at night. It is important to monitor such children closely to ensure an adequate airway is maintained, especially if the epiglottis is involved.[4] In the cases presented, vascular obstruction caused by enlarged lymph nodes may have also contributed to the laryngeal edema.

With bronchoscopy, the lesions most commonly seen in adults with laryngeal TB are found on the true vocal cords, the false vocal cords, the posterior commisure, and the arytenoids.[2,6] The epiglottis may also be involved, with increasing reports in the past 2 decades.[2] Lesions may appear as ulcers, papillomas, granulomas, or signs of nonspecific inflammation.[2,6] Single or multiple sites may be involved. In the cases presented, both children showed extensive swelling of the epiglottis and supraglottic tissue with no ulcers or papillomas. Without bronchoscopic investigation, the enlarged lymph nodes alone may have been implicated for the clinical presentation, without full appreciation of the extent of disease.

The standard therapy for pediatric laryngeal TB is the same 6-month 4-drug regimen used in complicated pulmonary TB. This includes rifampin, isoniazid, pyrazinamide, and ethambutol. Miliary TB significantly increases the likelihood of meningeal involvement, and therefore ethionamide may be substituted for ethambutol to increase CNS penetration in such cases.[10] With signs of airway compromise, steroids may help, although no specific trials support their use in laryngeal TB. Most patients will show prompt regression of symptoms on steroids and anti-TB therapy, with complete resolution by 3 months.[2,6] Repeat imaging and bronchoscopy are useful tools for monitoring disease improvement.

REFERENCES

1. Nelson J, Wells CD. Global epidemiology of childhood tuberculosis. *Int J Tuberc Lung Dis*. 2004;8:636–647.
2. Shin JE, Nam SY, Yoo SJ, et al. Changing trends in clinical manifestations of laryngeal tuberculosis. *Laryngoscope*. 2000;110:1950–1953.
3. Marais BJ, Gie RP, Schaaf HS, et al. Childhood pulmonary tuberculosis: old wisdom and new challenges. *Am J Respir Crit Care Med*. 2006;173:1078–1090.
4. Rizzo PB, Da Mosto MC, Clari M, et al. Laryngeal tuberculosis: an often forgotten diagnosis. *Int J Infect Dis*. 2003;7:129–131.
5. Kandiloros DC, Nikolopoulos TP, Ferekidis EA, et al. Laryngeal tuberculosis at the end of the 20th century. *J Laryngol Otol*. 1997;111:619–621.
6. Wang CC, Lin CC, Wang CP, et al. Laryngeal tuberculosis: a review of 26 cases. *Otolaryngol Head Neck Surg*. 2007;137:582–588.
7. Lim JY, Kim KM, Choi EC, et al. Current clinical propensity of laryngeal tuberculosis: review of 60 cases. *Eur Arch Otorhinolaryngol*. 2006;263:838–842.
8. Ulloa R, Avila ML, Soto M, et al. Laryngeal tuberculosis. *Pediatr Infect Dis J*. 1998;17:758–760.
9. Rupa V, Mathew J, Bhanu TS, et al. Paediatric laryngeal tuberculosis presenting with stridor. *J Laryngol Otol*. 1989;103:787–788.
10. Donald PR, Seifart HI. Cerebrospinal fluid concentrations of ethionamide in children with tuberculous meningitis. *J Pediatr*. 1989;115:483–486.

MELTING MUSCLES

NOVEL H1N1 INFLUENZA A ASSOCIATED RHABDOMYOLYSIS

Dimple D'Silva, MB BS, Saliya Hewagama, MB BS,†*
Richard Doherty, MB BS, FRACP,‡*
Tony M. Korman, MB BS, FRACP, FRCPA,†§
and Jim Buttery, MB BS, FRACP, MSc‡¶*

Abstract: We report the first case of myositis and rhabdomyolysis after infection with novel influenza A (H1N1/09) virus. The case demonstrates the novel virus' capacity for causing significant disease. Myositis and the possibility of rhabdomyolysis should be considered in any individual presenting with influenza-like symptoms in which severe myalgia or muscle weakness is apparent. It is likely that we will see severe clinical manifestations of infection with this novel influenza virus in the coming respiratory virus season.

Key Words: swine influenza, pandemic H1N1/09, viral myositis, rhabdomyolysis

Accepted for publication September 8, 2009.

From the *Departments of *Pediatric Infectious Diseases, †Infectious Diseases, ‡Pediatrics, and §Medicine, Monash Medical Centre, Victoria, Australia; and ¶Murdoch Children's Institute, Victoria, Australia.

Address for correspondence: Dimple D'Silva, MBBS, Department of Pediatric Infectious Diseases, Level 3, Monash Medical Centre, 246 Clayton Rd, Clayton, VIC 3168, Australia. E-mail: dimpledsilva@yahoo.com.

DOI: 10.1097/INF.0b013e3181c03cf2

Novel influenza A (subtype H1N1 or swine origin influenza) was first identified in April 2009 in symptomatic human infections in Mexico.[1] The virus rapidly spread to all continents except Antarctica, and was declared a pandemic strain by the World Health Organization in June 2009.[2] This new triple reassortment strain seems to have a higher secondary attack rate than seasonal flu, accounting for its rapid emergence as a pandemic infection, with an estimated reproductive number of 1.4 to 1.6.[3] Only individuals born before 1957 are anticipated to have prior immunity from similar circulating seasonal influenza A strains.[4] Although data on the full spectrum of illness are not yet available for novel pandemic influenza A (H1N1/09), complications described to date seem similar to seasonal influenza. Unlike previous influenza strains, however, the illness to date has been generally mild in a young, previously well, population.[5,6] We report the first case of rhabdomyolysis in an adolescent, resulting from influenza A H1N1.

CASE REPORT

A 16-year-old boy presented with severe myalgia on the background of a 3-day history of fever, cough, sore throat, and mild headache after likely exposure to swine flu at his school. Two confirmed cases of novel influenza A H1N1 infection had already been identified at his school, which had then been closed for a week under the "Contain" phase of the local public health response. Severe myalgia began at midnight of the morning of presentation, such that he was unable to move his arms and legs, walk, or stand. Despite adequate oral fluid intake and continued good urine output, he noted dark urine later that day, and presented to the Emergency Department. There was no history of vomiting or diarrhea.

His history was unremarkable except for mild asthma for which he was not receiving regular medication (including inhaled and oral steroids).

At presentation to hospital, he was distressed by myalgia. Vital signs were normal apart from a raised blood pressure of 140/78 mmHg. Respiratory examination was normal. Abdominal palpation revealed mild tenderness in the left hypochondrium and epigastrium without guarding or rigidity. He had marked tenderness bilaterally over the biceps and quadriceps muscles. He was noted to have dark colored urine.

He was admitted and received intravenous 0.9% normal saline to achieve a urine output of 2 mL/kg/h and morphine for controlled analgesia. Empiric intravenous cefotaxime, oral roxithromycin, and oral oseltamivir (75 mg twice daily) were commenced. Full blood count, coagulation profile and serum electrolytes, urea nitrogen, and creatinine were normal on admission. His serum creatine kinase was 164,149 U/L (normal <230 IU/L), with fractionated MB 1501 U/L (normal: 0–10 U/L), and serum troponin 0.03 mcg/L (normal <0.081 mcg/L). Urine collected at admission contained 1034.73 mg/L myoglobin. Electromyography and muscle biopsy were not performed. Novel influenza A H1N1 was identified on a nasopharyngeal swab by specific polymerase chain reaction.

With aggressive hydration and analgesia his renal function remained normal throughout, and he steadily improved clinically. His creatine kinase concentration peaked at 1,127,000 U/L on day 4 of his admission before gradually declining. By day 5, his urine was macroscopically clearer, and he was discharged after 8 days. At follow-up of 2 weeks post-discharge, he had no residual weakness or myalgia, and his creatine kinase value had decreased to 742 U/L. Renal function remained stable throughout.

DISCUSSION

Novel influenza A (H1N1) infection seems to have arisen from Mexico in April 2009 and has rapidly spread throughout the world.[1,5] Initial concern regarding the case fatality rate from Mexico has not been replicated elsewhere and this current infection has generally been associated with a mild illness in the majority of instances. However, deaths and severe respiratory illness continue to be reported worldwide. Other traditional extrapulmonary complications of influenza have yet to be described.

Myalgia is a classic symptom of acute influenza, and although less common in children than in adults, is still reported in up to 40% of cases.[6] A smaller proportion of children experience severe myositis and of these, about 3% develop rhabdomyolysis.[7,8]

Pediatr Radiol (2010) 40 (Suppl 1):S78
DOI 10.1007/s00247-009-1537-6

CLINICAL IMAGE

Tuberculous broncho-oesophageal fistula: images demonstrating the pathogenesis

Pierre Goussard · Savvas Andronikou

Received: 5 October 2009 / Revised: 24 November 2009 / Accepted: 28 November 2009 / Published online: 9 February 2010

An 18-month-old girl with known pulmonary tuberculosis, on treatment for 5 months, presented with a history of coughing after feeding and recurrent infections of the left lower lobe. Chest radiograph showed a large right-side mediastinal lymph node, patent airways and pneumonic changes in the right middle lobe. There was gaseous distension of the stomach. Flexible bronchoscopy confirmed a suspected broncho-oesophageal fistula (BOF) in the left main bronchus with caseating material eroding into the lumen. Gastroscopy visualised a calcified lesion in the oesophagus.

Barium swallow (Fig. 1) confirmed the left-side BOF with contrast medium demonstrated in the tracheo-bronchial tree during the 'swallow' phase (*arrow*), without evidence of palatopharyngeal aspiration. Contrast-enhanced CT scan of the chest (Fig. 2) showed enlarged, calcified subcarinal lymphadenopathy compressing the left main bronchus and bronchus intermedius with erosion into the oesophagus (*short arrow*). A fistula was demonstrated between the oesophagus and the left main bronchus (*long arrow*). There was bilateral hilar lymphadenopathy. A calcified lymph node was seen extending from the oesophagus to the left main bronchus in the position of the BOF.

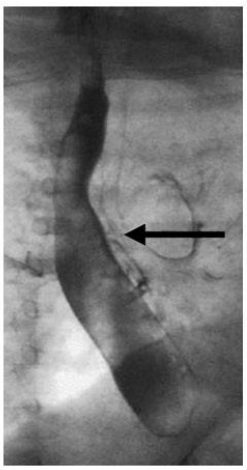

Fig. 1 Upper gastrointestinal contrast study

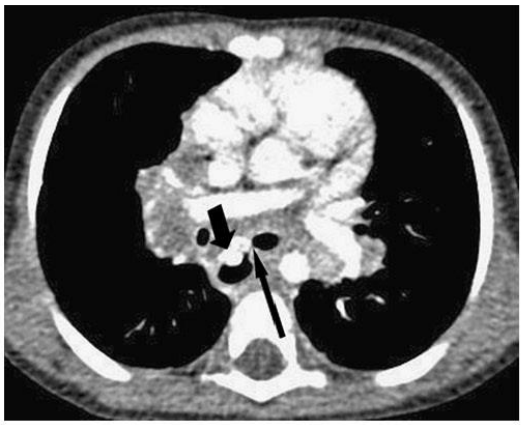

Fig. 2 Axial contrast-enhanced CT scan of the chest

These images confirm that BOF secondary to tuberculosis in children is most likely caused by glandular erosion of a lymph node into both the oesophagus and bronchus, although other explanations for BOF have been reported in adults [1, 2].

P. Goussard (✉)
Department of Paediatrics and Child Health,
University of Stellenbosch, Tygerberg Children's Hospital,
P.O. Box 19063, Tygerberg 7505, South Africa
e-mail: pgouss@sun.ac.za

S. Andronikou
Department of Radiology, University of Cape Town,
Cape Town, South Africa

References

1. Gie RP, Goussard P, Kling S et al (2004) Unusual forms of intrathoracic tuberculosis in children and their management. Paediatr Respir Rev 5(Suppl A):S139–141
2. Mahapatro S, Kane D, Dave S et al (2007) Post-tuberculous broncho-esophageal fistula. Ind J Thorac Cardiovasc Surg 23:161–163

JOURNAL OF TROPICAL PEDIATRICS, VOL. 56, NO. 5, 2010

Case Report

Paradoxical Tuberculosis associated Immune Reconstitution Inflammatory Syndrome Presenting with Chylous Ascites and Chylothorax in a HIV-1 Infected Child

by Helena Rabie,[1] Andrea Lomp,[2] Pierre Goussard,[1] Ettienne Nel,[1] *and* Mark Cotton[3]
[1]*Tygerberg Children's Hospital and University of Stellenbosch, Pediatrics and Child Health*
[2]*Division of Medicine, Imperial College, London*
[3]*Tygerberg Children's Hospital and Stellenbosch University, Pediatrics and Child Health and KIDCRU*

Correspondence: Helena Rabie, Tygerberg Children's Hospital and University of Stellenbosch, Pediatrics and Child Health. E-mail: <hrabie@sun.ac.za>

Summary

We present a case of tuberculosis (TB) paradoxical immune reconstitution inflammatory syndrome (IRIS) complicated by chylous ascites and chylothorax in a HIV-infected child. There are few descriptions of TB IRIS in children. This case extends the clinical spectrum of TB IRIS.

Key words: immune reconstitution inflammatory syndrome, HIV, tuberculosis, chylothorax, chylous ascites.

Introduction

Tuberculosis (TB) occurs commonly in HIV-infected children especially in the absence of anti-retroviral therapy (ART) [1]. Clinical deterioration of TB can occur despite appropriate anti-TB chemotherapy, once ART is initiated [paradoxical immune reconstitution inflammatory syndrome (IRIS)] these reactions are characterized by marked inflammatory phenomena [2]. Despite the fact that paradoxical IRIS due to TB is well recognized there are few clinical descriptions in children. We describe a unique case of paradoxical IRIS with abdominal TB.

Case report

A 3-year-old boy presented with extensive pulmonary, abdominal and pericardial TB. *Mycobacterium tuberculosis*, sensitive to isoniazid and rifampicin, was isolated from bone marrow and blood. HIV infection was confirmed by detecting HIV-specific antibodies (ELISA) and RNA. Severe CD4 T-cell depletion was noted. The CD4 count was 4 cells per mm^3 (2.6%). Baseline and subsequent data are shown in Table 1, baseline chest radiograph is shown in Fig. 1A.

Based on initial presentation, anti-TB therapy (rifampicin $20\,mg\,kg^{-1}\,day^{-1}$, isoniazid $15\,mg\,kg^{-1}\,day^{-1}$, pyrazinamide $25\,mg\,kg^{-1}\,day^{-1}$, ethambutol $25\,mg\,kg^{-1}\,day^{-1}$, ethionamide $20\,mg\,kg^{-1}\,day^{-1}$ and oral prednisone $2.5\,mg\,kg^{-1}\,day^{-1}$ were initiated. Other therapy included oral mycostatin, vitamin and mineral supplementation, broad spectrum antibiotics, blood transfusion and co-trimoxazole preventative therapy. Pericardial drainage was not required. The pyrexia resolved.

Highly active ART (HAART), consisting of stavudine 15 mg twice daily, lamivudine 50 mg twice daily and efavirenz 200 mg daily was commenced after 16 days. Eleven days later, the fever returned. Progressive abdominal distention due to ascites was noted. The fluid triglyceride level (FTL) at paracentesis was $>1.2\,mmol\,l^{-1}$ ($110\,mg\,dl^{-1}$), confirming chylous ascites. A low fat diet was prescribed and spironolactone was commenced. Prednisone continued unchanged but without resolution of fever and abdominal distention. After a further 22 days, a large right-sided pleural effusion was noted. An intercostal drain was inserted. Pleural fluid was confirmed as chylous (triglyceride level $21.5\,mmol\,l^{-1}$) (Fig. 1B and C). Echocardiography showed improvement of pericardial effusion and CT scan of the chest showed no adenopathy or features suggestive of Kaposi sarcoma.

Dietary fat restriction was made more stringent and pulsed methylprednisone at $10\,mg\,kg^{-1}\,day^{-1}$ was given intravenously for 3 days followed by oral prednisone at $2.5\,mg\,kg^{-1}\,day^{-1}$. The fever continued. Between 300 and 400 ml of chyle was lost

doi:10.1093/tropej/fmp141 Advance Access published on 25 January 2010

TABLE 1
Clinical and laboratory parameters as well as imaging at hospitalization, onset of ascites and onset of pleural effusion

	Presentation	Onset of ascites	Onset of pleural effusion
Days of hospitalization	0	27	49
Days on TB therapy	0	27	49
Days on HAART	0	11	33
Weight (WAZ)	10.5 (−2.65)	12.1 (−1.74)	14.1 (−0.51)
CD4 count/percentage	4/2.6		80 (8.4)
Log Viral load	5.6		3.04
Mantoux skin test	Non-reactive		Non-reactive
CXR	Miliary TB		Right-sided pleural effusion
CT Abdomen	Large glands		Extensive intra-abdominal adenopathy and ascites
CT Chest			No thoracic adenopathy
Complete blood count			
WBC($\times 10^6$/l)	2.33	17	
Hb (g dl^{-1})	5.1	8.4	
MCV (fl)	85.6		
PLT($\times 10^9$/l)	37	317	
Reticulocytes	1.64		
Absolute reticulocyte count	0.033		
Bone marrow aspirate	Granulomas, AFB[a] noted Culture: *M. Tuberculosis* sensitive to Rifampicin and Isoniazid		
Blood culture	Culture: *M. Tuberculosis*		
Echocardiograph	Pericardial effusion with diastolic dysfunction		Pericardial effusion improved
Ascites		Turbid, Milky	
Triglycerides (mmol l^{-1})		7.36	
Protein fluid ratio		>0.5	
Total Protein g l^{-1}		46	
Pleural fluid			Turbid, milky
Triglycerides (mmol l^{-1})			21.54
Total Protein (g l^{-1})			41
Albumin (g l^{-1})			21
Lactate dehydrogenase (U l^{-1})			805
pH			7.00
Adenosine deaminase (U l^{-1})			52.1
Leucocytes			13720

[a]Acid-fast bacilli.

daily. Sixteen days later, subcutaneous octreotide at 200 μg/dose 12 hourly was commenced with good effect. Fever resolved within 5 days. After 12 days, the intercostal drain could be removed (Fig. 1D). Prednisone was tapered after a further 2 weeks. No steroid side effects were noted. The total duration of hospitalization was 113 days.

Consent

Written informed consent was obtained from the parent for publication of this case report and accompanying images. A copy of the written consent is available for review by the Editor-in-Chief of this journal.

Discussion

Chlylothorax and chylous ascites are both rare entities. Triglyceride levels $\geq$1.2 mmol l^{-1} (110 mg dl^{-1}) are confirmatory [3, 4]. In children, TB rarely causes these phenomena [5, 6].

Abdominal mycobacterial infections lead to chylous ascites through two possible mechanisms: (i) obstruction of the lymphatic system through enlarged retroperitoneal glands with direct leakage of chyle through a lymphoperitoneal fistula, and (ii) increased retrograde pressure due to destruction of lymph node architecture with leakage of chyle from the dilated subserosal lymphatics into the peritoneal cavity [4].

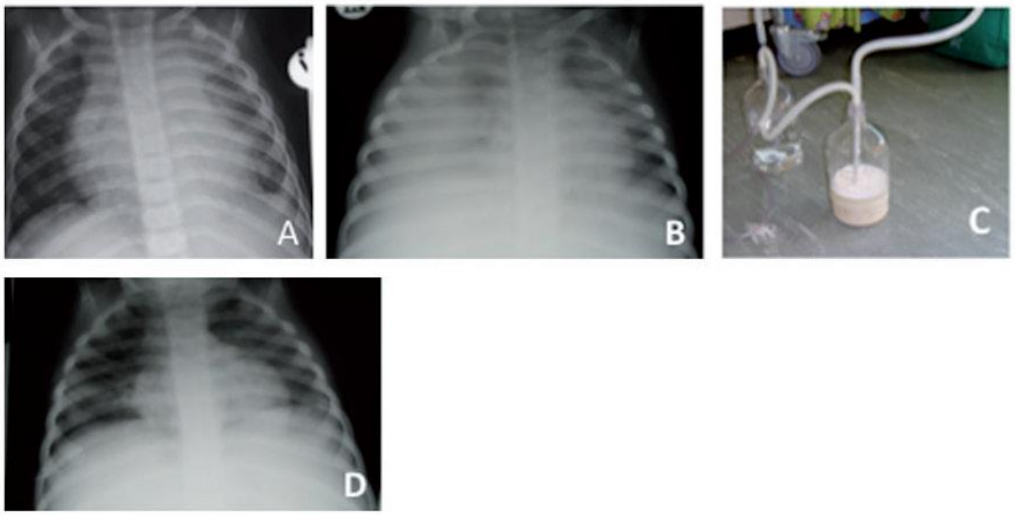

FIG 1. The course of illness from presentation to resolution of the cyclothorax. (**A**) Chest radiograph at presentation, (**B**) at the time of cyclothorax prior to insertion, (**C**) drainage from the intercostal drain and (**D**) after resolution and successful removal of the intercostal drain.

TB has been documented as causes of chylous ascites in HIV-infected adults [7, 8]. To our knowledge, the present report is the first documenting TB as a cause of chylous ascites in a HIV-infected child; this being despite the high prevalence of abdominal TB (10%) in children with culture positive disease [10].

The recrudescence of fever and new onset of chylous ascites and enlarging abdominal lymph nodes in this child on appropriate anti-TB therapy shortly after initiating HAART supports a diagnosis of paradoxical IRIS due to TB [2]. There are few case series describing TB-related paradoxical IRIS phenomena in children. MAC-related IRIS as a cause of chylous ascites in has been described in both adults and children [10, 11]. In a small series of 11 cases of TB IRIS in children, four were paradoxical, of which two had new pleural effusions, which were not further described [12]. There are no cases documenting abdominal TB IRIS in HIV-infected children, although other cases have been treated by the authors (E.D.N., H.R. and M.F.C.). No cases of deterioration of abdominal tuberculosis with subsequent chylous ascites in a child are reported in literature.

In children with TB, chylothorax is the result of lymph node compression or erosion of the thoracic duct, often identified on computerized tomography of the chest [13]. The development of chylothorax in the absence enlarged chest lymph nodes and presence of constrictive pericarditis in our case suggest that the chylothorax was secondary to the transdiaphragmatic movement of chylous ascites. This shunting across the diaphragm is a well described as a cause for chylothorax [14], possibly due to defects in the diaphragm [15].

Because both chylous ascites and IRIS are manifestation of an underlying disease, the prognosis depends on the treatment of the underlying disease and the success of the supportive care. Supportive care includes dietary manipulation with or without total parenteral nutrition, somatostatin or octreotide. Paracentesis and diuretics help to reduce discomfort. In selected cases, surgical intervention is indicated [4].

In adult case series of TB–HIV-associated chylous ascites, patients responded well to TB therapy and supportive care [7].

Management of TB IRIS includes the continuation of anti-TB therapy and HAART [2]. Data from a randomized trial in adults suggest that prednisone $1.5\,mg\,kg^{-1}\,day^{-1}$ (2 weeks) then $0.75\,mg\,kg^{-1}\,day^{-1}$ (2 weeks) improved symptoms and reduced the need for hospitalization and procedures. Due to the high rates of drug resistant TB and the inability to distinguish patients clinically, these authors recommend that undiagnosed resistance must be excluded prior to initiation of steroids [16]. In this case, severe IRIS developed despite being on high doses of steroids.

It is unclear whether the clinical response was due to octreotide use or, since fever improved in the same

time frame; the anti-TB therapy or pulsed doses of steroids.

Conclusion

We report the first case of paradoxical TB IRIS complicated by chyloperitoneum and secondary chylothorax. As access to HAART improves, more children with severe immune depletion and TB will initiate HAART. There is an urgent need to study the prevention and therapeutic interventions for these children.

References

1. Walters E, Cotton MF, Rabie H, *et al.* Clinical presentation and outcome of tuberculosis in human immunodeficiency virus infected children on anti-retroviral therapy. BMC Pediatrics 2008;8:1.
2. Boulware DR, Callens S, Pahwa S. Pediatric HIV immune reconstitution inflammatory syndrome. Curr Opin HIV AIDS 2008;3:461–7.
3. Buttiker V, Fanconi S, Burger R. Chylothorax in children: guidelines for diagnoses and management. Chest 1999;116:682–7.
4. Cardenas A, Chopra S. Chylous ascites. Am J Gastroenterol 2002;97:1896–900.
5. Gie RP, Goussard P, Kling S, *et al.* Unusual forms of intrathoracic tuberculosis in children and their management. Paediatr Respir Rev 2004;5(Suppl A):S139–41.
6. Jhittay PS, Wolverson RL, Wilson AO. Acute chylous peritonitis with associated intestinal tuberculosis. J Pediatr Surg 1986;21:5–76.
7. Sathiravikarn W, Apisarnthanarak A, Apisarnthanarak P, Bailey TC. Mycobacterium tuberculosis associated chylous ascites in HIV-infected patients: case report and review of the literature. Infection 2006;34:230–3.
8. Wu UI, Chen MY, Hu RH, *et al.* Peritonitis due to Mycobacterium avium complex in patients with AIDS: report of five cases and review of the literature. Int J Infect Dis 2009;13:285–90.
9. Schaaf HS, Marais BJ, Whitelaw A, *et al.* Culture-confirmed childhood tuberculosis in Cape Town, South Africa: a review of 596 cases. BMC Infect Dis 2007;7:140.
10. Phillips P, Lee JK, Wang C, *et al.* Chylous ascites: a late complication of intra-abdominal Mycobacterium avium complex immune reconstitution syndrome in HIV-infected patients. Int J STD AIDS 2009;20:285–7.
11. Berkowitz FE, Nesheim S. Chylous ascites caused by Mycobacterium avium complex and mesenteric lymphadenitis in a child with the acquired immunodeficiency syndrome. Pediatr Infect Dis J 1993;12:99–101.
12. Zampoli M, Kilborn T, Eley B. Tuberculosis during early antiretroviral-induced immune reconstitution in HIV-infected children. Int J Tuberc Lung Dis 2007;11:417–23.
13. Grobbelaar M, Andronikou S, Goussard P, *et al.* Chylothorax as a complication of pulmonary tuberculosis in children. Pediatr Radiol 2008;38:224–6.
14. Doerr CH, Allen MS, Nichols FCr, *et al.* Etiology of chylothorax in 203 patients. Mayo Clin Proc 2005; 80:867–70.
15. Lieberman FL, Hidemura R, Peters RL, *et al.* Pathogenesis and treatment of hydrothorax complicating cirrhosis with ascites. Ann Intern Med 1966; 64:341–51.
16. Meintjes G, Wilkinson R, Morroni C, *et al.* Randomized Placebo-controlled Trial of Prednisone for the TB Immune Reconstitution Inflammatory Syndrome. In: 16th Conference of Retrovirus and Opportunistic Infection February 8–11 2009; Montreal Abstract 34 www.retroconference.org/2009/ (June 2009, date last accessed).

Pediatric Pulmonology 46:1134–1136 (2011)

Case Report

Not All Children With Nodular Interstitial Lung Patterns in South Africa Have TB—A Rare Case of Paediatric "Bird Fanciers' Disease"

Savvas Andronikou, PhD,[1]* Pierre Goussard, MMed (Paed),[2] and Robert P. Gie, FCP (Paed)[2]

Summary. Bird Fancier's disease is an allergic alveolitis that is rare in children. We describe the relevance of adequate history for making the diagnosis in children and the difficulty distinguishing this entity on chest radiographs and CT from imaging patterns caused by infections such as tuberculosis and HIV in developing countries. **Pediatr Pulmonol. 2011;46:1134–1136.** © 2011 Wiley Periodicals, Inc.

Key words: extrinsic allergic alveolitis; chest radiograph; computed tomography; tuberculosis; HIV.

Funding source: none reported.

INTRODUCTION

"Bird Fancier's Disease" is the most common allergic alveolitis in adults[1] but is rare in children.[2,3] It may present acutely and progressively, intermittently or as recurrent disease[4] and eventual lung fibrosis.[2,5] It results from contact with pets,[1] sports birds,[6] game birds,[7] exotic birds, and feather duvets.[8,9] Imaging findings are common to tuberculosis (TB) and HIV.[10] A typical clinical and radiographic pattern, high index of suspicion and an environmental history are essential.[11] We present a boy diagnosed through a meticulous history and imaging.

CASE REPORT

A 12-year-old boy presented with weight loss, fever, and cough over 2 months. He was cyanotic, had finger clubbing and was tachypneoic. Crepitations were audible bilaterally. Screening for TB, mycoplasma, and clamydia was negative and there was no cardiac disease. Treatment with oxygen and ceftriaxcone was unsuccessful. Further questioning revealed the farther was a pigeon breeder and the boy cleaned the bird cages. IgG antibody test against pigeon serum antigens was negative. Treatment with oral corticosteroids was successful but he represented in 2 weeks with the same symptoms after not avoiding the cages. Chest radiograph demonstrated a diffuse fine nodular pattern but no air-space confluence or effusion. CT chest demonstrated mediastinal lymphadenopathy. High resolution reconstructions demonstrated a mosaic pattern with diffuse fine centrilobular nodules and a ground glass appearance in dependent areas consistent with acute hypersensitivity pneumonitis (Fig. 1). After treatment, the pigeons were removed and he had no further symptoms.

DISCUSSION

Bird Fancier's disease is a hypersensitivity pneumonitis (allergic alveolitis) induced by inhalation of bird antigens in sensitized individuals.[4,5,9] It can result from contact with birds[1,6,7] or feather duvets.[8,9] It is rare in

[1]Radiology Department, University of the Witwatersrand, Johannesburg, South Africa.

[2]Paediatric Pulmonology, Department of Paediatrics and Child Health, University of Stellenbosch, Western Cape, South Africa.

*Correspondence to: Savvas Andronikou, PhD, Harbouredge 700, 10 Hospital Street, Greenpoint 8005, Cape Town, South Africa.
E-mail: docsav@mweb.co.za

Received 11 January 2011; Revised 6 March 2011; Accepted 6 March 2011.

DOI 10.1002/ppul.21473
Published online 25 April 2011 in Wiley Online Library (wileyonlinelibrary.com).

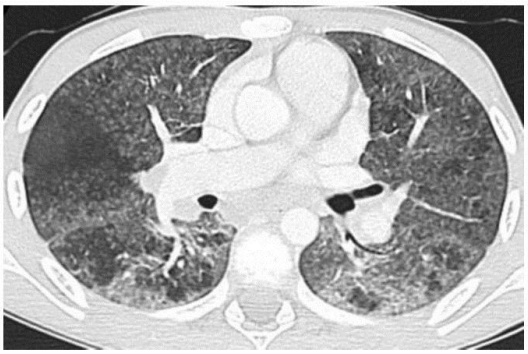

Fig 1. High resolution CT on lung window demonstrates a mosaic pattern with diffuse fine centrilobular nodules and a ground glass appearance in the dependent areas consistent with an acute hypersensitivity pneumonitis.

children[2,3] (38 paediatric cases reported in English).[2,3,5,12–16]

Prompt recognition and management is critical to prevent fibrosis.[2,5] Treatment primarily involves avoidance and oral prednisolone.[2,5] The varied clinical presentation, (acute progressive with breathlessness, cough, fever, shivering, and malaise <8 hr after exposure; intermittent non-progressive; recurrent non-acute)[4,5] makes diagnosis challenging. Children usually present with chronic insidious symptoms due to prolonged exposure to low amounts of antigen[5]—dyspnoea, anorexia, decreased energy, intermittent low-grade fever, and coughing.[5]

Radiographic findings range from widespread patchy consolidation (acute)[11] to a bilateral interstitial pattern (80% of patients),[12] (lower zone[7] micronodular[2] or peripheral reticular[8]). The micronodular pattern seen in our patient is typical in children.[5] HRCT findings include micronodules,[8] ground glass opacity (68%),[8,12] mosaic pattern (61%), and emphysema (17%).[12] In the late stages, fibrosis and honeycombing predominating at the bases may occur.[7,11]

Diffuse interstitial lung disease is rare in childhood and may be due to infection[5] (TB, HIV, aspergillosis)[17], chemicals, drugs, radiation, malignancy, collagen vascular disease, idiopathic fibrosis, alveolar proteinosis, pulmonary lymphangiectasia, and idiopathic haemosiderosis.[5,18,19] Primary TB on HRCT may present as miliary or larger nodules, groundglass, or consolidation,[10,17] centrilobular opacities, bronchiectasis, and air-trapping. Mediastinal lymphadenopathy as seen in our patient is typical of primary TB. In children with HIV, *Pneumocystis carinii* Pneumonia (PCP/PJP), lymphocytic interstitial pneumonitis and bacterial pneumonias also result in patchy airspace, groundglass, reticules, or nodules.[20] Our patients' imaging mimics infectious diseases. One publication by Madrenas and colleagues demonstrates that in the differentiation of patients with milliary TB and those with Bird Fancier's disease, the laboratory can make a clear distinction when the radiograph shows a nodular pattern.[21] They showed that low values for hemoglobin, red blood cell count, and hematocrit; alterations of leukocyte count and differential; hypoalbuminemia and hyponatremia in a patient with fever, supports the diagnosis of TB. Normal values for these parameters, with hypergammaglobulinemia is more in keeping with Bird Fancier's disease.[21]

CONCLUSION

In Africa, a child with cough, fever, weight loss, and malaise demonstrating a nodular radiographic pattern probably has TB[10] or HIV.[22,23] To diagnose "Bird Fancier's Disease" in a child in this setting, paediatricians must have a high index of suspicion, recognize the typical clinical and radiological appearances and routinely take a diligent environmental history.

REFERENCES

1. Hendrick DJ, Faux JA, Marshal R. Budgerigar–Fancier's Lung: the commonest variety of allergic alveolitis in Britain. BMJ 1978;2:81–84.
2. Stauffer Ettlin M, Pache JC, Renevey F, Hanquinet-Ginter S, Guinand S, Barazzone Argiroffo C. Bird breeders disease: a rare diagnosis in young children. Eur J Pediatr 2006;165:55–61.
3. Nacar N, Kiper N, Yalcin E, Dogru D, Dilber E, Ozcelik U, Misirligil Z. Hypersensitivity pneumonitis in children: pigeon Breeder's disease. Ann Trop Paediatr 2004;24:349–355.
4. Bourke SJ, Banham SW, Carter R, Lynch P, Boyd G. Longitudinal course of extrinsic allergic alveolitis in pigeon breeders. Thorax 1989;44:415–418.
5. Tsai E, Couture D, Hughes DM. A pediatric case of pigeon breeder's disease in Nova Scotia. Can Respir J 1998;5:507–510.
6. Bourke S, Boyd G. Pigeon Fancier's Lung—antigen avoidance and respiratory protection are the mainstays of management. BMJ 1997;315:70–71.
7. Partridge SJ, Pepperell JCT, Forrester-Wood C, Ibrahim NBN, Raynal A, Swinburn CR. Pheasant rearer's lung. Occup Med 2004;54:500–503.
8. Inase N, Ohtani Y, Endo J, Miyake S, Yoshizawa Y. Feather duvet lung. Med Sci Monit 2003;9:CS37-40.
9. Inase N, Ohtani Y, Sumi Y, Umino T, Usui Y, Miyake S, Yoshizawa Y. A clinical study of hypersensitivity pneumonitis presumably caused by feather duvets. Ann Allergy Asthma Immunol 2006;96:98–104.
10. Andronikou S, Vanhoenacker FM, De Backer AI. Advances in imaging chest tuberculosis: blurring of differences between children and adults. Clin Chest Med 2009;30:717–744, viii.
11. Tasaka S, Knanazawa M, Kawai C, Soejima K, Yamaguchi K, Takata A, Torikata C, Hata J. Fatal diffuse alveolar damage from Bird Fancier's Lung. Respiration 1997;64:307–309.
12. Morell F, Roger A, Reyes L, Cruz MJ, Murio C, Munoz X. Bird Fancier's Lung: a series of 86 patients. Medicine (Blatimore) 2008;87:110–130.

13. Yalcin E, Kiper N, Gocmen A, Ozcelik U, Dogru D, Misirligil Z. Pigeon Breeder's Disease in a child with selective IgA deficiency. Pediatr Int 2003;45:216–218.
14. Bahna SL. A custodian cured the doctor. Pediatrics 2000;105: E71.
15. Ceviz N, Kaynar H, Olgun H, Onbar O, Misirligil Z. Pigeon Breeder's Lung in childhood: is family screening necessary? Pediatr Pulmonol 2006;41:279–282.
16. Du Marche Sarvaas GJ, Merkus PJ, de Jongste JC. A family withextrinsic allergic alveolitis caused by wild city pigeons: a case report. Pediatrics 2000;105:E62.
17. Andronikou S, Wieselthaler N, Bertelsmann J. Paediatric HRCT of the chest-help for the general radiologist. SAJR 2005;9: 21–29.
18. Koh DM, Hansell DM. Computed tomography of diffuse interstitial lung disease in childhood. Clin Radiol 2000;55:659–667.
19. Copley SJ, Coren M, Nicholson AG, Rubens MB, Bush A, Hansell DM. Diagnostic accuracy of thin-section CT and chest radiography of paediatric interstitial lung disease. Am J Roentgenol 2000;174:549–554.
20. Kuhn JP, Brody AS. High resolution CT of pediatric lung disease. Radiol Clin North Am 2002;40:89–110.
21. Madrenas J, Curull V, Vidal R, Morell F. Non immunological analytic data fopr the differential diagnosis between military tuberculosis (MTBC) and bird breeder's disease (BBD). Allergol Immunopathol (Madr) 1985;13:301–304.
22. Theron S, Andronikou S, George R, du Plessis J, Goussard P, Hayes M, Mapukata A, Gie R. Non-infective pulmonary disease in HIV-positive children. Pediatr Radiol 2009;39:555–564.
23. George R, Andronikou S, Theron S, du Plessis J, Hayes M, Goussard P, Mapukata A, Gie R. Pulmonary infections in HIV-positive children. Pediatr Radiol 2009;39:545–554.

Pediatr Radiol (2013) 43:254–255
DOI 10.1007/s00247-012-2557-1

LETTER TO THE EDITOR

Tuberculous lymphadenopathy is not only obstructive but also inflammatory—it can erode anything it touches. Reply to Marchiori et al

Susan Lucas · Savvas Andronikou · Pierre Goussard · Robert Gie

Received: 12 September 2012 / Accepted: 13 September 2012 / Published online: 27 November 2012

Sir,

We thank Dr. Marchiori [1] and colleagues for taking an interest in our publication on lymphobronchial tuberculosis [2] and for contributing a case demonstrating the development of lymphobronchial fistula in a child with tuberculosis [1].

Members of our research group have reported the consequences of lymph node erosion into adjacent structures through inflammation and necrosis. These include erosion into the oesophagus [3, 4] with subsequent need for oesophageal stenting [5]; erosion into the pleural space with fibrin glue closure as a treatment option [6], erosion into the phrenic nerve with resulting palsy [7] and erosion into the thoracic duct causing chylothorax [8].

We have also performed a CT scan on a 5-month-old infant where the tuberculous lymphadenopathy eroded into the airway, leading to a significant amount of air detectable throughout the mediastinal structures and within the lymph nodes (Fig. 1). Bronchoscopy demonstrated a defect in the wall of the left lower lobe bronchus, allowing air to escape freely into the mediastinum (Fig. 2). These further examples emphasize the finding highlighted by Marchiori and colleagues [1], namely that the tuberculous lymphadenopathy is inflammatory and may cause a reaction and necrosis in adjacent structures leading to a wide variety of clinical problems in addition to the pressure effects and compression of the airways described previously [2].

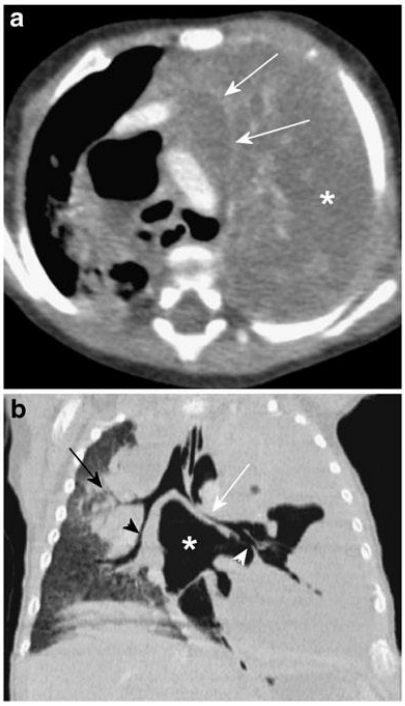

Fig. 1 CT of the chest in a 5-month old girl with lymphobronchial TB. **a** Axial image at the level of the carina after administration of contrast agent shows extensive pneumomediastinum as a result of a lymphobronchial fistula. Ghost-like enhancement (*arrows*) of superior mediastinal nodes is visible, as well as necrosis (non-enhancement, *white star*) of the left lung parenchyma. **b** Reformatted coronal thick-slab minimum-intensity projection of the CT scan shows significant narrowing of the left main bronchus (*white arrow*) and bronchus intermedius (*black arrowhead*). The extensive breakdown of the subcarinal nodal group is clearly visible (*white star*), as is the consolidation of right upper lobe (*black arrow*). The wide fistulous connection between the left lower lobe bronchus and the necrotic subcarinal nodes is indicated with a *white arrowhead*

S. Lucas (✉) · S. Andronikou
Department of Radiology, Faculty of Health Sciences,
University of Witwatersrand,
7 York Road, Parktown,
Johannesburg 2001, South Africa
e-mail: su.lucas@iburst.co.za

P. Goussard · R. Gie
Department of Paediatrics, Stellenbosch University,
Stellenbosch, South Africa

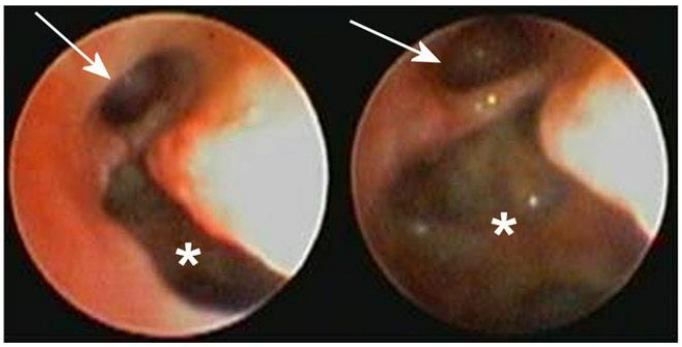

Fig. 2 Fiberoptic tracheobronchoscopy image taken from left main bronchus shows the left upper lobe bronchus (*white arrow*) and a very large cavity originating from a destroyed left lower lobe bronchus

References

1. Marchiori E, Francisco FAF, Zanetti G et al (2012) Lymphobronchial fistula: another complication associated with lymphobronchial tuberculosis in children. Pediatr Radiol doi:10.1007/s00247-012-2538-4
2. Lucas S, Andronikou S, Goussard P et al (2012) CT features of lymphobronchial tuberculosis in children, including complications and associated abnormalities. Pediatr Radiol 42:923–931
3. Erlank A, Goussard P, Andronikou S et al (2007) Oesophageal perforation as a complication of primary pulmonary tuberculous lymphadenopathy in children. Pediatr Radiol 37:636–639
4. Goussard P, Andronikou S (2010) Tuberculous broncho-oesophageal fistula: images demonstrating the pathogenesis. Pediatr Radiol 40 (Suppl 1):S78
5. Goussard P, Sidler D, Kling S et al (2007) Esophageal stent improves ventilation in a child with a broncho-esophageal fistula caused by *Mycobacterium tuberculosis*. Pediatr Pulmonol 42:93–97
6. Goussard P, Gie RP, Kling S et al (2008) Fibrin glue closure of persistent bronchopleural fistula following pneumonectomy for post-tuberculosis bronchiectasis. Pediatr Pulmonol 43:721–725
7. Goussard P, Gie RP, Kling S et al (2009) Phrenic nerve palsy in children associated with confirmed intrathoracic tuberculosis: diagnosis and clinical course. Pediatr Pulmonol 44:345–350
8. Grobbelaar M, Andronikou S, Goussard P et al (2008) Chylothorax as a complication of pulmonary tuberculosis in children. Pediatr Radiol 38:224–226

INT J TUBERC LUNG DIS 18(7):763–769

http://dx.doi.org/10.5588/ijtld.13.0892

Teaching chest X-ray reading for child tuberculosis suspects

J. A. Seddon,*† T. Padayachee,‡ A-M. Du Plessis,§ P. Goussard,¶ H. S. Schaaf,*¶ C. Lombard,‡ R. P. Gie*¶

*Desmond Tutu TB Centre, Department of Paediatrics and Child Health, Faculty of Medicine and Health Sciences, Stellenbosch University, South Africa; †Department of Paediatric Infectious Diseases, Imperial College London, London, UK; ‡Biostatistics Unit, Medical Research Council, Tygerberg, §Department of Radiology, Tygerberg Hospital, Tygerberg, ¶Tygerberg Children's Hospital, Tygerberg, South Africa

SUMMARY

SETTING: Cape Town, South Africa.

OBJECTIVE: To improve the reading of chest X-rays (CXRs) in child tuberculosis (TB) suspects.

DESIGN: We designed a reporting and recording form to assist in the diagnosis of childhood TB from CXRs. We then developed an image bank of antero-posterior and lateral CXR pairs, with each image pair assigned to one of four diagnostic categories. Finally, we designed and carried out a 1-day training course to teach clinicians how to read paediatric CXRs, with pre- and post-course assessments.

RESULTS: Of the 27 participants included, 17 (63%) were women. The median age was 38 years (interquartile range [IQR] 32.5–43.5). The median pre-training score was 16.0/30 (IQR 13.0–18.0) and the median post-training score was 17.0 (IQR 13.5–21.0). Sensitivity ($P = 0.09$) and specificity ($P = 0.06$) to detect TB did not change as a result of the course; however, the Wilcoxon signed ranks paired-sample test indicated an increase in the participants' overall ability to read CXRs ($P = 0.017$).

CONCLUSIONS: Teaching clinicians with a 1-day training course using a systematic approach and a standardised form led to a limited improvement in CXR reading ability.

KEY WORDS: paediatric; childhood; teaching; X-ray; TB

THE DIAGNOSIS of tuberculosis (TB) in adults is well established, and mostly relies on phenotypic or genotypic microbiological confirmation. In adult TB suspects who are smear- and culture-negative, the chest X-ray (CXR) remains an important diagnostic tool. To this end, validated epidemiological tools exist for standardised CXR reading in adults[1,2] and aids to improve radiological diagnosis have recently been published.[3]

In children, the situation is different. As children frequently develop paucibacillary disease, only a small proportion of cases with clinical evidence of disease have microbiological confirmation,[4] and clinical scoring systems have proved disappointing.[5,6] In addition, human immunodeficiency virus (HIV) infection can both increase the risk of TB as well as complicate the diagnosis due to clinical and radiological overlap. In the majority of children, diagnosis relies on the constellation of reported symptoms, history of TB exposure, clinical signs, immunological tests and CXR. In the highly industrialised regions of the world, complex, invasive and expensive imaging modalities, such as computerised tomography (CT) and magnetic resonance imaging or bronchoscopy, are available to assist in the diagnosis of TB in children.[7–11] In the majority of high TB incidence countries, however, the only type of imaging available is plain film CXR. This diagnostic challenge is further complicated by the lack of radiologists and high-quality radiographic services. Usually, therefore, in most high TB incidence countries of the world, a clinician must interpret the CXR after clinical assessment of the child TB suspect.

Many frontline clinicians and even paediatric specialists have limited training and expertise in reading paediatric CXRs, and many have little experience of interpreting lateral images. Over- and under-diagnosis occurs, and cases are either missed or treated unnecessarily. Intra- and inter-observer error is widespread, even among experts.[12–14] CXR reading scores are available to assist in the context of childhood pneumonia[15] and cystic fibrosis,[16] and for adults with suspected TB,[17] but none exist for childhood TB. Training courses have been demonstrated to improve CXR reading for children with severe pneumonia,[18] and although some general

Correspondence to: James Seddon, Department of Paediatric Infectious Diseases, Imperial College London, Norfolk Place, London W2 1NY, UK. Tel: (+44) 20 7594 3179. Fax: (+44) 20 7594 3984. e-mail: james.seddon@imperial.ac.uk
Article submitted 12 December 2013. Final version accepted 17 March 2014.

advice and guidance on reading CXR in childhood TB is available,[19–21] we are not aware of any training courses designed for clinicians working in a high TB-HIV context that have been formally evaluated and published.

We aimed to design and carry out a training course to teach physicians to better diagnose TB in children using CXR. We also sought to evaluate the course to determine if it was successful in its aim.

STUDY POPULATION AND METHODS

Setting and participants

This course was carried out at Stellenbosch University, Western Cape province, South Africa, with CXR images included from children treated at the Tygerberg Children's Hospital (TCH). Western Cape had a TB notification rate of 976 per 100 000 population in 2009.[22] The course was designed for doctors (non-radiologists) working in high TB-HIV prevalence settings; the only prerequisite was that they be responsible for the care of children with TB. As the course and its evaluation were considered routine teaching and training, participants were not asked to provide written consent, and ethical approval was not requested.

The childhood tuberculosis diagnosis reporting and recording form

A one-page form designed by the research team included the main CXR changes associated with childhood TB (Figure 1).[23] An assessment of adequacy (identification, inspiration, rotation and penetration) was included for both antero-posterior and lateral images. Changes in the parenchyma of the lungs were recorded using descriptive rather than anatomical position (three equal zones on each side rather than lung lobes); changes outside the parenchyma were also recorded. The form was developed from previous templates that have been used to report on childhood[23,24] and adult CXR.[2] The role of the form was to provide an *aide-mémoire* to assist systematic CXR reading as well as to provide a record to enable classification, severity of disease and monitoring over time. The final component of the form, to be completed once the CXR had been reviewed, was to assign one of the four following diagnostic categories: 'normal', 'abnormal, unlikely TB', 'abnormal, likely TB' or 'unreadable'.

Creation of the image bank

We created a bank of images divided into the four diagnostic categories, to be used for course evaluation. All images consisted of a pair of CXRs (antero-posterior and lateral) that had been taken from the hospital picture archiving and communication system (PACS). All image pairs were of children (aged <14 years) who had been admitted to TCH or seen at TCH from January to December 2010. A panel of experts (two paediatric respiratory specialists, two paediatric infectious disease specialists and one paediatric radiologist) reviewed the CXRs and discarded any image pairs that were not appropriate for the given category (Table 1). For the category of 'abnormal likely TB', the images of all children diagnosed with culture-confirmed TB at TCH in 2010 were reviewed, and only images of children with both culture-confirmed TB and CXR features characteristic of childhood TB were included. For the category of 'abnormal unlikely TB', a diagnosis other than TB had been determined. The final bank included 68 image pairs, divided roughly evenly between the four categories. All images were anonymised when extracted from the PACS.

Teaching strategy

A pilot course was conducted and the course then refined on the basis of teaching experience, participant feedback and interpretation of pre- and post-training course assessments. The 1-day (7-h) course was taught by five faculty members (the five authors who developed the image bank); mixed teaching methods, including lectures, videos and interactive sessions, were used. The course included an introduction; a pre-course test; teaching on the basics of radiology physics; chest anatomy and an assessment of adequacy; the use of a reporting and recording (R&R) form and a systematic approach to reading CXR;[19,21] a review of CXR features typical of paediatric TB (taught using a framework that followed the pathophysiology of childhood TB);[23] a facilitated, interactive session; and then a post-course test. Repeated examples of CXR demonstrating TB pathology were shown, as well as non-TB pathology that might be confused with a diagnosis of TB. Features that we taught as being highly suggestive of paediatric TB in the target context included hilar lymphadenopathy, large airways compression, Ghon complexes/foci, miliary picture and adult-type cavitations. We also demonstrated other findings (lobar opacification/collapse, hyperinflation, fibrosis, parenchymal infiltrates, bronchopneumonic changes, pleural effusions, tracheal deviation, as well as cardiac and spinal changes) that could indicate TB but might also be seen in other conditions. We taught that where there were multiple features suggestive of TB, the diagnosis of TB was more likely.

CXRs demonstrating pathology were presented alongside normal CXRs to highlight changes. For each CXR presented, a completed R&R form was shown to reinforce the value of the systematic approach to examine the CXR. Chest CT scans and bronchoscopic images were used in conjunction with the CXRs to reinforce the pathological changes resulting from TB in children. The course was

CXR code		CXR date	
Reader code		Date read	

Quality	AP/PA		Lateral	
	Readable	Unreadable	Readable	Unreadable
Identification				
Inspiration				
Rotation				
Penetration				

			AP/PA						Lateral		
	Yes	No	RUZ	RMZ	RLZ	LUZ	LMZ	LLZ	UZ	MZ	LZ
Lobar consolidation											
Bronchopneumonic											
Ghon focus											
Cavity											
Interstitial changes											
Nodular infiltration											
Calcification in lung											
Fibrosis											
	Yes	No	Right			Left			Lateral		
Hyperinflation											
Volume Loss											
Peri-hilar infiltration											
Peri-hilar nodes											
Paratracheal nodes											
Nodal calcification											
Airway compression											
Pleural fluid											
Pneumothorax											

	Yes	No		Yes	No
Tracheal deviation			Soft tissue changes		
Mediastinal deviation			Spine abnormality		
Cardiac abnormality			Other bony abnormality		
Displaced diaphragm			Artefact/FB		

	Normal	Abnormal – unlikely TB	Abnormal – likely TB	Unreadable
Diagnosis				

Figure 1 Reporting and recording form used in the training course. CXR = chest X-ray; AP = antero-posterior; PA = posteroanterior; RUZ = right upper zone; RMZ = right middle zone; RLZ = right lower zone; LUZ = left upper zone; LMZ = left middle zone; LLZ = left lower zone; UZ = upper zone; MZ = middle zone; LZ = lower zone; FB = foreign body; TB = tuberculosis.

conducted in a computer laboratory so that each participant had their own high-resolution monitor.

Evaluation of the course

Thirty pairs of CXR images were selected from the image bank using a randomly computer-generated numbering system. This included 7 'normal' pairs, 7 that were classed as 'abnormal, unlikely TB', 9 'abnormal, likely TB' and 7 'unreadable'. Following the introductory lecture, participants were given 2 min to view each of the 30 pairs of CXR images, and were then asked to assign one of the four diagnostic categories to each image pair. Following the training course, the participants were given the same CXR pairs to read, with 2 min for each pair. They were asked to complete one R&R form for each pair of CXR images and to select one of the diagnostic categories. As all images were anonymised, CXR pairs could not be evaluated for their identification; an assessment of adequacy was based on inspiration, rotation and penetration only. If either the antero-posterior or the lateral image had any features of poor adequacy, candidates were instructed to classify them as 'unreadable'.

Basic demographic data (age, sex, radiological and paediatric training, and experience) on each participant were collected. All data concerning course participants were dissociated from identifier details with unique course numbers.

Table 1 Criteria required to fulfil the diagnostic categories for an image pair to be included in the image bank

Image category	Criteria
Normal	Antero-posterior and lateral images present Optimal inspiration, rotation and penetration of both antero-posterior and lateral image (identification not used as all images were anonymous) No changes inconsistent with normal anatomy observed Physiological structures that are not always seen (such as a thymus) could be present
Abnormal, likely TB	Antero-posterior and lateral images present Optimal inspiration, rotation and penetration of both antero-posterior and lateral images Changes that were unlikely to be normal observed Changes consistent with the common presentations of childhood TB: Lymphadenopathy Cavitation Airways narrowing (compression) Miliary pattern
Abnormal, unlikely TB	Antero-posterior and lateral images present Optimal inspiration, rotation and penetration of both antero-posterior and lateral images Changes that were unlikely to be normal observed Changes inconsistent with the common presentations of childhood TB
Unreadable	Antero-posterior and lateral images present Adequacy significantly impaired by poor inspiration, rotation or under/over penetration of either antero-posterior or lateral image

TB = tuberculosis.

Statistical analysis

The data were analysed using *R* (R Computing, Vienna, Austria), an open-source programming language, through a series of tabulations, graphical displays and non-parametric statistical tests. Individuals were evaluated pre- and post-training. As such, paired comparisons involving the difference scores of the participants (post-training score minus pre-training score) were made. The distribution of difference scores warranted non-parametric tests (Figure 2). Wilcoxon signed ranks paired-sample tests were performed to test whether the median difference in scores was significantly greater than zero and, in addition, for difference in test scores by diagnostic category. To investigate whether certain individuals benefited more from the training than others, a linear model of the rank-transformed post-training scores was regressed onto the pre-training scores, and the indicator variables sex and previous paediatric or radiology training were fitted after establishing that the interaction between pre-training scores and previous paediatric or radiology training was not statistically significant.

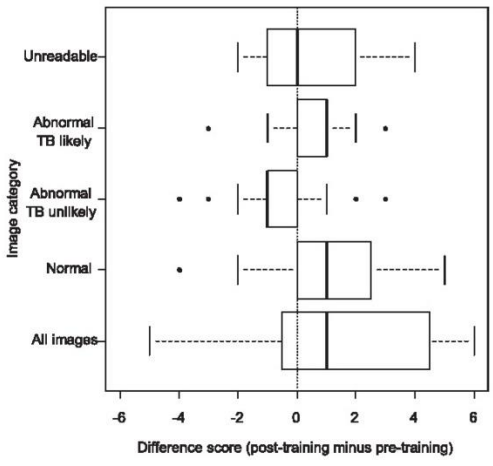

Figure 2 Box plot of difference scores by image category. TB = tuberculosis.

RESULTS

Of the 27 participants who undertook the course, 17 (63%) were women, 17 (63%) had undertaken previous training in either radiology or paediatrics, and 4 (15%) had attended a previous CXR reading course. The median age of the participants was 38 years (interquartile range [IQR] 32.5–43.5). The median number of years qualified was 11 (IQR 7.5–16.5), the median number of years spent in a TB clinic was 3 (IQR 1.0–6.0) and the median number of years of paediatric experience was 5.0 (IQR 2.0–10.0). The median pre-training score (out of 30) was 16.0 (IQR 13.0–18.0) and the median post-training score was 17.0 (IQR 13.5–21.0).

Figure 3 shows the number of individuals (out of 27) who correctly read each image pre- and post-training. The median number of individuals who correctly read each image pre- and post-training, in that order, for each image category were 'normal', 14 and 19, 'abnormal, unlikely TB', 13 and 12; 'abnormal, likely TB', 23 and 21; and 'unreadable',

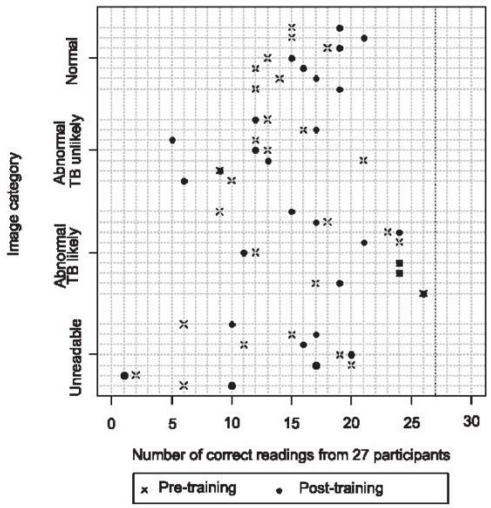

Figure 3 Dot plot of the number of correct readings per image for pre-and post-training test. TB = tuberculosis.

11 and 16. Table 2 demonstrates the median number of CXR images correctly identified by each participant per category. The median sensitivity to identify images 'abnormal, likely TB' before the training was 0.67 (IQR 0.56–0.83) and the median sensitivity after the training was 0.67 (IQR 0.67–0.89). The median specificity before and after the training was respectively 0.52 (IQR 0.48–0.62) and 0.48 (IQR 0.31–0.67). The median difference in sensitivity ($P = 0.087$) and the median difference in specificity ($P = 0.064$) were not significantly different from zero. The Wilcoxon signed ranks paired-sample test indicated an increase in the participants' overall ability to read CXRs ($P = 0.017$). The tests by image category also indicate an increase in ability to identify 'normal' ($P = 0.013$), 'abnormal, likely TB' ($P = 0.043$) and 'unreadable' ($P = 0.038$) images but a reduced ability to identify 'abnormal, unlikely TB' images ($P = 0.023$). In 43 instances, participants correctly identified CXR pairs as 'abnormal, unlikely TB' pre-course, but then changed their response post-course. In 3 they changed it to 'normal', in 35 to 'abnormal, likely TB' and in 5 to 'unreadable.'

Table 2 Median number of CXR images correctly identified by each participant per category

CXR category	Total number of CXR images in test	Pre-training	Post-training
Normal	7	4	6
Abnormal, unlikely TB	7	3	3
Abnormal, likely TB	9	6	6
Unreadable	7	3	3

CXR – chest X-ray; TB – tuberculosis.

When assessing the impact of participant characteristics on teaching impact, the model indicated a positive association between rank of post-training and pre-training ($P < 0.001$) and a positive association between rank of post-training and previous paediatric or radiology training ($P = 0.024$), keeping all other variables constant.

DISCUSSION

In this article we describe the design of a course to teach clinicians who regularly manage children with TB on how to interpret CXRs in high TB-HIV settings. We seem to have improved the participants' ability to correctly identify normal and unreadable CXR images, but made only minimal difference in their ability to correctly identify TB. We have shown that those with some paediatric or radiology training improved more than those with less training.

The implications of these findings are complex. It may mean either that we did not succeed in teaching reading skills or, alternatively, that with the evaluation system used we did not capture any improvements seen. It does appear that once a participant had identified an image as abnormal, they were more likely to classify it as TB following training; in a number of instances, participants correctly identified images as non-TB pre-training and then incorrectly labelled them as TB post-training. Spending a day reviewing mainly images that were consistent with TB may have increased the readiness of attendees to classify images as TB. Reading CXR is a complex skill; 7 h of training provides a foundation that can be built on with further experience and training, but it may not in itself be enough to improve reading skills. The implications of those with some experience benefiting more from the course may mean that such persons were building on knowledge and experience that they already had.

In most clinical practice, CXRs are interpreted following history taking and physical examination. However, we felt that it was important to read CXRs blinded to the clinical details. The probability of a patient having disease following a diagnostic test (post-test probability of disease) is dependent on the probability of a positive pre-test diagnosis (the pre-test probability), combined with the likelihood of a positive diagnosis given a positive test result (the likelihood ratio).[25] For most diagnostic tests, the pre-test probability and likelihood ratio are independent of each other, but if, as is often the case with CXRs, the likelihood ratio is influenced by pre-test probability, the utility of the test is difficult to interpret. By masking clinical details, we were able to determine the impact of training on the ability to diagnose TB using CXR rather than the ability to diagnose TB using a combination of clinical details and CXR. The composition of the bank used for testing is also

important, as it effectively influences the pre-test probability of TB disease. We tried to replicate these ratios in our teaching material, as the composition of teaching resources can influence interpretation.[26,27] However, we acknowledge that it is not possible to replicate the proportion of cases that are seen by a wide range of practitioners working in different contexts.

Our course and its evaluation had strengths and limitations. We were able to assess the impact of a training intervention on the ability of participants to interpret a diagnostic test, and we isolated the ability to read CXRs using other components of diagnosis by masking the clinical details of each case. However, we were only able to demonstrate a modest improvement and, due to the limited demographic data collected, we were unable to perform an extensive analysis of participant characteristics to determine who had benefited the most. We taught participants to reject CXR images with any features of poor adequacy, while acknowledging that in the real world this is frequently not practical or appropriate.[28] When teaching the course participants, we used a number of interventions: teaching background information, providing a systematic approach, using an R&R form, exposure to numerous CXR images, and group consolidation and review. It is unclear whether certain interventions provided benefit, whether some detracted or whether a combination was effective. We also did not assess the impact of our training over time. Finally, although we approached the classification of our diagnostic groups with rigour, including only culture-confirmed TB cases in the 'abnormal, likely TB' group, the gold standard against which we tested the participants was essentially expert opinion.

CONCLUSIONS

Teaching occurs in many contexts and is a fundamental component of medical training. However, teaching how to read CXRs in children is rarely assessed to determine if it achieves its aims. The evaluation of a teaching intervention not only helps in determining its benefits, it can also guide modifications for improving its impact. CXR reading and interpretation is challenging, and no training courses have previously been evaluated and published. The training course that we have developed is comprehensive, but it demonstrates only limited improvement in participant reading ability.

Acknowledgements

JAS was supported by a grant from the United States Agency for International Development Cooperative Agreement (TREAT TB: Agreement No GHN-A-00-08-00004-00) and by a fellowship from the Sir Halley Stewart Trust. The contents are the responsibility of the author(s) and do not necessarily reflect the views of the funders.

Conflict of interest: none declared.

References

1 Dawson R, Masuka P, Edwards D J, et al. Chest radiograph reading and recording system: evaluation for tuberculosis screening in patients with advanced HIV. Int J Tuberc Lung Dis 2010; 14: 52–58.
2 Den Boon S, Bateman E D, Enarson D A, et al. Development and evaluation of a new chest radiograph reading and recording system for epidemiological surveys of tuberculosis and lung disease. Int J Tuberc Lung Dis 2005; 9: 1088–1096.
3 Tuberculosis Coalition for Technical Assistance. Handbook for district hospitals in resource constrained settings for the quality improvement of chest X-ray reading in tuberculosis suspects. The Hague, The Netherlands: 2010. http://www.tbcta.org//Uploaded_files/Zelf/XRayQIHandbook1283938569.pdf Accessed April 2014.
4 Zar H J, Hanslo D, Apolles P, Swingler G, Hussey G. Induced sputum versus gastric lavage for microbiological confirmation of pulmonary tuberculosis in infants and young children: a prospective study. Lancet 2005; 365: 130–134.
5 Edwards D J, Kitetele F, Van Rie A. Agreement between clinical scoring systems used for the diagnosis of pediatric tuberculosis in the HIV era. Int J Tuberc Lung Dis 2007; 11: 263–269.
6 Hesseling A C, Gie R P. Scoring systems for the diagnosis of childhood tuberculosis: are we making progress? Int J Tuberc Lung Dis 2007; 11: 245.
7 Andronikou S. Pathological correlation of CT-detected mediastinal lymphadenopathy in children: the lack of size threshold criteria for abnormality. Pediatr Radiol 2002; 32: 912.
8 Andronikou S, Brauer B, Galpin J, et al. Interobserver variability in the detection of mediastinal and hilar lymph nodes on CT in children with suspected pulmonary tuberculosis. Pediatr Radiol 2005; 35: 425–428.
9 Andronikou S, Joseph E, Lucas S, et al. CT scanning for the detection of tuberculous mediastinal and hilar lymphadenopathy in children. Pediatr Radiol 2004; 34: 232–236.
10 Kim W S, Moon W K, Kim I O, et al. Pulmonary tuberculosis in children: evaluation with CT. AJR Am J Roentgenol 1997; 168: 1005–1009.
11 du Plessis J, Goussard P, Andronikou S, Gie R, George R. Comparing three-dimensional volume-rendered CT images with fibreoptic tracheobronchoscopy in the evaluation of airway compression caused by tuberculous lymphadenopathy in children. Pediatr Radiol 2009; 39: 694–702.
12 Hatherill M, Hanslo M, Hawkridge T, et al. Structured approaches for the screening and diagnosis of childhood tuberculosis in a high prevalence region of South Africa. Bull World Health Organ 2010; 88: 312–320.
13 De Villiers R V, Andronikou S, Van de Westhuizen S. Specificity and sensitivity of chest radiographs in the diagnosis of paediatric pulmonary tuberculosis and the value of additional high-kilovolt radiographs. Australas Radiol 2004; 48: 148–153.
14 Swingler G H, du Toit G, Andronikou S, van der Merwe L, Zar H J. Diagnostic accuracy of chest radiography in detecting mediastinal lymphadenopathy in suspected pulmonary tuberculosis. Arch Dis Child 2005; 90: 1153–1156.
15 Cherian T, Mulholland E K, Carlin J B, et al. Standardized interpretation of paediatric chest radiographs for the diagnosis of pneumonia in epidemiological studies. Bull World Health Organ 2005; 83: 353–359.
16 Conway S P, Pond M N, Bowler I, et al. The chest radiograph in cystic fibrosis: a new scoring system compared with the Chrispin-Norman and Brasfield scores. Thorax 1994; 49: 860–862.
17 Ralph A P, Ardian M, Wiguna A, et al. A simple, valid, numerical score for grading chest x-ray severity in adult smear-positive pulmonary tuberculosis. Thorax 2010; 65: 863–869.
18 Patel A B, Amin A, Sortey S Z, Athawale A, Kulkarni H. Impact

of training on observer variation in chest radiographs of children with severe pneumonia. Indian Pediatr 2007; 44: 675–681.
19 Arthur R. Interpretation of the paediatric chest X-ray. Paediatr Respir Rev 2000; 1: 41–50.
20 Gie R. Diagnostic atlas of intrathoracic tuberculosis in children—a guide for low income countries. Paris, France: International Union Against Tuberculosis and Lung Disease, 2003. http://www.theunion.org/what-we-do/publications/technical/english/pub_diagnostic-atlas_eng.pdf Accessed April 2014.
21 Raoof S, Feigin D, Sung A, Irugulpati L, Rosenow E C, 3rd. Interpretation of plain chest roentgenogram. Chest 2012; 141: 545–558.
22 South Africa Ministry of Health. South African Health Review 2010. Health and related indicators. Pretoria, South Africa: MoH, 2010. http://www.hst.org.za/sites/default/files/sahr10_21.pdf Accessed April 2014.
23 Marais B J, Gie R P, Schaaf H S, et al. A proposed radiological classification of childhood intra-thoracic tuberculosis. Pediatr Radiol 2004; 34: 886–894.
24 Graham S M, Ahmed T, Amanullah F, et al. Evaluation of tuberculosis diagnostics in children: 1. Proposed clinical case definitions for classification of intrathoracic tuberculosis disease. Consensus from an expert panel. J Infect Dis 2012; 205 (Suppl 2): S199–S208.
25 Fagan T J. Nomogram for Bayes's theorem. N Engl J Med 1975; 293: 257.
26 Boutis K, Pecaric M, Pusic M. Teaching X-ray interpretation: selecting the radiographs by the target population. Med Educ 2009; 43: 434–441.
27 Pusic M V, Andrews J S, Kessler D O, et al. Prevalence of abnormal cases in an image bank affects the learning of radiograph interpretation. Med Educ 2012; 46: 289–298.
28 Cook J V, Kyriou J C, Pettet A, Fitzgerald M C, Shah K, Pablot S M. Key factors in the optimization of paediatric X-ray practice. Br J Radiol 2001; 74: 1032–1040.

RESUME

CONTEXTE : Le Cap, Afrique du Sud.
OBJECTIF : Améliorer l'interprétation des radios pulmonaires (RP) des enfants avec une tuberculose (TB) présumée.
SCHÉMA : Nous avons élaboré un formulaire de rapport et d'enregistrement afin de contribuer au diagnostic de la TB de l'enfant à partir des RP. Nous avons ensuite conçu une banque d'images de RP de face et de profil, chaque paire de clichés étant assignée à une des quatre catégories de diagnostic. Enfin, nous avons conçu et réalisé une formation d'une journée pour apprendre aux cliniciens à lire les RP pédiatriques avec une évaluation avant et après le cours.
RÉSULTATS : Des 27 participants inclus, 17 (63%) étaient des femmes. L'âge médian était de 38 ans (plage interquartile [IQR] 32,5–43,5). Le score médian avant la formation était de 16,0 (sur 30) (IQR 13,0–18,0) et le score médian après le cours était de 17,0 (IQR 13,5–21,0). La sensibilité ($P = 0,09$) et la spécificité ($P = 0,06$) de la détection de la TB ne se sont pas modifiées après le cours, mais le test de Wilcoxon signed-ranks sur des échantillons appariés a mis en évidence une augmentation de la capacité des participants à lire les RP ($P = 0,017$).
CONCLUSIONS : Une formation d'une journée pour apprendre aux cliniciens à mieux lire les RP grâce à une approche systématique et un formulaire standardisé a mis en évidence une amélioration limitée de cette capacité de lecture.

RESUMEN

MARCO DE REFERENCIA: La Ciudad del Cabo en Suráfrica.
OBJETIVO: Mejorar la lectura de las radiografías de tórax (CXR) de los niños con presunción diagnóstica de tuberculosis (TB).
MÉTODOS: Se elaboró un formulario de registro y notificación destinado a facilitar el diagnóstico de la TB en los niños a partir de la CXR. Luego, se generó un banco de imágenes con parejas de imágenes anteroposterior y lateral y se asignó cada par a una de cuatro categorías diagnósticas. Por último, se preparó e impartió un cursillo de capacitación de un día con el fin de enseñar a los médicos la lectura de las CXR en pediatría; se llevaron a cabo evaluaciones antes del curso y después del mismo.
RESULTADOS: Se incluyeron 27 participantes en el estudio y 17 fueron mujeres (63%). La mediana de la edad fue 38 años (intervalo intercuartil [IIC] 32,5–43,5). La mediana de la puntuación antes de la capacitación fue 16,0 (sobre 30 puntos; IIC 13,0–18,0) y después de la capacitación la mediana fue 17,0 (IIC 13,5–21,0). La sensibilidad del método en la detección de la tuberculosis no se modificó después de la capacitación ($P = 0,09$) y tampoco su especificidad ($P = 0,06$), pero la prueba de Wilcoxon para datos emparejados indicó un aumento de la competencia global de los participantes para leer las CXR ($P = 0,017$).
CONCLUSIÓN: La capacitación de los médicos en un cursillo de un día mediante una estrategia sistematizada y un formulario normalizado aportó una discreta mejoría de la capacidad de lectura de las CXR.

Chapter 16

Priftis KN, Anthracopoulos MB, Eber E, Koumbourlis AC, Wood RE (eds): Paediatric Bronchoscopy.
Prog Respir Res. Basel, Karger 2010, vol 38, pp 173–181

Endobronchial Tuberculosis

Elif Dagli[a] · Robert P. Gie[b] · Zeynep Seda Uyan[a] · Pierre Goussard[b]

[a]Division of Paediatric Pulmonology, Marmara University, Istanbul, Turkey; [b]Desmond Tutu Tuberculosis Center, Department of Paediatrics and Child Health, Faculty of Health Sciences, Stellenbosch University, Stellenbosch, South Africa

Abstract

Childhood tuberculosis (TB) is characterized by enlarged mediastinal lymph nodes which compress and infiltrate the airways resulting in endobronchial tuberculosis (ETB). ETB has been reported in 41–63% of children suspected of pulmonary TB. In children the disease is typically pausibacillary, which hinders the microbiological confirmation of the diagnosis. Flexible bronchoscopy (FB) is a useful tool for the confirmation of paediatric ETB. Indications for performing FB in children suspected of having TB include: confirmation of the diagnosis, determination of the degree of airway compression in children with radiological evidence of airway obstruction, management of life-threatening airway obstruction and evaluation of the response to treatment. Common bronchoscopic presentations of ETB are airway compression (42–59%) and TB lymph node ulceration into the airway (18–29%). The most commonly involved site is the right main bronchus. The bronchoscopic presentation of ETB in HIV-positive and HIV-negative children does not differ. The diagnostic yield of the microbiological analysis of bronchoalveolar lavage fluid in childhood pulmonary TB is greatly enhanced when taking into account the endobronchial abnormalities that are detected by endoscopy. The diagnostic value of endobronchial and/or transbronchial biopsy has not been reported.

Childhood tuberculosis (TB) is a common disease that affects approximately 1 million children annually around the world and contributes by approximately 10–15% to the global TB case load. It is estimated that 75% of the affected children live in the 22 countries that have the highest burden of TB disease [1]. It should be noted that the technology required to make the diagnosis is quite limited in these countries. Unfortunately, the epidemiological data required to estimate the proportion of children with severe disease who would benefit from bronchoscopic intervention at a global level is lacking; therefore, the true extent to which airway endoscopy can benefit the management of pulmonary TB in children is unclear.

Pathogenesis of Childhood Tuberculosis

After inhalation, *Mycobacterium tuberculosis* causes a localized alveolitis, termed the Ghon focus, from which the bacilli spread to the hilar and mediastinal lymph nodes. The localized alveolitis and the enlarged mediastinal glands form the primary complex (Ghon complex). In children, when the infection is not contained, the lymph nodes enlarge and involve the central airways (fig. 1). The airway can be narrowed either by external compression from the enlarged lymph node(s) or by tuberculous infiltration of the airway due to this compression [2]. In case of tuberculous infiltration, the airway lumen is narrowed by the inflammatory reaction or by the intraluminal caseating material, granulation tissue or polyps that may follow the ulceration of the lymph node into the airway. The caseating material may cause airway obstruction or may be inhaled into a lung segment or lobe, thus resulting in a hypersensitivity pneumonia, which clinically presents as expansile pneumonia. The enlarged lymph nodes may not infiltrate only the airway, but also other intrathoracic structures such as the oesophagus, the phrenic nerve, the ductus thoracicus and various blood vessels, thus resulting in diverse clinical presentations; the common feature of these presentations is the airway involvement due to the tuberculous nodes.

The degree of airway obstruction is influenced by the severity of the disease and the age of the child. Indeed, younger children suffer more extended airway obstruction as compared to older ones; this is ascribed to the smaller airways and the more pliable cartilage rings at a young age. Infants with culture-proven pulmonary TB presented with airway compression diagnosed by chest radiography in 56% of cases [3]. The extrathoracic airway is rarely involved in childhood TB [4, 5].

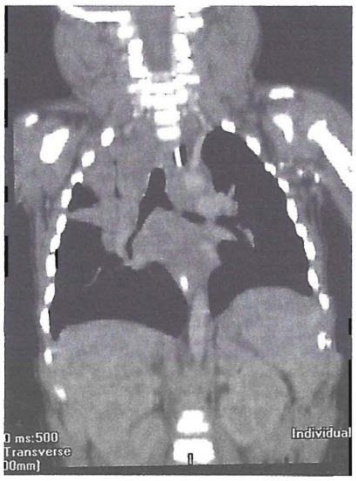

Fig. 1. Coronal reconstruction of a CT scan of the chest demonstrating compression of the left and right main bronchi by enlarged tuberculous lymph nodes. The importance of the enlarged subcarinal nodes in the airway compression is clearly demonstrated.

The diagnosis of TB in children can be quite challenging as it is extremely difficult to demonstrate acid-fast bacilli. Symptoms and signs of *M. tuberculosis* infection in children are often non-specific and can be misdiagnosed as other diseases such as HIV-related lung disease, intrathoracic lymphoma and fungal infections [6, 7]. For the diagnosis of TB, isolation of *M. tuberculosis* from culture is important. However, adequate diagnostic specimens are often difficult to obtain in children younger than 8 years of age due to lack of sputum production. In the majority of cases, the diagnosis is established using a combination of indirect evidence such as history of exposure to an adult with active TB, positive tuberculin skin test, positive chest radiograph and physical examination findings that are consistent with TB [8].

Definition of Endobronchial Tuberculosis

Endobronchial TB (ETB) is most often a complication of primary pulmonary TB. Since bronchoscopy is not routinely performed in all patients with TB, the exact incidence of ETB is unknown [9–11]. However, studies that investigated the results of flexible fibre-optic bronchoscopy (FB) in children with suspected TB have shown bronchial involvement in 41–63% of patients [11–13]. The pathogenesis of ETB is not yet fully understood. Sources of ETB may include: direct implantation of bacilli into a bronchus from an adjacent pulmonary parenchymal lesion, direct airway infiltration from an adjacent tuberculous mediastinal lymph node, erosion and protrusion of an intrathoracic tuberculous lymph node into the bronchus, haematogenous spread and extension to the peribronchial region by lymphatic drainage [9]. ETB has been classified according to the bronchoscopic findings as: extrinsic bronchial compression, actively caseating lesion, granuloma formation, polypoid mass lesion, lymph node protrusion, and mucosal erosion with ulceration [10, 11]. Early detection and effective treatment of ETB are important to decrease disease complications such as bronchiectasis and bronchial stenosis [13].

Unlike adults, the most common form of ETB in children is airway compression by enlarged lymph nodes. As a result, the term lymphobronchial tuberculosis has been suggested for childhood ETB as it describes more accurately the relevant pathology and thus helps to differentiate childhood from adult disease; this discrimination allows for better targeting of treatment and accuracy in prognosis.

Bronchoscopy in Suspected Pulmonary Tuberculosis

Indications

The role of FB in the investigation of paediatric airway disease continues to expand [7, 14]; it is most often used to investigate children with airway obstruction [introduction and chapter 1, this vol., pp. 12–21]. The use of FB in ETB has advantages such that smaller divisions of the airways can be reached and airway obstruction can be bypassed enabling the evaluation of the distal airway [15]. Therefore, FB offers a safe and rapid means of confirming the cause of obstruction by directly visualizing the airway abnormality [7, 14, 16–19].

Nevertheless, the use of bronchoscopy in the diagnosis and management of childhood TB remains controversial [20]. Most authors agree that the role of bronchoscopy is to exclude other possible causes of airway obstruction and coexistent opportunistic infections, especially in immunocompromised children. There are no officially endorsed indications for performing bronchoscopy in children with ETB, but the following propositions are generally agreed upon [15]:

1 in children suspected of having TB to confirm the diagnosis when this is not possible by other non-invasive techniques;

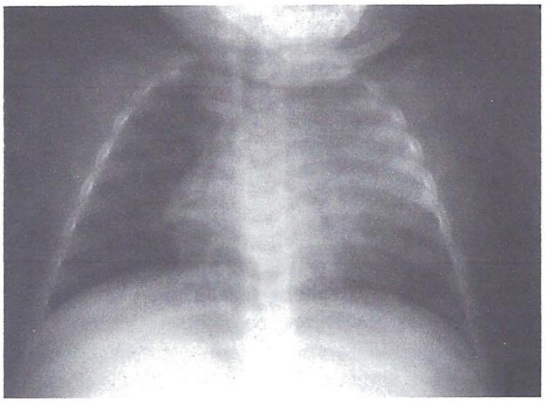

Fig. 2. Chest radiograph demonstrating the compression of the left main bronchus by enlarged tuberculous lymph nodes. Alveolar consolidation is visible in the left upper lobe.

2 in cases of airway obstruction that is visible on chest radiography to determine the degree, the cause and ultimately the management of the obstruction;
3 in children with life-threatening airway obstruction to determine the cause, the degree and the treatment of the obstruction;
4 in children being treated for ETB to determine the response to treatment.

Endoscopic Evaluation of Endobronchial Tuberculosis

The prevalence of ETB in children remains uncertain. In the prechemotherapeutic era, the incidence was stated to be 86%, with 28% of cases suffering bronchial perforation [2]. In more recent studies, the incidence of complicated lymph node disease varies from 8 to 38% (fig. 2); the low percentage was found in the community, while the high percentage was reported, not surprisingly, among hospitalized patients [21]. In paediatric studies, where FB was used to determine the presence of airway involvement, such involvement was found in 41–63% of patients [11–13]. The reported difference is not surprising as the degree of airway obstruction is underestimated when evaluated by chest radiography. There is a positive correlation between the frequency of airway involvement and the severity of the disease. In industrialized countries, where the majority of cases are diagnosed early in the course of the disease, the clinical presentation of TB and the airway compression are less severe. Conversely, in countries where children usually present with symptomatic disease, they are more likely to have more advanced disease, and a larger proportion is diagnosed with airway compression.

FB has been found to be useful not only in providing rapid confirmation of ETB, but also in excluding other causes of bronchial obstruction; indeed, ETB cases can be misdiagnosed as pneumonia, asthma or foreign-body aspiration [22–28]. Moreover, FB helped to diagnose ETB in patients in whom it was not suspected on the basis of their clinical findings and chest radiography [13].

FB has been proven to be valuable when making a decision between the conservative and the surgical approach to treat ETB. Corticosteroids are recommended in children with airway compression caused by mediastinal lymph node enlargement [15]. Although their role in the prevention of bronchial obstruction is controversial [29–32], there are studies that demonstrate the efficacy of adding corticosteroids to the routine anti-TB therapy in ETB [33–35]. The degree and the duration of the obstruction (as assessed by FB) are important factors in deciding which children would require surgical intervention [11].

FB is also used in children with TB to assess the response to treatment [13, 15]. The improvement, or the worsening, of the lymphobronchial lesion can be followed by repeat bronchoscopies [36]. It has been reported that some children with ETB have experienced initial worsening of airway compression and an increase in the size of granulation tissue when starting anti-TB treatment [13, 28]. This response is considered to be the result of a hypersensitivity reaction. Therefore, serial FBs have been suggested in order to assess the patient's response to therapy and to decide whether to continue anti-TB chemotherapy or resort to surgical treatment [36, 37].

The treatment of ETB remains uncertain, and there are many unanswered questions. The role of adjuvant corticosteroids, endobronchial or transthoracic enucleation of the lymph nodes eroding into or compressing the bronchus is not yet clear. In most cases, ETB is treated by 3 or 4 first-line anti-TB drugs, to which methylprednisolone (2 mg/kg/day) is added for the first month of treatment. The mean time to regression after initiation of treatment, as determined by FB, has been found to be 5.5 ± 2.7 months, while radiological improvement was observed in 5.3 ± 2.7 months [11]. The rate of regression is dependent on the grade of the bronchoscopic classification of the lymphobronchial lesions and the severity of the airway compression [10]. In cases with airway compression, resolution occurs in 9–90 days, while in 80% of cases with endoluminal granulation, tissue resolution was observed in 3–10 weeks [11]. Among children, in whom the airway compression is estimated to be greater than 75%,

approximately 33% fail to respond to medical therapy [P. Goussard, pers. observation]. Of 31 reported cases, 4 (12%) developed stenosis of the bronchi, with 1 requiring surgical intervention. This is considerably less than the reported frequency of 41% in adult patients who develop stenosis [38].

Bronchoalveolar Lavage and Endobronchial Biopsy

It has been argued that bronchoscopy is of limited value in the diagnosis of childhood TB due to the low diagnostic yield of cultured *M. tuberculosis* from bronchoalveolar lavage fluid (BALF). Numerous studies have demonstrated that the diagnostic yield of BALF is lower than that of gastric aspirate for *M. tuberculosis* culture [7, 39]. These results, however, do not take into account the lymphobronchial airway involvement, which can be visualized by the bronchoscope during the procedure.

In adults with pulmonary TB, the BALF culture has been reported to yield a higher recovery rate for *M. tuberculosis* than sputum cultures, especially in sputum-smear-negative patients [40]. In a study of children with suspected pulmonary TB, designed to investigate whether BALF is superior to gastric lavage for the isolation of *M. tuberculosis*, gastric lavage was found to perform better than BALF in the bacteriological confirmation of pulmonary TB [41]. However, in another study, Brown et al. [42] showed that the use of induced sputum samples was more sensitive than the use of gastric lavage or BALF samples for the diagnosis of TB in patients who could not expectorate spontaneously.

In their study of paediatric patients, Cakir et al. [11] demonstrated that the isolation rate of *M. tuberculosis* was 10% from gastric lavage, 12.8% from BALF, while it increased to 20% when both procedures were performed. When the authors reviewed the results of previous reports on the isolation rate of *M. tuberculosis* from samples obtained from different sites, they found that *M. tuberculosis* was isolated from gastric lavage in 14–47% of cases, and from BALF in 10–43% of cases [11]. Taking into account the available information, every effort, including BALF culture, should be made to recover the mycobacterium in order to perform anti-TB drug susceptibility testing, especially in regions where the prevalence of resistant *M. tuberculosis* is high. It is worth noting that in the study of Cakir et al. [11], while the total positive culture yield for *M. tuberculosis* was 20%, the frequency with which abnormalities due to ETB were visualized bronchoscopically reached 47%. Hence, when BALF culture of *M. tuberculosis* is the only means utilized to diagnose childhood TB, the diagnostic value of FB is grossly underestimated.

It is possible to perform endobronchial biopsy [chapter 4, this vol., pp. 42–53] of the airway sites affected by ETB. The size of the working channel is the limiting factor for the size of the biopsy that can be obtained, thus making the diagnosis more challenging. We routinely remove caseating material that herniates into the airway, and process it for culture and pathology. No study to date has systematically evaluated the diagnostic yield of endobronchial biopsy in children with ETB.

Use of Rigid versus Flexible Bronchoscopy

Since the working channel of the 2.8-mm flexible bronchoscope used in young children is small [chapter 1, this vol., pp. 12–21], interventional bronchoscopy using this instrument is quite limited. In cases where transbronchial enucleation of tuberculous lymph nodes ulcerating into the airways is required, the rigid bronchoscope can be very useful. This instrument has the added advantage that the patient can be ventilated throughout the procedure, thus giving more time to perform the procedure [chapters 2 and 8, this vol., pp. 22–29 and 83–94].

Bronchoscopy versus Computed Tomography

The modern multidetector computed tomography (CT) scanners make multiplanar reconstruction of the chest possible, thus allowing for accurate demonstration of airway narrowing in children [43; chapter 9, this vol., pp. 95–112]. In a study, in which 3-dimensional volume-rendered CT scans were used to determine airway narrowing caused by TB lymph node enlargement in children, the sensitivity of the examination was 92% and the specificity 85% when FB was used as the gold standard [44]. The 3-dimensional multidetector CT scan could not determine the tissue characteristics of the airway involvement and was less accurate when the airway compression was less than 50%. Where severe compression was present, its length could not be measured by FB, while it could be estimated from the CT scan images. These and other relevant data illustrate that the comprehensive management of patients suspected of having ETB should include both bronchoscopy and chest CT scan. Based on the above data, it is also evident that bronchoscopy should precede CT scan as the presence of less than 50% compression of the airway, as witnessed during FB, would indicate that the CT scan of the chest will most likely not contribute to the further management of the child, except in cases where the cause of the external compression is uncertain.

Studies Evaluating Flexible Bronchoscopy

There are three large series that have evaluated the role of FB in the diagnosis and treatment of ETB in children:

Chan et al. [13] investigated the usefulness of FB in the diagnosis and management of 36 children younger than 16 years of age with active pulmonary TB. ETB was detected in 41.7% of the patients, while one third of children thought to have primary uncomplicated TB, which was diagnosed by conventional means (i.e. history, physical examination and plain chest radiography), were found to have ETB by FB. *M. tuberculosis* was isolated from the gastric washing in 47.2% and from the BALF in 10.8% of the patients. None of the children had a major complication during or after the procedure.

De Blic et al. [12] evaluated 121 FB procedures in 54 children aged 3 months to 14 years who were suspected of having pulmonary TB. ETB was detected in 57% of the patients. FB helped to guide the use of oral corticosteroid therapy. It proved to be particularly useful in children with chest radiographs that were not suggestive of bronchial involvement, it indicated the need for resection of granulation tissue by rigid bronchoscopy in 3 cases, and its findings were crucial in the decision to proceed to surgical intervention in 2 children with persistent bronchial obstruction.

In their study, Cakir et al. [11] evaluated 70 TB patients aged 5 months to 15 years with suspected TB and an inadequate response to more than 8 weeks of anti-TB treatment. In patients with endobronchial lesions and extrinsic bronchial compression that obstructed the airway by more than 50% of the original lumen, methylprednisolone at a dose of 2 mg/kg/day was added to the standard anti-TB chemotherapy (20 patients), and FB was repeated every 2 months until resolution of the lesion. ETB was more common in children less than 3 years of age, in those with a history of contact with TB, and those with lymphadenopathy detected by chest CT scan. All of the patients in this series were treated without any complications, but 1 patient required surgical resection.

A separate evaluation of 193 FB procedures was carried out in 122 children, younger than 16 years of age with suspected pulmonary TB, at the paediatric pulmonary clinic of Marmara University Hospital. ETB was detected in 47.6% of the patients. In those with endobronchial lesions and/or extrinsic bronchial compression obstructing the airway by more than 50% of its original lumen, systemic corticosteroid treatment at a dose of 2 mg/kg/day was added to standard anti-TB chemotherapy, and serial FBs were performed every 2 months until resolution of the lesion. Among patients with ETB, 41.3% were found to have extrinsic bronchial compression, 31% actively caseating lesions (online suppl. videos 1 and 2), 13.7% granuloma formation (online suppl. videos 3 and 4), 3.4% protrusion of an enlarged lymph node (online suppl. video 5), 8.6% polypoid mass lesion (online suppl. videos 6 and 7), 1.7% mucosal erosion with ulceration and 13.7% more than one type of endobronchial lesion. During the follow-up, only a 1-year-old girl with a polypoid mass in the right main bronchus required surgical intervention to remove the endobronchial lesion and dilate the bronchial stenosis that complicated the surgical intervention (online suppl. videos 8–11).

Common Bronchoscopic Presentations of Endobronchial Tuberculosis

The most common lesion of ETB seen on bronchoscopy is compression of the airways (42–59%) [11, 12] (fig. 3). The few studies that have systematically investigated the compression of the airways by enlarged tuberculous lymph node(s) in children have found that the most common site of obstruction is the right main bronchus (58%), followed by the left main bronchus (21%) [11]. The degree of obstruction varies, but in most cases (79%) it is estimated to be less than 50% of the original airway lumen [11]. The next two most common lesions are granulation tissue at the site of lymph node ulceration into the airway (18–29%) and caseating material, which originates from the lymph node and protrudes into the airway (12–39%) [11, 12]. The least common lesion in children is polyp formation (6%) [11].

Another feature of childhood ETB is that airway involvement is multifocal (41%) [12] and commonly involves both the left and right bronchial trees (12%) [11].

These findings are similar to airway involvement as reported by chest CT scan in children with TB. The most common site of airway compression demonstrated by this modality was the left main bronchus (21%), followed by the right main bronchus (14%) and the bronchus intermedius (8%) [45].

Endobronchial Involvement in Children Infected with Human Immunodeficiency Virus

In children with severe immunosuppression, the deferential diagnosis of lymph node enlargement that involves the airway is expanded. Bronchoscopy in HIV-infected children is valuable for collecting specimens for culture, cytology and histopathology [chapters 3 and 4, this vol., pp. 30–41 and 42–53]. The bronchoscopic images of tuberculous

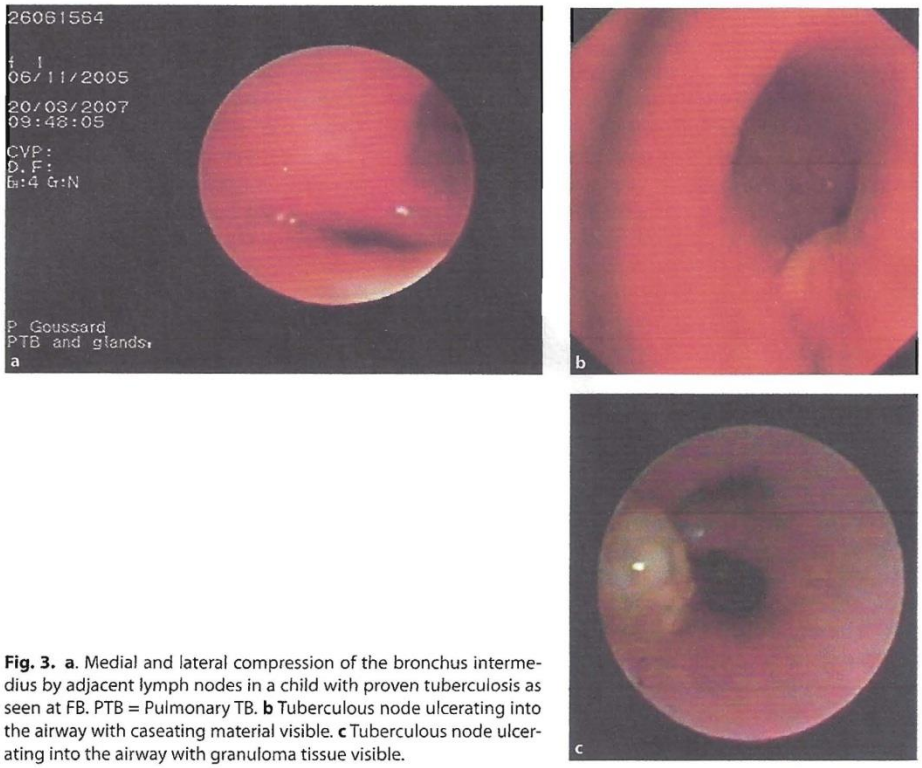

Fig. 3. **a**. Medial and lateral compression of the bronchus intermedius by adjacent lymph nodes in a child with proven tuberculosis as seen at FB. PTB = Pulmonary TB. **b** Tuberculous node ulcerating into the airway with caseating material visible. **c** Tuberculous node ulcerating into the airway with granuloma tissue visible.

lymphobronchial involvement in children have not been reported in the literature but in our experience it does not differ from that seen in children who are HIV negative. *Cryptococcus neoformans,* Karposi sarcoma and lymphoma cause lymph node enlargement, which can be confused with that of tuberculous aetiology.

The role of FB in the evaluation of immune reconstitution inflammatory syndrome has not been determined yet but it will most likely become an important additional investigation.

Unusual Cases of Endobronchial Tuberculosis

Expansile Pneumonia Caused by M. tuberculosis

Expansile pneumonia in children due to *M. tuberculosis* commonly presents with the clinical picture of a pneumonia that is not responding to treatment. The chest radiograph reveals a dense opacification, especially of the upper lobes (75%), with displacement of the fissures indicating an increase in volume of the involved lobe (fig. 4). The left (42%) and right (33%) upper lobes are the most commonly involved lobes [46]. The severity of this form of the disease is reflected by the fact that 88% of patients are culture positive for *M. tuberculosis.*

On FB, airway compression was present in 95% of patients, with the obstruction estimated to be more than 75% of the original airway lumen in 83% of the cases. In 21% of the children, the lumen occlusion was complete. Accompanying the airway compression were lymph nodes ulcerating into the airways in 21% of the patients, while tracheal compression was present in 63% of the cases [46].

The severity of the disease positively correlates with the degree of airway obstruction. In cases where the obstruction was greater than 75%, there was evidence of necrotic liquefaction of the affected lobe while this was not present in those where the airway obstruction was less than 75%.

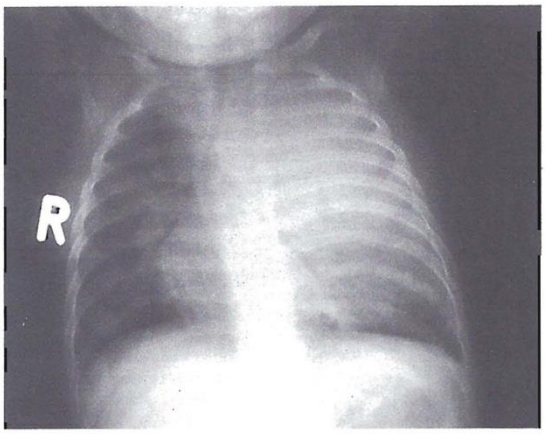

Fig. 4. Expansile pneumonia of the left upper lobe and lingula with compression of the left main bronchus and the trachea.

Often, the compression was so severe that 42% of children required enucleation of the tuberculous lymph node(s). Of the 10 cases that required nodular enucleation, this was achieved bronchoscopically in 3 cases [46].

Bronchoscopy is essential for the follow-up of children treated for expansile pneumonia due to *M. tuberculosis*. Transthoracic enucleation of the mediastinal lymph nodes should be carried out in those patients who, after 1 month of anti-TB therapy (to which oral steroids have been added), show no improvement of a bronchoscopically estimated airway obstruction which remains greater than 75%.

Broncho-Oesophageal Fistula Caused by M. tuberculosis

Tuberculous lymph nodes that involve the bronchi and the oesophagus can rupture into both structures, thus causing an acquired broncho-oesophageal fistula. Children with this form of fistula present clinically in one of two ways [5]:

The first clinical presentation is that of acute respiratory failure requiring assisted ventilation. When initiating mechanical ventilation, it becomes apparent that there is air leak into the gastrointestinal system. The presence of the suspected broncho-oesophageal fistula is best determined by FB. The fistula is visualized in the majority of cases in the medial wall of the left main bronchus. It needs to be blocked to ensure adequate ventilation. This is best achieved by placing a stent in the oesophagus at the level of the fistula [47].

The second is one of a child who coughs when fed, either prior to or after initiating anti-TB therapy. In these cases, FB demonstrates the fistula in the medial wall of the left main bronchus. Proving the patency of the fistula may present a challenge. However, the fistula can be demonstrated by injecting a dye (we use rifampicin) into the oesophagus and observe the dye enter from the oesophagus into the airway, through the fistula, during spontaneous ventilation.

Repeated bronchoscopy is useful in following the clinical course of these children. Although we have reported in the past that fistulas caused by *M. tuberculosis* in children do not resolve after 6 or more months of medical treatment, we have subsequently observed this to actually occur in children.

Laryngeal Tuberculosis

Laryngeal TB used to be common in adult patients with severe TB, especially prior to the modern chemotherapy era. In children this lesion is rare. We recently reported 2 cases of laryngeal TB with severe upper airway obstruction during sleep. When bronchoscoped, both children had severe supraglottic swelling with nodular compression of the proximal trachea [4]. The pathogenesis of these lesions is unclear. Both children had a miliary picture on a chest radiograph that was consistent with haematogenous spread, but the accompanying nodular compression of the trachea suggests that lymphatic spread may also have contributed to the pathogenesis.

Accompanying Intrathoracic Chest Disease

Tracheal compression, ball valve obstruction of the main bronchi [5], phrenic nerve palsy [48], chylothorax [49] and cold abscess of the thorax [5] have been associated with ETB. Bronchoscopy plays an important role in the diagnosis and management of such cases. In life-threatening airway obstruction, relief can be provided by endoscopically removing part of the lymph node ulcerating into the airway and the caseating material obstructing its lumen.

Future Trends

There is considerable debate regarding the value of FB in the investigation of a child suspected of pulmonary TB. Most studies have been performed in regions of the world where there is a low prevalence of disease. In reports originating from regions with a high prevalence of TB, FB plays an important role in the diagnosis and management of these children [11]. The exact role of endoscopy in high-burden countries needs to be explored.

With the continuous improvements in the image quality of FB and the potential increase in the size of the working channel, it may become possible to perform more invasive diagnostic procedures through this instrument. In adult patients transbronchial aspiration biopsies are feasible [50]. Children with nodal compression of the airways are probably ideal candidates for this procedure. Nevertheless, the precise role of FB in the diagnosis and management of pulmonary TB in children still needs to be determined.

References

1 Nelson LJ, Wells CD: Global epidemiology of childhood tuberculosis. Int J Tuberc Lung Dis 2004;8:363–647.
2 Marais BJ, Gie RP, Schaaf HS, Hesseling AC, Obihara CC, Enarson DA, Donald PR, Beyers N: The natural history of childhood intrathoracic tuberculosis: a critical review of the literature from the pre-chemotherapy era. Int J Tuberc Lung Dis 2004;8:392–402.
3 Schaaf HS, Gie RP, Beyers N, Smuts N, Donald PR: Tuberculosis in infants less than 3 months of age. Arch Dis Child 1993;69:371–374.
4 Gregg KK, Detjen AK, Goussard P, Gie RP: Laryngeal involvement in two severe cases of childhood tuberculosis. Pediatr Infect Dis J 2009;28: 1136–1138.
5 Gie RP, Goussard P, Kling S, Schaaf HS, Beyers N: Unusual forms of intrathoracic tuberculosis in childhood and their management. Pediatr Respir Rev 2004;5:S139–S141.
6 Starke JR, Taylor Watts KT: Tuberculosis in the pediatric population of Houston, Texas. Pediatrics 1989;84:28–35.
7 Bibi H, Mosheyev A, Shoseyov D, Feigenbaum D, Kurzbart E, Weiller Z: Should bronchoscopy be performed in the evaluation of suspected pediatric pulmonary tuberculosis? Chest 2002;122: 1604–1608.
8 Karadağ B: Pulmoner tüberkülozun klinik bulguları ve tanısı; in Dagli E, Karakoc F, (eds): Çocuk Göğüs Hastalıkları. Istanbul, Nobel Tıp Kitabevleri, 2007, pp 187–192.
9 Chung HS, Lee JH: Bronchoscopic assessment of the evolution of endobronchial tuberculosis. Chest 2000;117:385–392.
10 Lee JH, Park SS, Lee DH, Shin DH, Yang SC, Yoo BM: Endobronchial tuberculosis: clinical and bronchoscopic features in 121 cases. Chest 1992; 102:990–994.
11 Cakir E, Uyan ZS, Oktem S, Karakoc F, Ersu R, Karadag B, Dagli E: Flexible bronchoscopy for diagnosis and follow-up of childhood endobronchial tuberculosis. Pediatr Infect Dis J 2008;27: 783–787.
12 De Blic J, Azevedo I, Burren CP, Le Bourgeois M, Lallemand D, Scheinmann P: The value of flexible bronchoscopy in childhood pulmonary tuberculosis. Chest 1991;100:688–692.
13 Chan S, Abadco DL, Steiner P: Role of flexible fiberoptic bronchoscopy in the diagnosis of childhood endobronchial tuberculosis. Pediatr Infect Dis J 1994;13:506–509.
14 Wood RE: The emerging role of flexible bronchoscopy in pediatrics. Clin Chest Med 2001;2:311–317.
15 Goussard P, Gie R: Airway involvement in pulmonary tuberculosis. Pediatr Respir Rev 2007;8: 118–123.
16 Joos L, Patuto N, Chhajed PN, Tamm M: Diagnostic yield of flexible bronchoscopy in current clinical practice. Swiss Med Wkly 2006;136:155–159.
17 De Charnace G, de Lacourt C: Diagnostic techniques in paediatric tuberculosis. Paediatr Respir Rev 2001;2:120–126.
18 Donato L, Helms P, Barats A, Lebris V: Bronchoscopy in childhood pulmonary tuberculosis. Arch Pediatr 2005;12(suppl 2):S127–S131.
19 Charnace G, Delacourt C: Diagnostic techniques in paediatric tuberculosis. Paediatr Respir Rev 2001;2:120–125.
20 Shingadia D, Novelli V: Diagnosis and treatment of tuberculosis in children. Lancet Infect Dis 2003;3:624–632.
21 Marais BJ, Gie RP, Schaaf HS, Enarson D, Beyers N: The spectrum of disease in children treated for tuberculosis is a high endemic area. Int J Tubercl Lung Dis 2006;10:732–738.
22 Wood GS, Gonzalez C, Done S, Albus RA: Endobronchial tuberculosis in children: a case report and review. Int J Pediatr Otorhinolaryngol 1990;20:241–245.
23 Abdulla F, Dietrich KA: Endobronchial tuberculosis manifested as obstructive airway disease in a 4-month-old infant. South Med J 1990;83:715–717.
24 Uzuner N, Anal O, Karaman O, Sevinç C, Türkmen M, Canda T, Kazan E. Endobronchial tuberculosis complicated with *Staphylococcus aureus* pneumonia and empyema in a child. Turk J Pediatr 2003;45:254–257.
25 Park AH, Fowler SS, Challapalli M: Suspected foreign body aspiration in a child with endobronchial tuberculosis. Int J Pediatr Otorhinolaryngol 2000;53:67–71.
26 Caglayan S, Coteli I, Acar U, Erkin S: Endobronchial tuberculosis simulating foreign body aspiration. Chest 1989;95:1164.
27 Weiner GM, Batch AJ: Endobronchial tuberculosis masquerading as foreign body aspiration. J Laryngol Otol 1995;109:1192–1194.
28 Williams D, York E, Nobert E, Sproule B: Endobronchial tuberculosis presenting as asthma. Chest 1988;93:836–837.
29 Alzeer AH, FitzGerald JM: Corticosteroids and tuberculosis: risks and use as adjunct therapy. Tuber Lung Dis 1993;74:6–11.
30 Dooley DP, Carpenter JL, Rademacher S: Adjunctive corticosteroid therapy for tuberculosis: a critical reappraisal of the literature. Clin Infect Dis 1997;25:872–887.
31 Senderovitz T, Viskum K: Corticosteroids and tuberculosis. Respir Med 1994;88:561–565.
32 Rikimaru T: Therapeutic management of endobronchial tuberculosis. Expert Opin Pharmacother 2004;5:1463–1470.
33 Chan HS, Pang JA: Effect of corticosteroids on deterioration of endobronchial tuberculosis during chemotherapy. Chest 1989;96:1195–1196.
34 Chan HS, Sun A, Hoheisel GB: Endobronchial tuberculosis: is corticosteroid treatment useful? A report of 8 cases and review of the literature. Postgrad Med J 1990;66:822–826.
35 Toppet M, Malfroot A, Derbe MB, Toppet V, Spehl M, Dab I: Corticosteroids in primary tuberculosis with bronchial obstruction. Arch Dis Child 1990;65:1222–1226.
36 De Blic J: The value of flexible bronchoscopy in childhood pulmonary tuberculosis. Pediatr Pulmonol 1995;11(suppl):24–25.
37 Hsu HS, Hsu WH, Huang BS, Huang MH: Surgical treatment of endobronchial tuberculosis. Scand Cardiovasc J 1997;31:79–82.
38 Um SM, Yoon YS, Lee SM, Yim JJ, Yoo CG, Chung HS, Kim YW, Han SK, Shim YS, Kim DK: Predictors of airway stenosis in patients with endobronchial tuberculosis. Int J Tuberc Lung Dis 2007;12:57–62.
39 Abadaco D, Steiner P: Gastric lavage is better than bronchoalveolar lavage for isolation of *Mycobacterium tuberculosis* in childhood pulmonary tuberculosis. Pediatr Infect Dis J 1993;11: 735–738.
40 Norman E, Keistinen T, Uddenfeldt M, Perolof Rydstrom P, Lundgren R: Bronchoalveolar lavage is better than gastric lavage in the diagnosis of pulmonary tuberculosis. Scand J Infect Dis 1988;20:77–80.
41 Somu N, Swaminathan S, Paramasivan CN, Vijayasekaran D, Chandrabhooshanam A, Vijayan VK, Prabhakar R: Value of bronchoalveolar lavage and gastric lavage in the diagnosis of pulmonary tuberculosis in children. Tuber Lung Dis 1995;76:295–299.
42 Brown M, Varia H, Bassett P, Davidson RN, Wall R, Pasvol G: Prospective study of sputum induction, gastric washing and bronchoalveolar lavage for the diagnosis of pulmonary tuberculosis in patients who are unable to expectorate. Clin Infect Dis 2007;44:1415–1420.

43 Andronikou S, Wieselhaler N: Modern imaging of tuberculosis in children: thoracic, central nervous system and abdominal tuberculosis. Pediatr Radiol 2004;34:861–875.
44 Du Plessis J, Goussard P, Andronikou S, Gie R, George R: Comparing three-dimensional volume-rendered CT images with fibre-optic tracheobronchoscopy in the evaluation of airway compression caused by tuberculous lymphadenopathy. Pediatr Radiol 2009;39:694–702.
45 Andronikou S, Joseph E, Lucas S, Brachmeyer S, du Toit G, Zar H, Swingler G: CT scanning for the detection of TB mediastinal and hilar lymphadenopathy in children. Pediatr Radiol 2004;34:232–234.
46 Goussard P, Gie RP, Kling S, Beyers N: Expansile pneumonia in children caused by *Mycobacterium tuberculosis:* clinical, radiological and bronchoscopic appearances. Pediatr Pulmonol 2004;38:451–455.
47 Goussard P, Sidler D, Kling S, Andronikou S, Rossouw G, Gie R: Esophageal stent improves the ventilation in a child with broncho-esophageal fistula caused by *Mycobacterium tuberculosis*. Pediatr Pulmonol 2007;42:93–97.
48 Goussard P, Gie RP, Kling S, Andronikou S, Jansen J, Rossouw G: Phrenic nerve palsy in children associated with confirmed intrathoracic tuberculosis: diagnosis and clinical course. Pediatr Pulmonol 2008:44:345–350.
49 Cakir E, Gocmen B, Uyan ZS, Oktem S, Kiyau G, Karadoc F, Ersu R, Karadag B, Dagli T, Dagli E: An unusual case of chylothorax complicating childhood tuberculosis. Pediatr Pulmonol 2008; 43:611–614.
50 Cetinkaya E, Yildiz P, Kadakal F, Tekin A, Soysal T, Elibol S, Yilman V: Transbronchial needle aspiration in the diagnosis of intrathoracic lymphadenopathy. Respiration 2002;69:335–338.

Dr. Elif Dagli
Division of Paediatric Pulmonology, Marmara University
Istanbul (Turkey)
E-Mail esezginer@gmail.com

Chest radiograph findings in children with tuberculous meningitis

Solomons R[1*], Goussard P[1*], Visser DH[2], Marais BJ[3], Gie RP[1], Schoeman JF[1] and van Furth AM[2]

1. Department of Paediatrics and Child Health, Faculty of Medicine and Health Sciences, Stellenbosch University, South Africa
2. Department of Pediatric Infectious Diseases and Immunology, VU University Medical Center, Amsterdam, The Netherlands
3. Marie Bashir Institute for Infectious Diseases and Biosecurity Institute (MBI) and The Children's Hospital at Westmead, The University of Sydney, Australia.

*RS and PG contributed equally

Corresponding author: Dr Regan Solomons
Department of Pediatrics and Child Health, Faculty of Medicine and Health Sciences
PO Box 19063, Tygerberg, 7505, Cape Town, South Africa
Tel: +27 21 938-9891, Fax: +27 21 938-4858, Email: regan@sun.ac.za
Running head: The chest radiograph in childhood TBM

Text word count: 1795
Abstract word count: 170
Keywords: Central nervous system tuberculosis, diagnostics, chest X-ray

ABSTRACT

BACKGROUND: Tuberculous meningitis **(**TBM) is diagnosed based on a combination of clinical, laboratory, and radiological findings, including signs suggestive of tuberculosis (TB) on a standard chest radiograph.

METHODS: We describe the radiological features suggestive of intra-thoracic TB in children diagnosed with TBM during a prospective evaluation of meningitis suspects seen at Tygerberg Children's Hospital, Cape Town, South Africa.

RESULTS: Of 84 children treated for TBM, 31 (37%) had 'definite' TBM, 45 (55%) 'probable' TBM and 8 (9%) 'possible' TBM. In total, 37 (44%) TBM patients had chest radiograph findings suggestive of TB; 9 (11%) with disseminated (miliary) TB. Only 1 in 4.39 children ≤3 years of age with TBM had suggestive chest radiograph findings. The presence of complicated intra-thoracic lymph node disease was significantly higher in children ≤3 years of age, odds ratio 21.69 (95% confidence interval 2.73-172.67); $p < 0.01$. Among 6 HIV-infected children, 3 (50%) had intrathoracic lymphadenopathy.

CONCLUSION: The majority of children with TBM, including the very young, did not have signs suggestive of TB on chest radiograph.

INTRODUCTION

Globally there were an estimated 8.6 million new cases and 1.3 million deaths from tuberculosis (TB) in 2012[1]. TB is predominantly a pulmonary disease, but extrapulmonary involvement is particularly common in young children and in immunocompromised individuals[2]. Central nervous system (CNS) involvement, mostly tuberculous meningitis (TBM), accounts for approximately 1% of all TB cases[3]. TBM is the most devastating manifestation of TB and early treatment initiation is critical to achieve optimal outcomes[4]. In clinical practice, diagnosis is hampered by non-specific clinical features and sub-optimal accuracy of existing diagnostic methods[5-9], therefore TBM is mainly diagnosed based on a combination of clinical, laboratory, and radiological findings.

A uniform research case definition was proposed by an international panel of experts, categorizing patients as definite, probable, or possible TBM (Table 1)[10]. Chest radiograph findings are included within the scoring criteria. Previous observations suggest that chest radiograph findings consistent with active pulmonary TB are observed in 30% to 65% of adults with central nervous system TB[11-13]. Chest radiograph evidence of TB in children with TBM is usually considered to be more frequent, ranging from 70% of HIV-uninfected to 84% of HIV-infected children diagnosed with TBM[14]. In the group of children with TBM and HIV co-infection, hilar lymphadenopathy, pleural effusion and cavity formation was significantly increased compared to HIV uninfected children[14].

We aimed to describe the radiological features and frequency of chest radiograph signs suggestive of TB in children with TBM.

Methodology

This prospective descriptive cross-sectional study was conducted at Tygerberg Children's Hospital, South Africa, a major referral centre for Cape Town and surrounding areas. Children were enrolled between January 2010 and January 2014. Inclusion criteria were 1) age 3 months to 13 years 2) clinical suspicion of TBM 3) CSF evaluation 4) chest radiograph performed at admission 5) written consent from the caregiver and assent if the child was older than 7 years and competent to do so. The study was approved by the Human Research Ethics Committee of Stellenbosch University, South Africa (study nr. N11/01/006).

Clinical procedures

All patients underwent a comprehensive clinical evaluation. Routine investigations

included full blood count, basic biochemistry, human immunodeficiency virus (HIV) screening, tuberculin skin test (TST), microbiological analysis of sputum or gastric washings, bacterial blood culture, chest radiography and neuroimaging (if clinically indicated). Chest radiographs were independently interpreted by a pediatrician and an experienced pediatric pulmonologist, using a standard reporting form. Findings were categorized as certain TB, uncertain TB or not TB. Intra-thoracic lymph node disease was classified as either uncomplicated or complicated, accordingly to a radiological classification of childhood intrathoracic tuberculosis, using a structured approach to interpretation and recording chest radiograph findings[15]. Airway compression was defined as either compression of the trachea, left main bronchus or bronchus intermedius. Parenchymal changes were defined as either consolidation (including expansile pneumonia) or miliary.

Case definition of tuberculous meningitis

A diagnosis of TBM was based on the proposed uniform research case definition (Table 1)[10]. TBM was classified as 'definite' when CSF demonstrated acid-fast bacilli, positive *M. tuberculosis* culture and/or positive *M. tuberculosis* commercial nucleic acid amplification test (NAAT). TBM was classified as 'probable' when patients scored ≥ 12 when neuroimaging was available and ≥10 when neuroimaging was unavailable. TBM was classified as 'possible' when a patient had a diagnostic score of 6–11 when neuroimaging was available and 6–9 when neuroimaging was unavailable[10]. TBM was staged according to revised British MRC criteria as: Stage I) Glasgow Coma Scale (GCS) of 15 and no focal neurology, Stage IIa) GCS of 15 plus focal neurology, Stage IIb) GCS of 11-14 with focal neurology and Stage III) GCS <11[16,17]. All patients diagnosed with TBM were treated with a standard short-course regimen[18].

Statistical analysis

Data analysis was performed using SAS (Statistical analysis system) version 9.1 (SAS Institute Inc., Cary, North Carolina, USA). Frequencies were obtained for chest radiograph findings, stratified for TBM stage. An unweighted kappa statistic was used to assess inter-observer agreement. Comparison was made, using the X^2 test with a p-value <0.05 considered statistically significant. Chest radiograph criteria were further compared between children ≤3 years and age >3 years and odds ratios determined. A need to treat calculation was used to reflect the number of TBM patients ≤3 years of age with "certain TB" on chest radiograph evaluation.

RESULTS

In total 84 children met the inclusion criteria; 31 (37%) had 'definite/microbiologically-confirmed' TBM, 45 (55%) had 'probable' TBM and 8 (9%) had 'possible' TBM[10]. According to revised British MRC TBM staging criteria, 12 (14.3%) had stage I, 13 (15.5%) stage IIa, 30 (35.7%) stage IIb and 29 (34.5%) stage III disease. Tuberculin skin testing was positive in 24 (28.6%) TBM patients, of whom 11 had certain pulmonary TB on chest radiograph, 10 had no visible abnormality, and 3 had inconclusive signs. HIV co-infection was identified in 6 patients. Of these, 3 had no radiographic evidence of pulmonary TB. Of the three HIV-infected patients with abnormal chest radiograph, one had isolated lymph node involvement, one lymph node involvement plus lobar pneumonia and the third lymph node involvement plus a miliary picture.

A summary of chest radiograph findings is reflected in table 2. Inter-reviewer variability between the pediatrician and pediatric pulmonologist was minimal (unweighted kappa statistic 0.62 95% confidence interval (CI) 0.46-0.79); differences were resolved by consensus. The proportion of 'certain TB' and miliary TB on chest radiograph was 44% (37/84) and 11% (9/84) when including all TBM categories; 39% (12/31) and 13% (4/31) respectively in those with microbiologically-confirmed TBM. Among those with microbiologically-confirmed TBM, 1/31 (3%) had acid-fast bacilli on microscopy, 13/31 (42%) were *M. tuberculosis* culture positive, and 27/31 (87%) were confirmed by commercial NAAT (Either GenoType MTBDR*plus*® assay and/or GeneXpert MTB/RIF® assay). *M. tuberculosis* was cultured in gastric washings from 27 patients; 10 with microbiologically-confirmed and 17 with 'probable' TBM. No significant differences were observed when comparing chest radiograph findings in children with different stages of TBM.

Chest radiographs were more frequently indicative of TB in very young children (≤3 years of age) compared to older children (>3 yrs); 25/46 (54%) versus 12/38 (32%) (odds ratio (OR) 2.58 (95 % CI 1.05-6.33; p=0.04 (Table 3). Chest radiograph findings in children ≤3 years of age were more likely to include complicated intra-thoracic lymph node disease (OR 21.69; 95% CI 2.73-172.67), and the presence of airway compression (OR 17.90; 95% CI 2.24-143.27) than in older children. Despite the fact that chest radiographs were most informative in young children, only 1 in 4.39 children ≤3 years of age had "certain TB" on chest radiograph evaluation.

DISCUSSION

The main finding in this study is the lower percentage of chest radiograph findings highly suggestive of pulmonary TB in children with TBM, compared to the study by van Weert et al. (44% vs 70%)[14], with a need to treat calculation showing that only 1 in 4.39 children ≤3 years of age with TBM are likely to have 'certain TB' on chest radiograph. The lower proportion of 'certain TB' in our study compared to van Weert et al could potentially be explained by our 2 reviewers reaching consensus on chest radiograph findings, thereby minimizing the possibility of over-reporting of chest radiograph findings.[14] Another possible reason could be the difference in the study cohort, with 28% of our TBM group having positive tuberculin skin testing compared to 62% in the HIV-uninfected TBM group of the study by van Weert et al.[14]

A normal chest radiograph was found in almost half (46%) of children clinically diagnosed with TBM, and in 52% of cases with microbiologically-confirmed TBM. The poor diagnostic sensitivity of chest radiography in children with TBM implies that it cannot be used as a rule-out test, even in combination with TST and may impact the scoring of future diagnostic algorithms. The suggested uniform TBM research case definition incorporates chest radiograph findings as part of the scoring criteria[10]. The score weighting of a miliary pattern is higher than that of active TB on chest radiograph (excluding miliary TB). Our finding that hilar lympadenopathy is the more common finding of 'certain TB' on chest radiograph, in both suspected and definite TBM, suggests that its weighting may have to be reconsidered.

The most common radiological findings in young children (<5 years) with pulmonary TB is hilar or paratracheal lymph nodes[19]. This age group also has a higher risk for developing lympho-bronchial TB due to small airway size[15]. Our finding that intrathoracic lymph nodes, complicated lymph node disease and airway compression were significant more common in children ≤3 years, confirms that this is the predominant radiological finding in young children. TBM stage did not affect the radiographic picture. Although chest radiography has limited sensitivity, the fact that ~50% of patients do have suggestive chest radiograph findings and 16/84 (19%) had radiological evidence of airway compression highlights the need for pulmonary assessment, including flexible bronchoscopy if indicated[20]. The smaller percentage of TBM patients with airway compression, compared to those reported for all TB cases (41-63%)[21-23], could possibly be explained by differences in the immune response between pulmonary TB in isolation versus pulmonary TB in the setting of CNS involvement. A better understanding of immunology in CNS TB is warranted[3].

Inter-observer variability is a well-recognized problem in the interpretation of chest

radiographs in children with pulmonary TB. Swingler et al. have reported difficulty in distinguishing lymphadenopathy from a normal thymus and were not able to distinguish normal from pathological nodes[24]. The areas most reliable for lymphadenopathy were the right hilum and subcarinal area[25].

A limitation of our study was the small number of HIV co-infected patients (7%), which did not allow separate statistical analysis of this group. This low percentage is consistent with a previous study that found that only 7% of 123 children with clinically diagnosed TBM had HIV co-infection[26]. The number of microbiologically-confirmed TBM cases (31/84) were low, but is not unexpected in a cohort of this age group[5-9]. CSF NAATs offered improved sensitivity (27/84; 32.1%), compared to CSF culture (13/84; 15.5%) and a potential for same day diagnosis; described in detail in a separate manuscript[27]. A further limitation is that all the chest radiographs were from patients with TBM.

The main finding of this study is that about half of the children diagnosed with TBM had a normal chest radiograph. Significant chest radiograph findings in children ≤3 years of age were intrathoracic lymph nodes and the presence of airway compression. Apart from a lower proportion of airway compression, the radiological findings of pulmonary TB in the setting of TBM, irrespective of stage of disease, did not differ from those reported for pulmonary TB in isolation. Signs suggestive of TB on a chest radiograph provide valuable supportive evidence for TBM in a patient suspected of having the disease. In cases with a normal chest radiograph, the diagnosis of TBM is dependent on brain imaging, cerebrospinal fluid findings and microbiological confirmation.

FUNDING

This study was supported by a Vrije University-NRF Desmond Tutu PhD scholarship.

CONFLICT OF INTEREST

None of the authors declared a conflict of interest.

REFERENCES

1. World Health Organization. Global Tuberculosis Report. WHO report 2013. Geneva, Switzerland.
2. Perez-Velez CM, Marais BJ. Tuberculosis in children. N Engl J Med 2012; 367: 348-61.
3. Rock RB, Olin M, Baker CA, Molitor TW, Peterson PK. Central nervous system tuberculosis: pathogenesis and clinical aspects. Clin Microbiol Rev 2008; 21: 243-61.
4. Thwaites GE, Caws M, Chau TTH, et al. Comparison of conventional bacteriology with nucleic acid amplification (amplified mycobacterium direct test) for diagnosis of tuberculous meningitis before and after inception of antituberculosis chemotherapy. J Clin Microbiol 2004; 42: 996-1002.
5. Chaidir L, Ganiem AR, vander Zanden A, et al. Comparison of real time IS6110-PCR, microscopy, and culture for diagnosis of tuberculous meningitis in a cohort of adult patients in Indonesia. PLoS One 2012; 7(12): e52001.
6. Thwaites G, Chau TTH, Mai NTH, Drobniewski F, McAdam K, Farrar J. Tuberculous meningitis. J Neurol Neurosurg Psychiatry 2000; 68: 289-99.
7. Jönsson B, Ridell M. The Cobas Amplicor MTB Test for Detection of Mycobacterium tuberculosis Complex from Respiratory and Non-respiratory Clinical Specimens. Scand J Infect Dis 2003; 35(6-7): 372-7.
8. Hosoglu S, Geyik MF, Balik I, et al. Predictors of outcome in patients with tuberculous meningitis. Int J Tuberc Lung Dis 2002; 6(1): 64-70.
9. Solomons RS, van Elsland SL, Visser DH, et al. Commercial nucleic acid amplification tests in tuberculous meningitis - a meta-analysis. Diagn Microbiol Infect Dis 2014; 78(4): 398-403.
10. Marais S, Thwaites G, Schoeman JF, et al. Tuberculous meningitis: a uniform case definition for use in clinical research. Lancet Infect Dis 2010; 10(11): 803-12.
11. M Whiteman, L Espinoza, MJ Post, MD Bell, S Falcone. Central Nervous System Tuberculosis in HIV-Infected Patients: Clinical and Radiographic Findings. AJNR Am J Neuroradiol 1995; 16(6): 1319-27.
12. Sütlaş PN, Unal A, Forta H, Senol S, Kirbaş D. Tuberculous meningitis in adults: review of 61 cases. Infection 2003; 31(6): 387-91.
13. Thwaites GE, Duc Bang N, Huy Dung N, et al. The influence of HIV infection on clinical presentation, response to treatment, and outcome in adults with tuberculous meningitis. J Infect Dis 2005; 192(12): 2134-41.
14. van der Weert EM, Hartgers NM, Schaaf HS, et al. Comparison of diagnostic criteria

of tuberculous meningitis in human immunodeficiency virus-infected and uninfected children. Pediatr Infect Dis J 2006; 25(1): 65-9.

15. Marais BJ, Gie RP, Schaaf HS. A proposed radiological classification of childhood intra-thoracic tuberculosis. Pediatr Radiol 2004; 34: 886-94.
16. British Medical Research Council, Streptomycin treatment of tuberculous meningitis. Br Med J 1948; 1(6503): 582-96.
17. van Toorn R, Springer P, Laubscher JA, Schoeman JF. Value of different staging systems for predicting neurological outcome in childhood tuberculous meningitis. Int J Tuberc Lung Dis 2012; 16(5): 628-32.
18. van Toorn R, Schaaf HS, Laubscher JA, van Elsland SL, Donald PR, Schoeman JF. Short intensified treatment in children with drug-susceptible tuberculous meningitis. Pediatr Infect Dis J 2014; 33(3): 248-52.
19. Marais BJ. Childhood tuberculosis: epidemiology and natural history of disease. Indian J Pediatr 2011; 78(3): 321-27.
20. Goussard P, Gie R. The role of bronchoscopy in the diagnosis and management of pediatric pulmonary tuberculosis. Expert Rev Respir Med 2014; 8(1): 101-9.
21. Cakir E, Uyan ZS, Oktem S et al. Flexible bronchoscopy for the diagnosis and follow-up of childhood endobronchial tuberculosis. Pediatr Infect Dis J 2008; 27(9): 783-7.
22. De Blic J, Azevedo I, Burren CP et al. The value of flexible bronchoscopy in childhood pulmonary tuberculosis. Chest 1991; 100: 688-92.
23. Chan S,Abadco DL, Steiner P. Role of childhood endobronchial tuberculosis. Pediatr Infect Dis J 1994; 13: 506-9.
24. Swingler G, du Toit G, Andronikou S, van der Merwe L, Zar H. Diagnostic accuracy of chest radiography in detecting mediastinal lymphadenopathy in suspected pulmonary tuberculosis. Arch Dis Child 2005; 90(11): 1153-6.
25. Andronikou S, Brauer B, Galpin J, et al. Interobserver variability in the detection of mediastinal and hilar lymph nodes on CT in children with suspected pulmonary tuberculosis. Pediatr Radiol 2005; 35(4): 425-8.
26. Karande S, Gupta V, Kulkarni M, Joshi A, Rele M. Tuberculous Meningitis and HIV. Indian J Pediatr 2005; 72(9): 755-60.
27. Solomons RS, Visser DH, Friedrich SO, et al. Improved diagnosis of childhood tuberculous meningitis using more than one nucleic acid amplification test. Int J Tuberc Lung Dis (in press).

Table 1

Diagnostic criteria in the uniform TBM research case definition[10]

	Diagnostic score
Clinical criteria (Maximum category score=6)	
Symptom duration of more than 5 days	4
Systemic symptoms suggestive of TB (1 or more of): weight loss/(poor weight gain in children), night sweats or persistent cough > 2 weeks	2
History of recent close contact with an individual with pulmonary TB or a positive TST/IGRA in a child <10 years	2
Focal neurological deficit (excluding cranial nerve palsies)	1
Cranial nerve palsy	1
CSF criteria (Maximum category score=4)	
Clear appearance	1
Cells: 10–500 per µl	1
Lymphocytic predominance (>50%)	1
Protein concentration greater than 1 g/L	1
CSF to plasma glucose ratio of less than 50% or an absolute CSF glucose concentration less than 2·2mmol/L	1
Cerebral imaging criteria (Maximum category score=6)	
Hydrocephalus	1
Basal meningeal enhancement	2
Tuberculoma	2
Infarct	1
Pre-contrast basal hyperdensity	2
Evidence of tuberculosis elsewhere (Maximum category score=4)	

Chest X-ray suggestive of active TB (excluding miliary TB)	2
Chest X-ray suggestive of miliary TB	4
CT/ MRI/ US evidence for TB outside the CNS	2
AFB identified or *M.tuberculosis* cultured from another source i.e. lymph node, gastric washing, urine, blood culture	4
Exclusion of alternative diagnoses- An alternative diagnosis must be confirmed microbiologically, serologically or histopathologically	
Definite TBM = AFB seen on CSF microscopy, positive CSF *M.tuberculosis* culture, or positive CSF *M.tuberculosis* commercial NAAT in the setting of symptoms/signs suggestive of meningitis; or AFB seen in the context of histological changes consistent with TB brain or spinal cord together with suggestive symptoms/signs and CSF changes, or visible meningitis (on autopsy).	
Probable TBM = total score of ≥12 when neuroimaging available = total score of ≥10 when neuroimaging unavailable	
Possible TBM = total score of 6-11 when neuroimaging available = total score of 6-9 when neuroimaging unavailable	

TBM- tuberculous meningitis, TB- tuberculosis, TST- tuberculin skin test, IGRA- interferon gamma-release assay, CSF- cerebrospinal fluid, CT- computed tomography, MRI- magnetic resonance imaging, US- ultrasound, AFB- acid-fast bacilli, NAAT- nucleic acid amplification test

Table 2

Demographics and chest radiograph findings in 84 children with childhood TBM

Demographics	**n/N (%)**
Male	43/84 (51)
Age group	
≤3 years	46/84 (55)
>3 years	38/84 (45)
Chest radiograph findings	
Normal CXR	39/84 (46)
Abnormal CXR (not TB)	5/84 (6)
Abnormal CXR (Uncertain TB)	3/84 (4)
Abnormal CXR (certain TB)	37/84 (44)
Miliary TB	9/84 (11)
Parenchymal consolidation	15/84 (18)
Intrathoracic lymphadenopathy	32/84 (38)
Paratracheal	16/84 (19)
Hilar	24/84 (29)
Complicated lymph node disease	18/84 (21)
Airway compression	16/84 (19)
Bronchus intermedius	8/84 (10)
Left main bronchus	8/84 (10)

TBM= tuberculous meningitis, CXR= chest radiograph, TB= tuberculosis

Table 3

Chest radiograph findings in children investigated for TBM, comparing very young (≤3 years) to older children

	≤3 years (n=46)	>3 years (n=38)	Odds ratio (95% CI)	p-value
Normal CXR	17	22	0.43 (0.18-1.03)	0.06
Abnormal CXR (not TB)	3	2		
Abnormal CXR (Uncertain TB)	1	2		
Abnormal CXR (certain TB)	25	12	2.58 (1.05-6.33)	0.04
Miliary TB	5	4	1.04 (0.26-4.17)	0.96
Parenchymal consolidation	12	4	3.00 (0.88-10.24)	0.07
Intra-thoracic lymphadenopathy	23	9	3.22 (1.25-8.29)	0.02
Complicated lymph node disease	17	1	21.69 (2.73-172.67)	<0.01
Airway compression (any)	15	1	17.90 (2.24-143.27)	<0.01

TBM= tuberculous meningitis, CI= confidence interval, CXR= chest radiograph, TB= tuberculosis, LAD= lymphadenopathy

Funding

This project was made possible by the following generous contributions:

1. Astra Zeneca and the South African Thoracic Society - R50 000
2. Tygerberg Children`s Hospital Trust for donating a 4 mm bronchoscopy for interventional bronchoscopy

Acknowledgements

The work involved in this thesis could not have been carried out without enormous help from the following people:

My mentor:

Prof RP Gie

The father of pediatric bronchoscopy in South Africa. Without his ideas, help, encouragement and patience this thesis would have not been possible. I am grateful for his help and all the hard hours he has spent on this during the last 10 years.

Prof C Bollinger

For teaching us the art of TBNA

To the late Prof helping us to learn TBNA

Colleagues:

Prof S Kling

For her support, help and for advising on many ethical issues.

Dr Louis Heyns

For caring for many of these children in the intensive care unit and helping to find missing information through all his contacts in the Western Cape. We all miss him terribly.

Prof M Kruger and Prof P-L van der Merwe, Heads of Department of Pediatrics and Child Health

For their support and encouragement.

Department of Cardio-Thoracic Surgery:

Prof GJ Rossouw

Dr JT Janson

Thank you for your willingness to be part of this study and the professional way these patients were cared for. Your dedication and extremely good surgical skills have helped keep the complication rate very low.

Department of Anesthesiology and Critical Care:

For their help on Tuesdays in bronchoscopy theatre as well as for caring for these children during thoracotomy. To the late Dr Pieter le Roux for his help with the complicated airway cases as well as his jokes and “car talk” during bronchoscopies.

Department of Radiology

Prof S Andronikou

Prof R Pitcher

For conducting and reporting the Chest CT-scans of these children.

For Savvas for his sheer brilliance and his eagerness to get these projects done and published.

Bronchoscopy suite

To all the nursing personnel in bronchoscopy theatre, where most of the bronchoscopies was done.

Department of Anatomical Pathology

Dr P Schubert

Dr M Louw

For attendance at bronchoscopy and willingness to do onsite cytology.

Tygerberg Children's Hospital: Ward G9

To sister Lyners for always creating bed space for our patients and the excellent care they received under her supervision.

Pediatric registrars and pediatric pulmonology registrars

For doing most of the clinical work and arranging special investigations.

Anita Fourie, for her friendliness, willingness to help and her ability to sort everything out.

Secondary Hospitals (Paarl, Worcester, Helderberg and Karl Bremer)

For identifying and referring many of these cases.

Prof Martin Kidd

For his invaluable assistance with the statistical analysis.

I thank you

List of abbreviations

3D-VR	3-dimensional volume-rendered CT scans
ADA	adenosine deaminase
AIDS	acquired immunodeficiency syndrome
AP	anteroposterior
BAL	broncho-alveolar lavage
BALF	broncho-alveolar lavage fluid
BCG	Bacillus Calmette-Guerin
BEF	broncho-esophageal fistula
BI	bronchus intermedius
BOF	broncho-oesophageal fistula
BPF	bronchopleural fistula
CMV	convential mechanical ventilation
CPR	curved plane reformation
CRP	C-reactive protein
CT	computed tomography
CXR	chest radiograph
EBUS-TBNA	endobronchial ultrasound-guided TBNA
ECMO	extracorporeal membrane oxygenation
ETB	endobronchial TB
ETH	ethionamide
FB	fiberoptic bronchoscopy
FB	flexible bronchoscopy
FTB	fibreoptic tracheobronchoscopy
GA	gastric aspirate
HFOV	high frequency oscillatory ventilation
High-KV	high kilovolt
HIV	human immune deficiency
HU	Hounsfield unit
ICU	intensive care unit
INH	isoniazid
IRIS	immune reconstitution inflammatory syndrome
LA-PDM	local airway point distribution model
LBTB	lymphobronchial TB

LDA	linear discriminant analysis
LDH	lactate dehydrogenase
LLL	left lower lobe
LLLB	left lower lobe bronchus
LMA	laryngeal mask
LMB	left main bronchus
LOOCV	leave-one-out cross validation
LUL	left upper lobe
LULB	left upper lobe bronchus
MCV	mean corpuscular volume
MDCT	multidetector-row spiral computed tomography
MDR	multi-drug resistance
MIP/MinIP	maximum and minimum intensity projections
MMF	mycopheylate mofetil
MPR	multiplanar reformation
MRI	Magnetic resonance imaging
PCA	principal component analysis
PCP	Pneumocystis jiroveci pneumonia
PCR	polymerasechain reaction
PDM	point distribution models
PICU	pediatric intensive care unit
PTB	pulmonary tuberculosis
RLL	right lower lobe
RLLB	right lower lobe bronchus
RMB	right main bronchus
RML	right middle lobe
RMLB	right middle lobe bronchus
RMP	rifampicin
RUL	right upper lobe
RULB	right upper lobe bronchus
SA	South Africa
SSD	shaded surface display
TB	tuberculosis
TBNA	trans-bronchial needle aspiration
TPS	thin plate spline

TST	tuberculin skin test
VR	volume rendering
WHO	World Health Organization
ZN	Ziehl Neelsen